Elucidating the Functional Significance of Protein Interaction Networks Mediated by 19S Regulatory Particle of Proteasome

By

Indrajit Sahu

[LIFE09201004018]

Tata Memorial Centre,
Mumbai

A thesis submitted to the
Board of Studies in Life Sciences
In partial fulfilment of requirements

For the Degree of
DOCTOR OF PHILOSOPHY
Of
HOMI BHABHA NATIONAL INSTITUTE

March 2016

Homi Bhabha National Institute

Recommendations of the Viva Voce Committee

As members of the Viva Voce Committee, we certify that we have read the dissertation prepared by Mr. Indrajit Sahu entitled *"Elucidating the Functional Significance of Protein Interaction Networks Mediated by 19S Regulated Particle of Proteasome"* and recommend that it may be accepted as fulfilling the thesis requirement for the award of Degree of Doctor of Philosophy.

Chairman – Dr. S.V. Chiplunkar S.V. Chiplunkar **Date:** 22/3/2016

Guide – Dr. Prasanna Venkatraman V. Prasanna **Date:** 22/3/2016

Member 1 – Dr. Sorab Dalal S.N. Dalal **Date:** 22/3/2016

Member 2- Dr. Dibyendu Bhattacharyya D. Bhattacharyya **Date:** 22/3/16

External Examiner- Dr. Sandhya S. Visweswariah Sandhya S **Date:** 22.3.16

Final approval and acceptance of this thesis is contingent upon the candidate's submission of the final copies of the thesis to HBNI.

I/We hereby certify that I/we have read this thesis prepared under my/our direction and recommend that it may be accepted as fulfilling the thesis requirement.

Date: 22/3/16.

Place: Navi Mumbai

V. Prasanna

Signature

Dr. Prasanna Venkatraman

Guide

STATEMENT BY AUTHOR

This dissertation has been submitted in partial fulfilment of requirements for an advanced degree at Homi Bhabha National Institute (HBNI) and is deposited in the Library to be made available to borrowers under rules of the HBNI. Brief quotations from this dissertation are allowable without special permission, provided that accurate acknowledgement of source is made. Requests for permission for extended quotation from or reproduction of this manuscript in whole or in part may be granted by the Competent Authority of HBNI when in his or her judgment the proposed use of the material is in the interests of scholarship. In all other instances, however, permission must be obtained from the author.

Indrajit Sahu

DECLARATION

I, hereby declare that the investigation presented in the thesis has been carried out by me. The work is original and has not been submitted earlier as a whole or in part for a degree /diploma at this or any other Institution / University.

Indrajit Sahu

List of Publications arising from the thesis

Articles:

1. **Sahu I**, Sangith N, Ramteke M, Gadre R, Venkatraman P. (2014). A novel role for the proteasomal chaperone PSMD9 and hnRNPA1 in enhancing IκBα degradation and NF-κB activation – functional relevance of predicted PDZ domain–motif interaction. ***FEBS J***. Vol. 281 (11), 2688-2709.
2. Sangith N, Srinivasaraghavan K, **Sahu I**, Desai A, Medipally S, Somavarappu A. K, Verma C, Venkatraman P. (2014). Discovery of novel interacting partners of PSMD9, a proteasomal chaperone: Role of an Atypical and versatile PDZ-domain motif interaction and identification of putative functional modules. ***FEBS Openbio***. Vol 4, 571–583.

Conference Proceedings:

1. **Sahu I**, Sangith N, Ramteke M, Gadre R, Venkatrama P. (2014). A 19S proteasomal subunit-PSMD9 enhances IκBα degradation and NF-κB activation by interacting with hnRNPA1. ***Mol. Biol. Cell*** 25, 388 (Abstract P512).

CONFERENCES

1. Attended an International Conference "1st Global Cancer Genomics Consortium-Tata Memorial Centre Symposium" **(GCGC-2011**) on 10 – 12 November 2011 at ACTREC-TMC, Navi Mumbai.
2. Attended an International Conference "31st Annual Convention of Indian Association of Cancer Research (**IACR-2012)** and International Symposium of Cancer Genomics and its impact in the clinics" on 26 – 29 January 2012 at ACTREC-TMC, Navi Mumbai.
3. Attended an "International Symposium on Stem Cell Biology-2012" on 30th January 2012 at ACTREC-TMC, Navi Mumbai.

4. Attended an International Conference "2nd Global Cancer Genomics Consortium-Tata Memorial Centre Symposium" **(GCGC-2012**) on 19 – 20 November 2012 at ACTREC-TMC, Navi Mumbai.

5. Attended an meeting "International Conference on Radiation Biology and 11th Biennial Meeting of Indian Society for Radiation Biology **(ICRB-2012**)" on 22 – 24 November 2012 at ACTREC-TMC, Navi Mumbai.

6. **Won Best Poster Presentation Award** in an International Conference "32nd Annual Convention of Indian Association for Cancer Research **(IACR-2013)"** on 13-16 February 2013 at Delhi University, New Delhi, India.

7. Attended an International Symposium on "Conceptual Advances in Cellular Homeostasis Regulated by Proteases and Chaperons: The present, the Future and Impact on Human Diseases **ACPC-2013"** on 3 – 6 December 2013 at ACTREC-TMC, Navi Mumbai.

8. **Presented Poster** at an International Conference "The XXXVII All India Cell Biology Conference on Cell Dynamics and Cell Fate **(AICBC-2013)",** conducted by Indian Society for Cell Biology on 22 – 24 December 2013 at Indian Institute of Science, Bangalore, India.

9. **Presented Poster** at an International Conference "American Society of Cell Biology **(ASCB)/** International Federation for Cell Biology (IFCB) **Meeting-2014**" held on 6 – 10 December 2014 at Philadelphia, PA, US.

10. **Presented Poster** at an International Conference **"Carcinogenesis 2015"** organized by Carcinogenesis Foundation, USA and ACTREC-TMC, held on 11 – 13 February 2015 at ACTREC Navi Mumbai.

Dedicated to My Beloved

PARENTS

ACKNOWLEDGEMENT

I would like to take the opportunity to convey my heartiest regards to those who have contributed, supported and guided me throughout the entire duration of my PhD research.

Most importantly the very priority should be given to my guide, my mentor, my supervisor; Dr. Prasanna Venkatraman. I would like to convey my sincere and heart felt gratitude to her for the consistent guidance and motivation. Throughout my tenure she is been wonderful and inspiring to me and has taught me to a high. Her suggestions, experience and encouragement accompanied by the freedom of thought that she gave me, has helped me to discover my potential in science. Not only has she polished me intellectually but also professionally, to make me competent to this era. Ma'am, I have never thanked you enough for all that you have done for me and I have learned from you. With this, I am expressing my sincere thanks to you for giving me such a wonderful opportunity in the lab to pursue my early research carrier.

I would like to thank the Director of ACTREC Dr. S.V. Chipulnkar for providing me such a wonderful infrastructure to work with. I am thankful to Dr. Rajiv Sarin (Ex-Director, ACTREC) and Dr. Surekha Zingde (Ex-Deputy Director, ACTREC) for giving me such a great opportunity to pursue my PhD degree in this institute. I specially thank to Dr. Rajiv Sarin who helped me greatly during my bad time.

I would like to acknowledge my DC-members Dr. Sorab Dalal, Dr. Dibyendu Bhattacharyya and the Chairperson Dr. S.V. Chiplunkar for their timely suggestions and comments. I also thank Dr. Ullas Kolthur (TIFR, Mumbai) for his critical review of my work. Their sincere efforts; to make my research the finest and moves smoothly, are really appreciable.

I am expressing my deep regards to Dr. Neil D. Perkins (New Castle University, UK), Dr. D.C. Guttridge, (Ohio State University, USA), Dr. Robin Mukhopadhyay (Former scientist, ACTREC), Dr. Neelam Shirsat (ACTREC) and Dr. Sorab Dalal (ACTREC) for their help in various field that were indispensable for my research.

I am extremely thankful to ACTREC common instrument facility especially Mr. Dandekar for his constant support and help with instrumentation, imaging facility, genomic facility, Mass spectrometry, Flowcytometry, library, administration, accounts department and Students Council of ACTREC for their constant help and support.

I am very grateful towards the Sam-Mistry travel fund and HBNI international travel fund for supporting me for my international conference visit during my PhD tenure. I also acknowledge UGC for providing me the bread and butter – the "Fellowship".

I would like to express my heartiest thanks to all the Prasanna lab family members especially my seniors Dr. Amit Kumar Singh Gautam and Dr. Manoj Ramteke for their constant guidance, teaching and support which turned out to be very fruitful for my research tenure. Not only I learned many experiments from them in lab but also has acquired good ethics and lab practice as well. I would like to thank Padma, Nikhil for teaching me many techniques at initial stage of my PhD work. I would like to appreciate Ludbe Sir, Kamlesh, Vinita Ma'am, Priya, Burhan Mahalaxmi, Saim, other summer trainees and project JRFs for maintaining a very wonderful environment inside the lab. A special thanks to my two trainees Rucha and Minal, whose contribution to my research was indispensable. I have learned a lot while working with you people. Thank you so much.

I am expressing my heartiest thanks and warm regards for my fabulous batch mates JRF-2010. I had a great time with all my friends throughout the tenure which kept me refresh all the time. I would like to thank Saikat, Raja, Shyam, Asif (my Room-mate), Prasad, Poonam, Crismita for their both scientific and non-scientific contribution to my work. I would like to specially thank Richa for her critical analysis in my work and for her immense support throughout my PhD tenure. Discussing science with her has broadened my knowledge in various current fields of study, which helped me a lot to cope with people of different area of research. She stood beside me at every bad time and supported me immeasurably which replenished my concentration back. Her contribution towards my accomplishment of PhD is really appreciable and unforgettable.

I would like thank all the labs of ACTREC, which helped me in many different aspects for my work. I thank to all the fellow researchers of ACTREC for maintaining a good environment in the campus. I would like to thank those people in ACTREC who have offered me very happy and mesmerizing moments, especially my junior Pankaj Thapa who always kept me busy with his debatable and unanswerable question series.

And now the most important people of my life, "My parents and my sisters". Maa and Bapa you have always been my source of inspiration, motivation, encouragement and my greatest strength. Your sacrifices in every way for my life have only made it possible to achieve this goal. It is all because of your blessings and prayers I am getting the highest degree of my life. I owe all my sincere thanks to both of you and feel proud to be your son. I am expressing my heart-felt thanks to all my sisters and my brother-in-laws whose constant support and help contribute a lot to my 5 year journey and has made it fruitful. Thank you all for being in my life.

Thank you all for your contributions.

Indrajit Sahu

CONTENTS

CHAPTER-IV: Role of PSMD10 in Neural Stem cell Differentiation

Synopsis

Homi Bhabha National Institute

Ph.D. PROGRAMME

1. Name of the Student: Indrajit Sahu

2. Name of the Constituent Institution: Tata Memorial Centre (TMC), Advanced Centre for Treatment, Research and Education in Cancer (ACTREC)

3. Enrolment No. LIFE09201004018

4. Title of the Thesis: Elucidating the functional significance of protein interaction networks mediated by 19S regulatory particle of proteasome.

5. Board of Studies: Life Science

SYNOPSIS

Elucidating the functional significance of protein interaction network mediated by 19S regulatory particle of proteasome.

Introduction

Mammalian 26S proteasome consists of two 19S regulatory particles (RP) and one 20S core particle (CP). 19S-RP plays a major role in recognition and unfolding of the substrate-proteins and 20S-CP degrades the substrates by its three protease activity functions. Mammalian 19S-RP consists of 19 subunits comprising 6 ATPases and 13 non-ATPases. Among the non-ATPases, PSMD9 and PSMD10 primarily act as chaperons during the assembly of the 26S proteasome complex [1, 2]. Apart from the classical functions, these subunits exhibit some non-classical functions in mammalian cells.

PSMD9: PSMD9 contains an 88 amino acid long (aa108–aa195) PDZ–like domain [3]. Many PDZ domain containing proteins act as scaffolds to form supra molecular assemblies which allows them to function in signaling [4, 5]. Bridge1, the PSMD9 homolog in rats has been shown to act as a coactivator of insulin gene through interaction of its PDZ-like domain with transcription factors E12 and p300 [3, 6]. Since the structure and function of human PSMD9 has not yet well studied, we started investigating its function by searching novel interacting partners.

Using a novel structural bioinformatics method and peptide based screening we recently reported that hnRNPA1 is one among the novel interacting partners of PSMD9 [7]. We were intrigued by the report which demonstrated that, hnRNPA1 is responsible for IκBα degradation leading to NF-κB transcriptional activation in mouse cells [8]. Since the bigger and fundamental question of how IκBα is recruited to the proteasome for degradation remains largely unaddressed, it would be interesting to investigate

whether hnRNPA1 by interacting with PSMD9, involved in proteasomal degradation pathway in human cells. Furthermore, the mechanism by which ubiquitinated proteins are recruited to proteasome remains an active area of research throughout. Based on these background studies, we hypothesized that PSMD9 may have a role in NF-κB signaling pathway in mammalian cells.

PSMD10: PSMD10, a non-ATPase subunit of 19S RP and also called as Gankyrin, a seven ankyrin repeats containing protein of about 25 kDa. PSMD10 act as a chaperon and during assembly of 26S proteasome it interacts with two ATPase subunits PSMC4 and PSMC5. Gankyrin is now known as an oncoprotein found to be associated with many cancers. Gankyrin as an oncoprotein modulate several critical signal cascades by various mechanisms. Overexpression of gankyrin triggers the degradation of Rb and p53 by MDM2 and resulting cellular transformation [9, 10]. Gankyrin plays essential roles in Ras-induced Akt-RhoA/ROCK [11], PI3K/Akt in HCC progression [12], Rac1 activity [13] and IL-6/STAT3 signaling in cholangiocarcinoma [14]. Recently we have reported eight novel interacting partners of PSMD10 and established one of these interacting partners, CLIC1 in rewiring the network in cancer [15].

However, despite its oncogenic role, gankyrin also exhibits some normal functions in the cells. It binds to RelA and retains NF-κB in the cytoplasm hence decrease NF-κB activity [16]. Our initial microarray data indicated that PSMD10 overexpression in HEK293 cells, results in upregulation of neuron specific genes, Artemins, Neuregulin-1 (NRG1) and Neurogenin-1 (NGN1). Earlier studies suggested NGN1 promotes neuronal differentiation and prevents glial differentiation in rat cortical progenitor cells [17]. Based on these observations, we hypothesized that PSMD10 may be involved in neural stem cells differentiation process.

RESULTS

1. PSMD9:

PSMD9 interacts with C-terminus of hnRNPA1

Recently we have reported hnRNPA1 as a novel interacting partner of PSMD9 [7]. Further we proved that this interaction is mediated by the C-terminal residues of hnRNPA1. To test the *ex vivo* interaction we performed immunoprecipitation from HEK293 cell lysate and results indicated that C-terminus of hnRNPA1 is indeed essential for interaction with PSMD9 *ex vivo*.

PSMD9 protein levels influence basal and TNF-α mediated NF-κB activity

Since we found that PSMD9 interacts with hnRNPA1 *ex vivo* and hnRNPA1 reportedly influences NF-*κ*B activity [8], we asked if PSMD9 was involved in this pathway. When PSMD9 was overexpressed in HEK293 cells basal and TNF-*α* mediated NF-*κ*B activity was increased. This increase in NF-*κ*B activity was further validated by demonstrating nuclear translocation of NF-*κ*B (p65) and DNA binding activity assay (EMSA). Concomitantly upon PSMD9 knockdown a decrease in NF-*κ*B DNA binding activity was observed. In addition, five of NF-*κ*B target genes viz. ICAM1, IL6, I*κ*B*α*, A20 and COX2 were several fold upregulated in PSMD9 overexpression cells and downregulated in PSMD9 knockdown cells. These results suggest that PSMD9 is involved in both basal and signal mediated NF-*κ*B pathway.

PSMD9 overexpression increases NF-κB activity by enhancing IκBα proteasomal degradation

Since NF-*κ*B activity increased upon increase in the levels of PSMD9 in HEK293 cells, we hypothesized that PSMD9 may accelerate the degradation of I*κ*B*α*. Accordingly when PSMD9 was overexpressed, there was a visible decrease in half-life of I*κ*B*α*

protein i.e. from 18h to 4h. Upon knockdown of PSMD9, IκBα levels were found to be stable even after 24 hours of cycloheximide treatment. MG132 or Velcade treatment could significantly inhibit both basal and TNF-α mediated poly-ub-IκBα degradation in cells overexpressing PSMD9, which confirms the involvement of 26S proteasome in this degradation process. IκBα super-repressor (S32A-S36A) expression studies indicated that, phosphorylation of IκBα is not influenced by PSMD9 levels but it is indispensable for PSMD9 mediated IκBα degradation.

PSMD9 does not affect the IκBα ubiquitination and Proteasomal activity

Given its role as an assembly chaperone, PSMD9 expression may influence proteasomal activity which in turn may dictate the overall IκBα levels. We tested the activity of proteasome upon overexpression and silencing of PSMD9. Proteasomal activity was unaltered in these cells and remained uninfluenced by TNF-α treatment. Due to the importance of ubiquitination in IκBα degradation by the proteasome, we checked the influence of PSMD9 in this process. We performed experiment where we treated both control and PSMD9 knock-down cells with MG132 followed by CHX treatment. The results indicated that PSMD9 does not affect ubiquitination of IκBα but failed to degrade ubiquitinated IκBα efficiently not because of impaired proteasomal activity but due to the absence of PSMD9.

The PDZ domain of PSMD9 interacts with hnRNPA1

Point mutations in PDZ domain of PSMD9 affected *in vitro* binding to hnRNPA1 [7]. We checked if this domain-motif recognition is also a key determinant of interaction inside the cells. We showed by series of immunoprecipitation studies that Q181G and the β2 L124G/Q126G/E128G triple mutant abolished interaction with PSMD9 *ex vivo*. IκBα was detected only in the wild type PSMD9-hnRNPA1 complex suggesting that PSMD9 is probably linked to IκBα only through hnRNPA1. Unlike cells

overexpressing wild type PSMD9, in cells overexpressing PDZ mutants (Q181G and the β2 Triple mutant), IκBα was not efficiently degraded even after TNF-α treatment nor was there a significant change in NF-κB activity.

PSMD9 is linked to IκBα via hnRNPA1.

hnRNPA1 was previously shown to interact with IκBα through its RNA binding domain [8]. We demonstrated that PSMD9 interacts with hnRNPA1 through its C-terminus. And the PDZ mutation analysis indicates that interaction between PSMD9 and IκBα is likely through hnRNPA1. To determine the structural hierarchy of this tripartite interaction between PSMD9, hnRNPA1 and IκBα, we performed a series of *ex vivo* immunoprecipitation and *in vitro* Far western blot analysis. The results confirmed that there is no direct interaction between PSMD9 and IκBα, they can only interact through hnRNPA1, which uses different structural regions for these interactions that are not mutually exclusive.

Interaction between C-terminus of hnRNPA1 and PSMD9 is required for degradation of IκBα as well as NF-κB activity

We have demonstrated here a novel role of PSMD9 and its specific interaction with hnRNPA1. Now we asked if hnRNPA1 had any role to play in IκBα degradation and NF-κB activation in the absence of PSMD9 or when its interaction with PSMD9 is lost. When HA-WT-hnRNPA1 was overexpressed in HEK293 cells, degradation of IκBα and NF-κB activity were considerably enhanced which were not seen in HA-7ΔC-hnRNPA1 mutant case. Furthermore, when we silenced PSMD9 and overexpressed wild type HA-hnRNPA1, IκBα degradation and NF-κB activity was significantly reduced. These results suggest that PSMD9-hnRNPA1interaction is essential for the IκBα degradation as well as NF-κB activation and both PSMD9 and hnRNPA1 are in the same casecade of this signaling pathway.

PSMD9 anchors hnRNPA1-IκBα complex on 26S proteasome that facilitates proteasomal degradation of IκBα

We hypothesized that PSMD9 by virtue of its interaction with the proteasome on one hand and its interaction with hnRNPA1 on the other, would recruit IκBα to the proteasome for degradation. We first pulled down the whole 26S proteasomal and found both endogenous and transexpressed PSMD9 associated with proteasome. TNF-α treatment did not alter the levels of PSMD9, but increased the levels of proteasome-bound hnRNPA1 and further enhanced upon PSMD9 overexpression. In contrast when PSMD9 was silenced, no hnRNPA1 was found in the proteasome pull down complex even after TNF-α treatment.

Based on current evidence PSMD9 seems to harbour only the PDZ domain for protein- interaction, we tested whether the PDZ mutations affect association of PSMD9 with the proteasome. Affinity pull down of the 26S proteasome in cells over expressing PDZ mutant Q181G, indicated that this association was unimpaired so as the proteasomal activity. Since we found increased IκBα degradation upon hnRNPA1 overexpression with TNF-α treatment, we wanted to check the recruitment of overexpressed hnRNPA1 on 26S proteasome. Both endogenous and trans-expressed hnRNPA1 levels on proteasome were found to be increased upon TNF-α treatment, which correlates with the IκBα degradation. Furthermore total protein levels of hnRNPA1 remain unaltered upon PSMD9 overexpression or downregulation or after TNF-α treatment. A significant increase in association of polyubiquitinated-phospho-IκBα with 26S proteasome was observed, in proteasome pull down assay followed by MG132 treatment in PSMD9 overexpressing HEK293 cells confirming the PSMD9 role in this process.

Summary

We establish that PSMD9 through its PDZ domain interacts with the C-terminus of hnRNPA1, a novel interacting partner. This interaction is essential for degradation of IκBα by proteasome and therefore regulating the NF-κB activity in HEK293 cells. PSMD9 level neither affect phosphorylation or ubiquitination of IκBα nor the basal proteasome activity. However, the levels PSMD9 determine the rate of polyubiquitinated-phospho-IκBα recruitment on 26S proteasome and hence the rate of degradation. In this degradation process hnRNPA1 acts as a shuttle receptor while PSMD9 acts as the docking site on the 19S regulatory particle of Proteasome.

Based on our findings about the molecular details of interaction between the PDZ-domain of PSMD9 and hnRNPA1, we speculate a general role for PSMD9 in substrate recognition by the proteasome. IκBα may be one of the many examples of how ubquitinated substrates may be recruited on the proteasome through the PDZ domain of PSMD9. Since in the absence of any external stimuli, PSMD9 overexpression results in an increased basal activity of NF-κB, it remains to be seen whether PSMD9 acts as an internal signal for NF-κB activation.

Our study opens up new areas of investigation on the role of PSMD9 in cellular homeostasis. However, the generality of this interaction between hnRNPA1 and PSMD9 may propose the interface as a potential therapeutic drug target in tumor cells relying on high NF-κB activity for their survival.

2. PSMD10 (Gankyrin)

Characterization of the human Neural progenitor cells and differentiated cells

Human neural progenitor cells (hNPC) were grown on laminin coated plate in Neural stem cells maintenance media with EGF and FGF supplements. Expression of stem cell markers viz. Sox2, Nestin and Musashi were detected by immunofluorescence

and western blot analysis. When NPC cells were grown in Neural stem cells maintenance media without any growth factors for 12-15 days they differentiated into astrocytes, neurons and oligodendrocytes. Differentiated cell were characterized with Nuronal marker – β-III tubulin, astrocyte marker – GFAP (Glial fibrilliary acidic protein) and oligodendrocyte marker – O1 by immunofluorescence and western blot analysis.

Differential expression of Proteasomal subunits in human Neural progenitor cells

Transcript and protein levels of proteasomal subunits were analysed in undifferentiated and differentiated cells. The protein levels of proteasomal subunits α4, β7 and Rpt6 were found to be decreased. While PSMD9 levels remained unchanged, PSMD10 levels increased in differentiated cells. Similarly the mRNA levels of β1, β5, PSMD9 and PSMD4 were found to be decreased, β2 levels remained unchanged but PSMD10 transcript levels were found to be increased in differentiated cells.

Apart from the proteasomal subunits protein levels of *β*-catenin and mRNA levels of Neurogenin-1 (NGN1) was found to be increased in differentiated cells. When differentiated cell populations were analyzed by immunofluorescence, ~90% of cell population were found to be astrocytes. The day-wise studies of hNPCs differentiation indicated that, the levels of STAT3 and p-STAT3 seem to be increased during the early phase of differentiation process and decreased during the late phase. Whereas the levels *β*-catenin increased from the very early phase of the process and remained constant throughout the process. Most importantly the levels of PSMD10 kept on increasing during the process and remained stable at very late phase.

Effect of overexpression of Flag-PSMD10 in hNPCs

Third generation lentiviral particle of pTRIPZ-FLAG-PSMD10 was prepared and transduced in Neural progenitor cells. Immunofluorescence experiments indicated that,

~60% of FLAG-PSMD10 overexpressing hNPC cells were differentiated into astrocytes and rest of the cells (~40%) differentiated into neurons. Neuron counts of the total differentiated population increased to 2-2.5 fold upon PSMD10 overexpression validated by increase in βIII-tubulin levels in western blot analysis.

Summary

We could establish some preliminary results which suggest the possible role of PSMD10 in human neural progenitor cell differentiation process. PSMD10 might be promoting astrocyte differentiation by regulating STAT3 activity in the early days of differentiation process. However, the Co-expression of PSMD10, β-catenin and NGN1 in the latter part of differentiation process and increase in neuron counts suggest the possible involvement of PSMD10 in neuronal differentiation. Hence PSMD10 may be involved both in astrocyte as well as neuronal differentiation process of hNPC in a spatio-temporal manner. Nevertheless, further validation and detail mechanism of PSMD10 involvement in hNPC differentiation need to be deciphered. Gankyrin although established as an oncoprotein, our data suggests its normal function in neural differentiation process.

REFERENCES

1. Kaneko T, Hamazaki J, Iemura S, Sasaki K, Furuyama K, Natsume T, Tanaka K, Murata S: **Assembly pathway of the Mammalian proteasome base subcomplex is mediated by multiple specific chaperones**. *Cell* 2009, **137**(5):914-925.
2. da Fonseca PC, He J, Morris EP: **Molecular model of the human 26S proteasome**. *Mol Cell* 2012, **46**(1):54-66.
3. Thomas MK, Yao KM, Tenser MS, Wong GG, Habener JF: **Bridge-1, a novel PDZ-domain coactivator of E2A-mediated regulation of insulin gene transcription**. *Mol Cell Biol* 1999, **19**(12):8492-8504.
4. Jelen F, Oleksy A, Smietana K, Otlewski J: **PDZ domains - common players in the cell signaling**. *Acta Biochim Pol* 2003, **50**(4):985-1017.
5. Banz C, Munchow B, Diedrich K: **Bridge-1 is expressed in human granulosa cells and is involved in the activin A signaling cascade**. *Fertil Steril* 2010, **93**(4):1349-1352.
6. Lee JH, Volinic JL, Banz C, Yao KM, Thomas MK: **Interactions with p300 enhance transcriptional activation by the PDZ-domain coactivator Bridge-1**. *J Endocrinol* 2005, **187**(2):283-292.
7. Sangith N, Srinivasaraghavan K, Sahu I, Desai A, Medipally S, Somavarappu AK, Verma C, Venkatraman P: **Discovery of novel interacting partners of PSMD9, a proteasomal chaperone: Role of an Atypical and versatile PDZ-domain motif interaction and identification of putative functional modules**. *FEBS Open Bio* 2014, **4**:571-583.
8. Hay DC, Kemp GD, Dargemont C, Hay RT: **Interaction between hnRNPA1 and IkappaBalpha is required for maximal activation of NF-kappaB-dependent transcription**. *Mol Cell Biol* 2001, **21**(10):3482-3490.
9. Higashitsuji H, Itoh K, Nagao T, Dawson S, Nonoguchi K, Kido T, Mayer RJ, Arii S, Fujita J: **Reduced stability of retinoblastoma protein by gankyrin, an oncogenic ankyrin-repeat protein overexpressed in hepatomas**. *Nat Med* 2000, **6**(1):96-99.
10. Higashitsuji H, Itoh K, Sakurai T, Nagao T, Sumitomo Y, Masuda T, Dawson S, Shimada Y, Mayer RJ, Fujita J: **The oncoprotein gankyrin binds to**

MDM2/HDM2, enhancing ubiquitylation and degradation of p53. *Cancer Cell* 2005, **8**(1):75-87.

11. Man JH, Liang B, Gu YX, Zhou T, Li AL, Li T, Jin BF, Bai B, Zhang HY, Zhang WN *et al*: **Gankyrin plays an essential role in Ras-induced tumorigenesis through regulation of the RhoA/ROCK pathway in mammalian cells**. *J Clin Invest* 2010, **120**(8):2829-2841.
12. Fu J, Chen Y, Cao J, Luo T, Qian YW, Yang W, Ren YB, Su B, Cao GW, Yang Y *et al*: **p28GANK overexpression accelerates hepatocellular carcinoma invasiveness and metastasis via phosphoinositol 3-kinase/AKT/hypoxia-inducible factor-1alpha pathways**. *Hepatology* 2011, **53**(1):181-192.
13. Zhen C, Chen L, Zhao Q, Liang B, Gu YX, Bai ZF, Wang K, Xu X, Han QY, Fang DF *et al*: **Gankyrin promotes breast cancer cell metastasis by regulating Rac1 activity**. *Oncogene* 2013, **32**(29):3452-3460.
14. Zheng T, Hong X, Wang J, Pei T, Liang Y, Yin D, Song R, Song X, Lu Z, Qi S *et al*: **Gankyrin promotes tumor growth and metastasis through activation of IL-6/STAT3 signaling in human cholangiocarcinoma**. *Hepatology* 2014, **59**(3):935-946.
15. Nanaware PP, Ramteke MP, Somavarapu AK, Venkatraman P: **Discovery of multiple interacting partners of gankyrin, a proteasomal chaperone and an oncoprotein--evidence for a common hot spot site at the interface and its functional relevance**. *Proteins* 2014, **82**(7):1283-1300.
16. Chen Y, Li HH, Fu J, Wang XF, Ren YB, Dong LW, Tang SH, Liu SQ, Wu MC, Wang HY: **Oncoprotein p28 GANK binds to RelA and retains NF-kappaB in the cytoplasm through nuclear export**. *Cell Res* 2007, **17**(12):1020-1029.
17. Sun Y, Nadal-Vicens M, Misono S, Lin MZ, Zubiaga A, Hua X, Fan G, Greenberg ME: **Neurogenin promotes neurogenesis and inhibits glial differentiation by independent mechanisms**. *Cell* 2001, **104**(3):365-376.

Publication in Refereed Journal:

a. Published:

1. **Sahu I**, Sangith N, Ramteke M, Gadre R, Venkatrama P. (2014). A novel role for the proteasomal chaperone PSMD9 and hnRNPA1 in enhancing IκBα degradation and NF-κB activation – functional relevance of predicted PDZ domain–motif interaction. ***FEBS J.*** Vol. 281 (11), 2688-2709.
2. Sangith N, Srinivasaraghavan K, **Sahu I**, Desai A, Medipally S, Somavarappu A. K, Verma C, Venkatraman P. (2014). Discovery of novel interacting partners of PSMD9, a proteasomal chaperone: Role of an Atypical and versatile PDZ-domain motif interaction and identification of putative functional modules. ***FEBS Openbio***. Vol 4, 571–583.

b. Accepted: NA

c. Communicated: NA

d. Other Publication: (Conference proceedings)

1. **Sahu I**, Sangith N, Ramteke M, Gadre R, Venkatrama P. (2014). A 19S proteasomal subunit-PSMD9 enhances IκBα degradation and NF-κB activation by interacting with hnRNPA1. ***Mol. Biol. Cell*** 25, 388 (Abstract P512).

Signature of Student

Date: 22/01/15

Doctoral Committee:

S. No.	Name	Designation	Signature	Date
1.	Dr. S.V Chiplunkar	Chairperson		2/2/15
2.	Dr. Prasanna Venkatraman	Guide		28/01/15
4.	Dr. Sorab Dalal	Member		29/1/15
5.	Dr. Dibyendu Bhattacharyya	Member		29/01/15

Forwarded through:

Dr. S.V. Chiplunkar
Director ACTREC
Chairperson,
Academic & Training Programme

Dr. S. V. Chiplunkar
Director
Advanced Centre for Treatment, Research & Education in Cancer (ACTREC)
Tata Memorial Centre
Kharghar, Navi Mumbai 410210.

Dr. K. Sharma
Director, Academics
T.M.C.

PROF. K. S. SHARMA
DIRECTOR (ACADEMICS)
TATA MEMORIAL CENTRE,
PAREL, MUMBAI

List of Figures

List of Tables

List of Abbreviations

ATP	: Adenosine triphosphate
AAA-ATPase	: ATPases Associated with various cellular Activities
BME	: ß- Mercaptoethanol
bFGF	: basic Fibroblast Growth Factor
BSA	: Bovine Serum Albumin
cDNA	: complimentary Deoxyribonucleic acid
Dlg2	: Disc Large Homolog 2
DTT	: Dithiothreitol
EGF	: Epidermal Growth Factor
EMSA	: Electrophoretic Mobility Shift Assay
hNPCs	: human Neural Progenitor cells
KDa	: Kilodalton
mM	: Millimolar
Ni-NTA	: Nickel-nitriloacetic acid
MBP	: Maltose Binding Protein
GST	: Glutathione S-Transferase
hnRNPA1	: Heterogenous Ribonucleoprotein A1
PAGE	: Polyacrylamide Gel Electrophoresis
PCV	: Pack Cell Volume
PCR	: Polymerase Chain Reaction
PDZ	: PSD95, Dlg2 and ZO1
PSD95	: Post Synaptic Density 95
PSMD9	: Proteasome Macropain non-ATPase subunit 9
PSMD10	: Proteasome Macropain non-ATPase subunit 10
SDS	: Sodium Dodecyl Sulphate
TBST	: Tris Buffered Saline with 0.1% Tween-20
TEMED	: N,N,N’,N’ Tetramethyl Ethylene Diamine
ZO1	: Zonula Occludens1

CHAPTER-I

Introduction & Review of Literatures

1.1. THE PROTEASOME: Cellular degradation machine:

The proteasome, called as 26S-proteasome, the key player of Ubiquitin Proteasomal System (UPS), is responsible for the controlled degradation of proteins in eukaryotic cells. It is a very large energy dependent protease complex present both in cytoplasm and nucleus of the cell. The proteasome degrade unfolded, missfolded and ubiquitinated proteins in a well-regulated manner. 26S proteasome consists of two 19S and one 20S sub-complexes. The 19S regulatory particle is responsible for binding of polyubiquitylated proteins, releasing of ubiquitin chain, unfolding of the substrate-proteins and the regulated entry of the substrate into 20S complex. The 20S core particle is the catalytic chamber that degrades the substrates into amino acids and short peptides by the help of three catalytic subunits in it [1].

1.2. DISCOVERY OF UBIQUITIN PROTEASOME SYSTEM (UPS):

Eukaryotic cell maintain a protein homeostasis by balancing the equilibration between protein synthesis and protein degradation. For cell growth and maintenance, controlled protein degradation is equally important and necessary as protein synthesis. The first revolutionary finding in the field of protein degradation came in 1942, when Rudolph Schönheimer proposed that “proteins are being constantly build up and broken down”, in his book ‘The Dynamic State of Body Constituents’. The 20S proteasome was first observed in 1968 in electron micrographs of human erythrocyte lysates and, in view of its cylinder-shaped structure, was called “cylindrin” [2], but its function was unknown. Before the discovery of proteasome role, people believed that “Lysosomal degradation” is the major pathway of protein degradation in the cells. But during 1977 Joseph D. Etlinger and Alfred L. Goldberg, while working on reticulocyte that lack lysosomes on maturation, for the first time reported that there was also another pathway of protein degradation exists. They developed a cell-free extracts from rabbit

reticulocytes that rapidly hydrolyze abnormal globular protein in an ATP-dependent manner [3]. Along a different line, a particle called the “prosome” or the 19S ribonucleoprotein (RNP) was found ubiquitously in eukaryotes [4]. In 1988 however, it was established that the prosome particles are identical with a multicatalytic protease complex, latter on called as proteasome [5, 6]. The unifying name “Proteasome” more precisely the 20S proteasome was coined to highlight its proteolytic activity and complex structure [5].

After this break-through discovery people began exploring the role of this pathway in great details. Ciechanover and Hershko from Technion, Israel in 1987 fractionated the crude reticulocyte cell extract on an anion-exchange resin (DEAE-cellulose) as (APF)-I and II and found that combination of both the fractions reconstructed the energy-dependent proteolytic activity [7, 8]. Later, APF-II was further sub-fractionated into APF-IIa and APF-IIb. APF-IIb contained the E1-E3 ubiquitin conjugating enzymes and APF-IIa was shown to contain proteasomes [9]. APF-I was identified as ubiquitin [10]. Eventually, in 2004 Avram Hershko, Aaron Ciechanover and Irwin rose were awarded for Nobel Prize in Chemistry for the discovery of ‘Ub dependent degradation of protein’. After decades of research now it is known that this pathway is the major protein degradation pathway in eukaryotes and 26S proteasome is the main player in the process.

1.3 STRUCTURE OF 26S PROTEASOME:

26S proteasome is a multisubunit, multicatalytic protease complex. Structurally it is more or less a symmetrical and hollow cylindrical complex of molecular weight ~2600 KDa. It consists of 19S-20S-19S sub-complexes comprising total 64 no. of subunits. Purified proteasomes are always found as a mixture of free 20S, singly capped (19S-20S), and doubly capped (19S-20S-19S) forms (Figure-1.1) [11], while in vivo it seems

that in *S. cerevisiae* the majority of proteasomes are present as doubly capped forms [12]. In mammalian cells, the ratio of 19S to 20S is lower probably leading the presence of free 20S and to proteasomes with a single 19S [13].

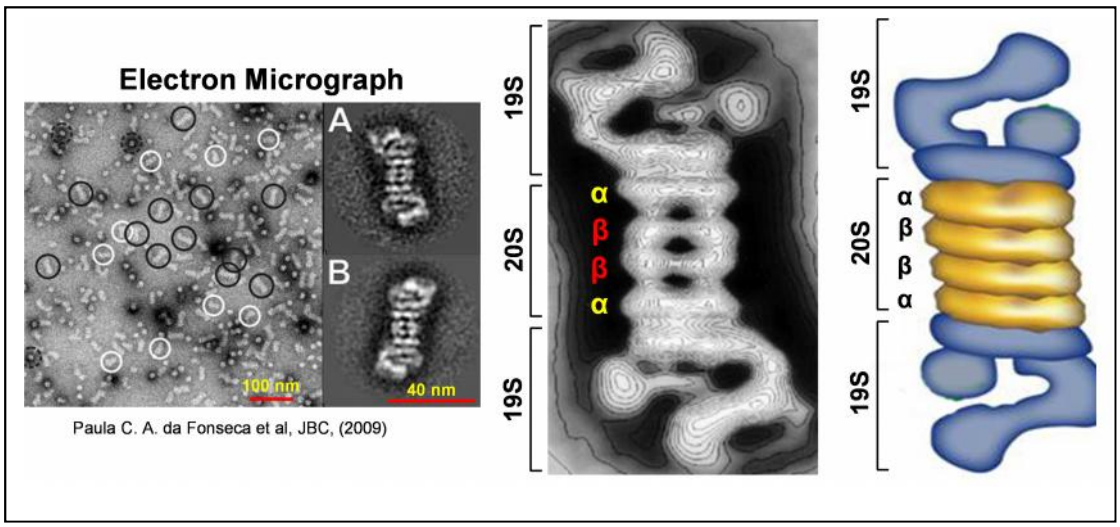

Figure-1.1: Electron micrograph of 26S proteasome: Electron micrograph of of a negatively stained 26S purified human proteasome sample. Examples of side views of double-capped and single-capped 26S proteasome images are identified with black and white circles, respectively. End views of 26S proteasome complexes are identified by black dashed circles. and B, class averages with 2-fold rotational symmetry characteristic of a projection along a C2 axis *(Left)*. Computerized magnified image of the electron micrograph of the left image *(Middle)*. Converted cartoon image of the 26S proteasome; blue colour corresponds to 19S and the yellow colour corresponds to 20S *(Right)*. *[Adopted from: Paula C. A. da Fonseca et. al., 2008]*

1.3.1 The 20S Core Particle (CP): The central 20S sub-complex of the 26S-proteasome, called as core particle (CP) of ~700 kDa is sandwiched between two 19S regulatory particles (RP) [14]. The 20S-CP can be found either isolated or associated with the 19S-RP in the eukaryotic cells. But the most abundant form of proteasome found in the eukaryotic cell is the 26S proteasome. 20S-CP is a hollow barrel-shaped structure which consists of total 28 subunits, arranged into four hetero-heptameric rings of ~150 Å X~120 Å dimension [15]. This complex is assembled from 14 no. of subunits into four stacked rings - two inner β rings and two outer α rings and exhibits twofold (C2) symmetry resulting an overall stoichiometry of α1-7–β1-7–β1-7–α1-7 (Figure-1.2). The inner surface of 20S CP forms a central channel divided into three

large cavities of of ~40 Å x ~50 Å dimension separated by narrow constrictions. The two cavities between the both α and β-subunit rings apparently store the substrate in unfolded conformation and the central catalytic cavity (of ~40 Å x ~55 Å in dimension) harbors the protease active sites [16, 17]. In eukaryotes only three of the seven β- type subunits harbour proteolytic activity making six active sites per 20S molecule. Each active site can cleave a broad range of peptide sequences, β1 cleaves after acidic residues (caspase like), β2 after basic residues (trypsin like), and β5 after hydrophobic residues (chymotrypsin like) [18]. 20S CP can also associate with other regulatory complexes like 11S and PA200 [14].

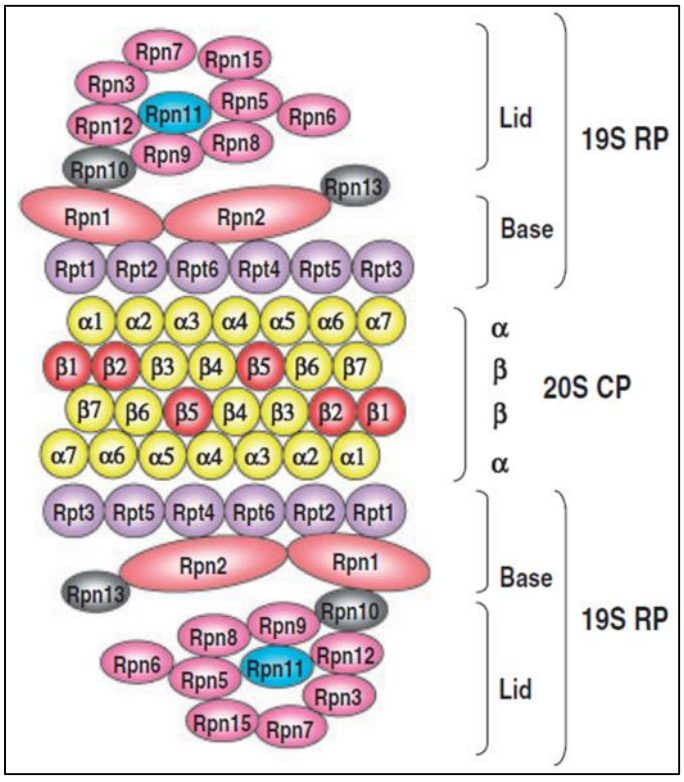

Figure-1.2: Cartoon representation of 26Sproteasome. Relative position of all the subunits of proteasome. Rpn10/13 are ubiquitin receptor, Rpn11 having deubiqutinating enzymatic activity, β1/2/5 (Red) contain the protease catalytic activity. [Adopted from: Keiji Tanaka, 2009]

1.3.2 The 19S Regulatory Particle (RP): (ATP dependent modulator of proteasome)

The 19S sub-complex of the proteasome is called as the regulatory particle (RP) since it regulates degradation of the substrates by guiding them into the 20S core particle. The 19S RP performs multiple roles in regulating proteasomal activity e.g.: (a)

substrates recognition, (b) substrate unfolding (c) substrate deubiquitination and (d) translocation to the 20S catalytic particle [14]. Although, different subunits of the 19S RP have been identified and assigned with specific functions, the organization of the 19S complex is still imprecise. However, recent cryo-EM map by single particle analysis has provided glimpse of the architecture of 26S holo-complex (9Å to 7.4Å) [19-21]. With the help of these EM maps, the position of ATPases and Ub binding domain containing subunits could be assigned in 26S proteasome.

Glickman, *et al*. biochemically characterized the 19S regulatory particle (RP), earlier termed as PA700 (due to its molecular weight speculated to be 700kDa) and found it to be composed of 18 subunits [22]. This 19S-RP may assemble at one or both ends of the 20S-CP [14]. The subunits of the 19S-RP can be divided into the `base' and the `lid' [11]. The base of the 19S, positioned proximal to the 20S core particle, comprises a ring of six AAA (ATPase associated with a variety of cellular activities)-ATPases, named Rpt1 to 6 (Regulatory particle triple A) in yeast [23-25]. The base consists of all the ATPases which form the ring like structure along with a few non-ATPases. The lid comprises of non-ATPases only, named Rpn.

1.3.2.1 The Base of the 19S:

The base of the 19S-RP is composed of four non-ATPase subunits (Rpn1, Rpn2, Rpn10 and Rpn13) and six ATPase subunits (Rpt1–6) that are members of the diverse AAA-ATPase family (Figure-1.2, 1.3 and 1.4). The Rpt1–6 ATPases form a hexameric ring in which the N-terminal domains project upward to contact other 19S RP subunits, and the ATPase cassettes lie close to the 20S CP α subunits. The C termini of Rpt2, Rpt3, and Rpt5, which are the ATPase subunits that display C-terminal HbYX motifs, dock at the α3/α4, α1/α2, and α5/α6 pockets, respectively [26, 27]

Known interactions between Rpt subunits indicate that such a hexameric ring should be orientated as Rpt1–2–6–3–4–5 in a clockwise manner in relation to the CP [28-32]. Due to the symmetry mismatch (seven *α* vs. 6 Rpt subunits), it is not expected that each Rpt will form a stable interaction with a single subunit. Reported CP-RP contacts include *α*1-Rpt6, *α*2-Rpt6, *α*4-Rpt2, *α*6-Rpt4, *α*2-Rpt4, *α*2-Rpt5, *α*4-Rpt4, and *α*7-Rpt4 [28, 29, 31, 33-37]. That the N-terminal tails of all seven subunits point directly into the centre of seven fold symmetry could explain how a single Rpt subunit can interact with more than one -subunit. Recently it has been solved and assigned that, the pore region of the ATPase subunits assemble into a spiral staircase-like arrangement, with the lowest and highest subunits, Rpt2 and Rpt3, respectively, separated by Rpt6 in an intermediate position [19, 20].

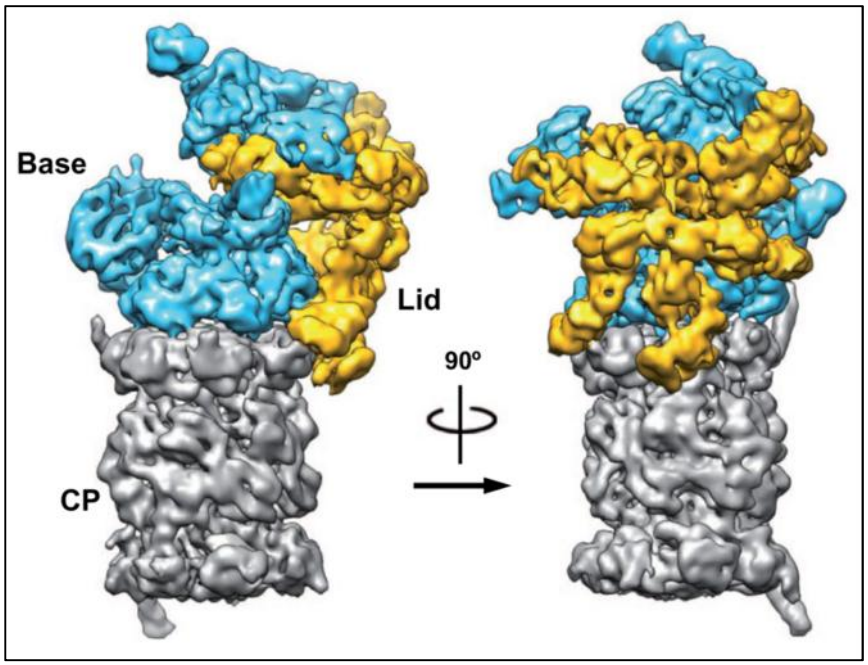

Figure-1.3: Subnanometre holoenzyme reconstruction of 19S-20S proteasome. The structure in cyan corresponds to the Base of 19S-RP. The structure in yellow corresponds to the lid of 19S-RP. [Adopted from: Lander et al. 2012]

The overall conservation of the RP subunits in eukaryotes is extraordinary. The Rpt subunits are the most conserved subunits of the RP, each of which is 66–76% identical between yeast and humans, pointing to their central and enzymatic role in

proteasome function. The six ATPases are roughly 40% identical to each other over the length of the protein, with the AAA domain at the centre showing a greater degree of identity [24]. These ATPases are distinct, as similar mutations in each result in unique phenotypes [11, 24]. This raises the idea that gene duplication plays a role in the composition of the contemporary proteasome.

The ATPases facilitate unfolding of the target proteins and have therefore been termed ‘reverse chaperones’ or ‘unfoldases’ [38]. Besides unfolding, these ATPases are presumably involved in the insertion of the target proteins into the gate of the core particle [39, 40]. Some of these ATPase subunits are responsible for regulating transcriptional activities [39]. Sug1 or PSMC5 acts as helicase and regulates transcription along with RNA polymerase II. S6a ATPase or PSMC3 acts as a coactivator of Class II MHC gene [41, 42]. Recently, it has been reported that Sug1, S7, and S6a form transcriptional activation complex along with RNA polymerase II, for the expression of the inflammatory gene CIITApIV [43].

The non ATPases of base subcomplex include four subunits viz., two scaffolding proteins Rpn1 and Rpn2 and two ubiquitin receptors Rpn10 and Rpn13 (Figure-3 and 4) [11]. Rpn1 and 2 are the largest proteasomal subunits (100kDa and 106kDa) containing proteasome cyclosome (PC) repeats [44]. In recent EM structure, the PC-domain of Rpn2 has been shown to interact with N-terminal end of the coiled-coil pair of Rpt6/Rpt3 while Rpn1 interact with Rpt1/Rpt2 [19]. The Ub binding subunits Rpn 10 and 13 have been assigned a position above the coiled coil of the Rpt4/5 and Rpt1/2 dimers, respectively. Rpn10 is tightly associated with the base, although it can also bind to the lid, or be found separate from the proteasome [22, 45-48]. Rpn10 has a role in stabilizing the interactions between the lid and the base subcomplexes of the RP. Based on the recent studies both Rpn13 and the UIM of

Rpn10 are located 70–80 Å, from the predicted position of the Rpn11 MPN domain, which could be bridged by a tetra Ub moiety [20]. This relative assignment of Ub receptors offers an explanation as to why polyubiquitin chains needs to be comprised of at least four Ub to function efficiently as a degradation signal. Similarly several Ub adaptor proteins (shuttle receptors) Rad23, Ddi1 and Dsk2 are expected to reside 80–120Å away from Rpn11, depending on where they bind Rpn1 because for receptor interaction, at least part of the ubiquitin chain has to be in an extended conformation with the hydrophobic patches exposed. Rad23, Dsk2, and Ddi1 share a common domain at their respective N-termini, known as ubiquitin-like domain (Ubl), and

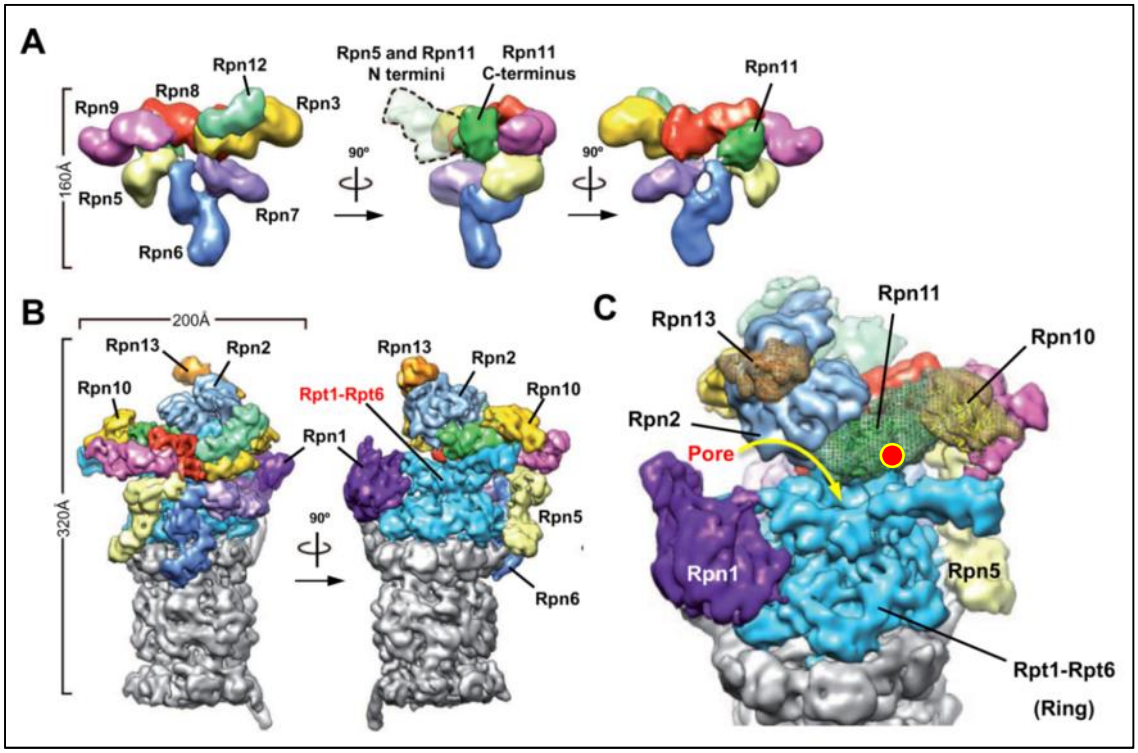

Figure-1.4: Three-dimensional reconstructions of the recombinant 19S subcomplex and the yeast 26S proteasome. (A) Negative-stain reconstruction of the isolated lid subcomplex at 15-Å resolution, coloured by subunit and shown from the exterior (left), the side (middle) and the interior, base-facing side (right). A dotted line (middle) indicates the highly variable electron density for the flexible N-terminal domains of Rpn5 and Rpn11. **(B)** Subnanometre cryoelectron microscopy reconstruction of the holoenzyme, shown in three views corresponding to the isolated lid and coloured as above, with the core particle in grey. **(C)** Side views of the regulatory particle, showing the locations of the ubiquitin receptors Rpn10 and Rpn13, and the DUB Rpn11 relative to the central pore. Crystal structures for Rpn10 (PDB ID: 2X5N), Rpn13 (PDB ID: 2R2Y), and an MPN domain homologous to Rpn11 (AMSH-LP, PDB ID: 2ZNR) are

shown docked into the electron microscopy density. The predicted active site of Rpn11 is indicated (red dot). *[Adopted from: Lander et. al.,2012]*

this domain mediates recognition by Rpn1 [49]. Moreover, both Rpn10 and Rpn13 bind between two consecutive ubiquitin moieties [50, 51] such that at least a tetra-ubiquitin chain would be required on a substrate to allow interaction with a receptor and simultaneous deubiquitination by Rpn11. In contrast, the function of Rpn2 is still not clear but it was found to interact with Hul5, a HECT-domain containing ubiquitin ligase [52].

1.3.2.2 The lid of the 19S:

The lid subcomplex is composed of only the non-ATPases; at least 9 non ATPase subunits (Figure-1.4). The subunits show a lower yet significant amount of sequence identity, typically in the range of 33–47% [14]. Based on amino acid sequence similarity, these subunits can be divided into two categories: (a) the MPN (Mpr1 and Pad1 in the N terminus) domain containing subunits Rpn8 and Rpn11 [25], (b) The PCI (Proteasome-COP9-eIf3) domain containing subunits Rpn3/5/6/7/9/12 [53]. Amongst all the nine lid subunits, the only subunit with a known catalytic activity is Rpn11. It has a metalloprotease-like deubiquitinating (DUb) activity which removes proximal ubiquitin from substrates [25]. Although the MPN domain of Rpn8 is very similar to that of Rpn11, it lacks crucial catalytic residues. In 26S holocomplex, Rpn8 interacts with Rpt3/6 pair while Rpn11 interacts with Rpn1 of base subcomplex. Some of the lid subunit have been shown to directly interact with AAA+, e.g. Rpn7 interact with AAA+ domain Rpt2 and Rpt6 while Rpn6 and Rpn5 with Rpt3 [19]. Lid subunits form hand-like structure where five PCI subunits (Rpn3, Rpn7, Rpn6, Rpn5 and Rpn9) form the fingers and Rnp11 palm [20] (Figure-1.4). Rpn8 not only connects Rpn3 and Rpn9 but also the palm of the hand Rpn11 [20]. The six PCI subunits form horseshoe-like structure covering a large part of the ATPase (Rpt3, Rpt6, and Rpt4) in form of a roof

[21]. The subunit order in the horseshoe heterohexamer is Rpn9/Rpn5/ Rpn6/Rpn7/Rpn3/Rpn12 [21]. The scaffold formed by PCI subunits positions the Rpn8/Rpn11 heterodimer in close vicinity to the mouth of ATPase ring, so that the engaged substrate can be deubiquitinated before entering translocation channel. The Rpn2 from base is thought to help in stabilization of lid conformation with the help of Rpn3, Rpn8 and the Rpn11 which extend towards the base. Unlike conventional model recent EM Map also showed that lid subunits interact directly with 20S CP [20]. It seems that the function of PCI subunit is to bring the essential machinery in 3D space, necessary for efficient degradation.

1.3.3 ATP independent modulator of 20S proteasome

1.3.3.1 PA28 or the 11S regulator:

PA28 or the 11S regulator (REG) was identified as another protein activator of the latent 20S proteasome [54]. Electron microscopic examination revealed that PA28 forms conical caps by associating with both ends of the central 20S CP [39]. PA28 complexes are composed of three structurally- related members designated α, β and γ; their primary structures display approximately 50% homology [55]. Whereas the PA28α and PA28β assemble into hetero-oligomeric complexes with alternating α and β subunits, the PA28γ appears to form homopolymeric complexes. Immunofluorescence analysis revealed that both PA28*α* and PA28*β* are located mainly in the cytoplasm, whereas PA28*γ* is located predominantly in the nucleus outside of the nucleolus [56]. X-ray crystallographic analysis of recombinant REG*α* (PA28*α*) revealed a heptameric complex [57], but the composition of PA28α and PA28β in the heteroheptameric (i.e., *α*3/*β*4 or *α*4/*β*3) complexes in cells, however, requires further investigation.

The PA28*α*/*β* containing proteasome functions as a processing enzyme responsible for the generation of major histocompatibility complex (MHC) class I

ligands, which are essential for the initiation of cell-mediated immunity in vertebrates [58-60]. The PA28*γ* containing proteasome functions as a regulator of cell proliferation and body growth in mice and demonstrated that neither PA28*α* nor PA28*β* compensates for the PA28*γ* deficiency in mice [61, 62]. A third type proteasome was discovered by immunoprecipitation analysis, which revealed that the PA28 and PA700 (19S) activators simultaneously bind to the 20S proteasome. PA28 and PA700 rings bind at opposite ends of the 20S particle, forming the PA700–20S–PA28 complex. This complex has been named the ‘‘hybrid proteasome’’ [63]. The hybrid proteasome seems to contribute to efficient proteolysis; intact substrate proteins may be first recognized by PA700 (19S-RP) and then fed into the cavity of the 20S proteasome, which shows markedly enhanced cleavage activity in the presence of the PA28α/β complex.

1.3.3.2 PA200 or Blm10:

Mammalian PA200 or the Yeast Blm10 (formally Blm3) are reported to regulate proteasome assembly and/or proteolytic activity, although there are discrepant reports about its precise roles [64, 65]. In the other hand Blm10 promotes proteasome maturation, presumably by stabilizing nascent 20S proteasomes [66]. The discrepancy in the two contradictory roles of Blm10 has not yet been explained. Interestingly, the Blm10-CP-RP complex (i.e., PA200-20S-PA700) is found predominantly in yeast cells. Electron microscopy (EM) studies have shown that Blm10 has a highly elongated, curved structure, and adapts to the end of the CP cylinder, where it is properly positioned to activate the autoinhibited closed-gate conformation of 20S proteasome by opening the axial channel into its proteolytic chamber [65]. In case of mammalian cells PA200 makes contact with all subunits except α7, and this interaction induces the opening of the axial channel through the α-ring, indicating that the activation mechanism of PA200 is expressed via its allosteric effects on the 20S-CP,

perhaps facilitating release of digestion products or the entrance of substrates. Recent reports suggested that the single-capped Blm10-CP shows peptide hydrolysis activity, whereas the peptide hydrolysis activity is repressed in double-capped Blm10-CP-Blm10, suggesting that that Blm10 distinguishes between gate conformations and regulates the activation of CP [67].

1.3.3.3 P131

PI31, known as an inhibitor of 20S proteasomes, prevents the activation of the proteasome by each of two proteasome regulatory proteins, PA700 and PA28, suggesting that it plays an important role in controlling proteasome function [68]. PI31 is a proline-rich protein, 26% of the amino acids are proline, particularly within its carboxyl-terminal half where it appears to have an extended secondary structure. This proline-rich domain of PI31 confirms the proteasome inhibition in the cells. However, it also is reported that PI31 represents a cellular regulator of proteasome formation and of proteasome mediated antigen processing, based on the observation that PI31 selectively interferes with the maturation of immunoproteasome precursor complexes [69].

1.3.3.4 Tissue specific proteasomes:

Although 26S proteasome ubiquitously expressed in all tissues, there are variants of proteasomal type exist in vertebrates in tissue specific manner. Vertebrates encode four additional catalytic β-subunits: three interferon-γ (IFN) inducible β1i, β2i, β5i immunosubunits and one thymus-specific β5t subunit, which are incorporated in the place of their most closely related β-subunits, thus forming distinct subtypes of proteasomes with altered catalytic activities. These are called immunoproteasomes and thymoproteasomes [58, 70, 71]. These alternative proteasomes play key roles in acquired immunity by altering antigen processing. The immunoproteasome has

increased chymotrypsin-like and trypsin-like activities, which are favourable for the production of antigenic peptides that bind to the groove of MHC class I molecules [58, 72]. The thymoproteasome has reduced chymotrypsin-like activity, which is thought to be important for the production of a unique peptide repertoire in the thymus [71, 73, 74]. By comparison, the 20S proteasome, including constitutively expressed catalytic subunits β1, β2 and β5, is often called the standard or constitutive proteasome. In Drosophila melanogaster, approximately one-third of the proteasome subunits are found to have testes specific isoforms [75]. One of these, proteasome subunit α6 testis-specific (PROSα6T), is required for spermatogenesis. However, whether there are specific mechanisms for the assembly of such testes-specific subtypes has not been explored. In mouse Rpn10 mRNA occurs in at least five distinct forms, Rpn10a–e, due to developmentally regulated alternative splicing [76]. These isoforms, with the exception of the universally expressed Rpn10a, are expressed in tissue-specific and/or developmental stage-specific manners. For example, Rpn10e is specifically expressed in the embryonic brain in mice, implying the existence of 'the brain-specific proteasome'. Knocking out the mouse Rpn10 gene was found to be embryonically lethal [77], although the specific reason was unknown.

1.4 PROTEASOMAL DEGRADATION PATHWAY:

The majority of cytosolic protein degradation in eukaryotes occurs via the UPS. In this process, cellular proteins targeted for degradation are tagged by multimers of an evolutionarily conserved protein known as ubiquitin and are degraded by the 26S proteasome. The crucial role that proteasome plays in the eukaryotic cells is to degrade proteins in a very regulated manner. The degradation process can be divided into two broader categories; (a) Ubiquitin dependent protein degradation and (b) ubiquitin independent protein degradation.

1.4.1 Ubiquitin dependent protein degradation:

“Ubiquitin” originally known as “ubiquitous immunopoietic polypeptide”, was first identified in 1975 by Goldstein, as an 8.5 kDa protein of unknown function expressed in all eukaryotic cells [78]. The basic functions of ubiquitin and other components of the ubiquitination process were explicated in the early 1980s at the Technion by Aaron Ciechanover, Avram Hershko, and Irwin Rose for which they were awarded Nobel Prize in Chemistry in 2004 [7]. Ubiquitin is a small protein (76 amino acids and has a molecular mass of about 8.5 KDa) that exists in all eukaryotic cells (Figure-1.5). It performs its innumerable functions through conjugation to a large range of target proteins. The feature for the ubiquitination process includes its C-terminal tail (Glycine) and the 7 lysine residues (K6, K11, K27, K29, K33, K48, and K63). It is highly conserved among eukaryotic species: Human and yeast ubiquitin share 96% sequence identity.

Ubiquitination is an enzymatic, post-translational modification (PTM) process in which an ubiquitin protein is attached to a substrate protein. This process most commonly binds the last (C-terminal) amino acid of ubiquitin (glycine 76) to a lysine residue on the substrate. An isopeptide bond is formed between the carboxylic acid group of the ubiquitin's glycine and the ε-amino group of the substrate's lysine [79]. Trypsin cleavage of an ubiquitin-conjugated substrate leaves a di-glycine "remnant" that is used to identify the site of ubiquitination [80, 81]. In a few rare cases nonlysine residues like cysteine, threonine and serine, have been identified as ubiquitination targets [82, 83]. The end result of this process is the addition of one ubiquitin molecule (monoubiquitination) or a chain of ubiquitin molecules (polyubiquitination) to the substrate protein [84].

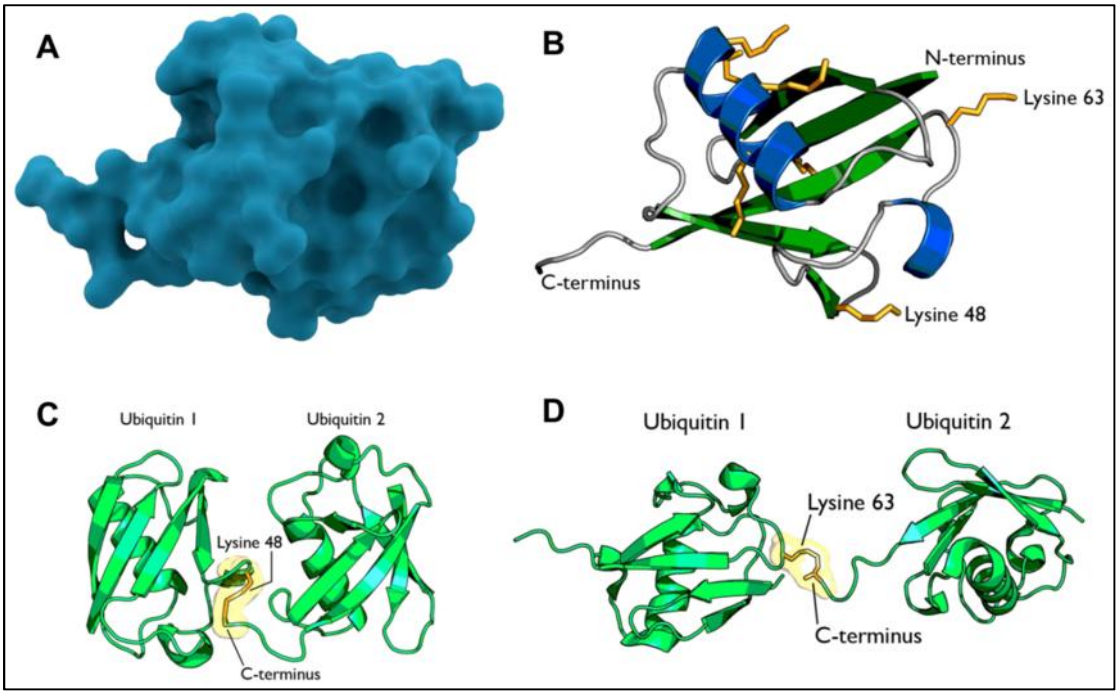

Figure-1.5: Ubiquitin Structure. **(A)**, Molecular surface representation of the protein ubiquitin, based on PDB 1UBQ (Author: Thomas Splettstoesser, 2004). **(B)** Cartoon representation of ubiquitin protein, highlighting the secondary structure. α-helices are coloured in blue and β-strands in green. The sidechains of the 7 lysine residues are indicated by orange sticks. The two best-characterised attachment points for further ubiquitin molecules in polyubiquitin chain formation (lysines 48 & 63) are labelled. Image was created using PyMOL from PDB id 1ubi. (Author: Rogerdodd, 2008). **(C)** A cartoon representation of a lysine 48-linked diubiquitin molecule. The two ubiquitin chains are shown as green cartoons with each chain labelled. The components of the linkage are indicated and shown as orange sticks. Image was created using PyMOL from PDB id 1aar. (Author: Rogerdodd, 2008). (D) A cartoon representation of a lysine 63-linked diubiquitin molecule. The two ubiquitin chains are shown as green cartoons with each chain labelled. The components of the linkage are indicated and shown as orange sticks. Image was created using PyMOL from PDB id 2jf5. (Author: Rogerdodd, 2008).

Ubiquitination requires three types of enzyme: ubiquitin-activating enzymes (E1), ubiquitin-conjugating enzymes (E2), and ubiquitin ligases (E3). The process consists of three main steps (a) activation, (b) conjugation and (c) ligation.

1.4.1.1 Activation: Ubiquitin is activated in a two-step reaction by an E1 ubiquitin-activating enzyme, which is dependent on ATP. The initial step involves production of an ubiquitin-adenylate intermediate. The E1 binds with ATP as well as ubiquitin and catalyses the acyl adenylation of the C-terminal glycine residue of the ubiqutin molecule. The second step transfers ubiquitin to an active site cysteine residue, with

release of AMP. This step results in a thioester linkage between the C-terminal carboxyl group of ubiquitin and the E1 cysteine sulfhydryl group (Figure-1.6) [79, 85]. The human genome contains two genes that produce enzymes capable of activating ubiquitin: UBA1 and UBA6 [86].

1.4.1.2 Conjugation: E2 ubiquitin-conjugating enzymes catalyse the transfer of ubiquitin from E1 to the active site cysteine of the E2 via a trans-(thio)-esterification reaction (Figure-1.6). In this reaction, the E2 binds to both activated ubiquitin and the E1 enzyme. Humans possess 35 different E2 enzymes, whereas other eukaryotic organisms have between 16 and 35. They are characterised by their highly conserved structure, known as the ubiquitin-conjugating catalytic (UBC) fold [87]. Glycine and lysine linked by an isopeptide bond.

1.4.1.3 Ligation: E3 ubiquitin ligases catalyse the final step of the ubiquitination process. Most commonly, they create an isopeptide bond between a lysine of the target protein and the C-terminal glycine of ubiquitin. In general, this step requires the activity of one of the hundreds of E3-ligases. E3 enzymes function as the substrate recognition modules of the system and are capable of interaction with both E2 and substrate. Some E3 enzymes also activate the E2 enzymes. E3 enzymes possess one of two domains: the homologous to the E6-AP carboxyl terminus (HECT) domain and the really interesting new gene (RING) domain (or the closely related U-box domain). HECT domain E3-ligases transiently bind ubiquitin in this process an obligate thioester intermediate is formed with the active-site cysteine of the E3, whereas RING domain E3-ligases catalyse the direct transfer from the E2 enzyme to the substrate (Figure-1.6) [88].

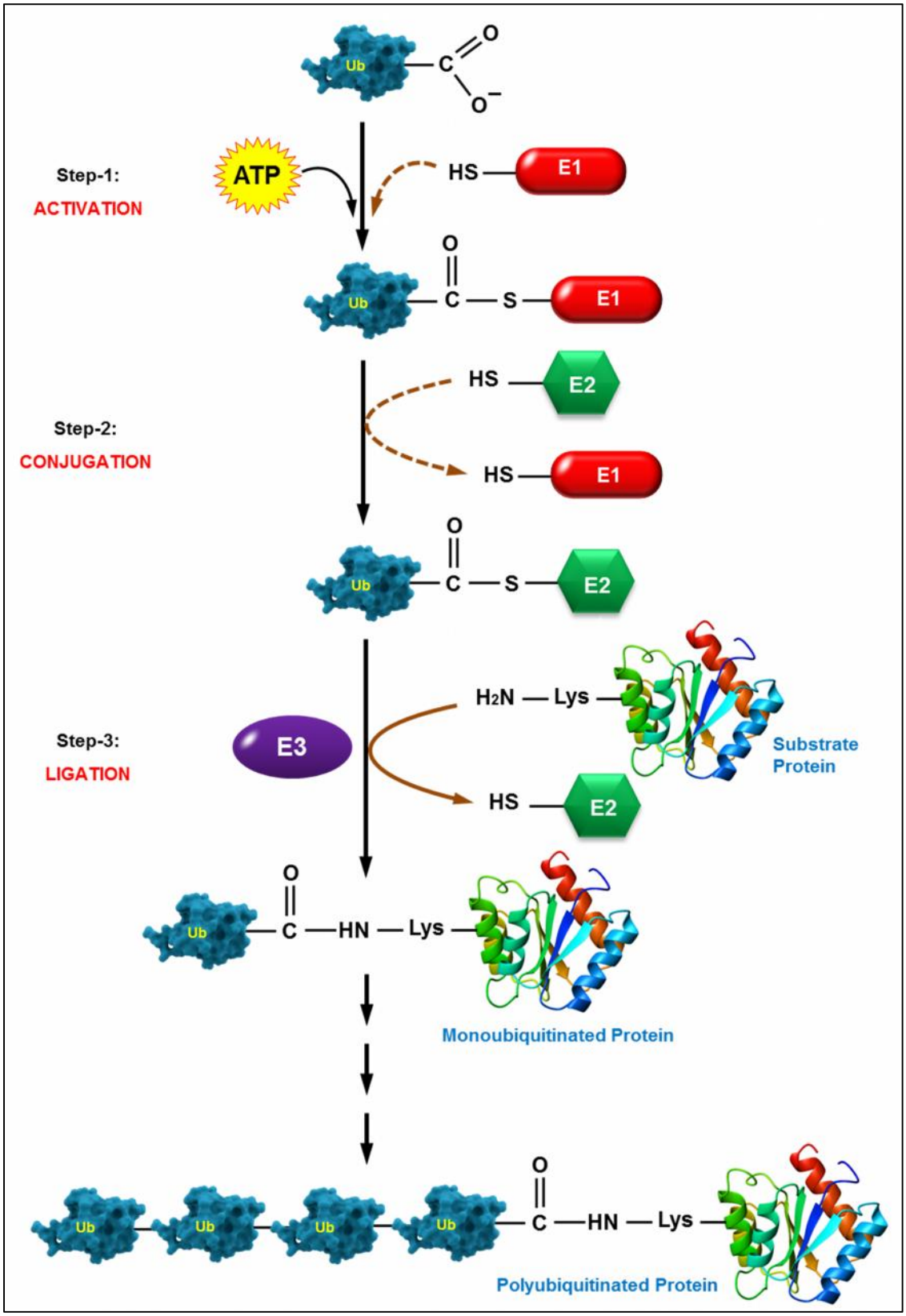

Figure-1.6: The protein ubiquitination pathway. Ubiquitin (Ub) is activated by E1 and transferred to the E2 enzyme and is, finally, conjugated to substrate proteins with a specific E3 ligase. Polyubiquitination occur in successive steps. [Adopted from; Dipankar Nandi, 2006]

In the ubiquitination cascade, E1 can bind with many E2, which can bind with hundreds of E3 in a hierarchical way. In this casecade of reactions monoubiquitination is the addition of one ubiquitin molecule to one substrate protein residue. Multi-monoubiquitination is the addition of one ubiquitin molecule to multiple substrate residues. The monoubiquitination of a protein can have different effects to the polyubiquitination of the same protein. The addition of a single ubiquitin molecule is thought to be required prior to the formation of polyubiquitin chains [89]. Monoubiquitination affects cellular processes such as membrane trafficking, endocytosis and viral budding [90, 91]. Polyubiquitination is the formation of an ubiquitin chain on a single lysine residue on the substrate protein. Following addition of a single ubiquitin moiety to a protein substrate, further ubiquitin molecules can be added to the first, yielding a polyubiquitin chain [89]. These chains are made by linking the glycine residue of an ubiquitin molecule to a lysine of ubiquitin bound to a substrate (Figure-1.5). Among the seven lysine residues Lysine 48-linked chains were the first identified and are the best-characterised type of ubiquitin chain. Lysine 48-linked polyubiquitin chains target proteins for destruction, by proteasomal degradation. At least four ubiquitin molecules must be attached to a lysine residue on the condemned protein in order for it to be recognised by the 26S proteasome. Lysine 63-linked chains are not associated with proteasomal degradation of the substrate protein. Instead, they allow the coordination of other processes such as endocytic trafficking, inflammation, translation, and DNA repair [90]. In cells, lysine 63-linked chains are bound by the ESCRT-0 complex, which prevents their binding to the proteasome. This complex contains two proteins, Hrs and STAM1 that contain a UIM, which allows it to bind to lysine 63-linked chains [92, 93].

1.4.2 Delivery of ubiquitynated substrates to the proteasome

After ubiquitination of the substrate protein, its delivery to the proteasome can occur in different ways. The ubiquitinated substrates can directly bind to the receptors on proteasome or some carrier protein may carry the substrates to proteasomal for degradation. Five ubiquitin receptors on the proteasome have been identified so far, including the intrinsic subunits Rpn10, Rpn13 and the shuttling factors Rad23, Dsk2, and Ddi1 [53]. The proteasome subunits Rpn10 was the first ubiquitin receptor identified and it has been shown that it can bind certain substrates directly in the free form as well as proteasome bound form [94]. The other intrinsic ubiquitin binding subunit is Rpn13 found on the proteasome RP [95]. In addition to the bona fide proteasome subunits Rpn10 and Rpn13, the UbL/UBA family of proteins has been suggested to recruit polyubiquitylated proteins to the proteasome. As outlined above, the UbL/UBA proteins Rad23, Dsk2, and Ddi1 are referred to as ‘shuttle factors’ that bind polyubiquitylated substrates to deliver them to the proteasome for their degradation, adding an additional layer of substrate selectivity to the ubiquitin/proteasome system [96-100], whereas the N-terminal UbL domain transiently interacts with the proteasome [101]. Consistent with this hypothesis was the finding that deletion of Dsk2 in yeast reduced ubiquitin-dependent proteasomal degradation (Funakoshi et al., 2002) and that Rad23 can promote binding of ubiquitynated proteins to the proteasome [96]. Interestingly, a large portion of Rpn10 in yeast is not associated with the proteasome. Similar to the function of Rad23, Dsk2, or Ddi1, it is intriguing to elucidate whether Rpn10 also act as a shuttles proteins to the proteasome, in addition to its function as an intrinsic ubiquitin receptor. However, free Rpn10 has been demonstrated to bind the ubiquitinated substrates as well as Dsk2’s UbL domain via its

UIM motif. These findings suggest that the free pool of Rpn10 may act as a shuttle receptor and also regulate the binding of Dsk2 to the proteasome [102].

Paradoxically, initial studies on the function of UbL/UBA proteins had suggested an inhibitory role in proteasomal degradation. For instance in vitro and in vivo experiments showed Rad23 inhibition in the formation of K48-linked polyubiquitin chains and stabilized proteasome substrates hence act as a negative regulator of proteasomal degradation. However, the function of shuttling factors is likely to strongly depend on their concentration since excessive amounts of Rad23 will decrease the probability that Rad23 loaded with ubiquitynated cargo will bind to the proteasome. In this respect it is noteworthy that each of these experiments was performed with either the addition of excess Rad23 to in vitro systems or by overexpression of Rad23 in vivo [103-105]. A subsequent study addressed this issue and indeed revealed that Rad23 can recruit polyubiquitylated proteins to the proteasome and facilitate their degradation [99].

Recently the chaperone Cdc48 has been emerged for its remarkable role in the delivery of substrates to the proteasome. In this pathway the polyubiquitylated substrate proteins, are escorted to the proteasome via a handover mechanism. Cdc48 as the central player in this pathway serves as a scaffolding platform that binds via its ubiquitin-binding co-factors polyubiquitynated proteins. It recruits multiple enzymes including E3 and E4 and DUBs, before the substates are delivered to the proteasome by the shuttle factors Rad23 or Dsk2 [106]. As discussed above, a possible role for the unfoldase activity of Cdc48 has been proposed in the context of substrate delivery. As such, initial unfolding of substrates before they encounter the proteasome has been found as a likely scenario and would combine Cdc48's functions in recruiting proteins and its unfoldase activity in targeting for proteasomal degradation [53, 107].

Although there exist numerous mechanisms for delivery of the substrate protein to proteasome for degradation, still the precise mechanism has not been fully understood yet. However, the role of some shuttle proteins like Rad23, Dsk2, Did1 and Cdc48 in delivering some ubiquitinated proteins contributes to the understanding of the phenomena to some extent. But cell must have a vast pool of substrate proteins in a given time point and it must be essential for the cell to degrade the committed protein in times. So to execute spatio temporal regulation of degradation, there may exist many more shuttle receptors or even alternate mechanisms of substrate delivery.

1.4.3. MECHANISM OF ACTION: Degradation of Ubiquitinated Substrates:

1.4.3.1 Ubiquitin recognition

Thousands of proteins are ubiquitinated in eukaryotic cells, but almost half of the ubiquitinated proteins are not targeted to the proteasome for degradation and it is not clear how the cell differentiates between the different ubiquitin signals [108]. Although the precise explanation is unavailable, recent studies have been highlighted some stoichiometry based descriptions. A polyubiquitin chain is synthesized on the majority of substrate proteins by a series of enzymes in the polyubiquitination process (as described in section 1.4.1, Figure-1.6 & 1.7) recognized by the proteasome. Monoubiquitination may serve as a cellular targeting or localization signal, but it does not seem to target proteins to the proteasome. But in case of polyubiqutination chains containing at least four molecules of G76-K48 isopeptide-linked ubiquitin are necessary for efficient binding to the proteasome [109] or its component S5a/ Rpn10 [110]. Evidently, the surface provided by the four-subunit structure of a polyubiquitin chain that is recognized by the proteasome, rather than a single ubiquitin molecule. It establishes some hydrophobic interactions that target the polyubiquitin signal and the

receptor site in the proteasome. For example, a hydrophobic cluster formed by a number of residues in the proximity of Ile-44 of ubiquitin is necessary for efficient proteasome-dependent degradation. Likewise, a hydrophobic patch at the C-terminal region of Rpn10 and its orthologs (within its UIM motif) binds to ubiquitin chains [111, 112]. The quaternary structure of ubiquitin polymers and the exact spatial relationship between each ubiquitin molecule is also critical for their ability to target substrates for degradation by the proteasome.

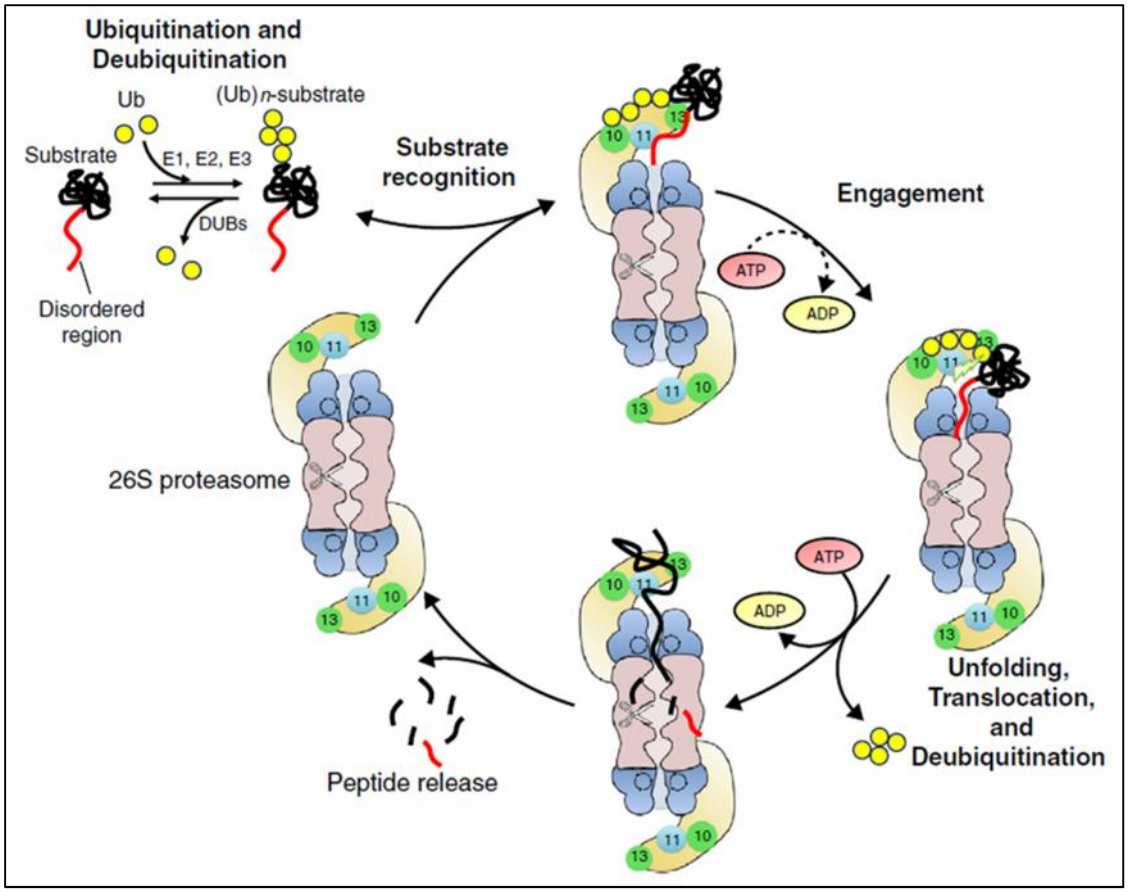

Figure-1.7: Schematic representation of the degradation cycle of the ubiquitin proteasome system. Proteins are targeted to the proteasome by a two-part degradation signal or degron. It consists of a disordered region within the substrate and reversibly attached polyubiquitin tag (Ubn). Polyubiquitin tag is attached by a E1–E2–E3 ubiquitination cascade and this process can be reversed by DUBs (top left). The proteasome recognizes its substrates at the ubiquitin tag through ubiquitin receptors (Rpn10 and Rpn13; green) (top) and initiates degradation at the unstructured region (right). Once the proteasome has engaged its substrate, it unravels the protein by translocating it into a central cavity in the core particle, where the protein is proteolysed (bottom). The polyubiquitin tag is cleaved off by the intrinsic DUB Rpn11 (skyblue) as unfolding and degradation begins. *[Adopted from: Tomonao Inobe et.al., Current Opinion in Structural Biology 2014, 24:156–164]*

It is important to note, that multiubiquitin chains linked via Lys-6, Lys-11, or Lys-48, also bind to the proteasomal subunit Rpn10/S5a with similar affinities [110]. Furthermore, linear ubiquitin fusions are competitive inhibitors of Lys-48-linked multiubiquiti- nated substrates for proteasomal binding, indicating they probably bind to the same site on the proteasome [109]. Purified proteasome binds the Lys63-linked polyubiquitin chain with almost the same affinity as the Lys48-linked polyubiquitin chain [92] and so specificity may come from accessory proteins. For example the ESCRT complex involved in membrane trafficking binds Lys63-linked polyubiquitin chains better than Lys48-linked chains whereas the UbLUBA proteins that can serve as non-stoichiometric ubiquitin receptors for the proteasome have the opposite preference [92]. Therefore, a Lys48-linked polyubiquitin chain has a greater chance to be delivered to the proteasome than the Lys63-linked polyubiquitin chain. These observations indicate that there is a separation between binding to the proteasome and correctly preparing a substrate for degradation.

To date only Rpn10 and 13 subunits are known for ubiquitin affinity recognition on proteasome. But reports suggested that Rpn10 functions in the proteasome independently of its ability to bind ubiquitin chains [14, 112]. In addition, as RPN10 or its orthologs are nonessential in S. cerevisiae, S. pombe, and moss, it was suggested that it does not function as the sole ubiquitin recognition site in the proteasome [48, 113, 114]. More than one proteasomal subunit might be necessary for recognition and binding of ubiquitin chains. Indeed, Rpn10 in combination with a comprised version of Rpn1 is essential, although it is unclear whether they share functions or merely interact with one another in the base [114].

Rpn10 may play overlapping roles with an unrelated protein, Rad23 [115]. Rad23 (as well as its human counterparts hHR23a and hHR23b) also binds tightly to

yeast or mammalian proteasomes through an NH2-terminal UBL (ubiquitin like) domain that shares homology with ubiquitin [116-118]. Mammalian hHR23 can bind Rpn10/S5a through this UBL domain, but it can also bind to the proteasome independently of Rpn10 [115], indicating that there might be an additional site for binding of ubiquitin or ubiquitin-like proteins in the 19S RP. It is not at all clear what is the role of Rad23 binding to the proteasome or to Rpn10, although it potentially links the proteasome to the DNA repair pathway by targeting the proteasome to sites of DNA damage. Whether the ability of Rad23 to interact with ubiquitinated substrates has anything to do with this function is yet to be shown [104, 117, 119]. A yeast two-hybrid screen has indicated that Rad23 can interact with Rpn1, a subunit of the base [120]. In addition, Rpn1 from C. elegans can interact with linear polyubiquitin while Rpn2 can interact with another UBLcontaining protein [28]. Thus Rpn1 and Rpn2 might be additional sites for polyubiquitin or UBL binding in the proteasome. hPLIC, which also contains a UBL domain, has been found to interact with the proteasome as well [121].

Similarly to the base, another hexameric ring of AAA ATPases VCP (also known as p97 in animals, Cdc48 in yeast, or VAT in archaea) has been shown to contain an unfoldase ability [122, 123]. VCP has been shown to physically bind both to the proteasome, as well as to polyubiquitinated substrates and polyubiquitinated chains directly [124]. It is not impossible, therefore, that members of the putative ring of Rpt ATPases in the base also have a certain affinity for polyubiquitin chains. Together this suggests that binding of polyubiquitin and ubiquitin-like domains occurs in the base, with at least some of this activity taken up by Rpn1, Rpn2, and Rpn10. Whether they each have unique affinities for different UBL domains or alternatively assembled polyubiquitin chains is unclear at this time, nor whether binding of all polyubiquitin chains and single UBL-domains occurs at the same subunits of the 19SRP.

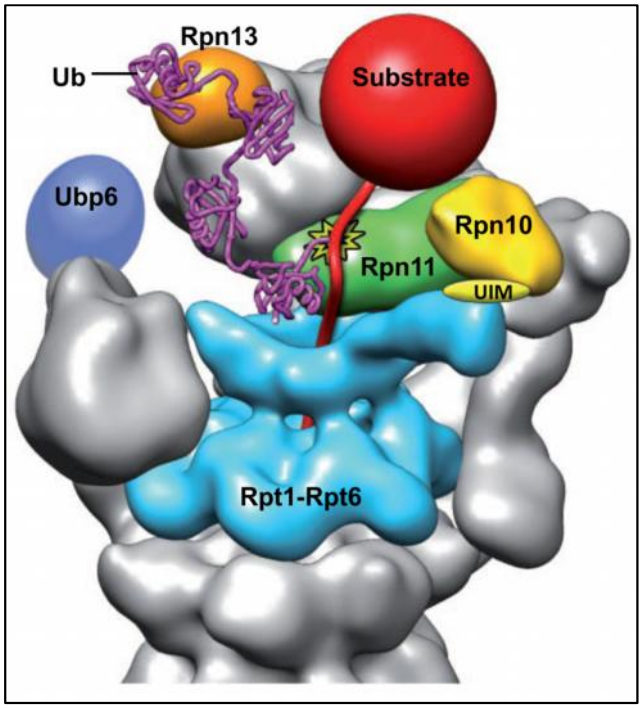

Figure-1.8: Binding of the substrate to 19S-RP. The tetra ubiquitinated substrate positioned itself perfectly on 19S. Rpn13 bind with the ub chain and the deubiquitinating enzyme Rpn11 cleaving the isopeptide bond. The unfoalded part of the substrate getting into the ATPase pore. *[Adapted from: Lander et al. 2012]*

1.4.3.2 Substrate binding

Rpn1 and Rpn2 make up the RP base together with the six Rpt ATPases. Both Rpn1 and Rpn2 contain multiple leucine-rich repeats (LRR), for protein-protein interaction [125]. The six ATPases of the base are also likely to function through protein-protein interaction with the substrates of the proteasome. Thus it is plausible that all eight components of the base may engage in direct interactions with substrates (Figure-1.8). Distinct functions of the base and the lid must be consistent with their location within the RP. The substrate must be properly positioned to be unfolded by the base and translocated into the CP; the distal positioning of the lid may ensure that the ubiquitin chain on the substrate does not occlude access of the target protein to the channel. Indeed, the base can bind to nonubiquitinated, unfolded substrates and promote their folding [126, 127]. PAN, an archaeal homolog of the base, can directly interact with

folded proteins and unfold them [128]. Whether interacting with substrates via their ub moieties or in a ubiquitin-independent manner reflects distinct mechanisms for preparing them for degradation remains to be seen.

1.4.3.3 Unfolding and translocation:

Not only the proteasomal assembly [129, 130], but also proteolysis of proteins by the proteasome is also strictly ATP dependent [11, 131, 132]. The conformational changes associated with this ATPase cycle could be used in three processes: 1) gating the channel defined by the NH2 termini of the core particle's α-ring subunits, 2) unfolding the substrate, and 3) threading the unfolded substrate through the channel into the lumen of the CP. The substrate docking onto the proteasome is followed by deubiquitylation and unfolding of the protein, two strictly coupled events [25, 133]. The mechanism of translocation of the substrate into the catalytic core is not yet clarified. A possible scenario suggests that unfolding is driven by translocation [134-138]. According to this model the proteasome would need an interaction site to apply mechanical force on the substrate, while the counteracting resistance for unravelling is provided by the narrow entry into the core particle. In line with this model it has been found that the proteasome needs an unstructured or disordered or loosely folded polypeptide of a certain length (20 to 30 amino acids) for initiation of degradation [139, 140]. Fully folded proteins might not reach deep (30-60 Å from the entry pore) enough into the centre of the ATPase ring in order to get processed to allow efficient degradation of the substrate [137]. Consistent with these results is the observation that the proteasome preferentially degrades those proteins out of complexes that carry an unstructured initiation site while leaving the other binding partners intact [141] and it has been proposed that this mechanism is responsible for the stability of some proteins that can interact with the proteasome

without facing destruction like shuttle factors delivering proteins for their degradation without facing destruction themselves [142].

1.4.3.4 Gating:

An important property of the base is that it is nearly as efficient as the intact RP in stimulating the degradation of peptides and a nonubiquitinated protein substrate by the CP, suggesting a role for proteasomal ATPases in preparing substrates for degradation [22]. One role of the RP might be to control opening and closing of this channel by forming competing interactions with the blocking α-subunit NH2-terminal tails [143]. Indeed, a substitution mutation in the ATP-binding site of a single ATPase (RPT2) severely lowers peptidase activity of the proteasome, probably due to hampering the ability of the RP to properly gate the channel into the CP [144]. This indicates that even the entry of small peptides, which do not need to be unfolded, can be controlled by the RP.

One reason for a gated channel in the CP could be to serve as a transition from one form of inhibition to another during assembly of the mature CP. In the final stage of CP assembly, self-compartmentalization is achieved by the association of two α7β7 half-CPs at the β-β interface. These half CPs are inactive due to propeptides in the critical β-subunits that mask their active site. As these half-CPs are joined, inhibition by β-subunit NH2 termini is relieved by autolysis [145] while inhibition by the blocking NH2 termini of the α-subunits is imposed. Binding of the RP relieves this inhibition by opening the channel, thus giving rise to the proteolytically active form of the complex [143, 144].

A second reason for a gated channel could be to regulate generation of different length of products by the proteasome. Under normal conditions product release is

slowed down by a gated channel to increase processivity and decrease average peptide length which are quickly removed from the cytoplasm. But under immune response, it might be beneficial to produce longer peptides that can play a regulatory role. The majority of peptides generated by the proteasome contain less than eight amino acids. A fraction of the peptides that are 8–10 amino acids in length can be transported through the ER and presented to the immune system by MHC class I [54, 146]. An increase in average peptide length of proteasome products could increase the efficiency of antigen presentation and, by extension, the efficiency of combating viral infection.

1.4.3.5 Proteolysis:

Under normal physiological condition, proteasomes cleave the protein substrates into small peptides varying between 3 and 23 amino acids in length [147, 148]. The median length of peptides generated by the proteasome are seven to nine amino acids long; however, in total peptides within this size range make up ~15% of the peptides generated by the proteasome. This process is processive such that a protein is hydrolyzed within the proteasome to the final products before the next substrate enters; thus the pattern of peptides generated from a specific protein is stable over time [148, 149]. However, each of the three active site-containing β-subunits preferentially cleaves after different amino acids: β1 cleaves after acidic or small hydrophobic amino acids, β2 cuts after basic or small hydrophobic amino acids, while β5 hydrolyzes the peptide bond after hydrophobic residues whether bulky or not [150]. The rules that govern the cleavage rate of the same peptide bond can be significantly altered when put into the context of the primary structure of the polypeptide [151]. An interesting feature of proteolysis by the proteasome is that the 20S CP and the proteasome holoenzyme generate different patterns of cleavage products [152], indicating that even the distal 19S RP affects the behavior of the CP. Furthermore, the CP contains specific

“noncatalytic” sites to which additional factors can bind and alter cleavage sites and product composition [153]. Understanding the precise rules regulating the makeup of peptides generated by the proteasome will have far-reaching consequences on predicting immunogenic peptides “hidden” within viral or tumorigenic proteins.

The peptide products of the proteasome are short lived and do not accumulate in the cell. Most likely, most of these peptides are rapidly hydrolysed by downstream proteases and aminopeptidases. Some of the peptides that are generated by the proteasome can be transported through the ER to be presented to the immune system by the MHC class I molecules [154].

1.4.3.5. Deubiqutination

As many other protein modifications, ubiquitylation is a reversible process. For this purpose, cells contain a number of proteases that can cleave the isopeptide bond connecting the ubiquitin molecule, leading to deubiquitylation of proteins [155]. While the vast majority of deubiquitylation enzymes (DUBs) are not associated with the proteasome, a few of these proteases are intrinsic subunits of the 26S proteasome. For example, Rpn11, a subunit of the 19S regulatory particle, removes whole polyubiquitin chains of substrates before degradation by hydrolyzing the isopeptide bond between the substrate’s lysine and the proximal ubiquitin molecule of the chain [25, 133]. Notably, deubiquitylation by Rpn11 and degradation are coupled events and thus only substrates that are fully committed for degradation are processed [25]. Two other DUBs associated with the proteasome can trim the polyubiquitin chain of substrates. In yeast, Uch37 and Ubp6 cleave single ubiquitin molecules or di-/ triubiquitin chains, respectively, from the distal end of a polyubiquitin chain [156]. By progressively shortening instead of removing entire chains, these DUBs are most likely responsible for reducing the affinity

of substrates for the proteasome. A likely model is that if degradation is not initiated before the entire chain has been removed, the protein will escape degradation and thus Uch37 and Ubp6 can negatively influence proteasomal degradation. However, Hul5, another proteasome-associated protein, is counteracting the DUB activity [157]. Hul5 is an E4 elongation factor responsible for further ubiquitylation of existing polyubiquitin chains on substrates, whereby it most likely, in concert with Uch37 and Ubp6, fine-tunes the selectivity of the degradation by the proteasome.

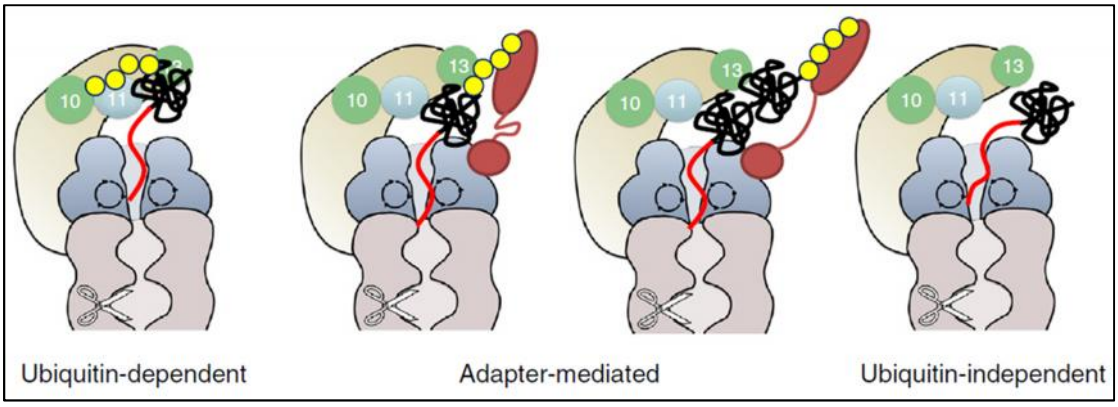

Figure-1.9: The proteasome recognizes substrates in three different modes; ubiquitin-dependent (left), adapter-mediated (middle), and ubiquitin-independent (right) modes. In all three modes, an intrinsically disordered region in the substrate is recognized by the ATPase motor to allow the proteasome to initiate degradation. This aspect of proteasomal degradation resembles the targeting mechanisms predominant with the bacterial and archaeal analogs of the proteasome. Ubiquitin tags can be either recognized by the two intrinsic proteasome receptors Rpn10 and Rpn13 (left), or by nonstoichiometric proteasome subunits that serve as substrate adaptors such as UbL-UBA proteins (middle). The UbL-UBA proteins might bind substrates by themselves (second right) or together with the intrinsic substrate receptors (second from left) and facilitate degradation of by positioning the disordered region properly. Finally, some substrates may be recognized only by their initiation sites. *[Adopted from: Tomonao Inobe et.al., Current Opinion in Structural Biology 2014, 24:156–164]*

1.4.2 Ubiquitin independent protein degradation:

Most of the cellular proteins undergo ubiquitination followed by proteasomal degradation. But recently it has been established that there are certain proteins whose turn over does not required ubiquitination. Those proteins very often happen to be oxidized or unfolded and do not require the 19S regulatory system for their degradation

process. The exposed hydrophobic regions of these substrate proteins presumably take over the function of polyubiquitin chain. In case of Ub independent degradation, the globular proteins are predominantly recruited to proteasome by ‘adaptor’ or ‘shuttling proteins’ [158] and degradation initiation, signals by the ‘unstructured region’ [137] (Figure-1.9). To delineate the molecular mechanism different model structures have been established to understand the process of degradation better in vitro. For instance, Using apomyoglobin, our lab provide first evidence for the natural ability of purified eukaryotic 26S proteasomes to directly recognize, unfold and degrade a globular protein in the absence of ubiquitin, extrinsic degradation tags or adaptor proteins [138].

There is a range of cellular proteins are degraded by the proteasome without being ubiquitinated [159] and the best understood example is ornithine decarboxylase (ODC) [118, 160]. Degradation of ODC requires ATP as well as an accessory protein called antizyme and begins a 37 amino acid long unstructured region at the C terminus of ODC [160]. To some extent, this ODC tail can function as a transferable degradation signal and induce the degradation of some proteins. One plausible explanation for the ubiquitin-independent degradation is that the unstructured regions themselves have bind sufficiently tightly to the ATPase ring loops so that ubiquitin is not required for proteasome association. Thus, this targeting mechanism can be taken as a variation of the conventional proteasome degron in which the ubiquitin tag component is missing and which resembles the degrons observed in the archaea and bacteria [161].

Several other proteasome substrates including p21/Cip1, c- Jun, c-Fos, p53, p73 IkBα T-cell antigen receptor chain a, Fra-1, and Hif-1a, can also be degraded in an ubiquitin- independent manner [162-164]. The mechanisms of these processes are not well understood and it is possible that these proteins are degraded by isolated 20S core particle in the absence of ATP [162], though in vivo perhaps more likely by 20S core

particle activated by alternative caps [163] or even by 26S proteasome [164]. The proteins in this group of ubiquitin-independent proteasome substrates are largely unstructured, but their degradation can still be regulated. The best understood example of this regulation is given by NQO1 [165, 166]. NQO1 is largely unstructured and can be degraded by 20S proteasome in vitro. Binding of NQO1's cofactor FAD stabilizes the protein's structure and inhibits its proteasomal degradation. Quite interestingly, FAD binding to NQO1 also stabilizes other ubiquitin-independent proteasome substrates, setting up a regulatory circuit controlled by the availability of FAD and thus the metabolic state of the cell.

1.5 Proteasomal degradation of proteins in signaling pathways

Decades of research on ubiquitin proteasomal system (UPS) and the degradation process suggests that, it is a highly regulated energy dependent protein degradation pathway. This comprises a large set of different proteins; includes the activators, modulators, direct interactors. This suggests eukaryotic cells invest much energy in synthesizing each individual subunit proteins, regulating them in an energy dependent fashion and maintained them till they die. However, in spite of all the expenses this process is indispensable for essential phenomena of cell physiology as well as cell homeostasis. Hence it will not be over exaggeration if we consider "UPS" the master regulator for almost all cellular signaling pathways. Nevertheless, numerous other vital modulators play important role in signalling pathway.

Signaling pathways in cells are mostly exhibited by different category of protein families; the external/internal (For outside-in/inside-out) signaling molecules, signaling receptors, intracellular modulators, adapters, secondary messengers, effectors, transcription co-activators and transcription factors. There is a definitive half-life or the

turn-over is confined to all these proteins in the cells and most of them are regulated by proteasome. The basal half-life or the induced half-life of these signalling molecules impact empirically on the signalling pathways although post-translational modification of signalling molecules is an essential phenomenon. Moreover, ubiquitination of the signalling molecules does not always confer the signal for degradation, in some circumstances it also act as a signal for various cellular activity. For instances monoubiqutination or polyubiquitination at K63 act as a signal for endocytic trafficking, inflammation, translation, and DNA repair [90].

1.5.1 Receptor protein degradation:

Many reports proposed that signal receptor proteins undergo ubiquitination at various site and are directed towards either lysosomal or proteasomal degradation or both. For instance EGFR is mostly reported as degraded by lysosomal pathway but its degradation is also responsive to MG132 as well [167-169]. Although most of the Seven-transmembrane receptors (7TMRs) get ubiquitinated, a very handful number of protein follow proteasomal degradation pathway. Two 7TMRs, namely, the metabotropic glutamate receptors (mGluR1 and mGluR5)70 and the human follitropin receptor also undergo ubiquitination and proteasomal degradation [170, 171]. Interestingly proteasomal inhibitors actually prevent the degradation of the receptors, which are well documented to occur in lysosomes. In the case of the single transmembrane growth hormone receptor (GHR), endocytosis occurs in the absence of ubiquitination but does require intact proteasomal activity [172]. Similarly, a functional proteasome ensures the optimal endocytosis and subsequent lysosomal degradation of the interleukin 2 receptor/ligand complex [173]. Studies also indicate that human κ opioid receptor, PAFR andβ2AR degradation can be reduced by both lysosomal and proteasomal inhibitors [174-176]. Reports suggest that glucocorticoid receptor (GR) and human estrogen receptor (ER)

follow proteasomal degradation pathway and regulate their transcriptional activity [177, 178]. The degradation of these receptor proteins resulting an alteration of the signaling output and cellular effects.

1.5.2 Adaptor, Modulator or regulator degradation:

In many signaling pathways the adaptors, the modulators or the regulatory molecules protein levels decides the directionality and the fate of the particular signaling cascade. These protein degrade in a controlled fashion resulting various modulation and cross talk within the pathways. Ubiquitination of these signaling molecules by the huge variety of E3-ligases regulate the downstream activity of the effector molecules. Most of the cases these molecules happen to be the inhibitors of different kinases or the inhibitors of transcription factors. Interestingly before ubiquitination these molecules very often undergo phosphorylation in specific sites which act as a signal for subsequent ubiquitination by the E3-ligases. The well-studied inhibitor protein IκBα sequesters the multidimensional transcription factor NF-κB in the cytoplasm and hence inhibit its transcriptional activity. After signal induction by TNF-α IKK complex phosphorylate IκBα followed by K48 polyubiqutination by the E3-ligase β-TrCP and proteasomal degradation results in NF-κB nuclear translocation and transcription activation.

1.5.2 Transcription factor degradation:

Transcription factors are regulated by the UPS both in cytoplasm and nucleus. For instances in β-catenin Wnt signaling pathway and p53 in apoptosis/cancer signaling pathway are degraded in the cytoplasm by the proteasome. In addition various transcription factors are sequestered in the cytoplasm by their inhibitors which undergo proteasomal degradation under certain circumstances and activate the transcription factors. Moreover, many transcription factors and transcription co-activators undergo

ubiquitination and proteasomal degradation in the nucleus. As a feedback loop or under continuous stimulus transcription factors get mono/polyubiquitinated by different E3 ligases in the nucleus and hence the transcriptional activity was regulated by nuclear proteasome. For instance while p53 is monoubiqutinated by MDM2 it shuttles back to cytoplasm, but when it is polyubiqutinated it is degraded by proteasome inside the nucleus.

1.6 Additional Function of Proteasome

1.6.1 Protein processing

Proteasome not only degrade the substrate proteins completely but also proteolytically process some proteins from their inactive form to active form. In some cases, the proteasome processes the substrate into a truncated form. Processing by the proteasome can serve as a potent regulatory tool for transforming a protein from one form into another, thus altering its cellular activities. The well-studied proteins amongst the known proteasomal substrate are of NF-κB family proteins. The p105 subunit (NFKB1) and p100 subunit (NFKB2) undergo proteasomal processing to form p50 (50kDa) and p52 (52kDa) protein subunits respectively [179-181]. After p105/p100 is ubiquitinated, probably within its COOH-terminal half, this half is proteolysed by the proteasome, and the 50/52-kDa NH2-terminal region is released as a stable and active subunit of the NF-κB transcription factor protein. In the case of p105/p100, the site of processing is determined in part by a glycine-rich region (GRR) in the middle of the protein [180, 182], as well as by specific interactions of certain amino acids within the p50/p52 domain that stabilize its three-dimensional structure, so it cannot be unfolded [181, 183]. The mechanisms of processing are far from being understood. For instance, it is not clear whether processing is a distinct event that occurs before proteolysis, or whether it is simply a termination of the processive proteolysis of a substrate.

1.6.2 Protein refolding and recovery

Different studies suggest that proteasome is also involved in protein refolding or recovery. At least *in vitro*, the proteasome can bind certain unfolded proteins, accelerate their refolding, and release them in their native form [126, 127]. The proteasome can also inhibit aggregation of misfolded proteins. These chaperone-like activities have been mapped to the ATPase-containing base of the RP. There is evidence that *in vivo*, the proteasome is involved in disassembly and rearrangement of the nuclear excision repair complex, without performing proteolysis [119]. Similarly, RP subunits, but not CP subunits, colocalize *in vivo* together with heat shock proteins and chaperones at sites of misfolded AR aggregates. Components of the RP function in nucleotide excision repair in yeast independent of proteolysis [184]. These may be in vivo examples of the in vitro observed chaperone-like activity of the RP.

1.6.3 Proteasome in chromatin modification:

Recent reports suggested that, there is good reason to believe that proteasomes are involved in proteolytic and non-proteolytic events that occur directly on, or in the immediate vicinity of, chromatin and impact genomic events in a direct and mechanistic way [185]. Various attempts to understand the proteasome role at chromatin proximity reveal many aspects like; proteasome components are present in the nuclei of actively-dividing eukaryotic cells [186], associated with chromatin [187], and enriched at specific sites in the genome [188-190] and in response to specific molecular events such as transcription [188] or DNA damage [191]. Moreover, inhibition of proteasome function results in profound changes in the distribution of ubiquitylated proteins on chromatin [192], implying that Ub-mediated proteolysis most likely occurs within the immediate confines of the chromatin environment in which these proteins act. Thus, although it is not always possible to directly and unambiguously tie proteasomes to the

biochemical operations of chromatin, strong circumstantial evidence places proteasome subunits and their activities at “the scene of the crime”.

Experimental evidences like; Chromatin immunoprecipitation (ChIP) experiments exploring the interaction of proteasome subunits with chromatin have produced contradictory results in terms of how 19S versus 20S subunits behave. Some studies have reported identical or overlapping patterns of binding for 19S and 20S proteins, others have focused specifically on 19S components, and others still have reported that 19S and 20S proteasome subunits behave differently in terms of chromatin association patterns, with significant disparity in ChIP signals of 19S versus 20S proteins. However using one or two subunit specific antibodies for the experimental validation and justification of the fact that 26S-proteasome as a whole, is involve in non-proteolytic functions in chromatin biology would be too early. Nevertheless, there are substantial evidences which suggest involvement of the individual subunits in chromatin modification and transcription regulation [185, 193, 194]. But further investigation is necessary to elucidate the precise molecular details regarding the substrates-proteasome interaction in nucleus, and explore more about the impact of 26S proteasomal action on chromatin biology.

1.7 Cellular localization of proteasomes:

Proteasome is ubiquitous in nature and express in all types of eukaryotic cells and with respect to human it is expressed in all tissues. In mammalian cells, proteasomes are primarily localized in cytosol and nucleus. They also display significant association with cytoskeletal elements, ER, nucleus and plasma membrane; however the ratios of proteasomes associated with different organelles varies in different cells [195]. Studies performed with GFP-tagged β1i (LMP2) in a human cell line revealed that proteasomes are distributed in both nucleus and cytoplasm, though they are excluded from nucleolus

and ER lumen. These experiments demonstrated that preformed proteasomes move from cytosol to nucleus in a slow and unidirectional manner. It is also possible that proteasomes from nucleus and cytosol mix after the breakdown of the nuclear envelope after mitosis [196]. In S. cerevisiae, proteasomes are mainly localized in the nuclear membrane-ER network [197]. However, localization of proteasomes at different times is dependent on the physiological state of the cell remarkably during cell cycle progression or responding to different external signals. Some of the α subunits harbour nuclear localization signals (NLS), which probably aid in nuclear targeting of proteasomes. In fact, T. acidophilum proteasomes when expressed in HeLa and 3T3 cells can translocate into nucleus [198]. In nucleus proteasomes are responsible for nuclear specific protein degradation especially the transcription factors and the chromatin modifiers [199]. Some of the nuclear substrates of proteasome are listed in the table Table-1.1.

Table-1.1: Substrates of the nuclear ubiquitin-proteasome system (nUPS):

Substrate	Nuclear structure and/or function
Far1	Cyclin-dependent kinase (CDK) inhibitor (Blondel et al., 2000)
Estrogen receptor α	Nuclear hormone receptor (Nawaz et al., 1999)
E1A	Nuclear oncoprotein (Ciechanover et al., 1991)
Fos	Nuclear oncoprotein (Ciechanover et al., 1991)
Jun	Nuclear oncoprotein (Ciechanover et al., 1991)
Myc	Nuclear oncoprotein (Ciechanover et al., 1991)
p53	Tumor suppressor (Ciechanover et al., 1991; Shirangi et al., 2002)
STAT1	Transcription factor (Kim and Maniatis, 1996)

GCN4	Transcription factor (Mayor et al., 2005)
Mat α2	Transcriptional repressor (Lenk and Sommer, 2000)
MyoD	Transcription factor (Floyd et al., 2001)
RNA polymerase II	Transcription (Beaudenon et al., 1999)
CREB-binding protein (CBP)	Histone acetylase/transcriptional co-activator (Jiang et al., 2003)
Histone H2A	Chromatin structure (Rockel and von Mikecz, 2002)
SmB/B	Spliceosomal component (Rockel and von Mikecz, 2002)
U1-70k	Spliceosomal component (Rockel and von Mikecz, 2002)
SC-35	Nucleoplasmic speckles/ splicing factor (Rockel and von Mikecz, 2002)
PML	PML body component/tumor suppressor (Rockel and von Mikecz, 2002)
DNA topoisomerase I	DNA topology (Desai et al., 1997; Chen et al., 2005)

In summary, the literature survey shed light on enormous researches in the past several decades which has been conducted to understand the structural complexity, the mechanistic prospective and the functional essentiality of ubiquitin proteasome system (UPS). Altogether Research is still going on to elucidate its contribution to cell physiology by both biochemical and cell biology approach. The structural complexity involving a large no of protein subunit, make this system more multifaceted and also interesting for researchers. Furthermore, the major player of UPS – 26S proteasome, is more complicated for its mode of action and large no of highly ordered protein subunits. The knowledge that currently we have about proteasome is, it's an indispensable

protease complex for life and regulate the cellular proteostasis by protein modification and protein degradation. However the large subunit-protein contents make the proteasome more dynamic and multifunctional in eukaryotic cells. Researches are still going on to elucidate the cooperative function of proteasomal subunits in making a fully assembled functional proteasome and the regulatory mechanism of protein degradation.

RATIONALE OF THE CURRENT STUDY

The primary function of 26S proteasome is to maintain protein homeostasis in eukaryotic cells by degrading cellular proteins.. In doing so the proteasome is responsible for regulatory functions of the cell such as signal transduction, transcription regulation, chromatin modification to name a few. In most cases a clear involvement of 26S proteasome and its associated degraded role in conjunction with the ubiquitin system is well established. In addition to this there have been reports on the role of isolated 19S regulatory particles, individual subunits of the proteasome in specific functions and in specific cell type. Their general role and significance is yet to be established. Among the well-studied examples are the proteasome associated proteins such as PSMD9, PSMD10, PSMD5 and PAAF1. These subunits are involved in assisting the complex formation between the base and the lid components of the priteasome in insulin and activin signaling (PSMD9), in the degradation of p53 and pRb (PSMD10), in stability of the 26S structure (Blm10) and in enhancing the activity of proteasome (SEM1, PSMD11).

Furthermore, recent studies provide substantial evidence on the involvement of proteasome in various diseases. Proteasome directly or indirectly affect both the pathogenesis as well as the prognosis of diseases such as cancers, Increase proteasome activity positively correlates with the progression of cancer and this association has

been exploited for therapy by developing active site inhibitor based drugs such as Velcade. On the contrary, in neurodegenerative disorders where the proteasome fails to degrade some unwanted proteins and thus contribute to the aetiology of the disease, such as prion and polyglutamine diseases, there is a need for activating the proteasome. Besides the proteasome components of UPS such as E3 ligases which are substrate specific and ubiquitin isopeptidases are also sought after drug targets. Interestingly protein interactions which are important for the assembly of the proteasome are also speculated to be targets for intervention. The emerging trend based on biology and the mechanism of action of the proteasome suggest that there are better ways to inhibit proteasome and avoid toxicity and side effects such as neuropathy seen with current day proteasome inhibitors.

Clearly this accumulated knowledge on the ubiquitin proteasome biology, is a product of intense research conducted by many investigators over the last several decades. At the same time there are many fundamental questions that remain to be addressed. For example a) the correlation between the structure and function of proteasome, b) the details on the mechanism of degradation including the structure, sequence requirement of the substrate c) signals that go beyond ubiquitin required for recognition and degradation d) the mechanism of subunit recruitment and the players involved e) the role of protein domains on 19S in substrate recognition f) the role of proteasome associated subunits when they are free, and g) the dynamics of the components of proteasome in various functions are some of the key questions that demand answers. It is with this background my thesis attempts to provide some answers to the role of proteasome associated subunits PSMD9 and PSMD10 in cellular functions.

Major Objectives:

1. To find out novel functions of PSMD9 and PSMD10 by their interactions with other putative binding partners.

2. To delineate their roles in the signaling networks due to their interactions, in mammalian cells.

CHAPTER-II

Materials and Methods

2.1 Materials:

2.1.1 Antibiotics:

Ampicillin (Sigma Aldrich): Used for bacterial clone selection. [Storage 4°C]

Doxycycline (Sigma Aldrich): Gene transcription induction in mammalian cells. [Storage 4°C]

G418 (Sigma Aldrich): Used for mammalian cells clone selection. [Storage 4°C]

Puromycin (Sigma Aldrich): Used for mammalian cells clone selection. [Storage -20°C]

2.1.2 Buffers:

Buffers made in Laboratory:

0.5M $CaCl_2$: For mammalian cells transfection. [Storage -20°C]

1X Protein Transfer Buffer (WB): (pH-No need to adjust) [Storage RT]

TRIS	25mM
Glycine	192mM
Methanol	20%
SDS	0.02-0.1%

1X Transformation Buffer: For competent cells preparation. [Storage 4°C]

PIPES Na-Salt	10mM
$CaCl_2$	15mM
KCl	250mM

Adjust pH using KOH to 6.7

Add 55mM $MnCl_2$. Filter sterilized.

2X BBS (pH 6.7): For mammalian cell transfection. [Storage -20°C]

BES	50 mM
NaCl	280 mM
Na2HPO4.2H2O	1.5 mM

3X Lamellae loading dye: For SDS-PAGE sample loading. [Storage RT]

TRIS	150mM
SDS	6%
Glycerol	30%
BME	3%
Bromophenol Blue	0.012%

5X TBE: For EMSA-native PAGE running. [Storage RT]

TRIS	450mM
Boric acid	27.5 g (for 1Ltr)
EDTA	5 mM

6X Gel Loading dye for DNA: [Storage 4°C]

Xylene Cyanol FF	0.25% (w/v) (migrates at 4160 bp with TAE)
Bromophenol blue	0.25% (w/v) (migrates at 370 bp with TAE)
Glycerol	30% (w/v)

10X Phosphate Buffer Saline: [Storage RT]

NaCl	1.37M
KCl	27mM
Na_2HPO_4. 2H2O	100mM
KH_2PO_4	18mM

10X SDS Running Buffer: (pH-No need to adjust) [Storage RT]

TRIS	250mM
Glycine	1920mM
SDS	1%

50X TAE: For Agarose electrophoresis. [Storage RT]

TRIS	2M
Acetic acid	114.2mL (for 1Ltr)
EDTA	50 mM

(pH was adjusted to 7.5 with NaOH and autoclaved)

Immunoprecipitation Buffer: [Storage 4°C]

TRIS	50mM (pH 7.5)
NaCl	150 mM
NP-40	0.4-0.6%
Protease inhibitor	1X

NP-40 Lysis Buffer: For Mammalian cell lysis. [Storage 4°C]

TRIS	50mM (pH 7.5)
NaCl	150 mM
NP-40	1%
DTT	1mM
Protease inhibitor	1X
NaF	10mM
Na_2VO_3	1mM
β-Glycerophosphate	10mM

Protein Purification buffers: [Storage 4°C]

10mM Sodium bicarbonate buffer (pH 9.3)

Sodium bicarbonate 0.42 g

Sodium carbonate 0.17 g

GST-protein lysis buffer (in Phosphate buffer saline pH 7.5)

NaCl	137 mM
KCl	2.7 mM
$Na2HPO_4$. 2H2O	10 mM
$KH2PO_4$	2 mM
Protease inhibitor	1X
DTT	1mM (To be added freshly)
TritonX100	0.1% (0.1% NP-40 can be used instead)

GST-fusion protein wash/binding buffer (Phosphate buffer saline pH 7.5)

NaCl	137 mM
KCl	2.7 mM
$Na2HPO_4$. 2H2O	10 mM
$KH2PO_4$	2 mM
DTT	1mM (To be added freshly)

GST-fusion protein elution buffer

TRIS	50 mM, (pH 8.0)
L- Glutathione reduced	10mM

MBP- fusion protein wash/binding buffer

TRIS	50 mM, (pH 8.0)
NaCl	150 mM
Protease inhibitor	1X (during lysis only)
BME	5 mM

Ni-NTA Lysis Buffer

TRIS	50 mM, (pH 7.5)
NaCl	150 mM
Imidazole	10 mM
Glycerol	10%
TritonX-100	0.1%
Protease inhibitor	1X
BME	50 mM

Ni-NTA Binding/Washing Buffer

TRIS	50 mM, (pH 8.0)
NaCl	150 mM

Imidazole	10 mM
Glycerol	10%
TritonX-100	0.1%
Protease inhibitor	1X (in lysis buffer only)
BME (14.3 M)	50 mM

Ni-NTA Elution Buffer

TRIS	50 mM, (pH 8.0)
NaCl	150 mM
Imidazole	250 mM
Glycerol	10%
TritonX-100	0.1%
Protease inhibitor	1X
BME	50 mM

Transport Buffer

HEPES	20mM, (pH 7.9)
Potassium acetate	110mM
Sodium acetate	5mM
EGTA	0.5mM
DTT	1mM DTT

TBST: For western blots washing. [Storage RT]

TRIS	25mM (pH 7.5)
NaCl	150 mM
Tween-20	0.1% (w/v)

Commercially available Buffer:

10X Restriction Digestion Buffer (Thermo)

10X Fast Digestion Buffer (Thermo)

10X Pfu Polymerase Buffer (Thermo)

10X Taq-polymerase Buffer (Thermo)

10X T4-DNA ligase Buffer (Thermo)

10X HF-Fusion Buffer (Thermo)

2.1.3 Reagents:

Antibodies: [Storage -20/4°C]

Primary antibodies; **anti-PSMD9** 1:2000 (mouse monoclonal, Sigma and rabbit polyclonal, abcam), Antibodies **anti-PSMD10** 1:1000 (mouse monoclonal, Sigma and rabbit polyclonal, Sigma), **anti-FLAG** 1:8000 (mouse monoclonal, sigma), **anti-hnRNPA1** 1:2000 (mouse monoclonal, Sigma and rabbit polyclonal, abcam), anti-HA in 1:1000 (rabbit polyclonal, abcam), **anti-IκBα** 1:1000 (rabbit polyclonal, Sigma), **anti-pIκBα** 1:1000 (mouse monoclonal, Sigma), **anti-β-actin** in 1:2000 (mouse monoclonal, Sigma), **anti-α-tubulin** 1:2000 (mouse monoclonal, Sigma), **anti-acetyl histone H4 K12** in 1:1000 (rabbit polyclonal, Cell Signaling), **anti-*β*7** 1:1000 (mouse monoclonal), **anti-*α*4** in 1:1000 (mouse monoclonal), **anti-*α*5** in 1:1000 (mouse monoclonal), **anti-Rpt6** 1:1000 (mouse monoclonal), **anti-ubiquitin** in 1:1000 (mouse polyclonal, sigma), **anti-p65** 1:1000 (rabbit polyclonal, abcam), **anti-HA** 1:1000 (rabbit polyclonal, abcam), **anti-β-III tubulin** 1:1000/1:100 (WB/IF) (Millipore polyclonal mouse), **anti-GFAP** 1:1000/1:100 (WB/IF) (Millipore polyclonal rabbit), **anti-nestin** 1:1000/1:100 (WB/IF) (Millipore monoclonal mouse), **anti-nestin** 1:1000/1:300 (WB/IF) (Sigma polyclonal rabbit), **anti-SOX2** 1:1000/1:100 (WB/IF) (Millipore polyclonal rabbit), **anti-Musashi** 1:1000/1:100 (WB/IF) (Millipore polyclonal rabbit), **anti-Oligodendrocyte marker O1** 1:1000 (Millipore monoclonal mouse), **anti-β-catenin** 1:1000 (mouse monoclonal, cell signalling), **Mouse IgG** (cell signalling, Millipore), **Rabbit IgG** (Cell signalling, Millipore).

Secondary antibodies; anti-mouse-HRP (GE-healthcare), anti-rabbit-HRP (GE healthcare), **anti-mouse-FITC** (Invitrogen), **anti-mouse-Alexaflour568** (Invitrogen), **anti-mouse-TR** (Invitrogen), **anti-rabbit-Alexaflour488** (Invitrogen), **anti-rabbit-Alexaflour568** (Invitrogen).

BME: For disulphide bond break. [Storage RT]

Bradford Reagent (BioRad)**:** Used for protein estimation

DTT (Dithiothretol): For disulphide bond break. [Storage 4°C]

Imidazole: For His tagged protein elution 250mM. [Storage 4°C]

IPTG (Isopropyl-D-thiogalactoside): For bacterial protein induction. Standard Concentration: 100mM. Working Concentration: 100µM. [Storage 4°C]

L-Gulathione reduced: For GST fused protein elution 10mM.

Luria-Bertani (LB) medium: For bacterial culture.

Maltose: For MBP fused protein elution 20mM.

SOB (Supra-optimal media): Used for Competent cell preparation.

2.1.4 Plasmids:

Mammalian expression vectors: **p3xFLAG-CMV10** vector (Sigma Aldich) a kind gift from Dr. Robin Mukhopadhyaya, Advanced Centre for Treatment, Research and Education in Cancer, Navi Mumbai, India; **pTRIPZ** vector (Invtrogen) a kind gift from Dr. Sorab Dalal, Advanced Centre for Treatment, Research and

Education in Cancer, Navi Mumbai, India; **pCDNA3.1-HA** vector (Invitrogeen) a kind gift from Dr. Sorab Dalal, Advanced Centre for Treatment, Research and Education in Cancer, Navi Mumbai, India were used for gene expression. Bacterial expression vectors: **pRSETA**, **pGEX4T1**, **pMALc5X** were used for recombinant protein expression. The phospho-mutant **pTRIPZ-IκBαSR** (S32A-S36A) vector (a kind gift from Dr. N. Shirsat, Advanced Center for Treatment, Research and Education in Cancer, Navi Mumbai, India and Dr. D.C. Guttridge, Ohio State University, USA) was used for NF-κB activity inhibition. **3x κB ConA luc** vector and **ConA luc control** vector (a kind gift from Dr. Neil D. Perkins, Newcastle University, UK) were used for the Luciferase reporter assay. **pBIND-Renilla-Luc** vector, **pEGFPN3** vector were used for transfection control and **pBSK3** vectors were used as filler DNA in mammalian cell transfection. **pJET3.1** (Thermo/Fermentas) vector was used for sub-cloning. PAX2 and MD2G packaging vectors were used for virus production.

2.1.5 Primers and Oligos:

Table-2.1: List of Cloning primers:

Gene name	Primers; Forward (Fw) and Reverse (Rv) (Sequences are in 5' to 3')
PSMD9 in pRSETA, pGEX4T1 and pMALc5X	Fw: GGATCCATGTCCGACGAGGAAGCGAG Rv: GAATTCGACAATCATCTTTGCAGAGG
PSMD9 in pCMV10-3X-FLAG	Fw: AAGCTTATGTCCGACGAGGAAGCGAG Rv: GAATTCGACAATCATCTTTGCAGAGG
FLAG-PSMD9 in pTRIPZ	Fw: ACCGGTCGCCACCATGGACTACAAAGACCATG Rv: GAATTCGACAATCATCTTTGCAGAGG

FLAG-PSMD10 in pTRIPZ	Fw: ACCGGTCGCCACCATGGACTACAAAGACCATG Rv: GAATTCTTAACCTTCCACCATTCTCTTG
hnRNPA1 in pGEX4T1 and pCDNA3.1	Fw: GGATCCATGTCTAAGTCAGAGTCT Rv: GAATTCTTAAAATCTTCTGCCAC
IκBα in pCMV10-3X FLAG	Fw: ATAAGCTTATGTTCCAGGCGGCCGAGCG Rv: GCGAATTCTCATAACGTCAGACGCTGGC
IκBα-ΔC in pCMV10-3X FLAG	Fw: ATAAGCTTATGTTCCAGGCGGCCGAGCG Rv: GCGAATTCTCAAGAATAGCCCTGGTAGG
IκBα in pMALc5X	Fw: ATGGATCCATGTTCCAGGCGGCCGAGCG Rv: GCCTCGAGTCATAACGTCAGACGCTGGC

Table-2.2: List of Real time primers:

Primer Name	Primer Sequence
GAPDH-Fwd	5'-ATCGTGGAAGGACTCATGACC-3'
GAPDH-Rv	5'-AGGGATGATGTTCTGGAGAGC-3'
PSMD9-Fwd	5'-AAGGCCAACTATGACGTGCTG-3'
PSMD9-Rv	5'-ATATGATGTTGTGCCTGGCG-3'
IκBα-Fwd	5'-CATCGTGGAGCTTTTGGTGTC-3'
IκBα-Rv	5'-AGCCCCACACTTCAACAGGAG-3'
IL6-Fwd	5'-GATGGCTGAAAAAGATGGATGC-3'
IL6-Rv	5'-GCTCTGGCTTGTTCCTCACTAC-3'
ICAM1-Fwd	5'-GGGCAGTCAACAGCTAAAACC-3'
ICAM1-Rv	5'-TGGCAGCGTAGGGTAAGGTTC-3'
COX2-Fwd	5'-TCCCTGAGCATCTACGGTTTG 3'
COX2-Rv	5'-GTCTGGAACAACTGCTCATCAC-3'

A20-Fwd	5’-GCGTTCAGGACACAGACTTGG-3’
A20-Rv	5’-TTCCGAGTATCATAGCAAAGCC-3’
α4-Fwd	5’- CGCTACATCGCCAGTCTGAAG -3’
α4-Rv	5’- GAGCCTAGGAGTGCCATCAAAG -3’
β1- Fwd	5’- AATCGAGTGACTGACAAGCTGAC -3’
β1-Rv	5’- CAGTGGAGGCTCATTCAGTTC -3’
β2-Fwd	5’- TGAAGGGATGGTTGTTGCTGAC -3’
β2-Rv	5’- GGAAGAAATGAGCTGGGTTGTC -3’
β5-Fwd	5’- CGGCAATGTCGAATCTATGAGC -3’
β5-Rv	5’- GCCTCTCTTATCCCAGCCACAG -3’
IL8-Fw	5’-TGCAGCTCTGTGTGAAGGTG -3’
IL8-Rv	5’-TGGTCCACTCTCAATCACTCTC -3’
NGN1-Fwd	5’- GACCTATCCGGCTTCCTCAC -3’
NGN1-Rv	5’- TCCTGCTCGTCGTCCTGTG -3’
NRG1-Fwd	5’-AGGTGAGAACGCCCAAGTC -3’
NRG1-Rv	5’-TCTCCTTCTCCGCACATTTTAC -3’
PSMD10-Fwd	5’- GCAGCTTCGAAAAACAGGCA -3’
PSMD10-Rv	5’- GGATGTTTGTGGATGCTTTG -3’
STAT3-Fwd	5’- TAAGACCCAGATCCAGTCCGT -3’
STAT3-Rv	5’- TACCTGGGTCAGCTTCAGGA -3’

2.2 METHODS (Experimental Methodology):

2.2.1 Molecular cloning:

For the current study various plasmids, constructs were either designed and prepared in-house or procured from outside labs. For cloning following materials and Methodologies were followed.

2.2.1.1 Competent cells preparation

For plasmid transformation *E Coli*, strains like DH5α and BL21 were used and the competent cells of these strains were prepared by following Methodology.

Reagents:

a) **SOB** (Supra-Optimal Broth) **Media (100mL):** For optimal growth of bacteria.

   (2% Bacto-tryptone, 0.5% Bacto-yeast extract, 0.05% Sodium chloride, 2.5 mM KCl, 10 mM MgCl2)

   10mM MgSO4 and 50mM KCl were prepared separately, autoclaved and added to the incomplete autoclaved SOB.

b) **Transfer Buffer (pH 6.7) 50mL:**

   (PIPES, $MnCl_2$, $CaCl_2$)

   Transfer buffer was prepared in autoclaved Milli-Q, pH was adjusted by adding 1N HCl and filter sterilized by 0.22µm syringe filter.

c) **DMSO:** Acting as a cryopreserving agent for competent cells.

d) **Liquid Nitrogen:** For snap freezing the freshly prepared competent cells.

Methodology:

i. Glycerol stock of *E. Coli* bacteria strain was streaked on a LB-agar plate and incubated at 37ºC/180rpm for overnight.

ii. Single colony was picked up and inoculated in 100mL of autoclaved complete SOB media and incubated at 18ºC/80rpm till the OD reaches upto 0.35 to 0.4. **Note: DO NOT** exceed the OD beyond 0.4.

iii. After the OD reaches bacteria culture were centrifuged at 4ºC/5000rpm for 10min.

iv. Cell pellet was dislodged and washed with 20mL of chilled sterilized transfer buffer twice, by intervenient centrifugation of 4ºC/5000rpm for 10min.

v. The washed pellet was reconstituted in 10mL of chilled transfer buffer.

vi. To this suspension 700µL of DMSO was added drop-wise by intervenient mixing on ice.

vii. This bacterial suspension was aliquoted (100µL) in MCT, snap-freezed in liquid nitrogen and stored at -80ºC.

2.2.1.2 PCR amplification:

For different gene plasmid constructs preparation the particular gene was PCR-amplified from either cDNA library or from another plasmid constructs, using different primer set containing required restriction enzyme sites.

Reagents

10X Pfu/Taq Polymerase Buffer

Forward and Reverse primers (10pmol)

dNTPs (10mM) (Working: 200µM)

MgCl2 (25mM) (Working: 500µM)

DNA template (~100ng)

Pfu Polymerase enzyme

Plasmids used for cloning: Mammalian expression vector – p3xFLAG-CMV-10, pCDNA3.1 and pTRIPZ. Bacterial expression vector – pRSETA, pGEX4T1, pMALc5X

2.2.1.3 Restriction Digestion:

PCR-amplified products or the plasmid constructs were digested with restriction enzymes as per requirements.

Reagents

1X Fast digestion Buffer *(Thermo/Fermentas)*

Restriction enzymes *(Thermo/Fermentas)*

Methodology

Required amount of DNA were digested with specific restriction enzymes at 37ºC for 1-2hr in water-bath. Reaction volume may vary from 20-50µL.

2.2.1.4 Agarose Gel Electrophoresis and DNA Extraction:

After PCR-amplification or restriction digestion the DNA products were analysed by agarose gel electrophoresis.

Reagents

a) 1X TAE buffer
b) Agarose powder *(Sigma/Himedia)*

Methodology

0.8% agaroge gel was prepared in 1X TAE buffer. DNA samples were run in the gel at 120V and 150mA. Required DNA products were gel extracted for further cloning process by using Quiagen Gel extraction Kit.

2.2.1.5 Ligation:

After gel extraction restricted digested cut vector and insert were ligated for preparation of recombinant plasmid constructs.

Reagents

1X Ligation Buffer *(Thermo/Fermentas)*

T4-DNA ligase enzymes *(Thermo/Fermentas)*

Methodology

Required amount of digested vector and inserts were ligated (according to the formula given) in presence of T4-DNA ligase enzyme and ATP in reaction mixture (20µL) at 22ºC for ~2-3hr in waterbath. In reaction volume vector: insert ratio may vary depending upon their size.

Amount of Insert (in ng) = [Amount of Vector (200ng) X Size of Insert (in KB) / size of vector (in KB)] X 3/1

2.2.1.6 Transformation:

After ligation, the ligation mixures were transformed into either DH5α (for plasmid preparation) or BL21 (for protein purification).

Reagents

a) LB broth/agar
b) Competent cells
c) Ligation mix
d) Ampicillin (100mg/mL)

Methodology

i. Competent cells were removed from -80ºC and placed on ice for 5min.

ii. Ligation mixture was mixed in the competent cells suspension and incubates on ice for 30min.

iii. Then the suspension was given heat shock at 42ºC for 90sec in water-bath and immediately placed on ice for 5min.

iv. 1mL of autoclaved LB broth was added to the suspension and incubated at 37ºC/180rpm for ~45min to 1hr.

v. After the incubation the bacteria suspension was centrifuged at 5000rpm at RT for 5min.

vi. Cell pellet was dislodged and resuspend with 50µL of LB broth, plated on ampicillin (100µg/mL of media) containing LB-agar plate and incubated at 37ºC for overnight.

2.2.1.6 Plasmid isolation (Mini prep/Maxi prep):

For selection of positive recombinant plasmid constructs and for transfection of mammalian cells plasmid isolation was performed.

Reagents

a) Miniprep Plasmid Extraxtion Kit *(Sigma)*

b) Maxiprep Plasmid Extraction Kit *(Quiagen)*

Methodology

i. After overnight incubation (from the Transformation step) the bacteria colonies were picked up, inoculated in (10mL for miniprep/500mL for maxi-prep) LB broth containing ampicillin (100µg/mL of media) and incubated incubated at 37ºC/180rpm for 14-16hr.

ii. Then the bacteria culture were pelleted down and proceed for plasmid extraction following the Kit manufacture Protocol.

2.2.1.7 Site directed Mutagenesis:

For the expression of mutant gene of PSMD9, hnRNPA1 and IκBα site directed mutagenesis Methodology was followed.

Reagents

a) 1X HF (High Fidelity) buffer *(Thermo)*

b) Forward and Reverse primer (10pmol)

c) dNTPs (10mM)

d) MgCl2 (25mM)

e) DMSO

f) Wild type Plasmid constructs (100ng)

g) High Fidelity polymerase enzyme *(Thermo)*

h) 1X Tango Buffer *(Fermentas/Thermo)*

i) DpnI restriction Digestion enzyme *(Fermentas/Thermo)*

j) Competent cells

k) LB broth and Agar

l) Plasmid isolation Kit (Mini/Maxi prep) *(Sigma/Quiagen)*

Primers used:

Table-2.3: List of SDM primers:

Name of the Gene	Primers; Forward (Fw) and Reverse (Rv)
PSMD9 L173G	Fw: CTTCCAGTCAGGGCATAACATTG Rv: CAATGTTATGCCCTGACTGGAAG
PSMD9 Q181G	Fw: GCAGTGTGGTGGGGCACAGTGAGGG Rv: CCCTCACTGTGCCCCACCACACTGC
PSMD9 Triple mutant	Fw:

(L124G/ Q126G/ E128G)	ATGAGCCGCAAAGGGGGTGGGAGTGGGAGCCA GGGCCCTCCACG Rv:CGTGGAGGGCCCTGCCCGCTCCCACTCCCA CCCCCTTTGCGGCTCAT
hnRNPA1ΔC in pGEX4T1	Fw: CAGCAGCAGTTAATAATATGGCAGTGGC Rv: GCCACTGCCATATTATTAACTGCTGCTG
IκBα-ΔC in pCMV10-3X FLAG	Fw: ATAAGCTTATGTTCCAGGCGGCCGAGCG Rv: GCGAATTCTCAAGAATAGCCCTGGTAGG

Methodology

i. Point mutations or deleted mutations were incorporated in the forward and reverse primer of the specific gene.

ii. PCR amplification (50µL reaction volume) was carried out using the primers and the specific wild type template by following PCR programme.

Initial denaturation at 95ºC for 5min

Denaturation at 95ºC for 1min

Annealing at 48ºC for 1min

Extension at 72ºC for X min (X= size of the vector/2)

Total cycle no. 18

iii. Then the PCR mixture was put for restriction digestion with DpnI enzyme at 37ºC for overnight in water-bath.

iv. Then the digested mix was transformed into the DH5α competent cells following the transformation Methodology (Described earlier).

2.2.1.8 shRNA Cloning:

To silence endogenous PSMD9, shRNA against the coding sequence of PSMD9 was designed and cloned in pTRIPZ vector under doxycycline inducible system.

Reagents

a) 1X Taq pol buffer *(Thermo)*
b) Forward and Reverse primer (100pmol)
c) dNTPs (10mM), MgCl2 (25mM), DMSO
d) Taq-Polymerase enzyme *(Thermo)*
e) 1X Fast digestion Buffer *(Fermentas/Thermo)*
f) Restriction Digestion enzyme (XhoI and EcoRI) *(Fermentas/Thermo)*
g) 1X Ligation Buffer *(Fermentas/Thermo)*
h) T4-DNA Ligase enzyme *(Fermentas/Thermo)*
i) pTRIPZ empty vector
j) Competent cells
k) LB broth and Agar
l) Plasmid isolation Kit (Mini/Maxi prep) *(Sigma/Qiagen)*

Primers of PSMD9-shRNA

Fwd primer (P9shRNA-2Fw) 75bp

5’ggctcgagGAAGGTATATTGCTGTTGACAGTGAGCGgcagatcaaggccaactatgaTAGTGAAGCCACAGATGT3’

Rev Primer (P9shRNA-2Rv) 69bp

5’gcgaattcCCGAGGCAGTAGGCAtcatagttggccttgatctgcTACATCTGTGGCTTCACTAgttatg3

shRNA Oligo sequence Map:

5'-Rest. Ezym-.mir30 flanking Seq.-Sense - miR-30 loop- Antisense- mir30 flanking Seq.- Rest. Ezym-3'

Oligo sequence:

5′ GGCTCGAGGAAGGTATATTGCTGTTGACAGTGAGCGGCAGATCAAGGCCAACTATGATAGTGAAGCCA
CAGATGTATCATAGTTGGCCTTGATCTGCTGCCTACTGCCTCGGGAATTCGC 3′

Figure-2.1: PSMD9 shRNA in Mir-30 cassette sequence Map.

Methodology

i. PCR amplification (50µL reaction volume) was carried out using the primer pair by following PCR programme.

Initial denaturation at 95ºC for 5min, Denaturation at 95ºC for 1min, Annealing at 55ºC for 2min, Extension at 72ºC for 1min, Total cycle no. 30

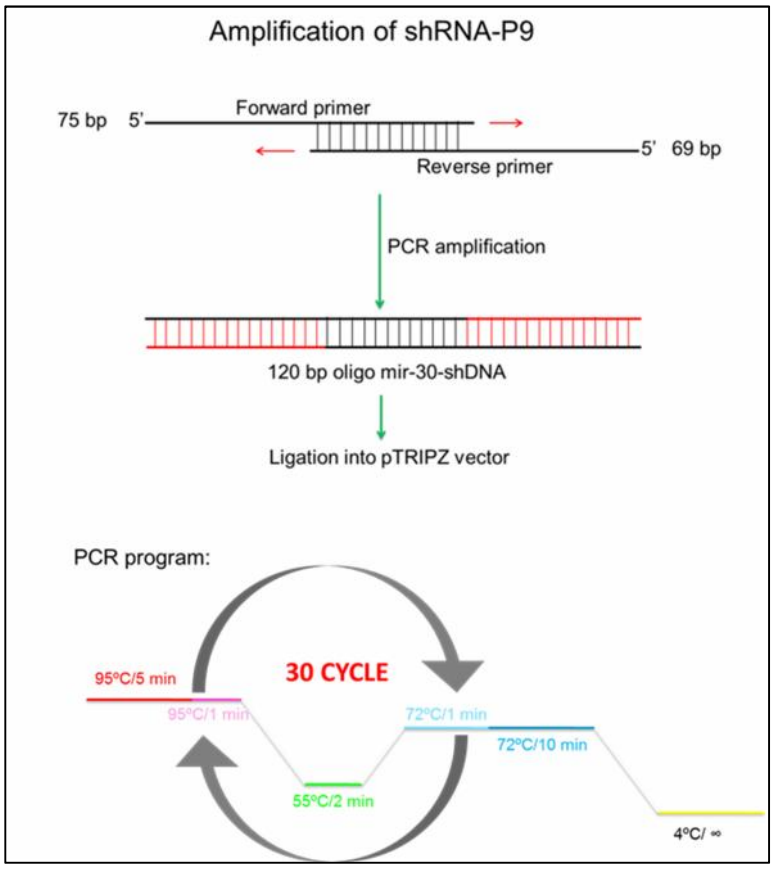

Figure-2.2: Amplification procedure of PSMD9 shRNA by PCR.

ii. Then the PCR mixture was run in an agarose gel for gel extraction.

iii. Gel extracted DNA put for restriction digestion with XhoI and EcoRI at 37ºC for 2hr in water bath.

iv. Then the digested mix was heat inactivated, diluted as per requirement and put for ligation with digested empty pTRIPZ vector in presence of T4-DNA ligase enzyme and ATP in reaction mixture (20µL) at 22ºC for ~2-3hr in water bath.

v. Ligation mixture was transformed into the DH5α competent cells following the transformation Methodology (Described earlier).

2.2.2 Mammalian Cell Culture and reagents:

Cell line used: HEK293 cells (Human Embronic Kidney cells) and human neuronal progenitor cells *(Millipore)*.

2.2.2.1 HEK293 culture:

HEK293 cells were grown on culture dish *(BD-Falcon)* in DMEM *(GIBCO)* supplemented with 10% FBS *(GIBCO)*, 37ºC, 5% CO2 and in humid condition.

Reagents

a) Culture Medium (DMEM): [Storage 4°C]

Dulbecco's Modified Eagle Medium (DMEM) containing high glucose, pyridoxine hydrochloride and sodium pyruvate (Invitrogen) was prepared as per the manufacturer's Protocol. Powdered medium was reconstituted in 800 ml autoclaved Milli-Q water under sterile conditions. 3.5 g sodium carbonate was added and pH was adjusted to 7.2 using 1 N HCl. The volume was made up to 1 L was filtered by a sterile filter assembly and stored at 4°C. 1.5mM HEPES, 10% FBS *(GIBCO-Invitrogen)*, and 1X antibiotic mixture (of 100IU of penicillin per ml, and 100µg of streptomycin per ml and amphotericin) *(Himedia)* was added to prepare the complete medium.

b) 1X sterile PBS [Storage 4°C].

c) 1X sterile trypsin made in 1X PBS [Storage 4°C].

d) DMSO *(Sigma)* [Storage RT].

Methodology

Revival of cryo-freeze cells:

i. The vial of cryo-freeze cells was removed from liquid nitrogen and incubated in a 37ºC water bath. The cells were closely monitored until completely thawed. **Note:** Maximum cell viability is dependent on the rapid and complete thawing of frozen cells. **IMPORTANT:** Do not vortex the cells.
ii. As soon as the cells were completely thawed, the outside of the vial was disinfected with 70% ethanol and proceeded immediately to the next step.
iii. In a laminar flow hood, the cells were transferred to a sterile 15 mL conical tube and onto that 5 mL of complete DMEM media (pre-warmed to 37ºC) was added drop wise. **IMPORTANT:** Do not add the whole volume of medium at once to the cells. This may result in decreased cell viability due to osmotic shock.
iv. The cell suspension was gently mixed by slow pipetting up and down twice to avoid introducing any bubbles. **IMPORTANT:** Do not vortex the cells.
v. The tube was centrifuged at 1000 Rpm for 2-3min to pellet the cells.
vi. Then the supernatant was decanted as much of as possible. **Note:** Steps iii – vi are necessary to remove residual cryo preservative (DMSO).
vii. The cells were resuspended in a total volume of 8 mL of complete DMEM media (pre-warmed to 37ºC).
viii. The above 8mL cell suspension was added onto the culture plate (90mm); that was pre-incubated in the 37ºC incubator.

ix. Then the cells were incubated at 37ºC in a 5% CO2 humidified incubator.

x. The next day, the medium was exchanged with fresh complete DMEM Medium (pre-warmed to 37ºC).

Sub-culturing/Passaging of cells:

i. Carefully remove the medium from the culture plate containing the confluent layer of HEK293 cells.

ii. Rinse the plate once with 1X PBS. **Note:** Add the PBS slowly from the side to avoid detaching the HEK293 cells.

iii. Aspirate the PBS.

iv. Apply 3-5 mL (90mm plate) of 1X pre-warmed trypsin and aspirate within 30seconds. Note: HEK293 cells were trypsinized very fast.

v. Apply 5 mL of complete DMEM Medium (pre-warmed to 37oC) to the plate.

vi. Gently mix the cell suspension. Transfer the dissociated cells to a 15 mL conical tube.

vii. Centrifuge the tube at 1000 RPM for 2-3 minutes to pellet the cells.

viii. Discard the supernatant.

ix. Apply 2 mL of complete DMEM Medium to the conical tube and resuspend the cells thoroughly. **Note:** Do not vortex the cells.

x. Count the number of cells using a haemocytometer.

xi. Plate the cells to the desired density into the appropriate fresh complete DMEM Medium. It was recommended that ~1.5 million cells be plated at on 90mm plate.

xii. The next day, exchange the medium with fresh complete DMEM Medium. The cells should be ready for passaging or harvesting 2 to 3 days after this step.

Freezing down the cells

i. The medium was carefully removed from the culture plate containing the 80% confluent layer of HEK293 cells. **Note:** For freezing 70-80% confluence was recommended.
ii. The plate was rinsed once with 1X PBS. **Note:** Add the PBS slowly from the side to avoid detaching the HEK293 cells.
iii. 3-5 mL of 1X pre-warmed trypsin (for 90mm plate) was added to the plate and aspirated within 30seconds. **Note:** HEK293 cells were trypsinized very fast.
iv. Then 5 mL of complete DMEM Medium (pre-warmed to 37ºC) was added to the plate.
v. Cell suspension was then gently mixed and transferred to a 15mL conical tube.
vi. The tube was centrifuged at 1000 RPM for 2-3 minutes to pellet the cells; the supernatant was discarded and kept on ice.
vii. Freezing media was prepared by adding 10% DMSO in FBS.
viii. 2 mL of freezing media (10% DMSO in FBS) was added to the conical tube slowly and the cells were resuspended thoroughly. **Note:** Do not vortex the cells.
ix. The cell suspension was aliquot into 2 cryo-vials and kept at -80ºC for overnight.
x. Next day the vials were transferred into liquid-N_2 for longer storage. **Note:** cells remain viable for more than 10years in this condition.

Other reagents (For different experiments):

Doxycycline (Sigma) 1-4 µg/mL of media, Cyclohexamide *(Sigma)* 50µg/mL of media, TNF-α *(Peprotech)* 20ng/mL of media, MG132 *(Sigma)* 10µM/mL of media and Velcade *(Johnson & Johnson)* 10µg/mL of media, E64d *(Calbiochem)* 10µg/mL of media were used for different experiments.

2.2.2.2 Transfection:

Reagents

a) Calcium phosphate method ($CaCl_2$ 0.5M, 2XBBS).
b) Lipofectamine 2000 *(Invitrogen)*
c) Xtremegene HP (*Roche)*
d) Dharmafect (Thermo)

Methodology (Calcium phosphate method):

i. 1 million HEK293 cells were seeded on a 60mm plate in complete DMEM media and allowed to grow for 24hr at 37ºC, 5% CO2 (for transfection 50-60% confluent plate was the optimum condition).
ii. The media was replaced with fresh complete media.
iii. 4-5hr of media change transfection procedures starts.
iv. 10µg of DNA+MQ was made upto 100µL; 100µL of 0.5M $CaCl_2$ was added, and then 200µL of 2X BBS was mixed with the DNA-$CaCl_2$ mix.
v. Then the solution was kept for 30min at RT.
vi. After the incubation the DNA-mix was added onto culture plate drop wise and was mixed properly.
vii. Or Cells were transfected by lipo-based techniqe according to manufacturer's protocol. 100µM of PSMD9 siRNA (Dharmacon, Thermo Scientific) or scramble siRNA (Dharmacon, Thermo Scientific) with lipofectamine-2000 was used for transfection.

2.2.2.3 Establishment of stable cell line:

Methodology: To generate clones stably expressing PSMD9,

i. HEK93 cells were transfected with p3xFLAG-CMV-10 and p3xFLAG-CMV-10-PSMD9 constructs using Lipofectamine 2000 (Invitrogen).

ii. After 24h, transfected cells were sub-cultured and kept under selection in DMEM supplemented with 10% FBS and 800 µg/ml of G418 *(Sigma).*

iii. After 2-4 weeks G418 resistant single colonies were picked up and grown in separate plates in DMEM supplemented with 10% FBS and 400 µg/ml of G418.

iv. Three different clones with high FLAG-PSMD9 expression (detected by WB) were selected for further studies.

v. For generating doxycycline inducible stable clones, HEK293 cells were transfected with pTRIPZ, pTRIPZ-3xFLAG-PSMD9, pTRIPZ-shRNA-PSMD9 using lipofectamine 2000.

vi. After 24h, transfected cells were sub-cultured and kept under selection in DMEM supplemented with 10% FBS and 800 ng/ml of puromycin *(Sigma).*

vii. After 10-15 days puromycin resistant single colonies were picked up and grown in DMEM supplemented with 10% FBS and 400 ng/ml of puromycin.

viii. Three clones with high FLAG-PSMD9 expression and three clones with maximum PSMD9 knock down upon doxycycline induction were selected for further studies.

2.2.2.4 Human Neural Progenitor Cells (hNPCs) culture: (ReNcell VM, Millipore)

- ReNcell VM was an immortalized human neural progenitor cells (hNPCs) line derived from the ventral mesencephalon region of human fetal brain tissue.
- ReNcell VM has the ability to readily differentiate into neurons and glial cells.
- Immortalized by retroviral transduction with the v-myc oncogene, grows rapidly on laminin with a doubling time of 20-30 hours.

- ReNcell VM retains a normal diploid karyotype in culture even after prolonged passage (>45 passages).
- ReNcell VM may be used for a variety of research applications such as studies of neurotoxicity, neurogenesis, electrophysiology, neurotransmitter and receptor functions.
- ReNcell VM cells have been validated for high level of expression of Nestin and Sox2 and for their self-renewal and multi-lineage differentiation capacities.

Reagents

a) **ReNcell NSC Maintenance Medium** *(Millipore)***:** [Storage -20ºC for long term] ReNcell Neural Stem Cell (NSC) Maintenance Medium was a defined serumfree, growth factor-free medium that has been optimized for the growth and in vitro differentiation of ReNcell immortalized human neural progenitor cells. When used in conjunction with FGF and EGF, the maintenance medium will allow for the proliferation of ReNcell immortalized VM and CX neural stem cells. Withdrawal of the growth factors from ReNcell NSC Maintenance Medium will result in the spontaneous differentiation of ReNcell immortalized neural progenitor cells.

Composition: ReNcell NSC Maintenance Medium contains DMEM/F12 w/o HEPES, L-glutamine, human serum albumin, human transferrin, putrescine dihydrochloride, human recombinant insulin, L-thyroxine, tri-iodo-thyronine, progesterone, sodium selenite, heparin, and corticosterone.

b) **ReNcell NSC Freezing Medium** *(Millipore)***:** [Storage -20ºC for long term] ReNcell NSC Freezing Medium was qualified for use with ReNcell immortalized human neural progenitor cell lines. The optimized formulation allows for consistent cryopreservation and high viability upon thawing and plating.

Composition: Serum-free formulation. Contains 10% DMSO

c) **Accutase** *(CHEMICON)***:** for enzymatic removal of cells from the culture plate. (Replacement of Trypsin).

d) **Basic Fibroblast growth factor (bFGF)** *(Sigma)*

e) **Epidermal growth factor (EGF)** *(Sigma)*

f) **Laminin** *(Sigma)*

g) **1X PBS**

Methodology: [Note: Methodology was adopted from *Millipore*]

i. Preparation of coated plates:

Coating tissue culture plastic- or glasswares with laminin that were used to culture ReNcell VM cells is essential for monolayer culture. Tissue culture plates should be coated on the same day that the ReNcell VM cells were thawed from liquid nitrogen or on the same day that the cells need to be passage. The following procedure was followed:

- Laminin was mixed with DMEM/F12 to 20µg/mL.
- Enough of the diluted laminin solution was added to the plate to cover the whole surface and incubated in a 37ºC, 5% CO2 incubator for at least 4 hours.

  Note: Use 3 mL for 60mm plates and 6.5 mL for 90mm plates.
- Just before use, laminin solution was aspirated and the plate was rinsed once with 1X PBS.
- Complete ReNcell NSC Medium with 20 ng/mL FGF-2 and 20 ng/mL EGF (8mL) was added to the laminin-coated 90mm plate and incubated in a 37ºC, 5% CO2 incubator. The laminin-coated plates were then ready to receive the cells.

ii. Thawing the cells:

- Exactly follow the thawing methodology described earlier for HEK293 cells. **Note:** Instead of complete DMEM, ReNcell NSC Maintenance Medium was used throughout the process.
- After seeding the hNPCs old medium was exchanged with fresh ReNcell NSC Maintenance medium containing FGF-2 and EGF every alternative day.

iii. Subculture:

- Fresh laminin-coated plates were prepared as described earlier.
- The hNPCs were sub-cultured exactly as describe earlier for HEK293 cells. **Note:** In place of complete DMEM, ReNcell NSC Maintenance Medium was used and instead of 1X trypsin, accutase was used for detaching hNPCs from the coated plate. During this process hNPCs were kept for 2-3 min in accutase at 37ºC for cell detachment.
- During sub-culturing the hNPCs, old medium was exchanged with fresh ReNcell NSC Maintenance medium containing FGF-2 and EGF every alternative day.

iv. Differentiation: (in 8-well chamber slide)

- The 8-well chamber slides should be coated with 20 µg/mL laminin (please refer to the section on Preparation of Coated plate).
- 30,000 cells were plated per well into an appropriately coated 8-well chamber slide in ReNcell NSC Maintenance Medium containing 20 ng/mL FGF-2 and 20 ng/mL EGF. Total volume per well = 0.5 – 0.75 mL. At this density the cells should be ~50% - 60% confluent by the next day. **Note:** To prevent overgrowth of the cells by the end of the two-week differntiation Methodology, it was best to avoid plating too many cells.

- The next day, differentiation was initiated by removing the medium from each well and replacing with fresh ReNcell NSC Maintenance Medium that does not contain FGF-2 and EGF.
- The old media was replaced with fresh ReNcell NSC Maintenance Medium every 2-3 days for two weeks. **Note:** It was important that FGF or EGF not be present in the basal medium.
- After two weeks, the cells were completely differentiated into different cell populations. (Then cells can be used for various experiments.)

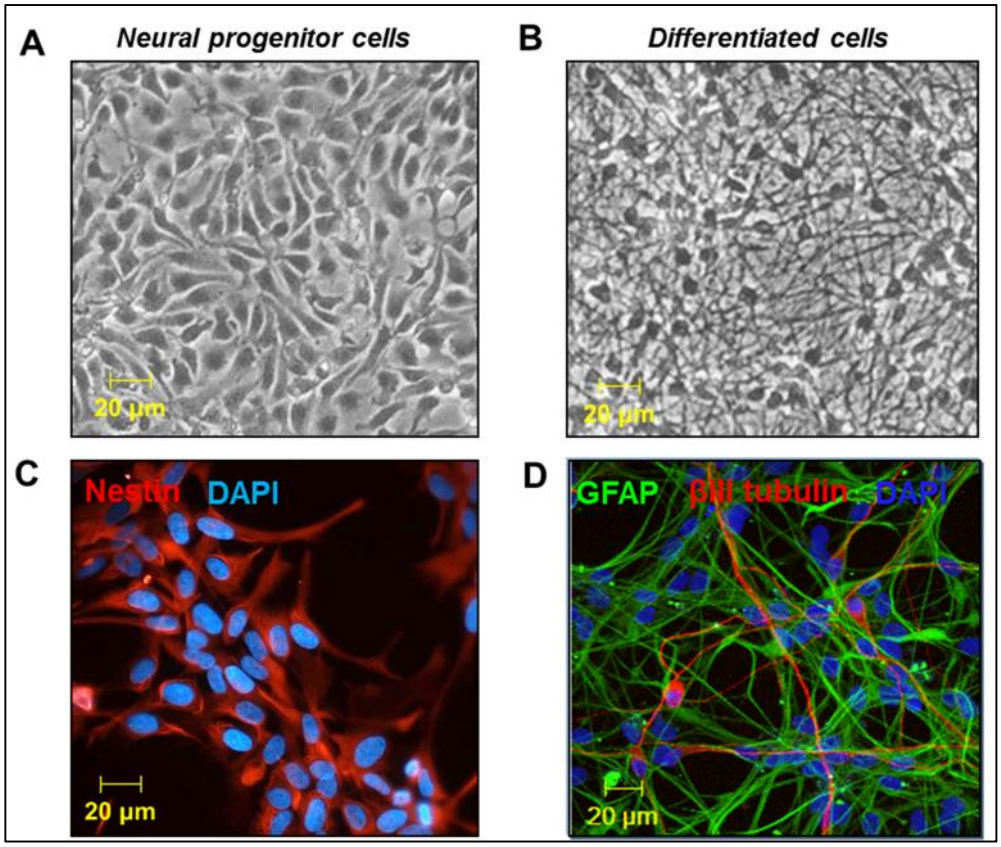

Figure-2.3 Phase contrast images and Immunostaining of human Neural progenitor cells (hNPCs) and differentiated cells. (A) Progenitor cells were grown on Laminin coated glass coverslips as described in the Methodology. Phase contrast image showing ~80-90% confluent monolayer cells. **(B)** The hNPCs were differentiated as described in the Methodology. Phase contrast image showing the network like differentiated cells (14 days). **(C)** Immunofluorescence was done following the Methodology described section 3.12. hNPCs were showing expression of Nestin (in red) **(D)** Immunofluorescence of above differentiated cells showing GFAP (in green) and β-III tubulin (in red) expression. DAPI was (in blue) used for nuclear staining. Images were acquired in Laser confocal microscope (Nikon-Meta510).

2.2.3 Mammalian cell lysis:

Methodology:

a) Cell were grown in culture till 80-90% confluent
b) Then the media was completely aspirated and plate was washed with 4mL 1X PBS.
c) 500µL chilled NP40-lysis buffer was added to the plate (90mm), cells were scrapped from the plate and collected in a MCT.
d) Then the suspension was vortexed for 10 seconds and incubated on ice for 30min.
e) After the incubation the suspension was again vortexed for 20 seconds.
f) Then it was centrifuged at 13000 rpm for 30 min at 4ºC.
g) The supernatant was collected and kept on ice; that is cell lysate.
h) The protein concentration of the cell lysate was measured by Bradford protein estimation method following the manufacturer protocol and Bradford reagent.

2.2.4 Immunoprecipitation:

Reagent:

a) Protein-G sepharose beads/ anti-FLAG-M2 Agarose beads/ anti-HA Agarose beads.
b) Antibodies (preferably polyclonal)
c) Mammalian cells (Minimum 10 million cells)
d) NP-40 lysis buffer
e) IP buffer

Methodology:

i. 1mL of chilled wash buffer (Wash buffer was NP-40 lysis buffer without NP-40) was added into 20µL of Protein-G sepharose beads.
ii. The beads were washed twice by gently inverting the tubes 4-5 times and then beads were pelleted down by centrifugation at 1000rpm for 2 min at 4°C.
iii. The wash buffer was discarded and the beads were esuspended in 1mL of wash buffer.
iv. 2-4µg of Ab/ IgG isotype was added into 20µL of Protein-G sepharose beads and kept for binding for 2h/overnight at 4°C on a rotater. (**IMPORTANT**: Do not follow this step for M2-agarose bead and anti-HA-beads).
v. Next day the cells wrew harvested from the culture plates by trypsinization and lysed by NP-40 Lysis Buffer.
vi. Pre-clear cell lysate was prepared by adding required amount of cell lysate into 20µL of Protein-A sepharose beads and keeping it for binding for 1h at 4°C on a roter. (**IMPORTANT**: Do not follow this step for M2-agarose bead and anti-HA-beads)
vii. Then pre-clear cell lysate was collected by centrifugation and was added into previously prepared Ab/IgG bound Protein-A sepharose beads.
viii. The total volume was made upto 1mL with lysis buffer and kept it for binding for 2h at 4°C on a roter.
ix. After binding the bead suspension was centrifuged at 1000 rpm for 2 min at 4°C and the supernatant was carefully separated.
x. The beads were washed (4 times) with chilled wash buffer by gently inverting 3-4 times and centrifugation at 1000 rpm for 2 min at 4°C.
xi. Finally the beads were resuspended with 20µL of wash buffer and 10µL of 3 X lamellae buffer (**Importantly without BME**) and boiled at 100°C for 5 min.

xii. Then the IP-suspensions and 5-10% input (cell lysate) were loaded on a SDS-PAGE and the proceeded towards the methodology of western blot.

2.2.5 Western Blotting

Reagents:

a) Cell lysate
b) 3X lamellae dye
c) SDS-PAGE
d) 1X SDS-running buffer
e) PVDF membrane
f) 1X transfer buffer
g) Antibodies
h) Luminiscence reagent (ECL-prime, GE-Healthcare)

Methodology:

i. Cell lysates were prepared in NP-40 lysis buffer mixed in 1X lamellae dye and boiled for 10 min at 100ºC dry bath.
ii. Then the samples were loaded and separated on SDS-PAGE in 1X SDS-running buffer (150V, 300mA and for 90min). **Note:** Run out the dye front from the gel.
iii. After a complete separation the samples were transferred onto a PVDF membrane in 1X transfer buffer at cold condition (120V, 300mA for 90min). **Note:** Avoid overheating.
iv. Membrane was then put in 3% BSA/5%milk for blocking for 1h at RT or ON at 4ºC.
v. Appropriate primary antibody dilution (in 1%BSA in TBST) was used for probing.

vi. For membrane washing 1X TBST was used and at least 4 washes were given for time period of 10 minutes each on rocker.

vii. HRP conjugated secondary Ab was used for probing the membrane for 1h at RT.

viii. Then membrane was washed in TBST and detection was done by following manufacturer protocol of ECL-prime.

ix. Various exposures were taken in X-ray film for analysis.

2.2.6 Immunofluorescence:

Reagents

a) TritonX-100
b) 3% Paraformaldehyde
c) TBST
d) 5%BSA-TBST
e) 1X PBS
f) Poly-Lysine and Laminin
g) Chamber-slides and Glass coverslips
h) Antibodies (primary & fluorophore labelled secondary) and DAPI
i) Mounting Media; Vectashield *(Vectorlabs)*
j) Nail paint

Methodology

i. HEK293 cells, hNPCs and differentiated cells were grown on sterile glass coverslips or in chamber slide according to the protocol described earlier.

Note: For better imaging cells should not be grown beyond 80% confluence.

ii. For HEK293 cells Coverslips were coated with 0.1mg/mL of poly-L-Lysine for 1h at RT inside the hood. Then washed with 1XPBS twice.

iii. For hNPCs chamber-slides or glass coverslips were coated with Laminin according to the protocol described previously.

iv. Culture media was removed from the monolayer cells carefully and immediately fixed with 4% paraformaldehyde (pre-warmed at 37ºC) for 20 min at RT.

v. Then the fixed cells were washed with 1X PBS (2mL for 35mm dish or 500µL for 4 well chamber-slides) for 2-3 times very carefully. (Washing time varies 2-3 min). **IMPORTANT:** Do not give vigorous washing or do not agitate the plate or slide.

vi. Cells were then permibilized with 0.3% TritonX-100 in 5% BSA-TBST for 2h at RT. **Note:** After permibilization 1 PBS wash can be given (but optional).

vii. Appropriate primary antibody dilutions (1:50 to 1:100) were prepared in above 5% BSA-TBST solution.

viii. Then the coverslip/chamber-slide was placed on parafilm layered moist chamber.

ix. The antibody dilution was apply on the cell monolayer carefully so that to cover the whole coverslip/well properly and were incubated for 1h at RT or overnight at 4ºC in a moist chamber. **Note:** For 1cm X 1cm coverslip 100µL and for 4well chamber-slide 50µL antibody dilutions are enough to cover the cells.

x. After incubation the antibody was decanted carefully and coverslip was placed back to the 35mm dish containing 2mL 1X PBS. The cells were then washed with 1X PBS for 2-3 times very carefully.

xi. Appropriate dilutions of secondary antibody (1:200 to 1:400) were prepared in 5% BSA-TBST solution. **Note: DO NOT** expose the secondary antibody to bright light and further steps should be done in dim light area.

xii. Then coverslip/slide was placed in moist chamber and cells were probed with fluorophore labelled secondary antibody for 1h at RT in dark then washed with PBS slowly as in step-x.

xiii. After the washing the PBS was aspirated carefully and the cells were then probed with 100µL/50µL of DAPI (1µg/mL) solution made in Milli-Q water, for 1min in dark. **Note:** This step was done in the 35mm dish only.

xiv. 2mL 1X PBS was then applied to cells (in 35mm dish).

xv. Finally coverslips were took out from PBS, extra PBS can be decanted to paper towel and mounted on a glass slide containing mounting media (20µL for 1cm X 1cm coverslip). **Note:** The mounting procedure for the chamber-slide was followed from the manufacturer protocol.

xvi. The coverslips were fixed permanently on glass slide by applying nail-paint to the four sides and proceeded for imaging immediately or kept at 4^{o}C dry and dark place for future use. **Note:** For long storage slides can be placed at -20^{o}C dry place, but in long storage the intensity of fluorophore gradually decreases.

xvii. Images were taken by laser confocal microscope (Nikon Meta510). A minimum of 5 fields from one coverslip were selected for imaging. The fluorophore intensity and the co-localization of proteins were measured by the software "Zeiss LSM Image Browser".

2.2.7 Luciferase Reporter Assay: [Using Promega Dual Luciferase Assay kit]

Reagents

a) Mammalian cells

b) Transfection reagents

c) Dual Luciferase kit (Promega)

Methodology:

i. HEK293 cells were co-transfected with ConA luc control or 3x κB ConA luc, pBIND-Renilla-Luc and other relevant vectors by calcium phosphate method.
ii. After 48 hours, cells were lysed and 10µg lysate was used for the assay.
iii. Luciferase assay was performed in 96 well white plate using Dual Luciferase Assay System (Promega) following the Methodology.
iv. In inducible stables clones of control pTRIPZ and pTRIPZ-3xFLAG-PSMD9 after 48 hours of doxycycline addition luciferase assay was performed as explained.
v. Luciferase reading was measure in 96-well luminescence plate reader.
vi. Renilla luciferase reading was used for transfection normalization.

2.2.8 RNA isolation: [Using Invitrogen TRIzol method]

Reagents:

a) TRIzol Reagent (Invitrogen)
b) Chloroform
c) Isopropyl alcohol
d) 75% ethanol (in DEPC-treated water) RNase-free water

Methodology:

i. Growth media was removed from culture plate.
ii. 1 mL TRIzol Reagent was added directly to the cells in the culture plate 90mm.
iii. Sample was vortxed and incubated for 5 minutes at room temperature.
iv. 0.2 mL of chloroform per 1 mL of TRIzol Reagent was added.
v. Then vigorously shaken by hand for 15 seconds then incubated for 2–3 minutes at room temperature.

vi. Centrifuged the sample at 12,000 × *g* for 15 minutes at 4°C. The mixture separates into a lower red phenol-chloroform phase, an interphase, and a colorless upper aqueous phase.

vii. The upper clear phase was collected and 0.5 mL of 100% isopropanol was added to the aqueous phase, per 1 mL of TRIzol Reagent.

viii. Incubated at room temperature for 10 minutes, Centrifuged at 12,000 × *g* for 10 minutes at 4°C. (Glycogen can be used to enhance the precipitation)

ix. The supernatant was discarded and the pellet was washed with 1 mL of 75% ethanol per 1 mL of TRIzol Reagent.

x. Then the RNA pellete was air dried for 5–10 minutes and resuspend with RNAse free water.

xi. RNA quality was checked by agarose electrophoresis.

2.2.9 cDNA synthesis: [Using Invitrogen cDNA synthesis kit]

Reagents:

a) CDNA synthesis mix

10X RT Buffer	2µl
25mM $MgCl_2$	4µl
0.1M DTT	2µl
RNaseOUT	1µl
Superscript III	1µl

b) RNaseH

Methodology:

i. The following mix was prepared:

up to 5 µg total RNA	n µL

Primer 50 µM oligo(dT)	1 µL
10 mM dNTP mix	1 µL
DEPC-treated water to	10 µL

ii. The above mix was incubated at 65°C for 5 min, then placed on ice for at least 1 min.

iii. cDNA mix was prepared by adding 10X RT buffer, 25 mM MgCl2, 0.1 M DTT, RNaseOUT , SuperScript III RT.

iv. 10 µL of cDNA Synthesis Mix was added to each RNA/primer mixture, mixed gently, and collected by brief centrifugation.

v. Incubated for 50 min at 50°C, then reaction was terminated at 85°C for 5 min.

vi. Chilled on ice then collected by brief centrifugation.

vii. RNase H added to each tube and incubated for 20 min at 37°C.

viii. Now cDNA was ready for detection.

2.2.10 Semi-quantitative RT-PCR

Reagents:

a) DyNazyme/Taq polymerase

b) DyNazyme/Taq Buffer

c) Primers (described in RT primer list)

Methodology:

i. mRNA levels of different genes were analysed by PCR amplification method.

ii. Amplified PCR products were analysed in 2% agarose gels containing 0.5 g/mL ethidium bromide.

2.2.11. Real Time PCR:

Reagents

a) cDNA

b) Primers

c) Syber green reagent (Kappa-Biosystem)

Methodology

i. Real time primers were designed using software GENE TOOL.

ii. Quantitative real-time polymerase chain reaction (qRT-PCR) was performed with the 12K-Flex Quant-Studio (Invitrogen) QPCR system using Syber green qRT-PCR Master Mix.

iii. Relative expression of different genes was calculated by normalizing to GAPDH.

2.2.12 Nuclear fractionation: [Using Sigma CelLytic NuCLEAR Extraction Kit]

Reagents

a) Mammalian cells.

b) 5X Lysis Buffer, isotonic

(50mM Tris HCl, pH 7.5, with 10 mM MgCl2, 15 mM CaCl2, and 1.5 M Sucrose)

c) Extraction Buffer

(20mM HEPES, pH 7.9, with 1.5 mM MgCl2, 0.42 M NaCl, 0.2 mM EDTA, and 25% (v/v) Glycerol)

d) Dithiothreitol (DTT)

e) Protease Inhibitor Cocktail

f) IGEPAL 10% Solution

Methodology

i. 1 M DTT solution was diluted with deionized, sterile water to a concentration of 0.1 M. For small-scale preparations (below 100 ml total) the 1 M DTT stock solution should be diluted to 0.01 M.

ii. 1X Isotonic Lysis Buffer (For fragile cells use) was prepared from the 5X Lysis Buffer. To 1mL of 1X Lysis Buffer 10µL of the prepared 0.1 M DTT solution and 10µL of the protease inhibitor cocktail were added.

iii. The HEK293 cells trypsinized and collected in a MCT. Then the packed cell volume (PCV) was estimated.

iv. 500µL (10X PCV) of 1X Lysis Buffer (including DTT and protease inhibitors) to was added to 50µL of PCV. The cell pellet was resuspended gently in a MCT.

v. Then the packed cells were incubated in the lysis buffer on ice for 20 minutes, allowing cells to swell.

vi. To the swollen cells in lysis buffer, 10% IGEPAL solution was added to a final concentration of 0.8% (8µL per 100µL of mixture) in the suspension. Then the cell suspension was vortexed vigorously for 10 seconds. **Note:** 5µL of the cells in the lysis buffer can be taken on a glass slide and observed under the microscope for detecting the cell membrane lysis.

vii. The lysate was centrifuge immediately at 8000rpm for 2min at 4ºC.

viii. The supernatant was transferred to a fresh tube. This fraction is the “Cytoplasmic fraction”.

ix. Then 1µL of the prepared 0.1 M DTT solution and 1µL of the protease inhibitor cocktail was added to 98µL of the Extraction Buffer.

x. The crude nuclei pellet was resuspended in ~50µL (5X PCV) of Extraction Buffer containing the DTT and protease inhibitor cocktail.

xi. The tube was then mounted on a vortex mixer and agitated at medium to high speed for 45min-60 minutes.

xii. The nuclear lysate was centrifuged at 13000 rpm for 10 minutes.

xiii. The supernatant was transferred to a clean tube; that is the "Nuclear extract".

xiv. The supernatant was aliquoted in MCTs, snap-freeze with liquid nitrogen and stored at –80°C for further study.

xv. The separation of nuclear and cytoplasmic fractions was evaluated by WB using cytoplasmic and nuclear specific markers such as α-tubulin and histone antibodies respectively.

2.2.13 Electrophoretic mobility shift assay (EMSA): (Using Thermo Scientific Kit):

For EMSA the main reagent DNA oligo can be radio labelled or biotin labelled. Here for our study we have biotinlyted the oligos at its 3' end using "Biotin 3' End DNA Labeling Kit- *Thermo*".

Reagents

a) <u>κB-binding DNA ologos:</u>

Wild type: 5'-AGTTGAG**GGG**ACTTTCCCAGGC-3'

5'-GCCTGGGAAAGT**CCC**CTCAACT-3'

Mutant: 5'-AGTTGAG**CTC**ACTTTCCCAGGC-3'

5'-GCCTGGGAAAGT**GAG**CTCAACT-3'

b) <u>Biotin 3' End DNA Labeling Kit:</u> [Storage -20°C]

- 5X TdT Reaction Buffer

  (500mM cacodylic acid, 10mM CoCl2, 1mM DTT, pH 7.2)

- Terminal Deoxynucleotidyl Transferase (TdT)

  (~20 U/µL in 100mM potassium phosphate, 10mM 2-mercaptoethanol, 50% glycerol, pH 6.9)

- Biotin-11-UTP

  (5µM in 10mM Tris-HCl, 1mM EDTA, pH 7.5; and minimize freeze-thaw cycles and exposure to light)

- Biotin-Control Oligo,

  (1µM in 10mM Tris-HCl, 1mM EDTA, pH 7.5)

c) LightShift EMSA Optimization Kit: [Storage -20°C]

- 10X Binding Buffer,

  (1mL, 100mM Tris, 500mM KCl, 10mM DTT; pH 7.5)

- Poly (dI-dC), 1µg/µL in 10mM Tris, 1mM EDTA; pH 7.5
- 50% Glycerol
- 1% NP-40
- 1 M KCl
- 100mM MgCl2
- 200mM EDTA
- 5X Loading Buffer.

d) Chemiluminescent Nucleic Acid Detection Module: [Storage 4°C]

- Stabilized Streptavidin-Horseradish Peroxidase Conjugate
- Chemiluminescent Substrate,
- Luminol/Enhancer Solution
- Stable Peroxide Solution
- Blocking Buffer
- 4X Wash Buffer

- Substrate Equilibration Buffer

e) 0.2M EDTA, pH 8.0

f) Chloroform:isoamyl alcohol (24:1)

g) Positively charged Nylon membrane

h) TE Buffer: 10mM Tris•HCl, 1mM EDTA, pH 8.0

i) 5X TBE (450mM Tris, 450mM boric acid, 10mM EDTA, pH 8.3)

j) Polyacrylamide gel in 0.5X TBE

k) 96-well microplate for preparing dilutions

l) UV lamp or cross-linking device equipped with 254nm bulbs or 312nm transilluminator

m) X-ray film

Methodology

Oligo 3'-Labeling Reaction:

i. All kit components were thawed except the TdT, and placed on ice. **Note:** Keep TdT at -20°C until needed.

ii. Just before use, a portion of the TdT stock was diluted in 1X TdT Reaction Buffer to a working concentration of 2 U/µL.

Note: Use the diluted TdT stock immediately. Do not store the diluted enzyme.

iii. The labelling reaction was prepared for the 5 pmol 3'-OH ends of the κB-oligo by adding components in the order listed below:

Components	Volume (µL)	Final Concentration
Ultrapure water	25	---
5X TdT Reaction Buffer	10	1X

Unlabelled κB-oligo (1μM)	5	100nM
Biotin-11-UTP (1μM)	5	0.5μM
Diluted TdT (2U/μL)	5	0.2U/μL
Total Volume	**50**	**---**

Note: Mix reactions gently. Do not vortex.

iv. Then reactions were incubated at 37°C for 30 minutes.

v. 2.5μL 0.2M EDTA was added to stop each reaction.

vi. Then 50μL of chloroform:isoamyl alcohol was added to each reaction to extract the TdT. The mixture was vortexed briefly then centrifuged for 1-2 minutes at high speed in a microcentrifuge to separate the phases. The top (aqueous) phase was removed and saved for further use.

vii. The labeling efficiency was detected by "Procedure for Estimating Labeling Efficiency" described in the next section. At this point, the DNA was ready to be used in the end application.

Note: For applications such as electrophoretic mobility shift assays (EMSA) that require biotin-labeled double-stranded DNA, complementary oligos should be end-labeled separately and then annealed before use. Oligos were annealed by mixing together equal amounts of labeled complementary oligos and incubating the mixture for 1 hour at room temperature. Oligonucleotides with high melting temperatures or secondary structure may require denaturation and slow cooling for optimal annealing (e.g., denature at 90°C for 1minute, then slowly cool and incubate at the melting temperature for 30 minutes). Then annealed oligos were freezed and stored at -20ºC. Removal of the unincorporated Biotin-11-UTP was not necessary for use in EMSA.

Estimating Labelling Efficiency:

Labelling efficiency can be determined by dot blots using either a dot/slot blotting apparatus or by hand spotting. The hand spotting methodology was followed using the detection reagents in the Light Shift Chemiluminescent EMSA Kit.

i. A positively-charged nylon membrane was hydrate/equilibrate in TE Buffer for at least 10 minutes.
ii. The biotin control oligos & control unlabelled oligos and the κB-labelled Oligos & κB-labelled Oligos (both wild type and mutant) stocks were diluted 20-fold in TE Buffer to make 50nM oligo working stocks.
iii. A series of oligo standards were prepared in microcentrifuge tubes, according to the following table:

Components	**%Biotin**			
	100	**75**	**50**	**25**
Biotin control oligo (50nM)	12	9	6	3
Unlabelled control oligo (50nM)	0	3	6	9
TE pH8.0	48	48	48	48
Total Volume	**60 µL**	**60 µL**	**60 µL**	**60 µL**

iv. 50µL of the oligo working stocks were pipetted into wells A1-A4 of a 96-well dilution plate.
v. In a microcentrifuge tube, 10-fold dilution of the κB-labelled oligo was made in TE Buffer to achieve a final concentration of 10nM (e.g., 6µL κB-labelled oligo + 54µL TE, pH 8.0).
vi. 50µL of each 10nM κB-labelled oligos (wt and mut) was placed into "A5 and A6". A series of two-fold dilutions were prepared removing 25µL aliquots from

all “A” wells and mixing them with the 25µL TE Buffer in corresponding “B” wells, continuing down the plate through the “E” wells.

vii. Then the equilibrated membrane was placed onto a clean, dry paper towel.

Note: Allow excess buffer to absorb into the membrane, but do not allow the membrane dry out.

viii. 2µL of samples and standards were spotted onto the membrane (resulting in 20 fmol 3'-OH ends in “A1” spots and 1.25 fmol in “E1” spots). The samples were allowed to absorb into the membrane.

i. Immediately the membrane was UV crosslinked at a distance of approximately 1cm from the membrane for 30 minutes with a hand-held UV lamp equipped with 254nm bulbs.

Note: The detection and analysis was done immediately, or the dried membrane was stored at room temperature until the detection Methodology can be performed.

Detection and Analysis: For detection methodology follow the section **“Detect Biotin-labeled DNA by Chemiluminescence”.** To determine the labelling efficiency, spot intensities of the sample lanes (κB-oligo) to those of the Biotin Control Oligo standards on the developed X-ray film, were measured by ImageJ software.

Note: The efficiency of TdT labelling was somewhat variable, even among different single-stranded oligonucleotides. This variability does not correlate directly to the identity of the 3' terminal base, but was related to the overall sequence. Typically, oligonucleotides with relatively inefficient labeling (< 50%) still produce good signal in subsequent chemiluminescent EMSA detection procedures.

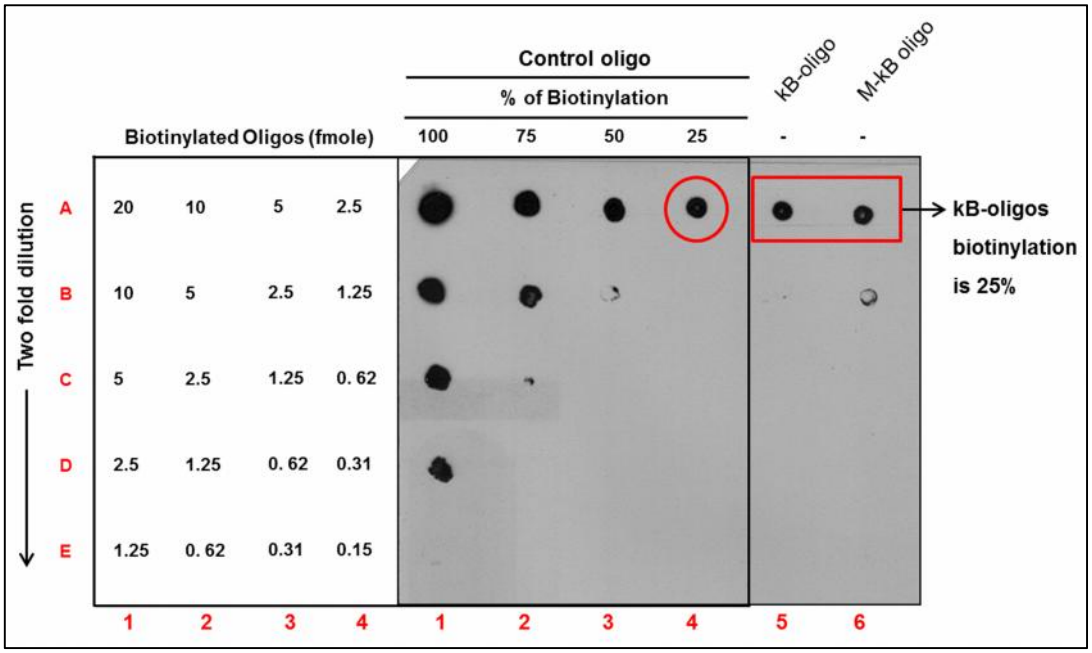

Figure-2.4: Detection of percentage of labelled κB oligos in the 3'end label reaction.

In our experiment we got ~25% of both the wild type and mutant *κ*B oligos were labelled with biotin.

Procedure for Electrophoretic Mobility Shift Assay:

ii. A native polyacrylamide gel was prepared in 0.5X TBE. The appropriate polyacrylamide percent depends on the size of the target DNA and the binding protein. Most systems use a 4 -6% polyacrylamide gel in 0.5X TBE.

iii. A complete set of binding reactions were prepared on ice as given in the table for an example. **IMPORTANT:** Do not vortex tubes at any time during this procedure.

Component	Final Amount	Control	Test
Ultrapure Water	---	12µL	7µL
10X Binding Buffer	1X	2µL	2µL
50% Glycerol	2.5%	1µL	1µL
100mM MgCl2	5mM	1µL	1µL

1% NP-40	0.05%	1µL	1µL
1µg/µL Poly (dI-dC)	50ng/µL	1µL	1µL
Biotin 3'-Labeled DNA oligo (10fmol/µL)	20fmol	2µL	2µL
Nuclear extract (if 4µg/ µL)	20µg	---	5µL
Total	**---**	**20µL**	**20µL**

iv. The above reaction mixtures were incubated at room temperature for 20 minutes.

v. Then 5µL of 5X Loading Buffer was added to each 20µL binding reaction and was mixed. **IMPORTANT:** DO NOT vortex or mix vigorously.

vi. The samples were run in the 6% PAGE (set to 100V for 8 × 8 × 0.1cm gel/45min) until the bromophenol blue dye had migrated approximately 2/3 to 3/4 down the length of the gel. **Note:** The free biotin-EBNA Control DNA duplex migrates just behind the bromophenol blue in a 6% polyacrylamide gel.

vii. Nylon membrane was soaked in 0.5X TBE for at least 10 minutes.

viii. The gel was sandwiched between nylon membrane and blotting paper, then placed in a clean electrophoretic transfer unit according the manufacturer's instructions. Use 0.5X TBE cooled to ~10ºC with a circulating water bath.

ix. The sample were put for transfer at 380mA (~100V) for 30 minutes. Typical transfer times were 30-60 minutes at 380mA using a standard tank transfer apparatus for mini gels (8 × 8 × 0.1cm).

x. When the transfer was complete, the membrane was placed with the bromophenol blue side up on a dry paper towel. (There should be no dye remaining in the gel.) The buffer was allowed on the membrane surface to absorb into the membrane. **IMPORTANT:** Do not let the membrane dry, immediately proceed to crosslinking.

xi. Immediately the membrane was UV crosslinked at a distance of approximately 1cm from the membrane for 30 minutes with a hand-held UV lamp equipped with 254nm bulbs.

Note: Continue with the detection and analysis immediately, or store the membrane dry at room temperature until the detection Methodology can be performed.

Detect Biotin-labeled DNA by Chemiluminescence:

i. Blocking Buffer and the 4X Wash Buffer were warmed to 37-50°C in a water bath until all particulate was dissolved. These buffers may be used between room temperature and 50°C as long as all particulate remains in solution. The Substrate Equilibration Buffer may be used between 4°C and room temperature.

ii. To block the membrane 20mL of Blocking Buffer was added and incubated for 15 minutes with gentle shaking.

iii. Conjugate/blocking buffer solution was prepared by adding 66.7µL Stabilized Streptavidin-Horseradish Peroxidase Conjugate to 20mL Blocking Buffer (1:300 dilutions).

Note: This conjugate/blocking buffer solution has been optimized by "*Thermo*" for the Nucleic Acid Detection Module and should not be modified.

iv. Blocking buffer was removed from the membrane and replaced with the conjugate/blocking solution. The membrane was incubated in the conjugate/blocking buffer solution for 15 minutes with gentle shaking.

v. 1X wash solution was prepared by adding 40mL of 4X Wash Buffer to 120mL of ultrapure water.

vi. Then the membrane was transfer to a new container and rinsed briefly with 20mL of 1X wash solution.

vii. Membrane was washed four times for 5 minutes each in 20mL of 1X wash solution with gentle shaking.

viii. Then the membrane was transferred to a new container, 30mL of Substrate Equilibration Buffer was added and incubated for 5 minutes with gentle shaking.

ix. Substrate Working Solution was prepared by adding 6mL Luminol/Enhancer Solution to 6mL Stable Peroxide Solution.

Note: Exposure to the sun or any intense light can harm the Working Solution. Working Solution should be kept in an amber bottle and avoid prolonged exposure to intense light. Short-term exposure to typical laboratory lighting will not harm the Working Solution.

x. Then the membrane was removed from the Substrate Equilibration Buffer, carefully blotting an edge of the membrane on a paper towel to remove excess buffer. Membrane was placed in a clean container or onto a clean sheet of plastic wrap placed on a flat surface.

xi. Substrate Working Solution was poured onto the membrane so that it completely covers the surface. Then membrane was incubated in the substrate solution for 5 minutes without shaking.

xii. Membrane was removed from the Working Solution and blotted an edge of the membrane on a paper towel for 2-5 seconds to remove excess buffer. **Note:** Do not allow the membrane to become dry.

xiii. The moist membrane was then wrapped in plastic wrapper, avoiding bubbles and wrinkles.

xiv. The membrane was exposed onto X-ray film to obtain the desired signal.

xv. Then the bands were subjected to ImageJ software to analyse it quantitatively.

2.2.14 Proteasomal Pull down assay:

Reagents

a) Mammalian cells

b) ATP-Buffer:

(50mM Tris (pH 7.6), 5mM $MgCl_2$, 1mM ATP, 10% Glycerol and 1X protease inhibitor cocktail (Sigma)).

Methodology

i. HEK293 cells were grown till 80% confluence. Cells can be treated with different inhibitors (MG132/Velcade/E64d) according to the experiment requirements.

ii. Protein-G sepharose beads were bound with β7-antibody following the standard protocol of" Immunoprecipitation" described earlier.

iii. Then cells were trypsinized and cell pellete was place on ice for further step.

iv. 500µL of ATP-Buffer was added to 50 PCV (pack cell volume), homogenized by quick vortexing and placed on ice for 10-15min. **IMPORTANT:** Presence of 1mM ATP in the buffer is essential for maintaining the proteasomal assembly and activity.

v. Then the cells were ultrasonicated on ice for 4 cycles of 20sec each (with 1 sec break after each 2 sec) at 30 kHz. **Note:** Excess sonication may break the proteasomal assembly. **IMPORTANT**: Do not vortex the cell suspension.

vi. The lysate then centrifuged at 13000 rpm for 10min at 4ºC.

vii. The supernatant lysates were collected into a microcentrifuge tube.

viii. The lysate were incubated in the β7-antibody bound Protein-G sepharose beads for 1h at 4ºC.

ix. Then for further steps the standard protocol of" Immunoprecipitation" (described earlier) was followed.

x. Then finally the detection of target proteins were analysed by WB as described earlier.

2.2.15 Proteasomal activity assay:

Reagents

a) Mammalian cells

b) ATP-Buffer:

(50mM Tris (pH 7.6), 5mM $MgCl_2$, 1mM ATP, 10% Glycerol and 1X protease inhibitor cocktail (Sigma)).

c) Suc-LLVY-7-amino, 4-methyl coumarin substrate

Methodology

i. Different stable clones or HEK293 cells were grown till 80% confluence. Cells can be transfected with different plasmid constructs according to the experiment requirements.

ii. Then cells were lysed in ATP-Buffer as described in above methodology.

iii. Reaction buffer was prepared by adding Suc-LLVY-7-amino, 4-methyl coumarin substrate to ATP-buffer to make a final concentration of 50µM.

iv. 70µL of reaction buffer was taken in a black-96 well plate *(Nunc)* and into that 10µg of cell lysate was added. (No cell lysate/equal volume of ATP buffer was added in control the well.)

v. The fluorescence reading was measured by the software- MicroWin-2000 in the instrument Berthhold technology- Mithras (LB 940) 96-well plate reader. The program for the assay is as follows:

Total time	300 sec
Counting time	0.33 sec
Cycle time	25sec
No.of cycle	13
Lamp energy	5000
Excitation	380nm
Emission	460nm

vi. The average reading in fluorescence unit/min was determined by normalizing with the concentration of lysate.

2.2.16 Virus production:

Reagents

a) Doxycycline inducible III-Generation lentiviral pTRIPZ empty vector and the construct pTRIPZ-FLAG-KZ-PSMD10.

b) Third generation packaging vectors PAX2 and MD2G.

c) Early passage HEK293FT cells.

d) 0.5M $CaCl_2$

e) 2X BBS

Methodology

i. Early passage HEK293FT cells were plated on four 90mm plates with 2million cells.

ii. The next day cells were transfected with pTRIPZ-empty/pTRIPZ-PSMD10 with the packaging vectors PAX2 and pMD2G in ratio 4:3:1 (8µg:6µg:2µg).

iii. 16h post transfection media was changed.

iv. 48h post transfection, the 10mL supernatant media was collected and stored at 4ºC.

v. 72h post transfection, the 10mL supernatant media was collected and stored at 4ºC.

vi. Supernatant was filtered in 0.2µm filter, and centrifuged at 30,000rpm/4ºC for 1h 30min.

vii. The supernatant media was discarded carefully.

viii. Virus pellet was resuspend in 200µL DMEM and stored at -80ºC.

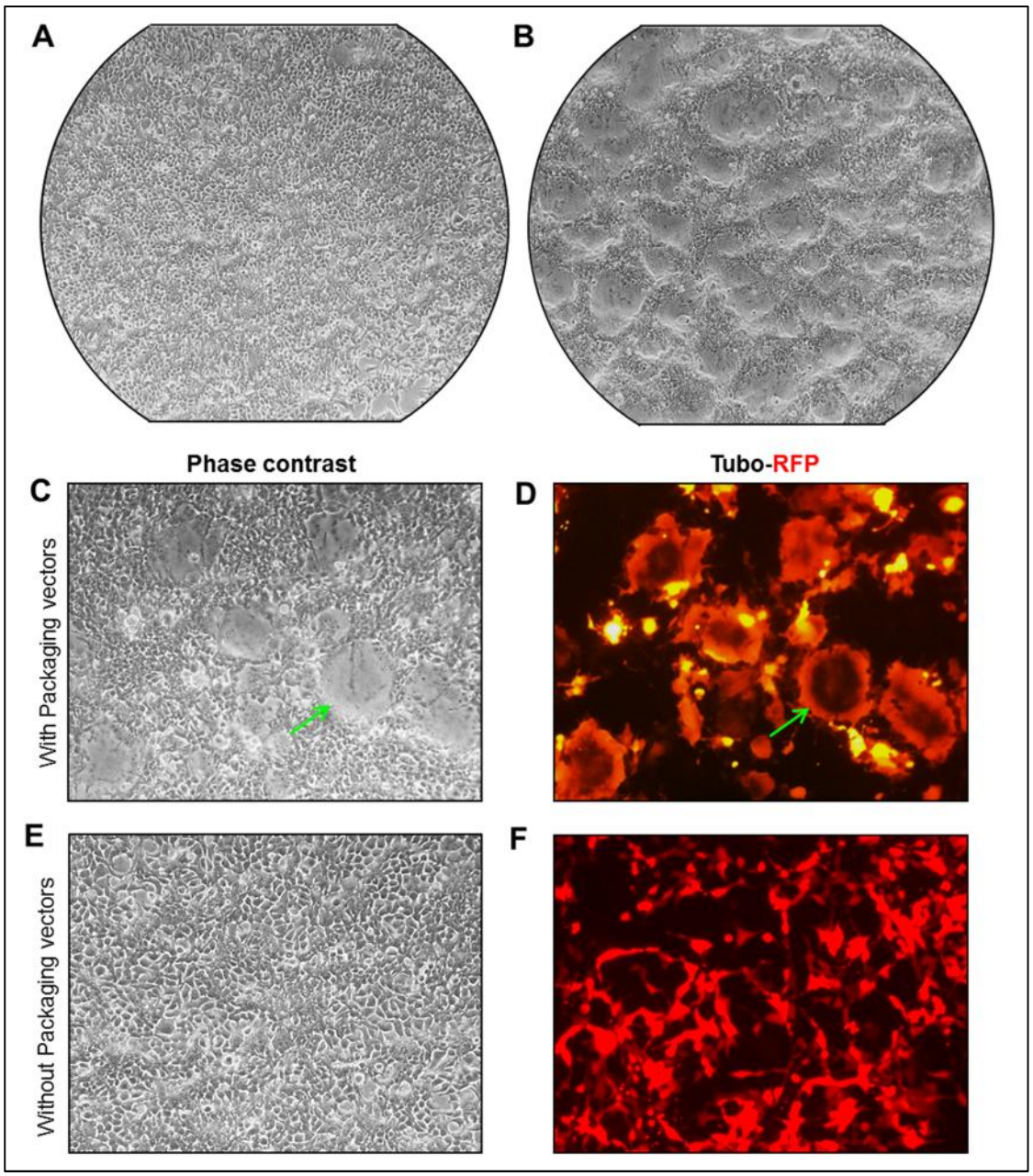

Figure-2.5: Syncytia formation after virus production. (A) Phase contrast image of HEK293FT cells transfected with only pTRPZ-FLAG-kz-PSMD10 (48h post transfection). **(B)** Phase contrast image of HEK293FT cells transfected with pTRPZ-FLAG-kz-PSMD10 and

packaging vectors (48h post transfection). Image shows syncytia after virus production. **(C), (D)** HEK293FT cells transfected with pTRPZ empty vector and packaging vectors (48h post transfection) and treated with doxycycline (1µg/mL of media). Arrow indicate syncytia expressing turbo-RFP. **(E), (F)** HEK293FT cells transfected with only pTRPZ empty vector (48h post transfection) and treated with doxycycline (1µg/mL of media). Image was showing only turbo-RFP but no syncytia formation.

Virus titer calculation:

- 0.5 Million HEK293 cells were palated on 35mm plate to reach 30-40% confluence.
- After 24 hr cells were transduced with the above concentrated viral particles (diluted then to 1:100 and 1:1000) of pTRIPZ control vector with 10µg of polybrene.
- Cells were treated with doxycycline 1µg/mL of media for 48h.
- RFP +ve cell were calculated by FACS analysis.
- Virus titer was calculated by given formula. An example of virus titer calculation was given bellow:

Virus Titer (TU) = (No of cell seeded X % of cell RFP+ve) X dilution factor
% of cell RFP+ve is 34% (for 48h virus) and 47% (for 72h virus) By **FACS analysis**
TU (for 48h) = 1.2×10^8 TU/mL and TU (for 72h) = 1.5×10^8 TU/mL

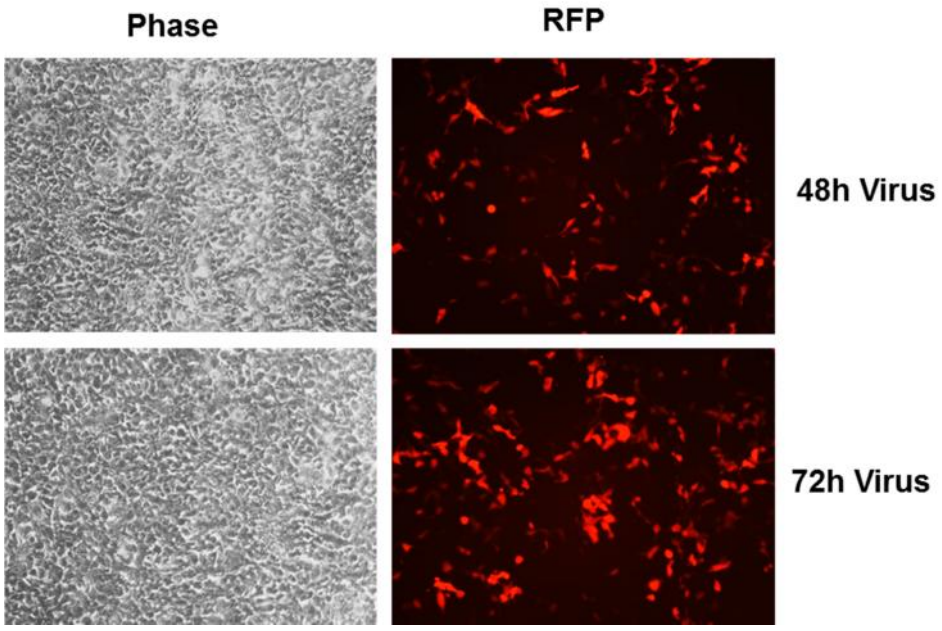

Figure-2.6: Virus titer calculation. HEK293 cell were transduced with viral particles of pTRIPZ empty vector (1:100 dilution). Image showing the RFP+ve cells after 48h of transduction with the 48h-viral particle and 72h-viral particle.

2.2.17 Transduction:

Reagents

a) Viral particles

b) Polybrene

Methodology

- 1 million hNPC cells were palated on Laminin coated 60mm plate to reach 30-40% confluence next day.
- After 24 hr cells were transduced with the concentrated viral particles with 10µg of polybrene in minimum amount of media in plae (2mL for 60mm plate).
- After 24hr of transduction media was replaced with fresh media.
- Cells were treated with doxycycline 1µg/mL of media for 48h.
- Expression of RFP or the target gene checked by microscopy observation or WB.

2.2.18 Recombinant Protein Purification:

All recombinant proteins (His-PSMD9, GST-PSMD9, GST-hnRNPA1, MBP-IκBα, GST and MBP) were expressed and purified by using Escherichia coli BL21 (DE3).

Reagent

a) LB media and LB agar Plate

b) Ampicillin (100mM): Working Concentration: 100µM

c) IPTG (100mM): Working Concentration: 100µM

d) Ni-NTA agarose beads *(Genetix),* GST beads and Amylose beads

e) Immidazole

f) Reduced glutathione

g) Maltose

h) Ni-NTA Lysis Buffer

i) Ni-NTA Binding/Wash Buffer

j) His-tagged, GST-tagged and MBP-tagged protein elution buffers

Methodology

i. Escherichia coli BL21 (DE3) strain cells were transformed with pRSETA-PSMD9/ pGEX4T1-PSMD9/ pGEX4T1-hnRNPA1or pMALc5X- MBP-IκB*α* following the standard transformation protocol.

ii. Next day single Colony was picked up and inoculated in 10 ml LB medium containing 100µg/ml ampicillin as starter culture and incubated at 37ºC /180 rpm shaker condition.

iii. After 10hr of growth the stater culture was inoculated into 1ltr sterile LB-amp medium and incubated at 37ºC/180 rpm shaker condition till the OD reach at 0.7-0.8. OD was checked at 600nm in spectrophotometer.

iv. At 0.7-0.8 OD (After ~3-4hr of starter culture inoculation) 100µL of 100mM IPTG was added for protein induction and was incubated at 18ºC/180 rpm shaker condition for 18hr. (Separated flask was kept for uninduced culture).

v. After completion of 18hr growth the bacterial cells were pelleted down by centrifugation at 5000 rpm for 15min at 4ºC then proceed for protein purification methodology.

His/GST/MBP tagged Protein Purification methodology

i. The cell pellet from 1ltr culture was resuspended in ice cold 20mL Ni-NTA lysis buffer/GST-PBS lysis buffer/MBP protein purification lysis buffer.

ii. Cell suspension was sonicated on ice at 50 khz, 20% amplitude for 20sec (in each 1sec sonication with break of 1sec) 10-15 cycles. **Note:** The no. of cycle may vary depending on the PCV (Pack cell volume) and till the suspension became comparatively clear. **DO NOT** sonicate for a longer time.

iii. The cell lysate was then centrifuged at 13000 rpm for 20min, and the supernatant was collected.

Note: Before proceed towards protein purification procedure, small scale cell lysis (From 10mL uninduced and induced bacterial culture) followed by protein induction was checked on SDS-PAGE.

iv. 2-3 mL of Ni-NTA agarose bead/GST bead/Amylose resin was added to a 50mL ECONO column (Bio-Rad) and washed twice with Ni-NTA wash buffer/GST-PBS wash buffer/MBP purification wash buffer.

v. Then the 20mL supernatant lysate was added to the column, mixed properly and kept at 4^{o}C with rotation for binding for 1hr.

vi. After binding the bead was allowed to settle down and the lysate was drained out from the bottom of the column.

vii. The bead was washed with 50mL Ni-NTA wash buffer/GST-PBS wash buffer/MBP purification wash buffer, thrice and the flow through was discarded. **Note:** The flow through can be collected for analysis.

viii. Then the bound His tagged protein/GST-protein/MBP-protein was eluted from the bead by 5mL elution buffer containing 250mM imidazole/20mM reduced glutathione in 50mM TRIS-pH8.0/10mM maltose. Elution buffer was added to bead 1mL each time followed by 2 minutes incubation. **Note:** The concentration of imidazole can be standardised depending on the purity of the eluted protein fractions. The pH is critical for GST-protein elution

ix. The eluted fractions were analysed in SDS-PAGE and quantitate for further purification process.

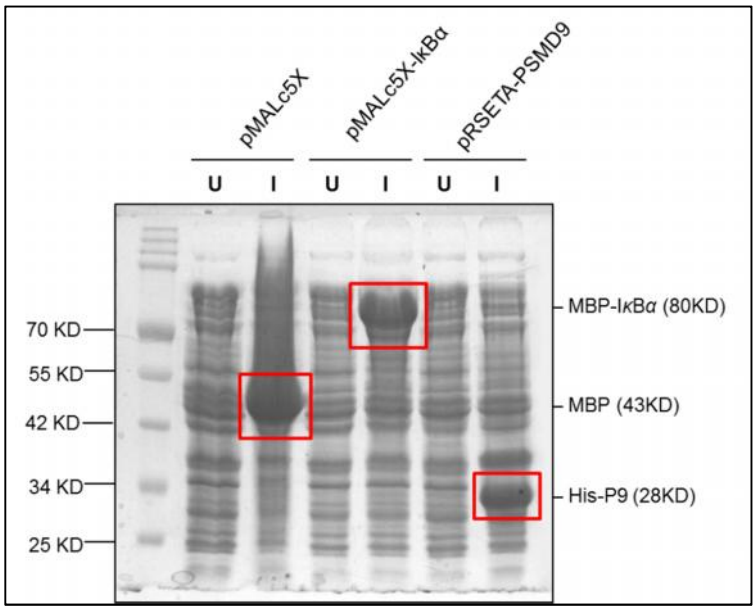

Figure-2.7: Recombinant protein Induction. Small scale bacteria culture (10mL) both for uninduced and induced cells were lysed by specific lysis buffer as described in the methodology. Cell lysate were run in a SDS-PAGE and stained with Coomassie. Image shows the protein induction of MBP, MBP- IκBα and His-PSMD9 (Red box). U-uninduced, I-induced.

Size exclusion chromatography methodology: (Gel Filtration of His-PSMD9)

The above bead eluted recombinant His PSMD9 was again purified by gel filtration sephadex-200 column (GE) because of two reasons; (1) His PSMD9 recombinant protein shows some level of contaminant proteins (Figure-2.8A) proved by WB (Figure-2.8B) and (2) His-PSMD9 was to be used as prey protein in Far western blot.

i. FPLC buffer for His tag protein purification was prepared (50mM TRIS pH7.5, 150mM NaCl, 50mM BME) and filtered through filter paper.
ii. The Sephadex-200 column fitted with FPLC (GE-Amersham) was equilibrated with the FPLC buffer for 3hr at a speed 0.5mL/min.
iii. ~6mg of the E2 fraction of eluted His-PSMD9 protein from Ni-NTA beads was injected to FPLC and run at a speed 0.3mL/min.

iv. The protein samples were collected from the collecting tube from 65th mL fraction to 95th mL fraction at every 1mL interval.

v. Then 10µL from each of the FPLC-fractions (65 to 95) were loaded in SDS-PAGE with lamellae dye and purity was checked by Coomassie staining (Figure-2.8D).

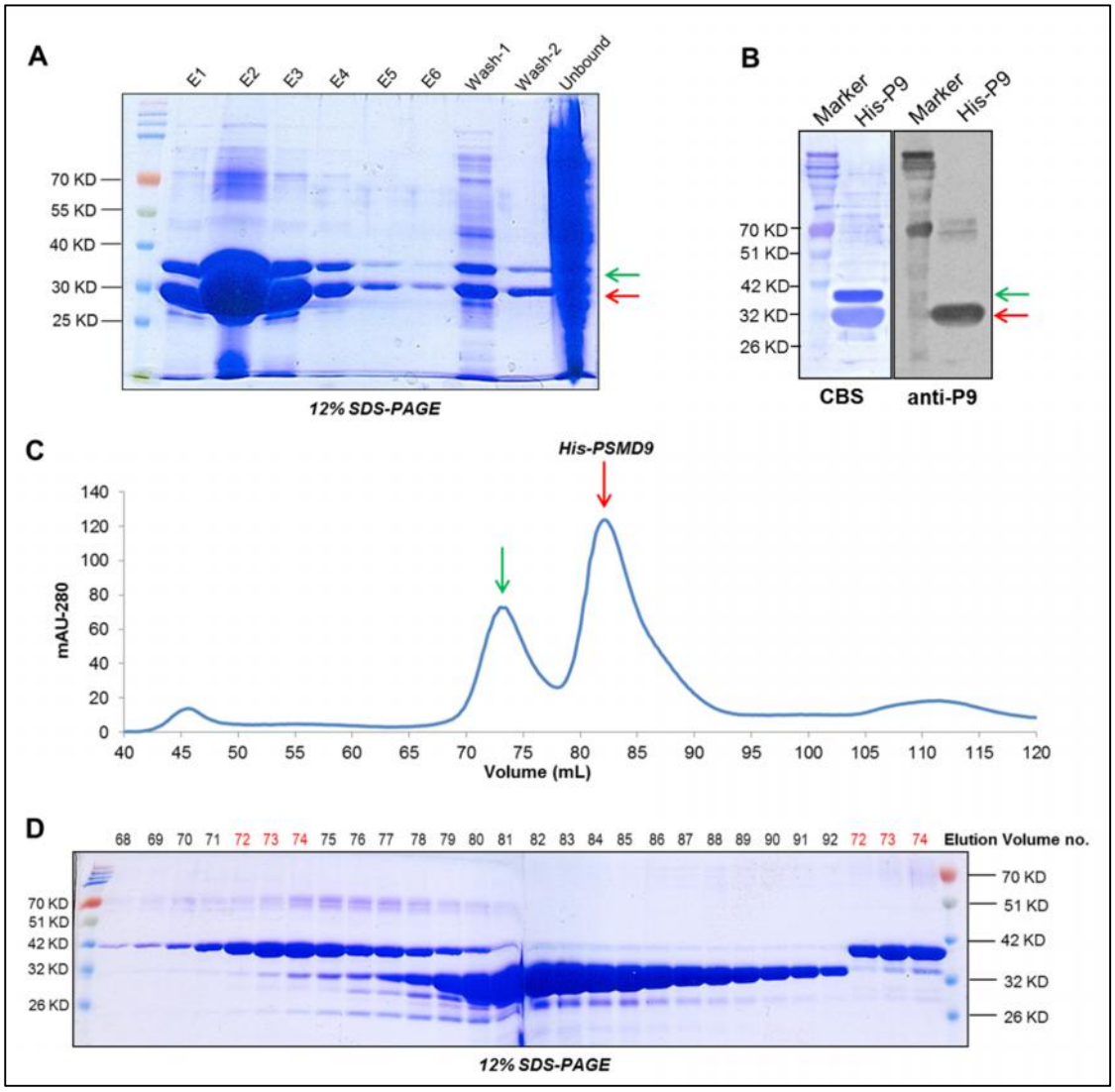

Figure-2.8: Recombinant His-PSMD9 protein Purification. (A) Different elutions of His-PSMD9 from the Ni-NTA beads (described in step viii of protein purification methodology) along with the flow-through wash (wash-1 and wash-2) from Ni-NTA beads & the unbound fraction were loaded (10µL from each sample) in SDS-PAGE and Coomassie stained. The green arrow corresponds to contaminant protein and the red arrow corresponds to His-PSMD9 **(B)** WB of the above eluted (E2 fraction) His-PSMD9 protein confirmed the lower band (red arrow) as His-PSMD9 protein. **(C)** ~6mg of Ni-NTA bead eluted (E2) His-PSMD9 fraction was injected to FPLC fitted with sephadex-200/200mL column. Gel filtration profile of the injected sample showing the upper contaminant protein (green arrow) separation from His-PSMD9 (red arrow) **(D)** Fractions (66mL fraction no. to 92mL fraction no.) of injected protein sample were

collected from FPLC and 10µL of the samples were loaded in SDS-PAGE and Coomassie stained. The later fractions (82-92) seems free from the upper contaminant protein.

[Approximate molecular weight detection of His-PSMD9: Since the calculated MW (28KDa) of His-PSMD9 differs from what it showed in SDS-PAGE, we determine the approximate MW by FPLC using different standard proteins. Pure BSA (2mg), Ovalbumin (2mg) and purified His-PSMD10 (2mg) mixture was injected to FPLC (Bio-Rad) and the MW-profile was determined. BSA (67KDa) was eluted at 63mL, Ovalbumin (45KDa) was eluted at 68 mL and His-PSMD10 (28KDa) was eluted at 75mL (Figure-2.9A).

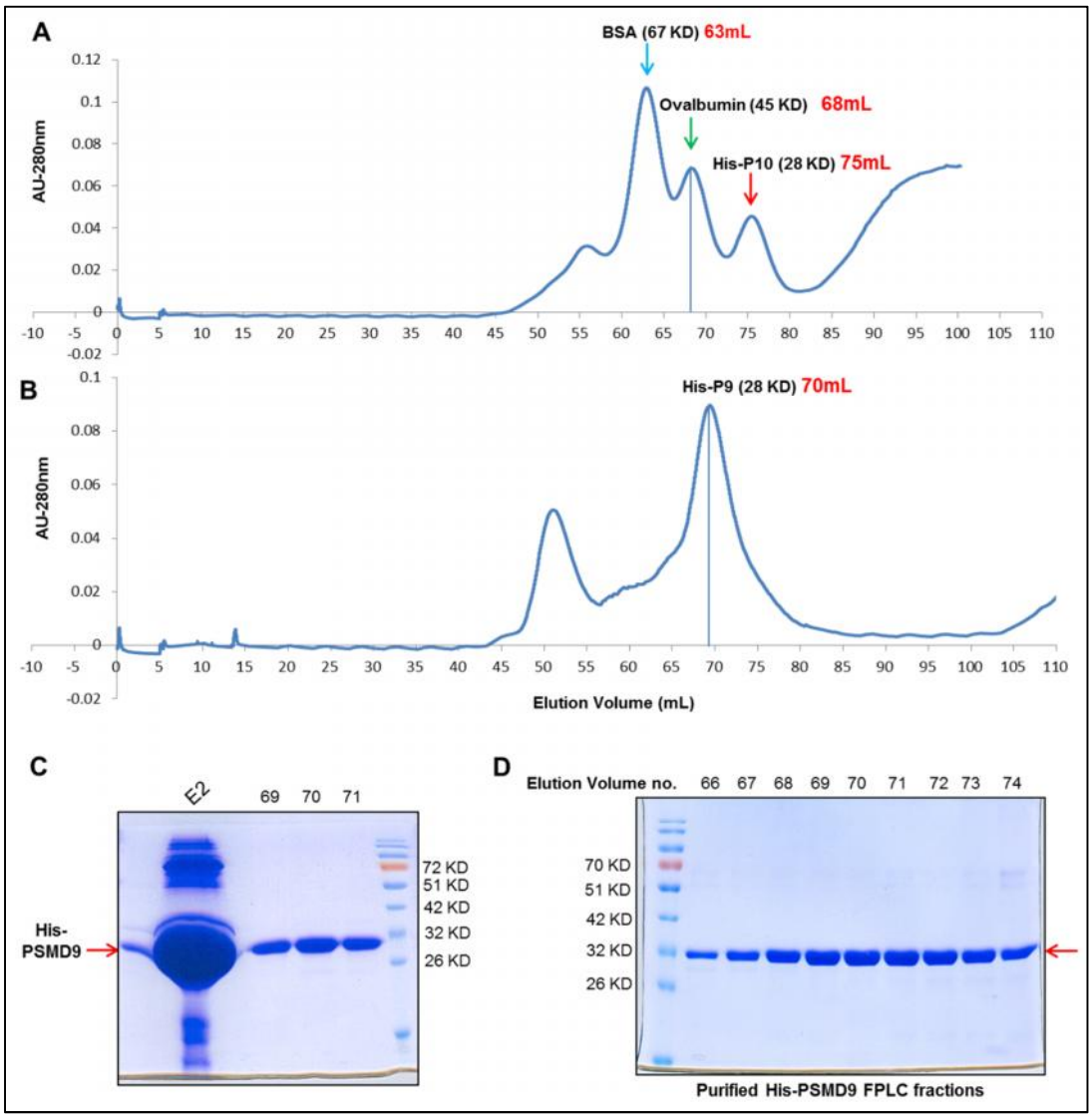

Figure-2.9: Approximate MW detection for His-PSMD9 protein. (A) Different standards such as Pure BSA (2mg), Ovalbumin (2mg) and purified His-PSMD10 (2mg) mixture were

injected to FPLC (Bio-Rad) fitted with sephadex-200/200mL column and FPLC profile was collected. **(B)** FPLC profile of injected ~4mg His-PSMD9 protein showing its elution at 70mL. **(C)** 10µL of Ni-NTA bead eluted (E2) His-PSMD9 fraction and the FPLC purified fractions of His-PSMD9 (69-71) were loaded in SDS-PAGE and Coomassie stained. **(D)** Fractions (66mL fraction no. to 74mL fraction no.) of injected protein sample were collected from FPLC and 10µL of the samples were loaded in SDS-PAGE and Coomassie stained. All the fractions are showing >95% pure recombinant His-PSMD9.

Then ~4mg of the E2 fraction of His-PSMD9 protein was injected into FPLC and run at a speed 0.3mL/min. The FPLC profile showed His-PSMD9 eluted at 70mL, after ovalbumin (Figure-2.9B). Furthermore SDS-PAGE showed His-PSMD9 run near 32KDa marker (Figure-2.9C & D). These results indicate an approximate MW of His-PSMD9 i.e 32KDa to 30KDa. However, further confirmation is necessary.]

2.2.19 Far western blot:

Reagents

a) Purified His-PSMD9, GST-PSMD9, His-hnRNPA1 and MBP-IκBα protein

b) PVDF membrane (GE-Healthcare)

c) 8M Guanidine-HCl and AC-Buffer

Table-2.4: Composition of AC-Buffer.

TABLE 1 | AC buffer with varying concentrations of guanidine–HCl used in denaturing and renaturing.

Concentration of guanidine–HCl (M)	6	3	1	0.1	0
Glycerol (ml)	2.5	2.5	2.5	2.5	2.5
5 M NaCl (ml)	0.5	0.5	0.5	0.5	0.5
1 M Tris, pH 7.5 (ml)	0.5	0.5	0.5	0.5	0.5
0.5 M EDTA (ml)	0.05	0.05	0.05	0.05	0.05
10% Tween-20 (ml)	0.25	0.25	0.25	0.25	0.25
Guanidine–HCl (8 M) (ml)	18.75	9.30	3.13	0.31	0
Milk powder (g)	0.5	0.5	0.5	0.5	0.5
1 M DTT (µl)	25	25	25	25	25
ddH_2O (ml)	2.45	12.82	18.07	20.89	21.20
Total volume (ml)	25	25	25	25	25
Time/temperature	30 min/room temperature (RT)	30 min/RT	30 min/RT	30 min/4 °C	1 h overnight/4 °C

Methodology

i. 2µg of Purified His-PSMD9/ GST-PSMD9/ His-hnRNPA1/ MBP-IκBα/ MBP or GST protein were denatured in SDS-Lamellae dye and run in SDS-PAGE according to standard protocol.

ii. Then the purified proteins were transferred onto a PVDF membrane following standard Transfer protocol. **Note:** These immobilized proteins in this case are called as Bait.

iii. Then the proteins were again denatured and renatured on the PVDF membrane using different concentration of Guanidine-HCl containing AC buffer (Table-2.5).

iv. First the PVDF membrane was treated with 6M-AC buffer keeping on rocker for 30min at RT.

v. Then the membrane was transferred to 3M AC-Buffer then subsequently 1M AC-buffer and incubated in each for 30min at RT on rocker.

vi. The membrane was then transferred to 0.1M AC-Buffer and incubated for 30min at 4^{o}C.

vii. Finally the membrane was put in 0M AC-buffer for overnight at 4^{o}C.

viii. Then the membrane was overlaid with the prey protein [His- PSMD9 (100nM)/ GST-hnRNPA1 (100nM)/ MBP-IκBα (100nM)] in 1% BSA-TBST buffer and incubated for 1h at RT in slow rocking condition.

ix. Membrane was washed with TBST twice (each for 5min) at slow rocking condition.

x. Then the membrane was probed with anti-prey antibody at required dilution and incubated for 1h at RT in slow rocking condition.

xi. Again membrane was washed with TBST twice (each for 5min) at slow rocking condition.

xii. Then the membrane was probed with secondary antibody at required dilution and incubated for 1h at RT in slow rocking condition followed by two washes with TBST (each for 5min) at slow rocking condition.

xiii. Membrane was developed onto X-Ray film following WB protocol.

2.2.20 Dot Blot:

Reagent

a) Purified His-PSMD9, GST-PSMD9, His-hnRNPA1 and MBP-IκBα protein

b) PVDF membrane (GE-Healthcare)

Methodology

i. 1µg of Purified His-PSMD9/ GST-PSMD9/ His-hnRNPA1/ MBP-IκBα/ MBP or GST protein spotted on moistened PVDF membrane.

ii. The membrane was air dried at 37ºC for 10-15 min and again activated in methanol for 2-3min.

iii. The membrane was then washed with Milli-Q water and then with TBST.

iv. The membrane was put for blocking in 3% BSA-TBST for 1h at RT.

v. Then the subsequent steps were same as Far western blot methodology.

Note: In this technique bait proteins are in their native conformation unlike far western blot.

2.2.21 Densitometric and Statistical analysis:

Densitometric quantitaion of scanned WB images was performed using Mac BioPhotonics ImageJ. Statistical analysis was performed using Graph Pad Prism 5. To evaluate the significance of values obtained, unpaired Student's t test was performed. $P < 0.05$ and $P > 0.05$ were considered as significant and non-significant data respectively. *** represents P value <0.001.

CHAPTER-III

PSMD9

(The novel role of PSMD9 in NF-κB signaling pathway)

3.1 INTROUDUCTION AND REVIEW OF LITRATURE

PSMD9, the proteasome (prosome, macropain) 26S subunit, non-ATPase9, is a non-ATPase subunit of 19S regulatory particle of human proteasome. It is also called as nas2 (in yeast) and Bridge-1 (in rat). It acts as a chaperone during the assembly of 19S regulatory particle on the 20S-core particle. Different studies on the 19S regulatory particle (PA700) revealed that a trimer modulator enhanced the association of the RP-complex with 20S and increased the protease activity [200]. Further characterization revealed that the trimeric complex composed of three subunits two of which were ATPases; Rpt4 (PSMC6) and Rpt5 (PSMC3) and a non-ATPase subunit p27 (human: PSMD9, rat: Bridge-1 and yeast: Nas2). The gene encoding p27 was mapped to the region q24.2-q24.3 of chromosome 12 [201]. Although PSMD9 is considered as a non-ATPase subunit of 19S-RP, no such reports has suggested the presence of PSMD9 on the 26S proteasome holocomplex. The cryo-EM structure did not show the presence of nas2 (yeast homolog) in the 26S proteasome holocomplex [20, 21, 202]. But in our current study we are showing the presence of human PSMD9 in the 26S proteasome *ex vivo* [203, 204].

3.1.1 Structure of PSMD9

PSMD9 is a 24.68 KDa protein with 223 amino acids run at 30 kDa marker in SDS-PAGE. Thomas et. al., in 1999 reported that the residues 138-178 of the rat homolog of PSMD9, Bridge-1 are conserved with well-known PDZ domain containing proteins. Rat Bridge-1 and human PSMD9 are highly homologous, with 70% identity (156 of 222 amino acids) and 82% similarity at the protein level. The two sequences diverge at the carboxy termini of the proteins. Comparison of the first 184 amino acids of rat Bridge-1 and p27 proteins shows 84% identity and 98% similarity. Homologies

with other proteins having PDZ domains ranged from 27 to 54% identity and 46 to 77% similarity [193].

Although the crystal structure of PSMD9 has not been solved, recently two groups have solved the partial crystal structure of nas2 [205, 206]. Nas2 is composed of 220 amino acid residues (whereas PSMD9 is of 223 amino acid residues), harboring an 80–90 residue-long C-terminal PDZ domain, which is often involved in the binding of target protein C termini [207]. Nas2 interacts with the C-terminal segment of Rpt5 [208]. The bioinformatics analysis of the Nas2 sequence using the program DISOPRED2 [209] identified a disordered region (residues 119–127, disorder probability score > 0.3) preceding the PDZ domain, suggesting that Nas2 consists of N- and C-domains connected by a flexible linker.

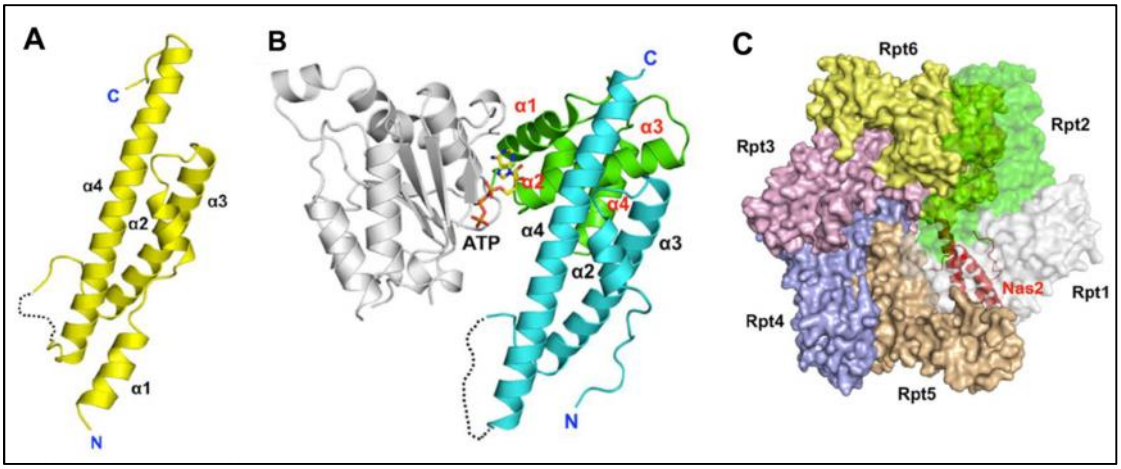

Figure-3.1: Crystal Structures of the Nas2 N-Domain Alone and Its Complex with the Rpt5 C-Domain. **(A)** A ribbon model of the Nas2N. The positions of the N and C termini are indicated by blue letters. Dotted lines indicate a disordered loop. **(B)** A ribbon model of the Nas2N-PAN-Rpt5C complex. The secondary structural elements of Nas2 and Rpt5 are labelled with black and red letters, respectively. Bound ATP is shown as stick models. **(C)** The Nas2N-Rpt5C complex structure was superimposed on an EM model of Rpt ATPase ring (PDB code: 4B4T). Nas2N is shown as red-colored ribbon models. The Rpt ring is shown as surface representations and is colored transparent gray (Rpt1), transparent green (Rpt2), pink (Rpt3), slate (Rpt4), wheat (Rpt5), and lemon (Rpt6). [Adopted from: Tadashi Satoh et. al., Structural Basis for Proteasome Formation Controlled by an Assembly Chaperone Nas2. *Structure* 22, 1–13, May 6, 2014]

Recently the Nas2 N-domain structure was solved by co-crystalization with PAN-Rpt5 (Figure-3.2) [206]. This report suggests that binding of the Nas2 N-domain to Rpt5 causes significant steric hindrances not only against 20S CP but also the Rpt1 and Rpt2 subunits of the 19S base because Nas2 touches the a3 helix of Rpt5, which corresponds to its Rpt5-interacting surface (Figure-3.1). This clearly explains why Nas2 dissociates from the base complex upon completion of the ATPase ring formation. Unlike other RP chaperones, Nas2 has been reported to be nonessential for scaffolding between Rpt4 and Rpt5. The NMR analysis and the crystal structure of Nas2-N suggested that this distinct mode of Nas2N-Rpt5C interaction is complemented with the Nas2 PDZ domain, which directly antagonizes the 20S CP-Rpt5 interaction by capping the C-terminal tail of Rpt5. The data also suggested that N-domain of Nas2 exists in monomeric form. Moreover, the structural data indicates that Nas2 operates as a proteasome activation blocker, preventing premature activation and acts as a check point during 26S proteasome assembly.

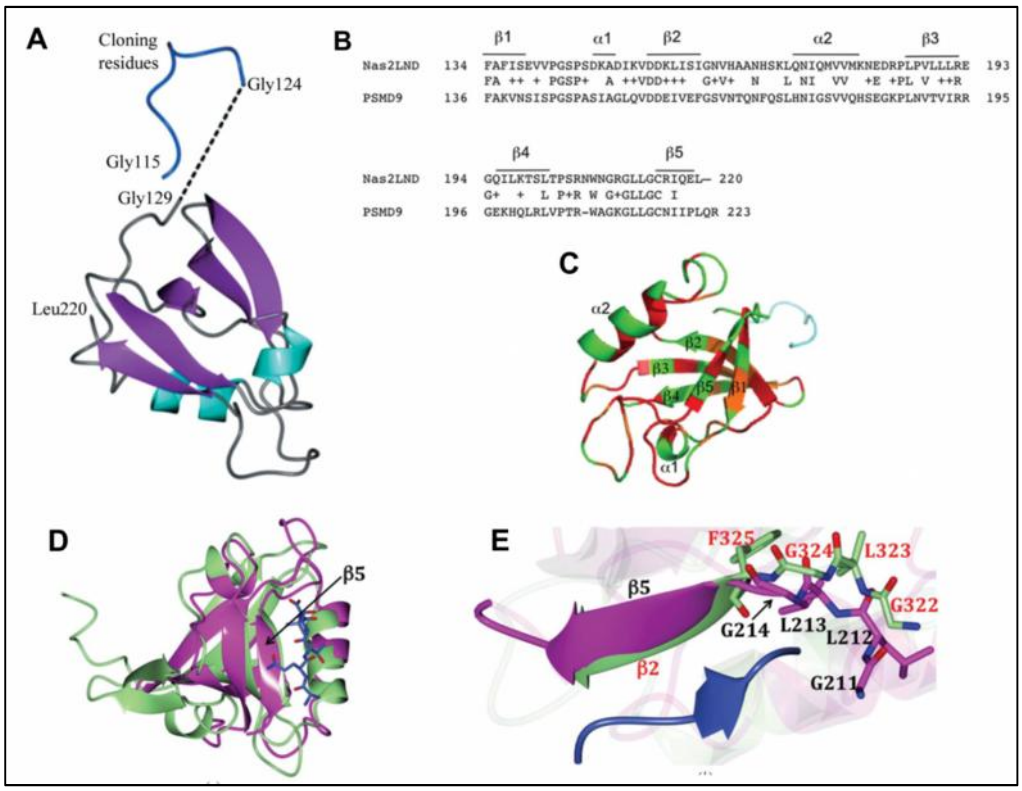

Figure-3.2: Crystal Structure of the Nas2 PDZ domain. (A) Asymmetric unit of Nas2LND colored by secondary structure: sheet, magenta; helix, cyan. The disordered region is indicated by the dashed line. N-terminal residues resulting from cloning are colored blue. **(B)** Alignment of Nas2 PDZ-domain residues with the human ortholog PSMD9. Residues modeled in the crystal structure of Nas2 were used in a BLASTp search against the human protein Ref Seq database. The top hit was the human ortholog of Nas2, PSMD9, showing 42% identity and 64% conserved residues (the latter are indicated with +). **(C)** Graphic structure of Nas2 in green. Based on an alignment between Nas2 and PSMD9, conserved residues were colored orange and identical residues red. The cloning-derived residues are in blue. **(D)** Superposition of Nas2LND (magenta) with a canonical PDZ domain (PDB entry 1be9, green). The peptide ligand for 1be9 is shown as blue cylinders. *β*-Sheet 5 of Nas2LND is indicated. Superposition of a canonical PDZ domain (PDB entry 1be9) with Nas2LND was conducted using GESAMT (Krissinel, 2012), which yielded an r.m.s.d. of 2.27 Å for 59 aligned residues. **(E)** Enlarged view of the *β*5/*α*2 region of Nas2LND superimposed with 1be9. The peptide ligand for 1be9 is shown as a blue ribbon. The GLGF (red) motif of 1be9 and similar residues in front of Nas2LND *β*-sheet 5, GLLG (black), are indicated. [Adopted from: Singh CR, Lovell S, Mehzabeen N, Chowdhury WQ, Geanes ES, Battaile KP, Roelofs J: 1.15 A resolution structure of the proteasome-assembly chaperone Nas2 PDZ domain. *Acta Crystallogr F Struct Biol Commun* 2014, 70(Pt 4):418-423]

In an independent study the structure of C-domain/PDZ-domain of Nas2 has been solved by 1.15Å resolution crystallography [205]. The crystal structure of the C-terminal region of Nas2 shows it contains a PDZ domain but, Nas2 lacks the GLGF motif commonly found just prior to *β*-strand-2 in PDZ domains. This motif interacts with the carboxy-termini of PDZ-binding partners [210]. The absence is not surprising as the Nas2 structure shows that *β* –strand-5, instead of the common *β*-strand-2, contributes to the putative peptide-binding groove, causing a different loop arrangement. In front of *β*-strand-5 a similar sequence is present (GLLG) (Figure-3.2). However, the role of this sequence in interactions with C-termini of Nas2-binding partners remains to be determined. In particular, the binding between Nas2 and Rpt5 does not appear to be affected by deletion of the Rpt5 C-terminal residue [208]. However, the reported Nas2 structure will provide the basis for further insights regarding the structure and function of Nas2 in proteasome assembly, as it will facilitate molecular docking of the tail of Rpt5 as well as enabling the design of Nas2 mutants based on the putative binding region.

Although Nas2 PDZ domain shows 42% identity and 64% conserved residues with the PDZ domain of PSMD9, there might be existing difference in the tertiary structure. However, Bridge-1 and human PSMD9 are highly homologous, with 70% identity and 82% similarity at protein level, but crystal structure of Bridge-1 has not been solved yet. Hence to facilitate the prediction for novel interacting partner of PSMD9 or to find out novel functions its structural detail is essential. So there is a scope of solving the crystal structure of human PSMD9.

3.1.1.1 PDZ domain:

In eukaryotic cells, diverse biological activities are regulated via dynamic interactions of modular protein domains (e.g., WW, SH3, SH2, PH, and PDZ) and their corresponding interacting partners [211]. PDZ domains are abundant protein interaction modules found in various species (Figure-3) [212-215]. They regulate multiple biological processes such as transport, ion channel signaling, and various signal transduction pathways [203, 207, 210, 216-228].

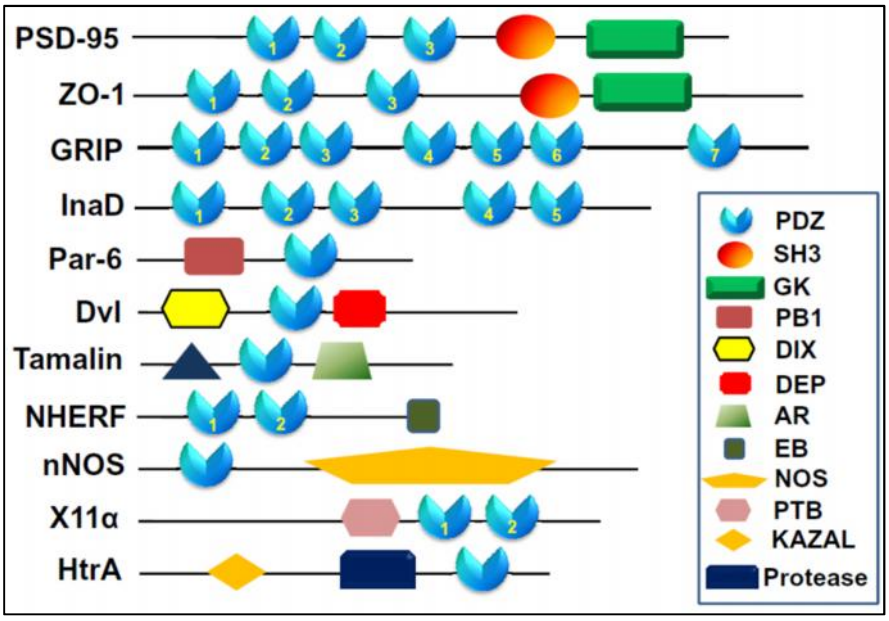

Figure-3.3 Examples of PDZ domain-containing proteins. Proteins are indicated by black lines scaled to the length of the primary sequence of the protein (from SMART [229]) [Adopted from: Lee and Zheng R, PDZ domains and their binding partners: structure, specificity, and modification *Cell Communication and Signaling* 2010, 8:8]

PDZ nomenclature has come from first letter of three proteins- Postsynaptic density protein-95 (PDZ-95), Disks large tumor suppressor (DLG) and Zonula occludens-1 (ZO-1), which were discovered as the initial PDZ containing protein, about two decades ago [230-232]. PDZ domains are small and often modular entities consisting of 5 or 6 β-stranded and 2 or 3 α-helical structures [233]. Canonical PDZ domains are usually 80-100 amino acid residues long and adopt a similar topology. Structural studies have revealed that canonical PDZ domains are usually composed of 6 β-strands (βA ~ βF), a short α-helix (αA) and a long α-helix (αB) (Figure-3.3) [21, 46, 47]. The N- and C-termini of canonical PDZ domains are in proximity to each other on the opposite side from the peptide-binding site in a groove between the αB-helix and βB-strand structures (Figure-3.3). Nas2 PDZ-domain crystal structure shows it has 5 β-strands and 2 α-helices and follows in the category of canonical PDZ domain [205]. Similar to canonical PDZ domains, the HtrA family, including HtrA, DegS, and DegQ, adopt a PDZ like fold consisting of 5 β-strands (β1-β5) capped by 2 α-helices (α2 and α3) and also 2 short β-strands at the N and C termini (βN and βC). The well-defined α-helix (α1) is formed in the region between the β1 & β2 loop of the PDZ-like domain (Figure 3.4) [225, 234].

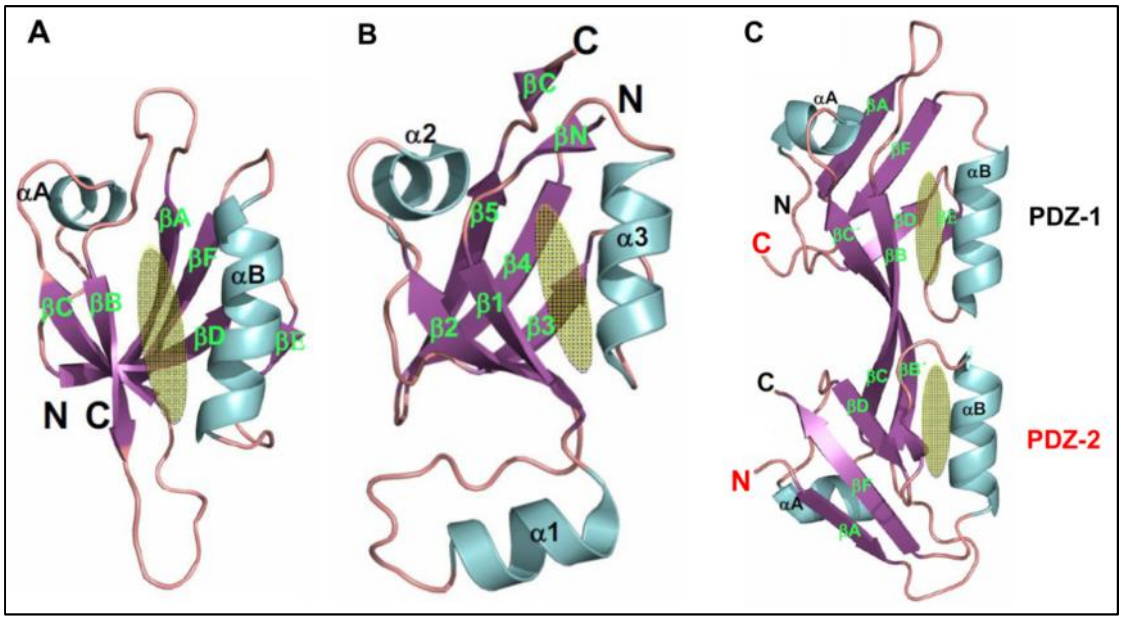

Figure-3.4 Structures of PDZ, PDZ-like, PDZ-PDZ dimer, and tandem PDZ domains. (A) Ribbon diagram of Dvl-1 PDZ (PDB code: 2KAW). **(B)** HtrA2 PDZ (PDB code: 1LCY). **(C)** ZO-1 PDZ2 (PDB code:2RCZ). The binding site of each PDZ domain is shown by a yellow oval. The structures were generated using the Pymol software. [Adopted from: Lee and Zheng R, PDZ domains and their binding partners: structure, specificity, and modification *Cell Communication and Signaling* 2010, 8:8]

PDZ domains typically recognize the extreme C-termini of target proteins [204, 235], but some also recognize the internal sequence motif of target proteins through a single binding site on the domains [236-238]. Based on the nature of the C-terminus they interact, PDZ domains are classified into three classes- class 1 (X-[T/S]X-Φ-COOH), class 2 (X-Φ-X-ΦCOOH) and class 3 (less common class) X-[E/D]-XϕCOOH where X is any residue and Φ is a hydrophobic residue [239-241]. PDZ domains have a single binding site in a groove between the αB and βB structural elements with a highly conserved carboxylate-binding loop (R/K-XXX-G-Φ-G- Φ motif, where X is any amino acid residue and Φ is hydrophobic residues) located before the βB strand [213, 240]. The first Gly residue in this motif is variable among canonical PDZ domains, and can be replaced by a Ser, Thr, or Phe residue [242]. The second and the fourth residues are hydrophobic, such as Val, Ile, Leu, or Phe. The side chains of both of these residues create the hydrophobic binding pocket of canonical PDZ domains [214].

3.1.2 Functions of PSMD9:

PSMD9 act as an assembly chaperone for 26S proteasome that interacts transiently with two ATPase subunits of 19S-RP i.e., Rpt4 (PSMC6) and Rpt5 (PSMC3). It plays an important role during the assembly of the 19S regulatory particle [243-245]. Apart from these two ATPase interacting partners there are no other known interacting partners amongst the 26S proteasomal subunits. However there are reports which suggest that, rat homolog Bridge-1 performs some other non-classical functions apart from the proteasomal assembly. Bridge-1 act as a coactivator of insulin gene transcription through interaction of its PDZ-like domain with transcription factors E12

and histone acetyl transferase, p300 [193, 194]. Bridge-1 modulates PDX-1 functions by interacting with it via the PDZ domain and regulates glucose-dependent insulin production and glucose metabolism [246]. In ovarian cells, changes in the levels of PSMD9 is known to alter activin signaling [247]. Overexpression of Bridge-1 increases pancreatic apoptosis with a reduction in the number of insulin-expressing beta cells leading to insulin deficiency and diabetes [248, 249].

It has been shown in mouse melanoma cells that, p27 (PSMD9) negatively regulate the activity and protein levels of Tyrosinase (Tyr) enzyme and Tyrosinase related protein 1 (Trp1) [250]. Increased level of p27 lower the activity of Tyr (and vice versa) may be by interacting with it and degrading it through proteasomal pathway shown by immunofluorescence and MG132 treatment experiments respectively. These results suggest that p27 (PSMD9) is directly involved in the regulation of melanin biosynthesis in mouse melanoma cell line.

In 2011 it has been demonstrated that, the expression of Bridge-1 increases both in RNA and protein levels in human breast carcinoma cell line MCF-7 by activin A stimulation [251]. The increased expression of Bridge-1 itself seems to influence activin A signaling in human breast carcinomas cells by affecting the expression of Smad2, 3 and 4. Moreover, recently in 2014 a clinical sample based study indicated that PSMD9 expression may predict radiotherapy benefit in human breast cancer, with low expression indicative of relative radio-sensitivity, the opposite of previous reports relating to 26S proteasome expression [252]. In support of this, the study showed knock-down of PSMD9 in breast cancer cell lines (MCF7 and MDA-MB-231), sensitized the cells to radiotherapy evaluated by colony forming assays after irradiation. These results altogether are compatible with use of proteasome inhibitors as radio-sensitizers, and highlights PSMD9 as a potential target for radio-sensitizing drugs.

The above findings suggests a substantial involvement of rat homolog Bridge-1 in non-degradation function in mammalian cells. However, there is enough scope for elucidating novel interacting partners and novel functions of human PSMD9.

3.1.3 NF-κB and the Signaling transduction pathway

The nuclear factor κB (NF-κB) is a family of transcription factors that regulates expression of various genes involved in inflammatory, anti-apoptotic and immune responses [253, 254]. NF-κB was discovered by Dr. Ranjan Sen in David Baltimore lab via its interaction with an 11-base pair sequence in the immunoglobulin κ-light-chain enhancer in B cells [255]. In addition to mammals, NF-κB is found in a number of simple animals as well including cnidarians, porifera, the single-celled eukaryote *Capsaspora owczarzaki* and insects [256].

3.1.3.1 NF-κB family proteins:

NF-κB is not a single gene but a family of closely related transcription factors that includes five genes NF-κB1 (p50/p105), NF-κB2 (p52/p100), RelA (p65), c-Rel and RelB (Figure-3.5). These five genes give raise to seven proteins that share a Rel Homology Domain (RHD) in their sequence. The RHD mediates their dimerization, interaction with their specific inhibitors, and DNA binding. There are two types of NF-κB proteins [257]: 1) RelA, c-Rel and RelB are synthesized in their mature forms and contain a transactivation domain which interacts with the transcriptional apparatus; and 2) NF-κB1-p105/p50 and NF-κB2-p100/p52 that are synthesized in a precursor form. The precursor forms (p100 and p105) contain C-terminal ankyrin repeats that are proteolysed by the proteasome resulting in the production of the mature (p50 and p52) proteins. Both p50 and p52 contain the DNA binding domain but lack a transactivation domain. [256, 258]. The p50 and p52 proteins have no intrinsic ability to activate

transcription and thus have been proposed to act as transcriptional repressors when binding κB elements as homodimers [259, 260]. Among the other IκB proteins, IκBβ, IκBε, p100 (precursors of p52) and p105 (precursors of p50) also undergo proteasomal degradation/endoproteolytic processing under induced and uninduced conditions [179, 261-264].

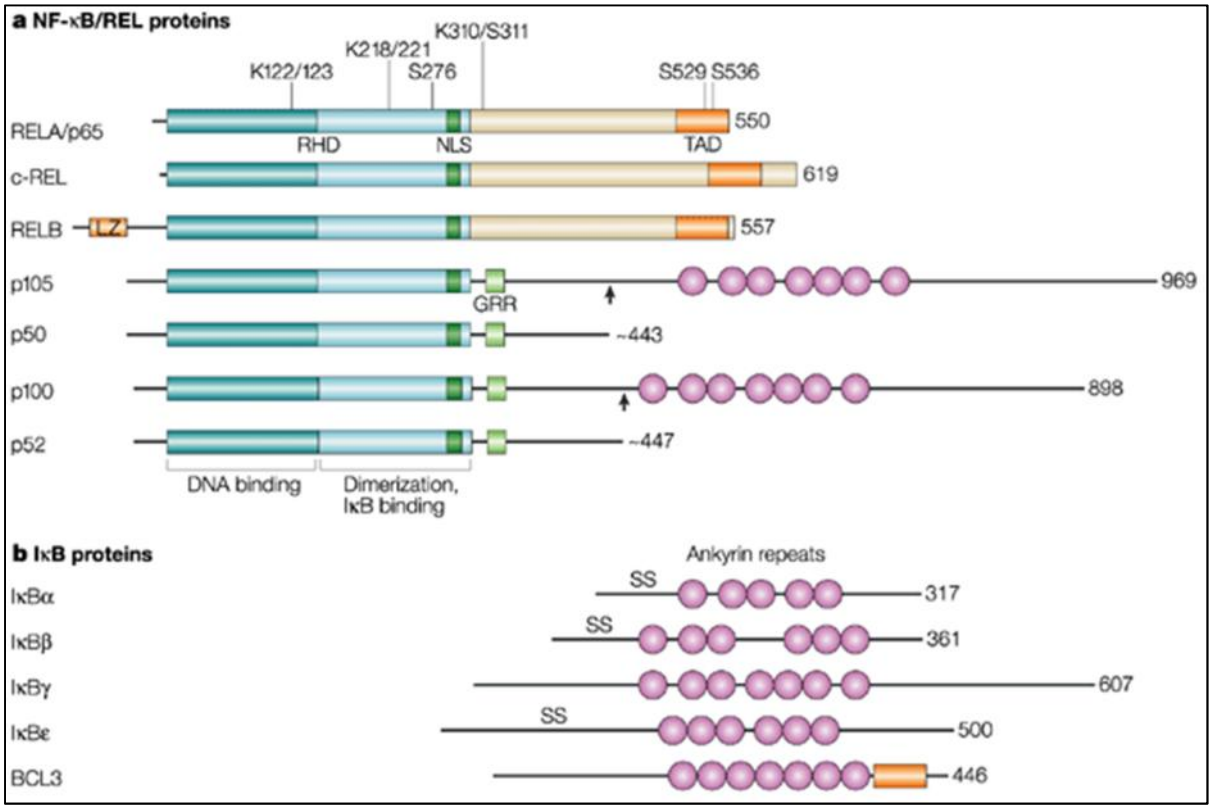

Figure-3.5: NF-κB and IκBα family proteins. [Adopted from: Chen LF at. al., Shaping the nuclear action of NF-kappaB. *Nat Rev Mol Cell Biol*. 2004 May;5(5):392-401]

NF-κB is important in regulating cellular responses because it belongs to the category of "rapid-acting" primary transcription factors, i.e., transcription factors that are present in cells in an inactive state and do not require new protein synthesis in order to become activated (other members of this family include transcription factors such as c-Jun, STATs, and nuclear hormone receptors). This allows NF-κB to be a first responder to harmful cellular stimuli like; reactive oxygen species (ROS), tumor necrosis factor alpha (TNFα), interleukin 1-beta (IL-1β), bacterial lipopolysaccharides

(LPS), isoproterenol, cocaine, and ionizing radiation. In higher eukaryotic cells NF-κB signaling pathway can be categorized into two main pathways; one is ubiquitously occur in all cells (canonical pathway) and other is predominantly immune cells specific (alternative pathway).

3.1.3.2 Canonical NF-κB signaling Pathway:

When cells are not stimulated, heterodimeric NF-κB complexes remain in the cytoplasm, where they are associated with an inhibitory molecule of the IκB family [265]. In mammalian species, six structural homologs of IκB have been identified viz. IκBα, IκBβ, IκBε, IκBγ, Bcl-3 and IκBζ (Figure-3.5) [266]. Among these, IκBα, the prototypical member of the IκB family has been extensively studied. The canonical NF-κB p65/p50 heterodimer is largely, though not exclusively, found in complex with its inhibitor IκBα in cytoplasm. Stimulation of cells with agonists such as tumor necrosis factor-α (TNF-α), interleukin-1β (IL-1β), lipopolysaccharide (Toll-like receptor-4 ligand) phorbol esters (e.g. phorbol 12-myristate 13-acetate), pervanadate, γ-radiation activates the canonical pathway of NF-κB activation (Figure-3.6). The signals transduced by the receptors for each of these ligands converge on the IκB kinase (IKK) complex, consisting of two catalytic subunits, IKKα and IKKβ (gets phosphorylated), and the regulatory subunit NF-κB essential modulator (NEMO, also known as IKKγ). IκBα undergoes phosphorylation by IKK complex at Ser32, Ser36 and/or Tyr42 followed by lysine-48 poly ubiquitination at Lys21 and Lys22 by βTrCP E3-ligase [267-270]. This leads to proteasomal degradation of the phosphorylated and ubiquitinated IκBα and nuclear translocation of free p50/p65, resulting in increased NF-κB transcription activity [253, 267, 271, 272]. One of the target genes potently upregulated by NF-κB is IκBα itself, which can enter the nucleus, displace NF-κB from DNA, and transport it back to the cytoplasm, forming a negative feedback loop. Therefore, without

persistent upstream activation signals, NF-κB is rapidly resequestered by IκBα. The traditional IκB proteins IκBα, IκBβ, and IκBε have similar but not entirely overlapping functions. Their differences likely result from temporal differences in their degradation and resynthesis [273]. However, apart from proteasomal degradation some reports suggest that in uninduced cells I*κ*B*α* undergoes non-proteasomal, calcium dependent proteolysis resulting in high and consistent NF-*κ*B activity [274-277]. Although the upstream processes of I*κ*B*α* degradation is extensively deciphered, the detailed mechanism of proteasomal degradation is still not clear.

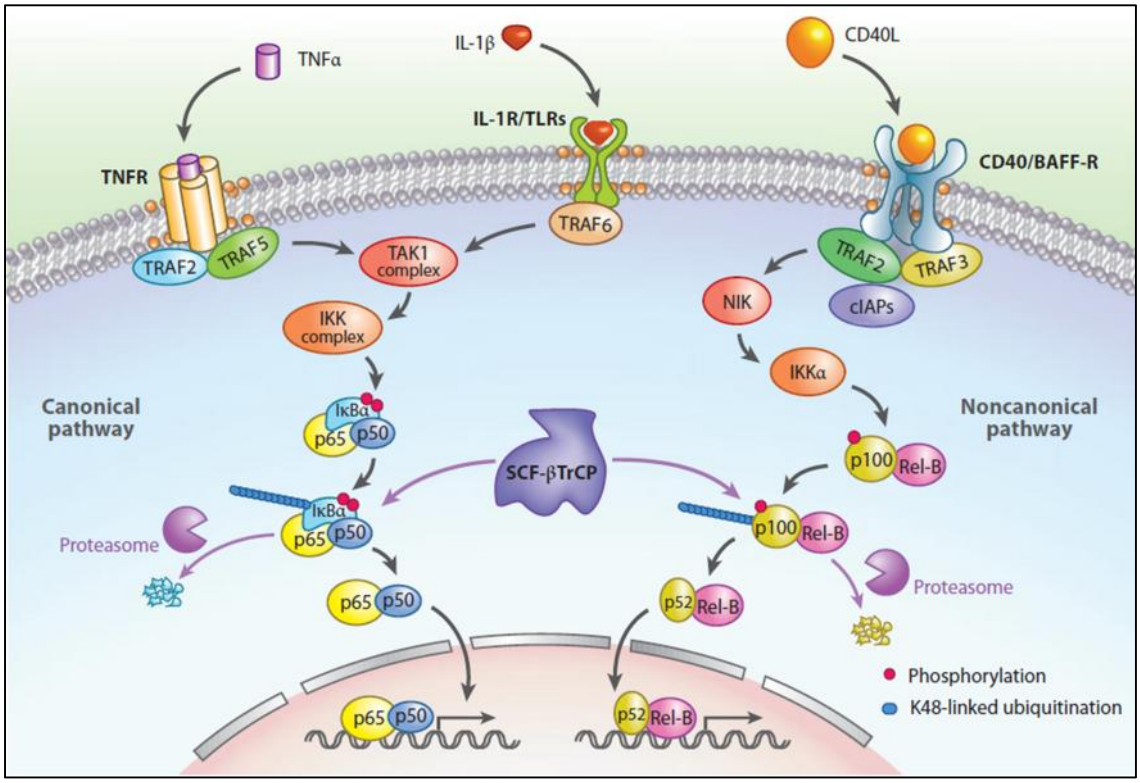

Figure 3.6: Two pathways leading to NF-κB activation. In canonical NF-κB activation (left), stimulation of the TNF receptor (TNFR), IL-1 receptor (IL-1R), and Toll-like receptors (TLRs) leads to activation of the TAK1 complex through TRAF proteins. TAK1 then activates IKK, which in turn phosphorylates IκB proteins and targets them for polyubiquitination by the SCF-βTrCP E3 ligase complex. Ubiquitinated IκB is degraded by the proteasome, allowing the p50/p65 NF-κB dimer to enter the nucleus and activate gene transcription. In noncanonical NF-κB activation (right), stimulation of a subset of receptors, including the BAFF receptor, leads to the stabilization of the kinase NIK, followed by activation of IKKα. IKKα phosphorylates p100, leading to its ubiquitination by the SCF-βTrCP complex. Ubiquitinated p100 is targeted for proteasomal processing to p52. The p52/REL-B dimer then translocates into the nucleus to activate gene transcription. [Adopted from: Brian Skaug et.al., The Role of Ubiquitin in NF-κB Regulatory Pathways. *Annu. Rev. Biochem*. 2009. 78:769–96]

3.1.3.3 Alternative NF-κB signaling Pathway:

A select set of cell-differentiating or developmental stimuli, such as lymphotoxin-α or β, B-cell-activating factor of the TNF family (BAFF), latent membrane protein (LMP)-1 of Epstein–Barr virus (EBV), RANKL or CD40 ligand, activate the non-canonical NF-κB pathway or the alternative pathway to induce NF-κB/RelB:p52 dimer in the nucleus [270, 278]. These signals stimulate another subset of TNF receptor (TNFR) superfamily members that induces NF-κB activation through another proteasome-dependent mechanism. In this pathway, activation of the NF-κB inducing kinase (NIK) upon receptor ligation leads to the phosphorylation and subsequent proteasomal processing of the NF-κB2 precursor protein p100 into mature p52 subunit in an IKK1/IKKa dependent manner (Figure-3.6). Then p52 dimerizes with RelB to appear as a nuclear RelB:p52 DNA binding activity and regulates a distinct class of genes [279]. In contrast to the canonical signaling that relies upon NEMO-IKK2 mediated degradation of IκBα, -β, -ε, the non-canonical signaling critically depends on NIK mediated processing of p100 into p52. Given their distinct regulations, these two pathways were thought to be independent of each other. However, recent analyses revealed that synthesis of the constituents of the non-canonical pathway, viz RelB and p52, is controlled by the canonical IKK2-IκB-RelA:p50 signaling [280]. Moreover, generation of the canonical and non-canonical dimers, viz RelA:p50 and RelB:p52, within the cellular milieu are also mechanistically interlinked [280]. These analyses suggest that an integrated NF-κB system network underlies activation of both RelA and RelB containing dimer and that a malfunctioning canonical pathway will lead to an aberrant cellular response also through the non-canonical pathway.

Proteasomal processing of p105 occurs cotranslationally and posttranslationally, and can result in its complete degradation or formation of p50. The prevalence of each

type of processing, as well as the role of ubiquitination in these processes, has been controversial. Processing of p105 to p50 was reconstituted in vitro and required ubiquitination and the proteasome [179]. Another group demonstrated that p50 is produced cotranslationally in a proteasome dependent process [281]. However, expression of a dominant-negative UBCH5 (an E2) inhibited IKKβ-dependent processing, but not basal processing [262], and it was recently shown that the 20S proteasome can process full-length p105 to p50 in a ubiquitin-independent process [264]. Thus, it appears that basal processing of p105 to p50 does not require ubiquitination, whereas signal-induced processing does.

But, "how does the proteasome distinguish between different regions of proteins, such that the C termini of p105 and p100 are degraded while the N termini remain intact?" To address this question, Jentsch and colleagues [282], proposed that proteasomal processing begins at a hairpin-like loop region within the protein, then proceeds in both the C-terminal and N-terminal directions. Both p100 and p105 contain a glycine-rich region, which appears to function as a processing signal [182] While degradation proceeds through the entire C terminus, N-terminal processing is halted by a region of stable tertiary structure and/or the presence of another associated protein, i.e., the other NF-κB subunit of a dimer. Indeed, initiation of proteasomal processing at an internal site was recently demonstrated using p105 and the yeast transcription factors Spt23 and Mga2 [264, 283].

3.1.3.4 The function and complexity of the NF-κB:

The central role played by NF-κB as a regulator of the immune response is illustrated by its conservation throughout evolution [256]. Drosophila melanogaster, for example, contains NF-κB -related proteins that regulate its immune system [284]. Gene knockouts in mice have confirmed the importance of NF-κB as a regulator of immune

cell function [285]. These experiments also revealed that RelA (p65) subunit of NF-κB is a crucial regulator of apoptosis – as a result of TNFa-induced apoptosis of liver cells, $RelA^{-/-}$ mice die in utero [285][9]. NF-κB also plays a central role in the inflammatory response, because it is induced by inflammatory molecules and also induces the expression of many cytokines and chemokines [286].

The regulation and function of NF-κB is highly complex and it is also an important regulator of many aspects of the cellular response to stimulation such as the stress response, cell adhesion, and proliferation. However, hundreds of inducers of NF-κB DNA-binding have been described [286]. Furthermore, given the almost ubiquitous presence of NF-κB in most cell types and the possibility that there will be hundreds of NF-κB target genes to regulate [286], the mechanisms controlling the NF-κB response are by necessity diverse and achieving the required specificity and selectivity with which it acts is very complex [287]. Therefore, the nature of the NF-κB response will differ, depending on the context in which it is found. This specificity is achieved through a combination of mechanisms [288]. Differential activation of NF-κB subunits can result in the regulation of different target genes through differences in DNA-binding affinity. Moreover, interactions with heterologous DNA-binding proteins, often resulting in cooperative DNA-binding, can determine which genes become activated by NF-κB. Finally, coactivator and co-repressor complexes are required for NF-κB function and their regulation will have effects on NF-κB itself. Therefore, NF-κB does not work alone; it functions as part of a network of coordinately regulated DNA-binding proteins and transcription factors that, together, determine the pattern of gene expression required for the response to a particular cellular stimulus. This complexity has led to many apparent contradictions in the scientific literature. There are many reports of both pro-apoptotic and anti-apoptotic activity of NF-κB [289]. Under some

circumstances, NF-κB can also induce pro-apoptotic genes such as Fas and Fas ligand [286, 289]. The ability to perform these apparently opposing functions is an example of how context, and possibly posttranslational modifications, can profoundly affect NF-κB function and the specificity of target genes. Interestingly, the β-catenin proto-oncogene represses NF-κB -mediated activation of Fas expression [290].

3.1.3.5 NF-κB signaling pathway inhibitors and drugs:

Since NF-κB is considered as a multifunctional transcription factor and involved in normal cell physiology as well as diseases and disorders, it's always being a target for therapy. Therefore, the NF-κB signaling pathway has also provided a focus for pharmacological intervention, primarily in situations of chronic inflammation or in cancer (discussed in section 3.1.3.5), where the pathway is often constitutively active and plays a key role in the disease. Now that many of the molecular details of the NF-κB pathway are known, it is clear that modulators of this pathway can act at several levels. As described in a collective study, over 750 inhibitors (Table-3.1) of the NF-κB pathway have been identified, including a variety of natural and synthetic molecules [291]. These compounds include antioxidants, peptides, small RNA/DNA, microbial and viral proteins, small molecules, and engineered dominant-negative or constitutively active polypeptides. Several of these molecules act as general inhibitors of NF-κB induction, whereas others inhibit specific pathways of induction. In addition, some compounds appear to target multiple steps in the NF-κB pathway. Compounds designed as specific NF-κB inhibitors are not yet in clinical use, but they are likely to be developed as treatments for certain cancers and neurodegenerative and inflammatory diseases. Moreover, the therapeutic and preventative effects of many natural products

Table-3.1: Classification of NF-κB inhibitors:

	Natural Products	*Proteins*	*Peptides*	*Synthetic compounds*	*Misc.*	*Inorganic Compounds*	*Antioxidants*	*Total Inhibitors*
S1: Upstream Target inhibitors	8	12	-	8	-	-	-	**28**
S2 – IKK and IκB phosphorylation inhibitors	90	19	2	57	1	1	-	**170**
S3– IκB degradation inhibitors	57	15	2	17	2	1	-	**94**
S4 – Proteasome and protease inhibitors	2	-	5	12	-	-	-	**19**
S5 – IκBα upregulation, NF-κB nuclear translocation and NF-κB expression inhibitors	51	21	3	23	1	-	-	**99**
S6 – NF-κB DNA-binding inhibitors	90	44	3	63	5	1	-	**206**
S7 – NF-κB transactivation inhibitors	33	6	-	18	1	-	-	**58**
S8 – Antioxidants	-	-	-	-	-	-	111	**111**
Total	**331**	**117**	**15**	**198**	**10**	**3**	**111**	**785**

[Adopted from: TD Gilmore et. al., Inhibitors of NF-jB signaling: 785 and counting. *Oncogene* (2006) 25, 6887–6899. For more details about the inhibitors, follow the reference supplementary data]

may, at least in part, be due to their ability to inhibit NF-κB. However, the inhibitory drugs primarily targeted for specific clinical use very often show side-effects. Hence there is a scope of designing and developing even better synthetic or natural-modified drugs that will target the specific molecule in the pathway and endorse the effect.

3.1.3.6 NF-κB in Cancer:

"The role of NF-κB in cancer": has been a highly demanding and interesting field of research since last two decades. The abundance of data indicates that NF-κB can act as both "Tumour promoter as well as Tumour suppressor" [287, 292]. Although it is context dependent still remains as a matter of debate. An important implication of the hypothesis that NF-κB can function as a tumor suppressor is that its behaviour in normal untransformed cells might be quite different from that in transformed and malignant tumor cells. Oncogenic stimulation of untransformed cells will not only activate DNA-binding and transcriptional activity of NF-κB but will also activate the tumor suppressor programs of the cell (Figure-3.7) [293-295]. These tumor suppressors, in particular p53 and ARF, can then act to inhibit the tumorigenic functions of NF-κB. In fact, the data suggest that they will actively utilize NF-κB subunits to repress the potentially tumorigenic genes normally induced by NF-κB activity [296, 297]. Thus, in the early stages of cancer, NF-κB might be tumor-suppressing rather than tumorpromoting. However, as the potential cancer cells accumulate more mutations, there will be selective pressure on them to lose the expression of tumor-suppressor genes. The effect on NF-κB will be a reversal of its role. The mechanisms for keeping the tumorigenic functions of NF-κB in check will no longer be in place. Rather its tumorpromoting activity will be unleashed, with NF-κB subunits becoming free to induce the expression of a wide range of genes that can promote the development of malignant and metastatic tumors. It should be acknowledged that, similar to the requirements for different tumor

suppressors and oncogenes, this two-step mechanism for NF-κB function in cancer development is probably both tumor and cell-type specific.

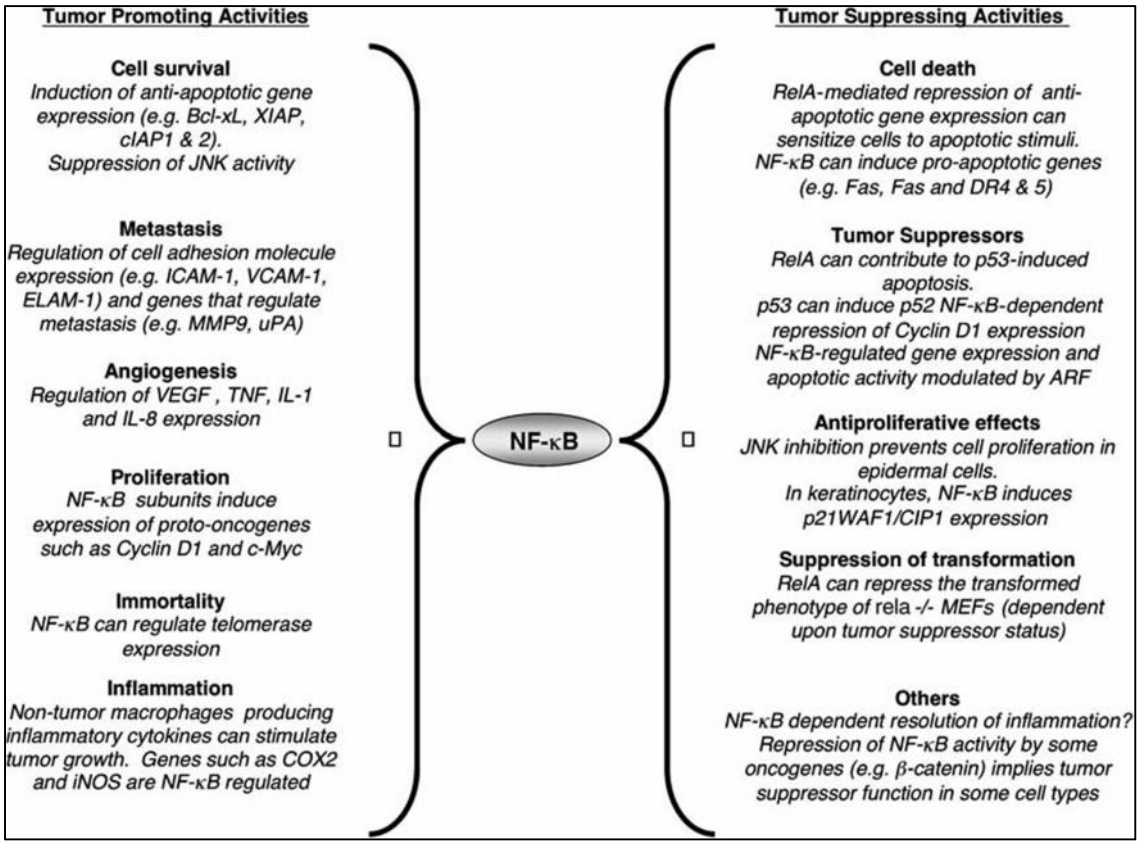

Figure-3.7: Different functions of NF-kB can have either tumor-promoting or tumor suppressing effects. On the left is a summary of the different tumorigenic processes to which aberrantly active NF-kB has been shown to contribute. In contrast, on the right is evidence indicating that under other circumstances active NF-kB can act to inhibit tumor growth and survival. [Adopted from: ND Perkins et. al., Good cop, bad cop: the different faces of NF-κB. *Cell Death and Differentiation,* (2006) 13, 759–772]

This hypothesis has implications for future NF-κB based therapy. It could be important to make sure that the right form of NF-κB is present in the tumor for the treatment to be effective. Indeed, if reagents can be developed, such as phospho-specific antibodies that can distinguish between the different forms of RelA, it will be important to investigate whether there is any correlation between the functional status of NF-κB and which tumours do or do not respond to both conventional and new forms of cancer therapy. Will drugs that inhibit NF-κB actually cause cancer? At this time, it seems

improbable that NF-κB is a sufficiently potent tumor suppressor, whereby its inhibition would result in the formation of cancer cells in humans. It is possible, however, that such drugs might stimulate the growth of tumours still undetected but present at early stages of development. Therefore, although inhibiting the activity of NF-κB represents a potentially exciting new therapy, it should be remembered that NF-κB performs functions that we might not want to inhibit and thus appropriate caution should be taken. However many reports suggests a high NF-κB activity persists and seems indispensable for tumerigenesis in many cancers. If that is the case, specific inhibitor can be developed to target critical steps/molecules in the signaling pathway without intervening the physiology of normal cells.

3.2 RATIONALE OF THE STUDY AND HYPOTHESIS:

Short Linear Sequence Motif (SLIM) have been identified as functionally relevant recognition motifs in SH2, SH3 domain containing proteins [298]. Based on the classical property of some PDZ domains to recognize 4-7 C-terminal residues or SLIMs in proteins, we recently identified several novel interacting partners of PSMD9 [204]. We also identified novel interacting partners of gankyrin (PSMD10), a chaperone of the proteasome (another non-ATPase subunit of 19S) and an oncoprotein by recognizing proteins which share EEVD, a conserved SLIM seen at the interface of gankyrin-S6 ATPase complex [299]. In addition we predicted the structure of the PDZ domain of PSMD9 and identified residues at the PDZ-interface which are important for recognizing the C-terminal residues of four novel interacting partners [204]. hnRNPA1, a RNA binding protein involved in mRNA export, splicing and protein translation was one of the novel interacting partners. This protein in mouse CB3 cells was reported to be responsible for IκBα degradation by an unknown mechanism leading to transcriptional activation of NF-κB [300]. This observation formed the premise of this

work which aims to establish the functional relevance of newly found PSMD9-hnRNPA1 interaction.

It is with this background that we were intrigued by the reports of Hay *et. al.*, who demonstrated interaction between ankyrin repeats of IκBα and hnRNPA1 which somehow seemed necessary for IκBα degradation and NF-κB transcriptional activity. But the identity of the protease involved and the role of proteasome in this process was not established. Since the bigger and fundamental question of how IκBα is recruited to the proteasome for degradation remains largely unaddressed, it would be interesting to investigate whether hnRNPA1, well known for its role in mRNA processing and transport [301], cross talks with the proteasomal degradation pathway in human cells. The mechanism by which ubiquitinated proteins are recruited to proteasome remains an active area of research. Hence, based on our finding that PSMD9 interacts with hnRNPA1 *in vitro* [204], and the reported role of hnRNPA1 in IκBα degradation and NF-κB activity, we hypothesized that **"PSMD9 may have a role in the degradation of IκBα by the proteasome and influence NF-κB activity in human cells"**.

To address the hypothesis we had set some fundamental questions to answer experimentally, that are as follows:

1. Whether PSMD9 and hnRNPA1 interact ex vivo?
2. Whether this interaction is PDZ domain-C-terminus specific?
3. Whether levels of PSMD9 in mammalian cells affect NF-κB activity?
4. Does the interaction between PSMD9 and hnRNPA1 promote IκBα degradation?
5. Whether this interaction influences NF-κB activity?
6. How exactly PSMD9 is involved in the IκBα degradation process?

To answer these questions we put forth following objectives:

1. To establish HEK293 cells as our model system
2. To generate stable clones in which PSMD9 will be overexpressed and silenced in an inducible system in HEK293 cells.
3. To monitor the NF-κB activity by various cell biology and biochemical studies.
4. To find out the molecular mechanism of PSMD9 involvement in the NF-κB signaling pathway.
5. To elucidate how important the PSMD9-hnRNPA1 interaction is for this biological process.

3.3 RESULTS:

3.3.1 Establishment of the Stable clones in HEK293 cells:

We established stable clones in HEK293 cells expressing human PSMD9 gene or human PSMD9-shRNA, following the antibiotic selection method described in Chapter-II (materials and methods). Accordingly we generated two types of stable clones under doxycycline inducible system: (1) which overexpress FLAG tagged human PSMD9; 3 no. of PSMD9-inducible Overexpression clones (P9-iOE clones) viz., TP9-C2, TP9-C3 & TP9-C9 and (2) which express human PSMD9-shRNA; 3 no. of PSMD9-inducible Knock Down clones (P9-iKD clones) viz., TP9-sh1, TP9-sh3 & TP9-sh11. The levels of expression of PSMD9 in all the different clones were detected by western blot and qRT-PCR techniques. In overexpression clones which was found to be 15-20 fold upregulation in protein levels and 20-30 fold upregulation in mRNA levels and in the knock down clones it is found to be 80-90% downregulation regulation in both protein and mRNA levels of PSMD9 (Figure-3.8).

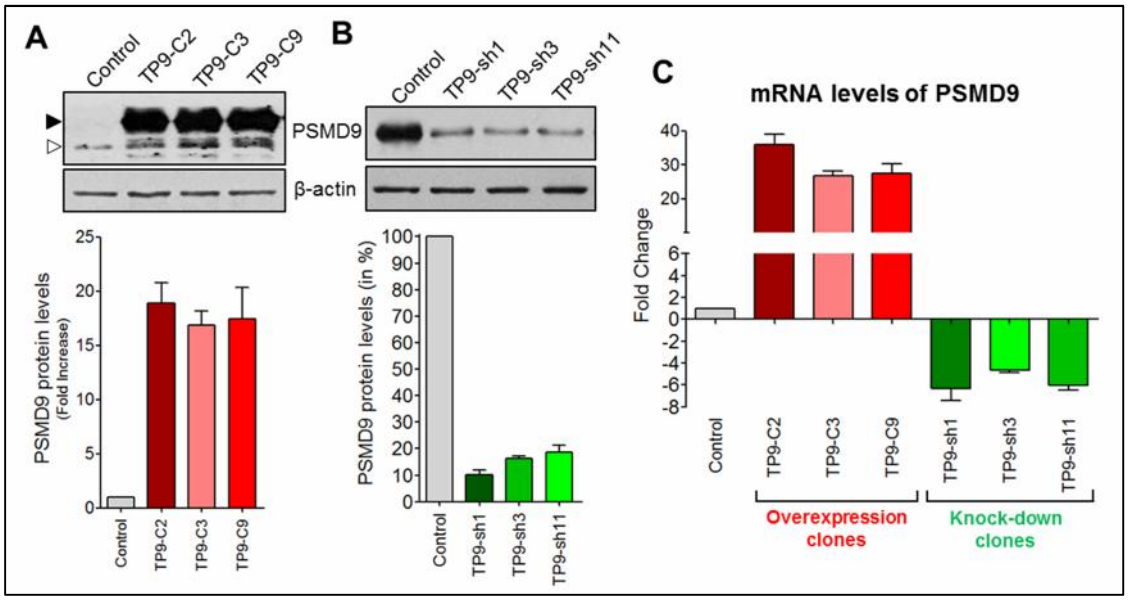

Figure 3.8 Expression levels of PSMD9 in the stable clones in HEK293 cells. (A) 3 clones of HEK293 cells inducibly expressing FLAG-PSMD9 were either treated with doxycycline or left untreated and the cell lysates were analyzed by western blot. The graph shows a 15-20 fold overexpression of PSMD9 protein levels in the clones. **(B)** 3 clones of HEK293 cells inducibly

expressing PSMD9-shRNA were either treated with doxycycline or left untreated and the cell lysates were analyzed by western blot. The graph shows a 80-90% downregulation of PSMD9 protein levels in the clones. **(C)** mRNA levels of PSMD9 in the P9-iOE and P9-iKD clones are quantitated by real time PCR.

3.3.2 PSMD9 interacts with C-terminus of hnRNPA1 endogenously:

Using a bioinformatics approach [204] and the knowledge that some PDZ domains interact with C-terminal regions of proteins [210], we predicted putative interacting partners of PSMD9, from the human proteome. This prediction was validated by screening C-terminal peptides for their ability to bind to pure recombinant PSMD9. Using this strategy we identified hnRNPA1 as a novel interacting partner of PSMD9 and further proved that this interaction is mediated by the C-terminal residues of hnRNPA1 [204]. To test if endogenous PSMD9 and hnRNPA1 interact with each other which would be physiologically relevant and important for function we perform a series of immunoprecipitation experiments. We used anti-PSMD9 antibody to immunoprecipitate PSMD9 from HEK293 cell lysate and probed for the presence of hnRNPA1 using anti-hnRNPA1 antibody. As expected, hnRNPA1 was found in the IP complex (Figure-3.9A). We further validated this endogenous interaction by performing a reverse-IP where hnRNPA1 antibody was used for immunoprecipitation and the complex was probed with anti-PSMD9 antibody (Figure-3.9B).

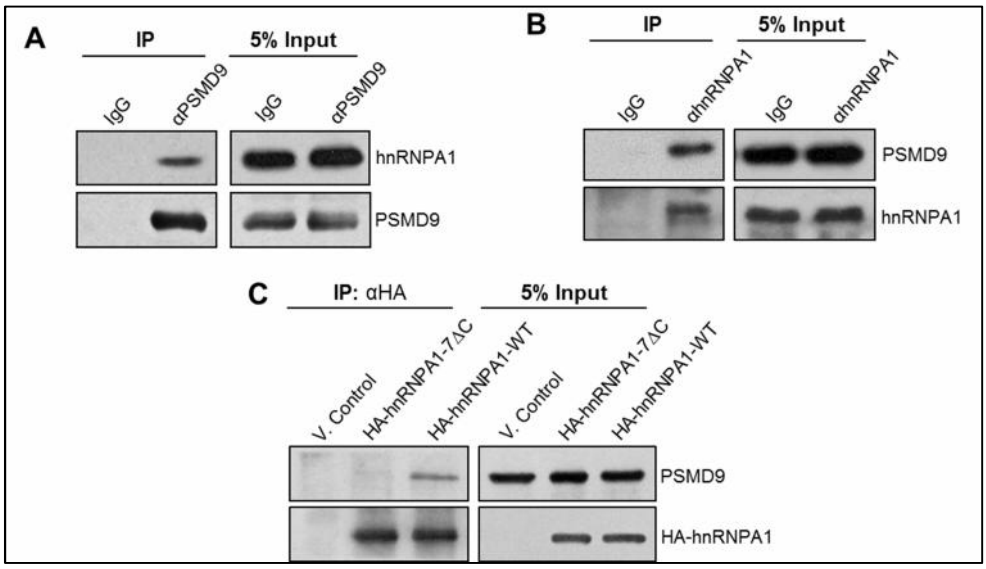

Figure-3.9 PSMD9 interacts with wild type hnRNPA1 but not with 7ΔC mutant of hnRNPA1 *ex vivo*. (A) HEK293 cell lysate was incubated either with anti-PSMD9 Ab-bound protein-G sepharose beads or mouse IgG (isotype control) bound protein-G sepharose beads. Pull down complexes were probed with anti-hnRNPA1 and anti-PSMD9 antibodies. **(B)** HEK293 cell lysate was incubated with either Anti-hnRNPA1 Ab-bound protein-G sepharose beads or mouse IgG isotype bound protein-G sepharose (isotype control). Then pull down complexes were probed with anti-PSMD9 and anti-hnRNPA1 antibodies and analysed by WB. **(C)** Wild type HA-hnRNPA1 or 7ΔC mutant HA-hnRNPA1 was transiently overexpressed in HEK293 cells and cell lysates were incubated with anti-HA Ab-bound protein-G sepharose beads. Pull down complexes were probed with anti-PSMD9 Ab and analyzed by WB.

We reconfirmed our earlier observation [204] that the C-terminus of hnRNPA1 interacts with PSMD9 in the cellular milieu. We trans-expressed wild type HA-hnRNPA1 and the mutant Δ7C –HA-hnRNPA1 in HEK293 cells. Immunoprecipitation was carried out using anti-HA antibody and when probed with anti-PSMD9 antibody, PSMD9 was only detected in wild type HA-hnRNPA1-IP not in case of C-terminal mutant hnRNPA1 (Figure-3.9C). These results again confirmed that PSMD9 interact with the C-terminal residues of hnRNPA1 endogenously.

3.3.3 Overexpression of PSMD9 enhances basal and TNF-*α* mediated NF-*κ*B transcriptional activity:

In CB3 cells, hnRNPA1 reportedly interacts with I*κ*B*α* and overexpression of hnRNPA1 enhances NF-*κ*B transcriptional activity [300]. No such role has been reported for hnRNPA1 in human cells. Since we found that PSMD9 interacts with hnRNPA1 *ex vivo* and hnRNPA1 reportedly influences NF-*κ*B activity, we asked if PSMD9 was involved in this pathway. If so, changes in the levels of PSMD9 must influence NF-*κ*B activity. Hence, PSMD9 was overexpressed under doxycycline inducible conditions in three different stable clones (P9-iOE clones) (Figure-3.10B), and NF-*κ*B transcriptional activity was measured by Luciferase reporter assay (Figure-3.10A). In all the three inducible clones NF-*κ*B activity was found to be 3-4 fold higher than that of the uninduced control cells (Figure-3.10C). In addition we regulated the

expression of PSMD9 using the inducible system in P9-iOE cells (Figure-3.10D) and found that doxycycline induced the expression of PSMD9 in a concentration dependent manner, which led to a corresponding increase in NF-κB transcriptional activity monitored using luciferase reporter assay (Figure-3.10E and F). In addition, when doxycycline induced or uninduced cells were treated with TNF-α (20ng/ml media), a potent signal for NF-κB activation [302], NF-κB transcriptional activity were increased. This increase was more pronounced in P9-iOE cells (Figure-3.10G). These results suggest there exists a correlation in PSMD9 overexpression and NF-κB basal and signal mediated activation in HEK293 cells.

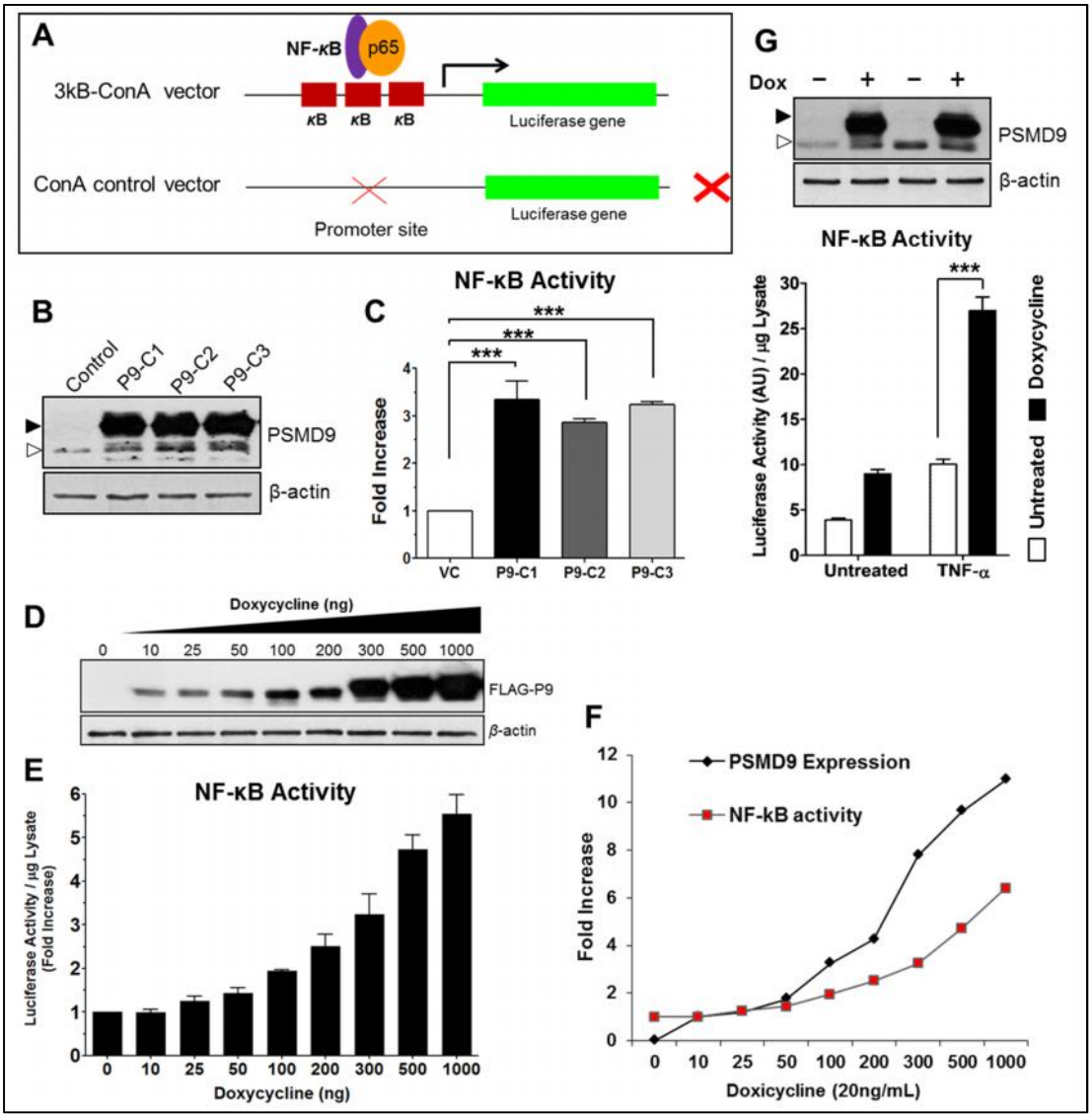

Figure-3.10 PSMD9 enhances basal and TNF-*α* mediated NF-*κ*B transcriptional activity. **(A)** NF-*κ*B transcriptional activity was measured by ConA-Luc Luciferase reporter vector. The vector contains 3*κ*B enhancer elements (NF-*κ*B binding site) at the promoter site upstream to the luciferase gene. The ConA-control vector does not have 3*κ*B enhancer elements. **(B)** Three P9-iOE clones of HEK293 cells inducibly expressing FLAG-PSMD9 were either treated with doxycycline or left untreated and the cell lysates were analyzed by western blot. **(C)** The above clones were transfected with 3x *κ*B ConA luc vector or ConA luc control vector and induced with doxycycline (1µg/mL of media). After 48h of induction NF-*κ*B activity was checked by measuring luciferase activity using dual luciferase substrate. Luciferase activity from firefly luciferase was normalized with renilla luciferase used as a transfection control. Data represents mean luciferase activity/µg of protein, ± SEM of two independent experiments done in triplicates. **(D)** P9-iOE cells were transfected with 3x *κ*B ConA luc vector or ConA luc control vector. Cells were induced with different concentrations (0-1000ng/mL of media) of doxycycline. After 48 hrs of induction, levels of FLAG-PSMD9 were analyzed by WB. **(E)** NF-*κ*B activity was checked by measuring luciferase activity of the above described (in (D)) cell lysates, using dual luciferase substrate. Luciferase activity from firefly luciferase was normalized with renilla luciferase used as a transfection control. Data represents mean luciferase activity/µg of protein, ± SEM of two independent experiments done in triplicates. **(F)** Graphical representation of the direct correlation between PSMD9 expressions and NF-*κ*B activity. **(G)** P9-iOE cells were transfected with 3x κB ConA luc vector or ConA luc control vector. Transfected cells were either treated with doxycycline (1µg/mL of media for 48h) and/or with TNF-α 12h or left untreated. NF-κB activity was determined by measuring firefly luciferase activity and normalized with renilla luciferase used as transfection control. Data represents mean luciferase activity/µg of protein ± SEM of two independent experiments done in triplicates. WB shows the level of PSMD9 expression in these cell lysates. Symbol ►corresponds to trans-expressed FLAG-PSMD9 and symbol Δ corresponds to the endogenous PSMD9.

3.3.4 Overexpression of PSMD9 enhances the nuclear translocation of NF-*κ*B (p65)

Increased NF-*κ*B activity is very often reflected by increase in nuclear translocation of the NF-*κ*B dimer p65-p50 [253]. Hence to validate our results we traced p65 translocation upon PSMD9 overexpression in our model system. The nuclear fraction of P9-iOE cells upon Doxycynline treated/untreated conditions were separated out and analysed by WB using anti-p65 antibody. In the Dox-treated cells nuclear p65 levels were found to be increased upto 2-2.5 fold (in all 3 clones) in comparison to Dox-untreated cells (Figure-3.11A). We also performed immunofluorescence experiment to check the p65 levels in the nucleus of P9-iOE cells. The IF-images showed 5-6 fold increased p65 levels in Dox-treated P9-iOE cell nuclei (Figure-3.11B). These experiments suggest NF-*κ*B p65-subunit translocation increased upon PSMD9 overexpression in HEK293 cells.

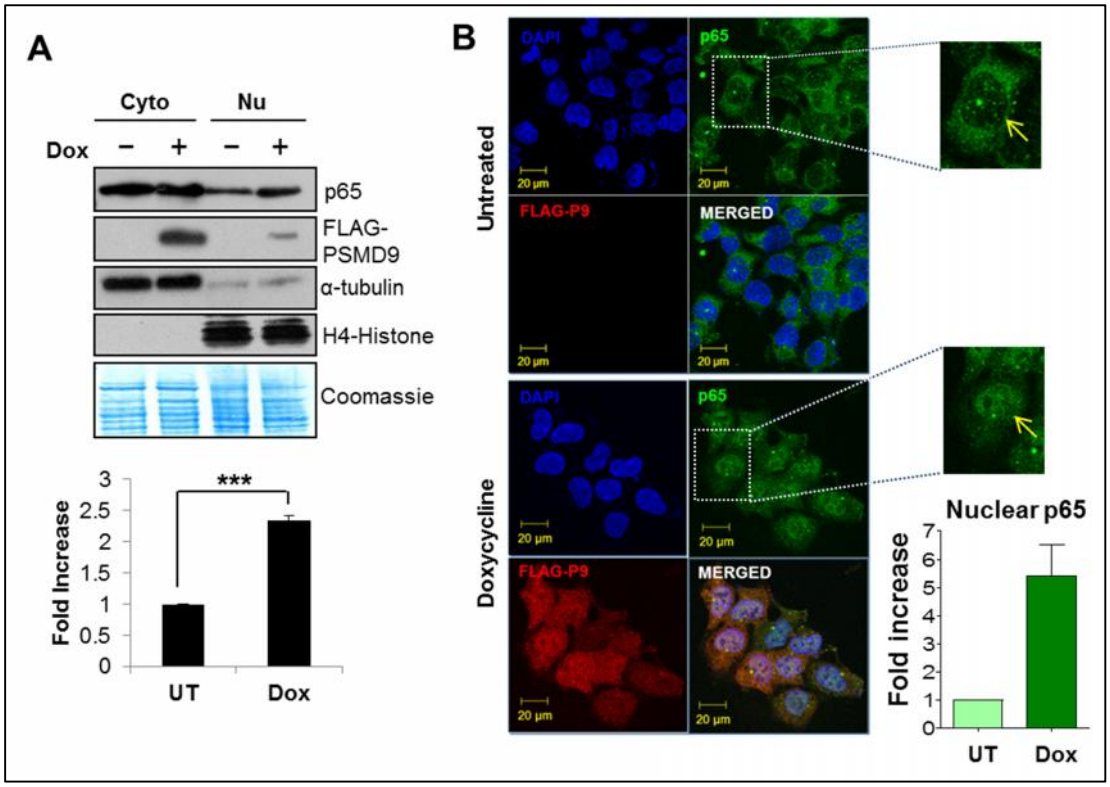

Figure-3.11 PSMD9 enhances p65 nuclear translocation. P9-iOE cells were either treated with doxycycline (1µg/mL of media for 48h) or left untreated. **(A)** Nuclear fractions from the above cells were prepared as described in materials and methods and analysed by WB. Graph represents mean fold increase of p65 nuclear translocation ± SEM of two independent experiments in three different stable clones. **(B)** Cells were grown on polylysine coated glass coverslip. Immunofluorescence staining was done following the protocol described in materials and method, using anti-p65 (with secondary Alexaflour-488) and anti-FLAG (with secondary Alexaflour-568). Images were taken Laser confocal microscope (Nikon LSM-meta510). Graph represents the mean fold increase of p65 intensity ± SEM of two different clones. Intensity was measured and calculated by LSM software analysis.

3.3.5 Overexpression of PSMD9 enhances NF-κB-p65 DNA-binding and transcriptional activity:

Influence of PSMD9 overexpression on NF-κB activity was further validated by demonstrating the increase in DNA binding activity of NF-κB (p65). Nuclear fractions from the P9-iOE cells were separated out and Electrophoretic Mobility Shift Assay (EMSA) was performed using biotinlyated κB-oligos. EMSA experiment showed binding of NF-κB to the κB enhancer element was increased significantly in Dox-treated P9-iOE cells, than the Dox-untreated cells (Lane 3, 8 and 13, Figure-3.12A).

This binding was further increased upon TNF-*α* treatment and more pronounced upon PSMD9 overexpression (Lane 14 & 15, Figure-3.12A). In addition this binding was competed out by unlabeled wild type *κ*B-oligos but not by mutant *κ*B-oligos which indicated the specificity of NF-*κ*B binding (Lane 4 & 5, Figure-3.12A) [303]. Furthermore when the reaction mixture was incubated with anti-p65 antibody, a supershift band was obtained which confirms the presence of p65 and its DNA binding activity (Lane 10, Figure-3.12A). In addition, five of NF-*κ*B target genes viz. ICAM1, IL6, I*κ*B*α*, A20 and COX2 [304] were found to be several fold upregulated in Dox-treated P9-iOE cells as compared to Dox-untreated cells (Figure-3.12B &C). These results altogether substantially indicate that overexpression of PSMD9 enhances both basal and signal mediated NF-*κ*B activity.

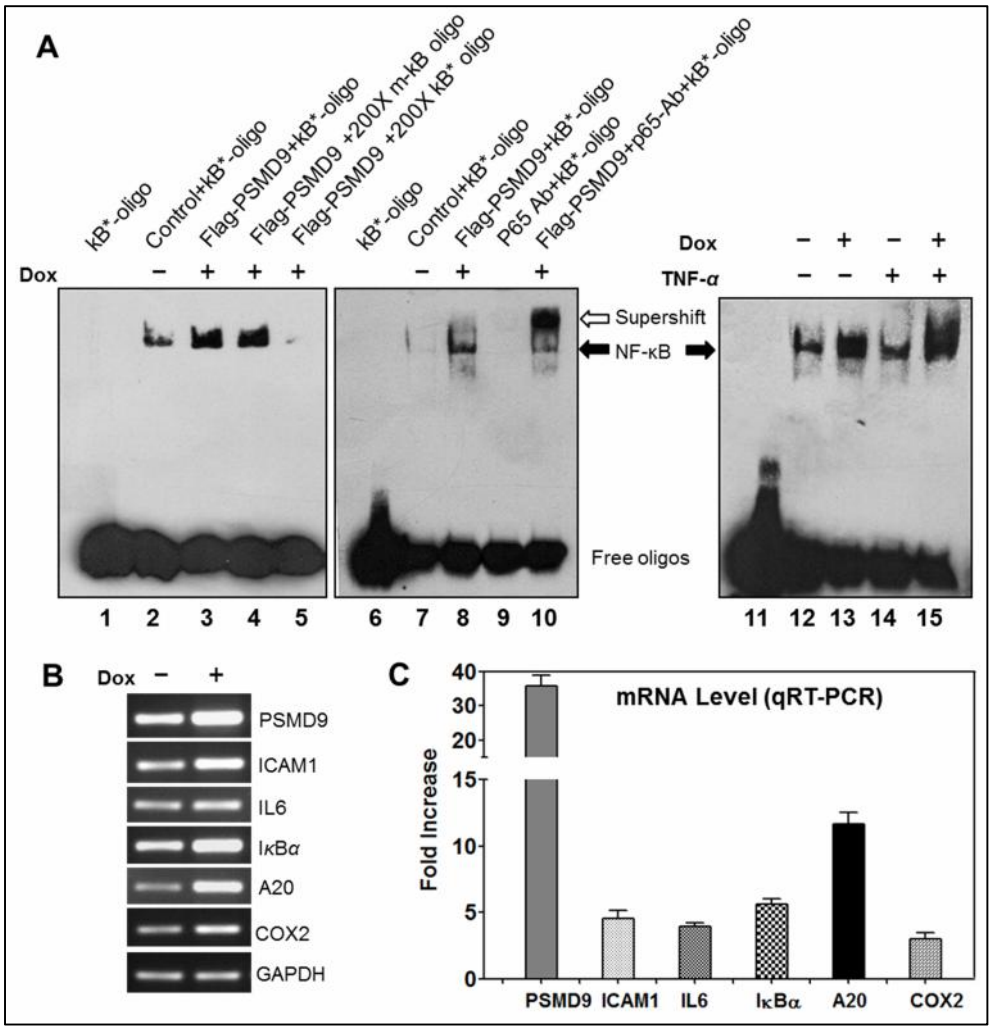

Figure-3.12 PSMD9 enhances p65-NF-κB DNA binding activity and transcriptional activity. (A) P9-iOE clone cells were either treated with doxycycline (1µg/mL of media for 48h) or left untreated. The nuclear fractions were subjected to EMSA (following the protocol described in material & methods). Lanes 1 and indicate biotinylated oligos only. The upper gel shift band (black arrow) indicates NF-κB DNA binding activity in doxycycline untreated (lanes 2 and 7) and treated (lanes 3 and 8) cells. NF-κB DNA binding specificity is shown by competing it with 200X unlabeled mutant oligos (lane 4) or WT oligos (lane 5). In lane 9 and 10 anti-p65 antibody was incubated with the binding reaction mix (with/without lysate) and the white arrow indicates the resulting supershift band. From lane 11-15, P9-iOE cells were either treated with doxycycline (1µg/mL of media for 48h) and/or with TNF-α (20ng.mL of media) for 12h or left untreated or left untreated. Lanes 11 and indicate biotinylated oligos only. The upper gel shift band (black arrow) indicates NF-κB DNA binding activity in doxycycline untreated (lanes 12 and 14) and treated (lanes 13 and 15) cells. Upon TNF-α treatment NF-κB DNA binding activity increased shown by the thick gel shift band (in Lane 14 and 15). **(B)** P9-iOE cells were either treated with doxycycline for 48h or left untreated. RNA was isolated and semi-quantitative reverse transcriptase PCR was performed for 5 different target genes and the PCR products were run in a 2% agarose gel. **(C)** Real-time PCR was performed for the same five different target genes. Graph represents GAPDH normalized mean fold increase in mRNA level of the genes ± SEM of three independent experiments done in duplicates.

3.3.6 PSMD9 overexpression accelerates degradation of IκBα:

In classical NF-κB pathway, upon signal induction, NF-κB bound IκBα is degraded by the 26S proteasome and hence NF-κB get released, translocate into nucleus and confer its activity [257, 261, 270, 288]. Since in our model system, NF-κB activity increased upon increase in the levels of PSMD9, we hypothesized that PSMD9 may accelerate the degradation of IκBα by the ubiquitin proteasomal pathway. Accordingly when PSMD9 expression was induced by doxycycline in the P9-iOE cells, there was a visible decrease in IκBα protein after 4-6h (half-life) of cycloheximide treatment whereas in uninduced cells reduction in the levels of IκBα is seen only after 18-24h of treatment (Figure-3.13A & C). Similarly signal mediated IκBα degradation was considerably enhanced 10 min post TNF-α treatment in P9-iOE cells induced to overexpress PSMD9 (Figure-3.13B & D). These results indicate that PSMD9 is involved in modulating IκBα levels presumably through proteasomal degradation in both basal as well as signal mediated NF-κB signaling pathway.

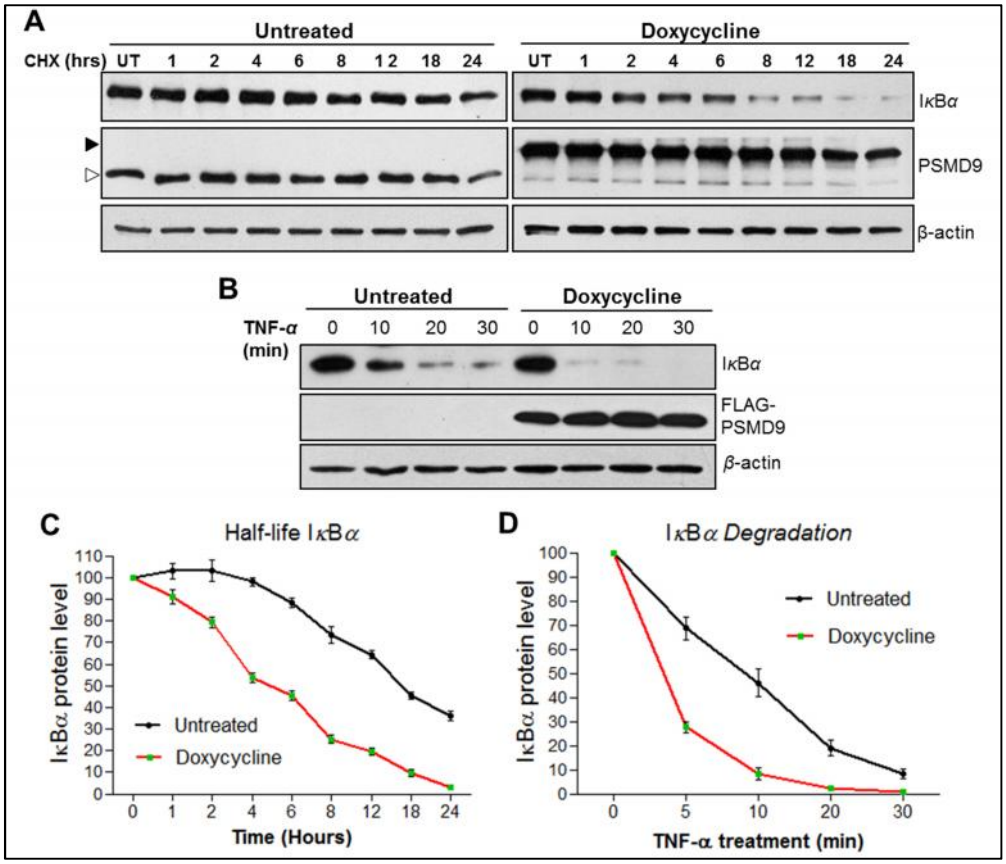

Figure-3.13 Overexpression of PSMD9 enhances IκBα degradation. (A) P9-iOE stable clones were either treated with doxycycline (1µg/mL of media for 48h) and/or cycloheximide (CHX) (50µg/mL of media for 1, 2, 4, 6, 8, 12, 18 and 24h) or left untreated. Cell lysates were prepared and analyzed by WB. **(B)** Both doxycycline treated or untreated P9-iOE clones were stimulated with TNF-α (20ng/mL of media) for 0, 10, 20 and 30 min. Cell lysates were subjected to WB. **(C)** Graphical representation of the WB data of (A) showing the half-life of IκBα. **(D)** Graphical representation of the WB data of (B) showing the IκBαdegradation upon TNF-α treatment.

3.3.7 Knockdown of PSMD9 decreases basal and signal mediated activation of NF-*κ*B and I*κ*B*α* degradation rate:

In order to validate the effect of trans-expressed PSMD9 in HEK293 cells on NF-*κ*B signaling pathway we knocked down endogenous PSMD9 in HEK293 cells (P9-iKD clones) under inducible conditions. Upon knockdown of PSMD9, I*κ*B*α* levels were found to be stable even after 24 hours of cycloheximide treatment (Figure-3.14A & B). In the same cells upon Dox-treatment a reduction in TNF-*α* induced I*κ*B*α* degradation was observed whereas in Dox-untreated cells I*κ*B*α* degradation was already apparent

after 20min of TNF-*α* treatment (Figure-3.14C & D). Concominantly a decrease in NF-*κ*B DNA binding activity was observed by EMSA both in TNF-*α* treated and untreated PSMD9 knockdown cells (Figure-3.14E). This was further confirmed by semi-quantitative RT-PCR and real time PCR of five different NF-*κ*B target genes viz. ICAM1, IL6, I*κ*B*α*, A20 and COX2, the levels of which decreased in PSMD9 knockdown cells as compared to the Dox-untreated cells (Figure-3.14F & G). These results indicate that endogenous PSMD9 indeed is responsible for the basal and signal induced degradation of I*κ*B*α* and subsequent increase in NF-*κ*B activity.

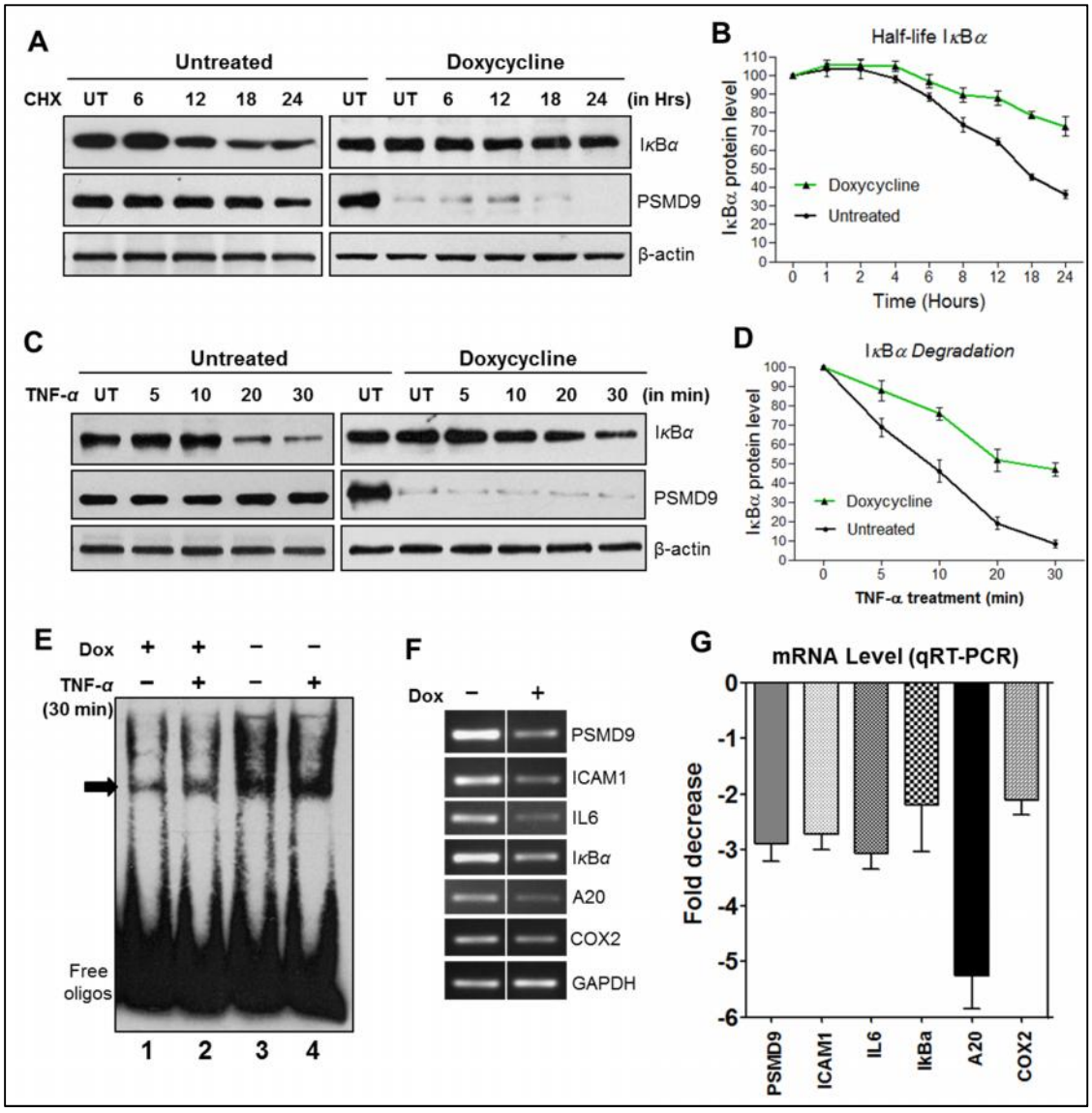

Figure-3.14 Knockdown of PSMD9 decreases IκBα degradation and NF-κB activation. (A) P9-iKD stable cells were either treated with doxycycline (4μg/mL of media for 48h) and/or CHX

(50µg/mL of media for 1, 2, 4, 6, 8, 12, 18 and 24h) or left untreated. Cell lysates were prepared and analyzed by WB. **(B)** Graphical representation of the WB data of (A) showing the half-life of IκBα **(C)** Both Dox-treated or untreated P9-iKD cells were stimulated with TNF-α (20ng/mL of media) for 0, 5, 10, 20 and 30 min. Cell lysates were subjected to WB. **(D)** Graphical representation of the WB data of (B) showing the IκBαdegradation upon TNF-α treatment. **(E)** Nuclear fractions of both doxycycline and TNF-α treated or untreated P9-iKD cells were subjected to EMSA. The upper band corresponds to NF-κB DNA binding activity in Dox +ve (lane 1 & 2) and Dox –ve (lane 3 & 4) cells. **(F)** P9-iKD cells were either treated with doxycycline for 48h or left untreated. RNA was isolated and semi-quantitative reverse transcriptase PCR was performed for 5 different target genes and the PCR products were run in a 2% agarose gel. **(G)** Real-time PCR was performed for the same five different target genes. Graph represents GAPDH normalized mean fold decrease in mRNA level of the genes ± SEM of three independent experiments done in duplicates.

3.3.8 PSMD9 mediated I*κ*B*α* degradation occurs via ubiquitin-proteasomal system:

Although there are substantial reports suggest that, I*κ*B*α* degradation is predominantly mediated by ubiquitin proteasomal system, there are studies indicating non-proteasomal way of I*κ*B*α* degradation preferably by calpain [274, 275, 277]. Hence to determine the role

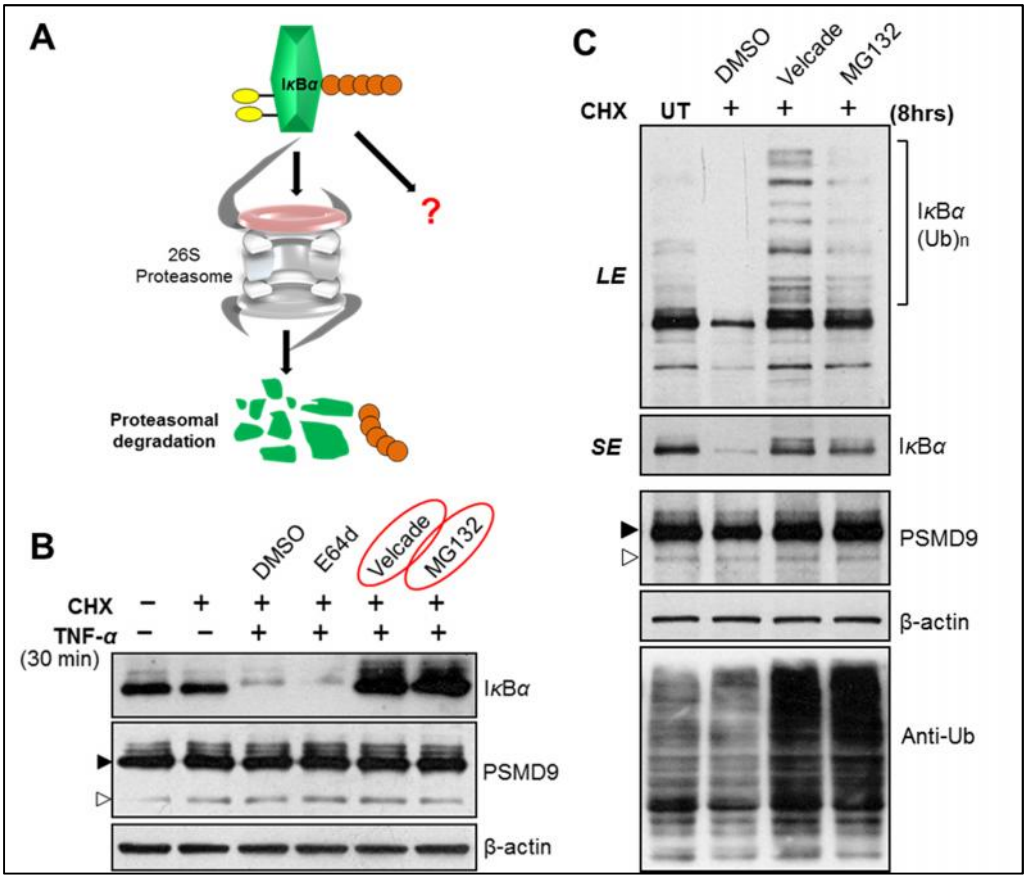

Figure-3.15 PSMD9 mediated IκBα degradation occurs via ubiquitin-proteasomal system. **(A)** Cartoon representation of possible degradation of IκBα via proteasome. **(B)** P9-iOE cells were treated with MG132 (10μM), velcade (10μg/mL of media), E64d (10μM) or 0.1% DMSO for 6h and either stimulated with TNF-α (20ng/mL of media) for 30 min or left unstimulated and the lysates were analyzed by WB. Symbol ►corresponds to trans-expressed FLAG-PSMD9 and symbol Δ corresponds to the endogenous PSMD9. **(C)** P9-iOE cells were either treated with doxycycline (1μg/mL of media), CHX (50μg/mL of media for 8h), (where indicated), and with MG132 (10μM), velcade (10μg/mL of media) or 0.1% DMSO for 6h and analyzed by WB. LE-long exposure and SE short exposure. At LE accumulation of polyubiqutinated IκBα is observed in case of velcade and MG132 treatment.

of proteasome in PSMD9 mediated degradation of I*κ*B*α*, we treated P9-iOE cells with proteasome inhibitors and calpain inhibitor under doxycycline induction. Treatment with MG132 or Velcade significantly inhibited both basal and TNF-*α* mediated I*κ*B*α* degradation in cells overexpressing PSMD9, but E64d (calpain inhibitor) could not inhibit the I*κ*B*α* degradation (Figure-3.15B & C). This suggests the involvement of 26S proteasome in the degradation process. In further support of proteasomal degradation, ubiquitinated I*κ*B*α* was also seen to accumulate when PSMD9 overexpressing cells were treated with both the proteasomal inhibitors (Figure-3.15C).

3.3.9 PSMD9 does not influence phosphorylation of I*κ*B*α* in the process:

It is also well established that degradation of I*κ*B*α* by the proteasome, upon signal induction, requires phosphorylation at sites S32 & S36 [253, 267]. Hence, we next determined whether the processing of I*κ*B*α* occurs through the same way in case of PSMD9 mediated degradation, and if PSMD9 is involved in the phosphorylation process in accelerating the degradation process. P9-iOE clone cells and P9-iKD clone cells were treated with doxycycline for 48hr and/or TNF-*α* (20ng/ml) for 5 minutes. WB from the above treated cell lyasates showed no difference in the levels phospho-I*κ*B*α* across different clones. This suggests PSMD9 does not influence the phosphorylation of I*κ*B*α* to enhance its degradation.

Next we wanted to test if at all phosphorylation is necessary at the particular site for this PSMD9 mediated IκBα degradation. We overexpressed a phospho-dead mutant IκBα super-repressor (S32A-S36A) in control cells as well as in P9-cOE cells. WB confirmed that after 30min of post TNF-α induction, super-repressor IκBα was not degraded even under PSMD9 overexpression condition, whereas endogenous IκBα got degraded significantly as seen in earlier experiments (Figure-3.16C). In accordance NF-κB activity is decreased significantly in these cells upon overexpression of the super-repressor irrespective of PSMD9 overexpression (Figure-3.16D). These results indicate that phosphorylation at S32 and S36 is necessary for the PSMD9 mediated IκBα degradation by the proteasome.

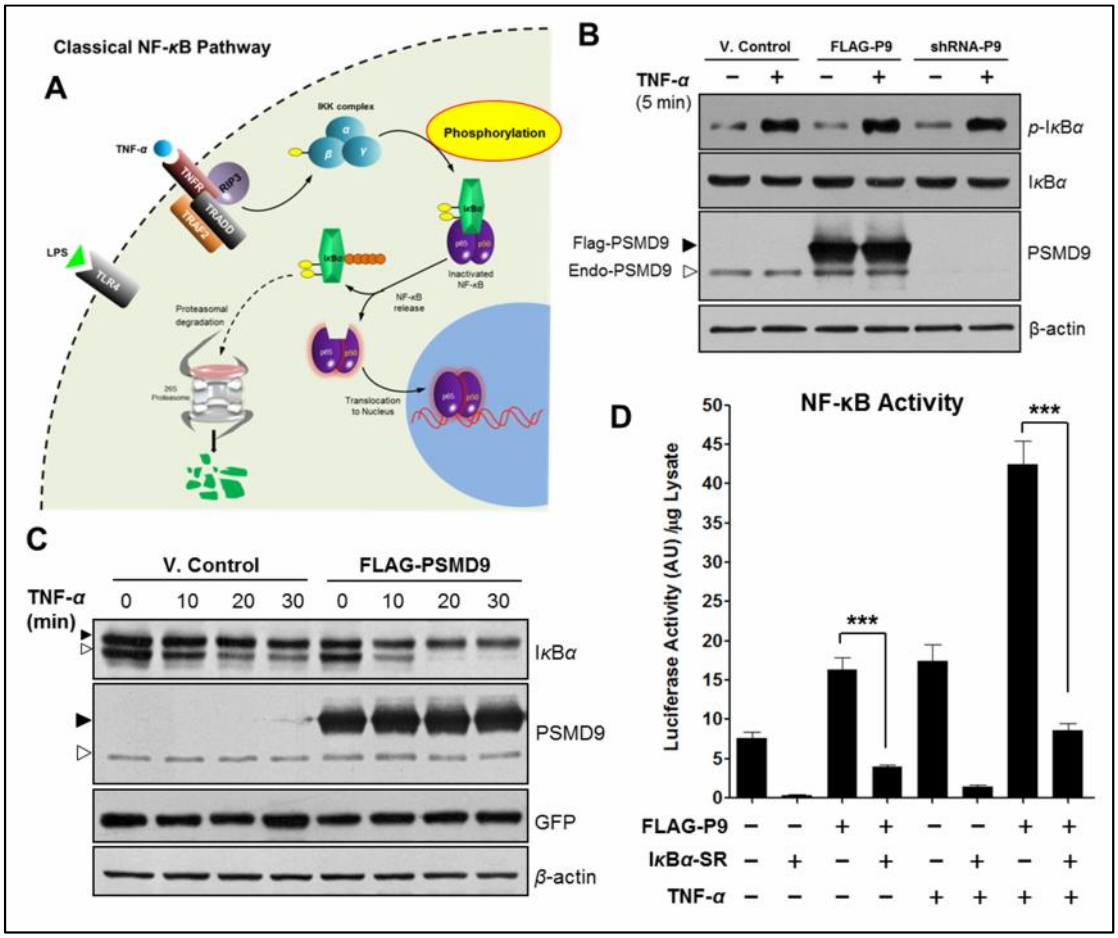

Figure-3.16 PSMD9 does not influence phosphorylation of IκBα. (A) Cartoon representation of classical NF-κB signaling pathway showing, IKK phosphorylate IκBα at S32 and S36. **(B)** Inducible stable clones of P9-iOE and P9-iKD cells were either treated with doxycycline and/or with TNF-α (20ng/ml) for 5min or left untreated, cell lysate were prepared and analysed by WB.

(C) HEK293 FLAG-PSMD9 constitutive stable clones (P9-cOE clones) and pCMV10 empty vector stable clones were transiently co-transfected with pTRIPZ-IκBα-SR and pEGFPN3 vector. Cells were induced with doxycycline (1µg/mL of media) for 48h and treated with TNF-α (20ng/mL of media) for 0, 10, 20 and 30 min. Cell lysates were prepare and analyzed by WB. Symbol ► corresponds to trans-expressed FLAG-IκBα-SR or FLAG-PSMD9 and symbol Δ corresponds to the endogenous IκBα or PSMD9. **(D)** P9-cOE stable clones and pCMV10 empty vector stable clones were co-transfected with pTRIPZ- IκBα-SR and 3x κB ConA luc vector or ConA luc control vector and induced with doxycycline (1µg/mL of media). After 36h of induction cells were either treated with TNF-α (20ng/mL of media) for 12h. Cell lysates were prepared and NF-κB activity was checked by measuring luciferase activity using dual luciferase substrate. Luciferase activity from firefly luciferase was normalized with renilla luciferase used as a transfection control. Data represents mean luciferase activity/µg of protein, ± SEM of two independent experiments done in duplicate.

3.3.9 PSMD9 neither influence ubiquitination of IκB*α* nor the proteasomal activity:

Due to the importance of ubiquitination of IκB*α* for its degradation by 26S proteasome, we checked the involvement of PSMD9 in this process. We treated both Dox-treated and untreated P9-iKD cells with MG132 for 2h followed by CHX treatment for 6h, 12h and 24h (Figure-3.16A). Initial Two hours of MG132 treatment resulted in 75% decrease in proteasomal activity. To ensure that after removal of MG132 and during the cycloheximide treatment (used to follow degradation of ubiquitinated IκB*α*) proteasomes were functional, activity was monitored at every assay point. 12h following removal of MG132, proteasomal activity was restored almost completely both in Dox-treated and untreated P9-iKD cells (Figure-3.16B). Coincident with the time period of CHX treatment and upon PSMD9 gene silencing, levels of ubiquitinated IκB*α* did not change significantly. Rather an increased accumulation of ubiquitinated IκB*α* was seen in these PSMD9 knockdown cells. In Dox-untreated cells there was a clear decrease in levels of ubiquitinated IκB*α* (Figure-3.16C & D). These results indicate that PSMD9 does not affect ubiquitination of IκB*α* and confirm that cells fail to degrade ubiquitinated IκB*α* efficiently not because of impaired proteasomal activity but due to the absence of PSMD9.

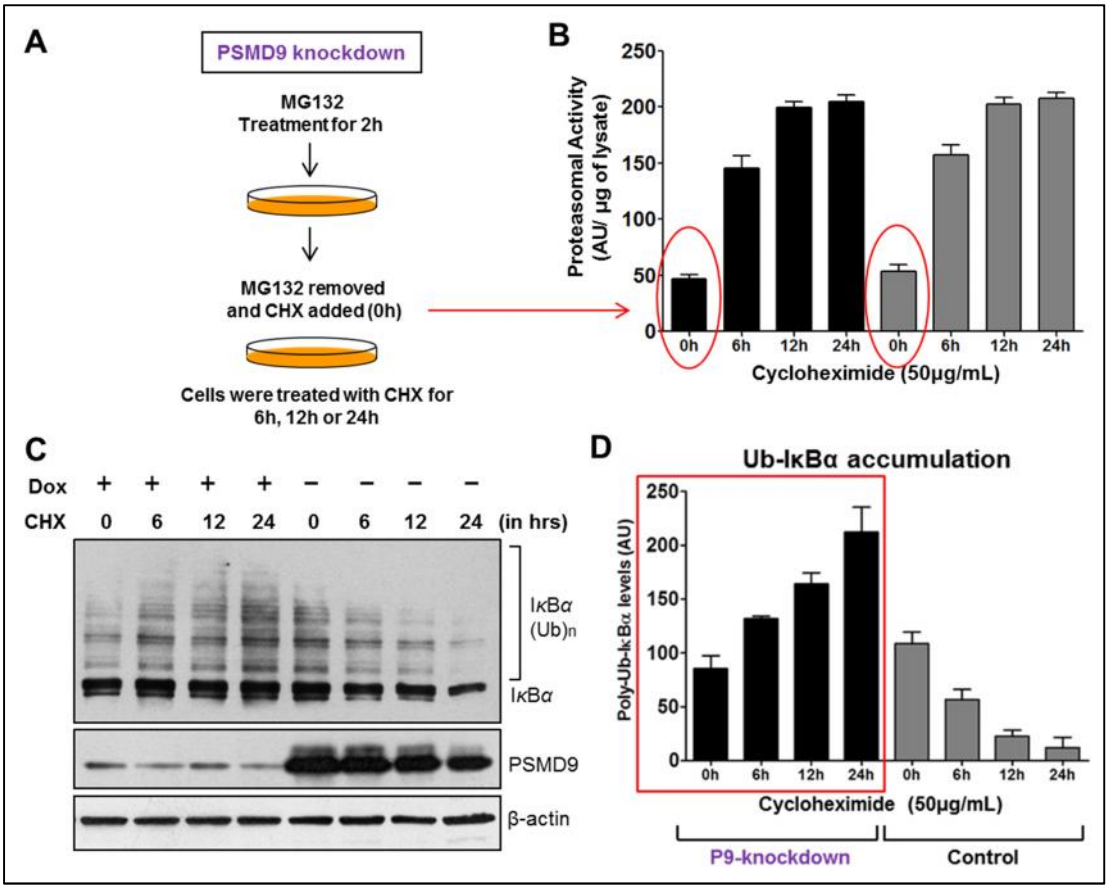

Figure-3.17 PSMD9 does not influence ubiquitination of IκBα (A) Cartoon represents the methodology for the pulse chase experiment. P9-iKD cells were either treated with doxycycline (4µg/mL of media for 48h) or left untreated. In addition cells were treated with MG132 (5µM) for 2h. Then the media was replaced with fresh media containing CHX (50µg/mL of media) for 0, 6, 12, 24h. Cell lysates were prepared for detection of proteasomal activity and WB following the protocol described in material and method. **(B)** The graph represents the proteasomal activity, measured as described in materials and methods, of cells for above experimental conditions. Data represents Suc-LLVY-AMC-proteasomal activity in arbitrary units (AU/µg of lysate) ± SEM of two independent experiments done in duplicates. **(C)** The above cell lysate were used for WB. **(D)** Graphical representation of the data from (C) showing the accumulation of ub-IκBα in above mentioned treated of P9-iKD cells. Data represents intensity of poly-ub- IκBα (in each lane) in arbitrary units (AU/µg of lysate) ± SEM of two independent experiments done in duplicates.

Given its role as an assembly chaperone, PSMD9 expression may influence proteasomal activity which in turn may dictate the overall I*κ*B*α* levels. We tested the activity of proteasome upon overexpression of PSMD9 and upon silencing the endogenous PSMD9. Proteasomal activity was unaltered in these cells and remained uninfluenced by TNF-*α* treatment (Figure-3.18A). Our observation that PSMD9 does not influence proteasomal activity is in line with a previous report by Shim et al. [305].

Here similar to our method the author used total cell lysates for monitoring proteasomal activity. In another study Keneko *et. al*., showed that knocking down PSMD9 results in reduced proteasomal activity [200]. Here in contrast to our method and those by Shim et.al, cell lysates were fractionated by glycerol gradient centrifugation and the fractions were monitored for proteasomal activity. Increase in proteasomal activity is seen in the presence of p27 modulator complex in reconstitution experiments involving subcomplexes of the proteasome. [243]. Role of this modulator seems to involve rescue of misassembled or damaged 19S particles to ensure correct orientation of the ATPase rings [306].

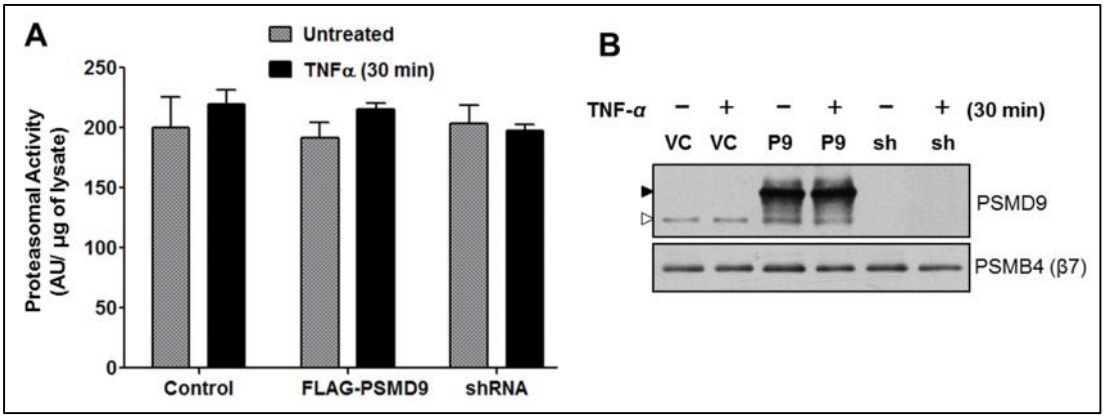

Figure-3.18 PSMD9 does not affect basal proteasomal activity in HEK293 cells. (A) Both P9-iOE and P9-iKD stable clones were either treated with doxycycline for 48h and/or with TNF-α (20ng/mL of media) for 30 min or left untreated. Cell lysates were prepared with ATP-Buffer as described in the materials and methods. Proteasomal activity was measured as described in the materials and methods. The "Control" panel in the graph represents the average value of doxycycline untreated control cells of both the stable clones. Data represents Suc-LLVY-AMC-proteasomal activity in arbitrary units (AU/µg of lysate) ± SEM of two independent experiments done in duplicates. **(B)** The WB showing the level expression of PSMD9 in above cell lysates and PSMB4 is taken as the loading control. Symbol ►corresponds to trans-expressed FLAG-PSMD9 and symbol Δ corresponds to the endogenous PSMD9.

3.3.10 The PDZ domain of PSMD9 interacts with hnRNPA1

Point mutations in PDZ domain of PSMD9 affected *in vitro* binding to hnRNPA1 [204]. Since hnRNPA1 interacts with PSMD9 through its C-terminal residues, this interaction represents a typical PDZ domain-motif interface. Hence, we wanted to determine if this

domain-motif recognition is also a key determinant of interaction inside the cells. As we recently reported that Q181G and the β2 L124G/Q126G/E128G triple mutant (all in the PDZ domain) abolished interaction with PSMD9 while L173G (also in the PDZ domain) did not affect binding [204]. To check functional relevance of these mutations, we overexpressed FLAG tagged wt-PSMD9, Q181G-PSMD9, L173G-PSMD9 or the β2 L124G/Q126G/E128G triple mutant in HEK293 cells. Endogenous hnRNPA1 was immunoprecipitated from each cell lysate and probed with anti-FLAG antibody. In accordance with the in vitro pull down assays [204], only wt-PSMD9 and L173G-PSMD9 were detected in the IP-complexes. However neither the Q181G mutant nor the triple mutant of PSMD9 could be detected in the hnRNPA1-IP complexes (Figure-3.19A).

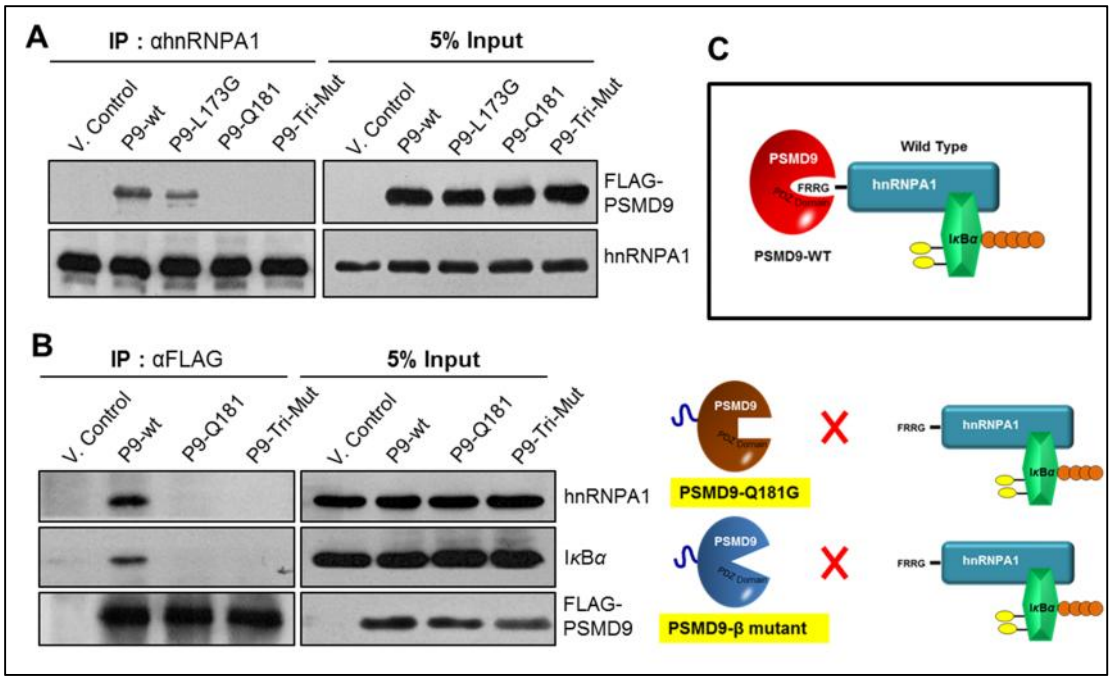

Figure-3.19 PSMD9 interact with hnRNPA1 via its PDZ-domain (A) HEK293 cells were transiently transfected with p3xFLAG-CMV-10-PSMD9, p3xFLAG-CMV-10-PSMD9(L173G), p3xFLAG-CMV-10-PSMD9(Triple mutant) or p3xFLAG-CMV-10-PSMD9(Q181G). Endogenous hnRNPA1 was immunoprecipitated from the cell lysates of the above transfected cells and probe with anti-FLAG antibody and analyzed by WB. **(B)** HEK293 cells were transiently transfected with p3xFLAG-CMV-10 empty vector/ p3xFLAG-CMV-10-wtPSMD9/ p3xFLAG-CMV-10-PSMD9(Q181G)/ p3xFLAG-CMV-10-PSMD9(Triple mutant) or. Cell lysates were incubated with anti-FLAG M2-Agarose beads and pull complexes were probed with anti-

hnRNPA1, anti-IκBα antibodies, anti-FLAG and analyzed by WB. **(C)** Cartoon image represents the probable mode of tripartite interaction between PSMD9, hnRNPA1 and IκBα.

We next probed for the presence of IκB*α* in the FLAG-PSMD9-IP-complex from cell lysates of HEK293 cells overexpressing wt-PSMD9, Q181G or the *β*2 L124G/Q126G/E128G triple mutant. IκB*α* was detected only in the wild type PSMD9-hnRNPA1 complex but not in PDZ Q181G and *β*2 L124G/Q126G/E128G triple mutant IP-complexes (Figure-3.19B) suggesting that PSMD9 is probably linked to IκB*α* through hnRNPA1.

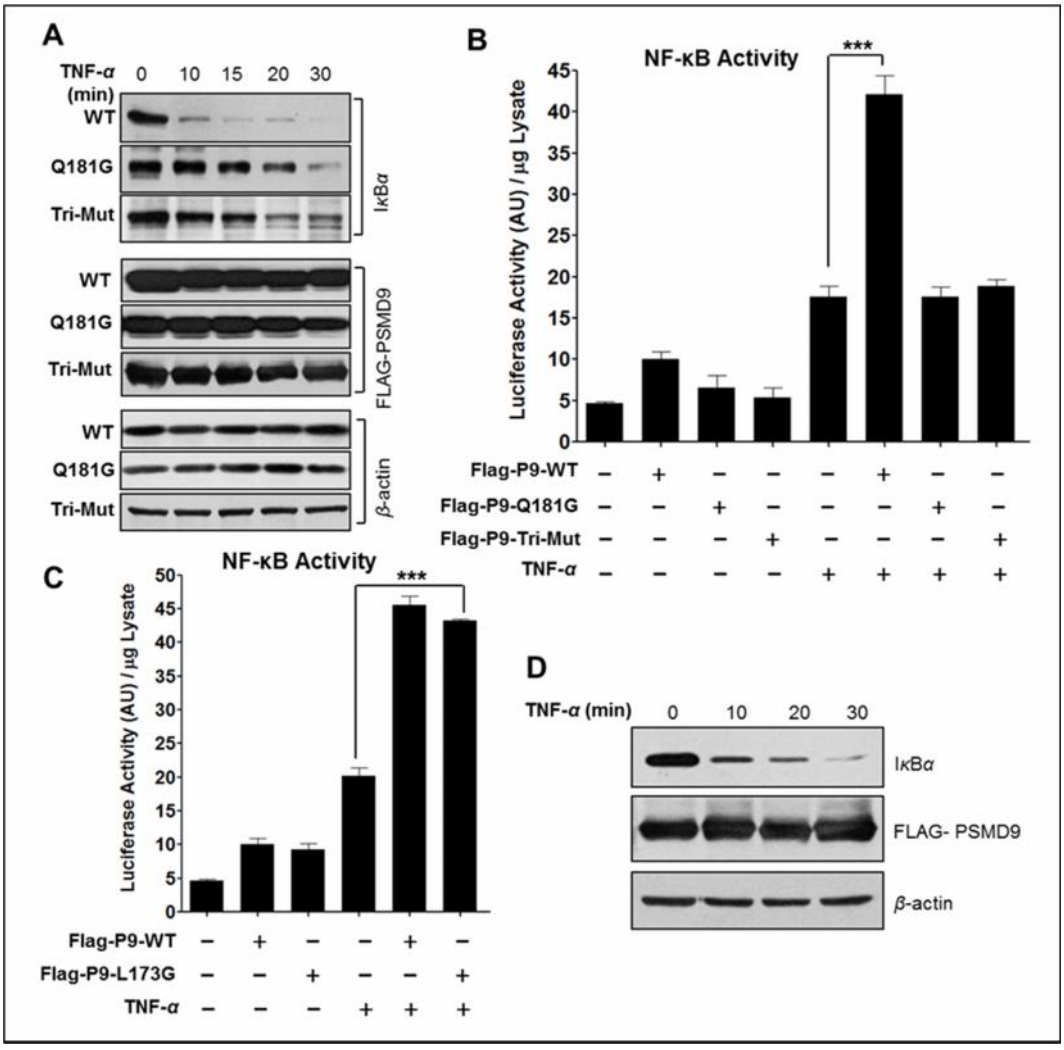

Figure-3.20 PDZ domain mediated interaction is crucial for IκBα degradation and NF-κB activity. (A) HEK293 cells were transiently transfected with p3xFLAG-CMV-10-PSMD9,/ p3xFLAG-CMV-10-PSMD9(Q181G)/ p3xFLAG-CMV-10-PSMD9(Triple mutant). After 48h of transfection cells were treated with TNF-α (20ng/mL of media) for 10, 15, 20, 30min or left untreated. Cell lysates were prepared and analyzed by WB. **(B)** HEK293 cells were co-

transfected with p3xFLAG-CMV-10 empty vector or p3xFLAG-CMV-10-PSMD9 (WT, Q181G, Triple mutant) and 3x κB ConA luc vector or ConA luc control vector. After 36h cells were either treated with TNF-α (20ng/mL of media) for 12h or left untreated. Cell lysates were prepared and NF-κB activity was determined by measuring firefly luciferase activity and normalized with renilla luciferase used as transfection control. Data represents mean luciferase activity/µg of protein ± SEM of two independent experiments done in duplicates. **(C)** HEK293 cells were co-transfected with p3xFLAG-CMV-10 empty vector or p3xFLAG-CMV-10-PSMD9 (WT or L173G) and 3x κB ConA luc vector or ConA luc control vector. After 36h cells were either treated with TNF-α (20ng/mL of media) for 12h or left untreated. Cell lysates were prepared and NF-κB activity was determined by measuring firefly luciferase activity and normalized with renilla luciferase used as transfection control. Data represents mean luciferase activity/µg of protein ± SEM of two independent experiments done in duplicates. **(D)** HEK293 cells were transiently transfected p3xFLAG-CMV-10-PSMD9(L173G). After 24h of transfection cells were treated with TNF-α (20ng/mL of media) for 12h or left untreated. Cell lysates were prepared and analyzed by WB.

To evaluate the functional relevance of the PDZ mediated interaction we checked the ability of these PSMD9-mutants in I*κ*B*α* degradation process. Unlike cells overexpressing wild type PSMD9, in cells overexpressing PDZ mutants (Q181G and the *β*2 Triple mutant), I*κ*B*α* was not efficiently degraded even after TNF-*α* treatment (Figure-3.20A) nor was there a significant change in NF-*κ*B activity (Figure-3.20B). In addition properties of L173G PSMD9 mutant was similar to that of wt-PSMD9 and cells expressing this mutant showed faster I*κ*B*α* degradation and enhanced NF-*κ*B activation (Figure-3.20C & D). These results confirm that specific residues on the PDZ domain of PSMD9 forms the interface for binding hnRNPA1 and this domain-motif interaction plays an important role in the NF-*κ*B activation pathway.

3.3. 11 PSMD9 is linked to I*κ*B*α* via hnRNPA1.

hnRNPA1 was previously shown to interact with I*κ*B*α* through its RNA binding domain [300]. We demonstrated that PSMD9 interacts with hnRNPA1 through its C-terminus. And the PDZ mutation analysis indicates that interaction between PSMD9 and I*κ*B*α* is likely through hnRNPA1. To determine the structural hierarchy of this tripartite interaction between PSMD9, hnRNPA1 and I*κ*B*α*, we performed both *ex vivo* and *in vitro* interaction studies. We first verified whether interaction of hnRNPA1 with

PSMD9 and IκBα is mutually exclusive or not. We trans-expressed HA tagged wild type hnRNPA1 and the mutant CΔ7hnRNPA1 (7 amino acid deleted from C-terminus) in HEK293 cells. Using anti-HA antibody we immunoprecipitated the trans-expressed wt and mutant HA-hnRNPA1 from the cell lysates. When the IP complexes were probed with anti-IκBα antibody it was detected in both the conditions (Figure 3.21A) suggesting that C-terminus deletion of hnRNPA1 does not affect binding to IκBα (Figure 3.21B). In contrast PSMD9 was found only in the wild type hnRNPA1-IP complex. As inferred from the failure of PDZ mutants to interact with IκBα in the absence of hnRNPA1 (Results 3.3.10 and Figure-3.19B), these results suggest that wt-PSMD9 and IκBα interaction is indirect and is through hnRNPA1. To further validate these observations we overexpressed both the FLAG tagged wt-IκBα and C-terminal deleted IκBα (253-372aa) in HEK293 cells. As discussed above C-terminal ankyrin repeats of murine-IκBα are necessary for interaction with hnRNPA1 [300]. When we immunoprecipitated the trans-expressed FLAG tagged IκBα, PSMD9 was found in the IP-complex of wild type IκBα where hnRNPA1 was present, but not in the mutant IκBα (which does not interact with hnRNPA1) IP-complex (Figure-3.21C & D). This suggested that hnRNPA1 mediates the indirect interaction between IκBα and PSMD9.

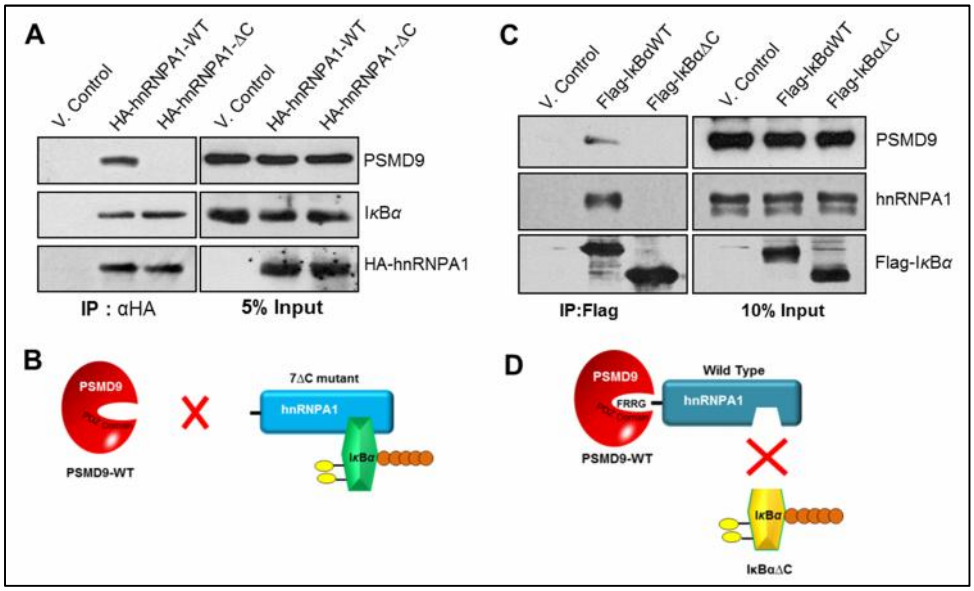

Figure-3.21 PDZ domain mediated interaction is crucial for IκBα degradation and NF-κB activity. (A) Wild type HA-hnRNPA1 and 7ΔC mutant HA-hnRNPA1 were transiently overexpressed in HEK293 cells and cell lysates were incubated with anti-HA Ab-bound protein-G sepharose beads. Pull down complexes were probed with anti-PSMD9 and anti-IκBα antibodies and analyzed by WB. **(B)** Cartoon represents the abrogation in interaction of mutant hnRNPA1 with PSMD9. **(C)** HEK293 cells were transfected with p3xFLAG-CMV-10-wtIκBα p3xFLAG-CMV-10-ΔCIκBα and cell lysates were incubated with anti-FLAG M2-Agarose beads. The pull complexes were probed with anti-PSMD9, anti-hnRNPA1 and anti-IκBα antibodies and analyzed by WB. **(D)** Cartoon represents the abrogation in interaction of mutant IκBα with hnRNPA1.

We performed a series of far western or overlay experiments using Recombinant proteins to substantiate these observations. Recombinant His-PSMD9, GST-PSMD9, GST-hnRNPA1 and MBP-I*κ*B*α* proteins were expressed in bacterial system and purified following the protocol described in materials and method. Recombinant GST-PSMD9 and GST-hnRNPA1 were immobilized on a PVDF membrane, followed by overlay of recombinant MBP-I*κ*B*α* protein and then probed with anti-I*κ*B*α* antibody. No I*κ*B*α* was detected in the GST-PSMD9 lane but was clearly visible in GST-hnRNPA1 lane (Figure-3.22C). Furthermore, when MBP-I*κ*B*α* and GST-hnRNPA1 were immobilized on PVDF membrane, overlaid with His-PSMD9 followed by probing with antiPSMD9 antibody, PSMD9 was clearly detected in GST-hnRNPA1 lane but not in MBP-I*κ*B*α* lane (Figure-3.22D). In a sandwich-dot blot assay we immobilized GST-PSMD9 on membrane, followed by overlay with GST or GST-hnRNPA1 and then with MBP-IκBα. When this sandwich was probed with anti-I*κ*B*α* antibody, MBP-I*κ*B*α* was found to interact with GST-PSMD9 only when hnRNPA1 was sandwiched in between these two proteins (Figure-3.22E). Furthermore this indirect interaction was validated by reversing the sandwich i.e. by immobilizing MBP-I*κ*B*α* and overlay of GST-or GST-hnRNPA1 followed by GST-PSMD9 (Figure-3.22F). These results altogether confirmed that there is no direct interaction between PSMD9 and I*κ*B*α* and they can only interact through hnRNPA1, which uses different structural regions for these interactions that are not mutually exclusive.

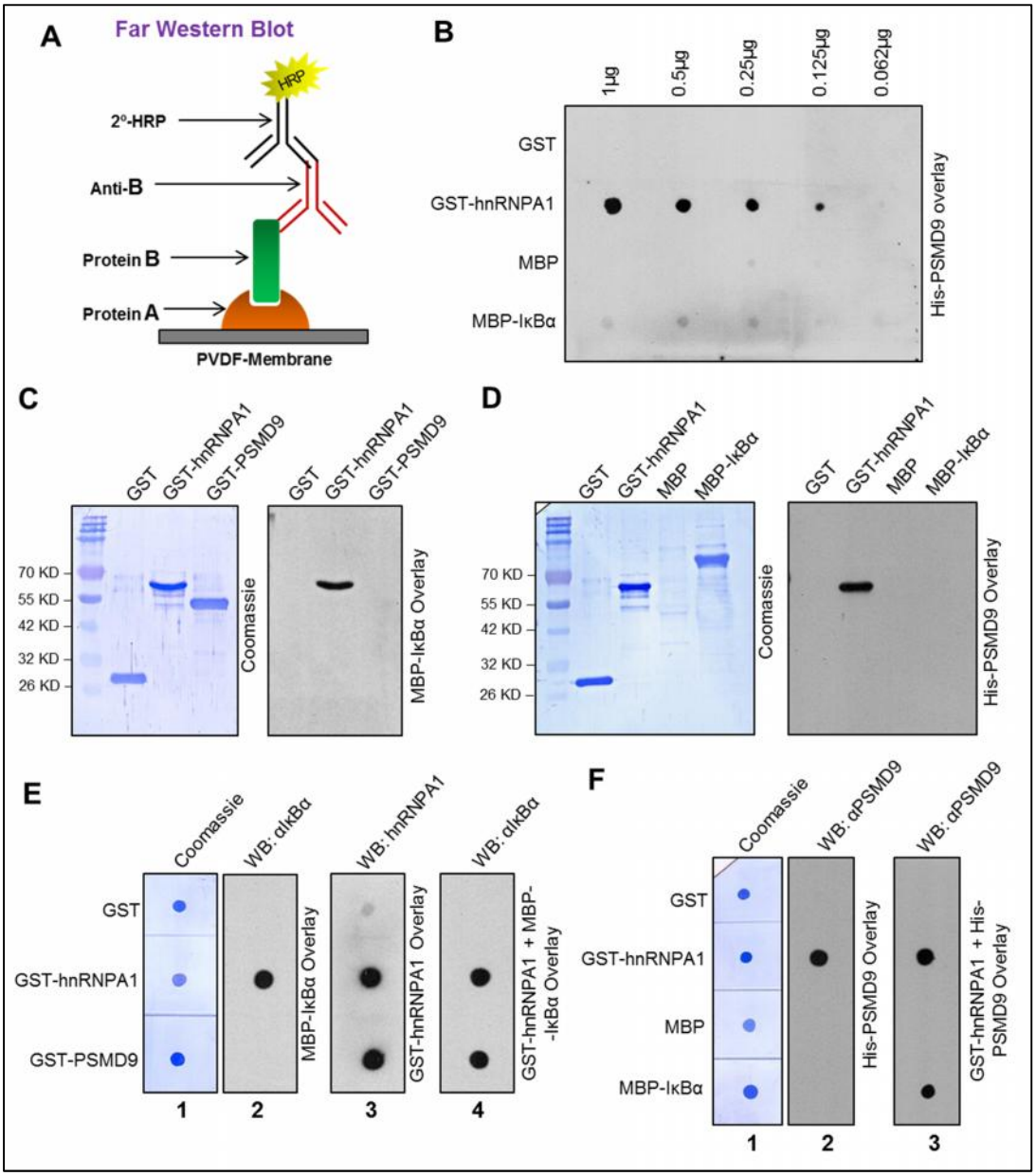

Figure-3.22 *In vitro* interaction of PSMD9, hnRNPA1 and IκBα. (A) The cartoon image represents the mode of protein binding in Far western blot. **(B)** Different amount of GST, GST-hnRNPA1 MBP and MBP-IκBα recombinant proteins were spotted on PVDF membrane. The membrane was overlaid with recombinant His-PSMD9 (100nM), probed with anti-PSMD9, and analyzed by WB. **(C)** 2µg of recombinant GST, GST-hnRNPA1 and GST-PSMD9 proteins were run in a SDS-PAGE, transfer onto a PVDF membrane and denature/renature the proteins on membrane using Guanidine-HCl AP-Buffer. Then the membrane was overlaid with recombinant MBP-IκBα (100nM), probed with anti-IκBα, and analyzed by by far western blot. **(D)** 2µg of recombinant GST, GST-hnRNPA1 MBP and MBP-IκBα proteins were run in a SDS-PAGE, transfer onto a PVDF membrane and denature/renature the proteins on membrane using Guanidine-HCl AP-Buffer. Then the membrane was overlaid with recombinant His-PSMD9 (100nM), probed with anti-PSMD9, and analyzed by WB. **(E)** 1µg of recombinant GST, GST-hnRNPA1 and GST-PSMD9 proteins were spotted on equilibrated PVDF membrane, blocked with 3% BSA-TBST. The membranes were overlaid with recombinant MBP-IκBα (100nM) and probed with anti- IκBα (Panel-2); overlaid with GST-hnRNPA1 (100nM) and probed with anti-hnRNPA1 (Panel-3); overlaid with both GST-hnRNPA1 (100nM) & MBP-IκBα (100nM) and probed with anti-IκBα (Panel-4). Panel-1 corresponds to the respective Coomassie stained

protein spots on membrane. **(F)** 1µg of recombinant GST, GST-hnRNPA1 MBP and MBP-IκBα proteins were spotted on equilibrated PVDF membrane, blocked with 3% BSA-TBST. The membranes were overlaid with recombinant His-PSMD9 (100nM) (Panel-2) or with both GST-hnRNPA1 (100nM) & His-PSMD9 (100nM) (Panel-3). Panel-1 corresponds to the respective Coomassie stained protein spots on membrane.

3.3.12 Interaction between C-terminus of hnRNPA1 and PSMD9 is required for degradation of IκBα as well as NF-κB activity:

The involvement of hnRNPA1 in IκBα degradation was previously shown by Hay et. al., group in 2001 [300]. We have demonstrated here a novel role of PSMD9 in NF-κB signaling pathway and a specific interaction between PDZ domain of PSMD9 and a SLIM at the C-terminus of hnRNPA1. Then we asked if hnRNPA1 had any independent role to play in IκBα degradation/NF-κB activation when interaction with PSMD9 is lost or in the absence of endogenous PSMD9. When HA-WT-hnRNPA1 was trans-expressed in HEK293 cells, degradation of IκBα was considerably enhanced after 10 minutes of TNF-α treatment. But, HA-7ΔC-hnRNPA1 mutant on the other hand had no influence on the degradation of IκBα (Figure-3.23A). Correspondingly, only the HA-WT-hnRNPA1 trans-expression in cells showed significant increase in NF-κB activity after TNF-α treatment. On the contrary cells expressing HA-7ΔC-hnRNPA1 mutant showed a lower NF-κB activity as compared to the control cells (Figure-3.23B). Furthermore when we silenced PSMD9 by PSMD9-siRNA in the background of wild type HA-hnRNPA1 overexpression, TNF-α mediated IκBα degradation was significantly reduced (Figure-3.22C). In addition, a considerable decrease (upto 40%) in NF-κB activity was also observed in these PSMD9 cells (Fig. 9D). These results suggest that both PSMD9 and hnRNPA1 are in the same pathway and only hnRNPA1 is not sufficient to exhibit the function; PSMD9 is essential for it. Moreover it further supports the role of PSMD9-hnRNPA1 interaction in IκBα degradation and NF-κB activation.

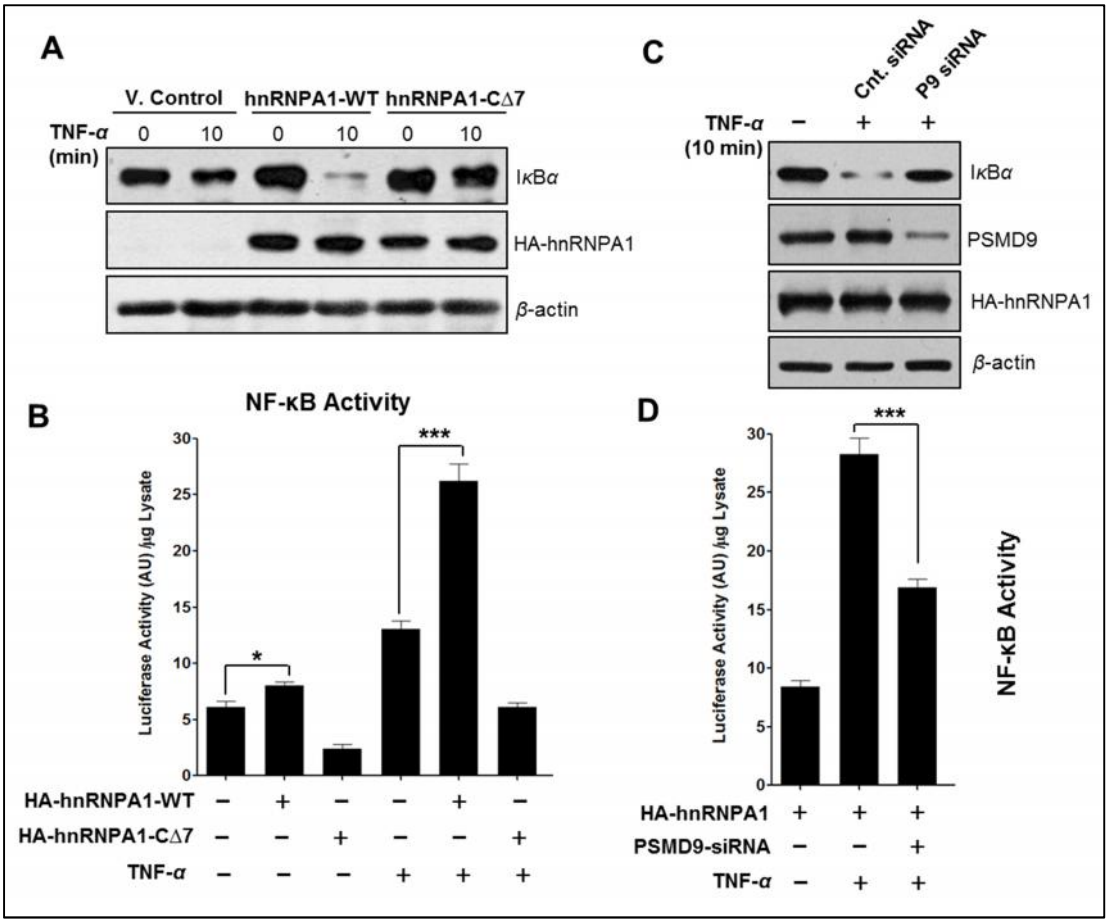

Figure-3.23 Interaction between hnRNPA1 and PSMD9 is essential for degradation of IκBα as well as NF-κB activity (A) Wild type HA-hnRNPA1 and 7ΔC mutant HA-hnRNPA1 were transiently overexpressed in HEK293 cells and after 48h cells were treated with TNF-α (20ng/mL of media) for 10 min or left untreated. Cell lysates were prepared along with vector control and subjected to WB analysis. **(B)** HEK293 cells were co-transfected with pCDNA3.1-HA-empty vector or pCDNA3.1-HA-hnRNPA1 (WT or 7ΔC mutant) and 3x κB ConA luc vector or ConA luc control vector. After 36h cells were either treated with TNF-α (20ng/mL of media) for 12h or left untreated. Cell lysates were prepared and NF-κB activity was determined by measuring firefly luciferase activity and normalized with renilla luciferase used as transfection control. Data represents mean luciferase activity/µg of protein ± SEM of three independent experiments done in duplicates. **(C)** HEK293 cells were transfected with PSMD9-siRNA/Control-siRNA (100µM) and after 48h cells were again transfected with pCDNA3.1-HA-wt-hnRNPA1. After 72h of siRNA transfection cells were either treated with TNF-α (20ng/mL of media) for 20min left untreated. Cell lysates were prepared and analyzed by WB. **(D)** HEK293 cells were transfected with PSMD9-siRNA/Control-siRNA (100µM) and after 48h cells were again transfected with pCDNA3.1-HA-wt-hnRNPA1 and 3x κB ConA luc vector or ConA luc control vector. After 60h of siRNA transfection cells were either treated with TNF-α (20ng/mL of media) for 12h or left untreated. Cell lysates were prepared and NF-κB activity was checked by measuring luciferase activity using dual luciferase substrate. Luciferase activity from firefly luciferase was normalized with renilla luciferase used as a transfection control. Data represents mean luciferase activity/µg of protein, ± SEM of two independent experiments done in duplicate.

3.3.13 PSMD9 anchors hnRNPA1-IκBα complex on 26S proteasome that facilitates proteasomal degradation of IκBα:

PSMD9 is known to be a chaperone of proteasome assembly and is reported to dissociate before the mature complex [243, 307, 308]. Nas2, the yeast homolog was not found in any of the cryo EM studies of the proteasome [20, 21, 202]. Like other classical chaperones PSMD9 or its homologs may only be transiently associated with the assembled proteasome. But we hypothesized that PSMD9 by virtue of its interaction with the proteasome on one hand and its interaction with hnRNPA1 on the other, would recruit IκBα to the proteasome for degradation. We first asked if endogenous or trans-expressed FLAG-PSMD9 could be located in the proteasome complex. We pulled down the whole 26S proteasomal complex using β7-subunit antibody. When probed for anti-PSMD9 antibody we found both endogenous and FLAG tagged PSMD9 in the complex (Figure-3.24A). To ensure that PSMD9 is associated with the intact 26S mature complex, we probed the complex for the presence of ATPase subunit (Rpt6), a marker for the base sub-complex and α5 subunit, a marker of 20S core particle. Results showed that β7-subunit antibody pulls down the intact 26S complex and PSMD9 is indeed associated with the mature proteasome. TNF-α treatment did not alter the levels of either endogenous or trans-expressed PSMD9 on proteasome. In addition the total protein levels of hnRNPA1 was not influenced either by the levels of PSMD9 or TNF-α treatment (Figure-3.24B & C). But, there was a definitive increase in the levels of proteasome bound hnRNPA1 in PSMD9 overexpressing cells which was further enhanced upon TNF-α treatment (Figure-3.24A). In contrast, when PSMD9 was silenced, no hnRNPA1 was found in the proteasome pull down complex even after TNF-α treatment. These results together indicate that recruitment of hnRNPA1 to the

proteasome requires the presence of PSMD9 and the levels of hnRNPA1 on proteasome positively correlate with the rate of IκBα degradation so as NF-κB activation.

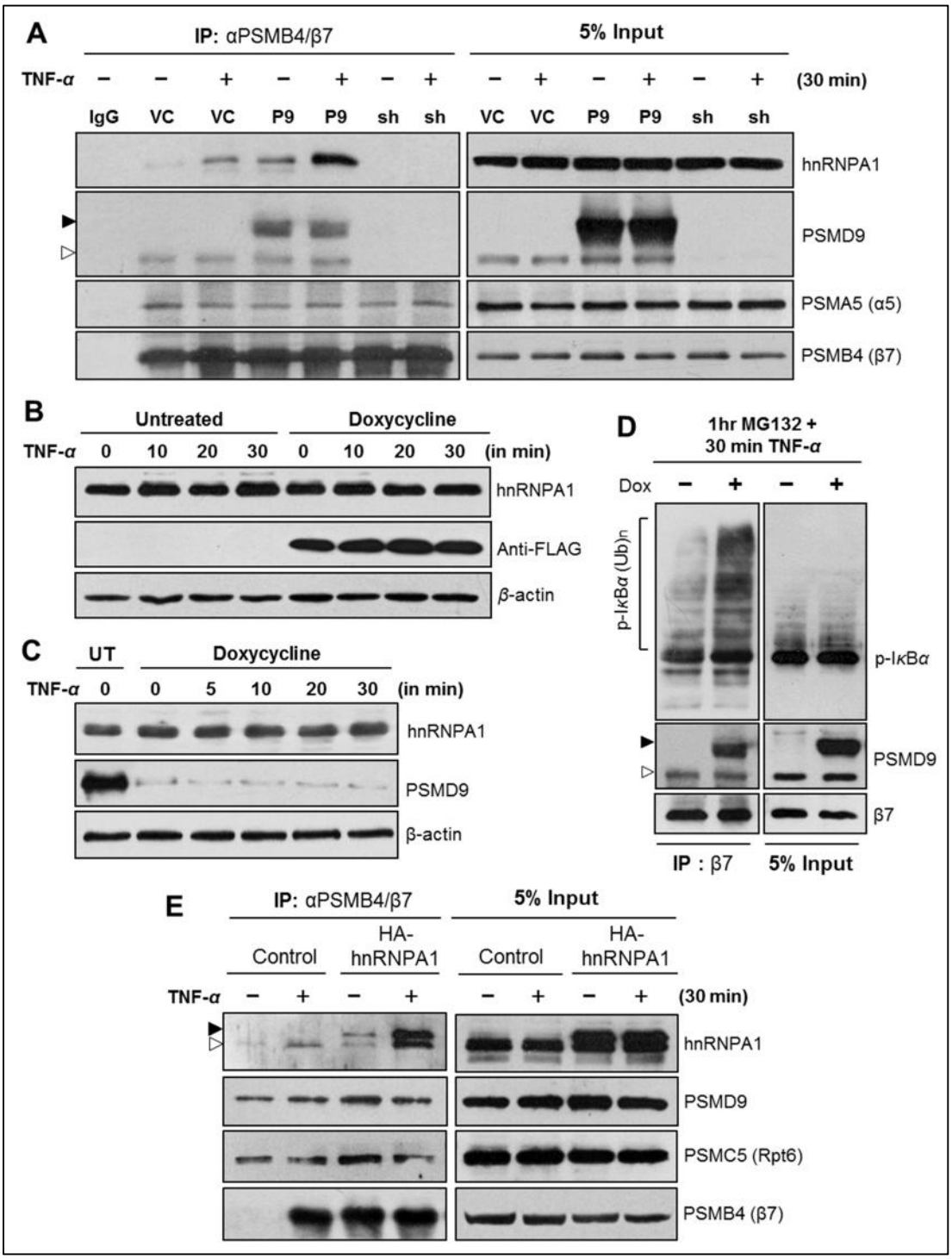

Figure-3.24 PSMD9 is crucial for the recruitment of hnRNPA1-IκBα complex on 26S proteasome (A) Both the overexpression (P9) and knockdown (sh) HEK293 inducible stable clones of PSMD9 were either treated with doxycycline for 48h and/or with TNF-α (20ng/mL of media) for the next 30 min or left untreated. Cell lysates were prepared with ATP-Buffer as described in the materials and methods. Whole 26S proteasome was pull down from the above cell lysates using β7 antibody and probed with different antibodies and analyzed by WB. Symbol

► corresponds to trans-expressed FLAG-PSMD9 and symbol Δ corresponds to the endogenous PSMD9. **(B, C)** The cell lysates prepared in the experiments described in Figure 3B and Figure 4B were probed with anti-hnRNPA1. **(D)** The P9-iOE cells were either treated with doxycycline or left untreated and MG132 (50μg/ml) for 1hr, with TNF-α (20ng/ml) for 30 min. Cell lysates were prepared with ATP-Buffer as described in the materials and methods. Whole 26S proteasome was pull down from the above cell lysates using β7 antibody and probed with different antibodies and analyzed by WB. **(E)** HEK293 cells were transfected with pCDNA3.1empty vector or pCDNA3.1-HA-wt-hnRNPA1 and after 48h of transfection cells were treated with TNF-α for 30min. Cell lysates were prepared in ATP-buffer (as described in the materials and methods), 26S proteasome was pulled down from the above cell lysates using β7 antibody and analyzed by WB. Symbol ► corresponds to trans-expressed HA-hnRNPA1 and symbol Δ corresponds to the endogenous hnRNPA1.

Since we found increased IκB*α* degradation and increased association of hnRNPA1 on proteasome upon overexpression of PSMD9, we wanted to check if IκB*α* recruitment increases under these conditions. We treated the P9-iOE cells with MG132 for 1hr and with TNF-*α* for 30 minute. Then 26S proteasome was pulled down using *β*7 antibody and the complex was probed with phospho-IκB*α* antibody. Results showed an increased levels of proteasome bound polyubiquitinated phospho-IκB*α* upon PSMD9 overexpression. These results indicate that PSMD9 might be providing a binding site on proteasome for polyUb-phospho-IκB*α* bound hnRNPA1. Furthermore, previous experiments suggested that hnRNPA1 overexpression enhances TNF-*α* mediated IκB*α* degradation in PSMD9 background. Hence we wanted to determine whether the overexpressed hnRNPA1 would have been recruited more on 26S proteasome. HA-hnRNPA1 was overexpressed in HEK293 cells and treated with TNF-*α* (20ng/ml of media for 30min). Cell lysates were prepared in ATP-Buffer and 26S proteasome was pulled down using *β*7 antibody. When the pull down complexes were probed with anti-hnRNPA1, both endogenous and trans-expressed hnRNPA1 levels were found to be increased upon TNF-*α* treatment, which correlates with the IκB*α* degradation (Figure-3.24E). These results are strongly suggestive of a mechanism which involves recruitment of hnRNPA1 to the proteasome complex during TNF-*α* signaling that would

result in more and more I*κ*B*α* degradation by the proteasome. And most importantly hnRNPA1 was not degraded during this process. Hence, taken together these results suggest that hnRNPA1 either recruits or represents I*κ*B*α* to the proteasome where hnRNPA1 act as a shuttle receptor which is transiently anchored by PSMD9 on the proteasome. While ubiquitinated I*κ*B*α* is degraded, hnRNPA1 in all probability is released intact. Moreover, it is possible that PSMD9-hnRNPA1 interaction shortens the distance between the substrate and the proteasomal ATPases or ensures that I*κ*B*α* is not prematurely released from the proteasome.

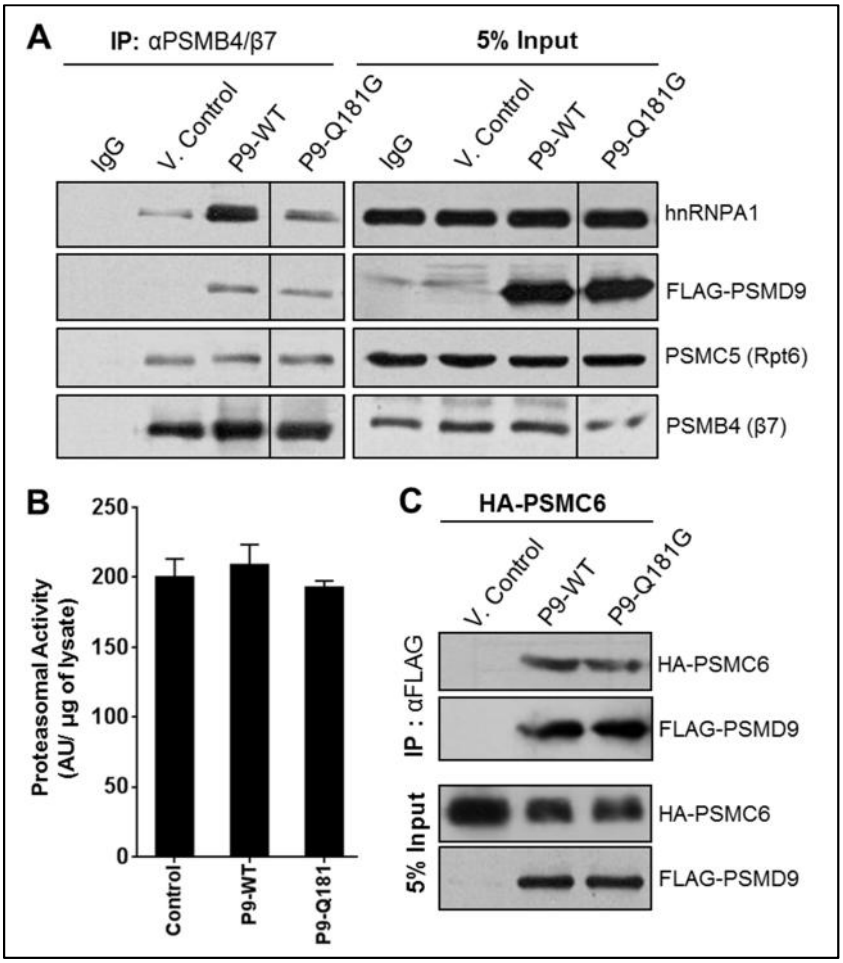

Figure-3.25 PDZ-domain of PSMD9 is not involved in proteasome and PSMD9 interaction. **(A)** HEK293 cells were transiently transfected with pCMV10 empty vector or pCMV10-PSMD9 (WT or mutants D157P/Q181G) and cell lysates were prepared in ATP-buffer in the materials and methods. 26S proteasome was pull down from the above cell lysates using β7 antibody and probe with different antibodies as indicated and analyzed by WB. **(B)** Proteasomal activity of the above mentioned (in (B)) cell lysates was measured as described in the materials and methods. Data represents Suc-LLVY-AMC-proteasomal activity in arbitrary units (AU/µg of lysate) ± SEM

of two independent experiments done in duplicates. The WB showing the expression of FLAG-PSMD9 in above cell lysates and PSMB4 is taken as the loading control. **(C)** HEK293 cells were co-transfected with pCDNA3.1-PSMC6 and p3X-FLAG-CMV-10, p3X-FLAG-CMV-10-wt-PSMD9 or p3X-FLAG-CMV-10-Q181G-PSMD9. After 48h of transfection cell lysates were used for pull down with anti-FLAG-M2Agarose beads and analysed by WB.

Furthermore, to enable degradation of IκBα by the proteasome, PSMD9 not only has to interact with hnRNPA1 but should also interact with the proteasome as demonstrated in previous experiments. However based on current evidence PSMD9 seems to harbour only the PDZ like domain for protein-protein interaction. Therefore it was important to test whether the PDZ mutations affect association of PSMD9 with the proteasome. Affinity pull down of the 26S proteasome in cells over expressing PDZ mutant Q181G, indicated that this association was unimpaired (Figure-3.25A), so as the proteasomal activity (Figure-3.25B). Probably there are other regions in PSMD9 that can interact with the proteasome. Although PSMD9 mutants cannot bind to hnRNPA1, because of the endogenous PSMD9 some hnRNPA1 could be still detected in the pull down complex as shown in the image (Figure-3.24A). These results further validate the role of PSMD9-PDZ domain in recruiting hnRNPA1 on proteasome for IκBα proteasomal degradation. In addition these results indicate that PSMD9 functions as an anchor rather than a chaperone and bridges IκBα bound hnRNPA1 to the proteasome. This specific interaction enables regulated degradation of IκBα and consequently modulates NF-κB activity.

While there is no clear evidence for the presence of PSMD9 on mature proteasomes or for the role of PDZ-domains in interaction with ATPase subunits in mammalian cells, the lack of any detectable effect of PDZ domain mutations on the association of PSMD9 with intact 26S proteasomes requires further explanation. To address this we analysed the primary sequence of PSMC6 (Rpt4) and PSMC3 (Rpt5).

GRRF was present in PSMC6 as an internal sequence. Intrigued we co-expressed wt-PSMD9 or PSMD9-Q181G mutant with wt-PSMC6 and performed co-immunoprecipitation studies. Results showed that Q181G mutation which inhibits binding to hnRNPA1 does not affect binding to PSMC6 (Figure-3.24D). This result in conjunction with the observation that the PDZ-mutations do not affect PSMD9 association with proteasome indicates that interaction with the mature proteasome may not involve Rpt4. Moreover Rpt5 C-terminus is known to interact with PSMD9-PDZ domain during assembly [208] and also play a key role in interaction with the 20S α subunit which opens the gate and activates the proteasome. Therefore, Rpt5 on mature proteasome is unlikely to interact with PSMD9. Hence further investigation is necessary to find out the interacting sites on PSMD9 and on proteasome for this whole degradation process to carry out.

3.4 DISCUSSION:

Protein-protein interactions are seminal to signal transduction. They are involved in spatio temporal regulation of cellular functions. Therefore identification of novel interactions can help in deciphering unknown functions of a protein. We have established a bioinformatic based methods for identification of unknown interacting partners of 19S subunits of the proteasome [204]. Using one such method we had identified hnRNPA1, a RNA binding protein involved in RNA metabolism and transport [301], as a novel interacting partner of PSMD9, a PDZ domain containing subunit of the proteasome. To test whether this interaction is physiologically relevant and to identify functions associated with this interaction, we searched for the reported functions of hnRNPA1. A singular report showed that N-terminal of hnRNPA1 binds to ankyrin repeats in IκB*α* and this interaction somehow influences the processing of IκBα, the nature or mechanism of which is unclear and enhanced NF-*κ*B activity [300]. Here

we reported a novel role of a proteasomal subunit- "PSMD9" in NF-κB signaling pathway and a detail mechanism of how IκBα is brought onto proteasome for degradation by a novel interaction between PSMD9 and hnRNPA1.

In this study we demonstrate that PSMD9 overexpression enhances both basal and TNF-α mediated NF-κB transcriptional activation in HEK293 cells. It increases the nuclear translocation as well as the DNA binding activity of NF-κB and regulates the transcription of some NF-κB target genes. This enhanced NF-κB activity was found to be the consequence of accelerated IκBα proteasomal degradation which falls in the category of canonical signaling pathway [253, 270, 273]. Furthermore, PSMD9 neither influence the phosphorylation nor the ubiquitination of IκBα to achieve this accelerated degradation. This suggests that, PSMD9 may not affect the kinase activity of IKK complex and the ligase activity of β-TrCP E3-ligase, indicating its role in the downstream not in the upstream events of the signaling pathway. However, further experimentation is required for a concrete conclusion. In addition, we demonstrate that PSMD9 also does not influence the basal proteasomal activity at all as reported previously [305]. Thereupon we performed a series of in vitro and ex vivo interaction studies which revealed the detail mechanistic overview of "how PSMD9 could enhance the rate of IκBα degradation on proteasome". We establish that, PSMD9 through its PDZ domain interacts with hnRNPA1 C-terminus and this domain-motif interaction is necessary for the proteasomal degradation of IκBα. We report a new role for hnRNPA1 as a shuttle receptor for the degradation of IκBα in HEK293 cells. PSMD9 contrary to its expected role as a chaperone, acts as a part of the 19S recognition module to facilitate delivery of ubiquitinated IκBα to the proteasome via hnRNPA1 as depicted in the model (Figure-3.26).

While our studies show how PSMD9 directly affects degradation of IκBα by the proteasome which helps in NF-κB activation, there are several upstream events that process IκBα for degradation. Possible role of PSMD9 in these processes have been somewhat addressed in this study. Since in the absence of any external stimuli, PSMD9 overexpression results in an increased basal activity of NF-κB, it remains to be seen whether PSMD9 acts as an "internal signal" for NF-κB activation. These may be dependent or independent of its interaction with hnRNPA1. Previously it is reported that, cells lacking hnRNPA1 (mouse leukemic cells) have a defective NF-κB activity [300]. And in this current study we have demonstrated that cells lacking PSMD9 show a lower NF-κB activity. Taken together, these studies suggest that PSMD9 and hnRNPA1 are probably not mutually exclusive in the context of NF-κB signaling pathway which may be explained by their ability to interact with each other.

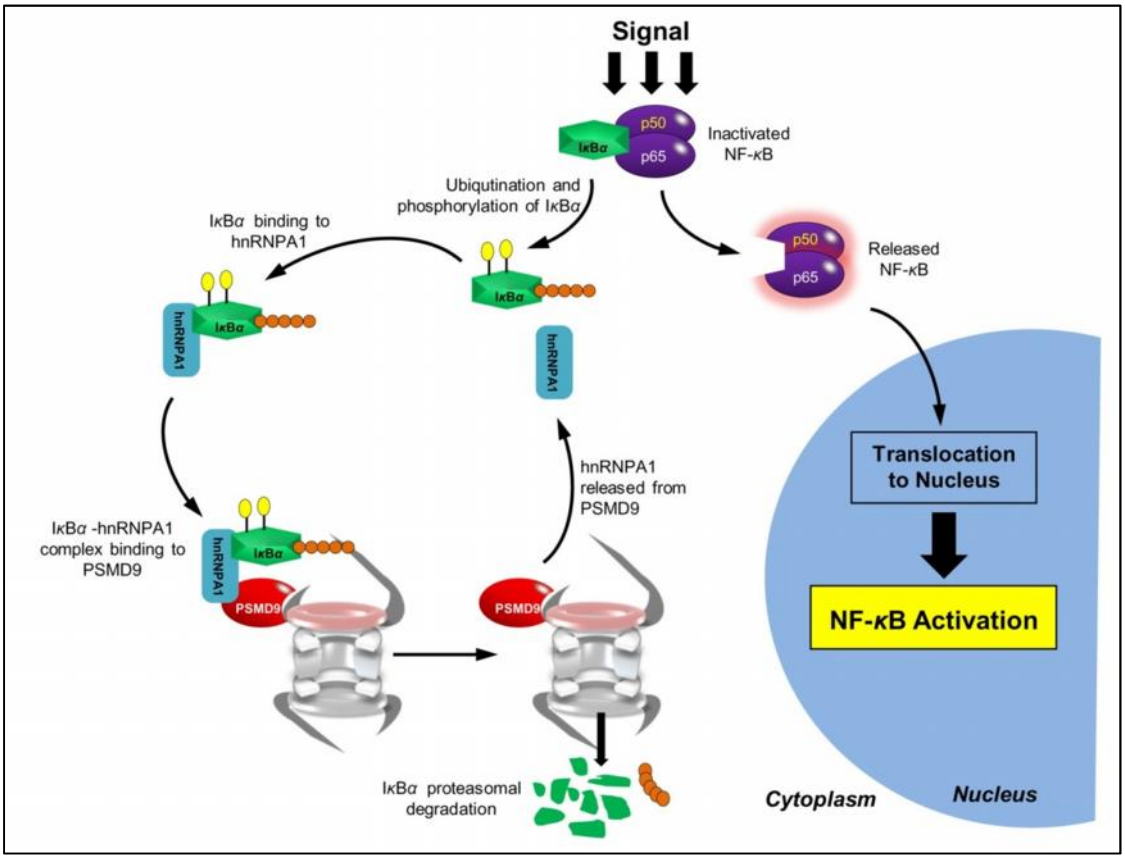

Figure-3.26 Model for the mechanism of IκBα presentation and degradation by 26S proteasome. Signal activated and modified IκBα binds to hnRNPA1 and this complex interacts

with PSMD9 on 26S proteasome. IκBα get degraded through proteasomal activity, hnRNPA1 shuttles back to bind with free IκBα and the cycle repeats.

Although degradation of I*κ*B*α* by the proteasome has been long established, the mechanism of how it is recruited to the proteasome is not well defined. Here we show how ubiquitinated I*κ*B*α* is targeted to the proteasome for degradation. This is important because how ubiquitinated substrates in general are recruited to the proteasome is an active area of research. So far two modes of substrate recognition have been well defined. In the direct mode, substrates are recognized by the ubiquitin binding motifs in 19S subunits like Rpn10 containing UIM domain, while Rpn13 binds via the pleckstrin motif [94, 95]. In the indirect mode of recognition, Rad23, Dsk2, and Ddi1 proteins called as 'shuttle receptors' bind proteasome through their UBL domains present at the N-terminus while their C-terminal ubiquitin association domain (UBA) bind to ubiquitin chains on the substrates [96, 309]. These shuttle receptors bind to the Rpn1 subunit of the proteasome in non-stoichiometric amounts and apparently dissociate with fast kinetics. In an in depth study, Deshaies group showed that Ddi1 is a proteasomal shuttle receptor that binds to the LRR1 domain of Rpn1 [49] and facilitates the degradation of Ufo1, a Ddi1 substrate. A UBA domain containing protein, p62 interacts with K63 ubiquitin chains of ubiquitinated tau and facilitates its proteasomal degradation by interacting with Rpt1 through its N-terminal PB1 domain [310]. HSP27 may also act as a shuttle receptor that recruits ubiquitinated I*κ*B*α* to the proteasome for degradation in cancer cells in response to stress signals [311]. In this report HSP27 was shown to bind ubiquitinated I*κ*B*α* and to the 19S regulatory particle of the proteasome to mediate this degradation. HSP27 recognizes covalently linked ubiquitin on I*κ*B*α* but how it interacts with the proteasome is unclear.

We describe our findings in the context of these reported mechanisms of substrate recognition and highlight unique features that are an outcome of our study. PSMD9 unlike HSP27 does not directly bind to ubiqutinated IκBα. This interaction is mediated by hnRNPA1 and therefore Ub-IκBα is targeted to the proteasome through the indirect pathway. Since hnRNPA1 level doesn't change under any conditions tested here, we argue that it acts as a shuttle receptor that brings in Ub-IκBα. Since hnRNPA1 lacks a UBL like domain, it does not bind to the proteasome in a classical manner like other shuttle receptors. Instead this function is mediated by a C-terminal region of the protein which acts as a recognition signal for the PDZ-domain of PSMD9 bound to the proteasome. PDZ domains can recognize native sequences in proteins typically through the C-terminal residues. Such a classical domain motif interaction for PSMD9-hnRNPA1 is established by our study. Nevertheless, the exact mechanism of hnRNPA1 release, the mode of binding of PSMD9 to the proteasome and molecular basis of this recognition remain to be investigated.

It will be important to see whether the mechanism of IκBα degradation and NF-κB activity is general to other cell types. While hnRNPA1 is a ubiquitous protein, PSMD9 may be expressed in cell or tissue specific manner [193]. Although PSMD9 deletion is not lethal in yeast [201], loss of PSMD9 expression may have phenotypic consequences in mammalian cells due to inhibition of NF-κB activity. Interestingly, preliminary data from our lab also suggest that PSMD9 modulate the cell proliferation and anchorage independent growth through this pathway. However, detail phenotypic study in mammalian cells has to be performed to corroborate the findings. Nevertheless, we have demonstrated that the PDZ domain mutants do not bind to hnRNPA1 and therefore their overexpression does not affect NF-κB activity. Thus small molecules that can target the interaction sites on PDZ domain of PSMD9 are likely to act as inhibitors

of NF-κB activity. Such molecules may be useful in targeting cancer cells that are dependent on a consistent high NF-κB activity for their survival [312, 313]. First step in this direction however, is to establish the role of PSMD9-hnRNPA1 interaction in this pathway in such cancer cells.

Based on our findings about the molecular details of interaction between the PDZ-domain of PSMD9 and hnRNPA1, we speculate a general role for PSMD9 in substrate recognition by the proteasome. For example IκBα may be one of the many examples of how substrates may converge on the proteasome through the PDZ domain of PSMD9. It is possible that other substrates are brought to the proteasome by a similar mechanism either through hnRNPA1 or other shuttle receptors that may carry a similar recognition motif. In addition by virtue of its binding to ATPase subunits, PSMD9 may be uniquely positioned on the surface of the 19S regulatory particles to ensure rapid unfolding, prevention of premature release of the substrates and translocation of the unfolded protein through the central channel that lines the ATPase ring. Another aspect of our finding is the nature and origin of the components involved in IκBα degradation – a chaperone from the proteasome pathway and a RNA binding protein. Thus it is speculated that there may be other functions mediated by this domain-motif interaction between PSMD9 and hnRNPA1 relevant to their respective network and/or the cross talk between different functional modules.

Regarding the involvement of the PDZ domain in interaction with the ATPase subunits, we find that mutations in the PDZ-domain that affect hnRNPA1 binding do not affect association with the proteasome. While we do not find any literature evidence for the role of PDZ domains in interaction with the ATPases in mammalian cells, Nas2 in yeast has been shown to interact with Rpt5 or PSMC3 via the C-terminal residues [208]. Although we have not tested the interaction of PSMD9 with PSMC3, interaction

of PSMD9 with PSMC6 is unaffected by the PDZ-mutations (current study). It is possible that the association of PSMD9 with the mature proteasome is different from its interaction with the ATPase subunits in the modular structure. It is obvious that we are from a clear understanding of the role of PSMD9 in the functioning of holo 26S proteasome and its interaction with the different subunits. More studies with detailed molecular characterization as reported in this current study would be necessary to clarify the complexity associated with these supramolecular structures.

3.5 SUMMARY AND CONCLUSION:

In summary, we establish that PSMD9, a proteasomal subunit, involve in the canonical NF-κB signaling pathway. PDZ domain of PSMD9 interacts with the C-terminus of hnRNPA1, a novel interacting partner and this interaction regulates degradation of IκBα and therefore NF-κB activity in HEK293 cells. PSMD9 without influencing the phosphorylation and ubiquitination of IκBα, degrade it by enhancing the rete of recruitment on proteasome. In this process hnRNPA1 acts as a shuttle receptor while PSMD9 is the docking site on the 19S regulatory particle. IκBα may be one of the many examples of how ubiquitinated substrates may be recruited on the proteasome through the PDZ domain of PSMD9. It is possible that features of the C-terminal sequence found in hnRNPA1 may be conserved in other shuttle receptors. Our study opens up new areas of investigation on the role of PSMD9 in cellular homeostasis. The generality of this interaction between hnRNPA1 and PSMD9 may propose the interface as a potential drug target in tumor cells relying on high NF-κB activity.

3.6 SIGNIFICANCE OF THE STUDY:

For the first time we have reported a novel function of a proteasomal subunit-PSMD9 in NF-κB signaling pathway. This is the first report where we explicate a novel interacting

partner of PSMD9 i.e. hnRNPA1 and the functional significance of this interaction. For the first time we have reported that PSMD9 found in the 26S proteasome holocomplex. “For IκBα proteasomal degradation, PSMD9 act as adaptor protein and hnRNPA1 as a shuttle receptor” may be one of the many example of how protein brought to proteasome for degradation. This study can be taken as an example for finding more proteins which follow same mechanism of substrate presentation to proteasome. Since the interaction site between PSMD9 and hnRNPA1 shown to be key determinant NF-κB activity, this hot spot site can be targeted for cancer therapy.

CHAPTER-IV

PSMD10 (Gankyrin)

(The role of PSMD10 in Neural Stem Cell differentiation)

4.1 INTROUDUCTION AND REVIEW OF LITRATURE

PSMD10, the proteasome (prosome, macropain) 26S subunit, non-ATPase10, is a non-ATPase subunit of 19S regulatory particle of human proteasome. It is commonly called as Gankyrin: Gann + ankyrin; “Gann” means cancer in Japanese. Initially it was identified as the p28 component (Nas6/PSMD10) of the 19S regulatory subunit of the 26S proteasome, which could function in the proteasome-mediated degradation in yeast [314]. Gankyrin was also discovered independently by constructing cDNA libraries from non-cancerous liver and hepatocellular carcinoma (HCC) in 2000 by Jun Fujita group [315]. Since this protein was reported for its tumorigenic potential in Hepatocellular carcinoma and was containing ankyrin repeats, given the name “Gankyrin” [315]. Since then PSMD10/gankyrin called as an oncoprotein and was found to be overexpressed in many cancers. However, studies indicated that, nas6 the yeast homolog of PSMD10 is not essential for cell-cycle progression or not required for spore germination in yeast [314]. PSMD10 expression in human tissue is ubiquitous in nature however, its mRNA levels are particularly high in pancreas, placenta, testis, heart and skeletal muscle [314]. Nas6 (PSMD10) acts as a chaperon during the assembly of 19S regulatory particle on the 20S-core particle [244, 316, 317]. In the assembly process it interacts with two ATPase subunits PSMC4 and PSMC5. Although PSMD10, a non-ATPase subunit of 19S-RP, is considered as the part of 26S proteasome (unlike PSMD9) [318], experimentally it has not yet been found in matured proteasome complex, rather found either free form or bound with the 19S sub-complex [319].

4.1.1 Structure of PSMD10:

PSMD10 is a 226 amino acid long protein, approx. MW is 24.7 KDa. The yeast homolog Nas6, was identified, cloned and sequenced for the first time during 1998 by Keiji Tanaka group [314]. Nas6 shares high sequence similarity with PSMD10.

Sequence comparison studies showed that PSMD10 possesses 35% identity and 52% similarity with Nas6 [320]. The sequence homologies between human and other mammals are higher than 90%, which is consistent with the fact that the proteasome system is highly conserved among mammals. While there is a homology of 72% between human and zebrafish gankyrin, the sequence homology between human and yeast is relatively low, 29%, however, most of residues important for the sketch structure of ankyrin repeats are conserved, implying that human and yeast gankyrin (Nas6) proteins could have a structural similarity higher than the sequence homology. The tertiary structure and the crystal structure of Nas6 or PSMD10 have been solved either alone or with their interacting partners by many independent groups during the period 2002-2007 [320-327].

4.1.1.1 Nas6 (yeast gankyrin) crystal structure:

Nas6 structure was solved for the first time in 2002 with a resolution of 2.3Å [320, 321]. The crystal structure of Nas6 composed of 228 residues was solved by the MIR method at 2.7-Å resolution and was refined to 2.3-Å resolution (Figure-4.1A). The tertiary structure of Nas6p is an elongated structure with overall dimensions 74 Å-36 Å-33 Å (Figure-4.1A). Nas6 consists of seven ankyrin repeats (ANK1 to ANK7 in Figure-4.1), each ankyrin repeat is formed by ~30 amino acid residues with a β-hairpin and helix-loop-helix motif (the only exception is ANK1, which lacks the β-strand β1). The seven ankyrin repeats in Nas6p possess uniform backbone conformations, as expected from the relatively high degree of sequence similarity between the motifs except for ANK7. ANK1 possesses a shorter linker region that connects ANK2 compared with the other repeats (ANK2–7). In ANK2, -3, and -5, the linker chain is relatively longer compared with that found in ANK1, -4, and -6. This insertion of a longer chain causes

more bending, and thus, the overall shape of Nas6p resembles a concave structure (called “banana-shaped” structure) [320].

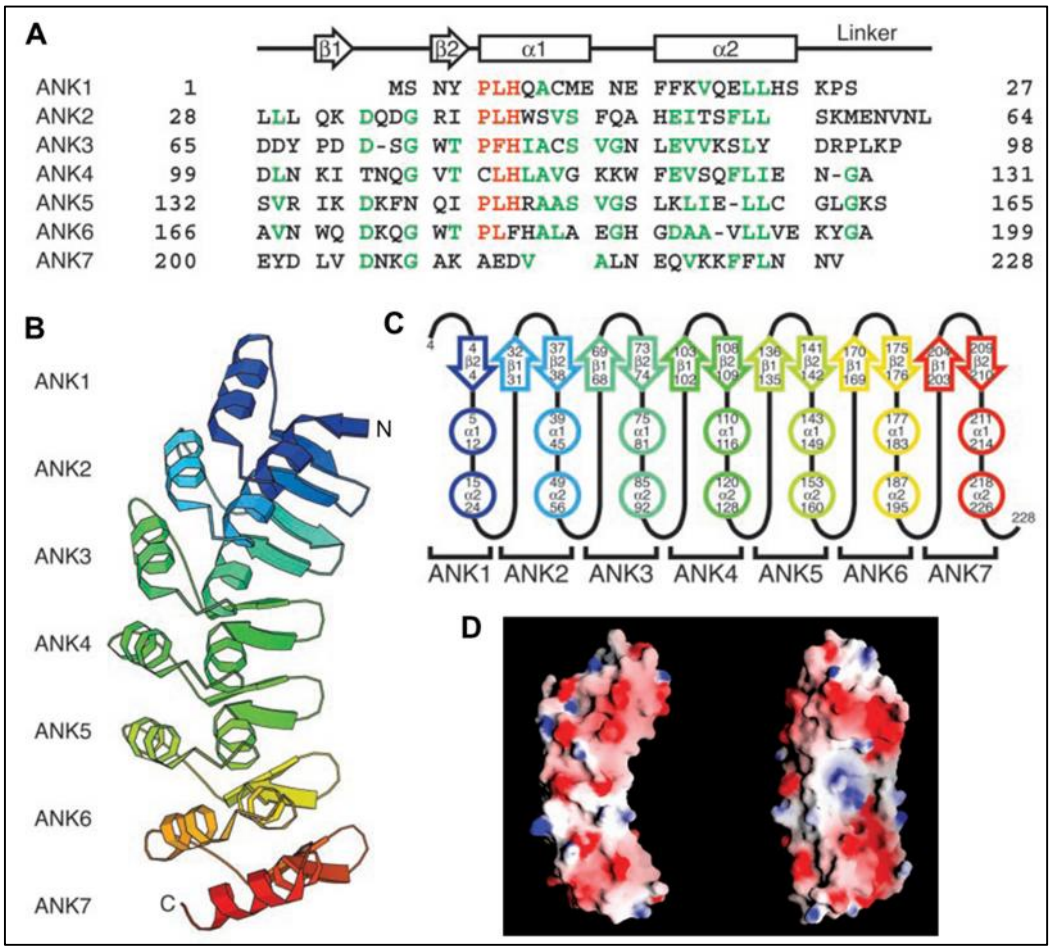

Figure-4.1: Crystal Structures of the Nas6. (A) structure-based sequence alignment of the seven ankyrin repeats of Nas6p. Positions of α-helices and β-strands are indicated *above* the sequences. *Red letters* indicate the conserved PLH motif except for AED in ANK7. *Green letters* indicate other identical or similar residues between each ankyrin repeat. **(B)** Ribbon representation of the tertiary structure of Nas6p. Each ankyrin repeat is indicated by ANK1–7. **(C)** Topological diagram of the secondary structure elements of the Nas6p protein. ANK1–7 indicates the seven ankyrin repeats. α-helices and β-strands are indicated by circles and arrows, respectively. Residue numbers are indicated at the start and end of each secondary structural element. **(D)** The “banana shaped structure” of nas6. The surfaces color-coded for calculated electrostatic surface potentials calculated by GRASP. Red, blue, and white represent acidic, basic, and neutral, respectively. Left panel is the same orientation as in (B). The orientation of the right panel is a 90° rotation about the vertical axis. [Adopted from: Padmanabhan B., et. al., 2004 [320]]

To better understand the molecular mechanism of protein interaction with nas6 and to elucidate the functional relevance of nas6 interaction, Nakamura group solved the co-crystal structure of nas6 with its novel interacting partner Rpt3 in 2007 [319, 326]. In

this study full length nas6 with the c-terminal domain of the ATPase-Rpt3 were crystalized with a resolution of 2.2Å. The modelled structure suggests that almost all of the ankyrin repeats of Nas6, ANK1-7, are involved in association with the Rpt3 protein (Figure-4.3A). Moreover, the structure of Nas6 in complex with Rpt3 uncovered the mechanisms for the exclusive interaction between Nas6 and the hetero-hexameric ATPase ring of the proteasome through the C-terminal domain of Rpt3. It also revealed that the recognition for a complex formation between Nas6 and Rpt3 occurred mainly through salt links and polar interactions. Structural and biochemical evidences presented in the study confirmed that Nas6 was indeed a subunit of the 26S proteasome, through its association with the Rpt3 subunit of the ATPase ring of the 19S regulatory particle [318]. The structural basis will aid in identification and characterization of possible substrates for 26S proteasome dependent protein degradation in yeast.

4.1.1.2 PSMD10 (Gankyrin) crystal structure:

Human PSMD10/gankyrin crystal structure was solved in two independent groups independently (2.0Å and 2.8Å resolution respectively) in the year 2003-2004 [322-324]. PSMD10 structure is very similar to that of nas6 (root mean square deviation = 1.7 Å for 224 common C_α atoms). The crystal structure reveals that the entire 226-residue gankyrin polypeptide folds into seven ankyrin repeat elements. Similar to nas6 structure the ankyrin repeats, consisting of an antiparallel β-hairpin followed by a perpendicularly oriented helix-loop-helix, stacked side-by-side together near linearly to form a helix bundle, and neighboring ankyrin repeats are linked by loops of varied size, which orientate perpendicularly to the axes of the helices of ankyrin repeats (Figure-4.2). While it is generally described as “linearly stacked”, a slight bending of the repeat stack toward the *β*-hairpin loop creating an extended curved structure with a groove running across the long concave surface. Like most of ankyrin repeat proteins, there is no

disulfide bond or long-range intramolecular interaction present in gankyrin, and the elongated structure is mainly stabilized through inter- and intra-ankyrin repeat hydrophobic interactions predominantly associated with conserved nonpolar residues in the helical regions as well as hydrogen bonding interactions between polar residues and the main chain atoms from adjacent ankyrin repeats [328, 329]. Furthermore, a solution structure of gankyrin is almost superimposable to that of gankyrin in complex with the C-terminal domain of S6 ATPase, implying that free gankyrin is in a biologically active conformation. [325].

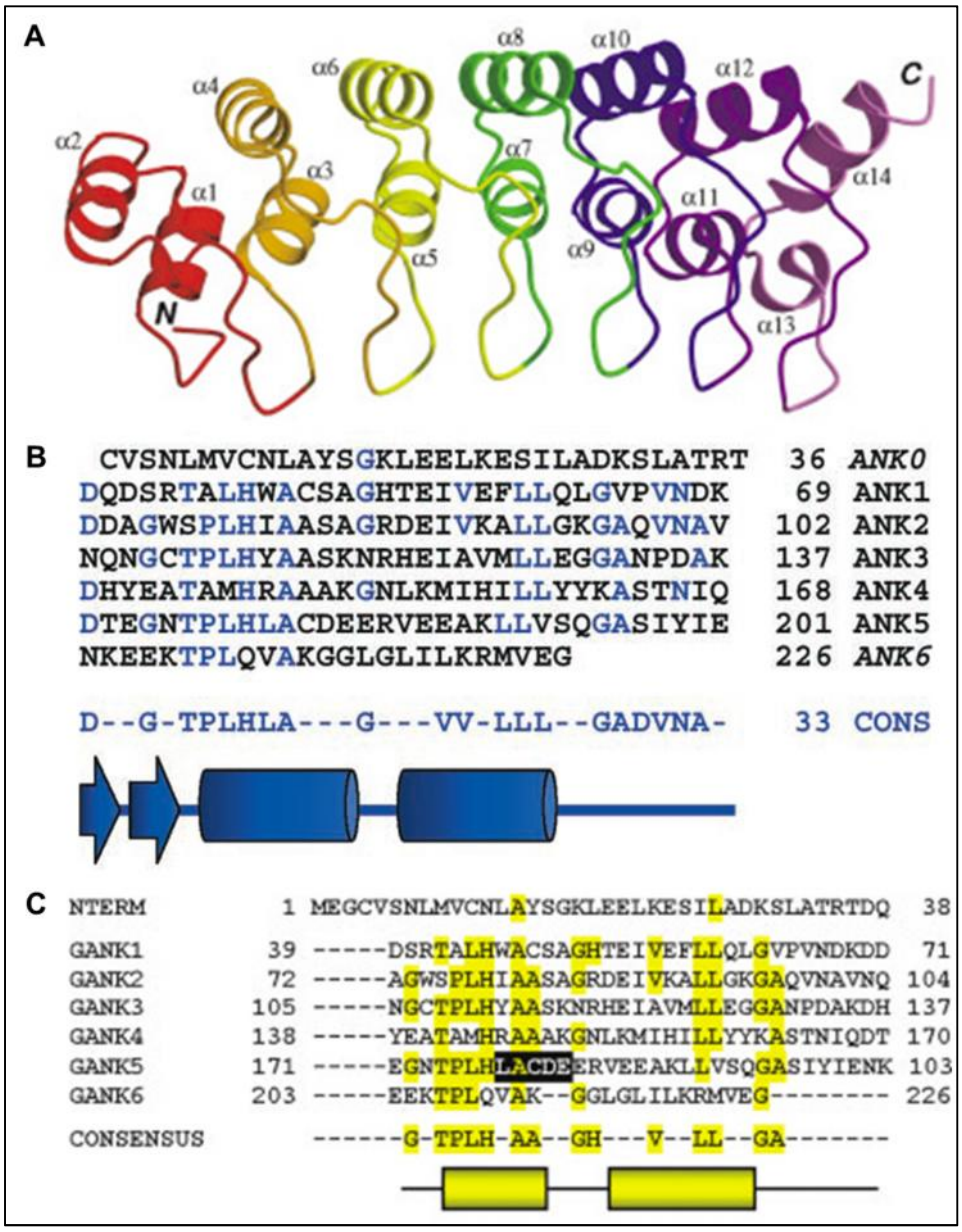

Figure-4.2: Crystal Structures of the PSMD10 (Gankyrin). (A) Ribbon diagram of human gankyrin. The N-terminal domain is coloured, and the six ankyrin repeats are colored individually. [Adopted from: Babu A. Manjasetty et al., 2004 [324]]. **(B)** Alignment of the five full ankyrin repeat sequences (ANK1-5) together with sequences at the N (ANK0) and C (ANK6) termini of the molecule, which in the structure adopts the ankyrin repeat fold (Reported by Szymon Krzywda et. al., 2004 [323]). The schematic below the alignment indicates the span of the α-helical and β-strand segments of the structure. A consensus ankyrin repeat sequence [330], is shown below the structure. Residues that match the consensus are in blue. (C) Sequence of human gankyrin reported by Babu A. Manjasetty et al., 2004 [324]. The six ankyrin repeats are aligned with the ankyrin consensus sequence [331]. In the fifth ankyrin repeat, the potentially Rb-interacting LXCXE sequence motif is highlighted. Below the sequence, the position of the α-helices are indicated.

Apart from these structural studies, mouse gankyrin was co-crystalized with its interacting partners S6-ATPase to elucidate the binding interface and relevant functions [326, 327]. The crystal structure of gankyrin in complex with the C-terminal domain of the S6-ATPase reveals that, gankyrin binds to the S6-ATPase through its concave region of ankyrin repeats. The structure of the complex suggested that all of the ankyrin repeats in

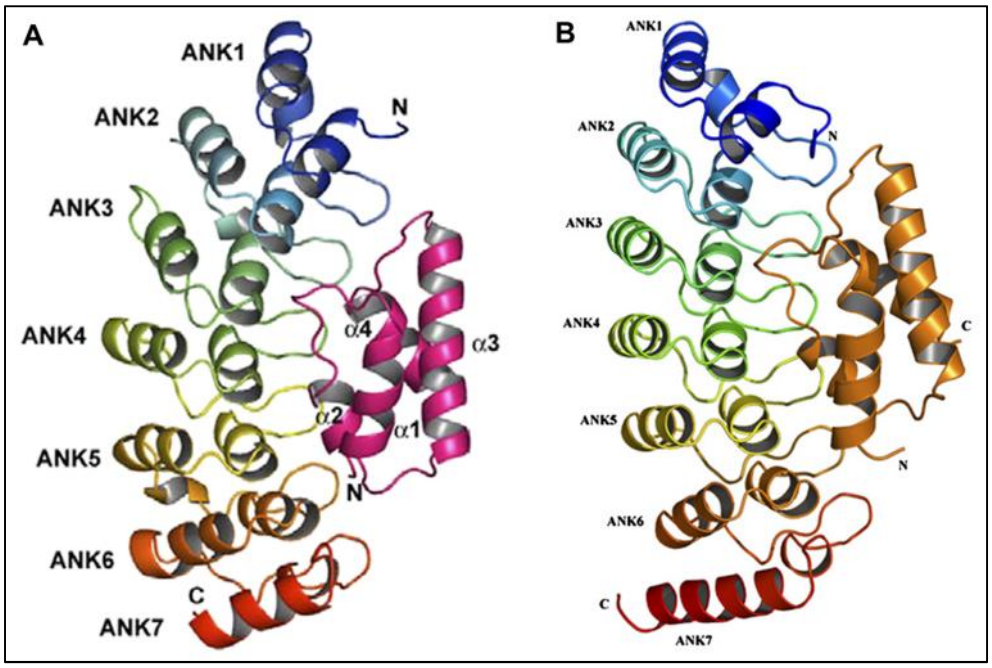

Figure-4.3: Structure of the Nas6/Rpt3 and Gankyrin/S6-C Complex. (A) Tertiary structure of the Nas6–Rpt3-C complex by ribbon diagram. Each ankyrin repeat of the gankyrin is indicated by ANK1-7 (blue to red). The Rpt3-C tertiary structure is in pink. The N and C termini of both molecules are indicated. **(B)** Ribbon representation of the mouse gankyrin/S6-C complex. Each ankyrin repeat of the gankyrin is indicated by ANK1-7 (blue to red). The S6-C tertiary structure is coloured orange. The N and C termini of both molecules are indicated. Structural figures were generated with PyMOL [Adopted from: Nakamura Y, et al., 2007 [318, 327]].

gankyrin are essential for the interaction with S6 ATPase which is consistent with a previous biochemical study that full-length nas6 is essential for the Rpt3 interaction [326], whereas the C-terminal domain of S6 ATPase alone is sufficient for association with its partner, gankyrin. (Figure-4.3A & B). A comparison of the structures between the gankyrin/S6-C complex and native gankyrin [323] indicated that gankyrin slightly bends to interact with the surface of S6-C [327]. The structure of the yeast homolog [320], Nas6p, also shows similar behaviour, as compared with that of the gankyrin in the gankyrin/S6-C complex. These results indicate that the gankyrin structure (and those of its homologs) is quite rigid and does not change much when it binds to S6 ATPase.

4.1.1.3 Comparison between Nas6 and PSMD10 structures:

The overall structures of the two homolog protein complexes; nas6 and PSMD10, as well as the mode of interactions with their counterparts, are similar (Fig. 4) [318]. The charged patches on the interface and the number of salt links are nearly conserved between these complexes. Most of the interacting residues responsible for making the complexes are also substantially conserved between them (Figs. 3 and 4A and B). Hence, the recognition modes for the interaction of these two complexes are essentially the same. A superposition of the two complexes with respect to ANK4 revealed that Nas6 in the Nas6–Rpt3 complex possesses more bent form as compared to gankyrin in the gankyrin–S6 ATPase complex (Fig. 4C). A comparison of the C-terminal domains of Rpt3 and S6 showed that the overall tertiary structures of these two domains are similar, and the interacting regions for complex formation with their partners also superposed well. However, the substantial bent observed in the Nas6 structure may influence in significant changes in the conformation and orientation of the side chains with respect to that found in the gankyrin structure of the gankyrin–S6C complex. Also, because of this bent, the Nas6 molecule appears to squeeze the Rpt3-C molecule

slightly downward when compared to the structure of the gankyrin–S6C complex. Thus, the variation in the curvature of the elongated structures observed in Nas6/gankyrin and the structural deviation in the loop region of Rpt3/S6 are likely to be unique features for selecting their specific partners in different species.

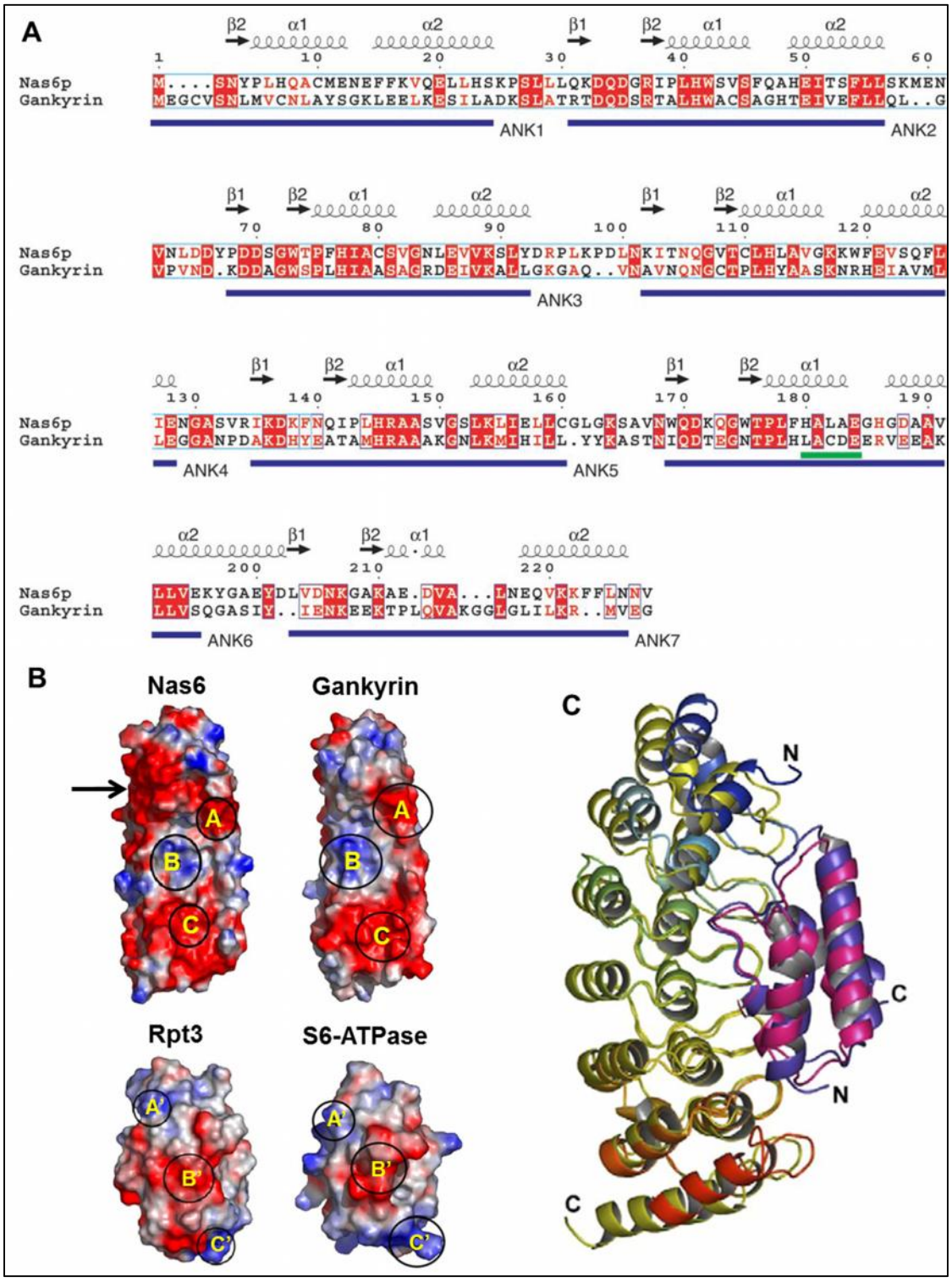

Figure-4.4: Comparison between Nas6 and PSMD10 (Gankyrin) structures. (A) Sequence alignment of Nas6p and gankyrin. Accession numbers of the amino acid sequences are P50086 (Nas6p) and O75832 (gankyrin). The α-helices and β-strands are indicated as helices and arrows, respectively, and ANK1–7 repeats are indicated by blue bars. Residues 1–27 and 200–228 in Nas6p are newly identified in this study as ANK1 and -7, respectively. Residues 1–138 in gankyrin (cyan box) are required for interaction with CDK4/6. Residues 178–182 in gankyrin (LXCXE motif (green bar)) are required for interaction with Rb (2, 3). The figure was generated by Espript (22). Identical or similar residues are defined as G; A, V, I, L; M; F, Y, W; P; C; S, T; N, Q; D, E; and H, K, R. [Adopted from: Padmanabhan B., et. al., 2004 [320]] **(B)** Charge distribution on the surfaces of Nas6, gankyrin, Rpt3-C and S6ATPase-C. The complementary surface patches responsible for complex formation are indicated by circles (labeled as A, B and C in Nas6/Gankyrin, and as A0, B0 and C0 in Rpt3-C/ S6ATPase-C, respectively). Red, blue and white represent acidic, basic, and neutral, respectively. An arrow indicates a proposed potential site for another Nas6 partner. **(C)** Superposition of ANK4 of the Nas6–Rpt3-C complex with that of the Gankyrin–S6C complex. The colouring code for the Nas6–Rpt3-C complex is the same as in Figure-4.3A, and for gankyrin and S6C are shown in yellow and violet, respectively. [Adopted from: Nakamura Y, et al., 2007 [318, 327]].

A sequence comparison between Nas6 and gankyrin revealed about 52 % sequence similarity (Figure-4.4A) [318, 320]. This relatively low similarity reflects the charge distribution on their surface regions. Although the charge distributions on the ATPase interacting surface (regions A, B and C) are well conserved, some other regions differ considerably. For instance, the N-terminal part of Nas6 is highly negative (indicated by an arrow in Figure-4.4B), whereas the corresponding region in gankyrin is relatively positive. As this region possesses a large charged surface patch, and the charge distribution in this region is quite different, it is possible that this may be another site for specific recognition of distinct protein partners for Nas6 and gankyrin.

4.1.2 Interacting partners of PSMD10:

As described earlier, gankyrin belongs to the ankyrin repeat protein class, and proteins in this class are involved in numerous physiological processes exclusively through mediating protein-protein interactions [328, 329]. A number of important proteins have been identified as physiological targets for gankyrin binding and modulating, some of which, such as pRb [315], MDM2 (HDM2 in human) [332], cyclin-dependent kinase-4 (CDK4) [319, 333], NF-κB-RelA [334], melanoma antigen (MAGE)-A4 [335] and

RhoGDI1 [336]; play pivotal roles in cell cycle progression, apoptosis, and tumorigenesis. Recently in our lab we reported seven novel interacting partners of gankyrin *in vitro* and *ex vivo* [337].

In 2000 Jun Fujita group reported that gankyrin binds to pRb through a conserved pRb binding motif LxCxE at its C-terminus, and such binding is essential for gankyrin-induced transformation of NIH 3T3 fibroblasts [315]. This was the first report for gankyrin interaction with its binding partner, here it is pRb. More importantly, overexpression of gankyrin led to increased pRb hyperphosphorylation (loss of suppressor activity), activation of the E2F transcription factors (activating the expression of DNA synthesis genes) and accelerated the degradation of pRb, suggesting that increased expression of gankyrin could promote tumorigenicity by targeting pRb to the proteasome (Figure-4.5) [338]. Interestingly, it has been shown that gankyrin is able to modulate the pRb pathway through an alternative mechanism. That is, gankyrin competes with p16 as well as other INK4 proteins for binding to CDK4 and preludes the INK4 inhibition to the kinase activity of CDK4, resulting in enhanced pRb phosphorylation and concomitant deregulation of E2F1-mediated transcription and cell cycle progression. Evidently, these studies indicate that gankyrin deregulate the pRb, a tumor suppressor, pathway at multiple levels, and facilitate tumorigenicity.

In 2005 the Jun Fujita group again reported another break-through finding, about the role of gankyrin, where it's tumorigenecity has been expanded to the disruption of the P53 tumor suppressor pathway [332, 338]. It has been shown that gankyrin binds to HDM2, an E3 ubiquitin ligase, enhances the ability of HDM2 to ubiquitinate P53 [332, 339]. Consequently, gankyrin recruits the HDM2 and P53 complex to the protease and fosters the turnover of P53 in an HDM2-dependent manner. In addition, it has been reported that pRb inhibits MDM2-mediated P53 ubiquitination in a gankyrin dependent

manner and the Rb-gankyrin interaction is critical for pRb-induced P53 stabilization [340]. Taken together, gankyrin functions as a dual-negative regulator in both pRb and P53 pathways hence consider as very potent oncoprotein (Figure-4.5).

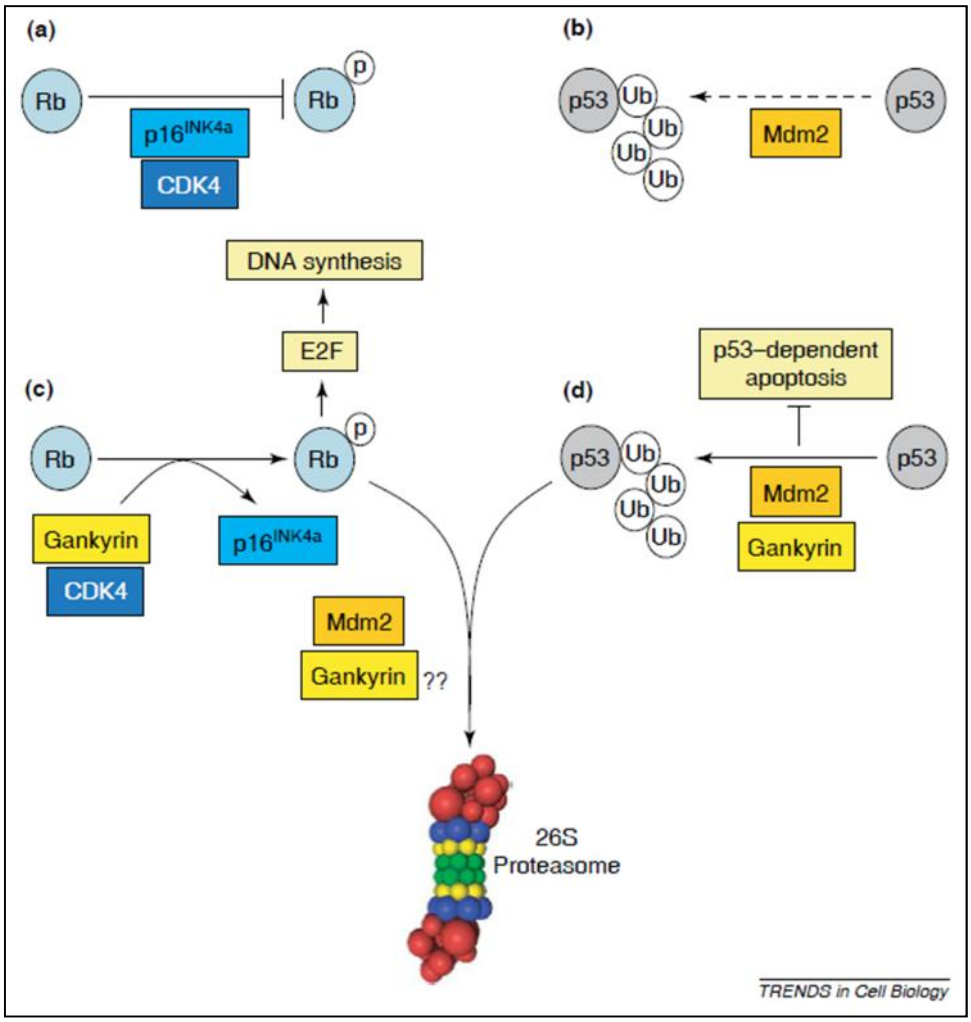

Figure-4.5 Current understanding of the activities of gankyrin in cell cycle regulation and apoptosis. In the absence of gankyrin (a) pRb is not hyperphosphorylated and (b) p53 is inefficiently ubiquitylated by MDM2 and poorly degraded. In the presence of gankyrin (c) pRb is hyperphosphorylated and degraded, whereas E2F transcription factors are released to trigger expression of DNA synthesis genes and (d) p53 is extensively ubiquitylated and degraded to inhibit p53 dependent apoptosis. Abbreviations: P, phosphate; Ub, ubiquitin. [Adopted from: Dawson, S. et. al., 2006 [338]]

In a pioneer work, Dawson et al., reported two novel interaction of gankyrin with cyclin dependent kinase-4 (CDK4) and proteasomal ATPase subunit-S6 (Rpt3) in a yeast-two hybrid screen [319]. Although gankyrin binds to CDK4, it is unlikely to interact with CDK4 and S6 ATPase simultaneously, as gankyrin uses the same region to

interact with CDK4 and S6 ATPase. Now as a proteasomal subunit, and interacting with C-terminal domain of the S6-ATPases gankyrin appears to be a shuttle protein for transporting ubiquitinated proteins, such as P53 to the proteasome for degradation [339]. Gankyrin structure suggests that, C-terminal region of gankyrin extends and bends toward the active center of CDK4. This free C-terminal region might interact with some target molecules and recruit them to CDK4 as substrates. The C-terminal region of gankyrin contains an LXCXE motif, which is responsible for the binding of Rb in vivo [315]. Again biochemical studies indicate that the LXCXE motif region of gankyrin is sufficient for Rb binding in vitro [333]. It has also been shown that the binding of CDK4/6 and Rb with gankyrin is independent to each other and occur at N- and C-terminal regions of gankyrin, respectively. [325, 333]. In addition the binding site for CDK4 and the phosphorylation site on pRb and the active site of CDK4 lies on the same site while both of them bind gankyrin simultaneously. And also studies have suggested that, the binding affinity between pRb and gankyrin was not influenced by the presence or absence of S6 ATPase and both shows different binding affinities to gankyrin [327]. Rb also interacts with E2F but opposite to its LXCXE binding motifs [341, 342]. Furthermore, overexpression of gankyrin enhances pRb phosphorylation and proteasomal degradation. Taken together the mode of interactions between Gankyrin, CDK4, S6-ATPase, pRb and E2F it can be hypothesized that, "*upon overexpression, gankyrin functions to carry pRb, which is phosphorylated by CDK4, to the 26S proteasome site. Then, gankyrin binds to S6 ATPase and subsequently releases pRb for its degradation at the 26S proteasome. And E2F gets free to transcribe cell cycle initiating genes*" (as depicted in Figure-4.6). However, the structure of the gankyrin/pRb complex and gankyrin/CDK4 complex are required to further understand the molecular mechanism of pRb degradation in detail.

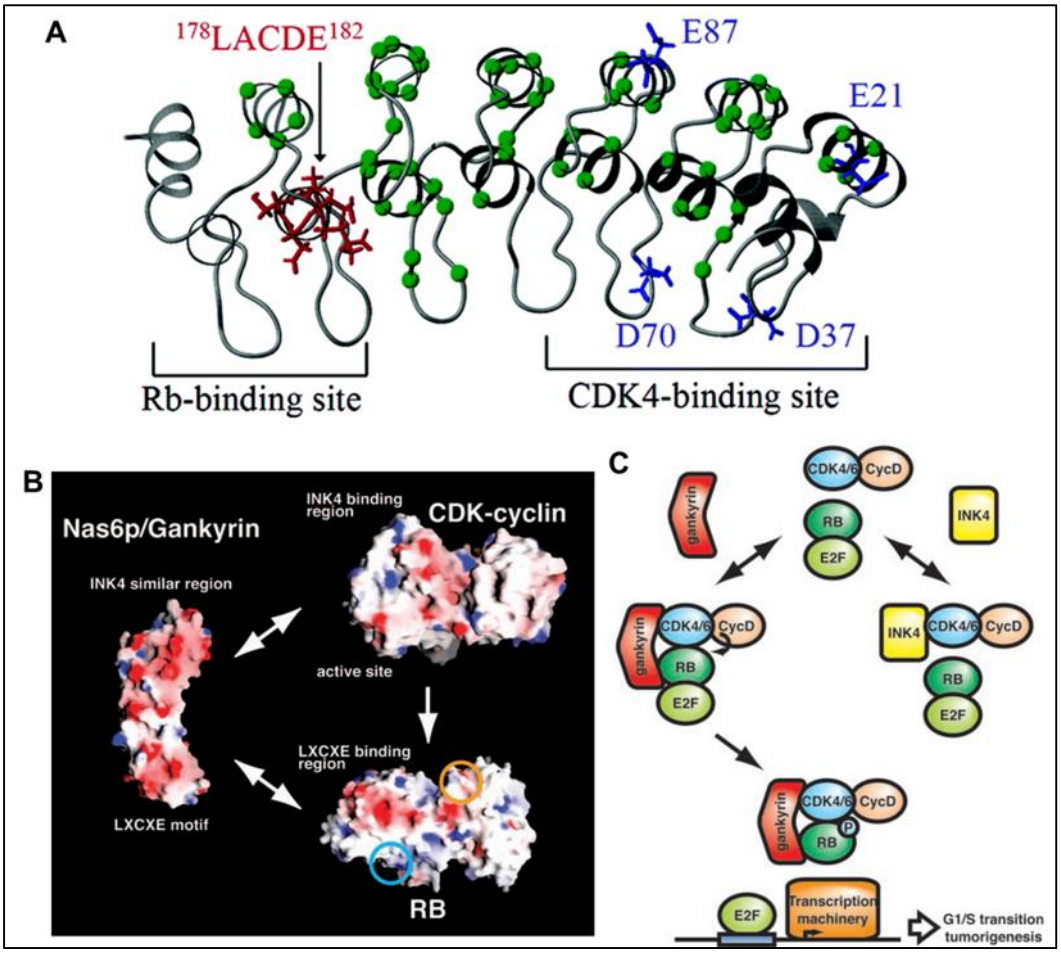

Figure-4.6 Prediction of gankyrin interaction with Rb and CDK4/6 based on the tertiary structure of Nas6p and biochemical and mutational studies. (A) Two different binding site for CDK4 and pRB on gankyrin. Amino acid residues mentioned are important for the binding. [Adopted from: Yuan C., et. al., 2004 [325]] **(B)** Structural model for the interaction among gankyrin homolog (Nas6p), CDKcyclin (PDB code: 1FIN), and Rb (PDB code: 1GUX). Corresponding regions to Thr-373 and Ser-780 in Rb are circled in orange and cyan, respectively. C and D were generated by GRASP (25). **(C)** Schematic representation of the Rb-phosphorylation pathway. Gankyrin interacts with CDK4/6 by competing with INK4 and then interacts with Rb and CDK4/6 simultaneously and promotes site-specific phosphorylation of Rb by CDK4/6. [Adopted from: Padmanabhan B., et. al., 2004 [320]].

In addition to the above mentioned role in the P53 and pRb pathways, gankyrin has been found to be able to interact with melanoma antigen (MAGE)-A4, a tumor specific antigen with potential in antitumor immunotherapy [335]. This interaction is mediated by the C-terminal half of MAGE-A4, and is very specific since other MAGE family proteins structurally similar to MAGE-A4, i.e. MAGE-A1, MAGE-A2, and MAGE-A12 do not bind to gankyrin. Studies suggested that gankyrin is also involved in

the regulation of the IκBα/NF-κB pathway [334, 343] but unlike PSMD9 it supress the activity of NF-κB. On one hand, gankyrin directly binds to NF-κB/RelA and exports RelA from nucleus through a chromosomal region maintanence-1 (CRM-1) dependent pathway, thus suppressing the nuclear translocation of NF-κB/RelA as well as its activity [334]. On the other hand, gankyrin can bind to NF-κB and negatively regulates its activity at the transcription level through modulating acetylation via SIRT1, a class III histone deacetylase [343].

Recently in our lab by a high through-put screening method we have reported seven novel interacting partners of PSMD10 (gankyrin) such as; NCK2, G-rich RNA sequence binding factor 1 (GRSF1), chloride intracellular channel protein 1 (CLIC1), eukaryotic initiation factor 4A-III (EIF4A3), dimethylarginine dimethylaminohydrolase 1 (DDAH1), and mitogen-activated protein kinase 1 (MAP2K1), heat shock protein 70 (Hsp70) and heat shock protein 90 (Hsp90) and the probable hotspot site for the interaction interface [337]. Taking the clue from the interaction interface sequence (EEVD in S6-ATPase) of the crystal structure of gankyrin/S6-ATPase, we screened the whole genome for EEVD containing proteins. By various in-silico screening (high rSASA value, and availability of crystal structure) and by in vitro and ex vivo studies, we proved seven novel interactions. Three of these interactions occur in HEK293 cells only when gankyrin is overexpressed but occur in breast cancer cells at endogenous levels. Furthermore, we experimentally showed the relevance of one of the interaction CLIC1-gankyrin in breast cancer. However, the rest of the interactions are to be validated for their functional significance further. Although we showed the importance of the consensus sequence for the interaction, further crystal structure of gankyrin with those proteins will shed light on the structural basis of the function of human gankyrin.

Since the discovery of the first gankyrin interacting partner in 2000, substantial number of interacting proteins has been identified during the one and half decade. Furthermore, two imperative characters make gankyrin a vital hub protein for protein interaction network in cancer and normal cells; such as (a) gankyrin has recently discovered as an oncoprotein and (b) it has potential ankyrin repeats (known for protein-protein interactions). Although many of the interactions were validated for their functional relevance lot more have to be elucidated. Hence there is a lot of scope to explicate novel interactions (including cancer specific interactions) and their functional significance, which might contribute towards therapeutic investigation for many diseases including cancer.

4.1.3 PSMD10 (gankyrin) in cancer:

Gankyrin appears to be one of few oncogenic proteins negatively modulating both pRb and P53 tumor suppressive pathways. Considering the fact that more than 90% of cancer cells have inactivated pRB and P53 pathways either directly or indirectly [338], the status of gankyrin in cells could be associated with the development of human cancers. “Gankyrin”, the non-ATPase subunit of 19S-RP, was in fact first identified as an oncoprotein in hepatocellularcarcinoma in 2000, and hence given the name accordingly [315]. The overexpression of this protein in HCC resulted in enhanced tumerogenic property in vivo. Moreover, overexpression of gankyrin was very often observed in many cancers like; esophageal squamous cell carcinoma (ESCC) [344], pancreatic cancer [345], colorectal cancer [346], cervical cancer [347], liposarcoma [348], middle ear cholesteatoma [349] and also in testicular germ cell tumor [350]. Gankyrin is frequently overexpressed in breast cancer and is associated with ErbB2 expression [351]. It has also been reported that, up-regulated gankyrin correlates with proliferation and poor prognosis of human glioma [352].

Gankyrin is not only overexpressed in cancer conditions but also modulate various signaling pathways in cancer. Gankyrin enhances Ras-mediated activation of Akt through interacting with RhoGDI. This interaction inturn increases RhoA-RhoGDI interaction and inhibits ROCK activity thereby decreases PTEN activity. That is how gankyrin plays an essential role in Ras-induced tumorigenesis [336]. Gankyrin promotes PI3K/Akt activation leading to enhanced HIF1α signaling pathway thereby increase HCC progression and metastasis [353]. Gankyrin promotes breast cancer cell metastasis via accelerating focal adhesion turnover by regulating Rac1 activity [354]. Gankyrin activates IL-8 to promote hepatic metastasis of colorecteal cancer [355]. Gankyrin plays an essential role in estrogen-driven and GPR30-mediated endometrial carcinoma cell proliferation via the PTEN/PI3K/AKT signaling pathway [356]. Gankyrin promotes tumor growth and metastasis through activation of IL-6/STAT3 signaling in human cholangiocarcinoma [357]. Our lab reported that, gankyrin by interacting with CLIC1, enhances migratory potential of breast cancer cells [337].

However, despite its oncogenic role, gankyrin also exhibits some normal functions in cells. As described earlier PSMD10 binds to RelA and retains NF-κB in the cytoplasm thus decreasing NF-κB activity [334]. Gankyrin reportedly stabilizes *β*-catenin cytoplasmic levels and also enhances the transcriptional activity of *β*-catenin/TCF3 complex [358]. Since, *β*-catenin/wnt signaling pathway is crucial for cellular differentiation,it can speculated that gankyrin may play some role in normal signaling pathways. In addition our recent study suggested an array of different proteins which interact with gankyrin both in normal and cancer scenario. Hence, although speculative, gankyrin might be modulating different signaling pathways for cellular homeostasis in normal cells.

4.1.4 NEURAL STEM CELLS (NSCs):

Neural stem cells (NSCs) are primary progenitor cells that give rise to neurons and glia in the embryonic, neonatal and adult brain [359]. The term “neural stem cell” is used to describe cells that; (1) can generate neural tissue or are derived from the nervous system, (2) have some capacity for self-renewal, and (3) can give rise to cells other than themselves through asymmetric cell division [360]. Moreover, central nervous system (CNS) development starts from a small number of highly plastic cells that proliferate, acquire regional identities and produce different cell types. These cells have been defined as neural stem cells on the basis of their ability to self-renew in vitro and to generate three major cell types such as neurons, oligodendrocytes and astrocytes. NSCs are specified in a space- and time-related manner , becoming spatially heterogeneous and generating progressively restricted repertoire of cell types [361]. Mammalian NSCs produce different cell types at different time points during development under the influence of multiple signaling pathways.

In recent years, we have learned three important things about these cells. First, NSCs correspond to cells previously thought to be committed glial cells. Second, embryonic and adult NSCs are lineally related: they transform from neuroepithelial cells into radial glia, then into cells with astroglial characteristics. Third, NSCs divide asymmetrically and often amplify the number of progeny they generate via symmetrically dividing intermediate progenitors [359]. The discovery of adult mammalian neural stem cells marks a milestone in the journey of our current understanding of adult brain plasticity. A previously long-held dogma maintained that neurogenesis in the adult mammalian CNS was complete, rendering it incapable of mitotic divisions to generate new neurons, and therefore lacking in the ability to repair damaged tissue caused by diseases (e.g. Parkinson’s disease, multiple sclerosis) or

injuries (e.g. spinal cord and brain ischemic injuries). However, there is now strong evidence that multipotent NSCs do exist, although only in specialized microenvironments, in the mature mammalian CNS. This discovery has fuelled a new era of research into understanding the tremendous potential that these cells hold for treatment of CNS diseases and injuries.

4.1.4.1 Identification of Neural Stem Cells:

Neurobiologists routinely use various terms interchangeably to describe undifferentiated cells of the CNS. The most commonly used terms are “stem cell”, “precursor cell” and “progenitor cell”. The inappropriate use of these terms to identify undifferentiated cells in the CNS has led to confusion and misunderstandings in the field of NSC and neural progenitor cell research. However, these different types of undifferentiated cells in the CNS technically possess different characteristics features and fates. For clarity, the terminology used here is:

Neural Stem Cells (NSCs): Multipotent cells which are able to self-renew and proliferate without limit, to produce progeny cells which terminally differentiate into neurons, astrocytes and oligodendrocytes. The non-stem cell progeny of NSCs are referred to as neural progenitor cells.

Neural Progenitor Cells: Neural progenitor cells have the capacity to proliferate and differentiate into more than one cell type. Neural progenitor cells can therefore be unipotent, bipotent or multipotent. A distinguishing feature of a neural progenitor cell is that, unlike a stem cell, it has a limited proliferative ability and does not exhibit self-renewal.

Neural Precursor Cells: As used here, this refers to a mixed population of cells consisting of all undifferentiated progeny of neural stem cells, therefore including both

neural progenitor cells and neural stem cells. The term neural precursor cells is commonly used to collectively describe the mixed population of NSCs and neural progenitor cells derived from embryonic stem cells and induced pluripotent stem cells.

Prior to 1992, numerous reports demonstrated evidence of neurogenesis and limited in vitro proliferation of neural progenitor cells isolated from embryonic tissue in the presence of growth factors [362-364]. While several sub-populations of neural progenitor cells had been identified in the adult CNS, researchers were unable to convincingly demonstrate the characteristic features of a stem cell, namely self-renewal, extended proliferative capacity and retention of multi-lineage potential. In vivo studies supported the notion that proliferation occurred early in life, whereas the adult CNS was mitotically inactive, and unable to generate new cells following injury. In the early 1990s, cells that responded to specific growth factors and exhibited stem cell features in vitro were isolated from the embryonic and adult CNS [365, 366]. With these studies, Reynolds and Weiss demonstrated that a rare population of cells in the adult CNS exhibited the defining characteristics of a stem cell: self-renewal, capacity to produce a large number of progeny and multilineage potential. The location of stem cells in the adult brain was later identified to be within the striatum [367], and researchers began to show that cells isolated from this region, and the dorsolateral region of the lateral ventricle of the adult brain, were capable of differentiating into both neurons and glia [368].

4.1.4.2 Neural Stem Cell Culture (*in vitro*) Systems:

In vitro culture methodologies develop to isolate, grow and functionally characterize NSC populations have revolutionized the understanding of neural stem cell biology, and increased our knowledge of the genetic and epigenetic regulation of NSCs [369]. Over the past several decades, a number of culture systems have been developed that attempt

to recapitulate the distinct in vivo developmental stages of the nervous system, enabling the isolation and expansion of different NPC populations at different stages of development. Here the commonly used culture systems are mentioned, for generating NPCs from pluripotent stem cells (PSCs), and for isolating and expanding NSCs from the early embryonic, postnatal and adult CNS.

4.1.4.2.1 Neural induction and differentiation of pluripotent stem cells: Early NPCs can be derived from mouse and human PSCs, which include embryonic stem cells (ESCs) and induced pluripotent stem cells (iPSCs), using appropriate neural induction conditions at the first stage of differentiation. While these neural differentiation protocols vary widely, a prominent feature in popular embryoid body-based protocols is the generation of neural “rosettes”, morphologically identifiable structures containing NPCs, which are believed to represent the neural tube. The NPCs present in the neural rosette structures are then isolated, and can be propagated to allow NPC expansion, while maintaining the potential to generate neurons and glial cells. More recently, studies have shown that neural induction of PSCs can also be achieved in a monolayer culture system, wherein human ESCs and iPSCs are plated onto a defined matrix, and exposed to inductive factors [370]. A combination of specific cytokines or small molecules, believed to mimic the developmental cues for spatiotemporal patterning in the developing brain during embryogenesis, can be added to cultures at the neural induction stage to promote regionalization of NPCs. These “patterned” NPCs can then be differentiated into mature cell types with phenotypes representative of different regions of the brain [371-376].

4.1.4.2.2 Neurosphere culture: The neurosphere culture system has been widely used since its development as a method to identify NSCs [377-380]. A specific region of the CNS is microdissected, mechanically or enzymatically dissociated, and plated in a

defined serum-free medium in the presence of a mitogenic factor, such as epidermal growth factor (EGF) and/or basic fibroblast growth factor (bFGF). In the neurosphere culture system, NSCs, as well as neural progenitor cells, begin to proliferate in response to these mitogens, forming small clusters of cells after 2 – 3 days. The clusters continue to grow in size, and by day 3 - 5, the majority of clusters detach from the culture surface and begin to grow in suspension. By approximately day seven, depending on the cell source, the cell clusters, called neurospheres, typically measure 100 - 200 μm in diameter and are composed of approximately 10,000 - 100,000 cells. At this point, the neurospheres should be passaged to prevent the cell clusters from growing too large, which can lead to necrosis as a result of a lack of oxygen and nutrient exchange at the neurosphere center. To passage the cultures, neurospheres are individually, or as a population, mechanically or enzymatically dissociated into a single cell suspension and replated under the same conditions as the primary culture. NSCs and neural progenitor cells again begin to proliferate to form new cell clusters that are ready to be passaged approximately 5 - 7 days later. By repeating the above procedures for multiple passages, NSCs present in the culture will self-renew and produce a large number of progeny, resulting in a relatively consistent increase in total cell number over time. Neurospheres derived from embryonic mouse CNS tissue treated in this manner can be passaged for up to 10 weeks with no loss in their proliferative ability, resulting in a greater than 100-fold increase in total cell number. NSCs and neural progenitors can be induced to differentiate by removing the mitogens and plating either intact neurospheres or dissociated cells on an adhesive substrate, in the presence of a low serum-containing medium. After several days, virtually all of the NSCs and progeny will differentiate into the three main neural cell types found in the CNS: neurons, astrocytes and oligodendrocytes. While the culture medium, growth factor requirements and culture

protocols may vary, the neurosphere culture system has been successfully used to isolate NSCs and progenitors from different regions of the embryonic and adult CNS of many species including mouse, rat and human.

4.1.4.2.3 Adherent monolayer culture: Alternatively, cells obtained from CNS tissues can be cultured as adherent cultures in a defined, serum-free medium supplemented with EGF and/or bFGF, in the presence of a substrate such as poly-L-ornithine, laminin, or fibronectin. When plated under these conditions, the neural stem and progenitor cells will attach to the substrate-coated cultureware, as opposed to each other, forming an adherent monolayer of cells, instead of neurospheres. The reported success of expanding NSCs in long-term adherent monolayer cultures is variable and may be due to differences in the substrates, serum-free media and growth factors used [369]. Recently, protocols that have incorporated laminin as the substrate, along with an appropriate serum-free culture medium containing both EGF and bFGF have been able to support long-term cultures of neural precursors from mouse and human CNS tissues [381-383]. These adherent cells proliferate and become confluent over the course of 5 - 10 days. To passage the cultures, cells are detached from the surface by enzymatic treatment and replated under the same conditions as the primary culture. It has been reported that NSCs cultured under adherent monolayer conditions undergo symmetric divisions in long-term culture [381, 384]. Similar to the neurosphere culture system, adherently cultured cells can be passaged multiple times and induced to differentiate into neurons, astrocytes and oligodendrocytes upon mitogen removal and exposure to a low serum-containing medium.

Several studies have suggested that culturing CNS cells in neurosphere cultures does not efficiently maintain NSCs and produces a heterogeneous cell population, whereas culturing cells under serum-free adherent culture conditions does maintain

NSCs [369]. In our lab for the current study we have used adherent monolayer culture of NPCs (procured from “Millipore”) and culture them following the protocol describe in materials and methods (Chapter-III).

4.1.4.3 In vivo differentiation of neural stem cells:

In vivo differentiation of NSCs or the active neurogenesis occurs during embryogenesis as well as in adult brain. In adult it primarily occurs in two regions of the adult mammalian brain: the subventricular zone (SVZ) of the lateral ventricles and the subgranular zone (SGZ) of the dentate gyrus (DG). During mammalian embryogenesis, CNS development begins with the induction of the neuroectoderm, which forms the neural plate and then folds to give rise to the neural tube. Within these neural structures there exists a complex and heterogeneous population of neuroepithelial progenitor cells (NEPs), the earliest neural stem cell type to form [385, 386]. As CNS development proceeds, NEPs give rise to temporally and spatially distinct neural stem/progenitor populations. During the early stage of neural development, NEPs undergo symmetric divisions to expand neural stem cell (NSC) pools. In the later stage of neural development, NSCs switch to asymmetric division cycles and give rise to lineage-restricted progenitors. Intermediate neuronal progenitor cells are formed first, and these subsequently differentiate to generate to neurons. Following this neurogenic phase, NSCs undergo asymmetric divisions to produce glial-restricted progenitors, which generate astrocytes and oligodendrocytes (Figure-4.7). The later stage of CNS development involves a period of axonal pruning and neuronal apoptosis, which fine tunes the circuitry of the CNS.

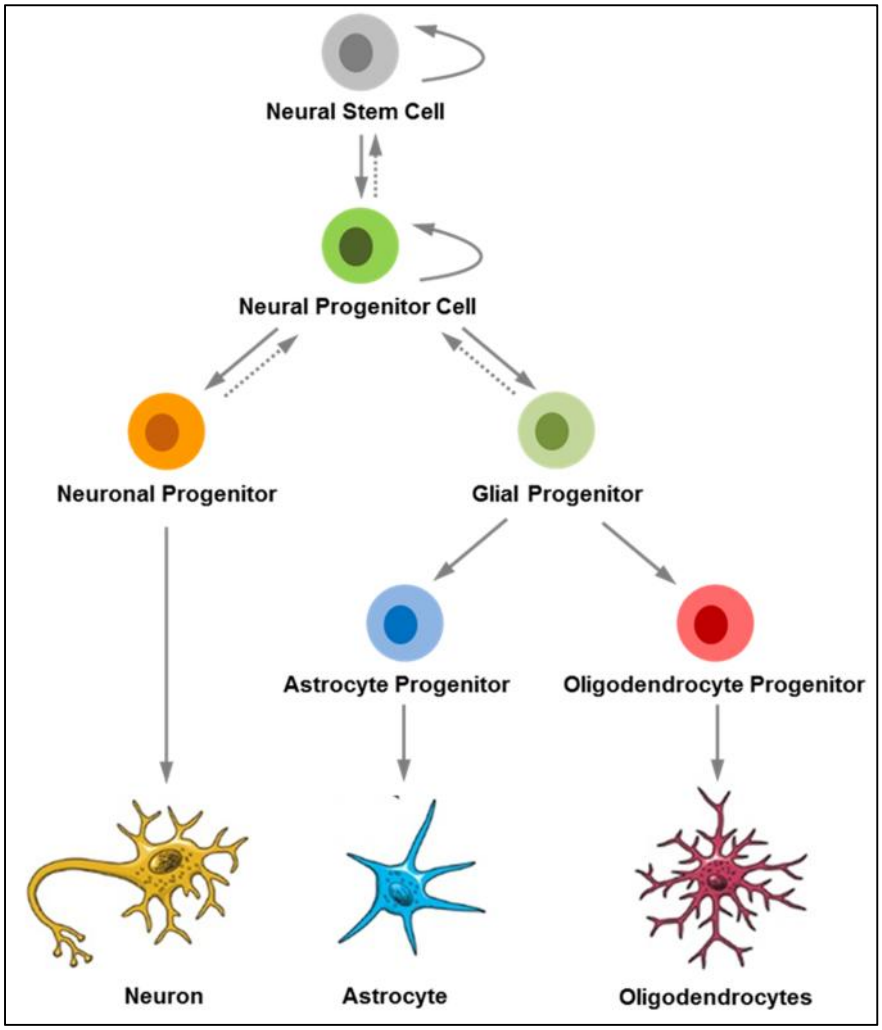

Figure-4.7 Model of neural stem cell differentiation process. [Adopted from: Jason T. Huse & Eric C. Holland, Nature, 2010 and Dragan Maric et al, Molecular Neurobiology, 2004].

4.1.4.4 Factors affecting differentiation of neural stem cells:

Neurogenesis in adults is dynamically regulated by a number of intrinsic as well as extrinsic factors [387]. Endogenous extrinsic factors in the local microenvironment, often referred to as the “neurogenic niche” or “stem cell niche”, include neural precursor cells, surrounding mature cells, cell-to-cell interactions, cilia, secreted factors, and neurotransmitters [388, 389]. Microenvironments of the subventricular zone (SVZ) and subgranular zone (SGZ), but not other brain regions, are thought to have specific factors that are permissive for the differentiation and integration of new neurons, as evidenced by a pivotal study showing that adult hippocampal astrocytes promote

neuronal differentiation of adult-derived hippocampal progenitor cells in vitro [390]. The importance of the stem cell niche in determining the fate of adult NSCs is highlighted by several different transplantation experiments [391].

Recently developed tools allowing inducible alteration of gene expression specifically within adult NSCs have provided new insights in the mechanisms regulating neurogenesis in vivo. Viral-mediated gene transfer in vivo enable inducible and cell-specific knock-out, knockdown, or overexpression of a specific gene of interest. With these and other techniques, several soluble and membrane-bound extracellular factors and their intracellular signaling cascades have recently been identified as determinants of the local microenvironment of the SVZ and SGZ, including Wnt, sonic hedgehog, Notch, BMPs, neurotrophins, and neurotransmitters [391]. Furthermore, cell-intrinsic mechanisms including transcription factors and epigenetic regulators of neurogenesis have recently been shown to be crucially involved in modulating neurogenesis in the adult brain (Table-4.1). Although the above mentioned signaling transduction pathways are critical for overall neural differentiation process, some of them are predominantly favours a particular lineage differentiation (Figure-4.8).

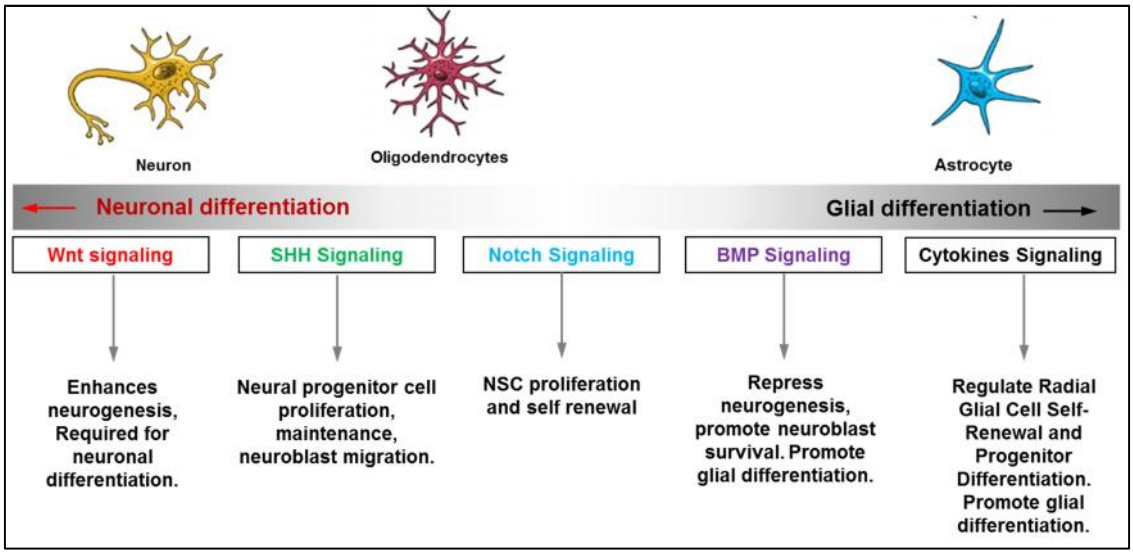

Figure-4.8 Signaling pathways biasness for particular lineage in neural stem cell differentiation process.

4.1.4.4.1 Regulatory Factors in Neuronal Fate Determination:

Main signaling pathways for neuronal fate determination:

Wnt signaling: During both NPCs expansion and neurogenic phases, Wnt ligands and receptors are expressed and impact drastically in the process [392]. *β*-catenin, a central player of Wnt signaling, exerts effects on proliferation and differentiation or both, depending on the context of other signaling cascades [393, 394]. Wnt signaling exhibits its neurogenic effects on late NPCs, because it causes cell cycle arrest and neuronal differentiation in developing neocortex.[392, 395]. The neurogenic effect of Wnt signaling is powerful in terms of induction of neuronal differentiation since nuclear accumulation

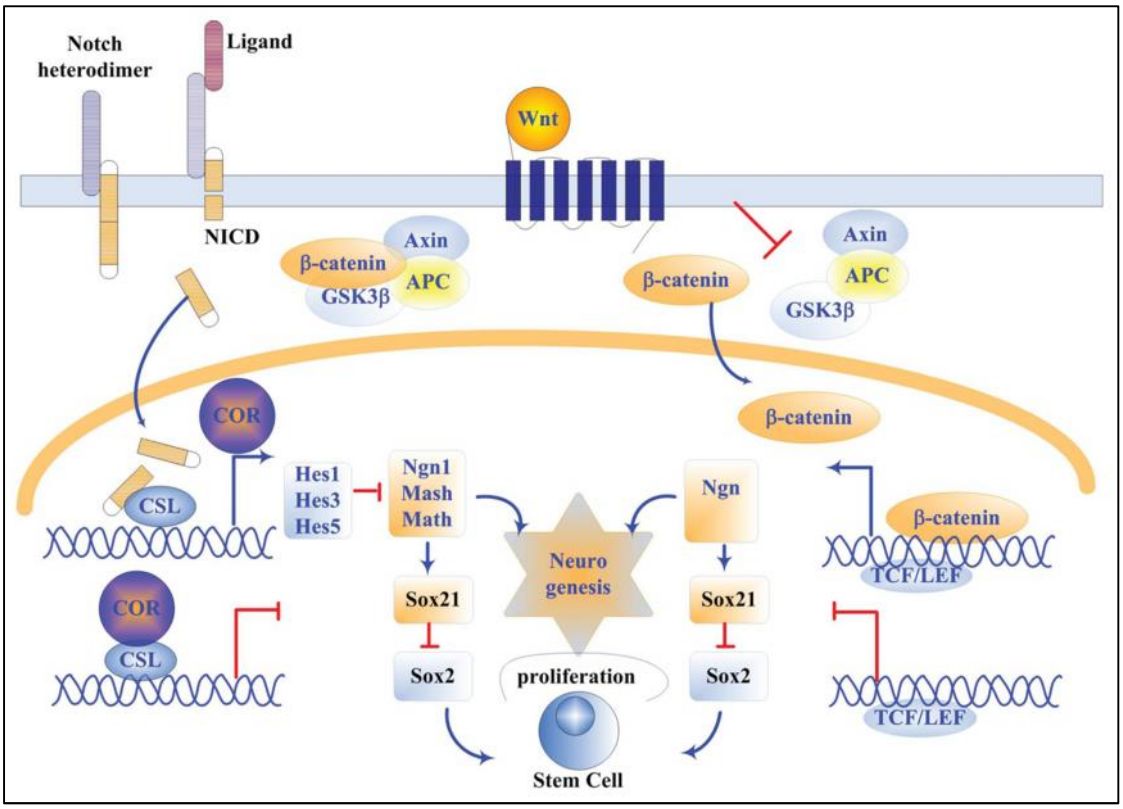

Figure-4.9 The involvement of Notch and Wnt signaling pathways and their relevant transcription factors in neurogenesis. The blue arrows indicate activating effects and the red

lines represent repressive effects. Notch is a negative signal while Wnt is a positive signal in neurogenesis through the mediation by bHLH and SOX transcription factors.

of β-catenin alone is sufficient to induce neuronal lineage commitment. Canonical Wnt pathway increases the expression of neurogenin1 (Ngn1) and Ngn2, a sort of proneural basic helix-loophelix (bHLH) proteins, through direct activation of their promoters by the β-catenin/TCF complex [392, 395]. In a subsequent study it was also shown that NeuroD1, a pro-neurogenic basic helix–loop–helix (bHLH) transcription factor, functions as a downstream mediator of Wnt-induced neurogenesis from adult hippocampal neural progenitors [396]. Moreover, these results indicate the instructive role of Wnt pathway in neurogenesis.

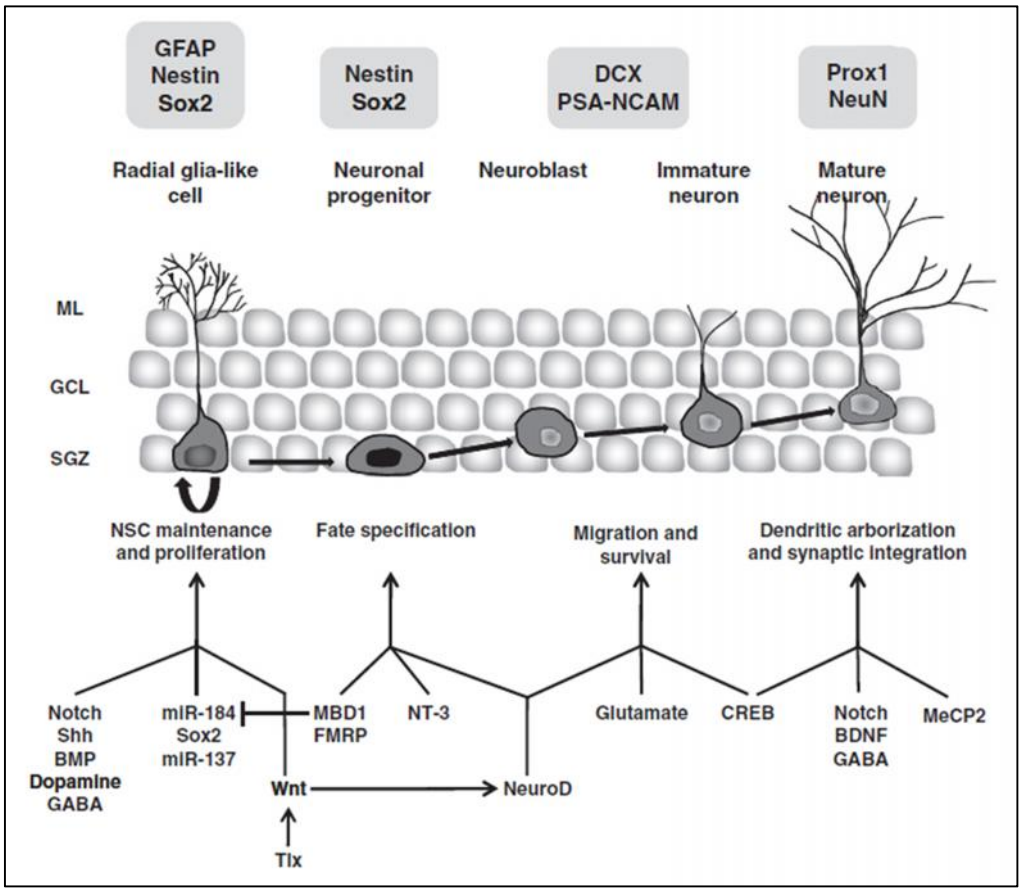

Figure-4.10: Regulation of adult neurogenesis in the dentate gyrus of the hippocampus of the lateral ventricle. Schematic diagram is illustrating the sequential steps underlying the process of neurogenesis in the adult hippocampus. Image shows the transition from a radial-like glia cell to neural progenitor cell in the adult SGZ, as well as subsequent stages of neuronal differentiation, maturation and migration.

Notch signaling: Notch receptors are single-pass trans-membrane heterodimers that are activated upon forming a binding complex with their membrane-bound ligands on the neighbouring cell, Delta and Jagged. Ligand binding results in gamma-secretase mediated cleavage of the trans-membrane domain, and subsequent release of the notch intracellular domain (NICD) into the cytosol. NICD is then translocated to the nucleus where it forms a complex with the DNA-binding protein RBPj. The NICD–RBPj complex in turn acts as a transcriptional activator and induces the expression of bHLH transcription factors, such as the hairy and enhancer of split (HES) and others [48].

While the role of Notch signaling in neurogenesis has previously been studied mainly during development, recent reports suggest that Notch has distinct roles in the maintenance and differentiation of NSCs in the adult nervous system. This signaling pathway maintains a NSCs pool in SVZ and regulates neuronal differentiation in a spatiotemporal manner. By a delimited mechanism called "*lateral inhibition*" Notch signals keep neurons in an appropriate proportion and initiate gliogenesis in time [397]. In this mechanism during vertebrate neurogenesis, proneural genes such as Mash1 and Ngns trigger transcriptional activation of the Notch receptor ligand Delta. This ligands activate the notch signaling in the neighbouring progenitor cells which resulting in the expression of Hes/ Her/Esr genes which, in turn, directly downregulate proneural gene expression, hence inhibit the cells to become neuron [397]. Therefore, the commitment to a neural fate by one cell had the consequence of inhibiting its neighbours to follow the same fate. Thus, Notch signaling is required to maintain a reservoir of undifferentiated cells and ensure ongoing neurogenesis during adult life. That's how notch singling regulates neurogenesis.

Sonic Hedgehog signaling: Sonic hedgehog (Shh) is a soluble extracellular signaling protein that was first discovered to have a role in cell differentiation in the neural tube

and limb bud [398]. Shh signaling has since been found to be crucial in regulating various processes during development of the nervous system, such as ventral forebrain neuronal differentiation, midbrain dopaminergic differentiation, and cerebellar neuronal precursor proliferation [399-401]. The Shh receptors Ptc and Smo are expressed in the adult hippocampus and in progenitors derived from this region. Furthermore, various components of the Shh signaling cascade are expressed in the early postnatal as well as the adult SVZ [402, 403]. This suggests the involvement of Shh in neurogenesis and neuronal progenitor cell proliferation. In addition Shh was recently found to serve as an important regulator of neuronal migration in the adult mammalian brain [404].

Neurotrophic factors, Growth factors and transcription factors: Neurotrophic factors are extracellular signaling proteins that play important roles in both the embryonic and adult neurogenesis. In mammals, four neurotrophic factors have been identified, namely nerve growth factor (NGF), brain-derived neurotrophic factor (BDNF), neurotrophin 3 (NT-3), and neurotrophin 4/5 (NT-4/5) [405]. Among the growth factors Fibroblast growth factor-2 (FGF-2), Insulin-like growth factor-1 (IGF-1), and Vascular endothelial growth factor (VEGF) contribute substantially towards neurogenesis. Several recent studies have implicated FGF-2 as a regulator of neurogenesis in the adult brain [406], IGF-1 increases the rate of neurogenesis in the adult hippocampus in vivo [407] and infusion of VEGF into the lateral ventricle of adult rats increases neurogenesis in the SVZ and the SGZ [408]. Among the transcription factors proneural gene encoding bHLH family transcription factors like; Mash1, NGN1, NGN2 and NGN3 play an important role in neurogenesis [397]. Neurogenin1 reportedly promote neuronal differentiation by transcribing the NeroD1 family genes and supressing the activity of STAT3 [409].

Table-4.1: Overview of signaling in adult neural stem cells: [Adopted from: Roland Faigle et al., Biochimica et Biophysica Acta 1830 (2013) 2435–2448]

Overview of signaling in adult neural stem cells

Signals	Effect on neurogenesis	Signals	Effect on neurogenesis
Extrinsic		*Intrinsic*	
Morphogens		Transcription factors	
Wnt	Increases neurogenesis	CREB	Required for neuronal survival, dendritic arborization
	Required for neuronal differentiation	Pax6	Promotes neuronal differentiation
	Stimulates NSC proliferation/self-renewal	Ascl1	Overexpression instructs oligodendrocyte fate
Notch	Required for NSC proliferation, maintenance	Dlx-2	Increases neuronal differentiation, migration velocity
	Required for dendritic arborization	Tlx	Required for NSC proliferation/self-renewal
Shh	Required for progenitor proliferation	Sox2	Required for NSC/neural progenitor cell proliferation
	Required for NSC maintenance	Tbr2	Required for differentiation of neuronal precursors
	Required for neuroblast migration	NeuroD	Necessary for survival, maturation of neuroblasts
BMP	Decreases neurogenesis	Epigenetic regulators	
	Promotes neuroblast survival	GADD45b	Mediates activity-induced NSCs proliferation
Growth factors		miR-124	Promotes neuronal differentiation
BDNF	Increases neurogenesis	MBD1	Required for neuronal differentiation
	Required for dendritic arborization	MeCP2	Required for neuronal maturation, dendrite formation
NT-3	Required for neuronal differentiation	miR-137	Required for NSC proliferation, maintenance
FGF-2	Increases neurogenesis	Bmi-1	Required for NSC proliferation, maintenance
IGF-1	Increases neurogenesis	Mll-1	Required for neuronal differentiation
	Required for neuroblast migration	FMRP	Required for neuronal differentiation
VEGF	Increases neurogenesis		Required for activity-dependent dendrite formation
Neurotransmitters			
Glutamate	Required for survival of migrating neuroblasts		
	Required for neuronal survival		
GABA	Decreases NSC proliferation		
	Required for dendritic arborization		
	Required for NSC quiescence		
Dopamine	Required for progenitor proliferation		

4.1.4.4.2 Regulatory Factors in astrocyte Fate Determination:

Main signaling pathways for astroglial fate determination: Signaling pathways involved in the induction of astrocyte specification are thought to be induced via cytokines such as CNTF, LIF and IL-6 as well as the signaling mediated by BMP and Notch proteins [410, 411].

STAT3 signaling: The typical effect of STAT3 signaling is to promote GFAP expression, a specific biomarker of glial cells. As a transcription factor, STAT3 induces GFAP expression via binding with STAT-responsive element in GFAP promoter region when activated by CNTF and LIF [412]. Among the genes activated by STAT1/3 in late embryonic NEPs, there are several composition elements of the Jak-Stat pathway itself, including gp130, Jak1, Stat1 and Stat3. Thus, STAT signaling triggers an auto-regulatory loop that reinforces itself and presumably tends to consolidate and stabilize the astrocyte phenotype [413].

BMP signaling: Bone morphogenetic proteins have been implicated in the development of gliocytes. It has been proved that BMPs are involved in astrocytic differentiation of neural precursor cells. In the nuclei, BMP-downstream transcription factors, i.e., Smad proteins, induce expression of astrocyte-specific genes in cooperation with another cytokine signaling [414].

Notch signaling: Notch directly promotes the differentiation of many glial subtypes except oligodendrocytes in an instructive manner. Notch1 could be detected in the nuclei of radial glial cells but not in neuronal precursor cells of the embryonic forebrain [415]. Various data suggest that Notch activation is essential for astrogenesis by inhibiting the tendency of neuronal formation. Notch appears to promote the astrocytic phenotype through its downstream effectors Hes1 and Hes5 which are known to

promote astrocytic differentiation via suppressing the function of proneural bHLHs [392].

Growth factors and transcription factors: The above mentioned factors like CNTF, LIF, IL6, the BMP family proteins including the TGF-β superfamily and to some extent growth hormone (GH) promote astrocyte differentiation over neuronal differentiation from the progenitor cells. Among the transcription factors STAT3, STAT1, smad1and Hes-5 are the major players for astroglial differentiation.

4.1.4..3 Regulatory Factors in Oligodendrocyte Fate Determination:

Main signaling pathways for astroglial fate determination:

Shh Pathway: Several studies demonstrated that sonic hedgehog (Shh) signaling was specificly required during oligodendrocyte development. For instance, Shh promotes NSCs to transform to oligodendrocyte progenitor/OLP [416, 417] and induces pMN-derived OLPs (progenitor of motor neurons derived oligodendrocyte progenitor) in primary cultures of dissociated forebrain NPCs [418, 419].

Notch signaling: Notch signaling is essential at the early stages of specification of the oligodendrocyte lineage, because constitutive activation of Notch signaling results in excess OLPs at the expense of motor neurons [420]. On the other hand, persistent Notch signaling can inhibit in vitro oligodendrocyte maturation, and loss of Notch signaling leads to premature differentiation of OLPs to oligodendrocytes in vivo [421]. These data thus suggest that Notch signaling might regulate both the specification of OLPs and oligodendrocytes maturation.

Opposite effects of BMPs signaling: BMP signaling is another element that influences oligodendrocytic fate determination but in an opposite way of Shh signaling. The members of the BMP family have been proposed to act as negative regulators of

oligodendrocyte specification because BMPs induce expression of Id proteins that interact with OLIG proteins to inhibit OLP differentiation and maturation [422].

Growth factors and transcription factors: Among the growth factors FGF2, insulin-like growth factor I (IGF-I), and IGF-II or Insulin has also been implicated to influence oligodendrocyte specification. The transcription factors like; neural basic helix-loop-helix (bHLH) transcription factors, Olig1 and Olig2 [418] along with Mash1 known to be involved in oligodendrocyte differentiation. In addition Nkx 6.1 and Nkx 6.2 the two homeodomain transcription factors which are induced by Shh in the ventral spinal cord [423] also regulate oligodendrocyte differentiation by regulating the expression of Olig2 in a dose dependent manner. Nkx2.2 is another homeobox transcription factor induced by shh signaling involved in oligodendrogenesis in the neural tube [424]. Moreover, the Sox E family transcription factors comprising Sox 9, Sox 8 and Sox 10, has a prominent role in oligodendrocyte development [425, 426].

4.1.4.5 Role ubiquitin proteasome system (UPS) in neural stem cell differentiation:

Increasing evidence suggests that the ubiquitin proteasome system (UPS) plays an important role in neural stem and progenitor cell differentiation and neurogenesis. Neural differentiation requires coordinated gene and protein regulation for controlled progression of neurons, astrocytes or oligodendrocytes formation. In this process, the neural stem cells either proliferate to maintain a pool of neural stem cells or exit the cell cycle to mature into neurons or glia. The neural stem cells are characterized by symmetrical cell division [427] and the expression of neural stem cell maintenance genes such as the SoxB1s [428], RE-1 silencing transcription factor (REST) [429] and Notch [430]. To form neurons or glia, neural stem cells undergo asymmetric cell divisions and a subset of proteins segregate differentially between the two daughter

cells, one of which remains a stem cell while the other cell differentiates [431-434]. In the differentiating cell, the levels of REST [435-437], Notch signaling and SoxB1s [438-441] are down-regulated by repression of their gene expression and post-translational modifications. As the interactions between proteins and signaling pathways restructure the proteome of the differentiating cell, the abundance of many proteins is regulated by targeted degradation by the ubiquitin–proteosome system.

If we revisit the detail progression of neural stem cell differentiation process, we will come across those five critical signaling pathways such as; Wnt, Shh, Notch, BMP and STAT3 signaling pathways controlling the whole process. All these pathways more or less regulated by spatio-temporal protein synthesis and degradation to modulate the differentiation process, and hence an involvement of UPS is attributed for the differentiation progression. For degradation point of view E3 ligases in UPS plays a pivotal role in this complex phenomenon of neural differentiation process.

4.1.4.5.1 Proteasomal degradation in the signaling pathways of differentiation process:

Notch signalling: In Notch signaling at least five E3 ubiquitin ligases: suppressor of deltex/ Itch [442], SCFFbxw7 [443, 444], ligand of numb-protein X (LNX) [445], neuralized [446, 447] and Mind bomb (MIB) [448, 449] fine-tune Notch-Delta signaling pathway. The HECT-type Ub ligase, neuralized, and the RING-type Ub ligase, MIB, are enriched at the plasma membrane of the differentiating cell and target the Notch ligands Delta and Serrate for ubiquitination and internalization In the differentiating cell, Notch signaling is down-regulated by ubiquitination and degradation of NICD and the NICD effector, Hes1, allowing for transient up-regulation of Delta. The decrease in Notch signaling is accomplished in part by degradation of the effector protein Hes1, which allows for the expression and stabilization of proneural genes, Neurogenin (Ngn).

Wnt signaling: In canonical Wnt signaling pathway the central player *β*-catenin get degraded via a destruction complex through proteasomal pathway while no extrinsic signal trigger the pathway for neurogenesis. In addition the *β*-catenin target genes such as NGN1 levels are regulated by proteasome in the nucleus during neuronal differentiation [450, 451].

Shh signaling: In Shh pathway the two critical transcription factors Gli2 and Gli3 get ubiquitinated, degraded and prevention of transcriptional activation in absence of Shh signal. Hence proteasomal degradation ensures the Gli-mediated target gene activation only occurs when Shh is present.

FGF signaling: In FGF pathway, which has a prominent role in anterior–posterior patterning of the neuroectoderm, the sprouty enhances the signaling by binding to and dissociating c-Cbl, a RING-type ubiquitin ligase, from the FGF receptor, thereby, allowing signaling to occur [452]. However, when Sprouty is ubiquitinated and degraded by NEDD4 ubiquitin ligase, c-Cbl interacts with the receptor, resulting in ubiquitination and degradation of the FGF receptor [453-455].

BMP signaling: In BMP signaling pathway three HECT-type E3 ligases smurf1, smirf2 (Smad ubiquitin regulatory factors), NEDD-4 regulate the proteasomal degradation of smard proteins; R-smard, smard-2, TGF- *β*-1 receptor and negatively regulate the pathway. Conversely other reports suggest, another RING-type ubiquitin ligase, Arkadia, enhances BMP signaling by inducing ubiquitination and degradation of inhibitory Smad7 transcription factor [456, 457].

Stem cell markers degradation: It has been reported that nestin the neural stem cell marker is degraded by UPS during the differentiation process. Another key player in neurogenesis REST, which regulates cell fate by preventing premature expression of neuronal genes in neural progenitors, get ubiquitinated by SCF^{TRCP} E3 ligase, whose

levels increases during neurogenesis, and consequently degraded by proteasome during neuronal differentiation. [429]. The SoxB1 group transcription factors, Sox1, Sox2, and Sox3, are important for the maintenance of neural progenitors [458-460]. Reports suggest as cells differentiate sox2 and sox3 expressions are down-regulated and their decrease promotes cell cycle exit and neuronal differentiation [439]. Conversely, constitutive expression of sox2 or sox3 maintains the proliferative capacity and inhibits neuronal differentiation of progenitors. Although SoxB1 degradation seems critical for differentiation, a very little literature exists about its post translational modification and proteasomal degradation. Not only SoxB1 many other stem cell markers must have been controlled by the UPS, which are still unrevealed.

All the above reports cumulatively suggest that there is a critical role of UPS exists in neural differentiation process by degrading cell fate deciding regulators in the progenitor cells. This is how; targeted protein degradation and ubiquitin E3 ligases provide a specific mechanism to eliminate key transcription factors and signaling pathways components important for neurogenesis and the development of the nervous system. Proteasomal regulation at the protein level allows for a rapid change in the proteome of the cells and the timely and ordered progression of neurogenesis, adding another layer of complexity to this already complex process. Nevertheless, this key role of proteasome seems critical for this differentiation process and appears a rapidly growing area of research. In comparison to the vast complexity of neural stem cell biology current knowledge about UPS role is in its infant stage. Hence there exist a lot of scopes for elucidating more about proteasomal role in neural stem cell maintenance and differentiation process.

4.2 RATIONALE OF THE STUDY AND HYPOTHESIS:

As we know from the review of literature, gankyrin is considered as a very potent oncoprotein which degrade pRb and p53. It contains ankyrin repeats, a potential protein-protein interacting domain and reportedly interacts with many proteins in many signalling pathways. Gankyrin acts as a hub protein which can rewire many signaling networks in cancer and may be important for regulating signaling cascades in normal cell to primarily regulate tissue development and differentiation, such as; NF-κB and Wnt/β-catenin signaling pathways. Reported studies (as mentioned in the section 4.1 Review of literature) and our preliminary data suggest that, gankyrin enhances the β-catenin transcriptional activity by stabilizing the protein. Upon overexpression of gankyrin a substantial increase of β-catenin protein levels are seen in HEK293 cells (Unpublished data from our lab). Wnt/β-catenin pathway predominantly influences neurogenesis in NSCs a. Furthermore, gankyrin influence IL6/STAT3 signaling pathway in cancer cells and perhaps in specific context in normal cells Indeed reports suggest a major role of STAT3 signaling pathway in gliogenesis of NSCs. Gankyrin is also involved in pathogenesis and poor prognosis of glioma. Glioma, is a product of disregulation in the genesis of glial cells and are dedifferentiatied glial progenitor cells. These literature reports speculate a probable role of gankyrin in neural differentiation process.

Preliminary results to develop our hypothesis:

As mentioned above we have shown a significant correlation between gankyrin and β-catenin. We observed a significant increase in IL8 mRNA expression and corresponding decrease in STAT3 mRNA levels upon gankyrin overexpression in HEK293 cells (Figure-4.9). These results suggest that, gankyrin may be influencing STAT3 activity negatively. Although increase in IL8 expression goes according to a

reported study [355] but the decrease in STAT3 activity is paradoxical to the report about the role of gankyrin in cholangiocarcinoma [357]. Whereas it has been reported that, gankyrin correlates with proliferation and poor prognosis of human glioma [352] and in glioblastoma STAT3 activity is inhibited and IL8 expression has increased [461] which correlates with our preliminary results. The both studies suggest, these contradictory fallouts could be a tissue specific response. However, these results altogether give an indication for the probable role of gankyrin mediated STAT3 activity for gliogenesis.

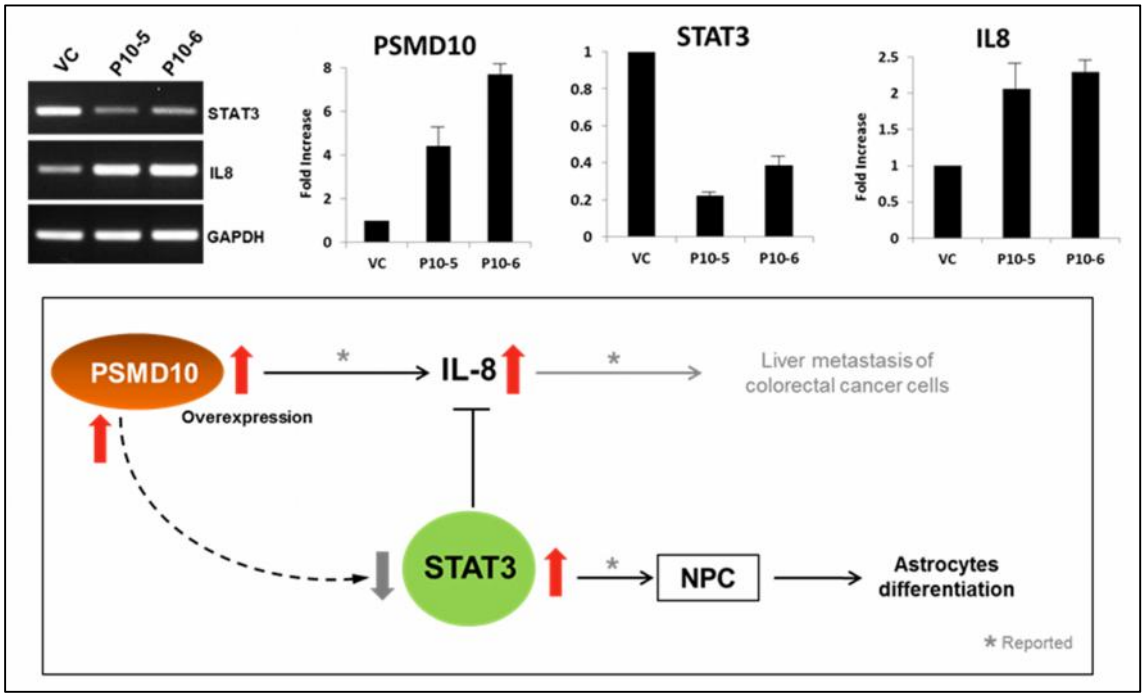

Figure-4.11 PSMD10 influence STAT3 signaling pathway in HEK293 cells.

Furthermore, microarray analysis of HEK293 cells over expressing gankyrin shows up regulation of at least 8 genes associated with neuronal differentiation (upto to 4-20 fold; Table-4.2). In the validation study two of these up-regulated genes NGN1 and NRG1 were confirmed to be over expressed by real-time qRT-PCR. According to literature NGN1 (Neurogenin1) is a basic helix-loop-helix transcription factor that predominantly promotes neurogenesis of the neural progenitor cells. In addition a positive correlation between β-catenin, which regulate NGN1 expression during

neurogenesis, and PSMD10 was observed in an independent experiment. One of the major interests in the lab is to understand the role of ubiquitin proteasome pathway in development and differentiation. We had chosen the human neural progenitor cells from Millipore the ReNcells to explore this possibility. Based on the literature evidence above and our own observations on gene regulation of PSMD10 in HEK293 cells, my hypothesis was to explore the potential role for PSMD10 in neural differentiation.

Table.4.2 Up-regulated gene list from the microarray data.

Gene Name	Protein	Type	Fold upregulation	Function
ARTN	Artemin	A member of the glial cell line-derived neurotophic factor	**20.69**	A member of the glial cell line-derived neurotophic factor (GDNF). Artemin regulate the development and maintenance of many neuronal populations in the mammalian nervous system.
NEFM	Neurofilament medium polypeptide	Cytoskeletal protein, type IV intermediate filament	**12.71**	Neuronal axon cargo transport, microtubule cytoskeleton organization and neurofilament bundle assembly.
NGN1	Neurogenin-1	Transcription Factor	**12.64**	Acts as a transcriptional regulator. Involved in the initiation of neuronal differentiation.
NPBWR1	Neuropeptides B/W receptor type 1	G-protein coupled receptor	**6.08**	Ligand of G-protein coupled receptor involved in neuroendocrine synaptic transmission
NRG1	Neuregulin-1	Receptor ligand of Neu/ErBb2	**5.8**	Regulate proliferation of CNS neuronal progenitor cells. controls Schwann cell migration and formation myelin sheath on neuronal axons.
SV2B	Synaptic vesicle glycoprotein 2B	Transmembrane protein	**5.33**	Act as a neurotransmitter transport protein and plays a role in the control of regulated secretion in neural and endocrine cells.
SYP	Synaptophysin	Transmembrane protein	**4.88**	Regulation of neuronal synaptic plasticity
NTRK2	Neurotrophic tyrosine kinase, receptor-2	Receptor protein of BDNF/NT-3	**3.7**	Receptor tyrosine kinase involved in the development and the maturation of the central and the peripheral nervous systems through regulation of neuron survival, proliferation, migration, differentiation, and synapse formation and plasticity.

Hence collectively basing upon the available literature and from our initial data (Figure-4.12) we hypothesize that, **"PSMD10 might be playing role in neural stem cell differentiation".**

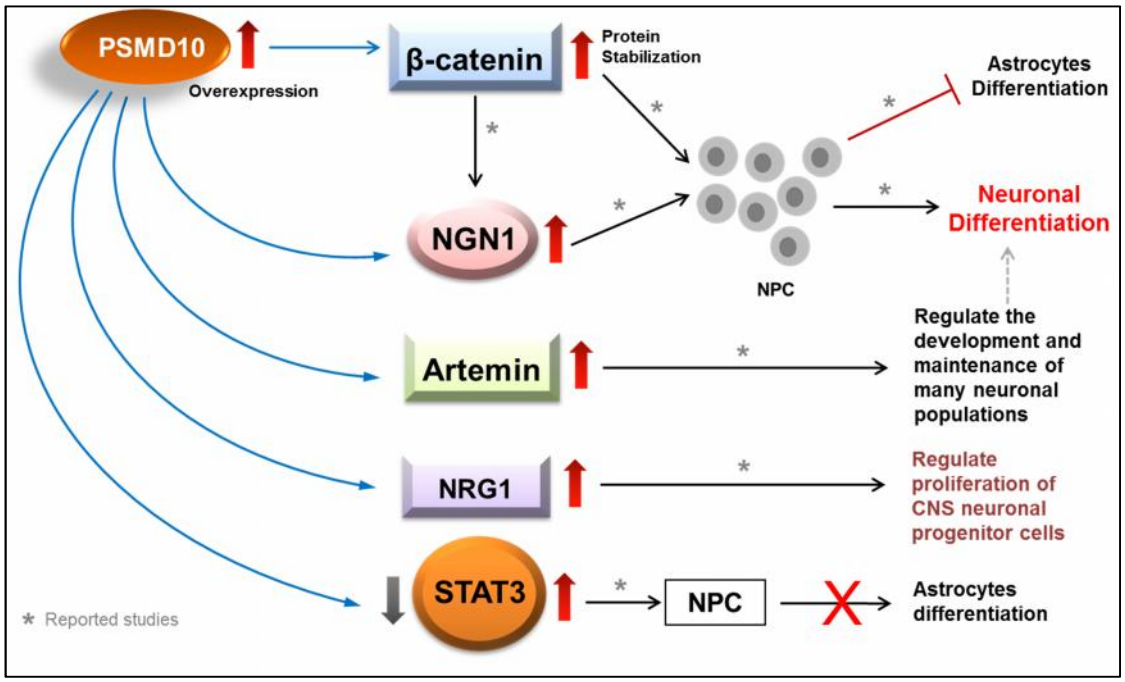

Figure-4.12 Hypothesis: PSMD10 might be playing role in Neural stem cell differentiation.

To test this hypothesis we put forth the following fundamental questions:

1. Whether endogenous PSMD10 levels vary during differentiation process?
2. Whether the levels of PSMD10 in progenitor cells influence the cell fate?
3. Is PSMD10 involved in the differentiation process process?
4. What may be the probable mechanism?

4.3 RESULTS:

4.3.1 In vitro culture of the human Neural Progenitor cells (hNPCs):

Human neural progenitor cells (hNPC) were commercially procured from Millipore. Since they grow in adherent fashion, we use Laminin for coating the culture plate. They grow on the coated plate in a mono layer fashion (Figure-4.13) in a specialized Neural stem cells maintenance media when supplemented with two growth factors; EGF and FGF. The doubling time of these cells is 20/30 hours and these cells maintain a proper diploid karyotype. They are sub-cultured for the next passage by an enzymatic de-adhesion method using acutase.

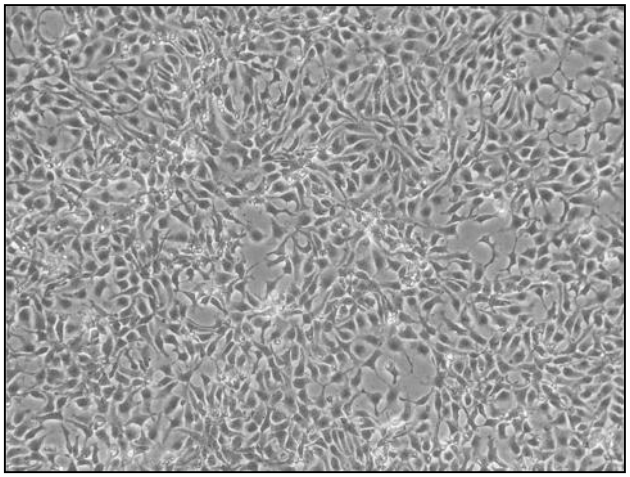

Figure-4.13 Phase Contrast image of human Neural progenitor cell. Cells were grown on Laminin coated plate in Neural stem cells maintenance media with supplement EGF (20ng/mL) and FGF (20ng/mL) for 72hr. Image shows >90% confluent mono layer cells.

4.3.2 Characterization of the human Neural progenitor cells (hNPCs):

Human neural progenitor cells (hNPC) were grown on laminin coated plate in Neural stem cells maintenance media with EGF and FGF supplements till 80% confluency. Expression of neural stem cell markers viz. Sox2 (a transcription factor), Nestin (a type VI intermediate filament (IF) protein) and Musashi (a RNA binding proteins) was confirmed by immunofluorescence. The IF-image showed nestin as filamentous structure, sox2 as nuclear localization and musashi as pan-cellular

localization, predominantly in cytoplasm. To validate the stemness we check the expression of some terminal differentiated cell markers such as a β-III tubulin a Neuronal marker –, and GFAP (Glial fibrilliary acidic protein) an astrocyte marker –. We did not detect cells expressing these differentiation markers within this pool of progenitor cells. These result suggested these progenitor cells retain the stem cell like characteristics in vitro.

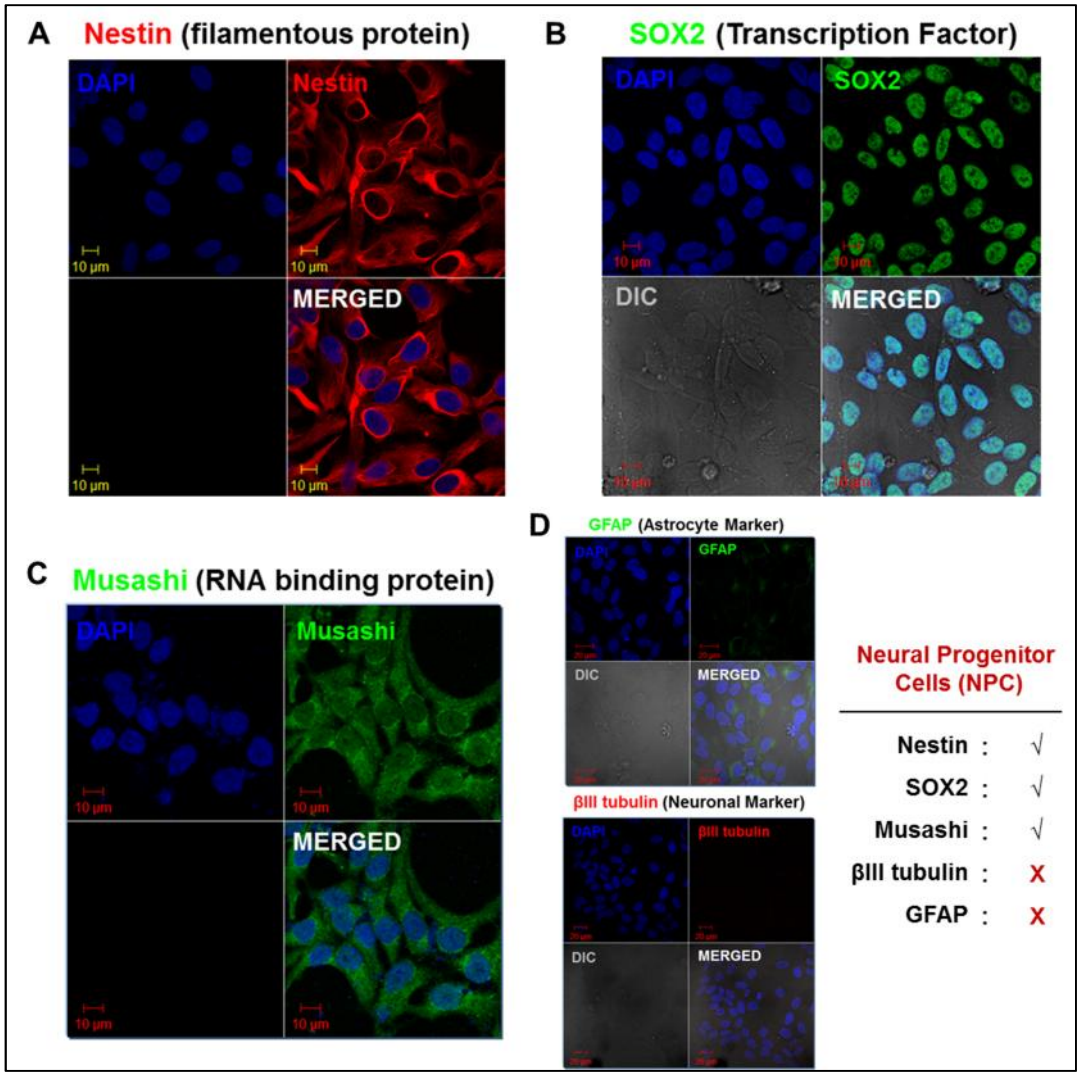

Figure-4.14 Expression of neural stem cells markers in human Neural progenitor cells (hNPCs). Progenitor cells were grown on Laminin coated glass coverslips till they reached ~80% confluence. Immunofluorescence was done following the protocol described in materials and methods. Cells are showing expression of **(A)** Nestin (in red) **(B)** Sox2 (in green) and **(C)** Mushashi (in green), but not showing the expression of **(D)** either GFAP or β-III tubulin. DAPI was (in blue) used for nuclear staining. Images were acquired in Laser confocal microscope (Nikon-Meta510).

4.3.3 In vitro differentiation of the human Neural progenitor cells:

Human neural progenitor cells (hNPC) were grown on laminin coated plate in Neural stem cells maintenance media with EGF and FGF supplements till 80% confluency. Then the media was replaced by fresh Neural stem cells maintenance media without any growth factors. When cells were allowed to grow in such condition for 12-14 days we observed microscopically that they stop dividing from the very first. During this process they started changing their morphology just after 24hr of growth factor withdrawn. The well-structured mono layer, flattened phenotype was changed to partial network like structure at the end of 48hr (Figure-4.16B). And at the end of 10^{th} day (from growth factor withdrawn) of differentiation process, cells showed a completely elongated network like structure with an altered N/C ratio (Figure-4.16A & B). It was observed that during the initial days of the differentiation process (by 3rd day) ~20-30% cell died, but at the later period (till the end of differentiation process) cell death was not observed and the cell no remained constant. Hence if we started with 80-90% confluent plate of progenitor cells, we end up with ~55-65% of differentiated cells. This phenomena was not confluency/cell number dependent. Furthermore the differentiation process occurs at both low and high confluency (at ~50% or ~90% of hNPC) (Figure-4.16A).

When the differentiated cells were observed under phase contrast microscope the three phenotypically different types of cell astrocytes, neurons and oligodendrocytes were detected as expected (Figure-4.16C, D & E). In the differentiated population oligodendrocytes seems favourably developed in low density confluency and found in clusters in the area where other two types of cells were present less in number. No such detectable behaviour was observed for neurons or astrocytes.

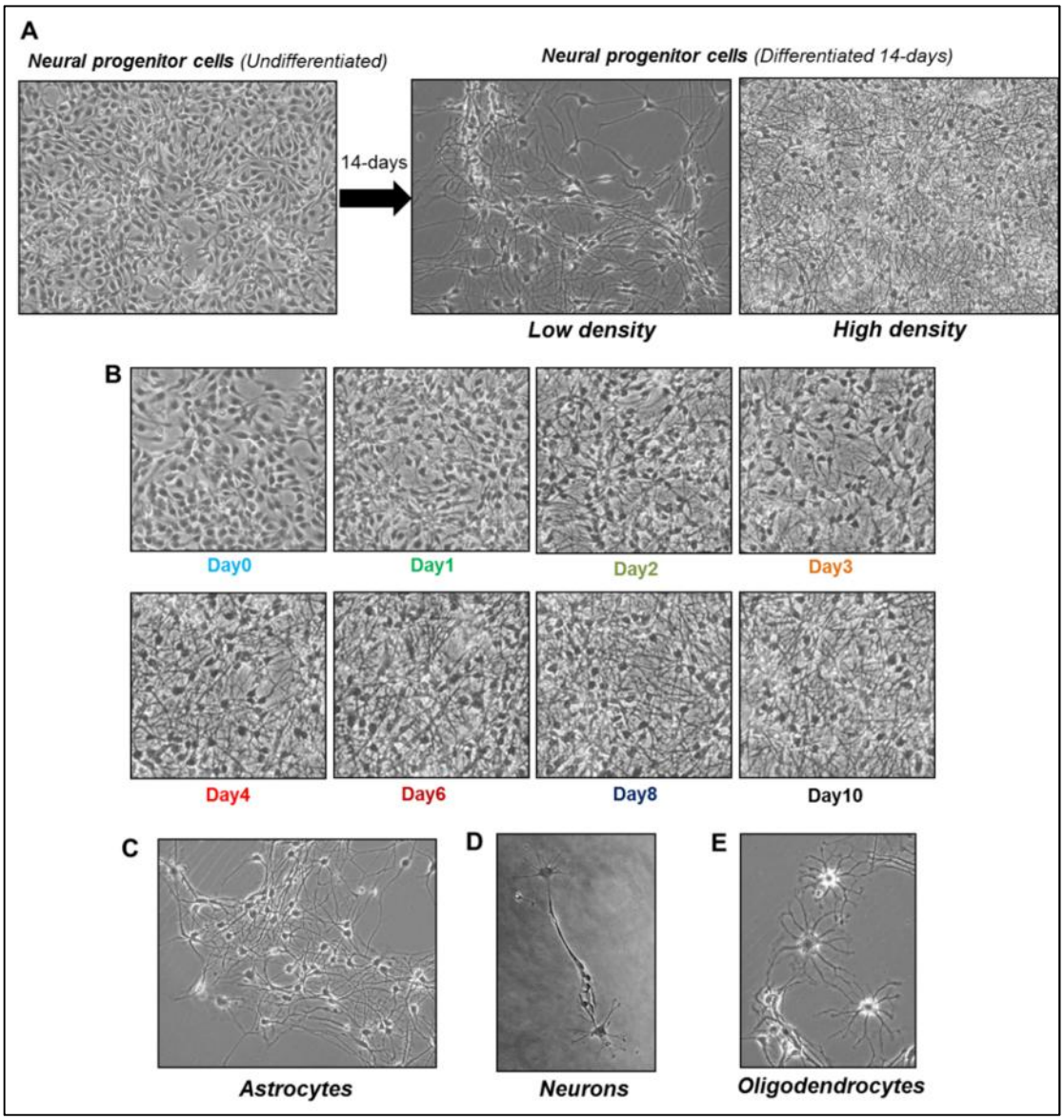

Figure-4.15 Differentiation of human Neural progenitor cells (hNPCs). Progenitor cells were grown on Laminin coated plates till they reached ~80% confluence. Then media was replaced with fresh media containing no EGF/FGF. In every alternative day media was changed. Images were taken by a phase-contrast microscope. **(A)** hNPCs differentiates in both low and high density conditions. **(B)** Day wise differentiation status of the hNPCs. **(C)** Astrocytes showing the network like structure, **(D)** Neurons showing the axon and cell body with dendritic processes, **(E)** Oligodendrocytes dendritic net like phenotype.

4.3.4 Characterization of the differentiated hNPCs:

Differentiated cell were characterized with Nuronal marker – β-III tubulin, astrocyte marker – GFAP (Glial fibrilliary acidic protein) and oligodendrocyte marker – O1 by immunofluorescence and western blot analysis. IF-image showed that out of all the differentiated population ~80-90% cells were astrocytes (GFAP+ve), ~10-15% cells are neurons (β-III tubulin+ve) and rest ~5% cells are oligodendrocytes (Figure-4.16A).

This suggests that, progenitor cells (hNPCs) predominantly give rise to astrocyte and less no of oligodendrocytes. WB shows predominant expression of stem cell markers in the progenitor cells and differentiated marker in the differentiated cells (Figure-4.16B). In contrast we did not see any changes in protein levels of O1 in both cell types.

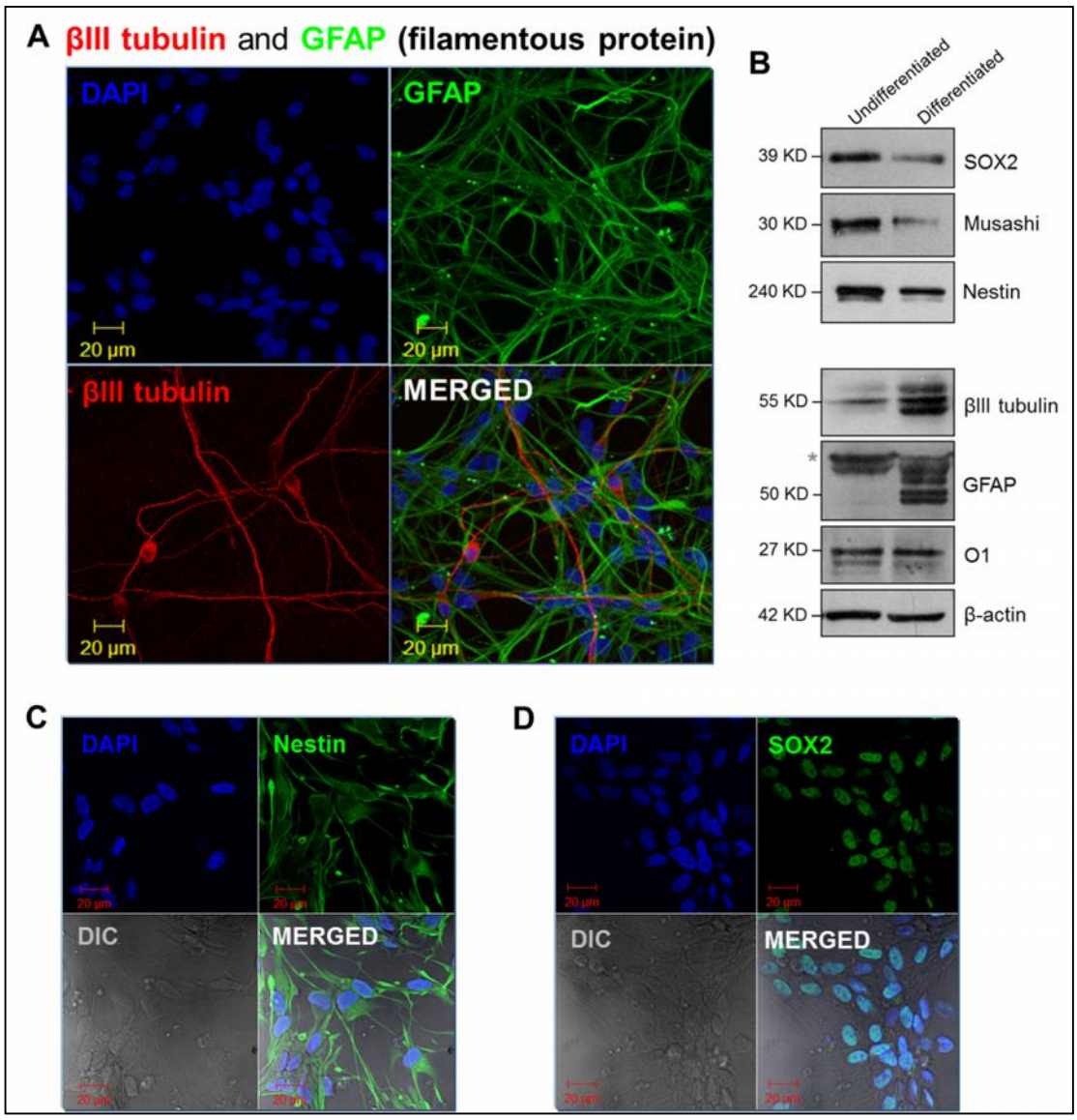

Figure-4.16 Characterization of Differentiated human Neural progenitor cells (hNPCs). Progenitor cells were grown on Laminin coated glass coverslips till they reached ~80% confluence. Then media was replaced with fresh media containing no EGF/FGF. In every alternative day media was changed. Immunofluorescence was performed following the protocol described in materials and methods. Cells are showing expression of **(A)** β-III tubulin (in red), and GFAP (in green). **(B)** WB showing the expression of stem cell markers and differentiation markers in the progenitor cells and differentiated cells. Differentiated cell shows **(C)** aberrant expression of nestin (in green) (D) less sox2 (in green). DAPI was (in blue) used for nuclear staining. Images were acquired in Laser confocal microscope (Nikon-Meta510).

4.3.5 Differential expression of Proteasomal subunits in hNPCs:

Literature study suggested that, proteasome plays a very critical role in neural stem cell biology. We prepared cell lysates and isolated RNA from the progenitor cells and 14 days differentiated cells. Transcript and protein levels of different proteasomal subunits were analysed in these cells. The protein levels of proteasomal subunits such as; (one α subunit) α4, (one β subunit) β7 and (one 19S ATPase subunit) Rpt6 were checked and found to be decreased in the differentiated cells (Figure-4.17A). PSMD10 levels were found to be increased in differentiated cells while PSMD9 levels remained unchanged. Similarly the mRNA levels of β1, β5, PSMD9 and PSMD4 were found to be decreased, β2 levels remained unchanged but PSMD10 transcript levels were also found to be increased to 5-6 fold in differentiated cells (Figure-4.17B & D). These results suggest the overall proteasome levels might be decreasing in the differentiated cells, although further investigation for all the 68 subunits is necessary. Paradoxically the level of PSMD10 is increased, which indicate there must be some proteasome independent role that PSMD10 is playing in the differentiated cells. This also suggests that, PSMD10 may be one of the crucial molecules which is essential for maintenance of cell physiology in differentiated cells.

Apart from the proteasomal subunits we also checked the expression levels of some important transcription factors in progenitor cells and differentiated cells. WB and real time QRT-PCR showed that protein levels of *β*-catenin (2-3 fold) and mRNA levels of Neurogenin-1 (NGN1) (>30 fold) was found to be increased in differentiated cells. But the levels of STAT3 mRNA levels were decreased (50%) in the differentiated cells. These results again validated the role of *β*-catenin and NGN1 in neurogenesis. In contrast decreased levels of STAT3 suggest that, in 14days differentiated cells the activity of STAT3 may not be essential. However further validation is necessary to confirm these results.

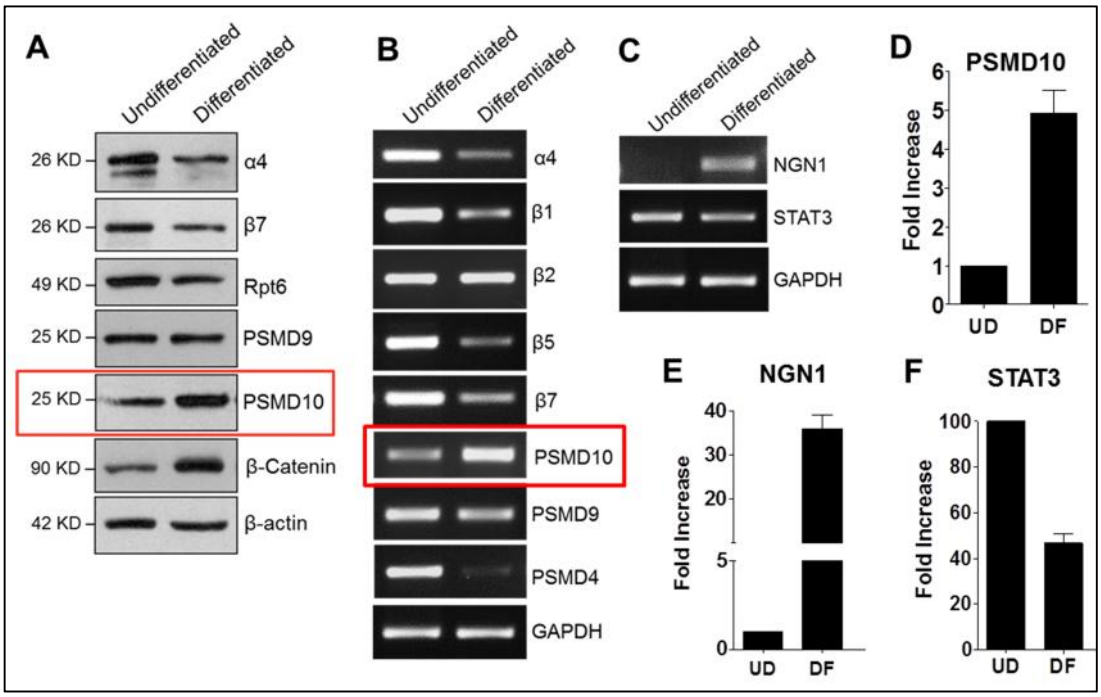

Figure-4.17 Differential protein levels in human Neural progenitor cells (hNPCs) and differentiated cells. (A) Progenitor cells were grown and allowed to differentiate for 14 days following the protocol described in Materials and methods. Cell lysates were prepared from both progenitor cells and differentiated cells and analysed by WB. **(B), (C)** mRNA was isolated from the above mentioned cells and semi-Q RT-PCT was carried out. Image shows the mRNA levels of different subunits of proteasome and transcription factors. **(D), (E), (F)** Real-time qRT-PCR was carried out showing the mRNA levels of PSMD10, NGN1 and STAT3 in those cells.

4.3.6 PSMD10 protein expression increases during differentiation process:

Since we specifically observed the high expression levels of PSMD10 in the 14 days differentiated cells, we then monitored its expression pattern during the time course of differentiation (from day 1-day 14). Because of the proposed relationship between PSMD10, *β*-catenin and STAT3 we monitored the expression of these proteins as well. This would establish a strong correlation between these proteins in the differentiation process and provide clues towards the players that may be required early during the differentiation process ie the commitment step and distinguish those that are required at later stages and perhaps associate these correlation with the cell type hNPCs cells were grown Laminin coated plates and were allowed for differentiation for 10 days. We collected cells at 8 different time-points in-days (from 8 plates) as mentioned in Figure-4.18 and analysed by WB.

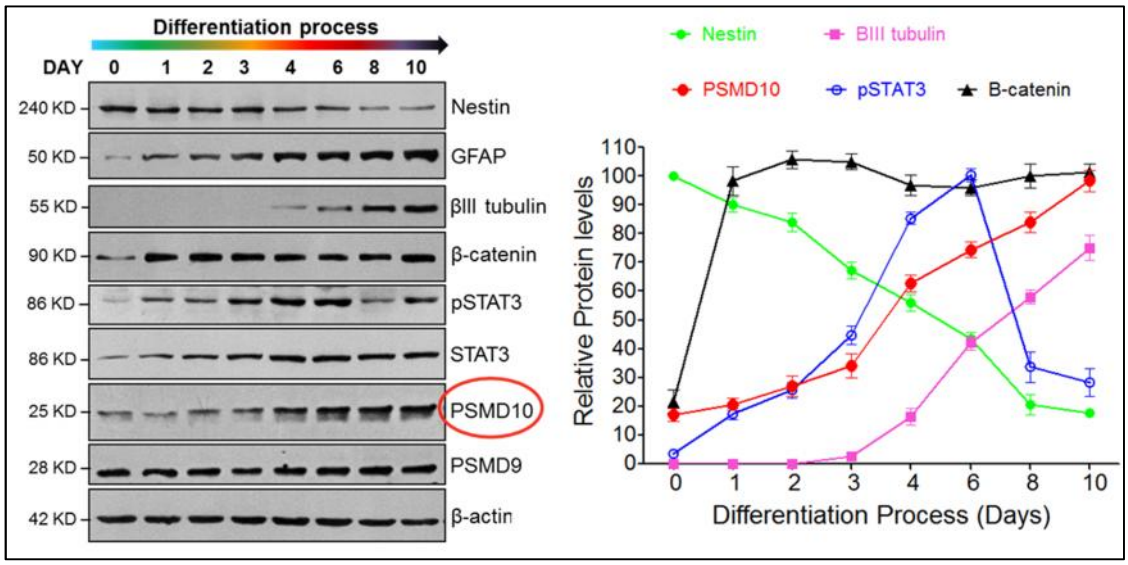

Figure-4.18 Differential protein expression during differentiation process in human Neural progenitor cells (hNPCs). Progenitor cells as well as the differentiated cells of 7 different time-points such as Day-1 to Day-10 were culture as described earlier. Cell lysate were prepared at each time points and analyses by WB. The line graph represents a correlation of the average protein levels at each time points during the differentiation process. Data represents mean intensity of proteins, ± SEM of three independent experiments.

The day-wise studies of hNPCs differentiation indicated that the stem cell marker; nestin expression gradually decreases. The differentiation marker GFAP (for astrocytes) was observed at the very first day (Day1) of the differentiation process and continued to oncrease till Day-4 and reamained stable during later stages. The neuronal marker β-III tubulin was detected at Day-4 of the differention process then increased gradually till the end of Day-10 (Figure-3.18). These results suggests while astrocyte differentiation is an early event and neuronal differentiation requires transcriptional changes that are either triggered late or is a slow cumulative response.

Results showed increase levels of *β*-catenin on the very first day of differentiation commensurate with the appearance of the astrocyte marker and remain constant presumably till the end of differentiation process (Figure-3.18). This suggests that, although *β*-catenin essential for neuronal differentiation, it also necessary for both initiation and progression of the overall differentiation process. Both STAT3 and p-STAT3 (transcriptional active STAT3) levels increased gradually till Day-6, and

subsequently STAT3 levels are stabilized but, pSTAT3 levels decrease (Figure-3.18). This indicates that for the initial differentiation stages (presumably for gliogenesis) STAT3 activity is required, as seen by increase in pSTAT3 levles in parallel with the GFAP expression. But after Day-6 decreased levels of pSTAT3 indicate that later stage of differentiation process (probably during neurogenesis) STAT3 activity may not essential. Since STAT3 itself is a target gene for STAT3 signaling pathway there was a corresponding increase of total STAT3 levels detected during the process. It is possible that STAT3 may be active in other post translationally modified form.

Most importantly, when we monitored PSMD10 in all these time-points, we observed a gradual increase in the expression of PSMD10 till Day-6 and remains stable for the next 8 days. Levels of PSMD9 did not change throughout the differentiation process. These results indicate that PSMD10 might be important for the later differentiation stages when neurogenesis begins, detected by β-III tubulin expression at the later part. However, there is a positive correlation observed between PSMD10, STAT3 expression and phosphorylation of STAT3 during Day-1 to Day-6. But, after Day-6 STAT3 phosphorylation (activity) decreases while PSMD10 expression reached to a high level. This might be indicating the probable role of PSMD10 in STAT3 pathway at initial stage (inducing) and at the later stage (inhibitory) as well. However, to validate of these results further experimentation is necessary.

4.3.7 Virus production and viral titre calculation (for Flag-PSMD10 construct):

Since, PSMD10 seems to be essential for the hNPCs differentiation process from the previous experiments; we wanted to check the direct effect of PSMD10 on this process by transexpressing it in the hNPCs and monitored the any alteration in differentiation.

For transexpressing PSMD10 in hNPCs we generate lentiviral particle of pTRIPZ-FLAG-PSMD10, expressed under doxycycline inducible condition, in HEK293FT cells and concentrate it for better transduction efficiency. After concentration virus titer was

found to be 1.2-1.5 X 10^8 TU/mL. The detail method of virus production and virus titer calculation is described in materials and methods (Chapter-III).

4.3.8 Transduction of Flag-PSMD10 in hNPCs:

The hNPCs were grown on laminin coated plate in Neural stem cells maintenance media with EGF and FGF supplements. At a confluence of ~30-40%, progenitor cells were transduced with pTRIPZ-FLAG-PSMD10 virus. Then the transexpression of PSMD10 was induced by doxycycline (1µg/mL) and checked via immunofluorescence using anti-FLAG antibody and also validated by WB. IF-images showed nNPCs were successfully transduced and ~20-30% of cells were expressing FLAG-PSMD10.

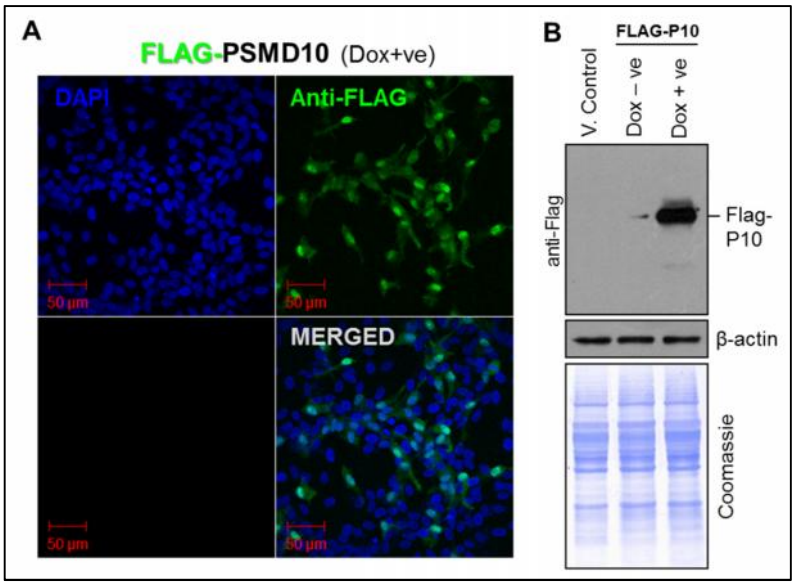

Figure-4.19 Trans-expression of FLAG-PSMD10 by transduction in human Neural progenitor cells (hNPCs). Progenitor cells were grown on Laminin coated glass coverslips till they reached ~30% confluence. Then cells were transduced with virus particle of pTRIPZ-FLAG-PSMD10 and cell were either treated with doxycycline (1µg/mL) for 48hr or left untreated. **(A)** Immunofluorescence was performed after 48h of transduction following the protocol described in materials and methods. Cells show expression of FLAG-PSMD10 (in green). DAPI was (in blue) used for nuclear staining. Images were acquired in Laser confocal microscope (Nikon-Meta510). (B) Cell lysate were prepared after 48h of transduction and analysed by WB.

4.3.9 Effect of overexpression of Flag-PSMD10 on differentiation of hNPCs:

Since we could successfully trans-express FLAG-PSMD10 by transduction method in hNPCs, we wanted to determine the effect of this trans-expression on differentiation process by tracing the FLAG-PSMD10 overexpressing cells in the differentiated

population (Figure-3.20A). So we transduced the hNPCs at ~30% confluency, maintained them in culture until they ~80% confluency, and allowed the progenitor cells to differentiate in presence doxycycline for 14 days. Immunofluorescence experiments indicated that, after the complete differentiation of the hNPCs, while ~60% of FLAG-PSMD10 overexpressing differentiated hNPCs (green cells) were co-localized with GFAP (red cells) rest of the PSMD10 overexpressing cells (~40%) were not co-localized with the GFAP staining. These results suggests that these ~40% cells may be neurons which could not be confirmed by tubulin staining due to other constraints. The ratio of astrocytic and neuronal population (3:2) was altogether different from what we observed in Dox-untreated cells (not expressing FLAG-PSMD10) i.e., ~80-90% astrocytes and ~10-20% neurons. These results indicated that PSMD10 overexpressing hNPCs acquired the tendency or the driving force to differentiate toward neuronal fate. However we did not find any oligodendrocyte population differentiating from the PSMD10 overexpressing cells.

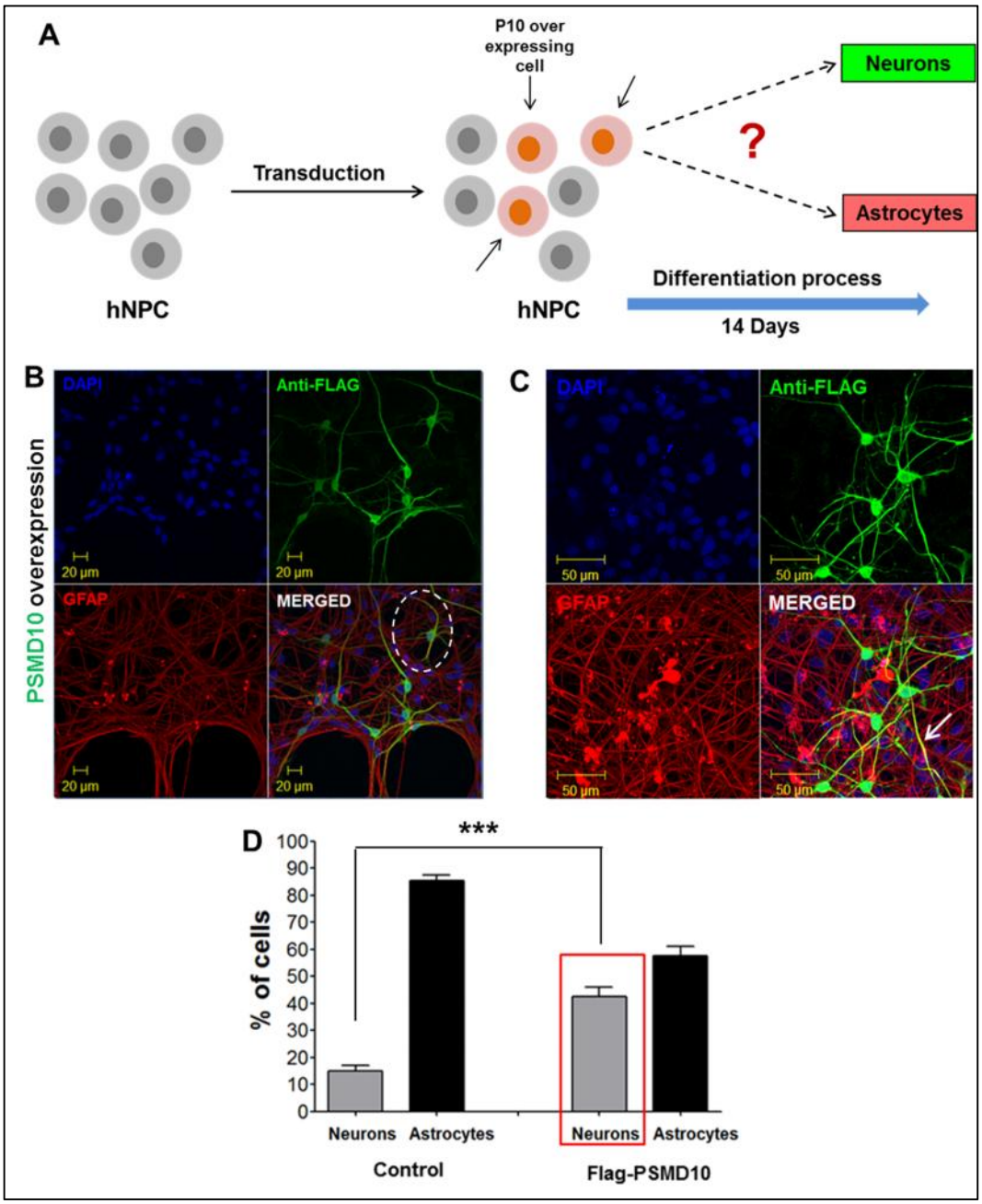

Figure-4.20 FLAG-PSMD10 trans-expression enhances neuronal differentiation. (A) A model for the for the experimental design to determine role of PSMD10 in the differentiation process. **(B), (C)** Progenitor cells were grown on Laminin coated glass coverslips till they reached ~30% confluence. Then cells were transduced with virus particle of pTRIPZ-FLAG-PSMD10, cell were either treated with doxycycline (1µg/mL) for 48hr or left untreated and allowed to differentiate for 14 days. Immunofluorescence was performed using anti-GFAP and anti-FLAG antibodies. The circle in (B) and the arrow in (C) are showing the co-localization of red and green. DAPI was (in blue) used for nuclear staining. Images were acquired in Laser confocal microscope (Nikon-Meta510). **(D)** Graph shows the average neuron to astrocyte ratios in both conditions, calculated by number of FLAG-PSMD10 expressing cells co-localizing with GFAP. Data represents the average number of cells from 10 different fields, done in three different experiments (10 X 3 = 30 fields).

Furthermore, we checked the overall effect of PSMD10 overexpression in the total pool of hNPCs, on the differentiation process. hNPCs were transduced with the virus, treated with doxycycline for 48h and then immunofluorescence was performed.

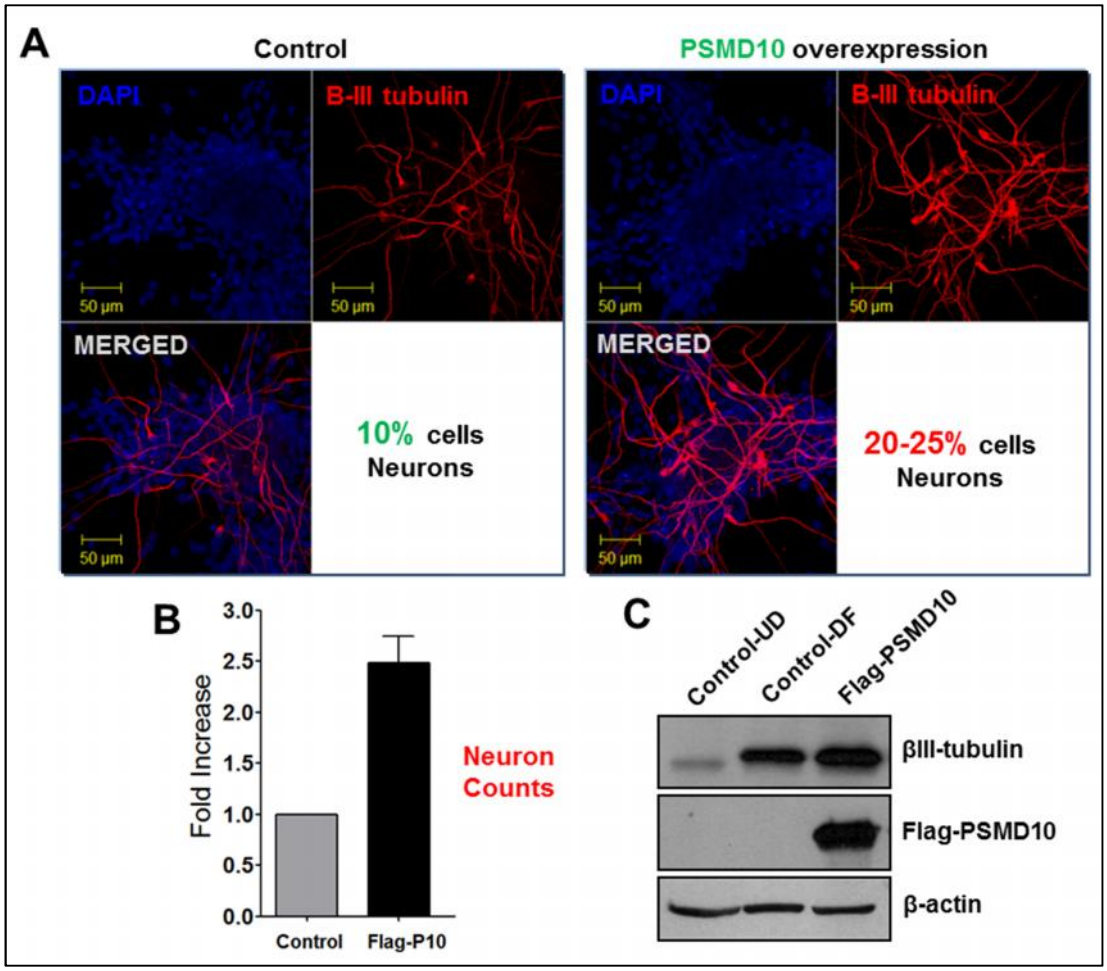

Figure-4.21 Overexpression of PSMD10 increases overall neuronal population. (A) Progenitor cells were grown on Laminin coated glass coverslips till they reached ~30% confluence. Then cells were transduced with virus particle of pTRIPZ-FLAG-PSMD10 and cell were either treated with doxycycline (1µg/mL) for 48hr or left untreated. **(A)** Immunofluorescence was performed after 48h of transduction following the protocol described in materials and methods. Cells show expression of FLAG-PSMD10 (in green). DAPI was (in blue) used for nuclear staining. Images were acquired in Laser confocal microscope (Nikon-Meta510). (B) Cell lysate were prepared after 48h of transduction and analysed by WB.

IF image showed upon PSMD10 overexpression neuron counts in the total differentiated population increased to ~20-25% from 10% (Dox-untreated) i.e. 2-2.5 fold increase (Figure-4.21A & B). In addition WB of Dox-treated/untreated differentiated cell lysate showed a significant increase in βIII-tubulin levels upon PSMD10 overexpression. These results altogether suggests PSMD10 overexpression somehow was triggering the

neuronal differentiation in hNPCs. However, further validation is required to substantial prove the effect of PSMD10 in neurogenesis.

4.4 DISCUSSION:

Over expression of PSMD10 in HEK 293 resulted in large scale changes in gene expression with the substantial number of significantly over expressed genes associated with neuronal differentiation. To investigate the possible involvement of PSMD10 in differentiation of stem cells into neurons, we established a model system using a human neural progenitor cell line (procured from Millipore) which grows as an adherent monolayer culture method, maintains stemness and has the capacity to generate all three terminally differentiated populations such as astrocytes, neurons and oligodendrocytes. Majority of the differentiated population were astrocytes (~80-90%) followed by neurons (~10-20%) and rest ~5% was oligodendrocytes. Using this model system we checked the endogenous levels of PSMD10 in progenitor cells before differentiation and after 14 days differentiation. Other proteasomal subunits and key proteins that are associated with differentiation were also measured. The protein levels as well as RNA levels of PSMD10 were found to be high in differentiated cells. Most of the other proteasomal subunits showed a decrease or no change (PSMD9 and β2) in their levels in going from the progenitor population to the differentiated cells.

There is a clear positive correlation between PSMD10 and markers of neuronal differentiation such as β-catenin and NGN1. PSMD10 reportedly stabilize the levels of β-catenin and vice-versa [358]. And β-catenin promotes neuronal differentiation through NGN1 expression [395]. We had also observed a substantial increase of NGN1 expression upon PSMD10 overexpression and upon trans-expression of PSMD10 in progenitor cells; we observed a significant enhancement of neuronal population. All these findings support the fact that PSMD10 favours neuronal differentiation of the

hNPCs. At the same time during early stages of differentiation process, a distinct correlation is seen between STAT3 activity and PSMD10 levels. And during this process PSMD10 seems to be negatively correlated with STAT3 signaling pathway, although it is too early to comment.

Considering the fact that, the hNPC differentiated population is a mix population of more astrocytes and less neurons, a role for PSMD10 in neuronal differentiation based on protein levels detected by western blot is speculative. Some of these are (a) a direct role for PSMD10 by modulating transcription; (b) activating signals in lateral progenitor cells within the niche to promote neurogenesis and inducing them to respond to paracrine and autocrine signals as is observed normally. We also observed that not all PSMD10 trans-expressing cells become neurons and all neurons are not positive for the trans expressed protein. This probably corroborates a role for PSMD10 in the above mentioned processes.

Although this current study provides a preliminary idea about the probable role of PSMD10 in the differentiation process, additional experiments are essential to achieve a concrete conclusion. Knock down of PSMD10 in the hNPC cells, challenging with different growth factors and neurotrophins, using inhibitors for either gliogenesis and neurogenesis and regulating some vital protein levels, it can be explicated the molecular mechanism behind the involvement of PSMD10 in neural differentiation process.

4.5 SUMMARY AND CONCLUSION:

In summary, we could establish some preliminary results which suggest a possible role of PSMD10 in human neural progenitor cell differentiation process. PSMD10 might be promoting astrocyte differentiation by regulating STAT3 activity in the early days of differentiation process. However, the Co-expression of PSMD10, β-catenin and NGN1 in the latter part of differentiation process and increase in neuron counts suggest the

possible involvement of PSMD10 in neuronal differentiation. Hence PSMD10 may be involved both in astrocyte as well as neuronal differentiation process of hNPC in a spatio-temporal manner. Gankyrin although established as an oncoprotein, our data imply a role for PSMD10 in a developmental/differentiation process. Some of the pertinent and provocative questions from this study are; (a) how does one explain the role of an oncoprotein, that normally leading to dedefferniation, in differentaion process? (b) the role of proteasome activity which is reportedly high during differentiation and therefore expected to show increase in levels of the subunits actually shows a reduction in this example. Hence further investigation is essential to decipher the molecular details of PSMD10 involvement in neural stem cell biology.

4.6 SIGNIFICANCE OF THE STUDY:

Although preliminary our results point towards a role for PSMD10 in neural differentiation process. If these observations are confirmed and if we can use PSMD10 to generate neurons in vivo, we may have a strategy to replenish neurons in in neurodegenerative disorders.

BIBILOGRAPHY

1. Baumeister W, Walz J, Zuhl F, Seemuller E: **The proteasome: paradigm of a self-compartmentalizing protease**. *Cell* 1998, **92**(3):367-380.
2. Harris JR: **Release of a macromolecular protein component from human erythrocyte ghosts**. *Biochim Biophys Acta* 1968, **150**(3):534-537.
3. Etlinger JD, Goldberg AL: **A soluble ATP-dependent proteolytic system responsible for the degradation of abnormal proteins in reticulocytes**. *Proc Natl Acad Sci U S A* 1977, **74**(1):54-58.
4. Schmid HP, Akhayat O, Martins De Sa C, Puvion F, Koehler K, Scherrer K: **The prosome: an ubiquitous morphologically distinct RNP particle associated with repressed mRNPs and containing specific ScRNA and a characteristic set of proteins**. *EMBO J* 1984, **3**(1):29-34.
5. Arrigo AP, Tanaka K, Goldberg AL, Welch WJ: **Identity of the 19S 'prosome' particle with the large multifunctional protease complex of mammalian cells (the proteasome)**. *Nature* 1988, **331**(6152):192-194.
6. Falkenburg PE, Haass C, Kloetzel PM, Niedel B, Kopp F, Kuehn L, Dahlmann B: **Drosophila small cytoplasmic 19S ribonucleoprotein is homologous to the rat multicatalytic proteinase**. *Nature* 1988, **331**(6152):190-192.
7. Ciehanover A, Hod Y, Hershko A: **A heat-stable polypeptide component of an ATP-dependent proteolytic system from reticulocytes**. *Biochem Biophys Res Commun* 1978, **81**(4):1100-1105.
8. Hough R, Pratt G, Rechsteiner M: **Purification of two high molecular weight proteases from rabbit reticulocyte lysate**. *J Biol Chem* 1987, **262**(17):8303-8313.
9. Hershko A, Ciechanover A, Rose IA: **Resolution of the ATP-dependent proteolytic system from reticulocytes: a component that interacts with ATP**. *Proc Natl Acad Sci U S A* 1979, **76**(7):3107-3110.
10. Wilkinson KD, Urban MK, Haas AL: **Ubiquitin is the ATP-dependent proteolysis factor I of rabbit reticulocytes**. *J Biol Chem* 1980, **255**(16):7529-7532.
11. Glickman MH, Rubin DM, Fried VA, Finley D: **The regulatory particle of the Saccharomyces cerevisiae proteasome**. *Mol Cell Biol* 1998, **18**(6):3149-3162.
12. Russell SJ, Steger KA, Johnston SA: **Subcellular localization, stoichiometry, and protein levels of 26 S proteasome subunits in yeast**. *J Biol Chem* 1999, **274**(31):21943-21952.
13. Brooks P, Fuertes G, Murray RZ, Bose S, Knecht E, Rechsteiner MC, Hendil KB, Tanaka K, Dyson J, Rivett J: **Subcellular localization of proteasomes and their regulatory complexes in mammalian cells**. *Biochem J* 2000, **346 Pt 1**:155-161.

14. Glickman MH, Ciechanover A: **The ubiquitin-proteasome proteolytic pathway: destruction for the sake of construction**. *Physiol Rev* 2002, **82**(2):373-428.
15. Groll M, Ditzel L, Lowe J, Stock D, Bochtler M, Bartunik HD, Huber R: **Structure of 20S proteasome from yeast at 2.4 A resolution**. *Nature* 1997, **386**(6624):463-471.
16. Ruschak AM, Religa TL, Breuer S, Witt S, Kay LE: **The proteasome antechamber maintains substrates in an unfolded state**. *Nature* 2010, **467**(7317):868-871.
17. Sharon M, Witt S, Felderer K, Rockel B, Baumeister W, Robinson CV: **20S proteasomes have the potential to keep substrates in store for continual degradation**. *J Biol Chem* 2006, **281**(14):9569-9575.
18. Borissenko L, Groll M: **20S proteasome and its inhibitors: crystallographic knowledge for drug development**. *Chem Rev* 2007, **107**(3):687-717.
19. Beck F, Unverdorben P, Bohn S, Schweitzer A, Pfeifer G, Sakata E, Nickell S, Plitzko JM, Villa E, Baumeister W *et al*: **Near-atomic resolution structural model of the yeast 26S proteasome**. *Proc Natl Acad Sci U S A* 2012, **109**(37):14870-14875.
20. Lander GC, Estrin E, Matyskiela ME, Bashore C, Nogales E, Martin A: **Complete subunit architecture of the proteasome regulatory particle**. *Nature* 2012, **482**(7384):186-191.
21. Lasker K, Forster F, Bohn S, Walzthoeni T, Villa E, Unverdorben P, Beck F, Aebersold R, Sali A, Baumeister W: **Molecular architecture of the 26S proteasome holocomplex determined by an integrative approach**. *Proc Natl Acad Sci U S A* 2012, **109**(5):1380-1387.
22. Glickman MH, Rubin DM, Coux O, Wefes I, Pfeifer G, Cjeka Z, Baumeister W, Fried VA, Finley D: **A subcomplex of the proteasome regulatory particle required for ubiquitin-conjugate degradation and related to the COP9-signalosome and eIF3**. *Cell* 1998, **94**(5):615-623.
23. Liu CW, Li X, Thompson D, Wooding K, Chang TL, Tang Z, Yu H, Thomas PJ, DeMartino GN: **ATP binding and ATP hydrolysis play distinct roles in the function of 26S proteasome**. *Mol Cell* 2006, **24**(1):39-50.
24. Rubin DM, Glickman MH, Larsen CN, Dhruvakumar S, Finley D: **Active site mutants in the six regulatory particle ATPases reveal multiple roles for ATP in the proteasome**. *EMBO J* 1998, **17**(17):4909-4919.
25. Verma R, Aravind L, Oania R, McDonald WH, Yates JR, 3rd, Koonin EV, Deshaies RJ: **Role of Rpn11 metalloprotease in deubiquitination and degradation by the 26S proteasome**. *Science* 2002, **298**(5593):611-615.
26. Tian G, Park S, Lee MJ, Huck B, McAllister F, Hill CP, Gygi SP, Finley D: **An asymmetric interface between the regulatory and core particles of the proteasome**. *Nat Struct Mol Biol* 2011, **18**(11):1259-1267.

27. Kish-Trier E, Hill CP: **Structural biology of the proteasome**. *Annu Rev Biophys* 2013, **42**:29-49.

28. Davy A, Bello P, Thierry-Mieg N, Vaglio P, Hitti J, Doucette-Stamm L, Thierry-Mieg D, Reboul J, Boulton S, Walhout AJ *et al*: **A protein-protein interaction map of the Caenorhabditis elegans 26S proteasome**. *EMBO Rep* 2001, **2**(9):821-828.

29. Fu H, Reis N, Lee Y, Glickman MH, Vierstra RD: **Subunit interaction maps for the regulatory particle of the 26S proteasome and the COP9 signalosome**. *EMBO J* 2001, **20**(24):7096-7107.

30. Gorbea C, Taillandier D, Rechsteiner M: **Mapping subunit contacts in the regulatory complex of the 26 S proteasome. S2 and S5b form a tetramer with ATPase subunits S4 and S7**. *J Biol Chem* 2000, **275**(2):875-882.

31. Hartmann-Petersen R, Tanaka K, Hendil KB: **Quaternary structure of the ATPase complex of human 26S proteasomes determined by chemical cross-linking**. *Arch Biochem Biophys* 2001, **386**(1):89-94.

32. Richmond C, Gorbea C, Rechsteiner M: **Specific interactions between ATPase subunits of the 26 S protease**. *J Biol Chem* 1997, **272**(20):13403-13411.

33. Gerlinger UM, Guckel R, Hoffmann M, Wolf DH, Hilt W: **Yeast cycloheximide-resistant crl mutants are proteasome mutants defective in protein degradation**. *Mol Biol Cell* 1997, **8**(12):2487-2499.

34. Satoh K, Sasajima H, Nyoumura KI, Yokosawa H, Sawada H: **Assembly of the 26S proteasome is regulated by phosphorylation of the p45/Rpt6 ATPase subunit**. *Biochemistry* 2001, **40**(2):314-319.

35. Zhang Z, Torii N, Furusaka A, Malayaman N, Hu Z, Liang TJ: **Structural and functional characterization of interaction between hepatitis B virus X protein and the proteasome complex**. *J Biol Chem* 2000, **275**(20):15157-15165.

36. Tomko RJ, Jr., Hochstrasser M: **Molecular architecture and assembly of the eukaryotic proteasome**. *Annu Rev Biochem* 2013, **82**:415-445.

37. Tomko RJ, Jr., Funakoshi M, Schneider K, Wang J, Hochstrasser M: **Heterohexameric ring arrangement of the eukaryotic proteasomal ATPases: implications for proteasome structure and assembly**. *Mol Cell* 2010, **38**(3):393-403.

38. Lupas A, Koster AJ, Baumeister W: **Structural features of 26S and 20S proteasomes**. *Enzyme Protein* 1993, **47**(4-6):252-273.

39. Coux O, Tanaka K, Goldberg AL: **Structure and functions of the 20S and 26S proteasomes**. *Annu Rev Biochem* 1996, **65**:801-847.

40. Zwickl P, Voges D, Baumeister W: **The proteasome: a macromolecular assembly designed for controlled proteolysis**. *Philos Trans R Soc Lond B Biol Sci* 1999, **354**(1389):1501-1511.

41. Fraser RA, Rossignol M, Heard DJ, Egly JM, Chambon P: **SUG1, a putative transcriptional mediator and subunit of the PA700 proteasome regulatory complex, is a DNA helicase**. *J Biol Chem* 1997, **272**(11):7122-7126.
42. Truax AD, Koues OI, Mentel MK, Greer SF: **The 19S ATPase S6a (S6'/TBP1) regulates the transcription initiation of class II transactivator**. *J Mol Biol* 2010, **395**(2):254-269.
43. Maganti N, Moody TD, Truax AD, Thakkar M, Spring AM, Germann MW, Greer SF: **Nonproteolytic roles of 19S ATPases in transcription of CIITApIV genes**. *PLoS One* 2014, **9**(3):e91200.
44. Kajava AV: **What curves alpha-solenoids? Evidence for an alpha-helical toroid structure of Rpn1 and Rpn2 proteins of the 26 S proteasome**. *J Biol Chem* 2002, **277**(51):49791-49798.
45. Haracska L, Udvardy A: **Mapping the ubiquitin-binding domains in the p54 regulatory complex subunit of the Drosophila 26S protease**. *FEBS Lett* 1997, **412**(2):331-336.
46. Saeki Y, Toh-e A, Yokosawa H: **Rapid isolation and characterization of the yeast proteasome regulatory complex**. *Biochem Biophys Res Commun* 2000, **273**(2):509-515.
47. Takeuchi J, Fujimuro M, Yokosawa H, Tanaka K, Toh-e A: **Rpn9 is required for efficient assembly of the yeast 26S proteasome**. *Mol Cell Biol* 1999, **19**(10):6575-6584.
48. van Nocker S, Sadis S, Rubin DM, Glickman M, Fu H, Coux O, Wefes I, Finley D, Vierstra RD: **The multiubiquitin-chain-binding protein Mcb1 is a component of the 26S proteasome in Saccharomyces cerevisiae and plays a nonessential, substrate-specific role in protein turnover**. *Mol Cell Biol* 1996, **16**(11):6020-6028.
49. Gomez TA, Kolawa N, Gee M, Sweredoski MJ, Deshaies RJ: **Identification of a functional docking site in the Rpn1 LRR domain for the UBA-UBL domain protein Ddi1**. *BMC Biol* 2011, **9**:33.
50. Schreiner P, Chen X, Husnjak K, Randles L, Zhang N, Elsasser S, Finley D, Dikic I, Walters KJ, Groll M: **Ubiquitin docking at the proteasome through a novel pleckstrin-homology domain interaction**. *Nature* 2008, **453**(7194):548-552.
51. Riedinger C, Boehringer J, Trempe JF, Lowe ED, Brown NR, Gehring K, Noble ME, Gordon C, Endicott JA: **Structure of Rpn10 and its interactions with polyubiquitin chains and the proteasome subunit Rpn12**. *J Biol Chem* 2010, **285**(44):33992-34003.
52. Kohlmann S, Schafer A, Wolf DH: **Ubiquitin ligase Hul5 is required for fragment-specific substrate degradation in endoplasmic reticulum-associated degradation**. *J Biol Chem* 2008, **283**(24):16374-16383.
53. Finley D: **Recognition and processing of ubiquitin-protein conjugates by the proteasome**. *Annu Rev Biochem* 2009, **78**:477-513.
54. Rechsteiner M, Realini C, Ustrell V: **The proteasome activator 11 S REG (PA28) and class I antigen presentation**. *Biochem J* 2000, **345 Pt 1**:1-15.

55. Tanahashi N, Yokota K, Ahn JY, Chung CH, Fujiwara T, Takahashi E, DeMartino GN, Slaughter CA, Toyonaga T, Yamamura K *et al*: **Molecular properties of the proteasome activator PA28 family proteins and gamma-interferon regulation**. *Genes Cells* 1997, **2**(3):195-211.
56. Wojcik C, Tanaka K, Paweletz N, Naab U, Wilk S: **Proteasome activator (PA28) subunits, alpha, beta and gamma (Ki antigen) in NT2 neuronal precursor cells and HeLa S3 cells**. *Eur J Cell Biol* 1998, **77**(2):151-160.
57. Whitby FG, Masters EI, Kramer L, Knowlton JR, Yao Y, Wang CC, Hill CP: **Structural basis for the activation of 20S proteasomes by 11S regulators**. *Nature* 2000, **408**(6808):115-120.
58. Tanaka K, Kasahara M: **The MHC class I ligand-generating system: roles of immunoproteasomes and the interferon-gamma-inducible proteasome activator PA28**. *Immunol Rev* 1998, **163**:161-176.
59. Kloetzel PM: **Antigen processing by the proteasome**. *Nat Rev Mol Cell Biol* 2001, **2**(3):179-187.
60. Rock KL, York IA, Saric T, Goldberg AL: **Protein degradation and the generation of MHC class I-presented peptides**. *Adv Immunol* 2002, **80**:1-70.
61. Murata S, Kawahara H, Tohma S, Yamamoto K, Kasahara M, Nabeshima Y, Tanaka K, Chiba T: **Growth retardation in mice lacking the proteasome activator PA28gamma**. *J Biol Chem* 1999, **274**(53):38211-38215.
62. Mao I, Liu J, Li X, Luo H: **REGgamma, a proteasome activator and beyond?** *Cell Mol Life Sci* 2008, **65**(24):3971-3980.
63. Tanahashi N, Murakami Y, Minami Y, Shimbara N, Hendil KB, Tanaka K: **Hybrid proteasomes. Induction by interferon-gamma and contribution to ATP-dependent proteolysis**. *J Biol Chem* 2000, **275**(19):14336-14345.
64. Ustrell V, Hoffman L, Pratt G, Rechsteiner M: **PA200, a nuclear proteasome activator involved in DNA repair**. *EMBO J* 2002, **21**(13):3516-3525.
65. Schmidt M, Haas W, Crosas B, Santamaria PG, Gygi SP, Walz T, Finley D: **The HEAT repeat protein Blm10 regulates the yeast proteasome by capping the core particle**. *Nat Struct Mol Biol* 2005, **12**(4):294-303.
66. Marques AJ, Glanemann C, Ramos PC, Dohmen RJ: **The C-terminal extension of the beta7 subunit and activator complexes stabilize nascent 20 S proteasomes and promote their maturation**. *J Biol Chem* 2007, **282**(48):34869-34876.
67. Lehmann A, Jechow K, Enenkel C: **Blm10 binds to pre-activated proteasome core particles with open gate conformation**. *EMBO Rep* 2008, **9**(12):1237-1243.

68. McCutchen-Maloney SL, Matsuda K, Shimbara N, Binns DD, Tanaka K, Slaughter CA, DeMartino GN: **cDNA cloning, expression, and functional characterization of PI31, a proline-rich inhibitor of the proteasome**. *J Biol Chem* 2000, **275**(24):18557-18565.
69. Zaiss DM, Standera S, Kloetzel PM, Sijts AJ: **PI31 is a modulator of proteasome formation and antigen processing**. *Proc Natl Acad Sci U S A* 2002, **99**(22):14344-14349.
70. Kloetzel PM: **Generation of major histocompatibility complex class I antigens: functional interplay between proteasomes and TPPII**. *Nat Immunol* 2004, **5**(7):661-669.
71. Murata S, Sasaki K, Kishimoto T, Niwa S, Hayashi H, Takahama Y, Tanaka K: **Regulation of CD8+ T cell development by thymus-specific proteasomes**. *Science* 2007, **316**(5829):1349-1353.
72. Rock KL, York IA, Goldberg AL: **Post-proteasomal antigen processing for major histocompatibility complex class I presentation**. *Nat Immunol* 2004, **5**(7):670-677.
73. Murata S, Takahama Y, Tanaka K: **Thymoproteasome: probable role in generating positively selecting peptides**. *Curr Opin Immunol* 2008, **20**(2):192-196.
74. Takahama Y, Tanaka K, Murata S: **Modest cortex and promiscuous medulla for thymic repertoire formation**. *Trends Immunol* 2008, **29**(6):251-255.
75. Zhong L, Belote JM: **The testis-specific proteasome subunit Prosalpha6T of D. melanogaster is required for individualization and nuclear maturation during spermatogenesis**. *Development* 2007, **134**(19):3517-3525.
76. Kawahara H, Kasahara M, Nishiyama A, Ohsumi K, Goto T, Kishimoto T, Saeki Y, Yokosawa H, Shimbara N, Murata S *et al*: **Developmentally regulated, alternative splicing of the Rpn10 gene generates multiple forms of 26S proteasomes**. *EMBO J* 2000, **19**(15):4144-4153.
77. Hamazaki J, Sasaki K, Kawahara H, Hisanaga S, Tanaka K, Murata S: **Rpn10-mediated degradation of ubiquitinated proteins is essential for mouse development**. *Mol Cell Biol* 2007, **27**(19):6629-6638.
78. Goldstein G, Scheid M, Hammerling U, Schlesinger DH, Niall HD, Boyse EA: **Isolation of a polypeptide that has lymphocyte-differentiating properties and is probably represented universally in living cells**. *Proc Natl Acad Sci U S A* 1975, **72**(1):11-15.
79. Pickart CM: **Mechanisms underlying ubiquitination**. *Annu Rev Biochem* 2001, **70**:503-533.
80. Marotti LA, Jr., Newitt R, Wang Y, Aebersold R, Dohlman HG: **Direct identification of a G protein ubiquitination site by mass spectrometry**. *Biochemistry* 2002, **41**(16):5067-5074.
81. Peng J, Schwartz D, Elias JE, Thoreen CC, Cheng D, Marsischky G, Roelofs J, Finley D, Gygi SP: **A proteomics approach to understanding protein ubiquitination**. *Nat Biotechnol* 2003, **21**(8):921-926.

82. Wang X, Herr RA, Chua WJ, Lybarger L, Wiertz EJ, Hansen TH: **Ubiquitination of serine, threonine, or lysine residues on the cytoplasmic tail can induce ERAD of MHC-I by viral E3 ligase mK3**. *J Cell Biol* 2007, **177**(4):613-624.
83. Cadwell K, Coscoy L: **Ubiquitination on nonlysine residues by a viral E3 ubiquitin ligase**. *Science* 2005, **309**(5731):127-130.
84. Dikic I, Robertson M: **Ubiquitin ligases and beyond**. *BMC Biol* 2012, **10**:22.
85. Schulman BA, Harper JW: **Ubiquitin-like protein activation by E1 enzymes: the apex for downstream signalling pathways**. *Nat Rev Mol Cell Biol* 2009, **10**(5):319-331.
86. Groettrup M, Pelzer C, Schmidtke G, Hofmann K: **Activating the ubiquitin family: UBA6 challenges the field**. *Trends Biochem Sci* 2008, **33**(5):230-237.
87. van Wijk SJ, Timmers HT: **The family of ubiquitin-conjugating enzymes (E2s): deciding between life and death of proteins**. *FASEB J* 2010, **24**(4):981-993.
88. Metzger MB, Hristova VA, Weissman AM: **HECT and RING finger families of E3 ubiquitin ligases at a glance**. *J Cell Sci* 2012, **125**(Pt 3):531-537.
89. Komander D: **The emerging complexity of protein ubiquitination**. *Biochem Soc Trans* 2009, **37**(Pt 5):937-953.
90. Miranda M, Sorkin A: **Regulation of receptors and transporters by ubiquitination: new insights into surprisingly similar mechanisms**. *Mol Interv* 2007, **7**(3):157-167.
91. Ikeda F, Dikic I: **Atypical ubiquitin chains: new molecular signals. 'Protein Modifications: Beyond the Usual Suspects' review series**. *EMBO Rep* 2008, **9**(6):536-542.
92. Nathan JA, Kim HT, Ting L, Gygi SP, Goldberg AL: **Why do cellular proteins linked to K63-polyubiquitin chains not associate with proteasomes?** *EMBO J* 2013, **32**(4):552-565.
93. Bache KG, Raiborg C, Mehlum A, Stenmark H: **STAM and Hrs are subunits of a multivalent ubiquitin-binding complex on early endosomes**. *J Biol Chem* 2003, **278**(14):12513-12521.
94. Deveraux Q, Ustrell V, Pickart C, Rechsteiner M: **A 26 S protease subunit that binds ubiquitin conjugates**. *J Biol Chem* 1994, **269**(10):7059-7061.
95. Husnjak K, Elsasser S, Zhang N, Chen X, Randles L, Shi Y, Hofmann K, Walters KJ, Finley D, Dikic I: **Proteasome subunit Rpn13 is a novel ubiquitin receptor**. *Nature* 2008, **453**(7194):481-488.
96. Chen L, Madura K: **Rad23 promotes the targeting of proteolytic substrates to the proteasome**. *Mol Cell Biol* 2002, **22**(13):4902-4913.
97. Elsasser S, Chandler-Militello D, Muller B, Hanna J, Finley D: **Rad23 and Rpn10 serve as alternative ubiquitin receptors for the proteasome**. *J Biol Chem* 2004, **279**(26):26817-26822.

98. Rao H, Sastry A: **Recognition of specific ubiquitin conjugates is important for the proteolytic functions of the ubiquitin-associated domain proteins Dsk2 and Rad23**. *J Biol Chem* 2002, **277**(14):11691-11695.

99. Verma R, Oania R, Graumann J, Deshaies RJ: **Multiubiquitin chain receptors define a layer of substrate selectivity in the ubiquitin-proteasome system**. *Cell* 2004, **118**(1):99-110.

100. Wilkinson CR, Seeger M, Hartmann-Petersen R, Stone M, Wallace M, Semple C, Gordon C: **Proteins containing the UBA domain are able to bind to multi-ubiquitin chains**. *Nat Cell Biol* 2001, **3**(10):939-943.

101. Elsasser S, Gali RR, Schwickart M, Larsen CN, Leggett DS, Muller B, Feng MT, Tubing F, Dittmar GA, Finley D: **Proteasome subunit Rpn1 binds ubiquitin-like protein domains**. *Nat Cell Biol* 2002, **4**(9):725-730.

102. Matiuhin Y, Kirkpatrick DS, Ziv I, Kim W, Dakshinamurthy A, Kleifeld O, Gygi SP, Reis N, Glickman MH: **Extraproteasomal Rpn10 restricts access of the polyubiquitin-binding protein Dsk2 to proteasome**. *Mol Cell* 2008, **32**(3):415-425.

103. Chen L, Shinde U, Ortolan TG, Madura K: **Ubiquitin-associated (UBA) domains in Rad23 bind ubiquitin and promote inhibition of multi-ubiquitin chain assembly**. *EMBO Rep* 2001, **2**(10):933-938.

104. Ortolan TG, Tongaonkar P, Lambertson D, Chen L, Schauber C, Madura K: **The DNA repair protein rad23 is a negative regulator of multi-ubiquitin chain assembly**. *Nat Cell Biol* 2000, **2**(9):601-608.

105. Raasi S, Pickart CM: **Rad23 ubiquitin-associated domains (UBA) inhibit 26 S proteasome-catalyzed proteolysis by sequestering lysine 48-linked polyubiquitin chains**. *J Biol Chem* 2003, **278**(11):8951-8959.

106. Richly H, Rape M, Braun S, Rumpf S, Hoege C, Jentsch S: **A series of ubiquitin binding factors connects CDC48/p97 to substrate multiubiquitylation and proteasomal targeting**. *Cell* 2005, **120**(1):73-84.

107. Beskow A, Grimberg KB, Bott LC, Salomons FA, Dantuma NP, Young P: **A conserved unfoldase activity for the p97 AAA-ATPase in proteasomal degradation**. *J Mol Biol* 2009, **394**(4):732-746.

108. Inobe T, Matouschek A: **Paradigms of protein degradation by the proteasome**. *Curr Opin Struct Biol* 2014, **24**:156-164.

109. Thrower JS, Hoffman L, Rechsteiner M, Pickart CM: **Recognition of the polyubiquitin proteolytic signal**. *EMBO J* 2000, **19**(1):94-102.

110. Baboshina OV, Haas AL: **Novel multiubiquitin chain linkages catalyzed by the conjugating enzymes E2EPF and RAD6 are recognized by 26 S proteasome subunit 5**. *J Biol Chem* 1996, **271**(5):2823-2831.

111. Young P, Deveraux Q, Beal RE, Pickart CM, Rechsteiner M: **Characterization of two polyubiquitin binding sites in the 26 S protease subunit 5a**. *J Biol Chem* 1998, **273**(10):5461-5467.

112. Fu H, Sadis S, Rubin DM, Glickman M, van Nocker S, Finley D, Vierstra RD: **Multiubiquitin chain binding and protein degradation are mediated by distinct domains within the 26 S proteasome subunit Mcb1**. *J Biol Chem* 1998, **273**(4):1970-1981.

113. Girod PA, Fu H, Zryd JP, Vierstra RD: **Multiubiquitin chain binding subunit MCB1 (RPN10) of the 26S proteasome is essential for developmental progression in Physcomitrella patens**. *Plant Cell* 1999, **11**(8):1457-1472.

114. Wilkinson CR, Ferrell K, Penney M, Wallace M, Dubiel W, Gordon C: **Analysis of a gene encoding Rpn10 of the fission yeast proteasome reveals that the polyubiquitin-binding site of this subunit is essential when Rpn12/Mts3 activity is compromised**. *J Biol Chem* 2000, **275**(20):15182-15192.

115. Lambertson D, Chen L, Madura K: **Pleiotropic defects caused by loss of the proteasome-interacting factors Rad23 and Rpn10 of Saccharomyces cerevisiae**. *Genetics* 1999, **153**(1):69-79.

116. Hiyama H, Yokoi M, Masutani C, Sugasawa K, Maekawa T, Tanaka K, Hoeijmakers JH, Hanaoka F: **Interaction of hHR23 with S5a. The ubiquitin-like domain of hHR23 mediates interaction with S5a subunit of 26 S proteasome**. *J Biol Chem* 1999, **274**(39):28019-28025.

117. Schauber C, Chen L, Tongaonkar P, Vega I, Lambertson D, Potts W, Madura K: **Rad23 links DNA repair to the ubiquitin/proteasome pathway**. *Nature* 1998, **391**(6668):715-718.

118. Murakami Y, Matsufuji S, Kameji T, Hayashi S, Igarashi K, Tamura T, Tanaka K, Ichihara A: **Ornithine decarboxylase is degraded by the 26S proteasome without ubiquitination**. *Nature* 1992, **360**(6404):597-599.

119. Russell SJ, Reed SH, Huang W, Friedberg EC, Johnston SA: **The 19S regulatory complex of the proteasome functions independently of proteolysis in nucleotide excision repair**. *Mol Cell* 1999, **3**(6):687-695.

120. Cagney G, Uetz P, Fields S: **Two-hybrid analysis of the Saccharomyces cerevisiae 26S proteasome**. *Physiol Genomics* 2001, **7**(1):27-34.

121. Kleijnen MF, Shih AH, Zhou P, Kumar S, Soccio RE, Kedersha NL, Gill G, Howley PM: **The hPLIC proteins may provide a link between the ubiquitination machinery and the proteasome**. *Mol Cell* 2000, **6**(2):409-419.

122. Golbik R, Lupas AN, Koretke KK, Baumeister W, Peters J: **The Janus face of the archaeal Cdc48/p97 homologue VAT: protein folding versus unfolding**. *Biol Chem* 1999, **380**(9):1049-1062.

123. Zwickl P, Baumeister W, Steven A: **Dis-assembly lines: the proteasome and related ATPase-assisted proteases**. *Curr Opin Struct Biol* 2000, **10**(2):242-250.

124. Dai RM, Li CC: **Valosin-containing protein is a multi-ubiquitin chain-targeting factor required in ubiquitin-proteasome degradation**. *Nat Cell Biol* 2001, **3**(8):740-744.

125. Lupas A, Baumeister W, Hofmann K: **A repetitive sequence in subunits of the 26S proteasome and 20S cyclosome (anaphase-promoting complex)**. *Trends Biochem Sci* 1997, **22**(6):195-196.

126. Braun BC, Glickman M, Kraft R, Dahlmann B, Kloetzel PM, Finley D, Schmidt M: **The base of the proteasome regulatory particle exhibits chaperone-like activity**. *Nat Cell Biol* 1999, **1**(4):221-226.

127. Strickland E, Hakala K, Thomas PJ, DeMartino GN: **Recognition of misfolding proteins by PA700, the regulatory subcomplex of the 26 S proteasome**. *J Biol Chem* 2000, **275**(8):5565-5572.

128. Navon A, Goldberg AL: **Proteins are unfolded on the surface of the ATPase ring before transport into the proteasome**. *Mol Cell* 2001, **8**(6):1339-1349.

129. Armon T, Ganoth D, Hershko A: **Assembly of the 26 S complex that degrades proteins ligated to ubiquitin is accompanied by the formation of ATPase activity**. *J Biol Chem* 1990, **265**(34):20723-20726.

130. Hoffman L, Rechsteiner M: **Activation of the multicatalytic protease. The 11 S regulator and 20 S ATPase complexes contain distinct 30-kilodalton subunits**. *J Biol Chem* 1994, **269**(24):16890-16895.

131. DeMartino GN, Moomaw CR, Zagnitko OP, Proske RJ, Chu-Ping M, Afendis SJ, Swaffield JC, Slaughter CA: **PA700, an ATP-dependent activator of the 20 S proteasome, is an ATPase containing multiple members of a nucleotide-binding protein family**. *J Biol Chem* 1994, **269**(33):20878-20884.

132. Hershko A, Leshinsky E, Ganoth D, Heller H: **ATP-dependent degradation of ubiquitin-protein conjugates**. *Proc Natl Acad Sci U S A* 1984, **81**(6):1619-1623.

133. Yao T, Cohen RE: **A cryptic protease couples deubiquitination and degradation by the proteasome**. *Nature* 2002, **419**(6905):403-407.

134. Kenniston JA, Baker TA, Fernandez JM, Sauer RT: **Linkage between ATP consumption and mechanical unfolding during the protein processing reactions of an AAA+ degradation machine**. *Cell* 2003, **114**(4):511-520.

135. Lee C, Schwartz MP, Prakash S, Iwakura M, Matouschek A: **ATP-dependent proteases degrade their substrates by processively unraveling them from the degradation signal**. *Mol Cell* 2001, **7**(3):627-637.

136. Pickart CM, Cohen RE: **Proteasomes and their kin: proteases in the machine age**. *Nat Rev Mol Cell Biol* 2004, **5**(3):177-187.

137. Prakash S, Tian L, Ratliff KS, Lehotzky RE, Matouschek A: **An unstructured initiation site is required for efficient proteasome-mediated degradation**. *Nat Struct Mol Biol* 2004, **11**(9):830-837.

138. Singh Gautam AK, Balakrishnan S, Venkatraman P: **Direct ubiquitin independent recognition and degradation of a folded protein by the eukaryotic proteasomes-origin of intrinsic degradation signals**. *PLoS One* 2012, **7**(4):e34864.

139. Takeuchi J, Chen H, Coffino P: **Proteasome substrate degradation requires association plus extended peptide**. *EMBO J* 2007, **26**(1):123-131.

140. Verhoef LG, Heinen C, Selivanova A, Halff EF, Salomons FA, Dantuma NP: **Minimal length requirement for proteasomal degradation of ubiquitin-dependent substrates**. *FASEB J* 2009, **23**(1):123-133.

141. Prakash S, Inobe T, Hatch AJ, Matouschek A: **Substrate selection by the proteasome during degradation of protein complexes**. *Nat Chem Biol* 2009, **5**(1):29-36.

142. Schrader EK, Harstad KG, Matouschek A: **Targeting proteins for degradation**. *Nat Chem Biol* 2009, **5**(11):815-822.

143. Groll M, Bajorek M, Kohler A, Moroder L, Rubin DM, Huber R, Glickman MH, Finley D: **A gated channel into the proteasome core particle**. *Nat Struct Biol* 2000, **7**(11):1062-1067.

144. Kohler A, Cascio P, Leggett DS, Woo KM, Goldberg AL, Finley D: **The axial channel of the proteasome core particle is gated by the Rpt2 ATPase and controls both substrate entry and product release**. *Mol Cell* 2001, **7**(6):1143-1152.

145. Chen P, Hochstrasser M: **Autocatalytic subunit processing couples active site formation in the 20S proteasome to completion of assembly**. *Cell* 1996, **86**(6):961-972.

146. Glickman MH: **Getting in and out of the proteasome**. *Semin Cell Dev Biol* 2000, **11**(3):149-158.

147. Kisselev AF, Akopian TN, Woo KM, Goldberg AL: **The sizes of peptides generated from protein by mammalian 26 and 20 S proteasomes. Implications for understanding the degradative mechanism and antigen presentation**. *J Biol Chem* 1999, **274**(6):3363-3371.

148. Nussbaum AK, Dick TP, Keilholz W, Schirle M, Stevanovic S, Dietz K, Heinemeyer W, Groll M, Wolf DH, Huber R *et al*: **Cleavage motifs of the yeast 20S proteasome beta subunits deduced from digests of enolase 1**. *Proc Natl Acad Sci U S A* 1998, **95**(21):12504-12509.

149. Kisselev AF, Akopian TN, Goldberg AL: **Range of sizes of peptide products generated during degradation of different proteins by archaeal proteasomes**. *J Biol Chem* 1998, **273**(4):1982-1989.

150. Dick TP, Nussbaum AK, Deeg M, Heinemeyer W, Groll M, Schirle M, Keilholz W, Stevanovic S, Wolf DH, Huber R *et al*: **Contribution of proteasomal beta-subunits to the**

cleavage of peptide substrates analyzed with yeast mutants. *J Biol Chem* 1998, **273**(40):25637-25646.

151. Holzhutter HG, Frommel C, Kloetzel PM: **A theoretical approach towards the identification of cleavage-determining amino acid motifs of the 20 S proteasome**. *J Mol Biol* 1999, **286**(4):1251-1265.
152. Emmerich NP, Nussbaum AK, Stevanovic S, Priemer M, Toes RE, Rammensee HG, Schild H: **The human 26 S and 20 S proteasomes generate overlapping but different sets of peptide fragments from a model protein substrate**. *J Biol Chem* 2000, **275**(28):21140-21148.
153. Schmidtke G, Emch S, Groettrup M, Holzhutter HG: **Evidence for the existence of a non-catalytic modifier site of peptide hydrolysis by the 20 S proteasome**. *J Biol Chem* 2000, **275**(29):22056-22063.
154. Michalek MT, Grant EP, Gramm C, Goldberg AL, Rock KL: **A role for the ubiquitin-dependent proteolytic pathway in MHC class I-restricted antigen presentation**. *Nature* 1993, **363**(6429):552-554.
155. Reyes-Turcu FE, Ventii KH, Wilkinson KD: **Regulation and cellular roles of ubiquitin-specific deubiquitinating enzymes**. *Annu Rev Biochem* 2009, **78**:363-397.
156. Hanna J, Hathaway NA, Tone Y, Crosas B, Elsasser S, Kirkpatrick DS, Leggett DS, Gygi SP, King RW, Finley D: **Deubiquitinating enzyme Ubp6 functions noncatalytically to delay proteasomal degradation**. *Cell* 2006, **127**(1):99-111.
157. Crosas B, Hanna J, Kirkpatrick DS, Zhang DP, Tone Y, Hathaway NA, Buecker C, Leggett DS, Schmidt M, King RW *et al*: **Ubiquitin chains are remodeled at the proteasome by opposing ubiquitin ligase and deubiquitinating activities**. *Cell* 2006, **127**(7):1401-1413.
158. Chattopadhyay MK, Murakami Y, Matsufuji S: **Antizyme regulates the degradation of ornithine decarboxylase in fission yeast Schizosaccharomyces pombe. Study in the spe2 knockout strains**. *J Biol Chem* 2001, **276**(24):21235-21241.
159. Baugh JM, Viktorova EG, Pilipenko EV: **Proteasomes can degrade a significant proportion of cellular proteins independent of ubiquitination**. *J Mol Biol* 2009, **386**(3):814-827.
160. Zhang M, Pickart CM, Coffino P: **Determinants of proteasome recognition of ornithine decarboxylase, a ubiquitin-independent substrate**. *EMBO J* 2003, **22**(7):1488-1496.
161. Sauer RT, Baker TA: **AAA+ proteases: ATP-fueled machines of protein destruction**. *Annu Rev Biochem* 2011, **80**:587-612.
162. Orlowski M, Wilk S: **Catalytic activities of the 20 S proteasome, a multicatalytic proteinase complex**. *Arch Biochem Biophys* 2000, **383**(1):1-16.
163. Chen X, Barton LF, Chi Y, Clurman BE, Roberts JM: **Ubiquitin-independent degradation of cell-cycle inhibitors by the REGgamma proteasome**. *Mol Cell* 2007, **26**(6):843-852.

164. Erales J, Coffino P: **Ubiquitin-independent proteasomal degradation**. *Biochim Biophys Acta* 2014, **1843**(1):216-221.

165. Asher G, Bercovich Z, Tsvetkov P, Shaul Y, Kahana C: **20S proteasomal degradation of ornithine decarboxylase is regulated by NQO1**. *Mol Cell* 2005, **17**(5):645-655.

166. Moscovitz O, Tsvetkov P, Hazan N, Michaelevski I, Keisar H, Ben-Nissan G, Shaul Y, Sharon M: **A mutually inhibitory feedback loop between the 20S proteasome and its regulator, NQO1**. *Mol Cell* 2012, **47**(1):76-86.

167. Ettenberg SA, Magnifico A, Cuello M, Nau MM, Rubinstein YR, Yarden Y, Weissman AM, Lipkowitz S: **Cbl-b-dependent coordinated degradation of the epidermal growth factor receptor signaling complex**. *J Biol Chem* 2001, **276**(29):27677-27684.

168. Levkowitz G, Waterman H, Zamir E, Kam Z, Oved S, Langdon WY, Beguinot L, Geiger B, Yarden Y: **c-Cbl/Sli-1 regulates endocytic sorting and ubiquitination of the epidermal growth factor receptor**. *Genes Dev* 1998, **12**(23):3663-3674.

169. van Kerkhof P, Govers R, Alves dos Santos CM, Strous GJ: **Endocytosis and degradation of the growth hormone receptor are proteasome-dependent**. *J Biol Chem* 2000, **275**(3):1575-1580.

170. Moriyoshi K, Iijima K, Fujii H, Ito H, Cho Y, Nakanishi S: **Seven in absentia homolog 1A mediates ubiquitination and degradation of group 1 metabotropic glutamate receptors**. *Proc Natl Acad Sci U S A* 2004, **101**(23):8614-8619.

171. Cohen BD, Bariteau JT, Magenis LM, Dias JA: **Regulation of follitropin receptor cell surface residency by the ubiquitin-proteasome pathway**. *Endocrinology* 2003, **144**(10):4393-4402.

172. Strous GJ, van Kerkhof P: **The ubiquitin-proteasome pathway and the regulation of growth hormone receptor availability**. *Mol Cell Endocrinol* 2002, **197**(1-2):143-151.

173. Yu A, Malek TR: **The proteasome regulates receptor-mediated endocytosis of interleukin-2**. *J Biol Chem* 2001, **276**(1):381-385.

174. Li JG, Benovic JL, Liu-Chen LY: **Mechanisms of agonist-induced down-regulation of the human kappa-opioid receptor: internalization is required for down-regulation**. *Mol Pharmacol* 2000, **58**(4):795-801.

175. Dupre DJ, Chen Z, Le Gouill C, Theriault C, Parent JL, Rola-Pleszczynski M, Stankova J: **Trafficking, ubiquitination, and down-regulation of the human platelet-activating factor receptor**. *J Biol Chem* 2003, **278**(48):48228-48235.

176. Shenoy SK, McDonald PH, Kohout TA, Lefkowitz RJ: **Regulation of receptor fate by ubiquitination of activated beta 2-adrenergic receptor and beta-arrestin**. *Science* 2001, **294**(5545):1307-1313.

177. Wallace AD, Cidlowski JA: **Proteasome-mediated glucocorticoid receptor degradation restricts transcriptional signaling by glucocorticoids**. *J Biol Chem* 2001, **276**(46):42714-42721.

178. Nawaz Z, Lonard DM, Dennis AP, Smith CL, O'Malley BW: **Proteasome-dependent degradation of the human estrogen receptor**. *Proc Natl Acad Sci U S A* 1999, **96**(5):1858-1862.

179. Palombella VJ, Rando OJ, Goldberg AL, Maniatis T: **The ubiquitin-proteasome pathway is required for processing the NF-kappa B1 precursor protein and the activation of NF-kappa B**. *Cell* 1994, **78**(5):773-785.

180. Orian A, Schwartz AL, Israel A, Whiteside S, Kahana C, Ciechanover A: **Structural motifs involved in ubiquitin-mediated processing of the NF-kappaB precursor p105: roles of the glycine-rich region and a downstream ubiquitination domain**. *Mol Cell Biol* 1999, **19**(5):3664-3673.

181. Heusch M, Lin L, Geleziunas R, Greene WC: **The generation of nfkb2 p52: mechanism and efficiency**. *Oncogene* 1999, **18**(46):6201-6208.

182. Lin L, Ghosh S: **A glycine-rich region in NF-kappaB p105 functions as a processing signal for the generation of the p50 subunit**. *Mol Cell Biol* 1996, **16**(5):2248-2254.

183. Hochstrasser M, Wang J: **Unraveling the means to the end in ATP-dependent proteases**. *Nat Struct Biol* 2001, **8**(4):294-296.

184. Gillette TG, Huang W, Russell SJ, Reed SH, Johnston SA, Friedberg EC: **The 19S complex of the proteasome regulates nucleotide excision repair in yeast**. *Genes Dev* 2001, **15**(12):1528-1539.

185. McCann TS, Tansey WP: **Functions of the proteasome on chromatin**. *Biomolecules* 2014, **4**(4):1026-1044.

186. Enenkel C: **Proteasome dynamics**. *Biochim Biophys Acta* 2014, **1843**(1):39-46.

187. Palmer A, Rivett AJ, Thomson S, Hendil KB, Butcher GW, Fuertes G, Knecht E: **Subpopulations of proteasomes in rat liver nuclei, microsomes and cytosol**. *Biochem J* 1996, **316 (Pt 2)**:401-407.

188. Geng F, Tansey WP: **Similar temporal and spatial recruitment of native 19S and 20S proteasome subunits to transcriptionally active chromatin**. *Proc Natl Acad Sci U S A* 2012, **109**(16):6060-6065.

189. Gonzalez F, Delahodde A, Kodadek T, Johnston SA: **Recruitment of a 19S proteasome subcomplex to an activated promoter**. *Science* 2002, **296**(5567):548-550.

190. Kitagawa T, Ishii K, Takeda K, Matsumoto T: **The 19S proteasome subunit Rpt3 regulates distribution of CENP-A by associating with centromeric chromatin**. *Nat Commun* 2014, **5**:3597.

191. Krogan NJ, Lam MH, Fillingham J, Keogh MC, Gebbia M, Li J, Datta N, Cagney G, Buratowski S, Emili A *et al*: **Proteasome involvement in the repair of DNA double-strand breaks**. *Mol Cell* 2004, **16**(6):1027-1034.

192. Catic A, Suh CY, Hill CT, Daheron L, Henkel T, Orford KW, Dombkowski DM, Liu T, Liu XS, Scadden DT: **Genome-wide map of nuclear protein degradation shows NCoR1 turnover as a key to mitochondrial gene regulation**. *Cell* 2013, **155**(6):1380-1395.

193. Thomas MK, Yao KM, Tenser MS, Wong GG, Habener JF: **Bridge-1, a novel PDZ-domain coactivator of E2A-mediated regulation of insulin gene transcription**. *Mol Cell Biol* 1999, **19**(12):8492-8504.

194. Lee JH, Volinic JL, Banz C, Yao KM, Thomas MK: **Interactions with p300 enhance transcriptional activation by the PDZ-domain coactivator Bridge-1**. *J Endocrinol* 2005, **187**(2):283-292.

195. Wojcik C, DeMartino GN: **Intracellular localization of proteasomes**. *Int J Biochem Cell Biol* 2003, **35**(5):579-589.

196. Reits EA, Benham AM, Plougastel B, Neefjes J, Trowsdale J: **Dynamics of proteasome distribution in living cells**. *EMBO J* 1997, **16**(20):6087-6094.

197. Enenkel C, Lehmann A, Kloetzel PM: **Subcellular distribution of proteasomes implicates a major location of protein degradation in the nuclear envelope-ER network in yeast**. *EMBO J* 1998, **17**(21):6144-6154.

198. Wang HR, Kania M, Baumeister W, Nederlof PM: **Import of human and Thermoplasma 20S proteasomes into nuclei of HeLa cells requires functional NLS sequences**. *Eur J Cell Biol* 1997, **73**(2):105-113.

199. von Mikecz A: **The nuclear ubiquitin-proteasome system**. *J Cell Sci* 2006, **119**(Pt 10):1977-1984.

200. DeMartino GN, Proske RJ, Moomaw CR, Strong AA, Song X, Hisamatsu H, Tanaka K, Slaughter CA: **Identification, purification, and characterization of a PA700-dependent activator of the proteasome**. *J Biol Chem* 1996, **271**(6):3112-3118.

201. Watanabe TK, Saito A, Suzuki M, Fujiwara T, Takahashi E, Slaughter CA, DeMartino GN, Hendil KB, Chung CH, Tanahashi N *et al*: **cDNA cloning and characterization of a human proteasomal modulator subunit, p27 (PSMD9)**. *Genomics* 1998, **50**(2):241-250.

202. Bohn S, Beck F, Sakata E, Walzthoeni T, Beck M, Aebersold R, Forster F, Baumeister W, Nickell S: **Structure of the 26S proteasome from Schizosaccharomyces pombe at subnanometer resolution**. *Proc Natl Acad Sci U S A* 2010, **107**(49):20992-20997.

203. Sahu I, Sangith N, Ramteke M, Gadre R, Venkatraman P: **A novel role for the proteasomal chaperone PSMD9 and hnRNPA1 in enhancing IkappaBalpha degradation and NF-kappaB activation - functional relevance of predicted PDZ domain-motif interaction**. *FEBS J* 2014, **281**(11):2688-2709.

204. Sangith N, Srinivasaraghavan K, Sahu I, Desai A, Medipally S, Somavarappu AK, Verma C, Venkatraman P: **Discovery of novel interacting partners of PSMD9, a proteasomal chaperone: Role of an Atypical and versatile PDZ-domain motif interaction and identification of putative functional modules**. *FEBS Open Bio* 2014, **4**:571-583.
205. Singh CR, Lovell S, Mehzabeen N, Chowdhury WQ, Geanes ES, Battaile KP, Roelofs J: **1.15 A resolution structure of the proteasome-assembly chaperone Nas2 PDZ domain**. *Acta Crystallogr F Struct Biol Commun* 2014, **70**(Pt 4):418-423.
206. Satoh T, Saeki Y, Hiromoto T, Wang YH, Uekusa Y, Yagi H, Yoshihara H, Yagi-Utsumi M, Mizushima T, Tanaka K *et al*: **Structural basis for proteasome formation controlled by an assembly chaperone nas2**. *Structure* 2014, **22**(5):731-743.
207. Hung AY, Sheng M: **PDZ domains: structural modules for protein complex assembly**. *J Biol Chem* 2002, **277**(8):5699-5702.
208. Lee SY, De la Mota-Peynado A, Roelofs J: **Loss of Rpt5 protein interactions with the core particle and Nas2 protein causes the formation of faulty proteasomes that are inhibited by Ecm29 protein**. *J Biol Chem* 2011, **286**(42):36641-36651.
209. Ward JJ, Sodhi JS, McGuffin LJ, Buxton BF, Jones DT: **Prediction and functional analysis of native disorder in proteins from the three kingdoms of life**. *J Mol Biol* 2004, **337**(3):635-645.
210. Lee HJ, Zheng JJ: **PDZ domains and their binding partners: structure, specificity, and modification**. *Cell Commun Signal* 2010, **8**:8.
211. Pawson T: **Dynamic control of signaling by modular adaptor proteins**. *Curr Opin Cell Biol* 2007, **19**(2):112-116.
212. Kennedy MB: **Origin of PDZ (DHR, GLGF) domains**. *Trends Biochem Sci* 1995, **20**(9):350.
213. Doyle DA, Lee A, Lewis J, Kim E, Sheng M, MacKinnon R: **Crystal structures of a complexed and peptide-free membrane protein-binding domain: molecular basis of peptide recognition by PDZ**. *Cell* 1996, **85**(7):1067-1076.
214. Morais Cabral JH, Petosa C, Sutcliffe MJ, Raza S, Byron O, Poy F, Marfatia SM, Chishti AH, Liddington RC: **Crystal structure of a PDZ domain**. *Nature* 1996, **382**(6592):649-652.
215. Ponting CP: **Evidence for PDZ domains in bacteria, yeast, and plants**. *Protein Sci* 1997, **6**(2):464-468.
216. Spaller MR: **Act globally, think locally: systems biology addresses the PDZ domain**. *ACS Chem Biol* 2006, **1**(4):207-210.
217. Garner CC, Nash J, Huganir RL: **PDZ domains in synapse assembly and signalling**. *Trends Cell Biol* 2000, **10**(7):274-280.

218. Sheng M, Sala C: **PDZ domains and the organization of supramolecular complexes**. *Annu Rev Neurosci* 2001, **24**:1-29.
219. Harris BZ, Lim WA: **Mechanism and role of PDZ domains in signaling complex assembly**. *J Cell Sci* 2001, **114**(Pt 18):3219-3231.
220. Bezprozvanny I, Maximov A: **PDZ domains: More than just a glue**. *Proc Natl Acad Sci U S A* 2001, **98**(3):787-789.
221. Fan JS, Zhang M: **Signaling complex organization by PDZ domain proteins**. *Neurosignals* 2002, **11**(6):315-321.
222. Zhang M, Wang W: **Organization of signaling complexes by PDZ-domain scaffold proteins**. *Acc Chem Res* 2003, **36**(7):530-538.
223. van Ham M, Hendriks W: **PDZ domains-glue and guide**. *Mol Biol Rep* 2003, **30**(2):69-82.
224. Roh MH, Margolis B: **Composition and function of PDZ protein complexes during cell polarization**. *Am J Physiol Renal Physiol* 2003, **285**(3):F377-387.
225. Kim DY, Kim KK: **Structure and function of HtrA family proteins, the key players in protein quality control**. *J Biochem Mol Biol* 2005, **38**(3):266-274.
226. Brone B, Eggermont J: **PDZ proteins retain and regulate membrane transporters in polarized epithelial cell membranes**. *Am J Physiol Cell Physiol* 2005, **288**(1):C20-29.
227. Dev KK: **PDZ domain protein-protein interactions: a case study with PICK1**. *Curr Top Med Chem* 2007, **7**(1):3-20.
228. Petit CM, Zhang J, Sapienza PJ, Fuentes EJ, Lee AL: **Hidden dynamic allostery in a PDZ domain**. *Proc Natl Acad Sci U S A* 2009, **106**(43):18249-18254.
229. Schultz J, Milpetz F, Bork P, Ponting CP: **SMART, a simple modular architecture research tool: identification of signaling domains**. *Proc Natl Acad Sci U S A* 1998, **95**(11):5857-5864.
230. Cho KO, Hunt CA, Kennedy MB: **The rat brain postsynaptic density fraction contains a homolog of the Drosophila discs-large tumor suppressor protein**. *Neuron* 1992, **9**(5):929-942.
231. Kim E, Niethammer M, Rothschild A, Jan YN, Sheng M: **Clustering of Shaker-type K+ channels by interaction with a family of membrane-associated guanylate kinases**. *Nature* 1995, **378**(6552):85-88.
232. Woods DF, Bryant PJ: **ZO-1, DlgA and PSD-95/SAP90: homologous proteins in tight, septate and synaptic cell junctions**. *Mech Dev* 1993, **44**(2-3):85-89.
233. Fanning AS, Anderson JM: **Protein-protein interactions: PDZ domain networks**. *Curr Biol* 1996, **6**(11):1385-1388.
234. Runyon ST, Zhang Y, Appleton BA, Sazinsky SL, Wu P, Pan B, Wiesmann C, Skelton NJ, Sidhu SS: **Structural and functional analysis of the PDZ domains of human HtrA1 and HtrA3**. *Protein Sci* 2007, **16**(11):2454-2471.

235. Saras J, Heldin CH: **PDZ domains bind carboxy-terminal sequences of target proteins**. *Trends Biochem Sci* 1996, **21**(12):455-458.

236. Cowburn D: **Peptide recognition by PTB and PDZ domains**. *Curr Opin Struct Biol* 1997, **7**(6):835-838.

237. Giallourakis C, Cao Z, Green T, Wachtel H, Xie X, Lopez-Illasaca M, Daly M, Rioux J, Xavier R: **A molecular-properties-based approach to understanding PDZ domain proteins and PDZ ligands**. *Genome Res* 2006, **16**(8):1056-1072.

238. Wang NX, Lee HJ, Zheng JJ: **Therapeutic use of PDZ protein-protein interaction antagonism**. *Drug News Perspect* 2008, **21**(3):137-141.

239. Nourry C, Grant SG, Borg JP: **PDZ domain proteins: plug and play!** *Sci STKE* 2003, **2003**(179):RE7.

240. Songyang Z, Fanning AS, Fu C, Xu J, Marfatia SM, Chishti AH, Crompton A, Chan AC, Anderson JM, Cantley LC: **Recognition of unique carboxyl-terminal motifs by distinct PDZ domains**. *Science* 1997, **275**(5296):73-77.

241. Stricker NL, Christopherson KS, Yi BA, Schatz PJ, Raab RW, Dawes G, Bassett DE, Jr., Bredt DS, Li M: **PDZ domain of neuronal nitric oxide synthase recognizes novel C-terminal peptide sequences**. *Nat Biotechnol* 1997, **15**(4):336-342.

242. Laskowski RA, Chistyakov VV, Thornton JM: **PDBsum more: new summaries and analyses of the known 3D structures of proteins and nucleic acids**. *Nucleic Acids Res* 2005, **33**(Database issue):D266-268.

243. Kaneko T, Hamazaki J, Iemura S, Sasaki K, Furuyama K, Natsume T, Tanaka K, Murata S: **Assembly pathway of the Mammalian proteasome base subcomplex is mediated by multiple specific chaperones**. *Cell* 2009, **137**(5):914-925.

244. Funakoshi M, Tomko RJ, Jr., Kobayashi H, Hochstrasser M: **Multiple assembly chaperones govern biogenesis of the proteasome regulatory particle base**. *Cell* 2009, **137**(5):887-899.

245. Park S, Tian G, Roelofs J, Finley D: **Assembly manual for the proteasome regulatory particle: the first draft**. *Biochem Soc Trans* 2010, **38**(Pt 1):6-13.

246. Stanojevic V, Yao KM, Thomas MK: **The coactivator Bridge-1 increases transcriptional activation by pancreas duodenum homeobox-1 (PDX-1)**. *Mol Cell Endocrinol* 2005, **237**(1-2):67-74.

247. Banz C, Munchow B, Diedrich K: **Bridge-1 is expressed in human granulosa cells and is involved in the activin A signaling cascade**. *Fertil Steril* 2010, **93**(4):1349-1352.

248. Volinic JL, Lee JH, Eto K, Kaur V, Thomas MK: **Overexpression of the coactivator bridge-1 results in insulin deficiency and diabetes**. *Mol Endocrinol* 2006, **20**(1):167-182.

249. Thomas MK, Tsang SW, Yeung ML, Leung PS, Yao KM: **The roles of the PDZ-containing proteins bridge-1 and PDZD2 in the regulation of insulin production and pancreatic beta-cell mass**. *Curr Protein Pept Sci* 2009, **10**(1):30-36.

250. Godbole D, Mojamdar M, Pal JK: **Increased level of p27 subunit of proteasomes and its co-localization with tyrosinase in amelanotic melanoma cells indicate its direct role in the regulation of melanin biosynthesis**. *Cell Biol Int* 2006, **30**(11):895-902.

251. Banz-Jansen C, Munchow B, Diedrich K, Finas D: **Bridge-1 is expressed in human breast carcinomas: silencing of Bridge-1 decreases Smad2, Smad3 and Smad4 expression in MCF-7 cells, a human breast cancer cell line**. *Arch Gynecol Obstet* 2011, **284**(6):1543-1549.

252. Langlands FE, Dodwell D, Hanby AM, Horgan K, Millican-Slater RA, Speirs V, Verghese ET, Smith L, Hughes TA: **PSMD9 expression predicts radiotherapy response in breast cancer**. *Mol Cancer* 2014, **13**:73.

253. Hayden MS, Ghosh S: **Shared principles in NF-kappaB signaling**. *Cell* 2008, **132**(3):344-362.

254. Li H, Lin X: **Positive and negative signaling components involved in TNFalpha-induced NF-kappaB activation**. *Cytokine* 2008, **41**(1):1-8.

255. Sen R, Baltimore D: **Multiple nuclear factors interact with the immunoglobulin enhancer sequences**. *Cell* 1986, **46**(5):705-716.

256. Ghosh S, May MJ, Kopp EB: **NF-kappa B and Rel proteins: evolutionarily conserved mediators of immune responses**. *Annu Rev Immunol* 1998, **16**:225-260.

257. Karin M, Ben-Neriah Y: **Phosphorylation meets ubiquitination: the control of NF-[kappa]B activity**. *Annu Rev Immunol* 2000, **18**:621-663.

258. Grilli M, Chiu JJ, Lenardo MJ: **NF-kappa B and Rel: participants in a multiform transcriptional regulatory system**. *Int Rev Cytol* 1993, **143**:1-62.

259. Plaksin D, Baeuerle PA, Eisenbach L: **KBF1 (p50 NF-kappa B homodimer) acts as a repressor of H-2Kb gene expression in metastatic tumor cells**. *J Exp Med* 1993, **177**(6):1651-1662.

260. Guan H, Hou S, Ricciardi RP: **DNA binding of repressor nuclear factor-kappaB p50/p50 depends on phosphorylation of Ser337 by the protein kinase A catalytic subunit**. *J Biol Chem* 2005, **280**(11):9957-9962.

261. Hoffmann A, Levchenko A, Scott ML, Baltimore D: **The IkappaB-NF-kappaB signaling module: temporal control and selective gene activation**. *Science* 2002, **298**(5596):1241-1245.

262. Cohen S, Achbert-Weiner H, Ciechanover A: **Dual effects of IkappaB kinase beta-mediated phosphorylation on p105 Fate: SCF(beta-TrCP)-dependent degradation and SCF(beta-TrCP)-independent processing**. *Mol Cell Biol* 2004, **24**(1):475-486.

263. Liang C, Zhang M, Sun SC: **beta-TrCP binding and processing of NF-kappaB2/p100 involve its phosphorylation at serines 866 and 870**. *Cell Signal* 2006, **18**(8):1309-1317.

264. Moorthy AK, Savinova OV, Ho JQ, Wang VY, Vu D, Ghosh G: **The 20S proteasome processes NF-kappaB1 p105 into p50 in a translation-independent manner**. *EMBO J* 2006, **25**(9):1945-1956.

265. Baeuerle PA, Baltimore D: **I kappa B: a specific inhibitor of the NF-kappa B transcription factor**. *Science* 1988, **242**(4878):540-546.

266. Beg AA, Baldwin AS, Jr.: **The I kappa B proteins: multifunctional regulators of Rel/NF-kappa B transcription factors**. *Genes Dev* 1993, **7**(11):2064-2070.

267. Chen Z, Hagler J, Palombella VJ, Melandri F, Scherer D, Ballard D, Maniatis T: **Signal-induced site-specific phosphorylation targets I kappa B alpha to the ubiquitin-proteasome pathway**. *Genes Dev* 1995, **9**(13):1586-1597.

268. Li N, Karin M: **Ionizing radiation and short wavelength UV activate NF-kappaB through two distinct mechanisms**. *Proc Natl Acad Sci U S A* 1998, **95**(22):13012-13017.

269. Mukhopadhyay A, Manna SK, Aggarwal BB: **Pervanadate-induced nuclear factor-kappaB activation requires tyrosine phosphorylation and degradation of IkappaBalpha. Comparison with tumor necrosis factor-alpha**. *J Biol Chem* 2000, **275**(12):8549-8555.

270. Hayden MS, Ghosh S: **Signaling to NF-kappaB**. *Genes Dev* 2004, **18**(18):2195-2224.

271. Alkalay I, Yaron A, Hatzubai A, Orian A, Ciechanover A, Ben-Neriah Y: **Stimulation-dependent I kappa B alpha phosphorylation marks the NF-kappa B inhibitor for degradation via the ubiquitin-proteasome pathway**. *Proc Natl Acad Sci U S A* 1995, **92**(23):10599-10603.

272. Tanaka K, Kawakami T, Tateishi K, Yashiroda H, Chiba T: **Control of IkappaBalpha proteolysis by the ubiquitin-proteasome pathway**. *Biochimie* 2001, **83**(3-4):351-356.

273. Hoffmann A, Baltimore D: **Circuitry of nuclear factor kappaB signaling**. *Immunol Rev* 2006, **210**:171-186.

274. Miyamoto S, Seufzer BJ, Shumway SD: **Novel IkappaB alpha proteolytic pathway in WEHI231 immature B cells**. *Mol Cell Biol* 1998, **18**(1):19-29.

275. Shumway SD, Berchtold CM, Gould MN, Miyamoto S: **Evidence for unique calmodulin-dependent nuclear factor-kappaB regulation in WEHI-231 B cells**. *Mol Pharmacol* 2002, **61**(1):177-185.

276. Shumway SD, Miyamoto S: **A mechanistic insight into a proteasome-independent constitutive inhibitor kappaBalpha (IkappaBalpha) degradation and nuclear factor kappaB (NF-kappaB) activation pathway in WEHI-231 B-cells**. *Biochem J* 2004, **380**(Pt 1):173-180.

277. Ponnappan S, Cullen SJ, Ponnappan U: **Constitutive degradation of IkappaBalpha in human T lymphocytes is mediated by calpain**. *Immun Ageing* 2005, **2**:15.

278. Bonizzi G, Karin M: **The two NF-kappaB activation pathways and their role in innate and adaptive immunity**. *Trends Immunol* 2004, **25**(6):280-288.

279. Bonizzi G, Bebien M, Otero DC, Johnson-Vroom KE, Cao Y, Vu D, Jegga AG, Aronow BJ, Ghosh G, Rickert RC *et al*: **Activation of IKKalpha target genes depends on recognition of specific kappaB binding sites by RelB:p52 dimers**. *EMBO J* 2004, **23**(21):4202-4210.

280. Basak S, Shih VF, Hoffmann A: **Generation and activation of multiple dimeric transcription factors within the NF-kappaB signaling system**. *Mol Cell Biol* 2008, **28**(10):3139-3150.

281. Lin L, DeMartino GN, Greene WC: **Cotranslational biogenesis of NF-kappaB p50 by the 26S proteasome**. *Cell* 1998, **92**(6):819-828.

282. Rape M, Jentsch S: **Productive RUPture: activation of transcription factors by proteasomal processing**. *Biochim Biophys Acta* 2004, **1695**(1-3):209-213.

283. Piwko W, Jentsch S: **Proteasome-mediated protein processing by bidirectional degradation initiated from an internal site**. *Nat Struct Mol Biol* 2006, **13**(8):691-697.

284. Govind S: **Control of development and immunity by rel transcription factors in Drosophila**. *Oncogene* 1999, **18**(49):6875-6887.

285. Gerondakis S, Grossmann M, Nakamura Y, Pohl T, Grumont R: **Genetic approaches in mice to understand Rel/NF-kappaB and IkappaB function: transgenics and knockouts**. *Oncogene* 1999, **18**(49):6888-6895.

286. Pahl HL: **Activators and target genes of Rel/NF-kappaB transcription factors**. *Oncogene* 1999, **18**(49):6853-6866.

287. Perkins ND: **NF-kappaB: tumor promoter or suppressor?** *Trends Cell Biol* 2004, **14**(2):64-69.

288. Perkins ND: **Achieving transcriptional specificity with NF-kappa B**. *Int J Biochem Cell Biol* 1997, **29**(12):1433-1448.

289. Barkett M, Gilmore TD: **Control of apoptosis by Rel/NF-kappaB transcription factors**. *Oncogene* 1999, **18**(49):6910-6924.

290. Deng J, Miller SA, Wang HY, Xia W, Wen Y, Zhou BP, Li Y, Lin SY, Hung MC: **beta-catenin interacts with and inhibits NF-kappa B in human colon and breast cancer**. *Cancer Cell* 2002, **2**(4):323-334.

291. Gilmore TD, Herscovitch M: **Inhibitors of NF-kappaB signaling: 785 and counting**. *Oncogene* 2006, **25**(51):6887-6899.

292. Perkins ND, Gilmore TD: **Good cop, bad cop: the different faces of NF-kappaB**. *Cell Death Differ* 2006, **13**(5):759-772.

293. Garg A, Aggarwal BB: **Nuclear transcription factor-kappaB as a target for cancer drug development**. *Leukemia* 2002, **16**(6):1053-1068.

294. Baldwin AS: **Control of oncogenesis and cancer therapy resistance by the transcription factor NF-kappaB**. *J Clin Invest* 2001, **107**(3):241-246.

295. Hanahan D, Weinberg RA: **The hallmarks of cancer**. *Cell* 2000, **100**(1):57-70.

296. Rocha S, Martin AM, Meek DW, Perkins ND: **p53 represses cyclin D1 transcription through down regulation of Bcl-3 and inducing increased association of the p52 NF-kappaB subunit with histone deacetylase 1**. *Mol Cell Biol* 2003, **23**(13):4713-4727.

297. Rocha S, Campbell KJ, Perkins ND: **p53- and Mdm2-independent repression of NF-kappa B transactivation by the ARF tumor suppressor**. *Mol Cell* 2003, **12**(1):15-25.

298. Ren S, Uversky VN, Chen Z, Dunker AK, Obradovic Z: **Short Linear Motifs recognized by SH2, SH3 and Ser/Thr Kinase domains are conserved in disordered protein regions**. *BMC Genomics* 2008, **9 Suppl 2**:S26.

299. Nanaware PP, Ramteke MP, Somavarapu AK, Venkatraman P: **Discovery of multiple interacting partners of gankyrin, a proteasomal chaperone and an oncoprotein-Evidence for a common hot spot site at the interface and its functional relevance**. *Proteins* 2013.

300. Hay DC, Kemp GD, Dargemont C, Hay RT: **Interaction between hnRNPA1 and IkappaBalpha is required for maximal activation of NF-kappaB-dependent transcription**. *Mol Cell Biol* 2001, **21**(10):3482-3490.

301. Dreyfuss G, Matunis MJ, Pinol-Roma S, Burd CG: **hnRNP proteins and the biogenesis of mRNA**. *Annu Rev Biochem* 1993, **62**:289-321.

302. Miyamoto S, Maki M, Schmitt MJ, Hatanaka M, Verma IM: **Tumor necrosis factor alpha-induced phosphorylation of I kappa B alpha is a signal for its degradation but not dissociation from NF-kappa B**. *Proc Natl Acad Sci U S A* 1994, **91**(26):12740-12744.

303. Reigstad CS, Lunden GO, Felin J, Backhed F: **Regulation of serum amyloid A3 (SAA3) in mouse colonic epithelium and adipose tissue by the intestinal microbiota**. *PLoS One* 2009, **4**(6):e5842.

304. Zhou A, Scoggin S, Gaynor RB, Williams NS: **Identification of NF-kappa B-regulated genes induced by TNFalpha utilizing expression profiling and RNA interference**. *Oncogene* 2003, **22**(13):2054-2064.

305. Shim SM, Lee WJ, Kim Y, Chang JW, Song S, Jung YK: **Role of S5b/PSMD5 in proteasome inhibition caused by TNF-alpha/NFkappaB in higher eukaryotes**. *Cell Rep* 2012, **2**(3):603-615.

306. Ferrell K, Wilkinson CR, Dubiel W, Gordon C: **Regulatory subunit interactions of the 26S proteasome, a complex problem**. *Trends Biochem Sci* 2000, **25**(2):83-88.

307. Chen C, Huang C, Chen S, Liang J, Lin W, Ke G, Zhang H, Wang B, Huang J, Han Z *et al*: **Subunit-subunit interactions in the human 26S proteasome**. *Proteomics* 2008, **8**(3):508-520.

308. da Fonseca PC, He J, Morris EP: **Molecular model of the human 26S proteasome**. *Mol Cell* 2012, **46**(1):54-66.

309. Su V, Lau AF: **Ubiquitin-like and ubiquitin-associated domain proteins: significance in proteasomal degradation**. *Cell Mol Life Sci* 2009, **66**(17):2819-2833.

310. Babu JR, Geetha T, Wooten MW: **Sequestosome 1/p62 shuttles polyubiquitinated tau for proteasomal degradation**. *J Neurochem* 2005, **94**(1):192-203.

311. Parcellier A, Schmitt E, Gurbuxani S, Seigneurin-Berny D, Pance A, Chantome A, Plenchette S, Khochbin S, Solary E, Garrido C: **HSP27 is a ubiquitin-binding protein involved in I-kappaBalpha proteasomal degradation**. *Mol Cell Biol* 2003, **23**(16):5790-5802.

312. Dolcet X, Llobet D, Pallares J, Matias-Guiu X: **NF-kB in development and progression of human cancer**. *Virchows Arch* 2005, **446**(5):475-482.

313. Ravi R, Bedi A: **NF-kappaB in cancer--a friend turned foe**. *Drug Resist Updat* 2004, **7**(1):53-67.

314. Hori T, Kato S, Saeki M, DeMartino GN, Slaughter CA, Takeuchi J, Toh-e A, Tanaka K: **cDNA cloning and functional analysis of p28 (Nas6p) and p40.5 (Nas7p), two novel regulatory subunits of the 26S proteasome**. *Gene* 1998, **216**(1):113-122.

315. Higashitsuji H, Itoh K, Nagao T, Dawson S, Nonoguchi K, Kido T, Mayer RJ, Arii S, Fujita J: **Reduced stability of retinoblastoma protein by gankyrin, an oncogenic ankyrin-repeat protein overexpressed in hepatomas**. *Nat Med* 2000, **6**(1):96-99.

316. Bedford L, Paine S, Sheppard PW, Mayer RJ, Roelofs J: **Assembly, structure, and function of the 26S proteasome**. *Trends Cell Biol* 2010, **20**(7):391-401.

317. Roelofs J, Park S, Haas W, Tian G, McAllister FE, Huo Y, Lee BH, Zhang F, Shi Y, Gygi SP *et al*: **Chaperone-mediated pathway of proteasome regulatory particle assembly**. *Nature* 2009, **459**(7248):861-865.

318. Nakamura Y, Umehara T, Tanaka A, Horikoshi M, Padmanabhan B, Yokoyama S: **Structural basis for the recognition between the regulatory particles Nas6 and Rpt3 of the yeast 26S proteasome**. *Biochem Biophys Res Commun* 2007, **359**(3):503-509.

319. Dawson S, Apcher S, Mee M, Higashitsuji H, Baker R, Uhle S, Dubiel W, Fujita J, Mayer RJ: **Gankyrin is an ankyrin-repeat oncoprotein that interacts with CDK4 kinase and the S6 ATPase of the 26 S proteasome**. *J Biol Chem* 2002, **277**(13):10893-10902.

320. Padmanabhan B, Adachi N, Kataoka K, Horikoshi M: **Crystal structure of the homolog of the oncoprotein gankyrin, an interactor of Rb and CDK4/6**. *J Biol Chem* 2004, **279**(2):1546-1552.

321. Adachi N, Padmanabhan B, Kataoka K, Kijima K, Yamaki M, Horikoshi M: **Purification, crystallization and preliminary X-ray diffraction analysis of yeast regulatory particle non-ATPase subunit 6 (Nas6p)**. *Acta Crystallogr D Biol Crystallogr* 2002, **58**(Pt 5):859-860.

322. Krzywda S, Brzozowski AM, Al-Safty R, Welchman R, Mee M, Dawson S, Fujita J, Higashitsuji H, Mayer RJ, Wilkinson AJ: **Crystallization of gankyrin, an oncoprotein that interacts with CDK4 and the S6b (rpt3) ATPase of the 19S regulator of the 26S proteasome**. *Acta Crystallogr D Biol Crystallogr* 2003, **59**(Pt 7):1294-1295.

323. Krzywda S, Brzozowski AM, Higashitsuji H, Fujita J, Welchman R, Dawson S, Mayer RJ, Wilkinson AJ: **The crystal structure of gankyrin, an oncoprotein found in complexes with cyclin-dependent kinase 4, a 19 S proteasomal ATPase regulator, and the tumor suppressors Rb and p53**. *J Biol Chem* 2004, **279**(2):1541-1545.

324. Manjasetty BA, Quedenau C, Sievert V, Bussow K, Niesen F, Delbruck H, Heinemann U: **X-ray structure of human gankyrin, the product of a gene linked to hepatocellular carcinoma**. *Proteins* 2004, **55**(1):214-217.

325. Yuan C, Li J, Mahajan A, Poi MJ, Byeon IJ, Tsai MD: **Solution structure of the human oncogenic protein gankyrin containing seven ankyrin repeats and analysis of its structure--function relationship**. *Biochemistry* 2004, **43**(38):12152-12161.

326. Nakamura Y, Umehara T, Tanaka A, Horikoshi M, Padmanabhan B, Yokoyama S: **Purification, crystallization and preliminary X-ray diffraction analysis of the non-ATPase subunit Nas6 in complex with the ATPase subunit Rpt3 of the 26S proteasome from Saccharomyces cerevisiae**. *Acta Crystallogr Sect F Struct Biol Cryst Commun* 2007, **63**(Pt 3):190-192.

327. Nakamura Y, Nakano K, Umehara T, Kimura M, Hayashizaki Y, Tanaka A, Horikoshi M, Padmanabhan B, Yokoyama S: **Structure of the oncoprotein gankyrin in complex with S6 ATPase of the 26S proteasome**. *Structure* 2007, **15**(2):179-189.

328. Mosavi LK, Cammett TJ, Desrosiers DC, Peng ZY: **The ankyrin repeat as molecular architecture for protein recognition**. *Protein Sci* 2004, **13**(6):1435-1448.

329. Li J, Mahajan A, Tsai MD: **Ankyrin repeat: a unique motif mediating protein-protein interactions**. *Biochemistry* 2006, **45**(51):15168-15178.

330. Sedgwick SG, Smerdon SJ: **The ankyrin repeat: a diversity of interactions on a common structural framework**. *Trends Biochem Sci* 1999, **24**(8):311-316.

331. Michaely P, Tomchick DR, Machius M, Anderson RG: **Crystal structure of a 12 ANK repeat stack from human ankyrinR**. *EMBO J* 2002, **21**(23):6387-6396.

332. Higashitsuji H, Itoh K, Sakurai T, Nagao T, Sumitomo Y, Masuda T, Dawson S, Shimada Y, Mayer RJ, Fujita J: **The oncoprotein gankyrin binds to MDM2/HDM2, enhancing ubiquitylation and degradation of p53**. *Cancer Cell* 2005, **8**(1):75-87.

333. Li J, Tsai MD: **Novel insights into the INK4-CDK4/6-Rb pathway: counter action of gankyrin against INK4 proteins regulates the CDK4-mediated phosphorylation of Rb**. *Biochemistry* 2002, **41**(12):3977-3983.

334. Chen Y, Li HH, Fu J, Wang XF, Ren YB, Dong LW, Tang SH, Liu SQ, Wu MC, Wang HY: **Oncoprotein p28 GANK binds to RelA and retains NF-kappaB in the cytoplasm through nuclear export**. *Cell Res* 2007, **17**(12):1020-1029.

335. Nagao T, Higashitsuji H, Nonoguchi K, Sakurai T, Dawson S, Mayer RJ, Itoh K, Fujita J: **MAGE-A4 interacts with the liver oncoprotein gankyrin and suppresses its tumorigenic activity**. *J Biol Chem* 2003, **278**(12):10668-10674.

336. Man JH, Liang B, Gu YX, Zhou T, Li AL, Li T, Jin BF, Bai B, Zhang HY, Zhang WN *et al*: **Gankyrin plays an essential role in Ras-induced tumorigenesis through regulation of the RhoA/ROCK pathway in mammalian cells**. *J Clin Invest* 2010, **120**(8):2829-2841.

337. Nanaware PP, Ramteke MP, Somavarapu AK, Venkatraman P: **Discovery of multiple interacting partners of gankyrin, a proteasomal chaperone and an oncoprotein--evidence for a common hot spot site at the interface and its functional relevance**. *Proteins* 2014, **82**(7):1283-1300.

338. Dawson S, Higashitsuji H, Wilkinson AJ, Fujita J, Mayer RJ: **Gankyrin: a new oncoprotein and regulator of pRb and p53**. *Trends Cell Biol* 2006, **16**(5):229-233.

339. Higashitsuji H, Liu Y, Mayer RJ, Fujita J: **The oncoprotein gankyrin negatively regulates both p53 and RB by enhancing proteasomal degradation**. *Cell Cycle* 2005, **4**(10):1335-1337.

340. Qiu W, Wu J, Walsh EM, Zhang Y, Chen CY, Fujita J, Xiao ZX: **Retinoblastoma protein modulates gankyrin-MDM2 in regulation of p53 stability and chemosensitivity in cancer cells**. *Oncogene* 2008, **27**(29):4034-4043.

341. Lee JO, Russo AA, Pavletich NP: **Structure of the retinoblastoma tumour-suppressor pocket domain bound to a peptide from HPV E7**. *Nature* 1998, **391**(6670):859-865.

342. Ikeda MA, Nevins JR: **Identification of distinct roles for separate E1A domains in disruption of E2F complexes**. *Mol Cell Biol* 1993, **13**(11):7029-7035.

343. Higashitsuji H, Liu Y, Masuda T, Fujita T, Abdel-Aziz HI, Kongkham S, Dawson S, John Mayer R, Itoh Y, Sakurai T *et al*: **The oncoprotein gankyrin interacts with RelA and suppresses NF-kappaB activity**. *Biochem Biophys Res Commun* 2007, **363**(3):879-884.

344. Ortiz CM, Ito T, Tanaka E, Tsunoda S, Nagayama S, Sakai Y, Higashitsuji H, Fujita J, Shimada Y: **Gankyrin oncoprotein overexpression as a critical factor for tumor growth in human esophageal squamous cell carcinoma and its clinical significance**. *Int J Cancer* 2008, **122**(2):325-332.

345. Meng Y, He L, Guo X, Tang S, Zhao X, Du R, Jin J, Bi Q, Li H, Nie Y *et al*: **Gankyrin promotes the proliferation of human pancreatic cancer**. *Cancer Lett* 2010, **297**(1):9-17.

346. Tang S, Yang G, Meng Y, Du R, Li X, Fan R, Zhao L, Bi Q, Jin J, Gao L *et al*: **Overexpression of a novel gene gankyrin correlates with the malignant phenotype of colorectal cancer**. *Cancer Biol Ther* 2010, **9**(2):88-95.

347. Liu Y, Zhang J, Qian W, Dong Y, Yang Y, Liu Z, Feng Y, Ma D, Zhang Z, Wu S: **Gankyrin is frequently overexpressed in cervical high grade disease and is associated with cervical carcinogenesis and metastasis**. *PLoS One* 2014, **9**(4):e95043.

348. Hwang JA, Yang HM, Hong DP, Joo SY, Choi YL, Park JH, Lazar AJ, Pollock RE, Lev D, Kim SJ: **Gankyrin is a predictive and oncogenic factor in well-differentiated and dedifferentiated liposarcoma**. *Oncotarget* 2014, **5**(19):9065-9078.

349. Kim KH, Lim HJ, Kim YJ, Kim SW, Kim YS, Tian C, Park K, Park TJ, Choung YH: **The oncoprotein, gankyrin, is up-regulated in middle ear cholesteatoma**. *Acta Otolaryngol* 2014, **134**(3):238-243.

350. Ando S, Matsuoka T, Kawai K, Sugita S, Joraku A, Kojima T, Suetomi T, Miyazaki J, Fujita J, Nishiyama H: **Expression of the oncoprotein gankyrin and phosphorylated retinoblastoma protein in human testis and testicular germ cell tumor**. *Int J Urol* 2014, **21**(10):992-998.

351. Kim YH, Kim JH, Choi YW, Lim SK, Yim H, Kang SY, Chung YS, Lee GY, Park TJ: **Gankyrin is frequently overexpressed in breast cancer and is associated with ErbB2 expression**. *Exp Mol Pathol* 2013, **94**(2):360-365.

352. Yang Y, Zhang C, Li L, Gao Y, Luo X, Zhang Y, Liu W, Fei Z: **Up-regulated oncoprotein P28GANK correlates with proliferation and poor prognosis of human glioma**. *World J Surg Oncol* 2012, **10**:169.

353. Fu J, Chen Y, Cao J, Luo T, Qian YW, Yang W, Ren YB, Su B, Cao GW, Yang Y *et al*: **p28GANK overexpression accelerates hepatocellular carcinoma invasiveness and metastasis via phosphoinositol 3-kinase/AKT/hypoxia-inducible factor-1alpha pathways**. *Hepatology* 2011, **53**(1):181-192.

354. Zhen C, Chen L, Zhao Q, Liang B, Gu YX, Bai ZF, Wang K, Xu X, Han QY, Fang DF *et al*: **Gankyrin promotes breast cancer cell metastasis by regulating Rac1 activity**. *Oncogene* 2013, **32**(29):3452-3460.

355. Bai Z, Tai Y, Li W, Zhen C, Gu W, Jian Z, Wang Q, Lin JE, Zhao Q, Gong W *et al*: **Gankyrin activates IL-8 to promote hepatic metastasis of colorectal cancer**. *Cancer Res* 2013, **73**(14):4548-4558.

356. Zhang J, Yang Y, Zhang Z, He Y, Liu Z, Yu Y, Wu S, Cai B, Feng Y: **Gankyrin plays an essential role in estrogen-driven and GPR30-mediated endometrial carcinoma cell proliferation via the PTEN/PI3K/AKT signaling pathway**. *Cancer Lett* 2013, **339**(2):279-287.

357. Zheng T, Hong X, Wang J, Pei T, Liang Y, Yin D, Song R, Song X, Lu Z, Qi S *et al*: **Gankyrin promotes tumor growth and metastasis through activation of IL-6/STAT3 signaling in human cholangiocarcinoma**. *Hepatology* 2014, **59**(3):935-946.

358. Dong LW, Yang GZ, Pan YF, Chen Y, Tan YX, Dai RY, Ren YB, Fu J, Wang HY: **The oncoprotein p28GANK establishes a positive feedback loop in beta-catenin signaling**. *Cell Res* 2011, **21**(8):1248-1261.

359. Merkle FT, Alvarez-Buylla A: **Neural stem cells in mammalian development**. *Curr Opin Cell Biol* 2006, **18**(6):704-709.

360. Gage FH: **Mammalian neural stem cells**. *Science* 2000, **287**(5457):1433-1438.

361. Wen S, Li H, Liu J: **Dynamic signaling for neural stem cell fate determination**. *Cell Adh Migr* 2009, **3**(1):107-117.

362. Bogler O, Wren D, Barnett SC, Land H, Noble M: **Cooperation between two growth factors promotes extended self-renewal and inhibits differentiation of oligodendrocyte-type-2 astrocyte (O-2A) progenitor cells**. *Proc Natl Acad Sci U S A* 1990, **87**(16):6368-6372.

363. Vescovi AL, Reynolds BA, Fraser DD, Weiss S: **bFGF regulates the proliferative fate of unipotent (neuronal) and bipotent (neuronal/astroglial) EGF-generated CNS progenitor cells**. *Neuron* 1993, **11**(5):951-966.

364. Ray J, Gage FH: **Spinal cord neuroblasts proliferate in response to basic fibroblast growth factor**. *J Neurosci* 1994, **14**(6):3548-3564.

365. Reynolds BA, Weiss S: **Generation of neurons and astrocytes from isolated cells of the adult mammalian central nervous system**. *Science* 1992, **255**(5052):1707-1710.

366. Reynolds BA, Tetzlaff W, Weiss S: **A multipotent EGF-responsive striatal embryonic progenitor cell produces neurons and astrocytes**. *J Neurosci* 1992, **12**(11):4565-4574.

367. Reynolds BA, Weiss S: **Clonal and population analyses demonstrate that an EGF-responsive mammalian embryonic CNS precursor is a stem cell**. *Dev Biol* 1996, **175**(1):1-13.

368. Morshead CM, Reynolds BA, Craig CG, McBurney MW, Staines WA, Morassutti D, Weiss S, van der Kooy D: **Neural stem cells in the adult mammalian forebrain: a relatively quiescent subpopulation of subependymal cells**. *Neuron* 1994, **13**(5):1071-1082.

369. Yan Y, Yang D, Zarnowska ED, Du Z, Werbel B, Valliere C, Pearce RA, Thomson JA, Zhang SC: **Directed differentiation of dopaminergic neuronal subtypes from human embryonic stem cells**. *Stem Cells* 2005, **23**(6):781-790.

370. Liem KF, Jr., Tremml G, Roelink H, Jessell TM: **Dorsal differentiation of neural plate cells induced by BMP-mediated signals from epidermal ectoderm**. *Cell* 1995, **82**(6):969-979.

371. Li XJ, Zhang X, Johnson MA, Wang ZB, Lavaute T, Zhang SC: **Coordination of sonic hedgehog and Wnt signaling determines ventral and dorsal telencephalic neuron types from human embryonic stem cells**. *Development* 2009, **136**(23):4055-4063.

372. Ye W, Shimamura K, Rubenstein JL, Hynes MA, Rosenthal A: **FGF and Shh signals control dopaminergic and serotonergic cell fate in the anterior neural plate**. *Cell* 1998, **93**(5):755-766.

373. Kim JE, O'Sullivan ML, Sanchez CA, Hwang M, Israel MA, Brennand K, Deerinck TJ, Goldstein LS, Gage FH, Ellisman MH *et al*: **Investigating synapse formation and function using human pluripotent stem cell-derived neurons**. *Proc Natl Acad Sci U S A* 2011, **108**(7):3005-3010.

374. Li XJ, Du ZW, Zarnowska ED, Pankratz M, Hansen LO, Pearce RA, Zhang SC: **Specification of motoneurons from human embryonic stem cells**. *Nat Biotechnol* 2005, **23**(2):215-221.

375. Fasano CA, Chambers SM, Lee G, Tomishima MJ, Studer L: **Efficient derivation of functional floor plate tissue from human embryonic stem cells**. *Cell Stem Cell* 2010, **6**(4):336-347.

376. Seaberg RM, van der Kooy D: **Adult rodent neurogenic regions: the ventricular subependyma contains neural stem cells, but the dentate gyrus contains restricted progenitors**. *J Neurosci* 2002, **22(**5):1784-1793.

377. Tropepe V, Sibilia M, Ciruna BG, Rossant J, Wagner EF, van der Kooy D: **Distinct neural stem cells proliferate in response to EGF and FGF in the developing mouse telencephalon**. *Dev Biol* 1999, **208**(1):166-188.

378. Tropepe V, Hitoshi S, Sirard C, Mak TW, Rossant J, van der Kooy D: **Direct neural fate specification from embryonic stem cells: a primitive mammalian neural stem cell stage acquired through a default mechanism**. *Neuron* 2001, **30**(1):65-78.

379. Conti L, Pollard SM, Gorba T, Reitano E, Toselli M, Biella G, Sun Y, Sanzone S, Ying QL, Cattaneo E *et al*: **Niche-independent symmetrical self-renewal of a mammalian tissue stem cell**. *PLoS Biol* 2005, **3**(9):e283.

380. Pollard SM, Wallbank R, Tomlinson S, Grotewold L, Smith A: **Fibroblast growth factor induces a neural stem cell phenotype in foetal forebrain progenitors and during embryonic stem cell differentiation**. *Mol Cell Neurosci* 2008, **38**(3):393-403.

381. Sun Y, Pollard S, Conti L, Toselli M, Biella G, Parkin G, Willatt L, Falk A, Cattaneo E, Smith A: **Long-term tripotent differentiation capacity of human neural stem (NS) cells in adherent culture**. *Mol Cell Neurosci* 2008, **38**(2):245-258.

382. Pollard SM, Conti L, Sun Y, Goffredo D, Smith A: **Adherent neural stem (NS) cells from fetal and adult forebrain**. *Cereb Cortex* 2006, **16 Suppl 1**:i112-120.

383. Pollard SM, Yoshikawa K, Clarke ID, Danovi D, Stricker S, Russell R, Bayani J, Head R, Lee M, Bernstein M *et al*: **Glioma stem cell lines expanded in adherent culture have tumor-specific phenotypes and are suitable for chemical and genetic screens**. *Cell Stem Cell* 2009, **4**(6):568-580.
384. Reynolds BA, Vescovi AL: **Brain cancer stem cells: Think twice before going flat**. *Cell Stem Cell* 2009, **5**(5):466-467; author reply 468-469.
385. Temple S: **The development of neural stem cells**. *Nature* 2001, **414**(6859):112-117.
386. Kriegstein A, Alvarez-Buylla A: **The glial nature of embryonic and adult neural stem cells**. *Annu Rev Neurosci* 2009, **32**:149-184.
387. Ma DK, Kim WR, Ming GL, Song H: **Activity-dependent extrinsic regulation of adult olfactory bulb and hippocampal neurogenesis**. *Ann N Y Acad Sci* 2009, **1170**:664-673.
388. Alvarez-Buylla A, Lim DA: **For the long run: maintaining germinal niches in the adult brain**. *Neuron* 2004, **41**(5):683-686.
389. Ma DK, Ming GL, Song H: **Glial influences on neural stem cell development: cellular niches for adult neurogenesis**. *Curr Opin Neurobiol* 2005, **15**(5):514-520.
390. Song H, Stevens CF, Gage FH: **Astroglia induce neurogenesis from adult neural stem cells**. *Nature* 2002, **417**(6884):39-44.
391. Faigle R, Song H: **Signaling mechanisms regulating adult neural stem cells and neurogenesis**. *Biochim Biophys Acta* 2013, **1830**(2):2435-2448.
392. Hirabayashi Y, Gotoh Y: **Stage-dependent fate determination of neural precursor cells in mouse forebrain**. *Neurosci Res* 2005, **51**(4):331-336.
393. Israsena N, Hu M, Fu W, Kan L, Kessler JA: **The presence of FGF2 signaling determines whether beta-catenin exerts effects on proliferation or neuronal differentiation of neural stem cells**. *Dev Biol* 2004, **268**(1):220-231.
394. Kasai M, Satoh K, Akiyama T: **Wnt signaling regulates the sequential onset of neurogenesis and gliogenesis via induction of BMPs**. *Genes Cells* 2005, **10**(8):777-783.
395. Hirabayashi Y, Itoh Y, Tabata H, Nakajima K, Akiyama T, Masuyama N, Gotoh Y: **The Wnt/beta-catenin pathway directs neuronal differentiation of cortical neural precursor cells**. *Development* 2004, **131**(12):2791-2801.
396. Kuwabara T, Hsieh J, Muotri A, Yeo G, Warashina M, Lie DC, Moore L, Nakashima K, Asashima M, Gage FH: **Wnt-mediated activation of NeuroD1 and retro-elements during adult neurogenesis**. *Nat Neurosci* 2009, **12**(9):1097-1105.
397. Bertrand N, Castro DS, Guillemot F: **Proneural genes and the specification of neural cell types**. *Nat Rev Neurosci* 2002, **3**(7):517-530.
398. Ruiz i Altaba A, Palma V, Dahmane N: **Hedgehog-Gli signalling and the growth of the brain**. *Nat Rev Neurosci* 2002, **3**(1):24-33.

399. Ericson J, Muhr J, Placzek M, Lints T, Jessell TM, Edlund T: **Sonic hedgehog induces the differentiation of ventral forebrain neurons: a common signal for ventral patterning within the neural tube**. *Cell* 1995, **81**(5):747-756.

400. Hynes M, Porter JA, Chiang C, Chang D, Tessier-Lavigne M, Beachy PA, Rosenthal A: **Induction of midbrain dopaminergic neurons by Sonic hedgehog**. *Neuron* 1995, **15**(1):35-44.

401. Wechsler-Reya RJ, Scott MP: **Control of neuronal precursor proliferation in the cerebellum by Sonic Hedgehog**. *Neuron* 1999, **22**(1):103-114.

402. Palma V, Lim DA, Dahmane N, Sanchez P, Brionne TC, Herzberg CD, Gitton Y, Carleton A, Alvarez-Buylla A, Ruiz i Altaba A: **Sonic hedgehog controls stem cell behavior in the postnatal and adult brain**. *Development* 2005, **132**(2):335-344.

403. Papanikolaou T, Lennington JB, Betz A, Figueiredo C, Salamone JD, Conover JC: **In vitro generation of dopaminergic neurons from adult subventricular zone neural progenitor cells**. *Stem Cells Dev* 2008, **17**(1):157-172.

404. Balordi F, Fishell G: **Hedgehog signaling in the subventricular zone is required for both the maintenance of stem cells and the migration of newborn neurons**. *J Neurosci* 2007, **27**(22):5936-5947.

405. Snider WD: **Functions of the neurotrophins during nervous system development: what the knockouts are teaching us**. *Cell* 1994, **77**(5):627-638.

406. Rai KS, Hattiangady B, Shetty AK: **Enhanced production and dendritic growth of new dentate granule cells in the middle-aged hippocampus following intracerebroventricular FGF-2 infusions**. *Eur J Neurosci* 2007, **26**(7):1765-1779.

407. Aberg MA, Aberg ND, Hedbacker H, Oscarsson J, Eriksson PS: **Peripheral infusion of IGF-I selectively induces neurogenesis in the adult rat hippocampus**. *J Neurosci* 2000, **20**(8):2896-2903.

408. Jin K, Zhu Y, Sun Y, Mao XO, Xie L, Greenberg DA: **Vascular endothelial growth factor (VEGF) stimulates neurogenesis in vitro and in vivo**. *Proc Natl Acad Sci U S A* 2002, **99**(18):11946-11950.

409. Sun Y, Nadal-Vicens M, Misono S, Lin MZ, Zubiaga A, Hua X, Fan G, Greenberg ME: **Neurogenin promotes neurogenesis and inhibits glial differentiation by independent mechanisms**. *Cell* 2001, **104**(3):365-376.

410. Nagao M, Sugimori M, Nakafuku M: **Cross talk between notch and growth factor/cytokine signaling pathways in neural stem cells**. *Mol Cell Biol* 2007, **27**(11):3982-3994.

411. Bauer S, Kerr BJ, Patterson PH: **The neuropoietic cytokine family in development, plasticity, disease and injury**. *Nat Rev Neurosci* 2007, **8**(3):221-232.

412. Moon C, Yoo JY, Matarazzo V, Sung YK, Kim EJ, Ronnett GV: **Leukemia inhibitory factor inhibits neuronal terminal differentiation through STAT3 activation**. *Proc Natl Acad Sci U S A* 2002, **99**(13):9015-9020.

413. Bonni A, Sun Y, Nadal-Vicens M, Bhatt A, Frank DA, Rozovsky I, Stahl N, Yancopoulos GD, Greenberg ME: **Regulation of gliogenesis in the central nervous system by the JAK-STAT signaling pathway**. *Science* 1997, **278**(5337):477-483.

414. Fukuda S, Taga T: **[Roles of BMP in the development of the central nervous system]**. *Clin Calcium* 2006, **16**(5):781-785.

415. Tokunaga A, Kohyama J, Yoshida T, Nakao K, Sawamoto K, Okano H: **Mapping spatio-temporal activation of Notch signaling during neurogenesis and gliogenesis in the developing mouse brain**. *J Neurochem* 2004, **90**(1):142-154.

416. Danesin C, Agius E, Escalas N, Ai X, Emerson C, Cochard P, Soula C: **Ventral neural progenitors switch toward an oligodendroglial fate in response to increased Sonic hedgehog (Shh) activity: involvement of Sulfatase 1 in modulating Shh signaling in the ventral spinal cord**. *J Neurosci* 2006, **26**(19):5037-5048.

417. Oh S, Huang X, Chiang C: **Specific requirements of sonic hedgehog signaling during oligodendrocyte development**. *Dev Dyn* 2005, **234**(3):489-496.

418. Tekki-Kessaris N, Woodruff R, Hall AC, Gaffield W, Kimura S, Stiles CD, Rowitch DH, Richardson WD: **Hedgehog-dependent oligodendrocyte lineage specification in the telencephalon**. *Development* 2001, **128**(13):2545-2554.

419. Kessaris N, Jamen F, Rubin LL, Richardson WD: **Cooperation between sonic hedgehog and fibroblast growth factor/MAPK signalling pathways in neocortical precursors**. *Development* 2004, **131**(6):1289-1298.

420. Rowitch DH: **Glial specification in the vertebrate neural tube**. *Nat Rev Neurosci* 2004, **5**(5):409-419.

421. Wang S, Sdrulla AD, diSibio G, Bush G, Nofziger D, Hicks C, Weinmaster G, Barres BA: **Notch receptor activation inhibits oligodendrocyte differentiation**. *Neuron* 1998, **21**(1):63-75.

422. Samanta J, Kessler JA: **Interactions between ID and OLIG proteins mediate the inhibitory effects of BMP4 on oligodendroglial differentiation**. *Development* 2004, **131**(17):4131-4142.

423. Cai J, St Amand T, Yin H, Guo H, Li G, Zhang Y, Chen Y, Qiu M: **Expression and regulation of the chicken Nkx-6.2 homeobox gene suggest its possible involvement in the ventral neural patterning and cell fate specification**. *Dev Dyn* 1999, **216**(4-5):459-468.

424. Qi Y, Cai J, Wu Y, Wu R, Lee J, Fu H, Rao M, Sussel L, Rubenstein J, Qiu M: **Control of oligodendrocyte differentiation by the Nkx2.2 homeodomain transcription factor**. *Development* 2001, **128**(14):2723-2733.

425. Stolt CC, Lommes P, Friedrich RP, Wegner M: **Transcription factors Sox8 and Sox10 perform non-equivalent roles during oligodendrocyte development despite functional redundancy**. *Development* 2004, **131**(10):2349-2358.

426. Cheung M, Briscoe J: **Neural crest development is regulated by the transcription factor Sox9**. *Development* 2003, **130**(23):5681-5693.

427. Gotz M, Huttner WB: **The cell biology of neurogenesis**. *Nat Rev Mol Cell Biol* 2005, **6**(10):777-788.

428. Pevny L, Placzek M: **SOX genes and neural progenitor identity**. *Curr Opin Neurobiol* 2005, **15**(1):7-13.

429. Gao Z, Ure K, Ding P, Nashaat M, Yuan L, Ma J, Hammer RE, Hsieh J: **The master negative regulator REST/NRSF controls adult neurogenesis by restraining the neurogenic program in quiescent stem cells**. *J Neurosci* 2011, **31**(26):9772-9786.

430. Zhou ZD, Kumari U, Xiao ZC, Tan EK: **Notch as a molecular switch in neural stem cells**. *IUBMB Life* 2010, **62**(8):spcone.

431. Egger B, Boone JQ, Stevens NR, Brand AH, Doe CQ: **Regulation of spindle orientation and neural stem cell fate in the Drosophila optic lobe**. *Neural Dev* 2007, **2**:1.

432. Egger B, Gold KS, Brand AH: **Notch regulates the switch from symmetric to asymmetric neural stem cell division in the Drosophila optic lobe**. *Development* 2010, **137**(18):2981-2987.

433. Prehoda KE: **Polarization of Drosophila neuroblasts during asymmetric division**. *Cold Spring Harb Perspect Biol* 2009, **1**(2):a001388.

434. Zhong W, Chia W: **Neurogenesis and asymmetric cell division**. *Curr Opin Neurobiol* 2008, **18**(1):4-11.

435. Ballas N, Grunseich C, Lu DD, Speh JC, Mandel G: **REST and its corepressors mediate plasticity of neuronal gene chromatin throughout neurogenesis**. *Cell* 2005, **121**(4):645-657.

436. Muraoka A, Maeda A, Nakahara N, Yokota M, Nishida T, Maruyama T, Ohshima T: **Sumoylation of CoREST modulates its function as a transcriptional repressor**. *Biochem Biophys Res Commun* 2008, **377**(4):1031-1035.

437. Westbrook TF, Hu G, Ang XL, Mulligan P, Pavlova NN, Liang A, Leng Y, Maehr R, Shi Y, Harper JW *et al*: **SCFbeta-TRCP controls oncogenic transformation and neural differentiation through REST degradation**. *Nature* 2008, **452**(7185):370-374.

438. Bylund M, Andersson E, Novitch BG, Muhr J: **Vertebrate neurogenesis is counteracted by Sox1-3 activity**. *Nat Neurosci* 2003, **6**(11):1162-1168.

439. Graham V, Khudyakov J, Ellis P, Pevny L: **SOX2 functions to maintain neural progenitor identity**. *Neuron* 2003, **39**(5):749-765.

440. Rogers CD, Archer TC, Cunningham DD, Grammer TC, Casey EM: **Sox3 expression is maintained by FGF signaling and restricted to the neural plate by Vent proteins in the Xenopus embryo**. *Dev Biol* 2008, **313**(1):307-319.

441. Savare J, Bonneaud N, Girard F: **SUMO represses transcriptional activity of the Drosophila SoxNeuro and human Sox3 central nervous system-specific transcription factors**. *Mol Biol Cell* 2005, **16**(6):2660-2669.

442. Cornell M, Evans DA, Mann R, Fostier M, Flasza M, Monthatong M, Artavanis-Tsakonas S, Baron M: **The Drosophila melanogaster Suppressor of deltex gene, a regulator of the Notch receptor signaling pathway, is an E3 class ubiquitin ligase**. *Genetics* 1999, **152**(2):567-576.

443. Oberg C, Li J, Pauley A, Wolf E, Gurney M, Lendahl U: **The Notch intracellular domain is ubiquitinated and negatively regulated by the mammalian Sel-10 homolog**. *J Biol Chem* 2001, **276**(38):35847-35853.

444. Wu G, Lyapina S, Das I, Li J, Gurney M, Pauley A, Chui I, Deshaies RJ, Kitajewski J: **SEL-10 is an inhibitor of notch signaling that targets notch for ubiquitin-mediated protein degradation**. *Mol Cell Biol* 2001, **21**(21):7403-7415.

445. Nie J, McGill MA, Dermer M, Dho SE, Wolting CD, McGlade CJ: **LNX functions as a RING type E3 ubiquitin ligase that targets the cell fate determinant Numb for ubiquitin-dependent degradation**. *EMBO J* 2002, **21**(1-2):93-102.

446. Deblandre GA, Lai EC, Kintner C: **Xenopus neuralized is a ubiquitin ligase that interacts with XDelta1 and regulates Notch signaling**. *Dev Cell* 2001, **1**(6):795-806.

447. Lai EC, Deblandre GA, Kintner C, Rubin GM: **Drosophila neuralized is a ubiquitin ligase that promotes the internalization and degradation of delta**. *Dev Cell* 2001, **1**(6):783-794.

448. Chen W, Casey Corliss D: **Three modules of zebrafish Mind bomb work cooperatively to promote Delta ubiquitination and endocytosis**. *Dev Biol* 2004, **267**(2):361-373.

449. Itoh M, Kim CH, Palardy G, Oda T, Jiang YJ, Maust D, Yeo SY, Lorick K, Wright GJ, Ariza-McNaughton L *et al*: **Mind bomb is a ubiquitin ligase that is essential for efficient activation of Notch signaling by Delta**. *Dev Cell* 2003, **4**(1):67-82.

450. Vosper JM, Fiore-Heriche CS, Horan I, Wilson K, Wise H, Philpott A: **Regulation of neurogenin stability by ubiquitin-mediated proteolysis**. *Biochem J* 2007, **407**(2):277-284.

451. Vosper JM, McDowell GS, Hindley CJ, Fiore-Heriche CS, Kucerova R, Horan I, Philpott A: **Ubiquitylation on canonical and non-canonical sites targets the transcription factor neurogenin for ubiquitin-mediated proteolysis**. *J Biol Chem* 2009, **284**(23):15458-15468.

452. Fong CW, Leong HF, Wong ES, Lim J, Yusoff P, Guy GR: **Tyrosine phosphorylation of Sprouty2 enhances its interaction with c-Cbl and is crucial for its function**. *J Biol Chem* 2003, **278**(35):33456-33464.

453. Edwin F, Anderson K, Patel TB: **HECT domain-containing E3 ubiquitin ligase Nedd4 interacts with and ubiquitinates Sprouty2**. *J Biol Chem* 2010, **285**(1):255-264.

454. Hall AB, Jura N, DaSilva J, Jang YJ, Gong D, Bar-Sagi D: **hSpry2 is targeted to the ubiquitin-dependent proteasome pathway by c-Cbl**. *Curr Biol* 2003, **13**(4):308-314.

455. Rubin C, Gur G, Yarden Y: **Negative regulation of receptor tyrosine kinases: unexpected links to c-Cbl and receptor ubiquitylation**. *Cell Res* 2005, **15**(1):66-71.

456. Koinuma D, Shinozaki M, Komuro A, Goto K, Saitoh M, Hanyu A, Ebina M, Nukiwa T, Miyazawa K, Imamura T *et al*: **Arkadia amplifies TGF-beta superfamily signalling through degradation of Smad7**. *EMBO J* 2003, **22**(24):6458-6470.

457. Liu W, Rui H, Wang J, Lin S, He Y, Chen M, Li Q, Ye Z, Zhang S, Chan SC *et al*: **Axin is a scaffold protein in TGF-beta signaling that promotes degradation of Smad7 by Arkadia**. *EMBO J* 2006, **25**(8):1646-1658.

458. Elkouris M, Balaskas N, Poulou M, Politis PK, Panayiotou E, Malas S, Thomaidou D, Remboutsika E: **Sox1 maintains the undifferentiated state of cortical neural progenitor cells via the suppression of Prox1-mediated cell cycle exit and neurogenesis**. *Stem Cells* 2011, **29**(1):89-98.

459. Holmberg J, Hansson E, Malewicz M, Sandberg M, Perlmann T, Lendahl U, Muhr J: **SoxB1 transcription factors and Notch signaling use distinct mechanisms to regulate proneural gene function and neural progenitor differentiation**. *Development* 2008, **135**(10):1843-1851.

460. Thiel G: **How Sox2 maintains neural stem cell identity**. *Biochem J* 2013, **450**(3):e1-2.

461. de la Iglesia N, Konopka G, Lim KL, Nutt CL, Bromberg JF, Frank DA, Mischel PS, Louis DN, Bonni A: **Deregulation of a STAT3-interleukin 8 signaling pathway promotes human glioblastoma cell proliferation and invasiveness**. *J Neurosci* 2008, **28**(23):5870-5878.

the FEBS Journal

A novel role for the proteasomal chaperone PSMD9 and hnRNPA1 in enhancing IκBα degradation and NF-κB activation – functional relevance of predicted PDZ domain–motif interaction

Indrajit Sahu, Nikhil Sangith, Manoj Ramteke, Rucha Gadre and Prasanna Venkatraman

Advanced Center for Treatment, Research and Education in Cancer, Tata Memorial Centre, Kharghar, Navi Mumbai, India

Keywords
hnRNPA1; IκBα degradation; NF-κB activity; PDZ domain; PSMD9

Correspondence
P. Venkatraman, Advanced Center for Treatment, Research and Education in Cancer, Tata Memorial Centre, Kharghar, Navi Mumbai 410210, India
Fax: 022 27405085
Tel: 022 27405091
E-mail: vprasanna@actrec.gov.in

(Received 30 October 2013, revised 27 February 2014, accepted 9 April 2014)

doi:10.1111/febs.12814

PSMD9 is a PDZ domain containing chaperone of proteasome assembly. Based on the ability of PDZ-like domains to recognize C-terminal residues in their interactors, we recently predicted and identified heterogeneous nuclear ribonucleoprotein A1 (hnRNPA1) as one of the novel interacting partners of PSMD9. Contingent on the reported role of hnRNPA1 in nuclear factor κB (NF-κB) activation, we tested the role of human PSMD9 and hnRNPA1 in NF-κB signaling. We demonstrated in human embryonic kidney 293 cells that PSMD9 influences both basal and tumor necrosis factor α (TNF-α) mediated NF-κB activation through inhibitor of nuclear factor κB α (IκBα) proteasomal degradation. PSMD9 mediates IκBα degradation through a specific domain–motif interaction involving its PDZ domain and a short linear sequence motif in the C-terminus of hnRNPA1. Point mutations in the PDZ domain or deletion of C-terminal residues in hnRNPA1 disrupt interaction between the two proteins which has a direct influence on NF-κB activity. hnRNPA1 interacts with IκBα directly, whereas PSMD9 interacts only through hnRNPA1. Furthermore, hnRNPA1 shows increased association with the proteasome upon TNF-α treatment which has no such effect in the absence of PSMD9. On the other hand endogenous and trans-expressed PSMD9 are found associated with the proteasome complex. This association is unaffected by PDZ mutations or TNF-α treatment. Collectively, these interactions between IκBα, hnRNPA1 and proteasome bound PSMD9 illustrate a potential mechanism by which ubiquitinated IκBα is recruited on the proteasome for degradation. In this process, hnRNPA1 may act as a shuttle receptor and PSMD9 as a subunit acceptor. The interaction sites of PSMD9 and hnRNPA1 may emerge as a vulnerable drug target in cancer cells which require consistent NF-κB activity for survival.

Introduction

Mammalian PSMD9 is known to form a stable subcomplex with PSMC3 and PSMC6, two of the AAA-ATPases, assisting in the assembly of the 20S and 19S particles to form the holo complex [1,2]. Structurally PSMD9 contains an 88 amino acid long (108–195) PDZ-like domain [3]. Many PDZ domain containing

Abbreviations
CHX, cycloheximide; COX-2, cyclooxygenase-2; EMSA, electrophoretic mobility shift assay; HEK293 cells, human embryonic kidney 293 cells; hnRNPA1, heterogeneous nuclear ribonucleoprotein A1; ICAM-1, intercellular adhesion molecule 1; IL, interleukin; IP, immunoprecipitation; IκBα, inhibitor of nuclear factor κB α; MBP, maltose bonding protein; NF-κB, nuclear factor κB; PVDF, poly(vinylidene difluoride); shRNA, small hairpin RNA; SLIM, short linear sequence motif; TNF-α, tumor necrosis factor α; WB, western blot; wt, wild type.

proteins act as scaffolds to form supramolecular assemblies which allow them to function in signaling, mediating adhesive properties of cells, and in ion transport [4,5]. Bridge-1, the PSMD9 homolog in rats, has been shown to act as a coactivator of insulin gene transcription through interaction of its PDZ-like domain with transcription factors E12 and histone acetyl transferase, p300 [3,6]. In ovarian cells, changes in the levels of PSMD9 are known to alter activin signaling [7]. Overexpression of Bridge-1 increases pancreatic apoptosis with a reduction in the number of insulin-expressing β-cells leading to insulin deficiency and diabetes [8].

Based on the classical property of some PDZ domains to recognize 4–7 C-terminal residues or short linear sequence motifs (SLIMs) in proteins, we recently identified several novel interacting partners of PSMD9 (*FEBS Open Bio*, submitted). Such SLIMs have been identified as functionally relevant recognition motifs in SH2, SH3 domain containing proteins [9]. We recently showed that a 13 residue A-helix acts as an anchor while a floppy F-helix acts as an initiator of ubiquitin independent degradation of apomyoglobin by the proteasome [10]. We also identified novel interacting partners of gankyrin, a chaperone of the proteasome and an oncoprotein, by recognizing proteins which share EEVD, a conserved SLIM seen at the interface of gankyrin-S6 ATPase complex [11]. In addition we predicted the structure of the PDZ domain of PSMD9 and identified residues at the PDZ interface which are important for recognizing the C-terminal residues of four novel interacting partners (*FEBS Open Bio*, submitted). Heterogeneous nuclear ribonucleoprotein A1 (hnRNPA1), an RNA binding protein involved in mRNA export, splicing and protein translation, was one of the novel interacting partners. This protein in the mouse CB3 cells was reported to be responsible for inhibitor of nuclear factor κB α (IκBα) degradation by an unknown mechanism leading to transcriptional activation of nuclear factor κB (NF-κB) [12]. This observation formed the premise of this work which aims to establish the functional relevance of the newly found PSMD9–hnRNPA1 interaction.

NF-κB is a family of transcription factors that regulate expression of various genes involved in inflammatory, anti-apoptotic and immune responses [13,14]. The NF-κB family or the Rel family of proteins includes p50 (p105), p52 (p100), p65 (RelA), c-Rel and Rel-B [15,16]. If cells are not stimulated, heterodimeric NF-κB complexes remain in the cytoplasm, where they are associated with an inhibitory molecule of the IκB family [17]. In mammalian species, six structural homologs of IκB have been identified: IκBα, IκBβ, IκBε, IκBγ, Bcl-3 and IκBζ [18]. Among these, IκBα, the prototypical member of the IκB family, has been extensively studied. The canonical NF-κB p65/p50 heterodimer is largely, although not exclusively, found in complex with its inhibitor IκBα in cytoplasm. In response to stimulation by various agents such as phorbol esters (e.g. phorbol 12-myristate 13-acetate), pervanadate, tumor necrosis factor α (TNF-α), interleukin-1a (IL-1a), γ-radiation and lipopolysaccharide, IκBα undergoes phosphorylation by the IKK complex at Ser32, Ser36 and/or Tyr42 followed by polyubiquitination at Lys21 and Lys22 [19–22]. This leads to proteasomal degradation of the phosphorylated and ubiquitinated IκBα and nuclear translocation of free p50/p65, resulting in NF-κB transcription activity [13,19,23,24]. Apart from proteasomal degradation some reports suggest that in uninduced cells IκBα undergoes non-proteasomal, calcium dependent proteolysis resulting in high and consistent NF-κB activity [25–28]. Among the other IκB proteins, IκBβ, IκBε, p100 (precursors of p52) and p105 (precursors of p50) also undergo proteasomal degradation/endoproteolytic processing under induced and uninduced conditions [29–33]. Although the upstream processes of IκBα degradation are extensively deciphered, the detailed mechanism of proteasomal degradation is still not clear.

It is with this background that we were intrigued by the reports of Hay *et al*., who demonstrated interaction between ankyrin repeats of IκBα and hnRNPA1 which somehow seemed necessary for IκBα degradation and NF-κB transcriptional activity [12]. But the identity of the protease involved and the role of proteasome in this process were not established. Since the bigger and fundamental question of how IκBα is recruited to the proteasome for degradation remains largely unaddressed, it would be interesting to investigate whether hnRNPA1, well known for its role in mRNA processing and transport [34], cross-talks with the proteasomal degradation pathway in human cells. The mechanism by which ubiquitinated proteins are recruited to proteasome remains an active area of research. Based on our finding that PSMD9 interacts with hnRNPA1 *in vitro* (*FEBS Open Bio*, submitted) and the reported role of hnRNPA1 in IκBα degradation and NF-κB activity, we hypothesized that PSMD9 may have a role in the degradation of IκBα by the proteasome and influence NF-κB activity in human cells. Here we provide evidence that in human embryonic kidney 293 (HEK293) cells, PSMD9 through its PDZ domain interacts with the C-terminus of hnRNPA1 and this tripartite interaction subjects ubiquitinated IκBα to proteasomal degradation enhancing both basal and signal mediated NF-κB activity. By a series of experiments we identify a novel role for hnRNPA1 as a shuttle receptor that recruits IκBα for degradation and

recognizes PSMD9 as a novel subunit receptor on the proteasome. Our results demonstrate an atypical function of hnRNPA1 which seems to integrate into the ubiquitin proteasome pathway through a specific interaction with proteasome bound PSMD9. We speculate about the general role of this interaction and the utility of the PDZ domain interface as a potential drug target.

Results

PSMD9 interacts with the C-terminus of hnRNPA1

Using a bioinformatics approach (*FEBS Open Bio*, submitted) and the knowledge that some PDZ domains interact with C-terminal regions of proteins [5], we predicted putative interacting partners of PSMD9, from the human proteome. This prediction was validated by screening C-terminal peptides for their ability to bind to pure recombinant PSMD9. Using this strategy we identified hnRNPA1 as a novel interacting partner of PSMD9 and further proved that this interaction is mediated by the C-terminal residues of hnRNPA1 (*FEBS Open Bio*, submitted). To test if PSMD9 and hnRNPA1 interact endogenously, as this would be physiologically and functionally relevant, we used PSMD9 antibody to immunoprecipitate PSMD9 from HEK293 cell lysates and probed for the presence of hnRNPA1 using hnRNPA1 antibody. As expected, hnRNPA1 was found in the immunoprecipitation (IP) complex (Fig. 1A). We further validated this endogenous interaction by performing a reverse IP where hnRNPA1 antibody was used for IP and the complex was probed with PSMD9 antibody (Fig. 1B). We reconfirmed our earlier observation that only wild type (wt) hnRNPA1 and not the C-terminal mutant can interact with PSMD9 (Fig. 1C).

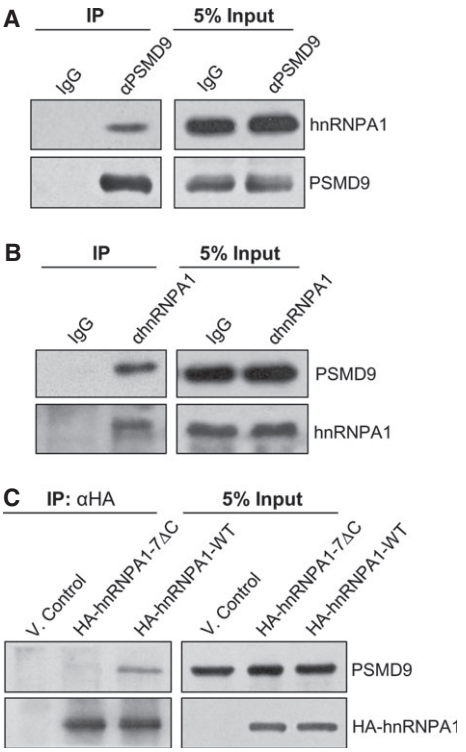

Fig. 1. PSMD9 interacts with wt-hnRNPA1 but not with the 7ΔC mutant of hnRNPA1 *ex vivo*. (A) HEK293 cell lysates were incubated either with PSMD9 antibody-bound Protein-G Sepharose beads or mouse IgG (isotype control) bound Protein-G Sepharose beads. Pull-down complexes were probed with hnRNPA1 and PSMD9 antibodies. (B) HEK293 cell lysates were incubated with either hnRNPA1 antibody-bound Protein-G Sepharose beads or mouse IgG isotype bound Protein-G Sepharose (isotype control). Then pull-down complexes were probed with PSMD9 and hnRNPA1 antibodies and analyzed by WB. (C) HA-wt-hnRNPA1 or 7ΔC mutant HA-hnRNPA1 was transiently overexpressed in HEK293 cells and cell lysates were incubated with HA antibody-bound Protein-G Sepharose beads. Pull-down complexes were probed with PSMD9 antibodies and analyzed by WB.

Overexpression of PSMD9 enhances basal and TNF-α mediated NF-κB activity

In CB3 cells, hnRNPA1 reportedly interacts with IκBα and overexpression of hnRNPA1 in these cells enhances NF-κB transcriptional activity [12]. No such role has been reported for hnRNPA1 in human cells. Since we found that PSMD9 interacts with hnRNPA1 *ex vivo* and hnRNPA1 reportedly influences NF-κB activity, we asked if PSMD9 was involved in this pathway. If so, changes in the levels of PSMD9 must influence NF-κB activity. PSMD9 was overexpressed under doxycycline inducible conditions in three different stable clones (Fig. 2A), and NF-κB transcriptional activity was measured by luciferase reporter assay. In all three inducible clones, NF-κB activity was found to be 3–4-fold higher than that of the uninduced control cells (Fig. 2B). In addition, we regulated the expression of PSMD9 using an inducible system in HEK293 cells (Fig. 2C) and found that doxycycline induced the expression of PSMD9 in a concentration dependent manner, which led to a corresponding increase in NF-κB transcriptional activity monitored using the luciferase reporter assay (Fig. 2D).

The influence of PSMD9 overexpression on NF-κB activity was further validated by demonstrating nuclear translocation of NF-κB (p65) and by electrophoretic mobility shift assay (EMSA). In PSMD9 overexpressing HEK293 cells, there was a significant increase in nuclear p65 in comparison with control cells (Fig. 2E). Upon

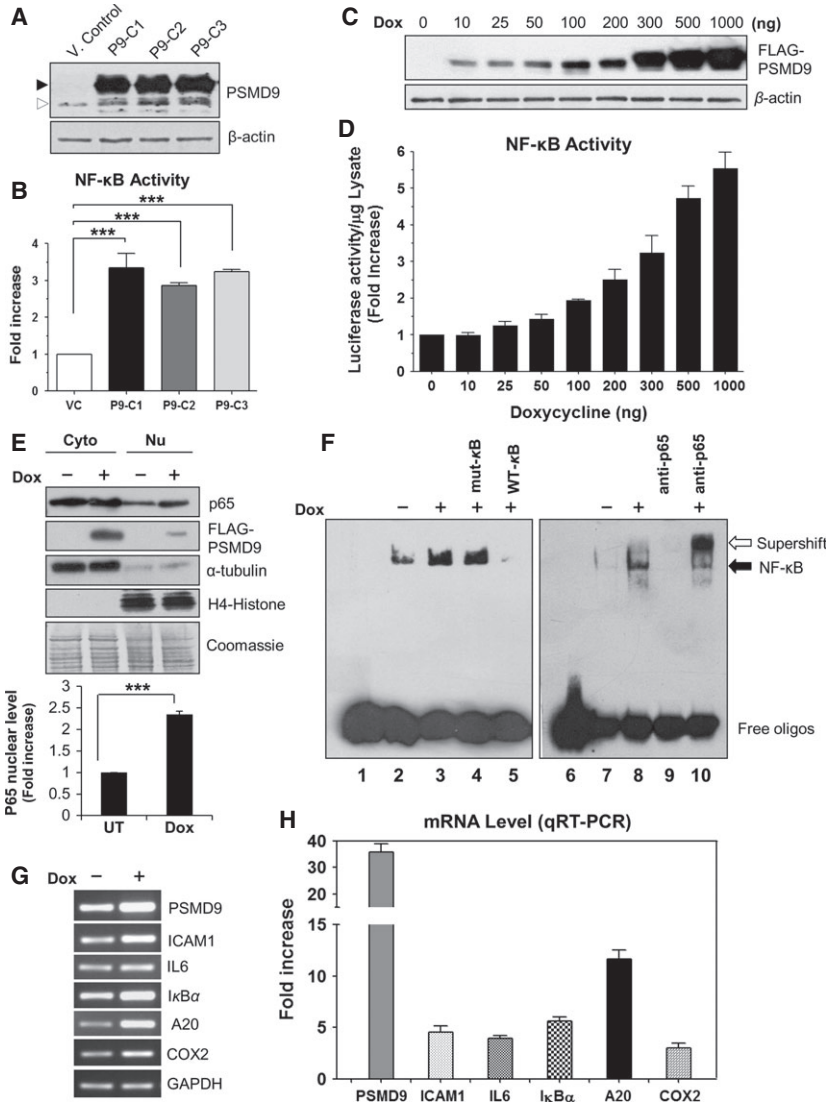

PSMD9 overexpression binding of NF-κB to the κB enhancer element was increased. This binding was competed out by unlabeled wt κB-oligos but not by mutant κB-oligos (Fig. 2F, lanes 4 and 5) [35]. Furthermore when the reaction mixture was incubated with p65 antibody, a supershift band was obtained which confirms the presence of p65 and its DNA binding activity (Fig. 2F, lane 10). In addition, five of the NF-κB target genes, namely intercellular adhesion molecule 1 (ICAM-1), IL-6, IκBα, A20 and cyclooxygenase-2 (COX-2) [36], were several-fold upregulated in PSMD9 overexpression cells compared with vector control cells (Fig. 2G,H). When doxycycline induced or uninduced cells were treated with TNF-α, a potent signal for NF-κB activation [37], both NF-κB DNA binding capacity and its transcriptional activity were increased. This increase was more pronounced in PSMD9 overexpressing cells (Fig. 3A,B, lane 5). These results suggest that PSMD9 is involved in both basal and the signal mediated NF-κB pathway.

PSMD9 overexpression increases NF-κB activity by enhancing degradation of IκBα by proteasome

In the classical NF-κB pathway, upon signal induction, NF-κB bound IκBα is degraded by the 26S proteasome. Since NF-κB activity increased with increase in the levels of PSMD9 in HEK293 cells (current study), we hypothesized that PSMD9 may accelerate the degradation of IκBα by the proteasome. Accordingly when PSMD9 expression was induced by doxycycline there was a visible decrease in IκBα protein after 4–6 h of cycloheximide (CHX) treatment, whereas in uninduced cells reduction in the levels of IκBα was

seen only after 18–24 h of treatment (Fig. 4A). Similarly signal mediated IκBα degradation was considerably enhanced 10 min post TNF-α treatment in cells induced to overexpress PSMD9 (Fig. 4B). These results indicate that PSMD9 is involved in modulating IκBα levels presumably through proteasomal degradation in both basal as well as the signal mediated NF-κB signaling pathway.

To determine the role of proteasome in PSMD9 mediated degradation of IκBα, we treated PSMD9 overexpressing HEK293 cells with proteasome inhibitors. Treatment with MG132 or Velcade significantly inhibited both basal and TNF-α mediated IκBα degradation in cells overexpressing PSMD9 (Fig. 4C,D). In further support of proteasomal degradation, ubiquitinated IκBα was also seen to accumulate when PSMD9 overexpressing cells were treated with the proteasomal inhibitors (Fig. 4C). It is well established that degradation of IκBα by the proteasome, upon signal induction, requires phosphorylation at sites S32 and S36 [13]. To determine whether the processing of IκBα occurs through the same way in the case of PSMD9 mediated degradation, we overexpressed IκBα super-repressor (S32A–S36A) in control cells as well as in PSMD9 overexpressing cells. After 30 min of TNF-α induction, super-repressor IκBα was not degraded even under PSMD9 overexpression conditions whereas endogenous IκBα got degraded significantly (Fig. 4E). In accordance with this, NF-κB activity is decreased significantly in the cells upon overexpression of the super-repressor irrespective of PSMD9 overexpression (Fig. 4F). These results indicate that the phosphorylation at S32 and S36 residues is necessary for the PSMD9 mediated IκBα degradation by the proteasome.

Endogenous PSMD9 is involved in basal and signal mediated activation of NF-κB and IκBα degradation

In order to demonstrate the role of endogenous PSMD9 in NF-κB activation, we knocked down PSMD9 in HEK293 cells using small hairpin RNA (shRNA) under inducible conditions. Upon knockdown of PSMD9, IκBα levels were found to be stable even after 24 h of CHX treatment (Fig. 5A). In the same cells, a reduction in TNF-α induced IκBα degradation was observed whereas in control cells IκBα degradation was already apparent after 20 min of TNF-α treatment (Fig. 5B). Concomitantly a decrease in NF-κB DNA binding activity was observed by EMSA both in TNF-α treated and untreated PSMD9 knockdown cells (Fig. 5C). This was further confirmed by semi-quantitative RT-PCR and real-time PCR of five different NF-κB target genes, namely ICAM-1, IL-6, IκBα, A20 and COX-2, the levels of which decreased in PSMD9 knockdown cells compared with control cells (Fig. 5D,E). These results indicate that endogenous PSMD9 is indeed responsible for the basal and signal induced degradation of IκBα and subsequent increase in NF-κB activity.

Fig. 2. Basal NF-κB activity increases upon PSMD9 overexpression in HEK293 cells. (A) Three clones of HEK293 cells inducibly expressing FLAG-PSMD9 were either treated with doxycycline or left untreated, and the cell lysates were analyzed by WB. (B) The above clones were transfected with 3x κB ConA luc vector or ConA luc control vector and induced with doxycycline (1 $\mu g \cdot mL^{-1}$ of medium). After 48 h of induction NF-κB activity was checked by measuring luciferase activity using dual luciferase substrate. Luciferase activity from firefly luciferase was normalized with renilla luciferase used as a transfection control. Data represent mean luciferase activity per microgram of protein ± SEM of two independent experiments done in triplicate. (C) HEK293 cells inducibly expressing FLAG-PSMD9 were transfected with 3x κB ConA luc vector or ConA luc control vector. Cells were induced with different concentrations (0–1000 $ng \cdot mL^{-1}$ of medium) of doxycycline. After 48 h of induction, levels of FLAG-PSMD9 were analyzed by WB. (D) NF-κB activity was checked by measuring luciferase activity of the above described (in C) cell lysates, using dual luciferase substrate. Luciferase activity from firefly luciferase was normalized with renilla luciferase used as a transfection control. Data represent mean luciferase activity per microgram of protein ± SEM of two independent experiments done in triplicate. (E) HEK293 cells inducibly expressing FLAG-PSMD9 were either treated with doxycycline (1 $\mu g \cdot mL^{-1}$ of medium for 48 h) or left untreated. Nuclear fractions were prepared as described in Materials and methods and analyzed by WB. The graph represents the mean fold increase of p65 nuclear translocation ± SEM of two independent experiments in three different stable clones. (F) HEK293 inducible FLAG-PSMD9 stable clones were either treated with doxycycline (1 $\mu g \cdot mL^{-1}$ of medium for 48 h) or left untreated. The nuclear fractions were subjected to EMSA (following the protocol described in Materials and methods). Lane 1 indicates biotinylated oligos only. The black arrow indicates NF-κB DNA binding activity in doxycycline untreated (lanes 2 and 7) and treated (lanes 3 and 8) cells. NF-κB DNA binding specificity is shown by competing it with 200× unlabeled mutant oligos (lane 4) or wt oligos (lane 5). In lanes 9 and 10 p65 antibody was incubated with the binding reaction mix (with/without lysate) and the white arrow indicates the resulting supershift band. (G) HEK293 inducible FLAG-PSMD9 stable clones either treated with doxycycline for 48 h or left untreated. RNA was isolated and semi-quantitative RT-PCR was performed for five different target genes; the PCR products were run in a 2% agarose gel. (H) Real-time PCR was performed for the same five different target genes. The graph represents glyceraldehyde-3-phosphate dehydrogenase (GAPDH) normalized mean fold increase in mRNA level of the genes ± SEM for three independent experiments done in duplicate.

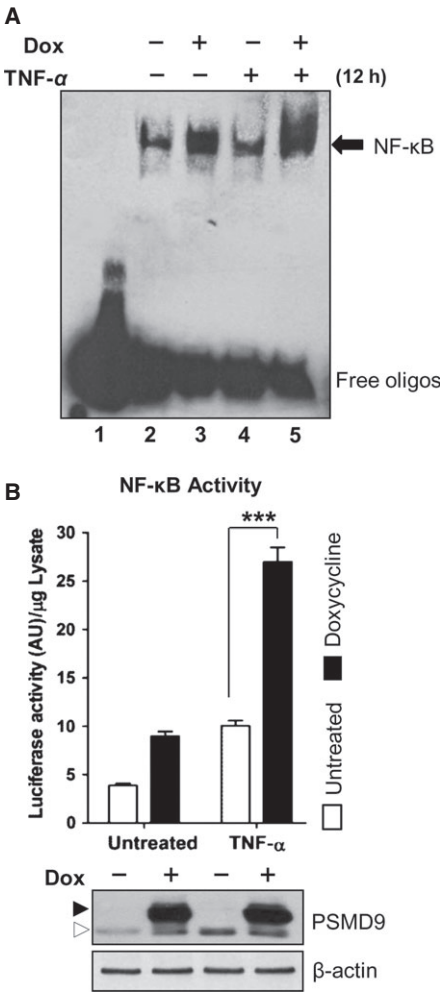

Fig. 3. TNF-α mediated NF-κB activity increases upon PSMD9 overexpression in HEK293 cells. (A) HEK293 inducible FLAG-PSMD9 stable clones were treated with doxycycline (1 $\mu g \cdot mL^{-1}$ of medium for 48 h) and/or with TNF-α (20 $ng \cdot mL^{-1}$ of medium for 12 h) or left untreated. The nuclear fractions were subjected to EMSA (following the protocol described in Materials and methods). Lane 1 indicates biotinylated oligos only. The black arrow indicates NF-κB DNA binding activity in doxycycline untreated (lanes 2 and 4) and treated (lanes 3 and 5) cells. Upon TNF-α treatment NF-κB DNA binding activity increased, shown by the thick gel shift band (in lanes 4 and 5). (B) HEK293 cells inducibly expressing FLAG-PSMD9 were transfected with 3x κB ConA luc vector or ConA luc control vector. Transfected cells were treated with doxycycline (1 $\mu g \cdot mL^{-1}$ of medium for 48 h) and/or with TNF-α for 12 h or left untreated. NF-κB activity was measured as described in Fig. 2B. Data represent mean luciferase activity per microgram of protein ± SEM of two independent experiments done in triplicate. WB shows the level of PSMD9 expression in these cell lysates. Symbol ▶ corresponds to trans-expressed FLAG-PSMD9 and ▷ symbol corresponds to the endogenous PSMD9.

PSMD9 does not affect the IκBα ubiquitination and proteasomal activity

Given its role as an assembly chaperone, PSMD9 expression may influence proteasomal activity which in turn may dictate the overall IκBα levels. We tested the activity of proteasome upon overexpression of PSMD9 and upon silencing the endogenous PSMD9. Proteasomal activity was unaltered in these cells and remained uninfluenced by TNF-α treatment (Fig. 6A). Our observation that PSMD9 does not influence proteasomal activity is in line with a previous report by Shim *et al.* [38]. Here similar to our method the authors used total cell lysates for monitoring proteasomal activity. In another study Keneko *et al.* showed that knocking down PSMD9 results in reduced proteasomal activity [1]. Here, in contrast to our method and those by Shim *et al.*, cell lysates were fractionated by glycerol gradient centrifugation and the fractions were monitored for proteasomal activity. Increase in proteasomal activity is seen in the presence of p27 modulator complex in reconstitution experiments involving subcomplexes of the proteasome [39]. The role of this modulator seems to involve rescue of improperly assembled or damaged 19S particles to ensure correct orientation of the ATPase rings [40].

Due to the importance of ubiquitination in IκBα degradation by the proteasome, we checked the requirement of PSMD9 in this process. We treated both doxycycline induced and uninduced cells with MG132 for 2 h followed by CHX treatment for 6, 12 and 24 h. The initial 2 h of MG132 treatment resulted in a 75% decrease in proteasomal activity. To ensure that after removal of MG132 and during the CHX treatment (used to follow degradation of ubiquitinated IκBα) proteasomes were functional, activity was monitored at every assay point. Then, 12 h following removal of MG132, proteasomal activity was restored almost completely both in PSMD9 knockdown cells and in control cells. Coincident with the time period of CHX treatment and upon PSMD9 gene silencing, levels of ubiquitinated IκBα did not change significantly. Rather an increased accumulation of ubiquitinated IκBα was seen in these PSMD9 knockdown cells. In control cells there was a clear decrease in levels of ubiquitinated IκBα (Fig. 6B). These results indicate that PSMD9 does not affect ubiquitination of IκBα and confirm that cells fail to degrade ubiquitinated IκBα efficiently not because of impaired proteasomal activity but due to the absence of PSMD9.

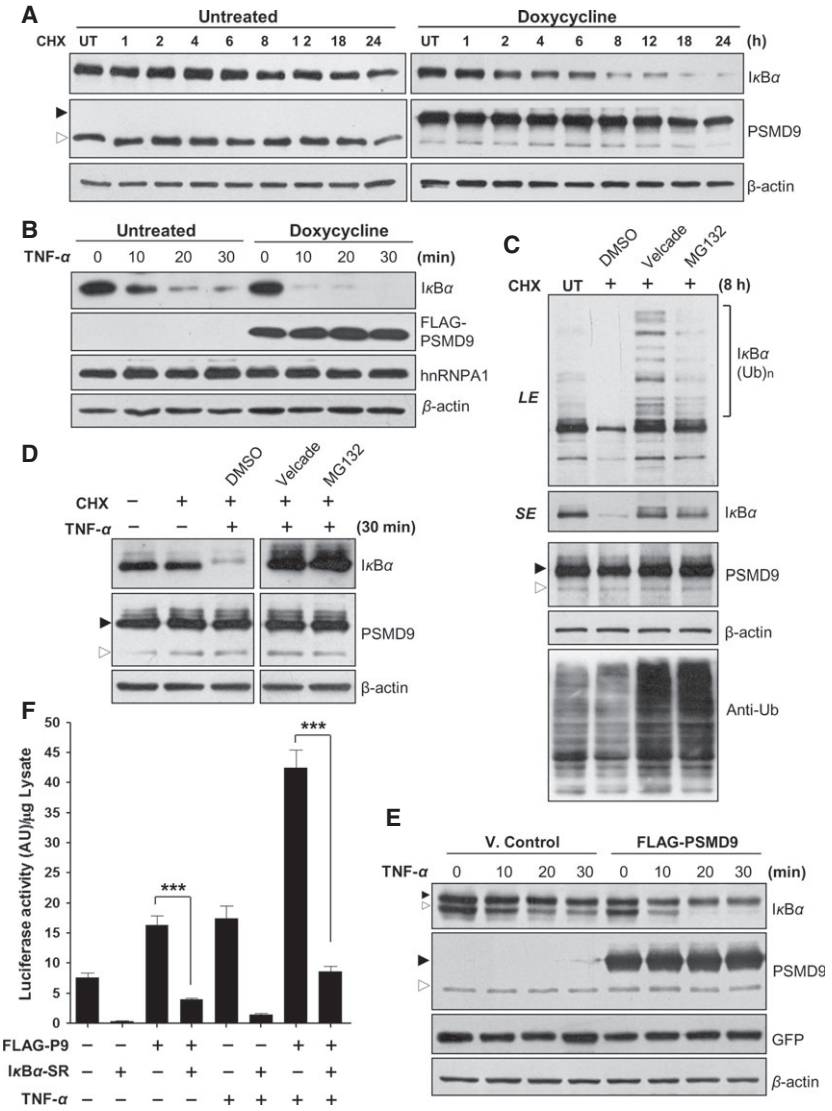

Fig. 4. PSMD9 overexpression accelerates basal and TNF-α mediated IκBα degradation. (A) HEK293 inducible FLAG-PSMD9 stable clones were treated with doxycycline (1 $\mu g \cdot mL^{-1}$ of medium for 48 h) and/or CHX (50 $\mu g \cdot mL^{-1}$ of medium for 1, 2, 4, 6, 8, 12, 18 and 24 h) or left untreated. Cell lysates were prepared and analyzed by WB. (B) Both doxycycline treated or untreated HEK293 inducible FLAG-PSMD9 stable clones were stimulated with TNF-α (20 $ng \cdot mL^{-1}$ of medium) for 0, 10, 20 and 30 min. Cell lysates were subjected to WB. (C) The above doxycycline induced stable clones were treated with CHX (50 $\mu g \cdot mL^{-1}$ of medium for 8 h) (where indicated) and with MG132 (10 μM), Velcade (10 $\mu g \cdot mL^{-1}$ of medium) or 0.1% dimethylsulfoxide for 6 h and analyzed by WB. LE, long exposure; SE, short exposure. At LE accumulation of polyubiquitinated IκBα is observed in the case of Velcade and MG132 treatment. (D) Cells were treated as described in (C) and either stimulated with TNF-α (20 $ng \cdot mL^{-1}$ of medium) for 30 min or left unstimulated and the lysates were analyzed by WB. Cropped image blots for each antibody are of the same exposure and from the same experiment, represented in a convenient manner. Symbol ► corresponds to trans-expressed FLAG-PSMD9 and symbol △ corresponds to the endogenous PSMD9. (E) HEK293 FLAG-PSMD9 stable clones and pCMV-10 empty vector stable clones were transiently co-transfected with pTRIPZ-IκBα-SR and pEGFPN3 vector. Cells were induced with doxycycline (1 $\mu g \cdot mL^{-1}$ of medium) for 48 h and treated with TNF-α (20 $ng \cdot mL^{-1}$ of medium) for 0, 10, 20 and 30 min. Cell lysates were prepared and analyzed by WB. Symbol ► corresponds to trans-expressed FLAG-IκBα-SR or FLAG-PSMD9 and symbol ▷ corresponds to the endogenous IκBα or PSMD9. (F) HEK293 FLAG-PSMD9 stable clones and pCMV-10 empty vector stable clones were co-transfected with pTRIPZ-IκBα-SR and 3x κB ConA luc vector or ConA luc control vector and induced with doxycycline (1 $\mu g \cdot mL^{-1}$ of medium). After 36 h of induction cells were treated with TNF-α (20 $ng \cdot mL^{-1}$ of medium) for 12 h. Cell lysates were prepared and NF-κB activity was measured as described in Fig. 2B. Data represent mean luciferase activity per microgram of protein ± SEM of two independent experiments done in duplicate.

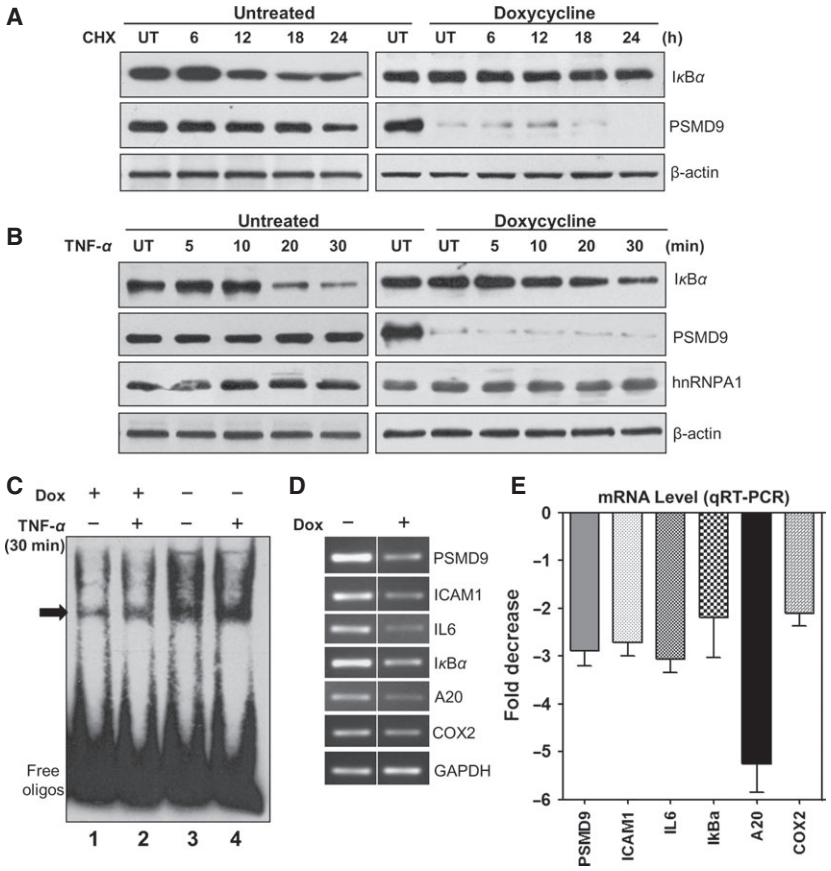

Fig. 5. PSMD9 knockdown reduces basal and TNF-α mediated IκBα degradation and NF-κB activation. (A) HEK293 inducible stable clones expressing PSMD9-shRNA were treated with doxycycline (4 $\mu g \cdot mL^{-1}$ of medium for 48 h) and/or CHX (50 $\mu g \cdot mL^{-1}$ of medium for 1, 2, 4, 6, 8, 12, 18 and 24 h) or left untreated. Cell lysates were prepared and analyzed by WB. (B) Both doxycycline treated or untreated PSMD9 knockdown inducible stable clones were stimulated with TNF-α (20 $ng \cdot mL^{-1}$ of medium) for 0, 5, 10, 20 and 30 min. Cell lysates were subjected to WB. (C) Nuclear fractions of both doxycycline and TNF-α treated or untreated PSMD9 knockdown stable inducible clones were subjected to EMSA. The upper band corresponds to NF-κB DNA binding activity in doxycycline positive (lanes 1 and 2) and doxycycline negative (lanes 3 and 4) cells. (D) PSMD9 knockdown inducible stable clones either treated with doxycycline for 48 h or left untreated. RNA was isolated and semi-quantitative RT-PCR was performed for five different target genes; the PCR products were run in a 2% agarose gel. (E) Real-time PCR was performed for the same five different target genes. The graph represents the glyceraldehyde-3-phosphate dehydrogenase (GAPDH) normalized mean fold decrease in mRNA level of the genes ± SEM for three independent experiments done in duplicate.

The PDZ domain of PSMD9 interacts with hnRNPA1

Point mutations in the PDZ domain of PSMD9 inhibit *in vitro* binding of hnRNPA1 (*FEBS Open Bio*, submitted). Since hnRNPA1 interacts with PSMD9 through its C-terminal residues, this interaction represents a typical PDZ domain–motif interface. We checked if this domain–motif recognition is also a key determinant of interaction inside the cells. We recently showed that Q181G and the β2 L124G/Q126G/E128G triple mutant (all in the PDZ domain) abolished interaction with PSMD9 while L173G (also in the PDZ domain) did not affect binding (*FEBS Open Bio*, submitted). To check the functional relevance of these mutations, we overexpressed FLAG-tagged wt-PSMD9, Q181G-PSMD9, L173G-PSMD9 or the β2 L124G/Q126G/E128G triple mutant in HEK293 cells. Endogenous hnRNPA1 was immunoprecipitated from each cell lysate and probed with FLAG antibody. In accordance with the *in vitro* pull-down assays, wt-PSMD9 and L173G-PSMD9 were detected in the IP complexes. However, neither the Q181G mutant nor the triple mutant of PSMD9 could be detected in these IP complexes (Fig. 7A).

Presence of IκBα was tested in the IP complex from cell lysates of HEK293 cells overexpressing wt-PSMD9, Q181G or the β2 L124G/Q126G/E128G triple mutant. IκBα was detected only in the wt-PSMD9–hnRNPA1

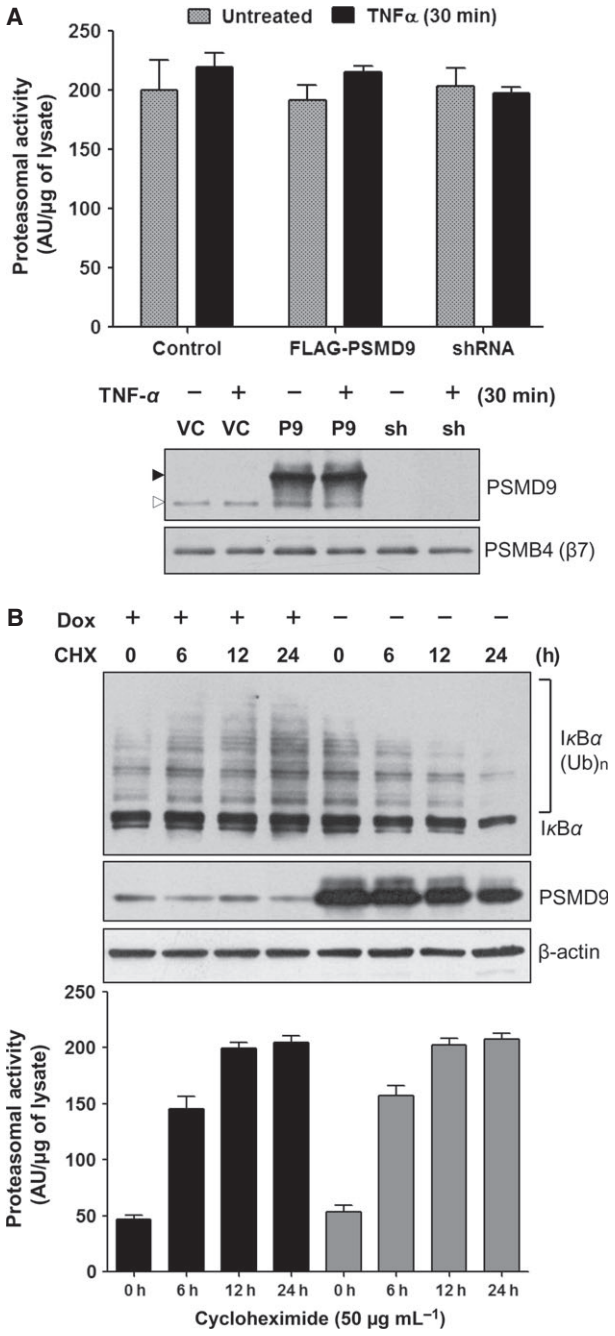

Fig. 6. PSMD9 does not affect proteasomal activity and IκBα ubiquitination. (A) Both the overexpression (FLAG-PSMD9) and knockdown (shRNA) HEK293 inducible stable clones of PSMD9 were treated with doxycycline for 48 h and/or with TNF-α (20 μg·mL^{-1} of medium) for 30 min or left untreated. Cell lysates were prepared with ATP buffer as described in Materials and methods. Proteasomal activity was measured as described in Materials and methods. The Control panel in the graph represents the average value of doxycycline untreated control cells of both the stable clones. Data represent Suc-LLVY-AMC proteasomal activity in arbitrary units (AU·μg^{-1} of lysate) ± SEM of two independent experiments done in duplicate. The WB shows the level expression of PSMD9 in the above cell lysates and PSMB4 is taken as the loading control. Symbol ▶ corresponds to trans-expressed FLAG-PSMD9 and symbol ▷ corresponds to the endogenous PSMD9. (B) HEK293 inducible stable clones expressing PSMD9-shRNA were either treated with doxycycline (4 μg·mL^{-1} of medium for 48 h) or left untreated. In addition cells were treated with MG132 (5 μM) for 2 h followed by treatment with CHX (50 μg·mL^{-1} of medium) for 0, 6, 12 and 24 h. Cell lysates were prepared and analyzed by WB. The graph represents the proteasomal activity, measured as described in Materials and methods, of cells for the above experimental conditions.

complex but not in PDZ Q181G and β2 L124G/Q126G/E128G triple mutant IP complexes (Fig. 7B) suggesting that PSMD9 is probably linked to IκBα through hnRNPA1. Unlike cells overexpressing wt-PSMD9, in cells overexpressing PDZ mutants (Q181G and the β2 triple mutant) IκBα was not efficiently degraded even after TNF-α treatment (Fig. 7C) nor was there a significant change in NF-κB activity (Fig. 7D). In addition, properties of L173G PSMD9 mutant were similar to those of wt-PSMD9 and cells expressing this mutant showed faster IκBα degradation and enhanced NF-κB activation (Fig. 7E,F). These results confirm that specific residues on the PDZ domain of PSMD9 form the interface for binding hnRNPA1 and this domain–motif interaction plays an important role in the NF-κB activation pathway.

PSMD9 is linked to IκBα via hnRNPA1

hnRNPA1 was previously shown to interact with IκBα through its RNA binding domain [12]. We demonstrated that PSMD9 interacted with hnRNPA1 through its C-terminus. And the PDZ mutation analysis indicates that the interaction between PSMD9 and IκBα is probably through hnRNPA1. To determine the structural hierarchy of this tripartite interaction between PSMD9, hnRNPA1 and IκBα, we performed both *ex vivo* and *in vitro* interaction studies. We first verified whether interaction of hnRNPA1 with PSMD9 and IκBα is mutually exclusive or not. When HA-tagged wt-hnRNPA1 and CΔ7hnRNPA1 mutant were pulled down, IκBα was detected in both the pull-down complexes (Fig. 8A) suggesting that C-terminus deletion of hnRNPA1 does not affect its interaction with IκBα. In contrast, PSMD9 was found only in the wt-hnRNPA1–IκBα complex. As inferred from the failure of PDZ mutants to interact with IκBα in the absence of hnRNPA1, these results suggest that wt-PSMD9 and IκBα interaction is indirect and is through hnRNPA1. To further validate these

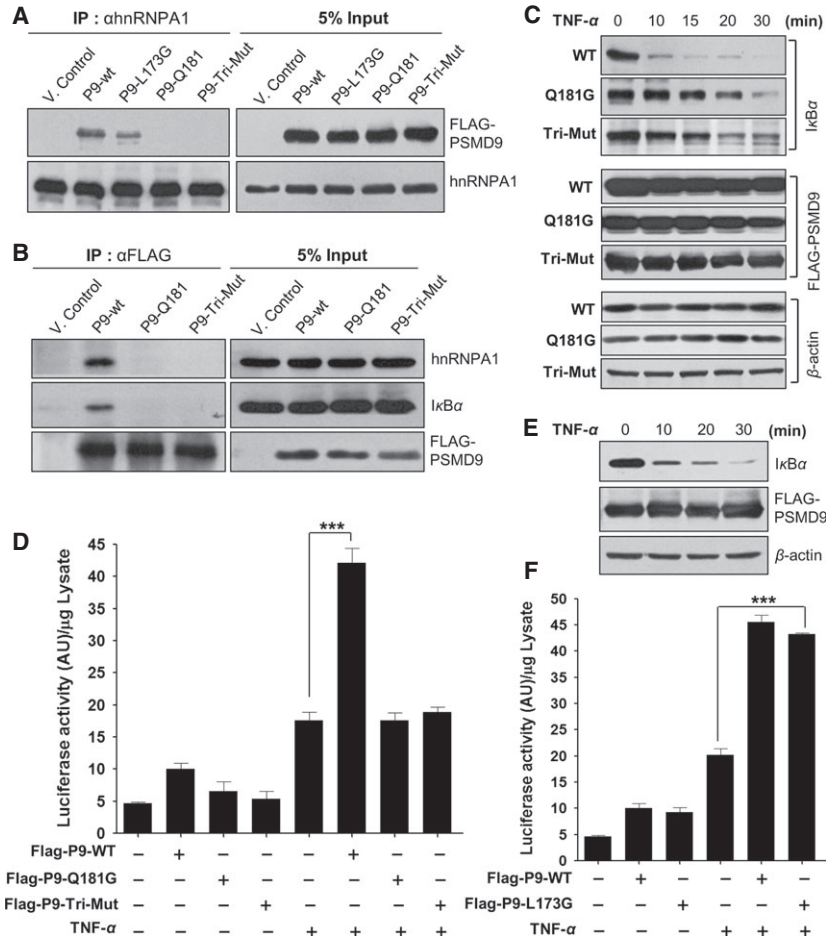

Fig. 7. The PDZ domain of PSMD9 is important for NF-κB activation and IκBα degradation. (A) HEK293 cells were transiently transfected with p3xFLAG-CMV-10-PSMD9, p3xFLAG-CMV-10-PSMD9(L173G), p3xFLAG-CMV-10-PSMD9(triple mutant) or p3xFLAG-CMV-10-PSMD9 (Q181G). Endogenous hnRNPA1 was immunoprecipitated from the cell lysates of the above transfected cells, probed with FLAG antibody and analyzed by WB. (B) HEK293 cells were transiently transfected with p3xFLAG-CMV-10 empty vector/p3xFLAG-CMV-10-wt-PSMD9/ p3xFLAG-CMV-10-PSMD9(Q181G)/p3xFLAG-CMV-10-PSMD9(triple mutant). Cell lysates were incubated with anti-FLAG M2 agarose beads and pull complexes were probed with hnRNPA1, IκBα, FLAG antibodies and analyzed by WB. (C) HEK293 cells were transiently transfected with p3xFLAG-CMV-10-PSMD9/p3xFLAG-CMV-10-PSMD9(Q181G)/p3xFLAG-CMV-10-PSMD9 (triple mutant). After 48 h of transfection cells were treated with TNF-α (20 ng·mL^{-1} of medium) for 10, 15, 20, 30 min or left untreated. Cell lysates were prepared and analyzed by WB. (D) HEK293 cells were co-transfected with p3xFLAG-CMV-10 empty vector or p3xFLAG-CMV-10-PSMD9 (wt, Q181G, triple mutant) and 3x κB ConA luc vector or ConA luc control vector. After 36 h cells were either treated with TNF-α (20 ng·mL^{-1} of medium) for 12 h or left untreated. Cell lysates were prepared and NF-κB activity was measured as described in Fig. 2B. Data represent mean luciferase activity per microgram of protein ± SEM of two independent experiments done in duplicate. (E) HEK293 cells were transiently transfected with p3xFLAG-CMV-10-PSMD9(L173G). After 24 h of transfection cells were treated with TNF-α (20 ng·mL^{-1} of medium) for 12 h or left untreated. Cell lysates were prepared and analyzed by WB. (F) HEK293 cells were co-transfected with p3xFLAG-CMV-10 empty vector or p3xFLAG-CMV-10-PSMD9 (wt or L173G) and 3x κB ConA luc vector or ConA luc control vector. After 36 h cells were either treated with TNF-α (20 ng·mL^{-1} of medium) for 12 h or left untreated. Cell lysates were prepared and NF-κB activity was measured as described in Fig. 2B. Data represent mean luciferase activity per microgram of protein ± SEM of two independent experiments done in duplicate.

observations we overexpressed both the FLAG-tagged wt-IκBα and C-terminal deleted IκBα (amino acids 253–372) in HEK293 cells. As discussed above, C-terminal residues in the ankyrin repeats of murine IκBα are necessary for interaction with hnRNPA1 [12]. When we pulled down the overexpressed FLAG-tagged IκBα, PSMD9 was found in the pull-down complex of wt protein where hnRNPA1 was present and not in the mutant IκBα (which does not interact with hnRNPA1) complex (Fig. 8B). This suggests that

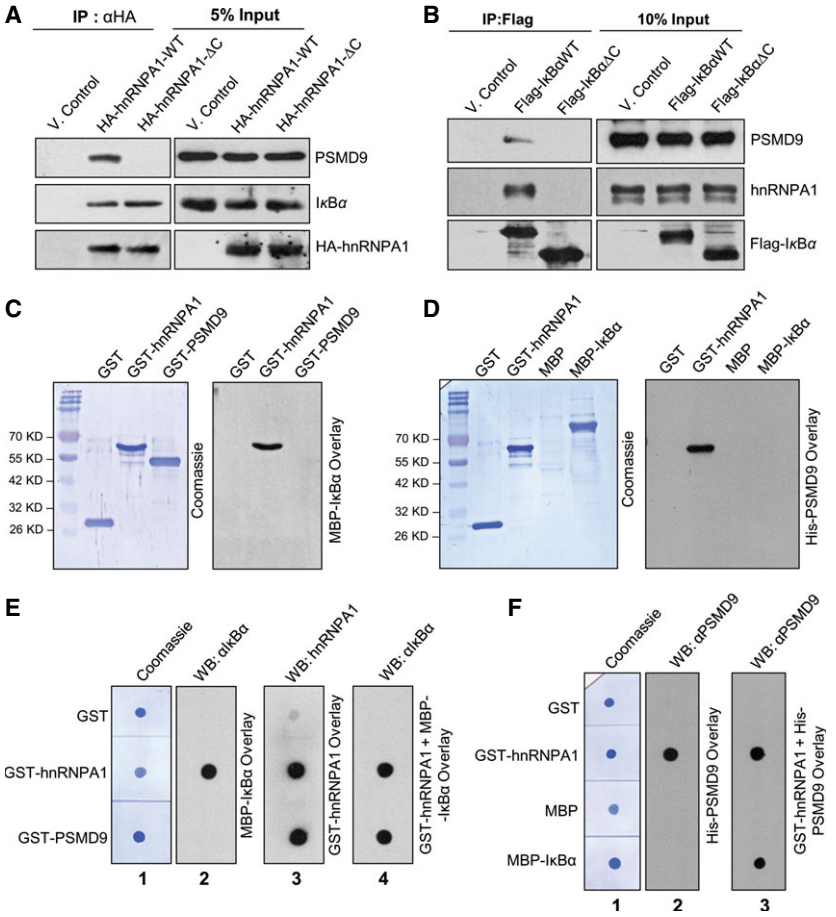

Fig. 8. PSMD9 is linked to IκBα via hnRNPA1. (A) HA-wt-hnRNPA1 and 7ΔC mutant HA-hnRNPA1 were transiently overexpressed in HEK293 cells and cell lysates were incubated with HA antibody-bound Protein-G Sepharose beads. Pull-down complexes were probed with PSMD9 and IκBα antibodies and analyzed by WB. (B) HEK293 cells were transfected with p3xFLAG-CMV-10-wt-IκBα p3xFLAG-CMV-10-ΔCIκBα and cell lysates were incubated with anti-FLAG M2 agarose beads. The pull-down complexes were probed with PSMD9, hnRNPA1 and IκBα antibodies and analyzed by WB. (C) 2 μg of recombinant GST, GST-hnRNPA1 and GST-PSMD9 proteins were run on SDS/PAGE, transferred onto a PVDF membrane and the proteins on the membrane were denatured/renatured using guanidine-HCl AP buffer. Then the membrane was overlaid with recombinant MBP-IκBα (100 nM), probed with IκBα antibody and analyzed by WB. (D) 2 μg of recombinant GST, GST-hnRNPA1 MBP and MBP-IκBα proteins were run on SDS/PAGE, transferred onto a PVDF membrane and the proteins were denatured/renatured on the membrane using guanidine-HCl AP buffer. Then the membrane was overlaid with recombinant His-PSMD9 (100 nM), probed with PSMD9 antibody and analyzed by WB. (E) 1 μg of recombinant GST, GST-hnRNPA1 and GST-PSMD9 proteins were spotted on equilibrated PVDF membrane, blocked with 3% BSA-TBST. The membranes were overlaid with recombinant MBP-IκBα (100 nM) and probed with IκBα antibody (panel 2); overlaid with GST-hnRNPA1 (100 nM) and probed with hnRNPA1 antibody (panel 3); overlaid with both GST-hnRNPA1 (100 nM) and MBP-IκBα (100 nM) and probed with IκBα antibody (panel 4). Panel 1 corresponds to the respective Coomassie stained protein spots on the membrane. (F) 1 μg of recombinant GST, GST-hnRNPA1 MBP and MBP-IκBα proteins were spotted on equilibrated PVDF membrane, blocked with 3% BSA-TBST. The membranes were overlaid with recombinant His-PSMD9 (100 nM) (panel 2) or with both GST-hnRNPA1 (100 nM) and His-PSMD9 (100 nM) (panel 3). Panel 1 corresponds to the respective Coomassie stained protein spots on the membrane.

the interaction between IκBα and PSMD9 is mediated by hnRNPA1.

We performed a series of far western or overlay experiments to substantiate these observations. Recombinant glutathione *S*-transferase (GST) PSMD9 and GST-hnRNPA1 were immobilized on a poly (vinylidene difluoride) (PVDF) membrane followed by overlay of recombinant maltose binding protein (MBP)-IκBα protein and were then probed with IκBα antibody. No IκBα was detected in the GST-PSMD9 lane but it was clearly visible in the GST-hnRNPA1 lane (Fig. 8C). Furthermore, when MBP-IκBα and GST-hnRNPA1 were immobilized on a PVDF membrane, overlaid with His-PSMD9 followed by probing

with PSMD9 antibody, PSMD9 was clearly detected in the GST-hnRNPA1 lane but not in the MBP-IκBα lane (Fig. 8D). In a sandwich dot blot assay, we immobilized GST-PSMD9 on the membrane, followed by overlay with GST or GST-hnRNPA1 and then with MBP-IκBα. When this sandwich was probed with IκBα antibody, MBP-IκBα was found to interact with GST-PSMD9 only when hnRNPA1 was sandwiched in between these two proteins (Fig. 8E). Furthermore, this indirect interaction was validated by reversing the sandwich, i.e. by immobilizing MBP-IκBα and overlay of GST or GST-hnRNPA1 followed by GST-PSMD9 (Fig. 8F). These results altogether confirmed that there is no direct interaction between PSMD9 and IκBα and they can only interact through hnRNPA1, which uses different structural regions for these interactions that are not mutually exclusive.

Interaction between C-terminus of hnRNPA1 and PSMD9 is required for degradation of IκBα as well as NF-κB activity

The involvement of hnRNPA1 in IκBα degradation was shown previously [12]. We have demonstrated here a novel role of PSMD9 and a specific interaction between the PDZ domain of PSMD9 and a SLIM at the C-terminus of hnRNPA1. We asked if hnRNPA1 has any role to play in IκBα degradation/NF-κB activation when interaction with PSMD9 is lost or in the absence of PSMD9. When HA-wt-hnRNPA1 was trans-expressed in HEK293 cells, degradation of IκBα was considerably enhanced after 10 min of TNF-α treatment (Fig. 9A). HA-7ΔChnRNPA1 mutant, on the other hand, had no influence on the degradation of IκBα. Correspondingly, only the HA-wt-hnRNPA1

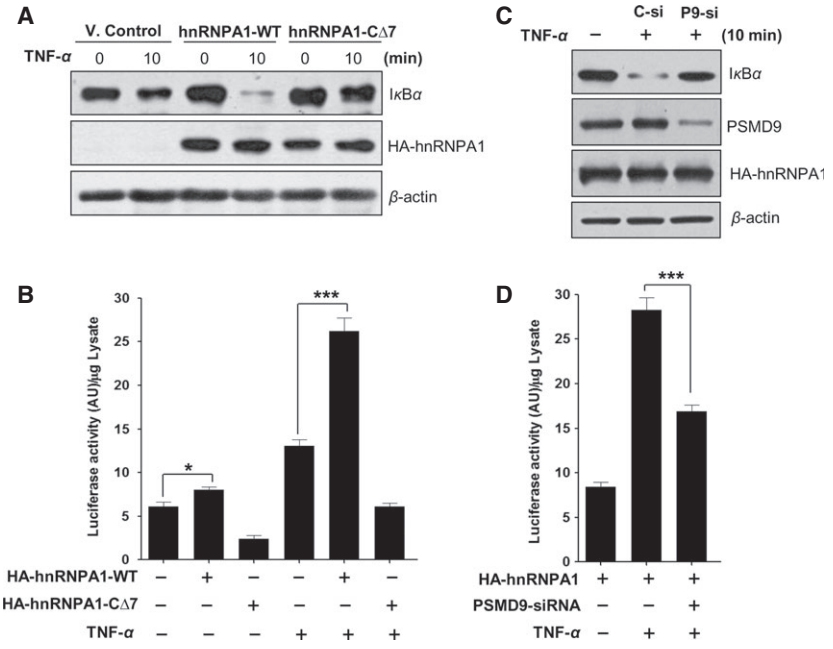

Fig. 9. C-terminus deleted hnRNPA1 mutant fails to enhance TNF-α mediated IκBα degradation and NF-κB activation. (A) HA-wt-hnRNPA1 and 7ΔC mutant HA-hnRNPA1 were transiently overexpressed in HEK293 cells and after 48 h cells were treated with TNF-α (20 ng·mL^{-1} of medium) for 10 min or left untreated. Cell lysates were prepared along with vector control and subjected to WB analysis. (B) HEK293 cells were co-transfected with pCDNA3.1-HA-empty vector or pCDNA3.1-HA-hnRNPA1 (wt or 7ΔC mutant) and 3x κB ConA luc vector or ConA luc control vector. After 36 h cells were either treated with TNF-α (20 ng·mL^{-1} of medium) for 12 h or left untreated. Cell lysates were prepared and NF-κB activity was measured as described in Fig. 2B. Data represent mean luciferase activity per microgram of protein ± SEM of three independent experiments done in duplicate. (C) HEK293 cells were transfected with PSMD9-siRNA/control-siRNA (100 μM) and after 48 h cells were again transfected with pCDNA3.1-HA-wt-hnRNPA1. After 72 h of siRNA transfection cells were either treated with TNF-α (20 ng·mL^{-1} of medium) for 20 min or left untreated. Cell lysates were prepared and analyzed by WB. (D) HEK293 cells were transfected with PSMD9-siRNA/control-siRNA (100 μM) and after 48 h cells were again transfected with pCDNA3.1-HA-wt-hnRNPA1 and 3x κB ConA luc vector or ConA luc control vector. After 60 h of siRNA transfection cells were either treated with TNF-α (20 ng·mL^{-1} of medium) for 12 h or left untreated. Cell lysates were prepared and NF-κB activity was measured as described in Fig. 2B. Data represent mean luciferase activity per microgram of protein ± SEM of two independent experiments done in duplicate.

transfected cells showed a significant increase in NF-κB activity after TNF-α treatment (Fig. 9B). In contrast, cells expressing HA-7ΔChnRNPA1 mutant showed a lower NF-κB activity compared with the control cells. Furthermore, when we silenced PSMD9 and overexpressed HA-wt-hnRNPA1, TNF-α mediated IκBα degradation was significantly reduced (Fig. 9C). In addition, a considerable decrease (up to 40%) in NF-κB activity was also observed in these cells (Fig. 9D). These results suggest that both PSMD9 and hnRNPA1 are in the same pathway and further support the role of PSMD9–hnRNPA1interaction in IκBα degradation and NF-κB activation.

PSMD9 anchors hnRNPA1–IκBα complex on 26S proteasome which facilitates proteasomal degradation of IκBα

PSMD9 is known to be a chaperone of proteasome assembly and is reported to dissociate before the mature complex [1,2,41]. Nas2, the yeast homolog, was not found in any of the cryo EM studies of the proteasome [42–44]. Like other classical chaperones, PSMD9 or its homologs may only be transiently associated with the assembled proteasome. We hypothesized that PSMD9, by virtue of its interaction with the proteasome on one hand and its interaction with hnRNPA1 on the other, would recruit IκBα to the proteasome for degradation. We first asked if endogenous or trans-expressed FLAG-PSMD9 could be located in the proteasome complex. We pulled down the whole 26S proteasomal complex using β7-subunit antibody. When probed for PSMD9 antibody we found both endogenous and FLAG-tagged PSMD9 in the complex. To ensure that PSMD9 is associated with the intact 26S mature complex, we probed the complex for the presence of ATPase subunit (Rpt6), a marker for the base subcomplex, and α5-subunit, a marker of 20S core particle. The results showed that β7-subunit antibody pulls down the intact 26S complex and PSMD9 is indeed associated with the mature proteasome (PSMD9 is not shown to interact with Rpt6). TNF-α treatment did not alter the levels of either endogenous or overexpressed PSMD9 in stable clones. But there was a definite increase in the levels of proteasome bound hnRNPA1 in PSMD9 overexpressing cells which were further enhanced upon TNF-α treatment (Fig. 10A). In contrast, when PSMD9 was silenced, no hnRNPA1 was found in the proteasome pull-down complex even after TNF-α treatment. These results together indicate that recruitment of hnRNPA1 to the proteasome requires the presence of PSMD9.

To enable the degradation of IκBα by the proteasome, PSMD9 not only has to interact with hnRNPA1 but should also interact with the proteasome as demonstrated above. However, based on current evidence PSMD9 seems to harbor only the PDZ-like domain for protein–protein interaction. Therefore it was important to test whether the PDZ mutations affect association of PSMD9 with the proteasome. Affinity pull-down of the 26S proteasome in cells overexpressing PDZ mutant Q181G indicated that this association was unimpaired (Fig. 10B). Proteasomal activity was also unaffected by this mutant (Fig. 10C). Probably there are other regions in PSMD9 that can interact with the proteasome. Although PSMD9 mutants cannot bind to hnRNPA1 because of the endogenous PSMD9, some hnRNPA1 could still be detected in the pull-down complex (Fig. 10B). These results further validate the role of the PDZ domain in proteasomal degradation of IκBα through interaction of PSMD9 with hnRNPA1. In addition these results indicate that PSMD9 functions as an anchor rather than a chaperone and bridges IκBα bound hnRNPA1 to the proteasome. This interaction enables regulated degradation of IκBα and modulates NF-κB activity.

While there is no clear evidence for the presence of PSMD9 on mature proteasomes or for the role of PDZ domains in interaction with ATPase subunits in mammalian cells, the lack of any detectable effect of PDZ domain mutations on the association of PSMD9 with intact 26S proteasomes requires further explanation. To address this we analysed the primary sequence of PSMC6 (Rpt4) and PSMC3 (Rpt5). GRRF was present in PSMC6. Intrigued we co-expressed wt-PSMD9 or PSMD9-Q181G mutant with wt-PSMC6 and performed co-immunoprecipitation studies. The results showed that the Q181G mutation which inhibits binding of PSMD9 to hnRNPA1 does not affect PSMD9 binding to PSMC6 (Fig. 10D). This result in conjunction with the observation that the PDZ mutations do not affect PSMD9 association with proteasome indicates that the interaction with the mature proteasome may not involve Rpt5. Moreover Rpt5 C-terminus is known to play a key role in interaction with the 20S α-subunit necessary for gate opening and activation of the proteasome. Therefore, Rpt5 on mature proteasome is unlikely to interact with PSMD9.

Since we found increased IκBα degradation upon hnRNPA1 overexpression with TNF-α treatment, we wanted to check the recruitment of overexpressed hnRNPA1 on 26S proteasome. HA-hnRNPA1 was overexpressed in HEK293 cells and treated with TNF-α (20 ng for 30 min). Cell lysates were prepared in ATP buffer and 26S proteasome was pulled down

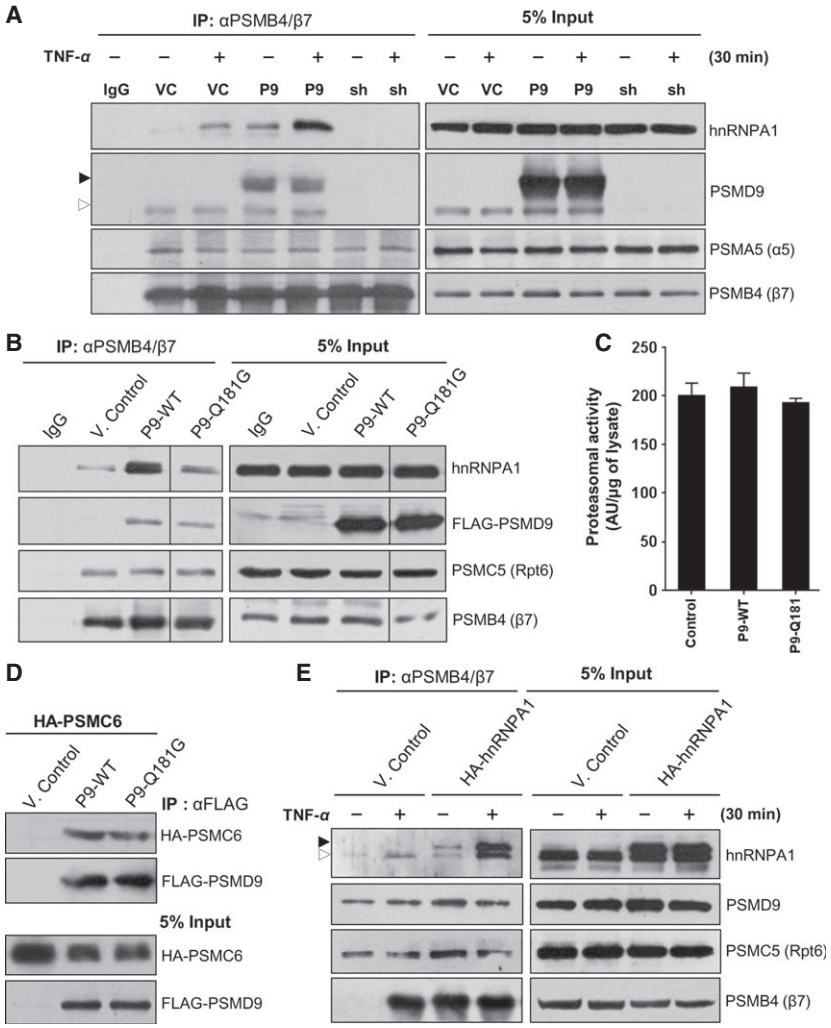

Fig. 10. PSMD9 is crucial for the recruitment of hnRNPA1-IκBα complex on 26S proteasome. (A) Both the overexpression (P9) and knockdown (sh) HEK293 inducible stable clones of PSMD9 were treated with doxycycline for 48 h and/or with TNF-α (20 ng·mL^{-1} of medium) for the next 30 min or left untreated. Cell lysates were prepared with ATP buffer as described in Materials and methods. Whole 26S proteasome was pulled down from the above cell lysates using β7 antibody and probed with different antibodies and analyzed by WB. Symbol ► corresponds to trans-expressed FLAG-PSMD9 and symbol ▷ corresponds to the endogenous PSMD9. (B) HEK293 cells were transiently transfected with pCMV-10 empty vector or pCMV-10-PSMD9 (wt or mutants D157P/Q181G) and cell lysates were prepared in ATP buffer as in Materials and methods. 26S proteasome was pulled down from the above cell lysates using β7 antibody and probed with different antibodies as indicated and analyzed by WB. (C) Proteasomal activity of the above mentioned (in B) cell lysates was measured as described in Materials and methods. Data represent Suc-LLVY-AMC proteasomal activity in arbitrary units (AU·μg^{-1} of lysate) ± SEM of two independent experiments done in duplicate. The WB shows the expression of FLAG-PSMD9 in the above cell lysates and PSMB4 is taken as the loading control. (D) HEK293 cells were co-transfected with pCDNA3.1-PSMC6 and p3X-FLAG-CMV-10, p3X-FLAG-CMV-10-wt-PSMD9 or p3X-FLAG-CMV-10-Q181G-PSMD9. After 48 h of transfection cell lysates were used for pull-down with anti-FLAG-M2 agarose beads and analyzed by WB. (E) HEK293 cells were transfected with pCDNA3.1 empty vector or pCDNA3.1-HA-wt-hnRNPA1 and after 48 h of transfection cells were treated with TNF-α for 30 min. Cell lysates were prepared in ATP buffer (as described in Materials and methods); 26S proteasome was pulled down using β7 antibody and analyzed by WB. Symbol ► corresponds to trans-expressed HA-hnRNPA1 and symbol ▷ corresponds to the endogenous hnRNPA1.

using β7 antibody. When the pull-down complexes were probed with hnRNPA1 antibody, both endogenous and trans-expressed hnRNPA1 levels were found to be increased upon TNF-α treatment, which correlates with the IκBα degradation (Fig. 10E). Furthermore levels of hnRNPA1 remain unaltered upon PSMD9 overexpression (Fig. 4B) or downregulation (Fig. 5B) or after TNF-α treatment. These results are strongly suggestive of a mechanism which involves recruitment of hnRNPA1 to the proteasome complex

during TNF-α signaling that would result in more and more IκBα degradation by the proteasome. Our attempts to substantiate this by capturing IκBα on 26S proteasome with/without TNF-α treatment under hnRNPA1 or PSMD9 overexpressing conditions failed perhaps due to its rapid degradation by the proteasome. Hence all these results suggest that hnRNPA1 either recruits or presents IκBα to the proteasome and this shuttle receptor hnRNPA1 is anchored by PSMD9 on the proteasome. While ubiquitinated IκBα is degraded, hnRNPA1 in all probability is released intact. It is possible that the PSMD9–hnRNPA1 interaction shortens the distance between the substrate and the proteasomal ATPases or ensures that IκBα is not prematurely released from the proteasome.

Discussion

Protein–protein interactions are seminal to signal transduction. They are involved in spatiotemporal regulation of cellular functions. Therefore, identification of novel interactions can help in deciphering unknown functions of a protein. We have established bioinformatics methods for identification of unknown interacting partners of 19S subunits of the proteasome (*FEBS Open Bio*, submitted). Using one such method we identified hnRNPA1, an RNA binding protein involved in RNA metabolism and transport [34], as a novel interacting partner of PSMD9, a PDZ domain containing a subunit of the proteasome. To test whether this interaction is physiologically relevant and to identify functions associated with the interaction, we searched for the reported functions of hnRNPA1. The N-terminal of hnRNPA1 binds to ankyrin repeats in IκBα and this interaction somehow influences the processing of IκBα, the nature or mechanism of which is unclear [12]. Here we demonstrate that PSMD9 through its PDZ domain interacts with hnRNPA1 C-terminus and this domain–motif interaction is necessary for the proteasomal degradation of IκBα. Overexpression of PSMD9 accelerates both basal and TNF-α mediated proteasomal degradation of IκBα. This results in increased NF-κB activation and expression of its target genes. We establish a new role for hnRNPA1 as a shuttle receptor for the degradation of IκBα in HEK293 cells. PSMD9, contrary to its expected role as a chaperone, acts as a part of the 19S recognition module to facilitate delivery of ubiquitinated IκBα to the proteasome via hnRNPA1, as depicted in the model (Fig. 11).

Although the degradation of IκBα by the proteasome has long been established, the mechanism of how it is recruited to the proteasome is not well defined. Here we show how ubiquitinated IκBα is targeted to the proteasome for degradation. This is important because how ubiquitinated substrates in general are recruited to the proteasome is an active area of research. So far two modes of substrate recognition have been well defined. In the direct mode, substrates are recognized by the ubiquitin binding motifs in 19S subunits like Rpn10 containing the UIM domain, or via motifs like pleckstrin in Rpn13 [45,46]. In the indirect mode of recognition, Rad23, Dsk2 and Ddi1 proteins called 'shuttle receptors' bind proteasome

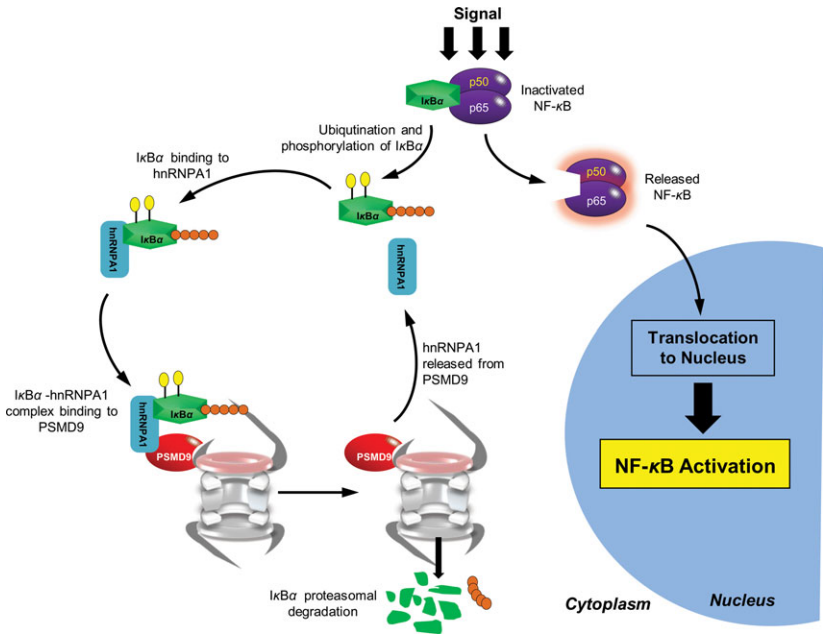

Fig. 11. Model for the mechanism of IκBα presentation and degradation by 26S proteasome. Signal activated and modified IκBα binds to hnRNPA1 and this complex interacts with PSMD9 on 26S proteasome. IκBα gets degraded through proteasomal activity hnRNPA1 shuttles back to bind with free IκBα and the cycle repeats.

through their UBL domains present at the N-terminus while their C-terminal ubiquitin association domain (UBA) binds to ubiquitin chains on the substrates [47,48]. These shuttle receptors bind to the Rpn1 subunit of the proteasome in non-stoichiometric amounts and apparently dissociate with fast kinetics. In an in-depth study, Deshaies group showed that Ddi1 is a proteasomal shuttle receptor that binds to the LRR1 domain of Rpn1 [49] and facilitates the degradation of Ufo1, a Ddi1 substrate. A UBA domain containing protein, p62, interacts with K63 ubiquitin chains of ubiquitinated tau and facilitates its proteasomal degradation by interacting with Rpt1 through its N-terminal PB1 domain [50]. HSP27 may also act as a shuttle receptor that recruits ubiquitinated IκBα to the proteasome for degradation in cancer cells in response to stress signals [51]. In this report HSP27 was shown to bind ubiquitinated IκBα and to the 19S regulatory particle of the proteasome to mediate this degradation. HSP27 recognizes covalently linked ubiquitin on IκBα but how it interacts with the proteasome is unclear. Recently we have demonstrated that non-ubiquitinated proteins can be directly recognized and degraded by 26S proteasome [10].

We describe our findings in the context of these reported mechanisms of substrate recognition and highlight unique features that are an outcome of our study. PSMD9 unlike HSP27 does not directly bind to ubiquitinated IκBα. This interaction is mediated by hnRNPA1 and, therefore, Ub-IκBα is targeted to the proteasome through the indirect pathway. Since the hnRNPA1 level does not change under any conditions tested here, we argue that it acts as a shuttle receptor that brings in Ub-IκBα. Since hnRNPA1 lacks a UBL-like domain, it does not bind to the proteasome in a classical manner like other shuttle receptors. Instead this function is mediated by a C-terminal region of the protein which acts as a recognition signal for the PDZ domain of PSMD9 bound to the proteasome. PDZ domains can recognize native sequences in proteins typically through the C-terminal residues. Such a classical domain–motif interaction for PSMD9–hnRNPA1 is established by our study. Nevertheless, the exact mechanism of hnRNPA1 release, the mode of binding of PSMD9 to the proteasome and the molecular basis of this recognition remain to be investigated.

While our studies show how PSMD9 directly affects the degradation of IκBα by the proteasome which helps in NF-κB activation, there are several upstream steps that process IκBα for degradation. A possible role of PSMD9 in these processes has been somewhat addressed in this study. Since in the absence of any external stimuli PSMD9 overexpression results in increased basal activity of NF-κB, it remains to be seen whether PSMD9 acts as an internal signal for NF-κB activation. This may be dependent or independent of its interaction with hnRNPA1. Previously it was reported that in cells lacking hnRNPA1 (mouse leukemic cells) NF-κB, activity is reduced [12]. Likewise in the current study we show that in cells lacking PSMD9 NF-κB, activity is reduced. Taken together, these studies suggest that PSMD9 and hnRNPA1 are probably not mutually exclusive in the context of the NF-κB signaling pathway which may be explained by their ability to interact with each other.

It will be important to see whether the mechanism of IκBα degradation and NF-κB activity is general to other cell types. While hnRNPA1 is a ubiquitous protein, PSMD9 may be expressed in a cell or tissue specific manner [3]. Although PSMD9 deletion is not lethal in yeast [52], loss of PSMD9 expression may have phenotypic consequences in mammalian cells due to inhibition of NF-κB activity. We have demonstrated that the PDZ domain mutants do not bind to hnRNPA1 and therefore their overexpression does not affect NF-κB activity. Thus small molecules that can target the interaction sites on the PDZ domain of PSMD9 are likely to act as inhibitors of NF-κB activity. Such molecules may be useful in targeting cancer cells that are dependent on a consistently high NF-κB activity for their survival [53,54]. The first step in this direction, however, is to establish the role of the PSMD9–hnRNPA1 interaction in this pathway in such cancer cells.

Based on our findings on the molecular details of the interaction between the PDZ domain of PSMD9 and hnRNPA1, we speculate about a general role for PSMD9 in substrate recognition by the proteasome. For example IκBα may be one of the many examples of how substrates may converge on the proteasome through the PDZ domain of PSMD9. It is possible that other substrates are brought to the proteasome by a similar mechanism through either hnRNPA1 or other shuttle receptors that may carry a similar recognition motif. In addition, by virtue of its binding to ATPase subunits, PSMD9 on the surface of the 19S regulatory particles may be uniquely positioned to ensure rapid unfolding, prevention of premature release of the substrates and translocation of the unfolded protein through the central channel that lines the ATPase ring. Another aspect of our finding is the nature and origin of the components involved in IκBα degradation – a chaperone from the proteasome pathway and an RNA binding protein. Thus it is speculated that there may be other functions mediated by this domain–motif interaction between PSMD9 and

hnRNPA1 relevant to their respective network and/or the crosstalk between different functional modules.

Two important points reported in the literature regarding the association of PSMD9 with proteasomes merit special attention: (a) chaperones such as PSMD9 and PSMD10 have not been found as part of the mature proteasome structure [43,44] and (b) Nas-2, the yeast homolog of PSMD9, has been shown to interact with Rpt5 through C-terminal residues implying a role for the PDZ domain in interaction. We believe PSMD9 or PSMD10 may transiently associate with the mature proteasome. It is likely that only few of the mature 26S proteasomes bind these chaperones at any given moment and they can be washed away under very stringent conditions during IPs or affinity purifications. It is interesting to note that reports on the interaction of shuttle receptors such as Ddi1 in yeast with the proteasome have been controversial. Ddi1 belongs to the UBA-UBL domain containing proteins that bind polyubiquitin chains in substrate proteins. Ddi1 is reported by some to physically interact with the intact proteasome while others question this finding. It is argued by Deshaies group, who find that Ddi1 does indeed interact with the proteasome in a specific and functionally relevant manner, that such discrepancies may be due to the qualitative nature of IP experiments and the rapid dynamics of UBL binding to and dissociation from the proteasome. The same could be true for the proteasomal chaperones such as PSMD9 or PSMD10.

Regarding the involvement of the PDZ domain in the interaction with the ATPase subunits, we find that mutations in the PDZ domain of PSMD9 that affect hnRNPA1 binding do not affect the association with the proteasome. While we do not find any literature evidence for the role of PDZ domains in interaction with the ATPases in mammalian cells, Nas2 in yeast has been shown to interact with Rpt5 or PSMC3 via the C-terminal residues [55]. Although we have not tested the interaction of PSMD9 with PSMC3, interaction of PSMD9 with PSMC6 is unaffected by the PDZ mutations (current study). It is possible that the association of PSMD9 with the mature proteasome is different from its interaction with the ATPase subunits in the modular structure. It is obvious that we are far from a clear understanding of the role of PSMD9 in the functioning of holo 26S proteasome and its interaction with the different subunits. More studies with detailed molecular characterization as reported in this current study will be necessary to clarify the complexity associated with these supramolecular structures.

In summary, we have established that PSMD9 through its PDZ domain interacts with the C-terminus of hnRNPA1, a novel interacting partner, and this interaction regulates degradation of IκBα and, therefore, NF-κB activity in HEK293 cells. hnRNPA1 acts as a shuttle receptor while PSMD9 is the docking site on the 19S regulatory particle. IκBα may be one of the many examples of how ubiquitinated substrates may be recruited on the proteasome through the PDZ domain of PSMD9. It is possible that features of the C-terminal sequence found in hnRNPA1 may be conserved in other shuttle receptors. Our study opens up new areas of investigation on the role of PSMD9 in cellular homeostasis. The generality of this interaction between hnRNPA1 and PSMD9 may propose the interface as a potential drug target in tumor cells relying on high NF-κB activity. Moreover, the interaction between hnRNPA1, a protein well known for mRNA transport and splicing, and PSMD9, a subunit chaperone of the proteasome, is intriguing. Although speculative, whether this interaction influences these well known functions of hnRNPA1 and whether there is crosstalk between the degradation pathway and the RNA metabolism remains to be seen.

Materials and methods

Plasmids

PSMD9 was amplified from PSMD9 cDNA (Origene Technologies) and cloned within *Hin*dIII and *Eco*RI in p3xFLAG-CMV-10 mammalian expression vector (Sigma, USA). For bacterial expression vector pRSETA, *Bam*HI and *Xho*I sites are used for cloning PSMD9. The PSMD9 (L173G), PSMD9(Q181G) and PSMD9(triple mutant L124G-Q126G-E128G) mutants were generated in p3xFLAG-CMV-10-PSMD9 construct by site directed mutagenesis. 3xFLAG-tagged PSMD9 was amplified from p3xFLAG-CMV-10-PSMD9 construct using the primers Fw 5′-ACCGGTCGCCACCATGGACTACAAAGACCATG-3′ and Rv 5′-GAATTCGACAATCATCTTTGCAGAGG-3′ cloned between *Age*I and *Eco*RI into doxycycline inducible vector pTRIPZ (a gift from S. Dalal, Advanced Center for Treatment, Research and Education in Cancer, Navi Mumbai, India). mir30 based shRNA of PSMD9 was PCR amplified using the primers Fw 3′-GGCTCGAGGAAGGTATATTGCTGTTGACAGTGAGCGGCAGATCAAGGCCAACTATGATAGTGAAGCCACAGATGT-3′ and Rv 5′-GCGAATTCCCGAGGCAGTAGGCAGCAGATCAAGGCCAACTATGATACA TCTGTGGCTTCACTATCATAG-3′. The PCR product was digested with *Xho*I and *Eco*RI and inserted into doxycycline inducible vector pTRIPZ. hnRNPA1 was PCR amplified from HEK293 cDNA library generated by RT-PCR of RNA from HEK293 cells and cloned within *Bam*HI and *Xho*I in HA-pCDNA3.1 mammalian expression vector (gift from S. Dalal, Advanced Center for

Treatment, Research and Education in Cancer, Navi Mumbai, India). For bacterial expression vector pGEX-4T-1, *Bam*HI and *Eco*RI sites were used for cloning hnRNPA1. The hnRNPA1(Δ7C) mutant was generated by deleting seven amino acids from the C-terminus. wt IκBα and ΔC mutant (1–252 amino acids) IκBα were amplified from HEK293 cDNA and were cloned into mammalian expression vector p3xFLAG-CMV-10 vector using *Hin*dIII and *Eco*RI sites. wt IκBα was cloned into bacterial expression vector pMALc5X within *Bam*HI and *Eco*RI sites. PSMC6 was PCR amplified from the HEK293 cDNA library generated by RT-PCR of RNA from HEK293 cells and cloned within *Bam*HI and *Xho*I in HA-pCDNA3.1 mammalian expression vector (gift from S. Dalal, Advanced Center for Treatment, Research and Education in Cancer, Navi Mumbai, India). The phospho-mutant pTRIPZ- IκBαSR (S32A–S36A) vector (gift from N. Shirsat, Advanced Center for Treatment, Research and Education in Cancer, Navi Mumbai, India, and D. C. Guttridge, Ohio State University, USA), pEGFPN3 vector and pBSK3 vectors were used for mammalian cell transfection. 3x κB ConA luc vector and ConA luc control vector (gift from N. D. Perkins, Newcastle University, UK) were used for the luciferase reporter assay.

Expression, purification of recombinant proteins

Recombinant His-PSMD9, GST-PSMD9, GST-hnRNPA1 and MBP-IκBα were expressed in *Escherichia coli* BL21 DE(3) using 100 μM isopropyl thio-β-D-galactoside at 18 °C for 18 h. His-PSMD9 and its mutant were purified by Ni-nitrilotriacetic acid column chromatography (Qiagen, Hilden, Germany) using 250 mM imidazole buffer; GST, GST-PSMD9 and GST-hnRNPA1 were purified using glutathione Sepharose beads (GE Healthcare Life Sciences, Amersham, UK) and MBP, MBP-IκBα were purified using amylose beads (NEB, UK) and 10 mM maltose buffer, according to the manufacturer's protocol. His-PSMD9 was FPLC purified using a Superdex-200 column (Amersham, GE Healthcare Life Science).

Far western blot and dot blot

Recombinant GST-PSMD9, GST-hnRNPA1 and MBP-IκBα proteins (2 μg each) were SDS denatured, run on an SDS/PAGE and transferred onto a PVDF membrane. The transferred proteins were denatured/renatured on the membrane using guanidine-HCl AC buffer with the protocol described in Yuliang Wu *et al.* [56]. For dot blot 1 μg of recombinant proteins (GST, GST-hnRNPA1, GST-PSMD9, MBP and MBP-IκBα) were spotted on a methanol equilibrated PVDF membrane. The spotted membranes were blocked in 3% BSA-TBST and overlaid with either His-PSMD9 or MBP-IκBα (100 nM in 1% BSA-TBST) for 1 h. Anti-PSMD9 (mouse monoclonal; Sigma) in 1 : 4000 dilution, anti-hnRNPA1 (mouse monoclonal; Sigma) in 1 : 4000 dilution and anti-IκBα (rabbit polyclonal; Sigma) in 1 : 4000 dilution were used for probing the overlaid proteins.

Cell culture, transfection and reagents

HEK293 cells were cultured in DMEM (Gibco, USA) supplemented with 10% fetal bovine serum (Gibco), 100 IU·mL^{-1} penicillin (Sigma) and 100 μg·mL^{-1} streptomycin (Sigma). For transfection Lipofectamine 2000 (Invitrogen, Carlsbad, CA, USA) or the calcium phosphate method were used according to the manufacturer's protocol. 100 μM of PSMD9 small interfering RNA (siRNA) (Dharmacon; Thermo Scientific, Waltham, MA, USA) or scrambled siRNA (Dharmacon; Thermo Scientific) with Lipofectamine 2000 was used for transfection. Doxycycline (Sigma) 1–4 μg·mL^{-1} of medium, CHX (Sigma) 50 μg·mL^{-1} of medium, TNF-α (Peprotech, Rocky Hill, NJ, USA) 20 ng·mL^{-1} of medium, MG132 (Sigma) 10 μM·mL^{-1} of medium and Velcade (Johnson & Johnson, NJ, USA) 10 μg·mL^{-1} of medium were used for different experiments.

Establishment of stable cell line

HEK293 cells were transfected with p3xFLAG-CMV-10 and p3xFLAG-CMV-10-PSMD9 constructs using Lipofectamine 2000 (Invitrogen) to generate PSMD9 overexpressing stable clones. After 24 h, transfected cells were subcultured and kept under selection in DMEM supplemented with 10% fetal bovine serum and 800 μg·mL^{-1} of G418 (Sigma). After 2–4 weeks G418 resistant single colonies were picked up and grown in DMEM supplemented with 10% fetal bovine serum and 400 μg·mL^{-1} of G418. Three different clones with high FLAG-PSMD9 expression were selected for further studies. For generating doxycycline inducible stable clones, HEK293 cells were transfected with pTRIPZ, pTRIPZ-3xFLAG-PSMD9, pTRIPZ-shRNA-PSMD9 using Lipofectamine 2000. After 24 h transfected cells were subcultured and kept under selection in DMEM supplemented with 10% fetal bovine serum and 800 ng·mL^{-1} puromycin (Sigma). After 5–7 days puromycin resistant single colonies were picked up and grown in DMEM supplemented with 10% fetal bovine serum and 400 ng·mL^{-1} puromycin. Three clones with high FLAG-PSMD9 expression and three clones with maximum PSMD9 knockdown upon doxycycline induction were selected for further studies.

Immunoprecipitation

Cells were pelleted, washed twice with NaCl/P_i and lysed in NP-40 lysis buffer [50 mM Tris pH 7.6, 150 mM NaCl, 0.5% NP-40 detergent, 10 mM NaF, 1 mM Na_2VO_5, 10 mM β-glycerophosphate and 1× protease inhibitor cocktail (Sigma,

P2714)]. For proteasomal pull-down, buffer containing 50 mM Tris (pH 7.6), 5 mM $MgCl_2$, 1 mM ATP, 10% glycerol and 1× protease inhibitor cocktail (Sigma) was used. Briefly, monoclonal antibodies (1 : 1000 vol/vol of antibody : cell lysate) were bound overnight to Protein-G Sepharose beads (GE Amersham) and pre-cleared cell extracts were incubated with antibody-bound Sepharose beads or anti-FLAG M2 agarose (Sigma) for 3 h at 4 °C. After extensive washing with washing buffer [50 mM Tris, pH 7.6, 150–450 mM NaCl, 10 mM NaF, 1 mM Na_2VO_5, 10 mM β-glycerophosphate and 1× protease inhibitor cocktail (Sigma, P2714)], immune complexes were separated by SDS/PAGE and analyzed by western blotting, following standard protocols.

Luciferase reporter assay

Stable clones of HEK293 harboring FLAG-PSMD9 and HEK293 cells transiently transfected with p3xFLAG-CMV-10/p3xFLAG-CMV-10-PSMD9/p3xFLAG-CMV-10-PSMD9 (D157P)/p3xFLAG-CMV-10-PSMD9(Q181G)/pcDNA3.1-HA-hnRNPA1/pcDNA3.1-HA-hnRNPA1(CΔ7) were co-transfected with ConA luc control or 3x κB ConA luc vectors by the calcium phosphate method. After 48 h, cells were lysed and luciferase assays were performed using the Luciferase Assay System (Promega, Fitchburg, WI, USA) in triplicate. In inducible stable clones of control pTRIPZ and pTRIPZ-3xFLAG-PSMD9 after 48 h of doxycycline addition luciferase assays were performed as explained.

Western blotting and antibodies

Cell lysates were prepared with NP-40 lysis buffer and separated on 12–15% SDS/PAGE gels, and western blot (WB) was performed following standard protocols. Antibodies anti-PSMD9 in 1 : 1000 (mouse monoclonal; Sigma, and rabbit polyclonal; Abcam, Cambridge, UK), anti-FLAG in 1 : 8000 (mouse monoclonal; Sigma), anti-hnRNPA1 in 1 : 1000 (mouse monoclonal; Sigma, and rabbit polyclonal; Abcam), anti-HA in 1 : 1000 (rabbit polyclonal; Abcam), anti-IκBα in 1 : 1000 (rabbit polyclonal; Sigma), anti-β-actin in 1 : 2000 (mouse monoclonal; Sigma), anti-α-tubulin in 1 : 2000 (mouse monoclonal; Sigma), anti-acetyl histone H4 K12 in 1 : 1000 (rabbit polyclonal; Cell Signaling, Danvers, MA, USA), anti-β7 in 1000 (mouse monoclonal), anti-α5 in 1 : 1000 (mouse monoclonal), anti-ubiquitin in 1 : 1000 (mouse polyclonal, Sigma) and anti-p65 in 1 : 1000 (rabbit polyclonal, Abcam) were used for western blotting experiments.

RT-PCR and real-time PCR

Total RNA was isolated from HEK293 cells, PSMD9 overexpression and knockdown clone by TRIzol® Reagent (Invitrogen) following the manufacturer's protocol. cDNA was prepared using SuperScript® III Reverse Transcriptase kit (Life Technologies, Invitrogen). Real-time PCR was performed using SYBR Green based Kappa-Biosystems kit (Woburn, MA, USA) and gene specific primers (Table S1).

Electrophoretic mobility shift assay

Nuclear fractions were extracted from HEK293 FLAG-PSMD9 stable clones, HEK293 inducible FLAG-PSMD9 stable clones and HEK293 inducible PSMD9-shRNA stable clones using N-XTRACT kit (Sigma) following the manufacturer's protocol. wt κB-oligo 5′-AGTTGAGGGGACTTTCCCAGGC-3′ and mutant κB-oligo 5′-AGTTGAGCTCACTTTCC CAGGC-3′ [35] were purchased from Sigma and biotin labeled at the 3′ end of the oligos using the Biotin 3′ End DNA Labeling Kit (Thermo Scientific) following the manufacturer's protocol. Both biotinylated complementary oligos were annealed at 65 °C for 10 min followed by incubation at room temperature for 30 min. Then 3–5 μg of nuclear extract was incubated with the biotinylated oligos and poly dI-dC for 20 min at room temperature. This binding reaction was carried out using LightShift® Chemiluminescent EMSA Kit (Thermo Scientific) following the manufacturer's protocol. Reactions were separated on 6% native PAGE, transferred onto positively charged nylon membrane and UV crosslinked for 30 min at 256 nm at 1 cm distance. The membrane was developed onto an X-ray film using Chemiluminescent Nucleic Acid Detection Module (Thermo Scientific) following the manufacturer's protocol.

Proteasomal activity assay

Cells were pelleted, washed twice with $NaCl/P_i$ and resuspended in buffer containing 50 mM Tris (pH 7.6), 5 mM $MgCl_2$, 1 mM ATP, 10% glycerol and 1× protease inhibitor cocktail (Sigma). Cell suspensions were ultrasonicated for four cycles of 20 s each (with 1 s break after each 2 s) at 30 kHz on ice. Proteasomal activity was measured using 25 nM Suc-LLVY-7-amino-4-methyl coumarin substrate and fluorescence readings were taken at excitation 355 nm/emission 460 nm.

Densitometric and statistical analysis

Densitometric quantitation of scanned images was performed using MAC BIOPHOTONICS IMAGEJ. Statistical analysis was performed using GRAPH PAD PRISM 5. To evaluate the significance of the values obtained, an unpaired Student's *t* test was performed. $P < 0.05$ and $P > 0.05$ are considered as significant and non-significant data respectively. In graphs the symbol *** represents P value < 0.001.

Acknowledgements

We thank Dr Neil D. Perkins for providing 3x κB ConA luc vector and ConA luc control vector, Dr Sorab Dalal for providing pTRIPZ and pCDNA3.1 vector, Dr N. Shirsat, Advanced Center for Treatment, Research and Education in Cancer, Navi Mumbai, India, and Dr D. C. Guttridge, Ohio State University, USA, for providing phospho-mutant pTRIPZ-IκBαSR (S32A–S36A) vector and Dr Amit Singh Gautam for discussions. This work was funded by ACTREC-TMH (Grant no. IRG.2657). IS is funded by UGC (University Grants Commission), India; NS is funded by Department of Biotechnology, India.

Author contributions

Indrajit Sahu: planned, performed, analyzed experiments and assisted in manuscript writing. Nikhil Sangith: planned, performed initial NF-κB activity experiments, some *in vitro* interactions and designed PDZ and C-terminal mutations. Manoj Ramteke: initial establishment of stable cell lines and transfection. Rucha Gadre: performed some cloning and *in vitro* interaction experiments. Prasanna Venkatraman: conceived, directed the project and wrote the manuscript.

References

1 Kaneko T, Hamazaki J, Iemura S, Sasaki K, Furuyama K, Natsume T, Tanaka K & Murata S (2009) Assembly pathway of the mammalian proteasome base subcomplex is mediated by multiple specific chaperones. *Cell* **137**, 914–925.

2 da Fonseca PC, He J & Morris EP (2012) Molecular model of the human 26S proteasome. *Mol Cell* **46**, 54–66.

3 Thomas MK, Yao KM, Tenser MS, Wong GG & Habener JF (1999) Bridge-1, a novel PDZ-domain coactivator of E2A-mediated regulation of insulin gene transcription. *Mol Cell Biol* **19**, 8492–8504.

4 Jelen F, Oleksy A, Smietana K & Otlewski J (2003) PDZ domains – common players in the cell signaling. *Acta Biochim Pol* **50**, 985–1017.

5 Lee HJ & Zheng JJ (2010) PDZ domains and their binding partners: structure, specificity, and modification. *Cell Commun Signal* **8**, 8.

6 Lee JH, Volinic JL, Banz C, Yao KM & Thomas MK (2005) Interactions with p300 enhance transcriptional activation by the PDZ-domain coactivator Bridge-1. *J Endocrinol* **187**, 283–292.

7 Banz C, Munchow B & Diedrich K (2010) Bridge-1 is expressed in human granulosa cells and is involved in the activin A signaling cascade. *Fertil Steril* **93**, 1349–1352.

8 Volinic JL, Lee JH, Eto K, Kaur V & Thomas MK (2006) Overexpression of the coactivator bridge-1 results in insulin deficiency and diabetes. *Mol Endocrinol* **20**, 167–182.

9 Ren S, Uversky VN, Chen Z, Dunker AK & Obradovic Z (2008) Short linear motifs recognized by SH2, SH3 and Ser/Thr kinase domains are conserved in disordered protein regions. *BMC Genomics* **9** (Suppl 2), S26.

10 Singh Gautam AK, Balakrishnan S & Venkatraman P (2012) Direct ubiquitin independent recognition and degradation of a folded protein by the eukaryotic proteasomes – origin of intrinsic degradation signals. *PLoS One* **7**, e34864.

11 Nanaware PP, Ramteke MP, Somavarapu AK & Venkatraman P (2013) Discovery of multiple interacting partners of gankyrin, a proteasomal chaperone and an oncoprotein – evidence for a common hot spot site at the interface and its functional relevance. *Proteins*. doi: 10.1002/prot.24494.

12 Hay DC, Kemp GD, Dargemont C & Hay RT (2001) Interaction between hnRNPA1 and IkappaBalpha is required for maximal activation of NF-kappaB-dependent transcription. *Mol Cell Biol* **21**, 3482–3490.

13 Hayden MS & Ghosh S (2008) Shared principles in NF-kappaB signaling. *Cell* **132**, 344–362.

14 Li H & Lin X (2008) Positive and negative signaling components involved in TNFalpha-induced NF-kappaB activation. *Cytokine* **41**, 1–8.

15 Grilli M, Chiu JJ & Lenardo MJ (1993) NF-kappa B and Rel: participants in a multiform transcriptional regulatory system. *Int Rev Cytol* **143**, 1–62.

16 Ghosh S, May MJ & Kopp EB (1998) NF-kappa B and Rel proteins: evolutionarily conserved mediators of immune responses. *Annu Rev Immunol* **16**, 225–260.

17 Baeuerle PA & Baltimore D (1988) I kappa B: a specific inhibitor of the NF-kappa B transcription factor. *Science* **242**, 540–546.

18 Beg AA & Baldwin AS Jr (1993) The I kappa B proteins: multifunctional regulators of Rel/NF-kappa B transcription factors. *Genes Dev* **7**, 2064–2070.

19 Chen Z, Hagler J, Palombella VJ, Melandri F, Scherer D, Ballard D & Maniatis T (1995) Signal-induced site-specific phosphorylation targets I kappa B alpha to the ubiquitin–proteasome pathway. *Genes Dev* **9**, 1586–1597.

20 Li N & Karin M (1998) Ionizing radiation and short wavelength UV activate NF-kappaB through two distinct mechanisms. *Proc Natl Acad Sci USA* **95**, 13012–13017.

21 Mukhopadhyay A, Manna SK & Aggarwal BB (2000) Pervanadate-induced nuclear factor-kappaB activation requires tyrosine phosphorylation and degradation of IkappaBalpha. Comparison with tumor necrosis factor-alpha. *J Biol Chem* **275**, 8549–8555.

22 Hayden MS & Ghosh S (2004) Signaling to NF-kappaB. *Genes Dev* **18**, 2195–2224.
23 Alkalay I, Yaron A, Hatzubai A, Orian A, Ciechanover A & Ben-Neriah Y (1995) Stimulation-dependent I kappa B alpha phosphorylation marks the NF-kappa B inhibitor for degradation via the ubiquitin−proteasome pathway. *Proc Natl Acad Sci USA* **92**, 10599–10603.
24 Tanaka K, Kawakami T, Tateishi K, Yashiroda H & Chiba T (2001) Control of IkappaBalpha proteolysis by the ubiquitin−proteasome pathway. *Biochimie* **83**, 351–356.
25 Miyamoto S, Seufzer BJ & Shumway SD (1998) Novel IkappaB alpha proteolytic pathway in WEHI231 immature B cells. *Mol Cell Biol* **18**, 19–29.
26 Shumway SD, Berchtold CM, Gould MN & Miyamoto S (2002) Evidence for unique calmodulin-dependent nuclear factor-kappaB regulation in WEHI-231 B cells. *Mol Pharmacol* **61**, 177–185.
27 Shumway SD & Miyamoto S (2004) A mechanistic insight into a proteasome-independent constitutive inhibitor kappaBalpha (IkappaBalpha) degradation and nuclear factor kappaB (NF-kappaB) activation pathway in WEHI-231 B-cells. *Biochem J* **380**, 173–180.
28 Ponnappan S, Cullen SJ & Ponnappan U (2005) Constitutive degradation of IkappaBalpha in human T lymphocytes is mediated by calpain. *Immun Ageing* **2**, 15.
29 Palombella VJ, Rando OJ, Goldberg AL & Maniatis T (1994) The ubiquitin−proteasome pathway is required for processing the NF-kappa B1 precursor protein and the activation of NF-kappa B. *Cell* **78**, 773–785.
30 Hoffmann A, Levchenko A, Scott ML & Baltimore D (2002) The IkappaB-NF-kappaB signaling module: temporal control and selective gene activation. *Science* **298**, 1241–1245.
31 Cohen S, Achbert-Weiner H & Ciechanover A (2004) Dual effects of IkappaB kinase beta-mediated phosphorylation on p105 Fate: SCF(beta-TrCP)-dependent degradation and SCF(beta-TrCP)-independent processing. *Mol Cell Biol* **24**, 475–486.
32 Liang C, Zhang M & Sun SC (2006) beta-TrCP binding and processing of NF-kappaB2/p100 involve its phosphorylation at serines 866 and 870. *Cell Signal* **18**, 1309–1317.
33 Moorthy AK, Savinova OV, Ho JQ, Wang VY, Vu D & Ghosh G (2006) The 20S proteasome processes NF-kappaB1 p105 into p50 in a translation-independent manner. *EMBO J* **25**, 1945–1956.
34 Dreyfuss G, Matunis MJ, Pinol-Roma S & Burd CG (1993) hnRNP proteins and the biogenesis of mRNA. *Annu Rev Biochem* **62**, 289–321.
35 Reigstad CS, Lunden GO, Felin J & Backhed F (2009) Regulation of serum amyloid A3 (SAA3) in mouse colonic epithelium and adipose tissue by the intestinal microbiota. *PLoS One* **4**, e5842.
36 Zhou A, Scoggin S, Gaynor RB & Williams NS (2003) Identification of NF-kappa B-regulated genes induced by TNFalpha utilizing expression profiling and RNA interference. *Oncogene* **22**, 2054–2064.
37 Miyamoto S, Maki M, Schmitt MJ, Hatanaka M & Verma IM (1994) Tumor necrosis factor alpha-induced phosphorylation of I kappa B alpha is a signal for its degradation but not dissociation from NF-kappa B. *Proc Natl Acad Sci USA* **91**, 12740–12744.
38 Shim SM, Lee WJ, Kim Y, Chang JW, Song S & Jung YK (2012) Role of S5b/PSMD5 in proteasome inhibition caused by TNF-alpha/NFkappaB in higher eukaryotes. *Cell Rep* **2**, 603–615.
39 DeMartino GN, Proske RJ, Moomaw CR, Strong AA, Song X, Hisamatsu H, Tanaka K & Slaughter CA (1996) Identification, purification, and characterization of a PA700-dependent activator of the proteasome. *J Biol Chem* **271**, 3112–3118.
40 Ferrell K, Wilkinson CR, Dubiel W & Gordon C (2000) Regulatory subunit interactions of the 26S proteasome, a complex problem. *Trends Biochem Sci* **25**, 83–88.
41 Chen C, Huang C, Chen S, Liang J, Lin W, Ke G, Zhang H, Wang B, Huang J, Han Z *et al.* (2008) Subunit−subunit interactions in the human 26S proteasome. *Proteomics* **8**, 508–520.
42 Bohn S, Beck F, Sakata E, Walzthoeni T, Beck M, Aebersold R, Forster F, Baumeister W & Nickell S (2010) Structure of the 26S proteasome from *Schizosaccharomyces pombe* at subnanometer resolution. *Proc Natl Acad Sci USA* **107**, 20992–20997.
43 Lander GC, Estrin E, Matyskiela ME, Bashore C, Nogales E & Martin A (2012) Complete subunit architecture of the proteasome regulatory particle. *Nature* **482**, 186–191.
44 Lasker K, Forster F, Bohn S, Walzthoeni T, Villa E, Unverdorben P, Beck F, Aebersold R, Sali A & Baumeister W (2012) Molecular architecture of the 26S proteasome holocomplex determined by an integrative approach. *Proc Natl Acad Sci USA* **109**, 1380–1387.
45 Deveraux Q, Ustrell V, Pickart C & Rechsteiner M (1994) A 26S protease subunit that binds ubiquitin conjugates. *J Biol Chem* **269**, 7059–7061.
46 Husnjak K, Elsasser S, Zhang N, Chen X, Randles L, Shi Y, Hofmann K, Walters KJ, Finley D & Dikic I (2008) Proteasome subunit Rpn13 is a novel ubiquitin receptor. *Nature* **453**, 481–488.
47 Su V & Lau AF (2009) Ubiquitin-like and ubiquitin-associated domain proteins: significance in proteasomal degradation. *Cell Mol Life Sci* **66**, 2819–2833.
48 Chen L & Madura K (2002) Rad23 promotes the targeting of proteolytic substrates to the proteasome. *Mol Cell Biol* **22**, 4902–4913.

49 Gomez TA, Kolawa N, Gee M, Sweredoski MJ & Deshaies RJ (2011) Identification of a functional docking site in the Rpn1 LRR domain for the UBA-UBL domain protein Ddi1. *BMC Biol* **9**, 33.
50 Babu JR, Geetha T & Wooten MW (2005) Sequestosome 1/p62 shuttles polyubiquitinated tau for proteasomal degradation. *J Neurochem* **94**, 192–203.
51 Parcellier A, Schmitt E, Gurbuxani S, Seigneurin-Berny D, Pance A, Chantome A, Plenchette S, Khochbin S, Solary E & Garrido C (2003) HSP27 is a ubiquitin-binding protein involved in I-kappaBalpha proteasomal degradation. *Mol Cell Biol* **23**, 5790–5802.
52 Watanabe TK, Saito A, Suzuki M, Fujiwara T, Takahashi E, Slaughter CA, DeMartino GN, Hendil KB, Chung CH, Tanahashi N *et al.* (1998) cDNA cloning and characterization of a human proteasomal modulator subunit, p27 (PSMD9). *Genomics* **50**, 241–250.
53 Dolcet X, Llobet D, Pallares J & Matias-Guiu X (2005) NF-kB in development and progression of human cancer. *Virchows Arch* **446**, 475–482.
54 Ravi R & Bedi A (2004) NF-kappaB in cancer – a friend turned foe. *Drug Resist Updat* **7**, 53–67.
55 Lee SY, De la Mota-Peynado A & Roelofs J (2011) Loss of Rpt5 protein interactions with the core particle and Nas2 protein causes the formation of faulty proteasomes that are inhibited by Ecm29 protein. *J Biol Chem* **286**, 36641–36651.
56 Wu Y, Li Q & Chen XZ (2007) Detecting protein–protein interactions by far western blotting. *Nature protocol* **2**, 3278–3284.

Supporting information

Additional supporting information may be found in the online version of this article at the publisher's web site:

Table S1. List of qRT-PCR primers.

FEBS Open Bio 4 (2014) 571–583

FEBS openbio

journal homepage: www.elsevier.com/locate/febsopenbio

Discovery of novel interacting partners of PSMD9, a proteasomal chaperone: Role of an Atypical and versatile PDZ-domain motif interaction and identification of putative functional modules

Nikhil Sangith [a], Kannan Srinivasaraghavan [b,c], Indrajit Sahu [a], Ankita Desai [a], Spandana Medipally [a], Arun Kumar Somavarappu [a], Chandra Verma [b,d,e], Prasanna Venkatraman [a,*]

[a] Advanced Centre for Treatment, Research and Education in Cancer (ACTREC), Tata Memorial Centre (TMC), Kharghar, Navi Mumbai 410210, India
[b] Bioinformatics Institute A*STAR, 30 Biopolis Street, #07-01 Matrix, Singapore 138671, Singapore
[c] Experimental Therapeutics Centre (A*STAR), 31 Biopolis Street, #03-01 Helios, Singapore 138669, Singapore
[d] School of Biological Sciences, Nanyang Technological University, 60 Nanyang Drive, Singapore 637551, Singapore
[e] Department of Biological Sciences, National University of Singapore, 14 Science Drive 4, Singapore 117543, Singapore

ARTICLE INFO

Article history:
Received 26 February 2014
Revised 20 May 2014
Accepted 24 May 2014

Keywords:
Proteasome
C-termini
PSMD9
PDZ

ABSTRACT

PSMD9 (Proteasome Macropain non-ATPase subunit 9), a proteasomal assembly chaperone, harbors an uncharacterized PDZ-like domain. Here we report the identification of five novel interacting partners of PSMD9 and provide the first glimpse at the structure of the PDZ-domain, including the molecular details of the interaction. We based our strategy on two propositions: (a) proteins with conserved C-termini may share common functions and (b) PDZ domains interact with C-terminal residues of proteins. Screening of C-terminal peptides followed by interactions using full-length recombinant proteins, we discovered hnRNPA1 (an RNA binding protein), S14 (a ribosomal protein), CSH1 (a growth hormone), E12 (a transcription factor) and IL6 receptor as novel PSMD9-interacting partners. Through multiple techniques and structural insights, we clearly demonstrate for the first time that human PDZ domain interacts with the predicted Short Linear Sequence Motif (SLIM) at the C-termini of the client proteins. These interactions are also recapitulated in mammalian cells. Together, these results are suggestive of the role of PSMD9 in transcriptional regulation, mRNA processing and editing, hormone and receptor activity and protein translation. Our proof-of-principle experiments endorse a novel and quick method for the identification of putative interacting partners of similar PDZ-domain proteins from the proteome and for discovering novel functions.

1. Introduction

Almost every cellular pathway involved in the biology and homeostasis of a eukaryotic organism is regulated by the Ubiquitin Proteasome System (UPS) [1]. Impairment in the function of UPS components results in the accumulation of proteins leading to cellular stress and apoptosis [2]. While the role of proteasome in normal biology and disease is by and large well studied, the precise mechanism, the sequence and the structural requirements for substrate recognition, direct and indirect protein–protein interactions required for recruiting a substrate to the proteasome, remain obscure [3]. The structure and the domain functions of various 19S subunits and their role in proteasome dependent and independent functions are unclear. We recently showed that a 13 residue peptide of the A-helix from myoglobin acts as an anchor while a floppy region, the 'F-helix' acts as an initiator of proteasome mediated ubiquitin independent degradation of apomyoglobin [4]. We identified new interacting partners of gankyrin, a chaperone of the proteasome assembly and an oncoprotein by recognizing proteins that share EEVD, a conserved Short Linear Sequence Motif (SLIM) seen at the gankyrin and S6 ATPase interface [5]. Interaction between gankyrin and chloride intracellular channel protein through the conserved hot spot site enhances the migratory potential of breast carcinoma cell line. In addition, we demonstrated a role for Sug 1, an ATPase of the proteasome in transcriptional regulation of MHC

Abbreviations: ELISA, enzyme linked immunosorbent assay; GH, growth hormone; hnRNPA1, heterogeneous nuclear ribonucleoprotein A1; IL6 receptor, interleukin 6 receptor; PSMD9, Proteasome Macropain non-ATPase subunit 9

* Corresponding author. Address: Protein Interactome Lab for Structural and Functional Biology, KS-244, ACTREC, Tata Memorial Centre (TMC), Kharghar, Navi Mumbai 410210, India. Tel.:+91 022 27405091; fax: +91 022 27405085.
E-mail address: vprasanna@actrec.gov.in (P. Venkatraman).

http://dx.doi.org/10.1016/j.fob.2014.05.005
2211-5463/

proteins [6]. We described a novel role of PSMD9–hnRNPA1 interaction in basal and signal induced NF-κB activation via enhanced proteasomal degradation of IκBα [7]. We show that in this signaling pathway, proteasome bound PSMD9 acts as a subunit acceptor and hnRNPA1 as a shuttle receptor that recruits IκBα for degradation. Here, we exploit the presence of PDZ domain in PSMD9, a non-ATPase subunit, and a chaperone, of proteasome assembly to identify novel interacting partners and suggest putative functions of this biologically important molecule.

2. Material and methods

2.1. Plasmids

PSMD9 cDNA (Origene Technologies) was amplified and ligated into pRSETA vector between BamHI and EcoRI sites. hnRNPA1 and S14 ribosomal protein cDNA was generated by RT-PCR from RNA extracted from HEK293 cells. E12, growth hormone and the FN3 domain of IL6 receptor were amplified from the cDNA obtained from Harvard Institute of Proteomics. hnRNPA1 was ligated in pGEX4T1 (GE Amersham). FN3 domain was cloned in pGEX4T1 between BamHI and XhoI. S14, ribosomal protein, growth hormone and E12 were cloned in pMALC5 between BamHI and EcoRI sites. Mutations generated by site directed mutagenesis were confirmed by sequencing. PSMD9 was cloned in pCMV10 3X FLAG between HindIII and EcoRI sites. In doxycycline inducible pTRIPZ vector, PSMD9 was cloned between AgeI and EcoRI sites. All the interacting partners of PSMD9 were cloned in HA-pcDNA3.1 (A gift from Dr. Sorab Dalal, ACTREC) between BamHI and XhoI sites. Also see primers (Table S6).

2.2. Expression and purification of recombinant proteins

All recombinant proteins were expressed in *E.coli* BL21 DE (3) using 100 μM IPTG at 20 °C for 16 h. His-PSMD9 and its mutants were purified by Ni-NTA chromatography (Qiagen); GST, GST-hnRNPA1, GST-FN3 and its mutants were purified using glutathione sepharose (GE Amersham); MBP and MBP-S14, E12 and growth hormone were purified using amylose resin (NEB), according to manufacturer's protocol.

2.3. ELISA with tetra-peptides

N-terminal biotinylated tetra-peptides were procured from GenPro Biotech, India, (Biotin-KGG-XXXX, where XXXX represents the tetra-peptide sequence) and reconstituted to 25 mM with 100% DMSO and further diluted to 5 mM with distilled water. Anti-PSMD9 (Abcam) antibody in 0.1 M sodium carbonate buffer, pH 9.5 was coated on Nunc-Immuno™ MicroWell™ 96 well solid plates and incubated for 16 h at 4 °C. Wells were blocked with 2% BSA in TBST (10 mM Tris pH8, 138 mM NaCl and 0.5% Tween-20) for 1 h at 37 °C. His-tagged PSMD9 or its mutant proteins (5 μg/ml), diluted in TBST (containing 0.1% BSA) were added and incubated at 37 °C for 1 h. Plates were washed, and biotinylated peptides (in TBST with 0.1% BSA) were added to the wells and incubated for 1 h at 37 °C. The plates were washed with TBST vigorously after each incubation step. Finally, streptavidin alkaline phosphatase (Sigma), at a dilution of 1:2000 in TBST containing 0.1% BSA was added to all wells. After incubation for 1 h at 37 °C, binding was detected by the addition of para-Nitro phenyl phosphate (PNPP) (Bangalore Genei, India), the substrate of alkaline phosphatase and color developed was read at 405 nm (Spectramax 190, Molecular Devices). Wells that lack PSMD9 and wells that lack anti-PSMD9 antibody were taken as negative controls.

2.4. ELISA for PSMD9-hnRNPA1 and PSMD9-growth hormone interaction

GST-hnRNPA1, its mutants and GST only (control; 5 μg/ml) or MBP-growth hormone and MBP only (control; 5 μg/ml) were coated as described for the PSMD9 antibody (Section3.2). All incubations were performed as described for the peptide ELISA (Section3.2). Different concentrations of His-tagged PSMD9 or its mutant proteins were (in TBST containing 0.1% BSA) added to the coated plates. After incubation, anti-his antibody (Cell Signaling) was added at a dilution of 1:2000, incubated and washed. HRP conjugated anti-mouse antibody (GE Amersham) (at 1:3000 dilution) was then added. After incubation and washes, HRP substrate TMB (1X) was added to all the wells. Reaction was stopped using 2 M sulfuric acid before recording the readings at 450 nm. Wells not coated with GST-hnRNPA1 and wells in which PSMD9 or the mutants were not added served as negative controls. For the competition assays, recombinant his-PSMD9 was incubated with different concentrations of GRRF/GRRG or SCGF/SCGG/SGGF peptides for 1 h at 37 °C and then added to wells containing GST-hnRNPA1 or MBP-GH respectively.

2.5. In vitro pull down assay

Recombinant GST, GST- hnRNPA1, and its mutants (baits) were allowed to bind with glutathione sepharose beads (GE Amersham) in Transport Buffer (TB, 20 mM HEPES pH 7.9, 110 mM potassium acetate, 5 mM sodium acetate, 0.5 mM EGTA and 1 mM DTT) for 1 h at 4 °C. Beads were washed, following which PSMD9 or its mutants (in TB 0.1% BSA) were incubated with each bait for 4 h at 4 °C. Binding was monitored by Western blot using anti-His antibody (Cell Signaling). Cell lysates of MBP, MBP-S14, growth hormone, E12 or their respective C-terminal mutants were allowed to bind with amylose resin (NEB) in Transport Buffer for 1 h at 4 °C. Further incubations with PSMD9 or mutants were performed as described above except that anti- His antibody (Cell Signaling) was used to detect bound PSMD9.

2.6. Homology modeling

There is currently no crystal structure available for PSMD9 protein. A homology model of PDZ domain of PSMD9 was thus constructed using comparative modeling method, by comparing the sequence of this target protein with sequence of other related proteins (template) for which experimental structures are available. BLAST search showed that the PDZ domain shares 42% sequence similarity with PDZ2 domain of harmonin and sequence alignment between the two reveals that this sequence similarity is distributed throughout the sequence. Solution structure of PDZ2 domain of harmonin bound with C-terminal peptide of cadherin23 (PDB code 2KBS) [8] was chosen as a template for the homology modeling. Modeller, a program for comparative protein structure modeling by satisfaction of spatial restraints [9] was used for generation of the homology model. Several homology models were built based on structural information from the template, and model that showed good stereochemical property was selected for further use.

2.7. Peptide docking

3D structure of peptides GRRF and SCGF was generated using Xleap module in Amber11 [10]. Peptide in its extended conformation was docked with the generated model of PDZ domain of PSMD9 protein. Peptide docking was carried out with two different docking programs, HADDOCK [11] and ATTRACT [12]. For HADDOCK, a binding site was defined using residues Leu124, Gly125, Gln126, Glu128 and Gln181 within the canonical pocket. No information regarding the binding site was given while using ATTRACT and a complete

blind docking was performed using this program. Both the docking programs were validated earlier, by docking a set of co-crystallized peptides into the canonical pocket of the corresponding PDZ domains, and the docked conformations of each peptide had rmsd values 1.5–2.5 A with the corresponding experimental structures.

2.8. Molecular dynamics simulations

Generated homology model of PDZ domain, peptide GRRF (derived from C-terminus of hnRNPA1) - PDZ complex (PDZ-GRRF) and peptide SCGF – PDZ complexes (PDZ-SCGF) (both the canonical and non-canonical binding mode) were used as the starting structure for MD simulations. Mutated structures of the protein Q181G and the*triple* β-sheet mutant L124G/Q126G/E128G were also generated by replacing (mutating) the respective residues in PyMol. Hydrogen atoms were added to the WT and mutant experimental structures using the Xleap module of the Amber11 package. N-terminus of the GRRF and SCGF peptide was capped by acetylation (ACE). Simulation systems were neutralized by the addition of counter ions. The neutralized system was solvated with TIP3P [13] water molecules to form a truncated octahedral box with at least 10 Å separating the solute atoms and the edges of the box. MD simulations were carried out with the Sander module of the AMBER11 package in combination with the parm03 force field [14]. All systems were first subjected to 100 steps of energy minimization. The protein was initially harmonically restrained (25 kcal mol^{-1} $Å^2$) to the energy minimized coordinates, and MD simulations were initiated by heating the system to 300 K in steps of 100 K followed by gradual removal of the positional restraints, and a 1 ns unrestrained equilibration at 300 K. The resulting system was used as starting structure for production MD run. For each case, three independent (using different initial random velocities) MD simulations were carried out starting from the well equilibrated structure. Each MD simulation was carried out for 100 ns and conformations were recorded every 10 ps. All MD simulations were carried out in explicit solvent at 300 K. During all the simulations, the long-range electrostatic interactions were treated with the particle mesh Ewald [15] method using a real space distance cutoff of 9 Å. The settle [16] algorithm was used to constrain bond vibrations involving hydrogen atoms, which allowed time step of 2 fs during the simulations. Simulation trajectories were visualized using VMD [17] and figures were generated using PyMol.

2.9. Immunoprecipitation

FLAG-PSMD9 and HA tagged interacting partners were overexpressed in HEK293 cells. Lysates were added either to M2-Agarose (Sigma) or to anti HA-agarose beads and incubated for 3 h at 4 °C to immunoprecipitate the complex. Either anti-HA antibody or anti-FLAG antibody (Sigma) was used for detection.

2.10. Circular dichroism of PSMD9 and its mutants

Far-UV CD spectrum (Jasco, J815) of PSMD9-WT and its mutant proteins were recorded between 260 nm and 190 nm in a 2 mm path length cuvette. A protein concentration of 2 μM, in a volume of 500 μl (10 mM phosphate buffer (pH 7.5)) was used for collecting data at 20 °C. Data were normalized to obtain molar ellipticity values and fitted using Dichroweb's CONTIN software.

2.11. Tryptophan fluorescence of PSMD9 and mutants

Tryptophan fluorescence of PSMD9-WT and PSMD9-PDZ-mutants was recorded at a concentration of 1.5 μM. Emission spectra between 310 and 400 nm were collected upon excitation at 295 nm with a slit width of 5 nm and scan speed of 50 nm/s using Fluorolog HORIBA fluorimeter.

2.12. Western blotting

Samples were separated on 15% SDS PAGE gels and Western blots were performed using standard protocols. Depending on the protein under study, anti-His antibody (mouse monoclonal, Cell Signaling), anti-FLAG antibody (rabbit polyclonal, Sigma) or anti-HA antibody (rabbit polyclonal, Sigma) were used.

3. Results

3.1. A screen for putative PSMD9 interacting partners and validation using full length proteins

Many methods capitalize on the ability of the PDZ domains to recognize C-terminal residues in proteins to primarily define their binding specificity [18–22]. Peptide libraries have been created, and peptides derived from the C-terminus of the human proteome have been used by various investigators [18,23–25]. We chose C-terminal peptides of the human proteome as baits to identify novel interacting partners of PSMD9. Premise for this study is that modification-independent, sequence specific recognition is central to many biological processes, and rules inherent to this recognition process can bring together proteins of very different functions under a master regulator. Chung et al., had classified proteome from drosophila/yeast/human by recognizing conserved C-terminal residues in some of these proteins [26]. These C-terminal peptides were tested here for the following reasons. (1) Most high-throughput studies are optimized for selecting peptides with high affinity while many protein–protein interactions are of low affinity and, therefore, are likely to be missed. (2) If the corresponding protein/proteins were to interact, one could quickly move to associated functions, and finally (3) such a guided approach prevents identification of those peptides that are not represented in the human proteome and, are physiologically irrelevant. Due to financial constraints, thirteen among the thirty conserved tetra peptides from the human proteome were chosen. These sequences differ in charge, hydrophobicity and size and represent some of the known sequence specificity seen with other PDZ domains. AGHM, the C-terminus of E12 transcription factor, the human homolog of rat E2, was specifically included. E12 was shown to interact with Bridge 1 (homolog of PSMD9 with a PDZ domain) during insulin signaling [27–29]. We cloned, expressed and purified human PSMD9 and used enzyme-linked immunosorbent assay (ELISA), to test for binding of the peptides. GRRF, SCGF and AGHM peptides bound to PSMD9 to an appreciable extent with SCGF demonstrating highest affinity (Fig. 1A and Fig. S1A and B). SCGF and GRRF resemble class III PDZ peptides with the sequence motif-X-[D/E/K/R]-X-Φ where Φ is hydrophobic, and X is any residue. GRRF forms the C-terminus of hnRNPA1 isoforms while SCGF belongs to growth hormone (CSH1; referred from henceforth as GH). To test if the corresponding full length proteins would interact with PSMD9, we cloned and expressed the longer isoform of hnRNPA1 as a GST fusion protein, GH and E12 as MBP fusion proteins. PSMD9 was expressed as a His-Tag protein. Affinity pull-down followed by Western blot showed that the three full length proteins interact with PSMD9 (Fig. 1B–D). While hnRNPA1 (Fig 1E andTable S4) and E12 binding (Fig 1C) were clearly affected by simple C-terminal substitution (Phe to Gly), GH binding to PSMD9 was not affected to any measurable extent (Fig. 1D). Deletion of C-terminal seven residues compromised binding of GH severely (Fig. 1D) and not surprisingly those of hnRNPA1 and E12, as well (Fig. 1B and C). These interactions were further confirmed using ELISA and the

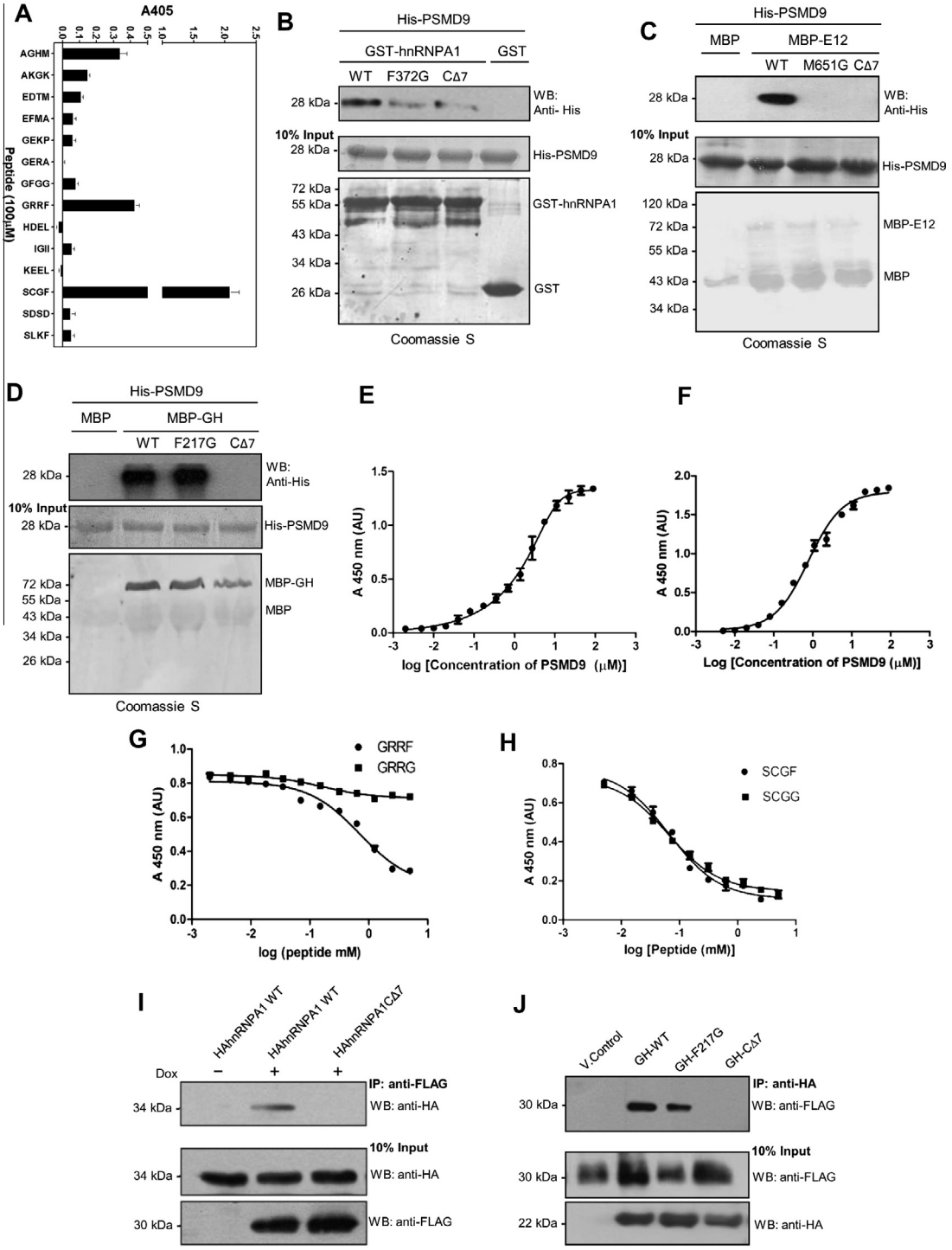

Fig. 1. Identification of putative interacting partners of PSMD9, and the importance of C-terminal residues in interaction. (A) Conserved C-terminal motifs in the form of tetra peptides were tested for binding to PSMD9 using ELISA (see Section2 for details). Values represent mean ± SEM (Standard Error of Mean) from three different experiments performed in duplicates.(B) Recombinant WT hnRNPA1 or hnRNPA1 C-terminal mutant (F372G or CΔ7) bound to GST served as baits to pull down PSMD9. (C) Interaction of recombinant E12 and its C-terminal mutants (MBP-fusions) with PSMD9 (His-tag) were tested by *in vitro* affinity pull-down using MBP-agarose (see Section2 for details). (D) Interaction of recombinant GH and its C-terminal mutants (MBP fusions) with PSMD9 was tested by *in vitro* affinity pull-down using MBP-agarose (see Section2 for details). (E) Interaction of PSMD9 with hnRNPA1 was monitored by ELISA (see Section2 for details). Data were best fit to one site specific binding using GraphPad Prism (commercial software, www.graphpad.com). The dissociation constant (K_d) for the interaction was found to be 1.33 ± 0.04 μM for hnRNPA1. Data from two independent experiments each done in duplicates is represented as mean ± SD (SD-standard deviation). (F) Interaction of PSMD9 with growth hormone. Data were fit to one site specific binding using PRISM. The dissociation constant (K_d) for the interaction was found to be 0.84 ± 0.07 μM for growth hormone. Measurements were done in duplicates and data is represented as mean ± SD (SD- standard deviation) for two independent experiments. (G) C-terminal peptide GRRF inhibits hnRNPA1-PSMD9 interaction. Prior to its incubation with hnRNPA1 coated plates, PSMD9 (0.65 μM) was incubated with GRRF or GRRG peptides. (H) C-terminal peptide SCGF and SCGG inhibit interaction of growth hormone with PSMD9. Prior to incubation with growth hormone, PSMD9 (0.65 μM) was incubated with SCGF or SCGG peptides. Ki for SCGF was calculated to be 36.7 ± 0.29 μM and for SCGG, it was 35.6 ± 0.24 μM. Data from two independent experiments each done in duplicates is represented as mean ± SD. (I) Interaction of hnRNPA1 and PSMD9 in mammalian cells. FLAG-tagged PSMD9 or its C-terminal mutant and HA- tagged hnRNPA1 were co-expressed in HEK293 cells. FLAG-PSMD9 was immunoprecipitated using M2-Agarose beads, followed by Western blot with anti-HA antibody. (J) Growth hormone and PSMD9 interact upon co-expression in mammalian cells. HA-Growth hormone or its C-terminal mutants and FLAG-PSMD9 were co-expressed in HEK293 cells and interaction was monitored by Co-IP as described in supplementary methods.

estimated dissociation constant K_d for PSMD9-hnRNPA1 interaction is 1.33 ± 0.16 μM and of PSMD9-GH interaction is 0.74 ± 0.04 μM and ΔG for the interaction between PSMD9 and WT-hnRNPA1 or GH were calculated to be 6.9 ± 0.04 and 7.1 ± 0.09 kcal/mol, respectively. Peptide GRRF and not GRRG inhibited hnRNPA1 binding (Ki of 326.5 ± 0.25 μM) confirming the importance of C-terminal residues (Fig. 1G) in this interaction. Again, as seen with the C-terminal substitutions of GH, inhibition of GH-PSMD9 interaction by SCGG was as good as SCGF and the Ki values for these peptides were 36.7 ± 0.29 and 35.6 ± 0.24 μM, respectively (Fig. 1H). These pairwise interactions and the role of C-terminal residues were confirmed in mammalian cells using co-immunoprecipitation assays (Fig. 1I and J).

3.2. The fine specificity of SCG derivatives

Unlike hnRNPA1 GRRG mutant, mutant GH with a C-terminal substituted SCGG binds to the PDZ domain of PSMD9 and interaction is inhibited only upon deletion of C-terminal residues (Δ7 mutant). To identify the minimal motif important for GH interaction, we engineered ΔGF, and ΔCGF mutants of GH and interaction with PSMD9 was tested by pull down and ELISA (Fig. 2 A and B and Table S4). While ΔGF mutant bound with PSMD9, deletion of one more residue, Cysteine, ΔGFC, impaired the interaction. By ELISA, the estimated K_d values were 0.8 ± 0.02 μM for ΔGF and 2.6 ± 0.011 μM for ΔCGF mutant. The % occupancy of GH was unaltered in the ΔGF mutant but was reduced to ~45% in the case of the ΔCGF mutant. This result emphasizes the importance of P−2 residue in interaction with PSMD9. The importance of the P−2 Cys was further confirmed by demonstrating the failure of peptide SGGF to inhibit the binding of GH to PSMD9 (Fig. 2C). As noted before both SCGF and SCGG can inhibit binding between the two proteins.

Our results help to clarify some of the observations made earlier with respect to Nas-2-Rpt5 interaction in yeast (PSMD9 homolog and the ATPase subunit of the 19S regulatory particle). Here, single C-terminal residue deletion in Rpt5 did not affect its binding to Nas-2 that made the authors conclude that the PDZ like domain of Nas2 may not confirm to the classical description [30]. Based on our results on human PSMD9 using similar pull down assays, other comparative studies and quantitative analysis, we show that the precise role of the C-terminal residues in the interaction is likely to be context dependent. In the case of hnRNPA1 (GRRF) and E12 (AGHM), bulk of the binding energy is derived from the C-terminal residue much like the classical PDZ domains. In GH with SCGF at the C-terminus, however, the terminal residue is less important. These differences are also reflected in the binding affinity of the three peptides to PSMD9. While GRRF binds weakly (K_d 651.7 ± 76 μM), peptide SCGF binds tightly to PSMD9 (K_d 8.6 ± 1.2 μM). One possible explanation is that these peptides may bind in different modes or orientations at the binding groove (discussed below). While results observed with the C-terminal peptides can be readily extrapolated to protein binding, stable binding of the full length protein may require additional interactions. It is also likely that, besides the canonical α–β groove, the protein, may bind elsewhere on PSMD9 perhaps at an allosteric site while the C-terminal sequence acts as initial recognition element that docks the protein at the canonical site.

3.3. Role of PDZ domain in interaction: modeling and site directed mutagenesis

To better understand the role of the C-terminal residues and PDZ domain in binding and recognition, we modeled the structure of PDZ and carried out extensive molecular dynamic simulations and peptide docking studies (supplementary methods). Several

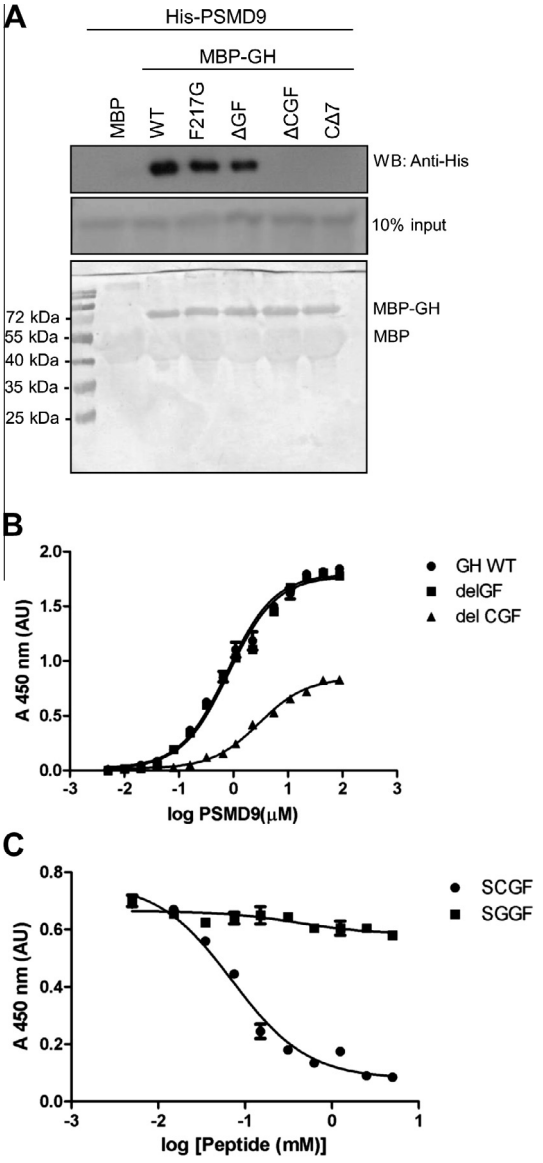

Fig. 2. Importance of Cysteine in growth hormone-PSMD9 interaction. (A) Interaction of recombinant GH and its C-terminal mutants F217G, ΔGF, ΔCGF and CΔ7 (MBP fusions) with PSMD9 was tested by *in vitro* affinity pull-down using MBP-agarose. (B) ELISA was used to monitor interaction between PSMD9 and GH or its C-terminal mutants. Data were fit to one site specific binding using PRISM. The dissociation constant (K_d) for the interaction of WT growth hormone, ΔGF and ΔGF with PSMD9 was found to be 0.74 ± 0.04 μM, 0.8 ± 0.03 and 2.64 ± 0.02 μM, respectively. Measurements were done in duplicates and data is represented as mean ± SD (SD-standard deviation) for two independent experiments (Also see Table S4). (C) C-terminal peptide SCGF and not SGGF inhibit interaction of growth hormone with PSMD9. Prior to incubation with growth hormone, PSMD9 (0.65 μM) was incubated with SCGF or SCGG peptides. Ki for SCGF was calculated to be 36.7 ± 0.29 μM. Data from two independent experiments each done in duplicates is represented as mean ± SD.

docking poses were created. Upon visual inspection of all the docked poses, a peptide-protein complex similar to that seen in the co-crystals of other PDZ-peptide complex with Phe at the fourth position was chosen. In this conformation, the peptide binds in an extended, antiparallel manner through canonical interactions that extend the beta sheet by an additional strand (Fig. 3A and B). The hydrophobic side chain of Phe4 of the peptide is deeply buried in the hydrophobic pocket formed by Leu124 from β_2, Val139, from β_3, Leu153 from β_4, Ile159, Phe 162, from β_4. The peptide further interacts with the beta sheet mainly through backbone/side chain

hydrogen bonds with residues Leu124, Gly125, Gln126, Glu128 of β_2 of the PDZ domain (Fig. 2B). In addition, the side chain of Arg2 of the peptide forms a salt bridge with the side chain of Glu128 from β_2. During MD simulation, the alpha/beta binding groove (canonical binding site) of apo PDZ showed increased flexibility (Supplementary Fig. S2). The α_2/β_2 binding pocket was partially deformed/destabilized (either collapses or widens), and is stabilized upon peptide binding. Increased flexibility of PDZ domains in their apo form have been reported by others [31]. The intrinsic flexibility of PDZ domains is a key determinant that allows them to recognize a wide repertoire of peptide ligands. Throughout the protein-peptide simulation, Phe4 remains deeply buried in the

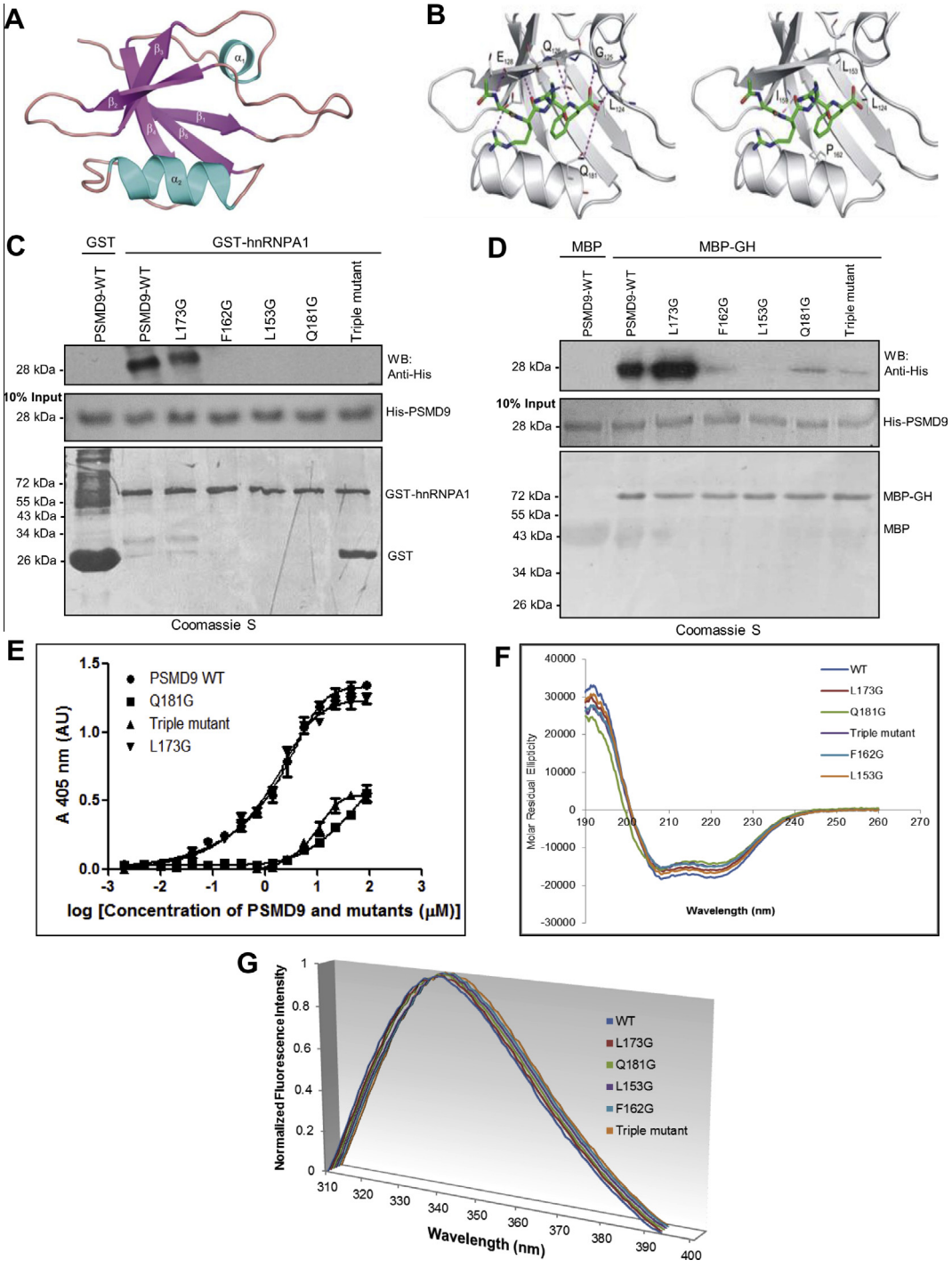

Fig. 3. Model of PDZ-domain of PSMD9 and residues important for interaction. (A) Cartoon representation of PDZ domain of PSMD9 built using PDZ2 domain of harmonin as the template. (B) Structure of PDZ domain bound to GRRF. A clear cleft that is bordered by α-helix and a β-strand can be seen in the PDZ domain similar to ligand bound PDZ structures. (C) Mutations of residues in the canonical pocket of PDZ domain [Q181G, the triple mutant (L124G/Q126G/E128G), L153G and F162G], abrogate binding to hnRNPA1 (D). Recombinant GH (expressed as MBP fusion) and PSMD9 (expressed as His-tagged) interact *in vitro*. Complex of PSMD9 or its mutants with GH was isolated using protocols described in methods. Mutations in the PDZ domain (as described in (C)) abrogate interaction. (E) WT-hnRNPA1 interaction with recombinant WT-PSMD9 or its mutant proteins was detected by ELISA. Three independent experiments each in duplicates were performed and data is represented as mean ± SD (SD- standard deviation). (F) Circular dichroism of PSMD9-WT and the PDZ mutants were recorded at 2 μM concentration between 260 nm and195 nm. Molar residual ellipticity is plotted against wavelength. (G) Fluorescence spectra of PSMD9-WT and its mutants were recorded between 310 nm and 410 nm (Excitation wavelength 295 nm). Data are represented as normalized fluorescence intensity against wavelength of emission.

hydrophobic pocket (Movie1:http://web.bii.a-star.edu.sg/bmad/PDZ/PDZ-PEP-WT-Top.mpg). Charge-charge interactions between Arg2 and Glu128 on β_2 are preserved during the 100 ns simulation. The bound conformation of the peptide was further stabilized via backbone hydrogen bond interactions with residues Leu124, Gly125, Gln126 and Glu128 from β_2 in the canonical binding site.

In the complex where Phe4 was mutated to Gly, the peptide unbinds from the canonical binding site within ~5–10 ns and doesn't bind again (Movie 2:http://web.bii.a-star.edu.sg/bmad/PDZ/PDZ-PEP_GRRG-Top.mpg). Although the peptide stays close to the canonical site due to charge-charge interactions with the protein residues, it undergoes translation and rotations that prevent it from rebinding in the canonical interaction mode. Thus, our MD simulations suggest that the burial of Phe in the hydrophobic pocket is crucial for the stabilization of this peptide in its bound conformation. Based on peptide docking and MD simulations (Movie 3:http://web.bii.a-star.edu.sg/bmad/PDZ/PDZPEP_L124G_Q126G_E128G-Top.mpg and Movie 4: http://web.bii.a-star.edu.sg/bmad/PDZ/PDZ-PEP_Q181G-Top.mpg), three single amino acid mutations F162G, L153G, Q181G and a triple mutation, L124G/Q126G/E128G were generated. *In vitro* pull-down shows that these mutations affect GH and hnRNPA1 binding to PSMD9 (Fig. 3C and D). Mutation of residue L173 (to Gly), part of the α2 helix, not involved in the interaction, did not affect the binding of peptide or the proteins (Fig. 3E and Table S1). MD simulations support this finding as the L173G PSMD9 mutant maintains the peptide in a stably bound form (not shown).

These results together, confirm the domain-motif interaction between PDZ domain of PSMD9 and the C-terminal region of the interacting proteins. The instability of the peptide-free forms is reflected in the secondary structure of these proteins determined by circular dichroism. While WT PSMD9 records 49% helicity, the L173G mutant shows 43% helical structure, Q181G mutant 39%, L153G mutant 45% and the F162G mutant shows 42% helical structure (Fig. 3F, Table 1 and Appendix Eq.(1)) [32]. Tryptophan fluorescence of these mutant proteins is less affected (Fig. 3G).

3.4. Identification of putative functional modules regulated by PSMD9

Although GRRF and SCGF were motifs under which several family members (12 and 13 respectively) were grouped by Chung et al., a detailed analysis and further curation using UniProt data (ftp://ftp.uniprot.org/pub/databases/uniprot/current_release/knowledgebase/) indicated that there was only one unique protein under each family. There are four isoforms within the GRRF family and ten isoforms within the SCGF family (Table S2). We re-analyzed other 28 families and found that, in the vast majority of the cases, the proteins grouped under each peptide family are primarily isoforms (Table S2). Although isoforms are homologous in sequence, their functions can be mutually exclusive or even counteractive [33,34]. To better define the role of C-terminus in functional grouping beyond isoforms, and predict the modules that may be regulated by PSMD9, we analyzed C-terminal variants of GRRF and SCGF from the human proteome. There are ten variants of GRRF where X is C, E, G I, K, L, N, P, Q or R (Table S3). SCGL at the C-terminus of IL6 receptor was a single variant of SCGF. We screened seven variants of GRRF (GRRG was already tested as a control) i.e., GRRC, GRRE, GRRI, GRRL, GRRN, GRRQ and GRRR as well as the SCGL peptide for binding to PSMD9 by ELISA (Fig. 4A, Table S5). Peptides GRRL, GRRI, GRRQ, GRRC, GRRR and SCGL bound to PSMD9. GRRI and GRRL binding affinity were comparable to GRRF. GRRI belongs to a hypothetical protein. GRRL belongs to S14. S14 is part of the ribosome and like hnRNPA1 is an RNA binding protein also involved in protein translation [35]. GRRC and GRRR surprisingly bound with 12–14-fold higher affinity than GRRF. GRRC belongs to endothelial receptor protein and GRRR to UPF2, a protein involved in mRNA metabolism. Like SCGF, SCGL (from IL6 receptor) bound to PSMD9 with better affinity than GRRF or its variants. We tested full length S14 and IL-6 receptor C-terminal domain for binding to PSMD9 using *in vitro* pull down assay, and both were found to interact with PSMD9. As in hnRNPA1, C-terminal substitution abrogated binding of S14 and remarkably as seen with GH, binding of IL-6 receptor was unaffected by the C-terminal Gly substitution but was inhibited upon deletion (Fig. 4B and D). Again, similar to hnRNPA1-PDZ interaction, all the PSMD9 PDZ mutants L153G, F162G, Q181G and the triple mutant L124G/Q126G/E128G, either did not recognize or bound less well to WT S14 and the FN3 domain of the IL6 receptor with intact C-terminal residues (Fig. 4C and E).

To test whether observed *in vitro* interactions can be extended to interactions within the cellular milieu, we cloned and trans-expressed S14 ribosomal protein and the FN3 domain of IL6 receptor and their respective C-terminal mutants, in HEK293 cells. Immunoprecipitation results clearly confirm all *in vitro* observations (Fig. 4F and G).

4. Discussion

Our results taken together indicate that PSMD9 carries a versatile PDZ domain and interacts with residues at the C-terminus of proteins that are non-homologous in sequence, but carry a signature Short Linear Sequence Motif. Although the number of peptides screened here is limited, substantial information can be inferred from the binding of peptides and proteins to the PDZ domain of PSMD9 and their mutant forms. Given that the information on the structure and functions of PSMD9 (and other 19S subunits) is minimal, the results reported here are highly significant. However, some amount of speculation drawing support from our own studies and those from the literature is necessary to appreciate the significance of the results.

4.1. On the origin of affinity differences

We had included 8 out of 10 C-terminal variants of GRRF, and SCGL a single variant of SCGF, from the human proteome and peptide AGHM from transcription factor E12, for their ability to

Table 1
Fraction of helicity of PSMD9 WT and mutants analyzed by circular dichroism.

Protein	$[\theta]_{222}$ (deg cm^2 d mol^{-1})	Helicity predicted by CONTIN(%)	Helicity predicted by formula*(%)
PSMD9 WT	−17281.7 ± 368.34	47.5 ± 0.96	52 ± 0.94
L173G	−15377.4 ± 327.75	41.93 ± 0.77	47.1 ± 0.8
Q181G	−13734.7 ± 292.14	38 ± 0.72	42.9 ± 0.7
Triple mutant L124G/Q126G/E128G	−14485.3 ± 308.74	40.13 ± 0.77	44.8 ± 0.7
F162G	−14863.4 ± 253.25	42.14 ± 0.65	45.8 ± 0.62
L153G	−16455.94 ± 362.63	45.3 ± 0.84	50.7 ± 0.66

* The fraction of α-helix present in PSMD9 and mutants were calculated using the CONTIN software available in DICHROWEB server and the helicity is also predicted by the formula $fH = ([\theta]_{222} - 3000)/(-36000 - 3000)$ (Appendix Eq.(1)) [21], where $[\theta]222$ is mean molar residual ellipticity at 222 nm.

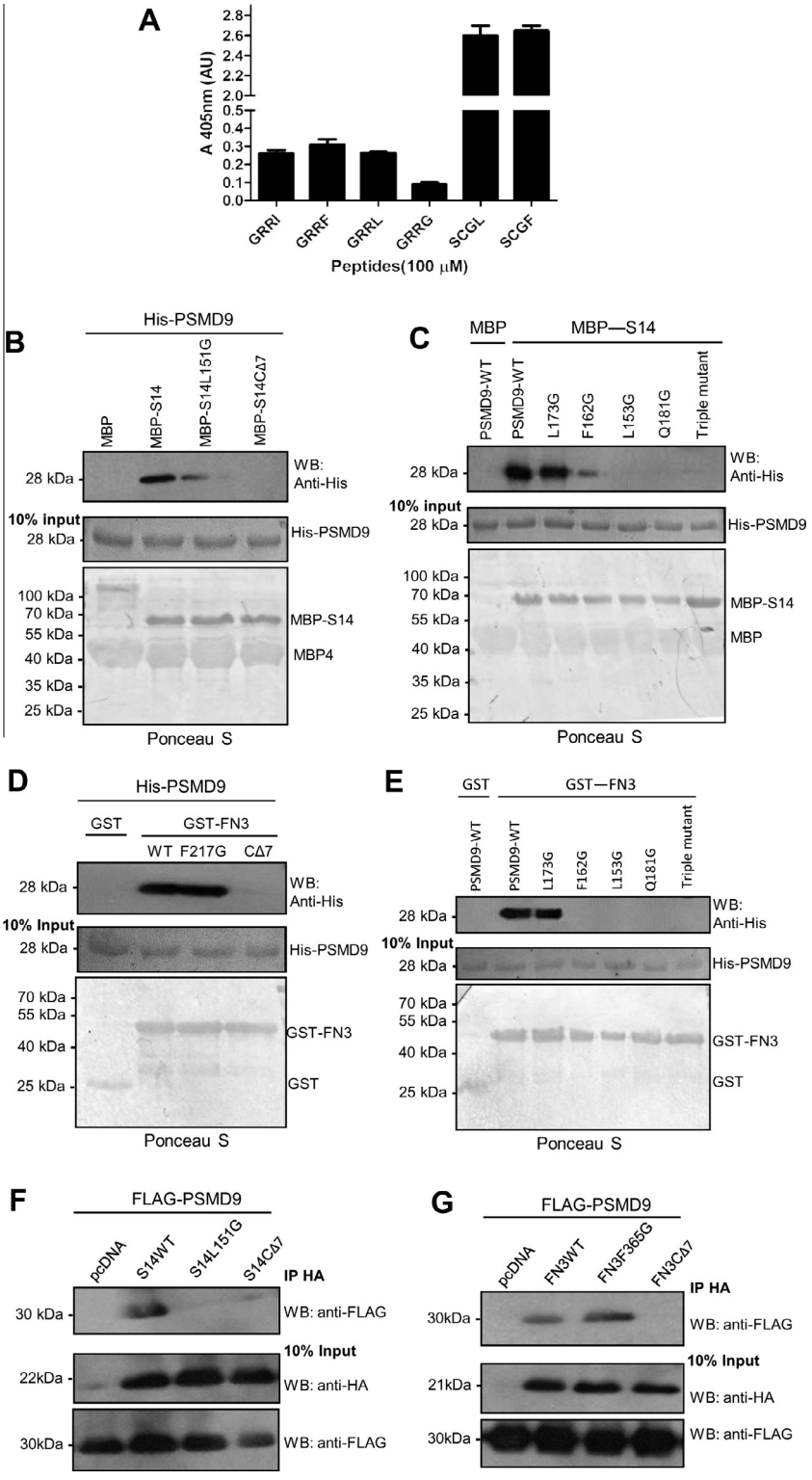

Fig. 4. Interaction of PSMD9 with C-terminal variants (from the human proteome) of hnRNPA1 and GH. (A) Binding of peptide variants GRRX to recombinant PSMD9. GRRX peptide (X = any residue) binding to PSMD9 was detected and measured by ELISA. Values from three experiments done in duplicates are represented as means ± SEM. (B) S14 ribosomal protein interacts with PSMD9 via its C-terminal residues. Complex formed between S14 wild type (MBP fusion), S14 L151G or C-terminal deletion mutant S14CΔ7 was isolated as described in methods. Any bound PSMD9 (His tagged) was detected using anti-His antibody (C) PDZ domain of PSMD9 is important for interaction with S14 ribosomal protein *in vitro*. *For* the *in vitro* pull-down, MBP-S14 fusion and his-PSMD9 or its mutant proteins were processed as described previously. (D) FN3 domain of IL6 receptor interacts with PSMD9 *in vitro*. GST-WTFN3, FN3 F365G mutant or C-terminal deletion mutant (FN3CΔ7) were used to pull down PSMD9 (His-tag) and probed for the presence PSMD9 using anti–His antibody. (E) PDZ domain of PSMD9 is important for interaction with the FN3 domain *in vitro*. (F) Interaction of S14 with PSMD9 in mammalian cells. HA-tagged WTS14 or its C-terminal mutants were co-expressed with FLAG-PSMD9, immunoprecipitated and the complexes were probed for FLAG-PSMD9. (G) Interaction of the FN3 domain of IL6 receptor with PSMD9 in mammalian cells. HA-tagged FN3 domain or its C-terminal mutants were co-expressed with Flag-PSMD9, co-immunoprecipitated and bound PSMD9 was detected using anti-Flag antibody.

interact with PSMD9. The K_d for each of these peptides is summarized in Table S3. Based on the affinity of the peptides, these variants can be classified into three groups – Group I or low affinity binders, Group II or high affinity binders and Group III tight binders or the top ranking peptides. In the Group I peptides, hydrophobic residues such as F, L, I at P0 provide specificity. In Group II peptides, Cys or Arg at P0 increases affinity by 10-fold as compared to that of Group I peptides. These two amino acids seem very different from each other and from the Group I peptides in terms of their physical properties and binding preference of the PSMD9 PDZ domain seems very intricate. The binding pocket of PSMD9 seems better adapted to bind to residues that are not bulky or highly hydrophobic explaining the high affinity binding of GRRR and GRRC. On the other hand, both Cys and Arg show characteristics of hydrophobic residues. For example, based on the hydrophobicity index Cys is classified along with Phe [36–39] and arginine, although one of the least hydrophobic amino acids, shows very interesting properties. Arginine solubilizes aggregation prone proteins helps in the elution of proteins bound to phenylsepharose column and has wide application in the purification and solubilization of inclusion bodies [40,41]. Arginine like GuHCL interacts with almost all amino acids and preferentially with aromatic residues [40], but unlike GuHCl, Arginine is not a denaturant [42]. This probably explains why these two amino acids like the hydrophobic residues occupy the P0 position. Arg substitution for a Phe in the interior of a protein will result in destabilization but less likely to do so at the protein interface.

Based on binding affinity, peptide AGHM will also fall under the Group I peptides, and methionine is known to be a hydrophobic residue. GRRE with a negatively charged C-terminus and GRRG with a small but relatively hydrophobic residue at P0 do not bind to PSMD9. These results indicate that P0 residue and not GRR is a major determinant of binding specificity in these peptides.

Compared to all peptides tested, the top ranking Group III peptides, SCG variants SCGF and SCGL bind with the highest affinity – K_d for the two peptides is four to five times less than the Group II peptides. The hydrophobicity of the C-terminal residue in SCGF and SCGL is clearly not important for binding and recognition as it can be readily replaced by a Gly. It seems that, in this set of peptides, the P−1, P−2 or P−3 residues are more important for high affinity interaction. By systematically deleting residues from the C-terminus, we identified Cys at P−2 position to be very important for interaction. In accordance with these results, peptide SGGF was unable to inhibit the interaction between GH and PSMD9.

It is clear that, in the absence of high resolution crystal structure of the complexes coupled with kinetic, thermodynamic studies using mutant peptides, it would be impossible to precisely define the molecular basis of affinity differences and positional occupancy of residues. In the absence of these details, we will have to consider different possibilities that may account for the binding preferences and affinity.

Reports from 20 complex structures of PDZ domains with C-terminal peptides of proteins indicate that the aminoacid at the P0 position has no specific conformational preference in the Ramachandran plot. In contrast the P−1, P−2 and P−3 residues show a strong preference and occupy either a strand or an extended conformation [43]. Such a conformational preference especially of the P−2 residue may explain the high affinity interaction seen with SCGX peptides. Alternatively, SCGF and SCGL peptides may mimic the internal sequences in proteins that bind PDZ domains and the Cys at P−2 may occupy the hydrophobic pocket formed by L153 and Phe 162 residues, mutations of which affect interaction. Flexibility in the binding modes is not uncommon to the peptide-PDZ domain interactions. For e.g., the P(−2) residue in some of the PDZ ligands are known to interact with αB-1 and αB-5 residues on the PDZ domain [43,44]. These residues normally interact with the P0 residues in the ligand. In the crystal structure of Dvl2 PDZ domain bound to a noncanonical C-terminal sequence, P−3 residue was seen to occupy the binding position utilized by a P−2 residue [45]. Secondary structure of the PSMD9 mutant proteins F162G (42%) and L153G (45%; very close to WT ∼48%) were not dramatically altered compared to other mutant proteins which bind the peptide (L173G 42%) or those that do not (Q181G 38%; Table 1).

Three modes of peptide binding to PDZ domains in proteins GRASP, PDLIM and MAST4 have been identified. In the structures of GRASP-peptide complexes, it is striking that the two chains of the protein bind to the same peptide in two different binding modes. Comparing these structures, a perpendicular mode, an intermediate mode – both speculated to be kinetic intermediates- and a stable canonical binding mode have been described [44]. We can draw parallels from these studies and propose the following: there exists a conformational ensemble of peptide-PSMD9 complexes. The Group I peptides, probably frequent the non-canonical or perpendicular orientation seen with other PDZ binding peptides. This orientation will rely heavily on the burial of the C-terminal residue for affinity. The Group II peptides GRRC and GRRR peptides probably frequent the intermediate population wherein the P0 residue is anchored. Peptides SCGF and SCGL populate the extended conformation in the canonical mode (although simulations propose a stable binding in the reverse orientation). The entropy cost of binding is probably paid for the SCGF and SCGL peptides as described for other protein derived C-terminal peptides bound to their cognate PDZ domain that may explain the high affinity interaction.

In our MD simulation studies, SCGF was unstable in the canonical binding mode but binds stably in a fully extended form, in the reverse orientation (Supplementary Fig. S3). Reverse binding modes of peptides have also been reported in literature, where the same peptide binds in opposite orientation i.e., N′–C′ or C′–N′ termini e.g., peptides binding to chaperone DnaK, Calmodulin and SH3 proteins [46–48]. If SCGF or SCGL peptides bind in a reverse orientation with the hydroxyl-group of the Ser residue substituting for the Phe carboxyl residue, mutation of F162 or L153 residues to Gly, will affect the binding, as seen in Supplementary Fig. S4. However, since the mutant peptide SGGF is unable to bind to PSMD9 or inhibit the binding of GH to PSMD9, the Ser residue seems unimportant for interaction. Therefore, binding of SCGF/L in the reverse orientation as a probable determinant of high affinity interaction seems less likely.

4.2. On the number of binding sites and the mechanism of binding

Mutation of the C-terminal Phe in GRRF, or Leu in GRRL or Met in AGHM, to Gly in the respective peptides or proteins inhibits interaction. Commensurate with these results, while GRRF competitively inhibits approximately 69% of the binding between hnRNPA1 and PSMD9 the mutant peptide GRRG, is unable to do so. However, substitution and even deletion of few C-terminal residues does not completely prevent binding of proteins. In all the cases, the fractional occupancy (like V_{max} in enzyme catalysis) is maximally affected by the C-terminal mutations while the affinity per se as determined by K_d (like Km for substrate binding) is less affected. In addition, the affinity differences between peptide or protein binding to PSMD9 is large. This difference is especially striking with the Group I peptides, the K_d of which are in the high μM range (∼600 μM) while the proteins bind with low micromolar affinity (1 μM). This vast discrepancy may be explained by the following: (a) C-terminal residues act primarily as signatures or bar codes that are read by the PDZ domain of PSMD9; (b) maximal affinity is contributed by a binding motif elsewhere in the protein or the binding of extended residues at the N-termini of the protein. Peptide affinity, however increases only marginally upon extension

of the N-terminal residues. For example, the nine residue C-terminal sequence of E12, with the tetrapeptide motif AGHM, interacts approximately two times more strongly than the short tetrapeptide AGHM (data not shown); and (c) the C-terminal sequences are stabilized by the structure of the full length protein. Based on these possibilities we propose a two state binding model for the interaction between PSMD9 and its client proteins – an initial weak recognition phase mediated by the C-terminal residues which act as specificity determinants followed by its consolidation via interaction of a secondary binding motif. Initial recognition of C-terminal residues in proteins by the PDZ domain may allow binding of the secondary site to an allosteric pocket on PSMD9 (Supplementary Fig. S5). These may or may not be accompanied by conformational changes in the proteins. The binding disparity between Group II peptides or the SCGF and SCGL peptides and their corresponding proteins although is much less (of the order of 8-fold), the fractional occupancy of the C-terminal deletion mutant, ΔCGF of GH is ∼45% of WT indicating that the same mechanism is probably operational. The plasticity of the PDZ domain and contribution of the overall structure to the binding is well illustrated in [31,49]. The partial loss in affinity upon mutations of residues present in different secondary structural elements of the PSMD9-PDZ domain is probably a reflection of the same paradigm.

It is also possible that the binding affinities are a reflection of the associated functions of the proteins. For example, we have demonstrated that hnRNPA1 acts as a novel shuttle receptor [7] that recruits IκBα for degradation by the proteasome. PSMD9 by interacting with hnRNPA1 and the 26S proteasome helps in anchoring IκBα and accelerating degradation. In this process, hnRNPA1 is likely to be recycled. By analogy, S14 may also act as a shuttle receptor that recruits proteins like MDM2 for degradation (Fig. 5B, see Section 4.3 for details) and must itself be released intact. Therefore, the C-terminus of these proteins may bind weakly to PSMD9. GH and IL6 receptors are the proposed direct substrates of the proteasome (Fig. 5D see Section 4.3 for details). In addition to the polyubiquitin binding, initial recognition of the C-terminal residues by PSMD9 with high affinity may be very important for the stable binding of such direct substrates to provide fatal directionality for degradation (Fig. 5D).

4.3. On the functional annotation of PSMD9 and its role in quality control by the proteasome

In this third part, we speculate on the probable regulatory role of PSMD9 by inferring on the role of its interacting partners. It is interesting that these proteins perform very different functions in the cell. At first glance, these interactions seem unusual, and the real physiological relevance may not be apparent. But detailed literature study provides substantial support for the plausible physiological role of these interactions in mammalian cells. hnRNPA1 is known to interact with IκBα in murine cells, and this interaction somehow accelerates degradation of IκBα resulting in NF-κB activation [50]. A possible functional conservation can be expected in human cells, and one may anticipate PSMD9 to regulate NF-κB signaling via IκBα degradation. In the manuscript that we published recently, we show that hnRNPA1 is a shuttle receptor that recruits IκBα for degradation and PSMD9 acts as a subunit acceptor and anchors hnRNPA1 to facilitate degradation of IκBα by the proteasome [7]. Association of proteasome with ribosome has been documented in the literature [51–53]. Whether S14 and PSMD9 interaction provides the structural scaffold for this interaction and what may be the functional consequence of this interaction in protein translation will be an interesting future investigation. In addition, S14 is known to bind to MDM2, which prevents the ability of this E3 ligase to ubiquitinate p53 thereby preventing proteasomal degradation of p53, leading to stabilization and activation of p53 [54]. Depending on whether or not the interaction between PSMD9 and S14, S14 and MDM2 are mutually exclusive, PSMD9 may influence ubiquitination, stability and functions of p53. By drawing a parallel from our studies on hnRNPA1 and PSMD9 interaction in IκBα degradation, we provide an alternate possibility for the fate of MDM2 and p53. We speculate that S14, similar to hnRNPA1 may also act as a shuttle receptor which recruits MDM2 for degradation by the proteasome (may be under similar stress conditions). Proteasome associated PSMD9 may anchor S14 (like it does hnRNPA1) to facilitate degradation of MDM2 (like IκBα) by the proteasome.

GRRR as mentioned before belongs to UPF2, yet another protein involved in RNA metabolism. UPF2 is part of a post-splicing multiprotein complex which regulate mRNA nuclear export and responsible for the detection of exported mRNAs with truncated open reading frames, resulting in nonsense-mediated mRNA decay [55].

Two other PSMD9 interacting partners GH (CHS1) and IL6 receptor are implicated in chemokine signaling [56,57]. However both GH and the IL6 receptor with SCGL at the C-termini created by alternate splicing are soluble, secreted proteins. In order to be exported out of the cell, these proteins must follow the ER-Golgi traffic [58]. Secreted proteins are inserted co-translationally into the ER lumen. Upon achieving their final folded state and post-translational modifications, these proteins are transported out of ER, through Golgi and finally out of the plasma membrane. However under stress or stimuli induced signaling, when the load on ER is more, quality control mechanisms must ensure that misfolded proteins are degraded. Misfolded and immature proteins are retro translocated by ER resident translocon and aided by ubiquitin or specialized proteins like Kar2p/BiP they are actively pulled out. These proteins are bound by the ER associated proteasomes and degraded [59–65]. Here, we speculate that while other ubiquitin binding proteins on the 19S regulatory complex of the proteasome may bind to the polyubiquitinated GH or IL6 as classically demonstrated for other proteins, PSMD9 would trap the misfolded GH or IL6R (and other such ERAD proteins) via the specific interaction of the PDZ domain with the respective C-terminal motif. Such interaction would prevent their premature release back into ER, ensure directionality and rapid clearance by the proteasome. Degradation is likely to occur at a basal rate as a routine quality control measure. The rate would be accelerated upon signal induction to truncate and attenuate the signaling process upon withdrawal of the stimuli or in response to ER stress. Therefore, PSMD9 may act as a general molecular chaperone that exerts quality control.

Soluble IL6R formed by splicing or proteolysis also bind to gp130 present on cells that lack the IL6 receptors. Soluble IL6R-IL6 complex is involved in what is called as the 'trans-signaling' an important mediator of inflammation and chemokine signaling in cancer [66]. Signaling may be attenuated by the receptor mediated endocytosis [67]. By binding to its receptor, GH may also follow receptor mediated endocytosis. The fate of such proteins engulfed by the process of endocytosis and how these may encounter the proteasome is described elegantly [60,68–71]. Some of these proteins routed by endocytosis may become shared substrates of the 'cytosolic' proteasomes and lysosomal enzymes. Different parts of the same sequence may be degraded by these degradation machineries. Our experiments designed to verify the binding of these proteins to PSMD9 in HEK293 cells upon co-expression is justified as these interactions are likely to be post endocytosis or post extraction events. Future lines of exciting studies include the characterization of the subcellular loci of these proteins and their ultimate and probably differential fate at the 'hands' of proteasome and lysosomes. GRRC belongs to endothelial receptor protein, yet another type I transmembrane protein, involved in signaling by EPCR [72].

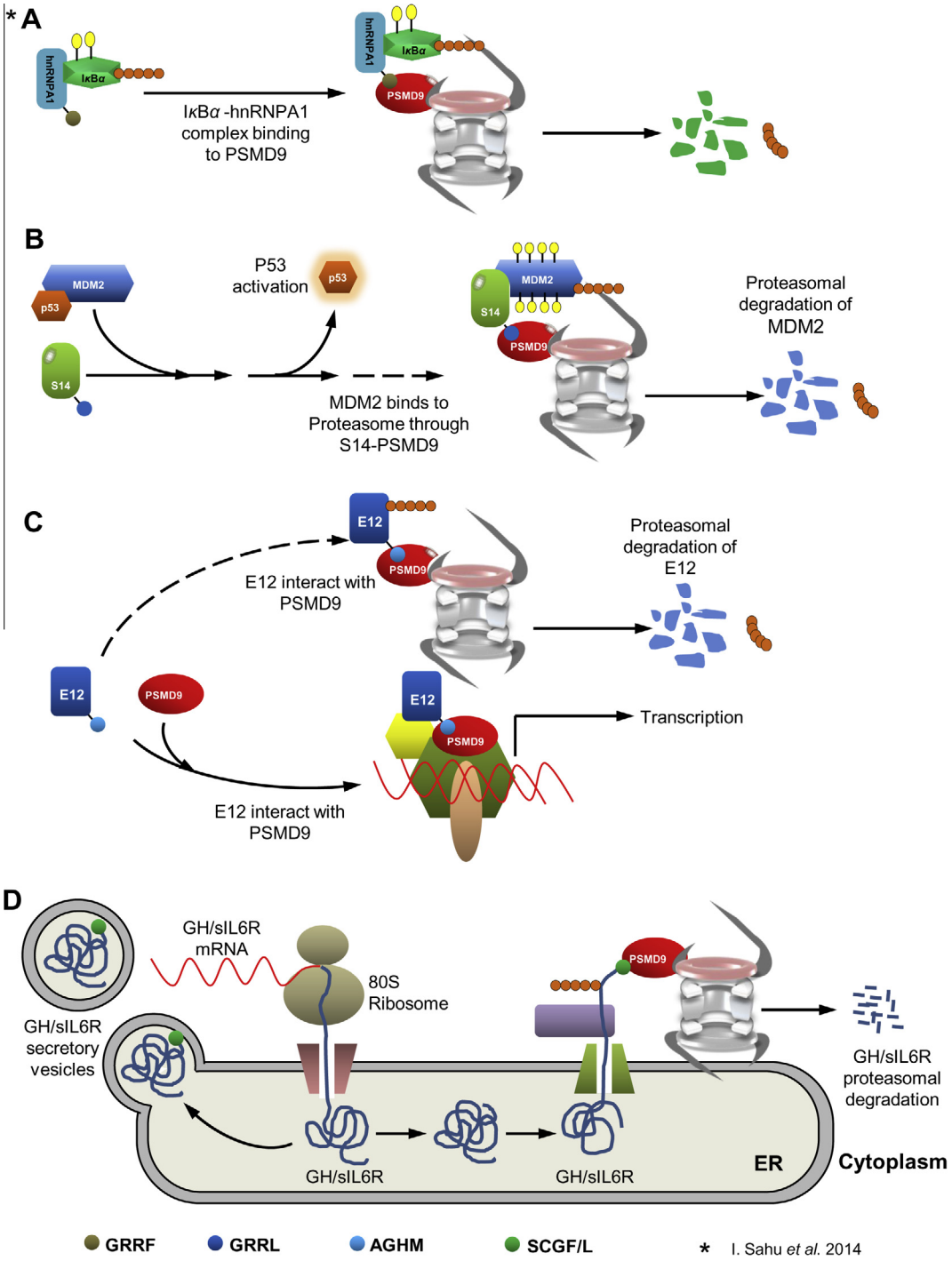

Fig. 5. Putative functional modules of PSMD9 and the probable role of PSMD9 in proteasome mediated quality control. (A) Role of PSMD9 in IκBα degradation. hnRNPA1 is assumed to be an adaptor protein or a shuttle receptor that recruits ubiquitinated IκBα to the proteasome by interacting with PDZ-PSMD9 via its C-terminus. PSMD9 acts as the subunit acceptor that helps to anchor IκBα via hnRNPA1. (B) Probable role of PSMD9 in regulating the stability of p53. S14 interacts with MDM2 and regulates the stability of p53. PSMD9 may modulate the ability of MDM2 to regulate p53 activity in two different ways (please see the Section 4 for details). (C) PSMD9-E12 interaction may be relevant for transcriptional coactivation/repression of many genes. PSMD9 may also play a regulatory role in proteasomal degradation of E12 to terminate transcription. (D) Model showing the probable role of PSMD9 in ER associated proteasomal degradation. Misfolded or aggregated secretory proteins like IL6 receptor and growth hormone are retro-translocated from ER and to ER associated proteasome for degradation. PSMD9 may help in anchoring the translocated substrate by capturing the C-terminal residues.

E12-PSMD9 interaction is likely to influence transcriptional regulation (like Bridge-1 in insulin signaling). PSMD9 may act either as a coactivator or as a repressor of many transcription events. Whether this regulatory role would involve 19S, or the entire 26S proteasome again or a proteasome independent role at the chromatin remains to be seen.

With all these examples, the grand or unifying role of PSMD9 seems to be to ensure quality control and regulate the magnitude of signaling or transcriptional programs (working model Fig. 5). The probable mechanism is likely to involve the proteasome and its proteolytic components. However, other regulatory steps involving an independent pool of PSMD9 and its interacting part-

ners within the protein–protein interaction network cannot be ruled out.

5. Conflict of interest

Authors declare that there is no conflict of interest.

Acknowledgements

The project was funded by Department of Science and Technology (DST), Government of India and Intra Mural Grant (IRG, ACTREC, TMC); N.S. acknowledges funding by the Department of Biotechnology, Government of India and A.K.S. by IRG no. 2691, ACTRC/TMC.

Appendix A.

$$f\mathrm{H} = \left([\theta]_{222} - 3000\right)/(-36000 - 3000), \quad (1)$$

where fH is the fraction of helicity, $[\theta]_{222}$, where $[\theta]_{222}$ is the mean molar residual ellipticity at 222 nm (deg cm^2 d mol^{-1}).

Appendix B. Supplementary data

Supplementary data associated with this article can be found, in the online version, at http://dx.doi.org/10.1016/j.fob.2014.05.005.

References

[1] Glickman, M.H. and Ciechanover, A. (2002) The ubiquitin-proteasome proteolytic pathway: destruction for the sake of construction. Physiol. Rev. 82, 373–428.
[2] Groll, M. and Clausen, T. (2003) Molecular shredders: how proteasomes fulfill their role. Curr. Opin. Struct. Biol. 13, 665–673.
[3] Ravid, T. and Hochstrasser, M. (2008) Diversity of degradation signals in the ubiquitin-proteasome system. Nat. Rev. Mol. Cell Biol. 9, 679–690.
[4] Singh Gautam, A.K., Balakrishnan, S. and Venkatraman, P. (2012) Direct ubiquitin independent recognition and degradation of a folded protein by the eukaryotic proteasomes-origin of intrinsic degradation signals. PLoS One 7, e34864.
[5] Nanaware, P.P., Ramteke, M.P., Somavarapu, A.K. and Venkatraman, P. (2013) Discovery of multiple interacting partners of gankyrin, a proteasomal chaperone and an oncoprotein – evidence for a common hot spot site at the interface and its functional relevance. Proteins.
[6] Inostroza-Nieves, Y., Venkatraman, P. and Zavala-Ruiz, Z. (2012) Role of Sug1, a 19S proteasome ATPase, in the transcription of MHC I and the atypical MHC II molecules, HLA-DM and HLA-DO. Immunol. Lett. 147, 67–74.
[7] Sahu, I., Sangith, N., Ramteke, M., Gadre, R. and Venkatraman, P. (2014) A novel role for the proteasomal chaperone PSMD9 and hnRNPA1 in enhancing IkappaBalpha degradation and NF-kappaB activation – functional relevance of predicted PDZ domain-motif interaction. FEBS J..
[8] Pan, L., Yan, J., Wu, L. and Zhang, M. (2009) Assembling stable hair cell tip link complex via multidentate interactions between harmonin and cadherin 23. Proc. Natl. Acad. Sci. U.S.A. 106, 5575–5580.
[9] Sali, A. and Blundell, T.L. (1993) Comparative protein modelling by satisfaction of spatial restraints. J. Mol. Biol. 234, 779–815.
[10] Case, D. (2010). Amber 9. University of California Sanfrancisco.
[11] Dominguez, C., Boelens, R. and Bonvin, A.M. (2003) HADDOCK: a protein-protein docking approach based on biochemical or biophysical information. J. Am. Chem. Soc. 125, 1731–1737.
[12] Zacharias, M. (2003) Protein-protein docking with a reduced protein model accounting for side-chain flexibility. Protein Sci. 12, 1271–1282.
[13] Jorgensen, W. (1983) Comparison of simple potential functions for simulating liquid water. J. Chem. Phys. 79, 926–935.
[14] Duan, Y. et al. (2003) A point-charge force field for molecular mechanics simulations of proteins based on condensed-phase quantum mechanical calculations. J. Comput. Chem. 24, 1999–2012.
[15] Darden, T. (1993) Particle mesh Ewald: an N•log(N) method for Ewald sums in large systems. J. Chem. Phys. 98, 10089–10092.
[16] Miyamoto, S. (1992) Settle: an analytical version of the SHAKE and RATTLE algorithm for rigid water models. J. Comput. Chem. 13, 952–962.
[17] Humphrey, W., Dalke, A. and Schulten, K. (1996) VMD: visual molecular dynamics. J. Mol. Graph. 14 (33–8), 27–28.
[18] Fuh, G., Pisabarro, M.T., Li, Y., Quan, C., Lasky, L.A. and Sidhu, S.S. (2000) Analysis of PDZ domain-ligand interactions using carboxyl-terminal phage display. J. Biol. Chem. 275, 21486–21491.
[19] Sidhu, S.S., Fairbrother, W.J. and Deshayes, K. (2003) Exploring protein–protein interactions with phage display. ChemBioChem 4, 14–25.
[20] Sidhu, S.S. and Koide, S. (2007) Phage display for engineering and analyzing protein interaction interfaces. Curr. Opin. Struct. Biol. 17, 481–487.
[21] Stiffler, M.A., Grantcharova, V.P., Sevecka, M. and MacBeath, G. (2006) Uncovering quantitative protein interaction networks for mouse PDZ domains using protein microarrays. J. Am. Chem. Soc. 128, 5913–5922.
[22] Chen, J.R., Chang, B.H., Allen, J.E., Stiffler, M.A. and MacBeath, G. (2008) Predicting PDZ domain-peptide interactions from primary sequences. Nat. Biotechnol. 26, 1041–1045.
[23] Rodi, D.J., Makowski, L. and Kay, B.K. (2002) One from column A and two from column B: the benefits of phage display in molecular-recognition studies. Curr. Opin. Chem. Biol. 6, 92–96.
[24] Sharma, S.C., Memic, A., Rupasinghe, C.N., Duc, A.C. and Spaller, M.R. (2009) T7 phage display as a method of peptide ligand discovery for PDZ domain proteins. Biopolymers 92, 183–193.
[25] Tonikian, R. et al. (2008) A specificity map for the PDZ domain family. PLoS Biol. 6, e239.
[26] Chung, J.J., Yang, H. and Li, M. (2003) Genome-wide analyses of carboxyl-terminal sequences. Mol. Cell. Proteomics 2, 173–181.
[27] Thomas, M.K., Yao, K.M., Tenser, M.S., Wong, G.G. and Habener, J.F. (1999) Bridge-1, a novel PDZ-domain coactivator of E2A-mediated regulation of insulin gene transcription. Mol. Cell. Biol. 19, 8492–8504.
[28] Lee, J.H., Volinic, J.L., Banz, C., Yao, K.M. and Thomas, M.K. (2005) Interactions with p300 enhance transcriptional activation by the PDZ-domain coactivator Bridge-1. J. Endocrinol. 187, 283–292.
[29] Johnson, J.D. et al. (2006) Insulin protects islets from apoptosis via Pdx1 and specific changes in the human islet proteome. Proc. Natl. Acad. Sci. U.S.A. 103, 19575–19580.
[30] Lee, S.Y., De la Mota-Peynado, A. and Roelofs, J. (2011) Loss of Rpt5 protein interactions with the core particle and Nas2 protein causes the formation of faulty proteasomes that are inhibited by Ecm29 protein. J. Biol. Chem. 286, 36641–36651.
[31] Munz, M., Hein, J. and Biggin, P.C. (2012) The role of flexibility and conformational selection in the binding promiscuity of PDZ domains. PLoS Comput. Biol. 8, e1002749.
[32] Morrisett, J.D., David, J.S., Pownall, H.J. and Gotto Jr., A.M. (1973) Interaction of an apolipoprotein (apoLP-alanine) with phosphatidylcholine. Biochemistry 12, 1290–1299.
[33] Haendeler, J. et al. (2013) Two isoforms of Sister-Of-Mammalian Grainyhead have opposing functions in endothelial cells and in vivo. Arterioscler. Thromb. Vasc. Biol. 33, 1639–1646.
[34] Hakre, S., Tussie-Luna, M.I., Ashworth, T., Novina, C.D., Settleman, J., Sharp, P.A. and Roy, A.L. (2006) Opposing functions of TFII-I spliced isoforms in growth factor-induced gene expression. Mol. Cell 24, 301–308.
[35] Terada, N., Patel, H.R., Takase, K., Kohno, K., Nairn, A.C. and Gelfand, E.W. (1994) Rapamycin selectively inhibits translation of mRNAs encoding elongation factors and ribosomal proteins. Proc. Natl. Acad. Sci. U.S.A. 91, 11477–11481.
[36] Janin, J. (1979) Surface and inside volumes in globular proteins. Nature 277, 491–492.
[37] Wolfenden, R., Andersson, L., Cullis, P.M. and Southgate, C.C. (1981) Affinities of amino acid side chains for solvent water. Biochemistry 20, 849–855.
[38] Kyte, J. and Doolittle, R.F. (1982) A simple method for displaying the hydropathic character of a protein. J. Mol. Biol. 157, 105–132.
[39] Rose, G.D., Geselowitz, A.R., Lesser, G.J., Lee, R.H. and Zehfus, M.H. (1985) Hydrophobicity of amino acid residues in globular proteins. Science 229, 834–838.
[40] Das, U. et al. (2007) Inhibition of protein aggregation: supramolecular assemblies of arginine hold the key. PLoS One 2, e1176.
[41] Tsumoto, K., Ejima, D., Nagase, K. and Arakawa, T. (2007) Arginine improves protein elution in hydrophobic interaction chromatography. The cases of human interleukin-6 and activin-A. J. Chromatogr. A 1154, 81–86.
[42] Tsumoto, K., Abe, R., Ejima, D. and Arakawa, T. (2010) Non-denaturing solubilization of inclusion bodies. Curr. Pharm. Biotechnol. 11, 309–312.
[43] Lee, H.J. and Zheng, J.J. (2010) PDZ domains and their binding partners: structure, specificity, and modification. Cell Commun. Signal. 8, 8.
[44] Elkins, J.M., Gileadi, C., Shrestha, L., Phillips, C., Wang, J., Muniz, J.R. and Doyle, D.A. (2010) Unusual binding interactions in PDZ domain crystal structures help explain binding mechanisms. Protein Sci. 19, 731–741.
[45] Zhang, Y., Appleton, B.A., Wiesmann, C., Lau, T., Costa, M., Hannoush, R.N. and Sidhu, S.S. (2009) Inhibition of Wnt signaling by Dishevelled PDZ peptides. Nat. Chem. Biol. 5, 217–219.
[46] Zahn, M., Berthold, N., Kieslich, B., Knappe, D., Hoffmann, R. and Strater, N. (2013) Structural studies on the forward and reverse binding modes of peptides to the chaperone DnaK. J. Mol. Biol. 425, 2463–2479.
[47] Brokx, R.D., Lopez, M.M., Vogel, H.J. and Makhatadze, G.I. (2001) Energetics of target peptide binding by calmodulin reveals different modes of binding. J. Biol. Chem. 276, 14083–14091.
[48] Feng, S., Chen, J.K., Yu, H., Simon, J.A. and Schreiber, S.L. (1994) Two binding orientations for peptides to the Src SH3 domain: development of a general model for SH3-ligand interactions. Science 266, 1241–1247.
[49] Liu, J. et al. (2008) Conformational change upon ligand binding and dynamics of the PDZ domain from leukemia-associated Rho guanine nucleotide exchange factor. Protein Sci. 17, 1003–1014.

[50] Hay, D.C., Kemp, G.D., Dargemont, C. and Hay, R.T. (2001) Interaction between hnRNPA1 and IkappaBalpha is required for maximal activation of NF-kappaB-dependent transcription. Mol. Cell. Biol. 21, 3482–3490.
[51] Stavreva, D.A. et al. (2006) Potential roles for ubiquitin and the proteasome during ribosome biogenesis. Mol. Cell. Biol. 26, 5131–5145.
[52] Ding, Q., Dimayuga, E., Markesbery, W.R. and Keller, J.N. (2006) Proteasome inhibition induces reversible impairments in protein synthesis. FASEB J. 20, 1055–1063.
[53] Lopez, A.D., Tar, K., Krugel, U., Dange, T., Ros, I.G. and Schmidt, M. (2011) Proteasomal degradation of Sfp1 contributes to the repression of ribosome biogenesis during starvation and is mediated by the proteasome activator Blm10. Mol. Biol. Cell 22, 528–540.
[54] Zhou, X., Hao, Q., Liao, J., Zhang, Q. and Lu, H. (2013) Ribosomal protein S14 unties the MDM2-p53 loop upon ribosomal stress. Oncogene 32, 388–396.
[55] Maquat, L.E. and Serin, G. (2001) Nonsense-mediated mRNA decay: insights into mechanism from the cellular abundance of human Upf1, Upf2, Upf3, and Upf3X proteins. Cold Spring Harb. Symp. Quant. Biol. 66, 313–320.
[56] Mehrotra, S. et al. (2004) Antigen presentation by MART-1 adenovirus-transduced interleukin-10-polarized human monocyte-derived dendritic cells. Immunology 113, 472–481.
[57] Garzon, R., Soriano, S.F., Rodriguez-Frade, J.M., Gomez, L., Martin de Ana, A., Sanchez-Gomez, M., Martinez, A.C. and Mellado, M. (2004) CXCR4-mediated suppressor of cytokine signaling up-regulation inactivates growth hormone function. J. Biol. Chem. 279, 44460–44466.
[58] Corsi, A.K. and Schekman, R. (1996) Mechanism of polypeptide translocation into the endoplasmic reticulum. J. Biol. Chem. 271, 30299–30302.
[59] Bonifacino, J.S. and Weissman, A.M. (1998) Ubiquitin and the control of protein fate in the secretory and endocytic pathways. Annu. Rev. Cell Dev. Biol. 14, 19–57.
[60] Strous, G.J. and Govers, R. (1999) The ubiquitin-proteasome system and endocytosis. J. Cell Sci. 112 (Pt 10), 1417–1423.
[61] Mayer, T.U., Braun, T. and Jentsch, S. (1998) Role of the proteasome in membrane extraction of a short-lived ER-transmembrane protein. EMBO J. 17, 3251–3257.
[62] Lord, J.M. (1996) Go outside and see the proteasome. Protein Degrad. Curr. Biol. 6, 1067–1069.
[63] Christianson, J.C. and Ye, Y. (2014) Cleaning up in the endoplasmic reticulum: ubiquitin in charge. Nat. Struct. Mol. Biol. 21, 325–335.
[64] Hampton, R.Y. (2002) ER-associated degradation in protein quality control and cellular regulation. Curr. Opin. Cell Biol. 14, 476–482.
[65] Shamu, C.E., Story, C.M., Rapoport, T.A. and Ploegh, H.L. (1999) The pathway of US11-dependent degradation of MHC class I heavy chains involves a ubiquitin-conjugated intermediate. J. Cell Biol. 147, 45–58.
[66] Levine, S.J. (2004) Mechanisms of soluble cytokine receptor generation. J. Immunol. 173, 5343–5348.
[67] Jostock, T. et al. (2001) Soluble gp130 is the natural inhibitor of soluble interleukin-6 receptor transsignaling responses. Eur. J. Biochem. 268, 160–167.
[68] Ortiz-Lazareno, P.C. et al. (2008) MG132 proteasome inhibitor modulates proinflammatory cytokines production and expression of their receptors in U937 cells: involvement of nuclear factor-kappaB and activator protein-1. Immunology 124, 534–541.
[69] Peiretti, F., Canault, M., Bernot, D., Bonardo, B., Deprez-Beauclair, P., Juhan-Vague, I. and Nalbone, G. (2005) Proteasome inhibition activates the transport and the ectodomain shedding of TNF-alpha receptors in human endothelial cells. J. Cell Sci. 118, 1061–1070.
[70] Levine, S.J. et al. (2005) Proteasome inhibition induces TNFR1 shedding from human airway epithelial (NCI-H292) cells. Am. J. Physiol. Lung Cell. Mol. Physiol. 289, L233–L243.
[71] van Kerkhof, P., Alves dos Santos, C.M., Sachse, M., Klumperman, J., Bu, G. and Strous, G.J. (2001) Proteasome inhibitors block a late step in lysosomal transport of selected membrane but not soluble proteins. Mol. Biol. Cell 12, 2556–2566.
[72] Riewald, M. and Schuepbach, R.A. (2008) Protective signaling pathways of activated protein C in endothelial cells. Arterioscler. Thromb. Vasc. Biol. 28, 1–3.